INTERNATIONAL JOURNAL OF CHEMISTRY

CCSE

Canadian Center of Science and Education®

Editorial Board

Contents

Contents

Diastereoselective Spiroannulation of Phenolic Derivatives: Effect of the o-Alkoxy Substituent on the Diastereoselectivity

Guy L. Plourde (Corresponding author)

Department of Chemistry, University of Northern British Columbia

3333 University Way, Prince George, BC, V2N 4Z9, Canada

Tel: 1-250-960-6694 E-mail: plourde@unbc.ca

Lyndia M. Susag

College of New Caledonia

3330 22nd Avenue, Prince George, BC, V2N 1P8, Canada

Tel: 1-250-562-2131 ext: 5509 E-mail: susagl@cnc.bc.ca

Abstract

This study was aimed at determining the effect, if any, that steric factors may have on the diastereoselectivity in the spiroannulation of simple phenols. A series of phenols bearing different size substituents *ortho* to the phenolic hydroxyl were synthesized and spiroannulated to the corresponding spiroethers in good to excellent yields (76-94%). However, the diastereoselectivity of the reaction remain mostly unchanged suggesting that stereoelectronic rather than steric factors influence the diastereoselectivity in this reaction.

Keywords: Spironannulation, Diastereoselectivity, Asymmetric, Phenols, Oxidation, Lead tetraacetate

1. Introduction

The spiroannulation (or spirocyclization) of simple 4-substituted phenols has been known for more than 50 years, (Cha *et al*, 2009; Frie *et al*, 2009; Moriarty *et al*., 2001; Pierce *et al*, 2008) yet the asymmetric version of the reaction in which the stereochemistry of the newly formed spirocarbon is controlled lack in examples. For the past 10 years our focus has been to develop methods to accomplish the asymmetric spiroannulation of simple phenols in order to use these methods in the asymmetric synthesis of natural products such as the Aranorosins (Mukhopadhyay *et al*., 1997; Roy *et al*., 1992; Watanabe *et al*., 2003), Gymnastatins (Amagata *et al*., 1998a; Amagata *et al*., 1998b; Numata *et al*., 1997; Phoon *et al*., 2004) and Manumycins (Hu *et al*., 2001; Sattler *et al*., 1998). We have previously shown that the synthesis of spirocompounds from simple phenols can be accomplished diastereoselectively, albeit with only moderate diastereoselectivity (4:1 ratio of diastereomers for **1**) (Plourde, G.L. 2002a; Plourde, G.L. 2003a; Plourde, G.L. 2003b; Plourde, G.L. 2003c). Other studies have also shown the importance of the presence of electron donating groups (EDG) such as methoxy or amide *ortho* to the phenolic hydroxyl as shown in compounds **1-3** in Figure 1 (Plourde *et al*., 2005; Plourde *et al*., 2007; Plourde *et al*., 2008). Such groups not only increase the overall chemical yield of the spiroannulation reaction, but also appear to favour a higher diastereoselectivity as well. Furthermore, it was also shown that when the EDG is located *meta* to the phenolic hydroxyl as shown in **4**, the spiroannulation reaction is no longer diastereoselective (product **5** is produced in 45% yield with a 1:1 ratio of diastereomers from **4**) suggesting that an electronic effect may be the cause of the enhanced diastereoselectivity in the case of the *ortho* substituted phenols (Plourde *et al*., 2005). We speculated that this may be the result of the stabilization of a phenoxenium ion by the EDG in the transition state. A similar effect has also been observed in the oxidative carbon-based nucleophilic substitution of phenols (Quideau *et al*., 1999). We have recently studied the effect that the size of the *ortho*-alkoxy substituent may have on the diastereoselectivity of this reaction and our results are summarized below.

2. Experimental

2.1 General

Melting points were determined on a hot stage instrument and are uncorrected. Infrared spectra were obtained on a Perkin Elmer System 2000 FTIR. ^{1}H-NMR spectra were recorded on a Bruker AMX300 spectrometer at 300 MHz and chemical shifts are expressed in ppm using TMS as internal standard. ^{13}C-NMR spectra were recorded on a

Bruker AMX300 spectrometer at 75.4 MHz and chemical shifts are expressed in ppm using residual solvent signal as internal standard. Mass spectra were recorded on a Varian CP-3800 GC system with a Saturn 2200 MS station.

2.2 Synthesis of phenols 9a-d

2.2.1 (1E)-1-[4-(benzyloxy)-3-hydroxyphenyl]-4,4-dimethyl-1-en-3-one (**7**)

To a solution of mono-protected benzaldehyde **6** (1.61g, 7.1mmol) in 1:1 mixture of tetrahydrofuran/ethanol (150mL) was added sodium hydroxide (0.86g, 21.6mmol) and pinacolone (3.1g, 31.2mmol). The mixture was refluxed for 24 hours at which point thin layer chromatography showed an incomplete reaction. Additional quantities of sodium hydroxide (0.75g, 2.7mmol) and pinacolone (3.1g, 30.9mmol) were added and the mixture was refluxed for an additional 24 hours. The resulting dark red mixture was cooled to room temperature, acidified with 10% HCl (150mL), concentrated *in vacuo* and extracted with dichloromethane (4 x 50mL). The organic fractions were combined, dried (MgSO$_4$) and the solvent was evaporated *in vacuo* to give an amber oil that solidified upon standing. Chromatography on silica gel using 15% ethyl acetate/hexanes as eluent afforded a light yellow solid (1.72g, 79%). mp: 92-93°C. IR (KBr) cm^{-1}: 3406, 1673. ^{1}H-NMR (CDCl$_3$) δ: 1.22 (s, 9H, ^{t}Bu), 5.15 (s, 2H, OCH$_2$), 5.71 (s, 1H exchangeable with D$_2$O, OH), 6.99 (d, 1H, J=15.5Hz, H$_2$), 7.24 (m, 8H, aromatic Hs), 7.59 (d, 1H, J=15.5Hz, H$_1$). ^{13}C-NMR (CDCl$_3$) δ: 26.8, 43.6, 71.5, 112.3, 113.4, 119.6, 122.8, 128.3, 129.0, 129.2, 137.0, 143.0, 146.4, 148.0, 204.7. MS (rel %) for C$_{20}$H$_{22}$O$_3$: 310 [M$^+$] (17), 251 (100), 219 (51), 162 (22), 91 (36), 57 (58).

2.2.2 1-(4-benzyloxy-3-ethoxyphenyl)-4,4-dimethylpent-1-ene-3-one (**8a**)

To a solution of **7** (0.45g, 1.5mmol) in acetonitrile (30mL) was added iodoethane (0.80g, 5.1mmol) and potassium carbonate (0.69g, 5mmol). The mixture was reflux for 24 hours, cooled to room temperature, washed with distilled water (30mL), concentrated *in vacuo* and extracted with dichloromethane (3 x 30mL). The organic fractions were combined, dried (MgSO$_4$) and the solvent evaporated *in vacuo*. The crude reaction product was purified by chromatography on silica gel using 10% ethyl acetate/hexanes as eluent to afford a light yellow solid (0.46g, 95%). mp: 88-90°C. IR (KBr) cm^{-1}: 1678. ^{1}H-NMR (CDCl$_3$) δ: 1.22 (s, 9H, ^{t}Bu), 1.49 (t, 3H, J=7.1Hz, ethyl CH$_3$), 4.18 (q, 2H, J=7.1Hz, ethyl CH$_2$), 5.19 (s, 2H, OCH$_2$), 7.04 (d, 1H, J=15.6Hz, H$_1$), 7.24 (m, 9H, aromatic Hs), 7.59 (d, 1H, J=15.6Hz, H$_2$). ^{13}C-NMR (CDCl$_3$) δ: 15.1, 26.6, 65.1, 71.1, 113.2, 114.4, 118.9, 122.6, 127.3, 128.1, 128.8, 137.0, 143.1, 149.4, 150.8, 204.4. MS (rel %) for C$_{22}$H$_{26}$O$_3$: 338 (M$^+$) (100), 281 (56), 191 (18), 91 (8).

2.2.3 1-(4-benzyloxy-3-isopropoxyphenyl)-4,4-dimethylpent-1-ene-3-one (**8b**)

To a solution of **7** (0.44g, 1.4mmol) in acetonitrile (30mL) was added 2-bromopropane (0.64g, 5.2mmol) and potassium carbonate (0.71g, 5.1mmol). The mixture was reflux for 24 hours, cooled to room temperature, washed with distilled water (30mL), concentrated *in vacuo* and extracted with dichloromethane (3 x 30mL). The organic fractions were combined, dried (MgSO$_4$) and the solvent evaporated *in vacuo*. The crude reaction product was purified by chromatography on silica gel using 10% ethyl acetate/hexanes as eluent to afford a white solid (0.49g, 98%). mp: 59-60°C. IR (KBr) cm^{-1}: 1678. ^{1}H-NMR (CDCl$_3$) δ: 1.22 (s, 9H, ^{t}Bu), 1.37 (d, 6H, J=6.2Hz, isopropyl CH$_3$), 4.57 (m, 1H, isopropyl CH), 5.17 (s, 2H, OCH$_2$), 6.97 (d, 1H, J=15.5Hz, H$_1$), 7.30 (m, 8H, aromatic Hs), 7.60 (d, 1H, J=15.5Hz, H$_2$). ^{13}C-NMR (CDCl$_3$) δ: 22.4, 26.6, 43.4, 71.1, 72.7, 114.8, 117.6, 119.0, 123.1, 127.3, 128.1, 128.8, 137.1, 143.0, 148.2, 152.2, 204.1.

2.2.4 1-(4-benzyloxy-3-isopropoxyphenyl)-4,4-dimethylpent-1-ene-3-one (**8c**)

To a solution of **7** (0.28g, 0.9mmol) in acetonitrile (30mL) was added bromomethylcyclohexane (0.49g, 2.8mmol) and potassium carbonate (0.69g, 5.0mmol). The mixture was reflux for 24 hours, cooled to room temperature, washed with distilled water (30mL), concentrated *in vacuo* and extracted with dichloromethane (3 x 30mL). The organic fractions were combined, dried (MgSO$_4$) and the solvent evaporated *in vacuo*. The crude reaction product was purified by chromatography on silica gel using 10% ethyl acetate/hexanes as eluent to afford a light yellow solid (0.25g, 70%). mp: 103-105°C. IR (KBr) cm^{-1}: 1678. ^{1}H-NMR (CDCl$_3$) δ: 1.22 (s, 9H, ^{t}Bu), 1.25 (m, 6H cyclohexyl Hs), 1.83 (m, 5H, cyclohexyl Hs), 3.86 (d, 2H, J=6.0Hz, cyclohexyl OCH$_2$), 5.15 (s, 2H, OCH$_2$), 6.97 (d, 1H, J=15.5Hz, H$_1$), 7.30 (m, 8H, aromatic Hs), 7.61 (d, 1H, J=15.5Hz, H$_2$). ^{13}C-NMR (CDCl$_3$) δ: 26.1, 26.7, 30.1, 37.9, 43.3, 71.2, 75.0, 113.3, 114.7, 118.9, 122.5, 127.3, 128.1, 128.7, 137.2, 143.3, 149.9, 150.9, 204.4. MS (rel %) for C$_{29}$H$_{34}$O$_3$: 406 (83), 349 (100), 318 923), 253 (28), 220 (33), 91 (10), 57 (8).

2.2.5 1-(4-benzyloxy-3-(2,6-dichlorobenzyloxy)phenyl)-4,4-dimethylpent-1-ene-3-one (**8d**)

To a solution of **7** (0.45g, 1.5mmol) in acetonitrile (30mL) was added 2,6-dichlorobenzylbromide (0.73g, 3.1mmol) and potassium carbonate (0.83g, 6.0mmol). The mixture was reflux for 24 hours, cooled to room temperature, washed with distilled water (30mL), concentrated *in vacuo* and extracted with dichloromethane (3 x 30mL). The organic fractions were combined, dried (MgSO$_4$) and the solvent evaporated *in vacuo*. The crude reaction product was purified by chromatography on silica gel using 10% ethyl acetate/hexanes as eluent to afford a light yellow oil

(0.57g, 84%). IR (neat) cm^{-1}: 1679. ^{1}H-NMR (CDCl$_3$) δ: 1.23 (s, 9H, ^{t}Bu), 5.17 (s, 2H, OCH$_2$), 5.42 (s, 2H, OCH$_2$), 6.98 (d, 1H, J=15.6Hz, H$_1$), 7.30 (m, 11H, aromatic Hs), 7.60 (d, 1H, J=15.6Hz, H$_2$). ^{13}C-NMR (CDCl$_3$) δ: 26.6, 43.4, 67.3, 71.3, 114.9, 115.9, 119.2, 124.2, 127.5, 128.1, 128.7, 130.0, 130.6, 132.5, 136.9, 137.3, 142.8, 149.1, 151.8, 204.4.

2.2.6 (±)-1-(3-ethoxy-4-hydroxyphenyl)-4,4-dimethylpentan-3-ol (9a)

To a solution of **8a** (0.41g, 1.2mmol) in ethyl acetate (30mL) was added 5% Pd/C (0.24g) and the mixture was shaken at room temperature in an hydrogenator with a H$_2$ pressure maintained at 30-35 psi. The mixture was filtered through Celite®, dried (MgSO$_4$), and the solvent was evaporated *in vacuo*. The crude reaction mixture was dissolved in ethanol (30mL) and sodium borohydride (0.14g, 3.8mmol) was added. The mixture was stirred at room temperature for 3 hours. The solution was acidified (10% HCl) and allowed to stir overnight. The solution was washed with water (10mL), extracted with dichloromethane (3 x 25mL), dried (MgSO$_4$) and the solvent was evaporated *in vacuo*. The crude product was purified by chromatography on silica gel using 20% ethyl acetate/hexanes as eluent to afford a slightly yellow oil (0.27g, 90%). IR (neat) cm^{-1}: 3422. ^{1}H-NMR (CDCl$_3$) δ: 0.89 (s, 9H, ^{t}Bu), 1.44 (t, 3H, J=6.8Hz, ethyl CH$_3$), 1.54 (m, 1H, H$_{2a}$), 1.61 (broad s, 1H exchangeable with D$_2$O, OH), 1.80 (m, 1H, H$_{2b}$), 2.54 (m, 1H, H$_{1a}$), 2.85 (m, 1H, H$_{1b}$), 3.22 (broad d, 1H, J=10.5Hz, H$_3$), 4.10 (q, 2H, J=6.8Hz, ethyl CH$_2$), 5.54 (s, 1H exchangeable with D$_2$O, OH), 6.71 (m, 2H, ArH$_2$ and ArH$_6$), 6.84 (d, 1H, J=8.6Hz, ArH$_5$). ^{13}C-NMR (CDCl$_3$) δ: 15.1, 25.9, 33.3, 33.9, 35.1, 79.6, 112.2, 114.4, 121.0, 134.5, 144.0, 145.8. MS (rel %) for C$_{15}$H$_{24}$O$_3$: 252 [M$^+$] (100), 165 (19), 151 (37).

2.2.7 (±)-1-(4-hydroxy-3-isopropoxyphenyl)-4,4-dimethylpentan-3-ol (9b)

To a solution of **8b** (0.42g, 1.2mmol) in ethyl acetate (30mL) was added 5% Pd/C (0.27g) and the mixture was shaken at room temperature in an hydrogenator with a H$_2$ pressure maintained at 30-35 psi. The mixture was filtered through Celite®, dried (MgSO$_4$), and the solvent was evaporated *in vacuo*. The crude reaction mixture was dissolved in ethanol (30mL) and sodium borohydride (0.12g, 3.1mmol) was added. The mixture was stirred at room temperature for 3 hours. The solution was acidified (10% HCl) and allowed to stir overnight. The solution was washed with water (10mL), extracted with dichloromethane (3 x 25mL), dried (MgSO$_4$) and the solvent was evaporated *in vacuo*. The crude product was purified by chromatography on silica gel using 10% ethyl acetate/hexanes as eluent to afford a slightly yellow oil (0.26g, 81%). IR (neat) cm^{-1}: 3420. ^{1}H-NMR (CDCl$_3$) δ: 0.89 (s, 9H, ^{t}Bu), 1.36 (d, 6H, J=6.2Hz, isopropyl CH$_3$), 1.54 (m, 1H, H$_{2a}$), 1.67 (broad s, 1H exchangeable with D$_2$O, OH), 1.80 (m, 1H, H$_{2b}$), 2.53 (m, 1H, H$_{1a}$), 2.83 (m, 1H, H$_{1b}$), 3.21 (broad d, 1H, J=10.8Hz, H$_3$), 4.58 (m, 1H, J=6.2Hz, isopropyl CH), 5.60 (s, 1H exchangeable with D$_2$O, OH), 6.71 (m, 2H, ArH$_2$ and ArH$_6$), 6.84 (d, 1H, J=8.0Hz, ArH$_5$). ^{13}C-NMR (CDCl$_3$) δ: 22.5, 25.9, 33.2, 33.9, 35.1, 71.8, 79.5, 113.9, 114.5, 121.2, 134.4, 144.0. MS (rel %) for C$_{16}$H$_{26}$O$_3$: 266 [M$^+$] (100), 249 (35), 205 (8), 165 (33), 123 (44).

2.2.8 (±)-1-(4-hydroxy-3-methylcyclohexyloxyphenyl)-4,4-dimethylpentan-3-ol (9c)

To a solution of **8c** (0.22g, 0.5mmol) in ethyl acetate (30mL) was added 5% Pd/C (0.20g) and the mixture was shaken at room temperature in an hydrogenator with a H$_2$ pressure maintained at 30-35 psi. The mixture was filtered through Celite®, dried (MgSO$_4$), and the solvent was evaporated *in vacuo*. The crude reaction mixture was dissolved in ethanol (30mL) and sodium borohydride (0.12g, 3.1mmol) was added. The mixture was stirred at room temperature for 3 hours. The solution was acidified (10% HCl) and allowed to stir overnight. The solution was washed with water (10mL), extracted with dichloromethane (3 x 25mL), dried (MgSO$_4$) and the solvent was evaporated *in vacuo*. The crude product was purified by chromatography on silica gel using 20% ethyl acetate/hexanes as eluent to afford a slightly yellow oil (0.08g, 43%). IR (neat) cm^{-1}: 3419. ^{1}H-NMR (CDCl$_3$) δ: 0.89 (s, 9H, ^{t}Bu), 1.0-1.8 (m, 13H, cyclohexyl Hs, H$_{2a}$ and H$_{2b}$), 2.54 (m, 1H, H$_{1a}$), 2.83 (m, 1H, H$_{1b}$), 3.22 (broad d, 1H, J=10.5Hz, H$_3$), 3.82 (d, 2H, J=7.1Hz, OCH$_2$), 5.53 (s, 1H exchangeable with D$_2$O, OH), 6.71 (m, 2H, ArH$_2$ and ArH$_6$), 6.84 (d, 1H, J=8.5Hz, ArH$_5$). ^{13}C-NMR (CDCl$_3$) δ: 25.9, 26.0, 26.7, 30.1, 33.3, 33.9, 35.1, 37.9, 74.4, 79.6, 112.1, 114.3, 120.9, 134.5, 144.0, 146.1. MS (rel %) for C$_{20}$H$_{32}$O$_3$: 319 (100), 218 (21), 123 (16).

2.2.9 (±)-1-(3-(2,6-dichlorobenzyloxy)-4-hydroxyphenyl)-4,4-dimethylpentan-3-ol (9d)

To a solution of **8d** (0.53g, 1.1mmol) in ethyl acetate (30mL) was added 5% Pd/C (0.37g) and the mixture was shaken at room temperature in an hydrogenator with a H$_2$ pressure maintained at 30-35 psi. The mixture was filtered through Celite®, dried (MgSO$_4$), and the solvent was evaporated *in vacuo*. The crude reaction mixture was dissolved in ethanol (30mL) and sodium borohydride (0.19g, 4.9mmol) was added. The mixture was stirred at room temperature for 3 hours. The solution was acidified (10% HCl) and allowed to stir overnight. The solution was washed with water (10mL), extracted with dichloromethane (3 x 25mL), dried (MgSO$_4$) and the solvent was evaporated *in vacuo*. The crude product was purified by chromatography on silica gel using 25% ethyl acetate/hexanes as eluent to afford a slightly yellow oil (0.20g, 46%). IR (neat) cm^{-1}: 3497. ^{1}H-NMR (CDCl$_3$) δ:

0.92 (s, 9H, ^{t}Bu), 1.57 (m, 1H, H$_{2a}$), 1.85 (m, 1H, H$_{2b}$), 2.61 (m, 1H, H$_{1a}$), 2.85 (m, 1H, H$_{1b}$), 3.25 (broad d, 1H, J=10.4Hz, H$_3$), 5.35 (s, 2H, OCH$_2$), 5.69 (s, 1H exchangeable with D$_2$O, OH), 6.85 (m, 3H, aromatic Hs), 7.35 (m, 3H, aromatic Hs). ^{13}C-NMR (CDCl$_3$) δ: 25.9, 33.2, 33.9, 35.1, 66.6, 79.6, 113.8, 114.9, 122.3, 128.8, 130.9, 132.0, 134.6, 137.1, 144.6, 145.5. MS (rel %) for C$_{20}$H$_{24}$Cl$_2$O$_3$: 382 (63), 365 (100), 282 (17), 219 (7).

2.3 Synthesis of spiroethers 10a-d

2.3.1 (±)-2-tert-butyl-7-ethoxy-1-oxospiro[4.5]deca-6,9-diene-8-one (**10a**)

To a cold (0°C) solution of alcohol **9a** (59mg, 0.23mmol) in acetone (35mL) was added lead (IV) acetate (264mg, 0.58 mmol). The resulting mixture was stirred at 0°C for 2.5 hours, filtered through Celite® and ethylene glycol (4 drops) was added. The resulting mixture was stirred at room temperature overnight, filtered through Celite® and the solvent was evaporated *in vacuo*. ^{1}H-NMR data was obtained at this stage in order to determine the diastereomeric ratio of the mixture by using the signals for H$_6$ of the major and minor isomers. The diastereomeric ratio was determined to be 76/24. The crude product was then purified by chromatography on silica gel using 25% ethyl acetate/hexanes as eluent to afford a slightly yellow oil (49mg, 92%). Whenever distinguishable, data for both isomers are given. In this case the data for the minor isomer of the mixture is listed in [square brackets]. IR (neat) cm^{-1}: 1677. ^{1}H-NMR (CDCl$_3$) δ: 0.94 [0.95] (s, 9H, ^{t}Bu), 1.42 (t, 3H, J=7.1Hz, ethyl CH$_3$), 1.95-2.07 (m, 4H, H$_3$ and H$_4$), 3.91 (m, 3H, ethyl CH$_2$ and H$_2$), 5.66 (d, 1H, J=2.7Hz, H$_6$) [5.76, d, J=2.7Hz, H$_6$], 6.12 (d, 1H, J=9.9Hz, H$_9$) [6.14, d, J=9.9Hz, H$_9$], 6.78 (dd, 1H, J=2.7, 9.9Hz, H$_{10}$) [6.87, dd, J=2.7, 9.9Hz, H$_{10}$]. ^{13}C-NMR (CDCl$_3$) δ: 14.5, 26.1, 27.7, 33.8, 38.4, 63.4, 79.7, 88.9, 118.0, 126.4, 149.1, 150.7, 181.4. MS (rel %) for C$_{15}$H$_{22}$O$_3$: 250 [M$^+$] (75), 167 (100), 165 (29), 139 (33), 91 (7).

2.3.2 (±)-2-tert-butyl-7-isopropoxy-1-oxospiro[4.5]deca-6,9-diene-8-one (**10b**)

To a cold (0°C) solution of alcohol **9b** (55mg, 0.21mmol) in acetone (35mL) was added lead (IV) acetate (240mg, 0.54 mmol). The resulting mixture was stirred at 0°C for 2.5 hours, filtered through Celite® and ethylene glycol (4 drops) was added. The resulting mixture was stirred at room temperature overnight, filtered through Celite® and the solvent was evaporated *in vacuo*. ^{1}H-NMR data was obtained at this stage in order to determine the diastereomeric ratio of the mixture by using the signals for H$_6$ of the major and minor isomers. The diastereomeric ratio was determined to be 71/29. The crude product was then purified by chromatography on silica gel using 25% ethyl acetate/hexanes as eluent to afford a slightly yellow oil (41mg, 76%). Whenever distinguishable, data for both isomers are given. In this case the data for the minor isomer of the mixture is listed in [square brackets]. IR (neat) cm^{-1}: 1676. ^{1}H-NMR (CDCl$_3$) δ: 0.94 [0.95] (s, 9H, ^{t}Bu), 1.31[1.34] (d, 6H, J=6.5Hz, isopropyl CH$_3$), 2.06 (m, 4H, H$_3$ and H$_4$), 3.92 [4.35] (m, 2H, isopropyl CH and H$_2$), 5.67 (d, 1H, J=2.8Hz, H$_6$) [5.77, d, J=2.7Hz, H$_6$], 6.11 (d, 1H, J=10.0Hz, H$_9$) [6.13 (d, J=10.0Hz, H$_9$], 6.76 (dd, 1H, J=2.7, 10.0Hz, H$_{10}$) [6.84 (dd, H=2.7, 10.0Hz, H$_{10}$]. ^{13}C-NMR (CDCl$_3$) δ: 21.9, 26.3, 34.0, 38.6, 79.9, 89.1, 119.8, 126.7, 147.9, 150.6, 182.2. MS (rel %) for C$_{16}$H$_{24}$O$_3$: 264 [M$^+$](100), 205 (11), 165 (58), 123 (51).

2.3.3 (±)-2-tert-butyl-7-methylcyclohexyloxy-1-oxospiro[4.5]deca-6,9-diene-8-one (**10c**)

To a cold (0°C) solution of alcohol **9c** (37mg, 0.12mmol) in acetone (35mL) was added lead (IV) acetate (138mg, 0.30 mmol). The resulting mixture was stirred at 0°C for 2.5 hours, filtered through Celite® and ethylene glycol (4 drops) was added. The resulting mixture was stirred at room temperature overnight, filtered through Celite® and the solvent was evaporated *in vacuo*. ^{1}H-NMR data was obtained at this stage in order to determine the diastereomeric ratio of the mixture by using the signals for H$_6$ of the major and minor isomers. The diastereomeric ratio was determined to be 65/35. The crude product was then purified by chromatography on silica gel using 25% ethyl acetate/hexanes as eluent to afford a slightly yellow oil (14mg, 38%). Whenever distinguishable, data for both isomers are given. In this case the data for the minor isomer of the mixture is listed in [square brackets]. IR (neat) cm^{-1}: 1678. ^{1}H-NMR (CDCl$_3$) δ: 0.95 [0.96] (s, 9H, ^{t}Bu), 1.26 (m, 4H, cyclohexyl Hs), 1.84-2.06 (m, 11H, cyclohexyl Hs, H$_3$ and H$_4$), 3.53 (m, 2H, OCH$_2$), 3.93 (m, 1H, H$_2$), 5.62 (d, 1H, J=2.7Hz, H$_6$) [5.74, d, J=2.7Hz, H$_6$], 6.12 (d, 1H, J=9.9Hz, H$_9$) [6.14, d, J=9.9Hz, H$_9$], 6.77 (dd, 1H, J=2.7, 9.9Hz, H$_{10}$) [6.87, dd, H=2.7, 9.9Hz, H$_{10}$]. ^{13}C-NMR (CDCl$_3$) δ: 26.1, 26.7, 27.5, 30.2, 33.8, 37.2, 38.1, 73.3, 79.7, 88.7, 117.8, 126.5, 149.5, 150.4, 181.3. MS (rel %) for C$_{20}$H$_{30}$O$_3$: 316 (100), 204 (12), 123 (7).

2.3.4 (±)-2-tert-butyl-7-(2,6-dichlorobenzyloxy)-1-oxospiro[4.5]deca-6,9-diene-8-one (**10d**)

To a cold (0°C) solution of alcohol **9d** (51mg, 0.13mmol) in acetone (35mL) was added lead (IV) acetate (151mg, 0.33 mmol). The resulting mixture was stirred at 0°C for 2.5 hours, filtered through Celite® and ethylene glycol (4 drops) was added. The resulting mixture was stirred at room temperature overnight, filtered through Celite® and the solvent was evaporated *in vacuo*. ^{1}H-NMR data was obtained at this stage in order to determine the diastereomeric ratio of the mixture by using the signals for H$_6$ of the major and minor isomers. The diastereomeric ratio was

determined to be 51/49. The crude product was then purified by chromatography on silica gel using 20% ethyl acetate/hexanes as eluent to afford a slightly yellow oil (47mg, 94%). Whenever distinguishable, data for both isomers are given. In this case the data for the minor isomer of the mixture is listed in [square brackets]. IR (neat) cm^{-1}: 1677. ^{1}H-NMR (CDCl$_3$) δ: 0.96 [0.97] (s, 9H, ^{t}Bu), 2.05 (m, 4H, H$_3$ and H$_4$), 3.97 (m, 1H, H$_2$), 5.08 (s, 2H, OCH$_2$), 5.88 (d, 1H, J=2.7Hz, H$_6$) [5.98, d, J=2.7Hz, H$_6$], 6.13 (d, 1H, J=10.0Hz, H$_9$) [6.14, d, J=10.0Hz, H$_9$], 6.79 (dd, 1H, J=2.7, 10.0Hz, H$_{10}$) [6.87, dd, H=2.7, 10.0Hz, H$_{10}$], 7.3 (m, 3H, aromatic Hs). ^{13}C-NMR (CDCl$_3$) δ: 26.1, 27.6, 33.8, 38.1, 65.0, 79.6, 88.9, 119.5, 126.5, 128.6, 130.8, 131.4, 137.4, 149.1, 150.4, 180.7. MS (rel %) for C$_{20}$H$_{22}$Cl$_2$O$_3$: 381 [M$^+$] (100), 205 (66).

3. Results and Discussion

In order to study the influence that the size of the alkoxy group may have on the diastereoselectivity of the reaction we synthesized a series of four phenols **9a-d** bearing alkoxy functions *ortho* to the phenolic hydroxyl as shown in Scheme 1. These compounds were synthesized in three steps following a procedure similar to one that we have already published starting from the mono-protected benzaldehyde **6** (Plourde, G.L., 2002a; Plourde *et al*., 2002b; Plourde *et al*., 2005). Yields were comparable to those previously obtained in similar syntheses and are shown in Scheme 1.

The spiroannulation reaction of these phenols was carried out using the same method as previously described in order to allow for comparison of results as shown in Scheme 2 (Plourde, G.L. 2002a; Plourde, G.L. 2003a; Plourde, G.L. 2003b; Plourde, G.L. 2003c). Yields ranging from 38 to 94% were obtained for these spiroethers. It should be noted that we have not attempted to optimize these yields, especially for **10c** which was the lowest at 38%. Furthermore, in order to maintain consistency with our previous work, we used the integration of the ^{1}H-NMR signal for H-6 to calculate the diastereomeric ratios obtained in these reactions. These ratios were calculated from the crude reaction mixture prior to any purification of the material recovered and are shown in Scheme 2. As can be seen from the results in Scheme 2 as well as the partial ^{1}H-NMR spectra for **10a-d** shown in Figure 2, the diastereomeric ratio does not appear to be affected in a positive manner by the change of the alkyl function located on the ether oxygen in **9**. Instead, a slight decrease in the diastereomeric ratio is observed as the alkoxy group increases in size. This is clearly observed from the diagram shown in Figure 2. For comparison, the optimized diastereomeric ratio originally obtained with a methoxy group as substituent was 81/19 (Plourde, G.L., 2002a). The diastereoselectivity of the reaction even disappeared completely when the 2,6-dichlorobenzyl substituent was used (**10d**). While there may be a steric effect associated with this change, it is most likely due to the electron withdrawing character of this group which may be destabilizing the transition state. The possibility that a combination of both steric and electronic factors may influence the diastereomeric ratio in **10d** also exists. The effect appears somewhat similar to that of halogen substituents in electrophilic aromatic substitution, *i.e.* the halogen deactivates the ring by induction yet favours ortho/para substitution due to resonance stabilization. We are presently in the process of making the necessary phenols bearing halogens *ortho* to the phenolic hydroxyl to support this hypothesis.

4. Conclusions

We have prepared a series of four spiroethers bearing increasingly larger substituents in order to ascertain whether the reaction would be affected by the steric factors associated with those substituents. While we were hoping for an increase in diastereoselectivity, we observed the opposite trend *i.e.* the diastereoselectivity appears to decrease (although only slightly) with an increase in size of the substituents used. Furthermore, the results obtained with the 2,6-dichlorobenzyl group *ortho* to the phenolic hydroxyl in **9d** suggest that electronic factors are more important for the diastereoselectivity of this reaction and while weakly electron withdrawing groups still allow for the spiroannulation reaction to take place, this reaction is no longer diastereoselective. We are presently attempting to confirm this hypothesis. This finding appears to support our previously published work suggesting a stabilization effect by electron donating groups *ortho* to the phenolic hydroxyl (Plourde and English, 2005).

References

Amagata, T., Doi, M., Ohta, T., Minoura, K., Numata, A. (1998a). Absolute stereostructures of novel cytotoxic metabolites, gymnastatin A-E from a *Gymnascella* species separated from a *Halichondria* sponge. *JCS, Perkin Trans. 1*, 3585-3599.

Amagata, T., Minoura, K., Numata, A. (1998b). Gymnasterones, Novel cytotoxic metabolites produced by a fungal strain from a sponge. *Tet. Lett*., 39, 3773-3774.

Cha, J.Y., Huang, Y., Pettus, T. (2009). Total Synthesis of TK-57-164A, Isariotin F, and their Putative Progenitor Isariotin E. *Ang. Chem., Int. Ed.*, 48, 9519-9521.

Frie, J.L., Jeffrey, C.S., Sorensen, E.J. (2009). A Hypervalent Iodine-Induced Annulation Enables a Concise Synthesis of the Pentancyclic Core Structure of the Cortistatins. *Org. Lett.*, 11, 5394-5397.

Hu, Y., Floss, H.G. (2001). New Type II Manumycins produced by *Streptomyces nodosus* ssp. *Asukaensis* and their biosynthesis. *J. Antibiot.*, 54, 340-348.

Moriarty, R.M., Prakash, O. (2001). Oxidation of phenolic compounds with organohypervalent iodine reagents. *Organic Reactions*, Hoboken, NJ, USA, 57pp.

Mukohopadhyay, T., Bhat, R.G., Roy, R., Yijayakumar, E.K.S., Ganguli, B.N. (1997). Aranochlor A and aranochlor B, two new metabolites from *Pseudoarachniotus roseus*: Production, isolation, structure elucidation and biological properties. *J. Antibiot.*, 51, 439-441.

Numata, A., Amagata, T., Minoura, K., Ito, T. (1997). Gymnastatins, Novel cytotoxic metabolites produced by a fungal strain from a sponge. *Tet. Lett.*, 38, 5675-5678.

Phoon, C.W., Somanadhan, B., Heng, S.C.H., Ngo, A., Ng, S.B., Butler, M.S., Buss, A.D., Sim, M.M. (2004). Isolation and total synthesis of Gymnastatin N, a POLO-like kinase 1 active constituent from the fungus *Arachniotus punctatus*. *Tetr.*, 60, 11619-11628.

Pierce, J.G., Kasi, D., Fushimi, M., Cuzzupe, A., Wipf, P. (2008). Synthesis of Hydroxylated Bicyclic Amino Acids from L-Tyrosine: Octahydro-1H-indole Carboxylates. *J.O.C.*, 73, 7807-7810.

Plourde, G.L. (2002a). Studies towards the diastereoselective spiroannulation of phenolic derivatives. *Tet. Lett.*, 43, 3597-3599.

Plourde, G.L.; Spaetzel, R.R. (2002b). Regioselective Protection of the 4-Hydroxyl of 3,4-Dihydroxybenzaldehyde. *Molecules*, 7, 697-705.

Plourde, G.L. (2003a). (+/-)-2-^{t}Butyl-7-methoxy-1-oxaspiro[4,5]deca-6,9-diene-8-one. *Molbank*, M322.

Plourde, G.L. (2003b). (+/-)-7-Methoxy-2-^{i}propyl-1-oxaspiro[4,5]deca-6,9-diene-8-one *Molbank*, M319.

Plourde, G.L. (2003c). (+/-)-7-Methoxy-2-methyl-1-oxaspiro[4,5]deca-6,9-diene-8-one *Molbank*, M316.

Plourde, G.L., English, N.J. (2005). Diastereoselective Spiroannulation of Phenolic Substrates: Synthesis of (+/-)-2-*tert*-Butyl-6-methoxy-1-oxaspiro[4.5]deca-6,9-diene-8-one. *Molecules*, 10, 1335-1339.

Plourde, G.L., Spaetzel, R.R., Kwasnitza, J.S., Scully, T.W. (2007). Diastereoselective Spiroannulation of Phenolic Substrates: Advances Towards the Asymmetric Formation of the Manumycin m-C_7N Core Skeleton. *Molecules*, 12, 2215-2222.

Plourde, G.L., Susag, L.M., Dick, D.G. (2008). Determination of the Absolute Configurations of (+)-N-((3S)-3-{[(4-methylphenyl)sulfonyl]amino}-1-oxaspiro[4.5]deca-6,9-dien-2,8-dion-7-yl) Acetamide and Benzamide. *Molbank*, M579.

Quideau, S., Looney, M.A., Pouysegu, L. (1999). Oxidized Arenol Intermediates in Intermolecular Carbon-Carbon Bond Formation. Naphathoid 2,4-Cyclohexadienones via Oxidative Nucleophilic Substitution. *Org. Lett.*, 1, 1651-1654.

Roy, K., Vijayakumar, E.K.S., Mukhopadhyay, T., Chattaerjee, S., Bhat, R.G., Blumbach, J., Ganguli, B.N. (1992). Aranorosinol A and aranorosinol B, two mew methobolites from *Pseudoarachiniotus roseus*: Production, isolation, structure elucidation and biological properties. *J. Antibiot.*, 45, 1592-1598.

Sattler, I., Thiericke, R., Zeeck, A. (1998). The Manumycin-group metabolites. *Nat. Prod. Rep.*, 221-240.

Wanatabe, T., Hashimoto, Y, Yamamoto, K., Hirao, K., Ishihama, A., Hino, M., Utsumi, R. (2003). Isolation and characterization of inhibitors of the essential histidine kinase, YycG in *Bacillus subtilis* and *Staphylococcus aureus*. *J. Antibiot.*, 56, 1045-1052.
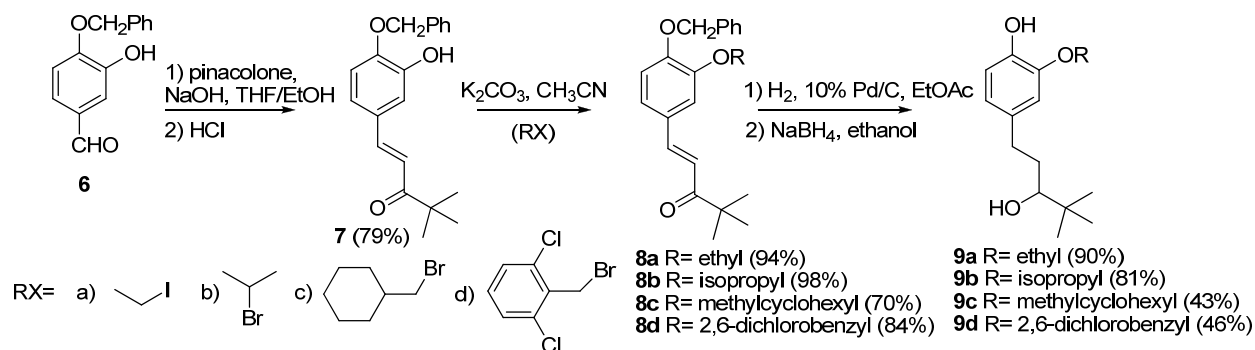
Scheme 1. Synthesis of phenols **9a-d**
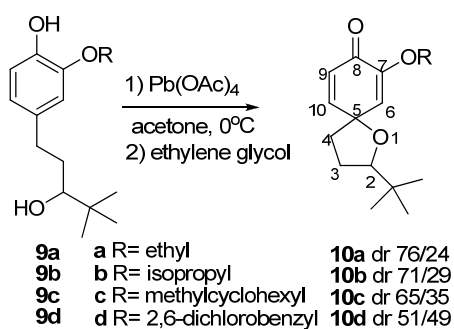
Scheme 2. Spiroannulation of **9a-d**
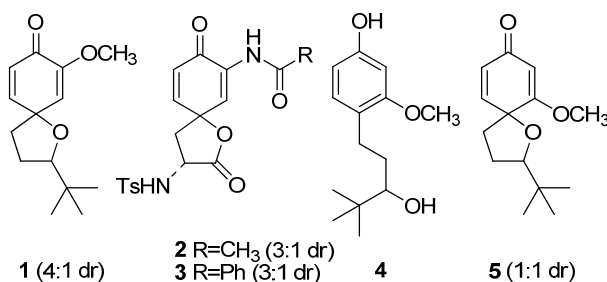
Figure 1. Diastereomeric ratios of spirocompounds
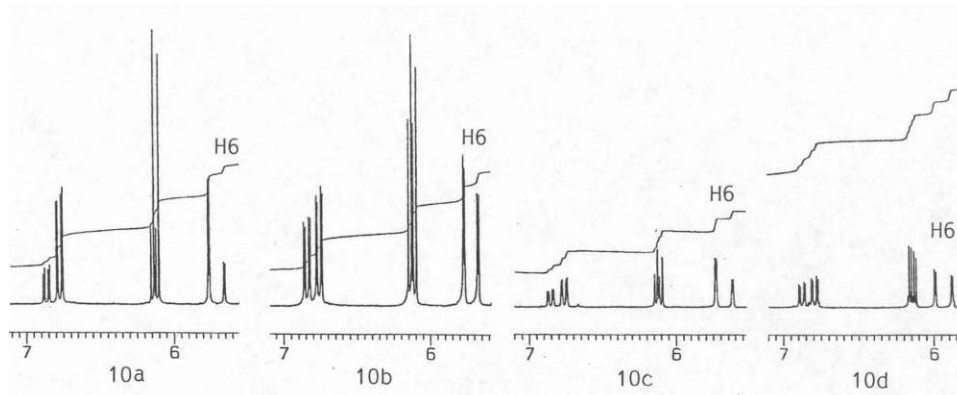
Figure 2. Partial ^{1}H-NMR spectra for **10a-d** showing the diastereomeric ratios

Dansyl - Substituted Aza Crown Ethers: Complexation with Alkali, Alkaline Earth Metal Ions and Ammonium

Nelly Mateeva (Corresponding author)

Department of Chemistry, Florida A&M University, 444 Gamble St. #204, Tallahassee, FL 32307, USA

Tel: 1-850-412-5662   E-mail: nelly.mateeva@famu.edu

Shihab Deiab

Department of Chemistry, Florida A&M University, 444 Gamble St. #204, Tallahassee, FL 32307, USA

Tel: 1-850-412-5662   E-mail: diab_pd@yahoo.com

Edikan Archibong

Department of Chemistry, Florida A&M University, 444 Gamble St. #204, Tallahassee, FL 32307, USA

Tel: 1-850-412-5662   E-mail: edikan18@yahoo.com

Donka Tasheva

Department of Chemistry, University of Sofia, 1 James Bourchier Ave. 1164 Sofia Bulgaria

Tel: 011-359-2-8161-303   E-mail: dtasheva@chem.uni-sofia.bg

Bereket Mochona

Department of Chemistry, Florida A&M University, 444 Gamble St. #204, Tallahassee, FL 32307, USA

Tel: 1-850-599-3285   E-mail: bereket.mochona@famu.edu

Madhavi Gangapuram

College of Pharmacy and Pharmaceutical Sciences, Florida A&M University

1415 S. Marthin L.King, Jr. Blvd., Tallahassee, FL 32307, USA

Tel: 1-850-561-2200   E-mail: madhavi.gangapuram@famu.edu

Kinfe Redda

College of Pharmacy and Pharmaceutical Sciences, Florida A&M University

1415 S. Marthin L.King, Jr. Blvd., Tallahassee, FL 32307, USA

Tel: 1-850-561-2200   E-mail: kinfe.redda@famu.edu

Abstract

The present study investigates the binding properties of four dansyl substituted aza-crown ethers with alkali, alkaline earth metal ions and ammonium. The influence of the solvent polarity and protonation on the photophysical properties of the compounds was studied by UV/Vis and fluorescence methods. The host species caused only slight changes on the absorption spectra of the ligands. The fluorescence changes were more pronounced and concentration dependent thus allowing to calculate the binding constants of the process. The most stable complex under our working conditions was the one between Ba^{2+} and DNS18C6.

Keywords: Aza-crown ethers, Complexation, Metal ions, Fluorescence, Absorption

1. Introduction

Dansyl chloride is a reagent very often used to react with primary and secondary amines in order to introduce a fluorescent moiety in a molecule. Amino acid derivatization is widely employed in HPLC chromatography in order to identify the N- terminal residue of peptides and proteins as well as to utilize a fluorescent detector for amino acid separation.

A typical example for the above mentioned method is shown in [Wang, Y., 2007]. An accurate, simple, and sensitive reversed-phase high-performance liquid chromatographic method, with loratadine as internal standard (IS) and UV detection at 286 nm, has been developed for determination of cystine in human urine. Amino acids fluorescently tagged with dansyl chloride were used in capillary electrophoresis study of amino acid separation. [Yin, D., 2008]

In molecular recognition chemistry, labeling of either guest or the host is often needed in order to create a chemosensor for detection of the investigated phenomena.

Modified cyclodextrins bearing fluorescent moieties have been used by Ueno and coworkers [Ueno, A., 1999] as sensors for a wide variety of organic guests, including chiral molecules. Roper et al., [Roper, E.D., 2007] reported a fluorogenic derivative of *1,3-alternate* calix[4]arenebis- (crown-6) containing a dansyl group in the protonionizable side arm has been employed in selective sensing of Tl^+ and Cs^+ at low concentration levels in MeCN-H_2O (1:1) mixed solvent.

Recognition and sensing of heavy and transition metal ions via artificial receptors are of current interest in supramolecular chemistry because of their significant importance in chemical, biological, and environmental assays. Of particular interest in this regard are fluorescent sensors, because they have both high sensitivity and ease of signal transduction. A practical fluorescent sensor for targeting ions of specific importance should at least have the following properties: simplicity, high selectivity, strong signal output, wide conditions of coordination and recognition in aqueous environments. Chen et al. [2004] reported a new fluorescent chemosensor for Hg^{2+} based on a dansyl amide-armed calix[4]-aza-crown. It exhibits high sensitivity and selectivity toward Hg^{2+}, and the detection limit for Hg^{2+} was found to be 4.1 x10^{-6}mol/L. [Chen, Q.-Y., 2004] More applications involving calixarines as well as peptide synthesis were reported elsewhere. [Casnati, A., 2001; Ten Brink H. T., 2006]

To the best of our knowledge, there are only a few examples of dansyl-modified crown ethers. Tsunooka et al. [1997] described the synthesis and cation-binding behavior of anionic polymers bearing both crown ether units and dansyl units. The structure of the anionic moieties in polymers strongly affects the cation-responsive fluorescence. [Shirai, M., 1997]

Ossowski et al., investigated the influence of alkaline, alkaline earth metal ions as well as number of heavy metals ions on the spectroscopic properties of the dansyl group covalently linked to crown ether or diazacrown ethers. Interaction of the alkali metal ions with all fluoroionophores studied was weak, while alkaline earth metal ions interact strongly causing about 50% quenching of dansyl fluorescence. The Cu^{2+}, Pb^{2+} and Al^{3+} cations interact very strongly with dansyl chromophore regardless of the crown ether type, causing a major change in absorption spectrum of the chromophore and forming non-fluorescent complexes. The Co^{2+}, Ni^{2+}, Zn^{2+}, Mg^{2+} and Ag^+ cations interact moderately with all fluoroionophores studied causing about 20% of fluorescence quenching of dansyl. The quenching efficiency of didansylated fluoroionophores by the alkali metal ions and alkaline earth metal ions is weaker than monodansylated ones. [Warmke, H., 2000; Sulowska, H., 2002]

In earlier studies we investigated the synthesis and complexation properties of aza-crown ether containing chromo- and fluoroionophores where the complexation was done in excess of the guest and in anhydrous solvents [Mateeva, N., 1994; Mateeva, N., 1995; Antonov, L., 1996]

In the present study we utilized four dansyl aza-crown ether derivatives and quantified their binding properties with alkaline, alkaline earth metal ions and ammonium. We report the binding constants and spectroscopic changes accompanying the complexation process.

2. Experimental

2.1 Materials and Methods

All chemicals were purchased from Sigma Aldrich and were ACS grade. They were used without further purification. Melting points were determined on Mel Temp 3.0 instrument and were uncorrected. ^{1}H NMR spectra were recorded on a Varian Gemini HX 300 MHz spectrometer using CDCl$_3$ as a solvent and the chemical shifts are expressed in parts per million (δ, ppm) downfield from TMS as an internal standard. Infrared spectra (IR) were recorded, for KBr discs, on a Perkin-Elmer FTIR 1430 spectrometer. Elemental analyses were performed for C, H,

and N (Galbraith Laboratories, Inc., Knoxville, TN, USA) and were within ± 0.4% of the theoretical values. The UV/Vis absorption of the solutions was measured using the Shimadzu UV-2401 PC spectrophotometer instrument. Fluorescence measurements were done on the Perkin Elmer LS55 Fluorescence spectrofluorimeter.

2.2 Synthesis

The compounds utilized in this study were synthesized according to Ossowski et al [Warmke, H., 2000; Sulowska, H., 2002]. The proton NMR, IR data and elemental analysis confirm the structure and are also in agreement with published data.

Figure 1 shows the structures of the aza-crown ether derivatives used in this study.

DNS2N218C6: ^{1}H NMR (CDCl$_3$) 2.85 (s, 6H, CH$_3$); 3.45-3.55 (m, 24H, crown); 7.17 (d, 1H, J = 7.8 Hz, Ar H); 7.40 (dd, 1H, J1 = 8.0Hz, Ar H);

7.50 (dd, 1H, J1 = 8.2 Hz, Ar H); 8.10 (d, 1H, J = 8.2Hz, Ar H); 8.20 (d, 1H, J = 8.7Hz, Ar H); 8.45 (d, 1H, J = 8.9Hz, Ar H).

IR: (ν cm^{-1}): (KBr) : 2820-2950, 1620, 1550, 1150

Elemental analysis: (C$_{24}$H$_{37}$N$_3$O$_6$S): (%calculated/found): C:58.16/58.25; H:7.52/7.20; N: 8.48/8.75

DNSN218C6: ^{1}H NMR (CDCl$_3$) 2.85 (s, 12H,CH$_3$); 3.45-3.55 (m, 24H, crown); 7.16 (d, 2H, J = 7.8Hz, Ar H); 7.45(dd, 2H, J = 8.0 Hz, Ar H); 7.54 (dd, 2H, J= 7.8 Hz, Ar H); 8.18 (d, 2H, J = 6.3 Hz, Ar H); 8.20 (d, 2H, J = 8.7 Hz, Ar H); 8.49 (d, 2H, J = 8.1 Hz, Ar H).

IR: (ν cm^{-1}) : (KBr) : 2830-2970, 1610, 1544, 1160

Elemental analysis: (C$_{36}$H$_{48}$N$_4$O$_8$S$_2$): (%calculated/found): C:59.32/59.45, H: 6.64/6.75, N: 7.69/7.30

DNS15C5: ^{1}H NMR (CDCl$_3$) 2.85 (s, 6H, CH$_3$); 3.40-3.55 (m, 20H, crown); 7.20 (d, 1H, J = 7.15 Hz, Ar H); 7.50 (dd, 1H, J = 8.7 Hz, Ar H); 7.57 (dd, 1H, J = 8.4 Hz, Ar H); 8.10 (d, 1H, J = 8.4 Hz, Ar H); 8.35 (d, 1H, J = 8.4 Hz, Ar H); 8.52 (d, 1H, J = 8.1 Hz, Ar H).

IR: (ν cm^{-1}) : (KBr) : 2820-2970, 1615, 1550, 1155

Elemental analysis: (C$_{22}$H$_{32}$N$_2$O$_6$S): (%calculated/found), C: 58.39/58.45, H: 7.13/7.25, N: 6.19/6.30

DNS18C6: ^{1}H NMR (CDCl$_3$) 2.90 (s, 6H, CH$_3$); 3.50-3.65 (m, 24H, crown); 7.26 (d, 1H, J = 8.8, Ar H) 7.50 (dd, 1H, J = 8.7 Hz, Ar H); 7.57 (dd, 1H, J = 8.4 Hz, Ar H); 8.15 (d, 1H, J = 8.3 Hz, Ar H); 8.30 (d, 1H, J = 8.3Hz, Ar H); 8.52 (d, 1H, J = 8.2 Hz, Ar H).

IR: (ν cm^{-1}) : (KBr) : 2820-2960, 1620, 1550, 1160

Elemental analysis: (C$_{24}$H$_{36}$N$_2$O$_7$S): (%calculated/found) C: 58.04/58.25, H: 7.31/7.40, N: 5.64/5.75

2.3 Spectroscopic Studies

All crown ether solutions (1-3x10^{-5}M) were prepared from a stock solution in acetonitrile (spectroscopic grade, Sigma Aldrich). The solutions of the guest were also prepared in acetonitrile and different volumes were added to the host solutions. The concentration of the DNS crown ethers was kept constant while the concentration of the metal salts was changing. The corresponding volumes of the guest and the host were mixed in 25 mL volumetric flasks and the volume adjusted to the mark with acetonitrile. All measurements were performed at 25 ^{0}C.

3. Results and Discussion

3.1 Protonation of the DNS chromophore. Absorption and fluorescence in presence of HCl and H$_2$O

Addition of hydrochloric acid causes decrease in absorption intensity at both absorption maxima. (Figure 2) This is consistent with protonation at both dimethylamino and macrocyclic nitrogen atom. Addition of hydrochloric acid causes fluorescence quenching at the emission maximum at 520 nm however no significant shift in the emission maximum wavelength has been observed indicating that the changes are consistent with protonation rather than changing the polarity of the medium. (Figure 3)

3.2 Effect of cations on the absorption and emission properties of the DNS chromophore

The complexation properties of the ligands were investigated in acetonitrile. The amount of host was kept constant and the absorption and emission spectra were recorded in presence of increasing amounts of the guest. Metal ions cause only a slight decrease in the absorption intensity (ΔA==0.05-0.1) of the charge transfer band combined with a slight hypsochromic shift ($\Delta\lambda$= 1-5 nm) (Figure 4)

Metal ions induce slight hypsochromic change and decrease in absorption intensity. Similarly to the previous study on the NBD chromophore [Mateeva, N., 2010] the absorption changes are very small and sometimes inconsistent with the concentration changes of the guest.

The majority of ions studied in this paper caused only minor changes in the molar absorption coefficients of the long- and short-wave absorption bands in the spectrum of dansyl chromophore. Such changes can be explained by the modification of environment polarity caused by the excess salt added and interaction of metal ions with fluoroionophores. The influence of the environment polarity on the absorption and emission spectra of the dansyl chromophore is well known.

A clear trend in the absorption spectra is increase in the absorption maximum at about 260 nm due to the complex formation. No clear trend however was observed in terms of correlation between ionic size, crown ether size and changes in the absorption spectra.

Upon complex formation a strong fluorescence quenching was observed with all metal ions observed. The dansyl substituted monoaza- crown ethers as well as monosubstituted diaza crown ether derivatives exhibit stronger fluorescence quenching than the disubstituted diaza compound.

Emission spectra of all fluoroionophores studied are typical of dansyl emission in organic solvent with maximum at about 520 nm. Incorporation of the ionophore moiety does not change the shape and position of dansyl amide fluorescence spectrum. An addition of metal ions causes the decrease of dansyl fluorescence intensity and simultaneously a small batochromic shift of the fluorescence spectrum compared to the free ligand as shown in for different fluoroionophores. (Figure 5)

Quenching efficiency of metal ions studied depends on the kind of metal ion as well as the properties of macro-cycle moiety: cavity size, number of nitrogen atoms and number of dansyl substituents. The quenching efficiency of other ions depends on the size of macrocyclic moiety, as well as on the atomic radius of the metal.

For ions Li^+, Na^+, K^+, and Mg^{2+} only a weak quenching of dansyl fluorescence (not higher than a several percent) is observed. Generally the quenching is higher for monodansylated macrocycle than didansylated ones. Double-charged ions exhibited much stronger binding than the single charged; however, K^+ seems to have much stronger affinity toward DNS18C6 compared to the other investigated compounds. (Tables 1 & 2).

The calculation of the binging constants was performed on the basis of the fluorescence spectra of the ligands and complexes similarly to the calculations performed for the corresponding NBD substituted compounds [Mateeva, N., 2010]. The results are summarized in Tables 1&2.

The complexation process can be described by the following:

$$M + L \rightarrow ML$$

$$\frac{I_0}{I_0 - I} = \frac{a}{K_f M} + a \tag{1}$$

The apparent formation constant K_f was calculated according to Valeur et al [Valeur, B, 2002] using the equation (1) where a is a constant incorporating the factors of molar absorptivities and fluorescence quantum yields for the free ligand and complex. C_M and C_1 are the concentrations of the metal ion and the ligand. Under the conditions of $C_M >> C_1$ and hence, $[M] \sim CM$, a plot of $I_0/(I - I_0)$ versus $1/C_M$ is linear, and K_f is found as a ratio of the intercept at the OY axis and the slope.

From the data shown in Tables 1 and 2 it can be seen that 18-crown-6 containing compounds form stronger complexes than the 15-crown-5 analogs. Alkaline earth metal ions form more stable complexes than the alkaline metal ions. The effect is due from one side, to the higher charge and from another, to the closeness in size to the ligand cavity. Exception is potassium complexation with DNS18C6 which is related probably to better size fit to the size of the crown cavity. The data for magnesium complexation were inconsistent due probably to the presence of more than one equilibrium in the solution.

There is not enough evidence in the literature to support the actual participation of the dansyl chromophore in the complexation. We assume that the function of the dansyl moiety in this study is to only detect the binding process due to the changes in its fluorescent characteristics.

4. Conclusions

DNS modified crown ethers were synthesized, purified and their structure confirmed by proton NMR, IR and elemental analysis. Absorption spectra were only slightly affected by the presence of the hosts, however, fluorescence changes were significant and concentration dependant. Double charged ions exhibited higher affinity

toward 18C6 containing ligands and the strongest binding was between Ba^{2+} and DNS18C6. The similarity of the crown ether cavity and the size of the K^+ ion is probably the reason for the greater stability of this complex compared to the other single charged ions.

References

Antonov, L., Mateeva, N., Mitewa, M., & Stoyanov, St. (1996). Spectral properties of aza-15-crown-5 containing styryl dyes. *Dyes and Pigments*, 30, 235-243.

Casnati, A., Giunta, F., Sansone, F., Ungaro, R., Montalti, M., Prodi, L., & Zaccheroni, N. (2001). Synthesis, complexation and photophysics of 1,3-alternate calix[4]arene-crowns-6 bearing fluorophoric units on the bridge. *Supramolecular Chemistry*, 13, 419-434.

Chen, Q.-Y., & Chen, C.-F. (2004). A new Hg^{2+}-selective fluorescent sensor based on a dansyl amide-armed calix[4]-aza-crown. *Tetrahedron Letters*, 46, 165-168.

Mateeva, N., Deiab, S., Archibong, E., Jackson, M., Mochona, B., Gangapuram, M., & Redda, K. (2010). N-(4-amino-7-nitrobenzaoxa-1,3-diazole) - Substituted Aza Crown Ethers: Complexation with Alkali, Alkaline Earth Metal Ions and Ammonium. *J. Inclus. Phenom. Macromol. Chem.*, in press.

Mateeva, N., Deligeorgiev, T., Mitewa, M., Simova, S., & Dimov, I. (1994). Synthesis and Spectral Properties of New Benzothiazolic Chromofluoroionophore Containing Aza-18-Crown-5 Macrocyclic Moiety. *Journal of Inclusion Phenomena and Molecular Recognition in Chemistry*, 17, 81-91.

Mateeva, N., Enchev, V., Antonov, L., Deligeorgiev, T., & Mitewa, M. (1995). Spectroscopic study of the complexation of an aza-15-crown-5 containing chromofluoroionophore with Ba^{2+} and Ca^{2+} cations. *Journal of Inclusion Phenomena and Molecular Recognition in Chemistry*, 20, 323-333.

Roper, E.D., Talanov, V.S., Gorbunova, M.G., Bartsch, R.A., & Talanova, G. G. (2007). Optical Determination of Thallium(I) and Cesium(I) with a Fluorogenic Calix[4]arenebis(crown-6 ether) Containing One Pendent Dansyl Group. *Anal. Chem.*, 79, 1983-1989.

Shirai, M., Matoba, Y., & Tsunooka M. (1997). Cation-Responsive Fluorescence Of Dansyl-Labeled Polyanions Bearing Crown Ether Units. *Journal of Fluorescence,* 7, 245-250.

Sulowska, H., Wiczk, W., Młodzianowski, J., Przyborowska, M., & Ossowski, T. (2002). Synthesis and fluorescence behavior of crown and azacrown ethers carrying the dansyl fluorophore as a pendant in acetonitrile solution. *Journal of Photochemistry and Photobiology A: Chemistry*, 150, 249-255.

Ten Brink H. T., Meijer J. T, Geel, R. V, Damen M., Lowik, D. W. P. M., & van Hest J. C M. (2006). Solid-phase synthesis of C-terminally modified peptides. *Journal of peptide science: an official publication of the European Peptide Society,* 12, 686-92.

Ueno, A., Ikeda, A., Ikeda, H., Ikeda, T., & Toda, F. (1999). Fluorescent Cyclodextrins Responsive to Molecules and Metal Ions. Fluorescence Properties and Inclusion Phenomena of Nα-Dansyl-L-lysine-β-cyclodextrin and Monensin-Incorporated Nα-Dansyl-L-lysine-β-cyclodextrin. *J. Org. Chem*.**,** 64*,* 382-387.

Valeur, B. (2002). *Molecular Fluorescence. Principles and Applications.* Wiley-VCH: Weinheim, Germany, pp 341-342.

Wang, Y., Kang, X.-J., Wei-Hong Ge, W.-H., Sun, X.-Z., & Peng, J. (2007). Simple, rapid, and accurate RP-HPLC method for determination of cystine in human urine after derivatization with dansyl chloride. *Chromatographia*, 65, 527-532.

Warmke, H., Wiczk, W., & Ossowski, T. (2000). Interactions of metal ions with monoaza crown ethers A15C5 and A18C6 carrying dansyl fluorophore as pendant in acetonitrile solution. *Talanta,* 52, 449-456.

Yin, D., Xiea, C., Zhanga, L., Liua, B., Zhoua, X., Wang, P., & Wua, M. (2008). Development of a novel capillary electrophoresis chemiluminescence system for amino acid analysis. *Luminescence*, 23, 434-438.

Table 1. Apparent formation constants K_f for the complexation between DNS crown ethers, alkaline metal ions and ammonium

Ion	Li$^+$	Na$^+$	K$^+$	NH$_4^+$
Ligand	K_f	K_f	K_f	K_f
DNS15C5	195	160	41	217
DNS18C6	98	155	2.56×10^4	412
DNSN218C6	9.63	24.3	350	200
DNS2N218C6	N/A	0.77	1.55	0.56

Table 2. Apparent formation constants K_f for the complexation between DNS crown ethers, and alkaline earth metal ions

Ion	Mg^{2+}	Ca^{2+}	Sr^{2+}	Ba^{2+}
Ligand	K_f	K_f	K_f	K_f
DNS15C5	N/A	222	345	1.6×10^3
DNS18C6	N/A	2.6×10^4	6.4×10^3	1.9×10^5
DNSN218C6	N/A	3.5×10^2	7.5×10^4	2.9×10^3
DNS2N218C6	N/A	55	4.61	23
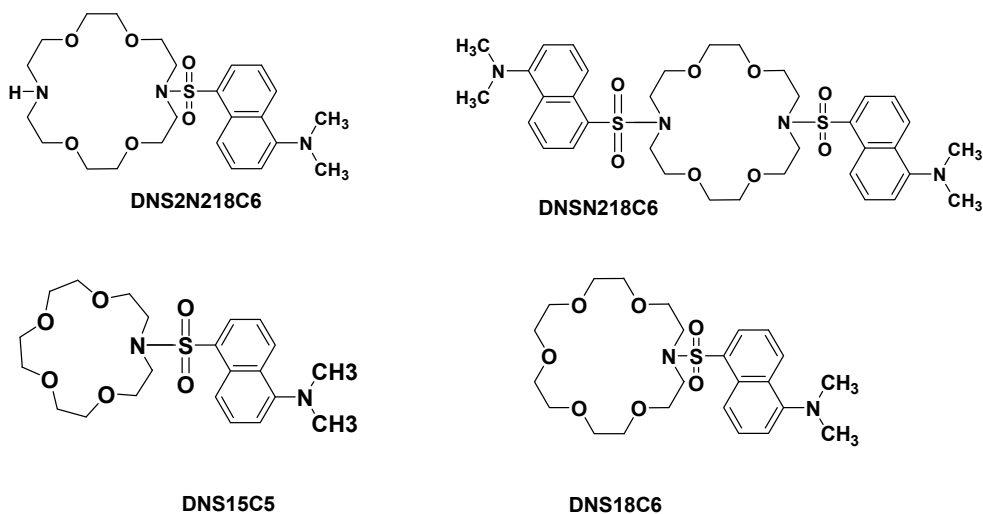
Figure 1. Dansyl aza-crown ethers used in the study
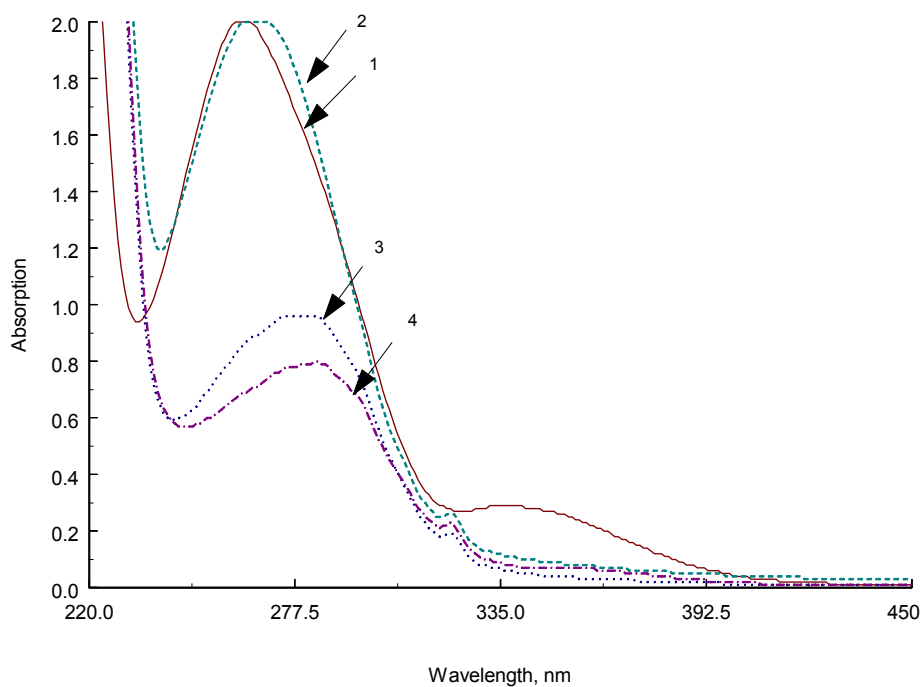
Figure 2. Absorption spectra of DNS18C6 ($1.0x10^{-5}$M) in acetonitrile in presence of increasing amounts of $1.0x10^{-5}$M hydrochloric acid (1→4)
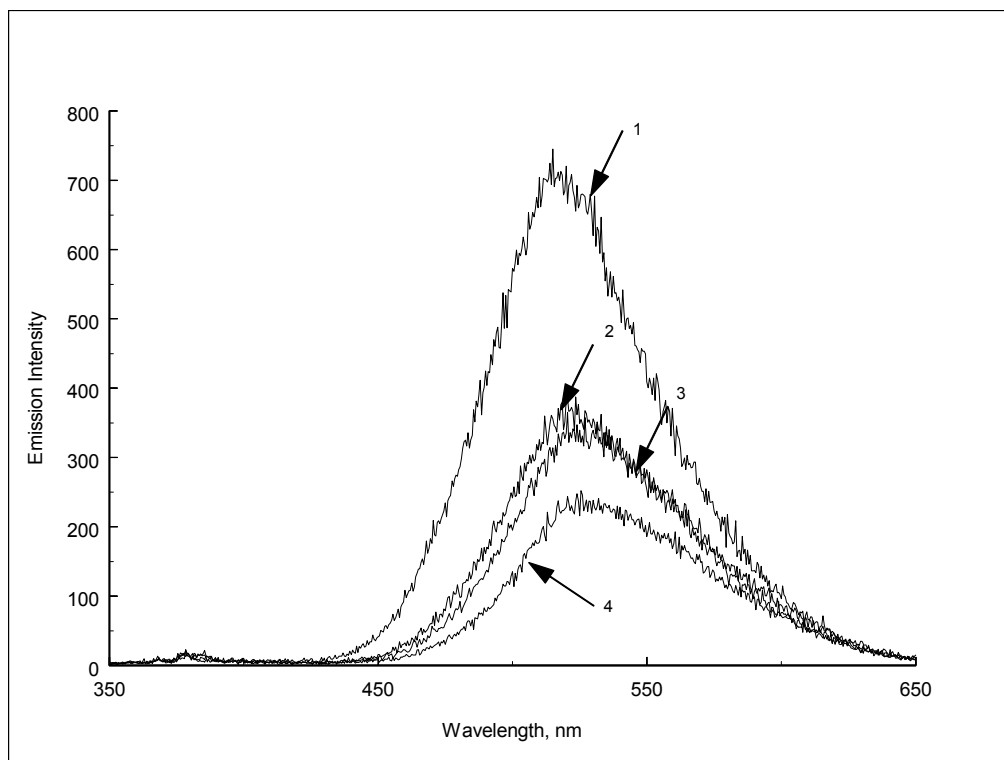
Figure 3. Emission spectra of DNS18C6 ($1x10^{-5}$ M) in acetonitrile presence of increasing amounts of $1x10^{-5}$ M hydrochloric acid (1→4)
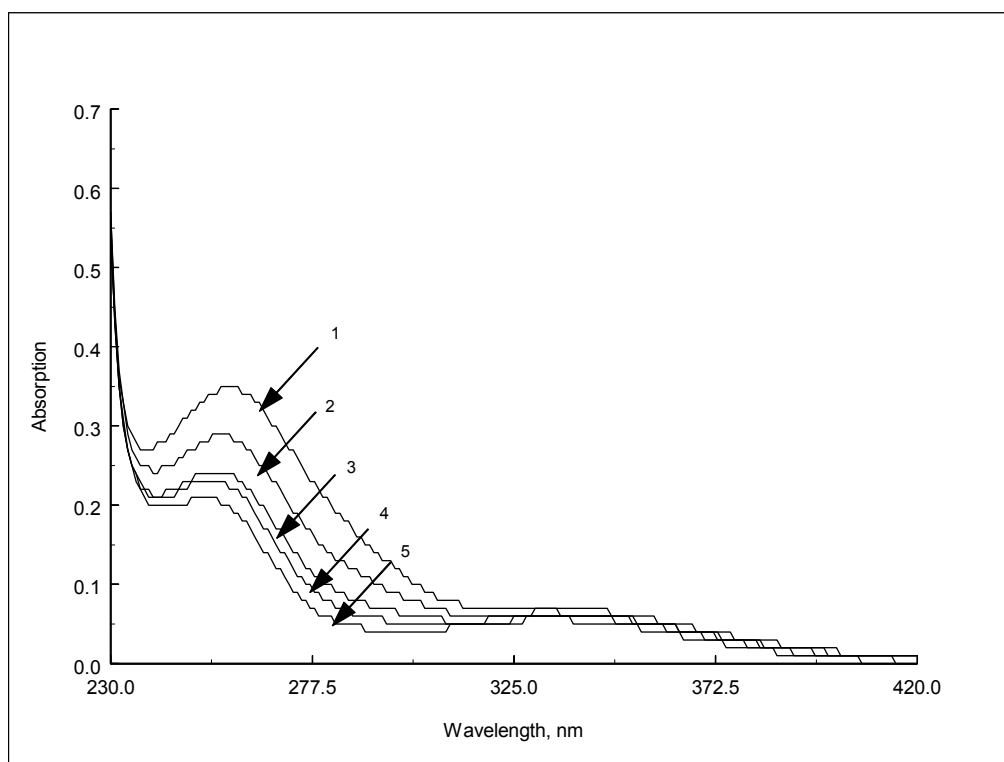
Figure 4. Absorption spectra of DNSN218C6 ($1x10^{-5}$M) in presence of increasing amounts of 1M LiClO$_4$ in acetonitrile
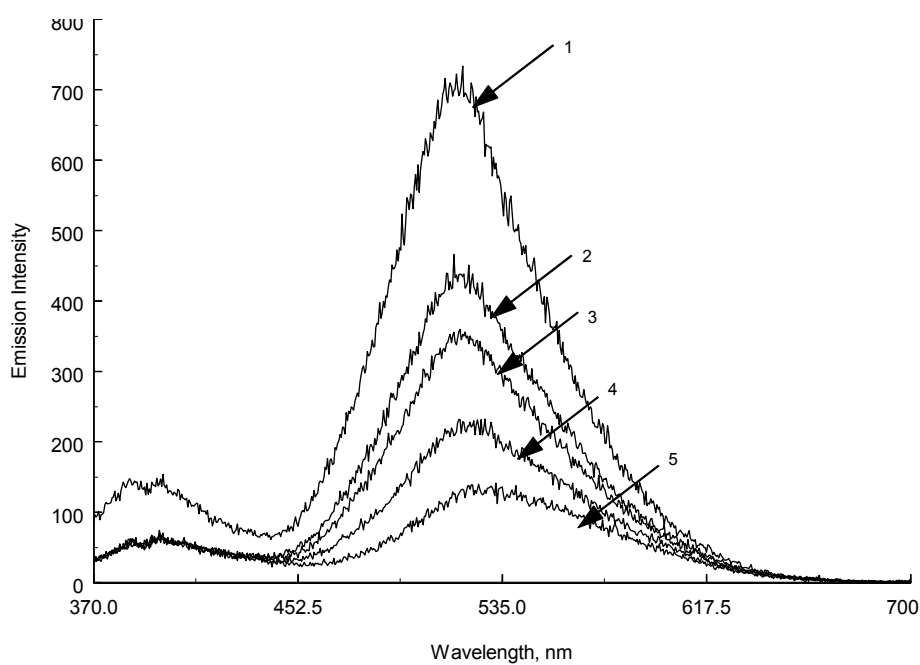
Figure 5. Emission spectra of DNS18C6 ($1x10^{-5}$M) in acetonitrile in presence of increasing amounts ($1\rightarrow5$) of BaClO$_4$ ($1x10^{-4}$M stock solution)

Kinetic and Thermodynamic Studies on the Adsorption of Zn^{2+} onto Chitosan-aluminium Oxide Composite Material

Zhiguang Ma, Na Di, Fang Zhang, Peipei Gu, Suwen Liu & Pan Liu (Corresponding author)

College of Chemistry and Environmental Science, Hebei University

Baoding 071002, China

Tel.: 86-312-507-9795   E-mail: hbumzg@163.com

Abstract

This study presents kinetic and thermodynamic studies on the adsorption of Zn^{2+} onto chitosan-aluminium oxide composite material. The adsorption of Zn^{2+} onto chitosan-aluminium oxide composite material was found to follow pseudo-second-order kinetic model and the apparent adsorption activation energy (Ea) was measured to be 37.20kJ/mol. Adsorption was mainly chemical adsorption. Thermodynamic data supported Langmuir adsorption model and the enthalpy of adsorption (ΔH^{θ}) and the entropy of adsorption (ΔS^{θ}) were found to be 17.81kJ/mol and 109.77J/(mol·K), respectively. The adsorption Gibbs free energy (ΔG^{θ}) decreased with the increase of temperature.

Keywords: Chitosan, Composite material, Adsorption, Kinetic, Thermodynamic

1. Instruction

Chitosan is a linear polysaccharide composed of randomly distributed β-(1-4)-linked D-glucosamine and N-acetyl-D-glucosamine. It has high adsorption capacity for a variety of heavy metals including zinc, copper, and mercury (Majeti, N V., & Ravi, K. 2000; Chu, K H. 2002; Burke, A., Yilmaz, E., & Hasirci, N. 2002; Dhakal, R P., Inoue, K., & Yoshizuka, K. 2005). Furthermore, chitosan can be easily synthesized through chitin deacetylation with low cost. These two characteristics make chitosan an excellent candidate for manufacturing commercial adsorbent for wastewater treatment and heavy metal enrichment and recycling (Mayumi, M., Hiroaki, M., Shoichiro, Y., & Nobuharu, Y J. 2004; Veera, M. B., Drishnaiah, A., Jonathan, L. T., & Edgar, D S. 2003). As an organic compound, chitosan has poor sulfuric acid resistance and weak mechanical strength, thus limiting its commercial applications. In addition, the presence of large amount of hydrogen bonding within chitosan could decrease its adsorption capacity. Aiming to overcome these limitations, it has been demonstrated that synthesis of chitosan-inorganic composite material can be a promising approach for the design of new chitosan adsorbents. For example, Xie et al (Xie, G. Y., & Du, C Q. 2009) prepared the chitosan-aluminium oxide composite material using chitosan and isopropanol aluminum and found that the adsorption capacity of such composite towards copper ions and mercury ions had been greatly improved.

In this study, we focus on a better understanding towards the fundamental aspects of the adsorption of heavy metal such as zinc onto chitosan-aluminium oxide composite and present a thorough kinetic and thermodynamic investigation of the adsorption process. We hope our results help to provide valuable insights for a better design of chitosan-inorganic composite materials.

2. Experimental

2.1 reagents

Chitosan (>90%, Zhejiang Golden-shell Biochemical Co., Ltd. China), Isopropanol aluminum (>99.5%,Sinopharm Chemical Reagent Co., Ltd. China), $ZnSO_4·6H_2O$(>99.5%,Sinopharm Chemical Reagent Co., Ltd. China), EDTA, Ammonium chloride, Ammonia water, Eriochrome balck T, Toluene, Ethanol, All reagents used were of analytical reagent grade.

2.2 Experimental methods

Chitosan-aluminum oxide composite material was prepared according to the procedure described in previous study (Xie, G. Y., & Du, C Q. 2009). Briefly, 3g of isopropanol aluminum was added into 100ml of toluene in a three-neck bottle equipped with reflux condenser. The mixture was kept at 50 ℃ under nitrogen protection and stirring for 30min. Then 10g chitosan was added into the mixture and the mixture was kept at 112 ℃ for 5h. The crude product first went through leaching and washing with toluene, ethanol, and distilled water, and then dried at 80 ℃ in an oven.

Adsorption experiments were carried out in a flask placed in a water bath oscillator. 0.5000g composite material was added into $ZnSO_4$ solution to carry the adsorption study. The oscillator oscillated at 130r/min. EDTA titration was used to quantify the amount of Zn^{2+} onto the composite material. Adsorption was calculated by according to equation (1)

$$Q = (C_0\text{-}C) \times V / m \tag{1}$$

Where Q is adsorption capacity, C_0 and C are the initial concentration and the final concentration of Zn^{2+}, V is the solution volume, and m is the adsorbent mass.

For each adsorption experiment, the average of three replicates was recorded.

3. Result and discussion

3.1 Kinetic studies on the adsorption of Zn^{2+} onto chitosan-aluminum oxide composite material

Fig. 1 shows the adsorption kinetic curve of Zn^{2+} from a 0.04mol.L^{-1} solution onto the chitosan-aluminum oxide composite material at different temperatures. The results demonstrated that the composite material had better adsorption properties compared with previous results. This adsorption procedure was generally consistent with the three-step adsorption behavior usually observed from porous adsorbents (Huang, Y. R., Li, Z. J., Wang, H. F., Miao, Z .C., & Liu, J. G. 2009). Initially, the adsorption rate was fast, and then decreased over time, after about 480 minutes later, the adsorption reached equilibrium. This adsorption behavior was attributed to that: at the beginning, the adsorption of Zn^{2+} onto composite material mainly occurred on the external surface of composite material and the adsorption rate was rapid. The concentration of Zn^{2+} then began to decrease over time as adsorption progressed. Meanwhile, adsorbed zinc ions diffused inward into the composite material through the micropore, and the resistance of diffusion increased. Adsorption rate was mainly controlled by diffusion at this stage, so the rate of adsorption was becoming small. At the final stage, the adsorption mainly occurred on the inner surface of adsorbent while the concentration of zinc in the solution became smaller, and the adsorption reached equilibrium at the last stage. Temperature had a positive effect on the adsorption. When the temperature increased, the rate of adsorption increased correspondingly since the percentage of activated molecules increased.

Pseudo second order kinetics model was used to fit the kinetic data. This model is based on assumption of that: the rate of adsorption is determined by the square of the number of vacancies (Sun, X. L., Zeng, Q. X., & Feng, C. G. 2009). The formula is:

$$dQ_t/dt = k\ (Q_{eq}\text{-}Q_t)^2 \tag{2}$$

Integration of equation (2) under boundary conditions resulted in equation (3)

$$t/Q_t = t/Q_{eq} + 1/kQ_{eq}^2 \tag{3}$$

where Q_t (mmol·g^{-1}) is the absorption amount at time t (minute); and Q_{eq} (mmol·g^{-1}) is the absorption amount at equilibrium; k is the adsorption rate constant (g.$mmol^{-1}$.min^{-1}).

If adsorption procedure conforms to pseudo-second-order equation, t / Q_t and t could have a linear relationship. Fitting the data in fig. 1 by the pseudo-second-order-kinetic equation resulted in a straight line as shown in fig 2. Correlation coefficients R^2 are all better than 0.999, and speed constant k and the enhancement of initial concentration of solution also have good relevance. Therefore, the pseudo-second-order equation is a suitable model to describe this adsorption procedure. Because the pseudo-second-order equation is usually used to describe chemical adsorption process, we hypothesize that the adsorption procedure in our study was primarily chemical adsorption (Ho, Y. S. 2006). We can also obtain the values of Q_{eq} and k from the slope and intercept, as listed in Table 1.

Temperature study (lnk versus 1/T) showed a R^2 value of 0.9967. This indicated that the relationship between temperature and the rate of absorption obeyed the Arrhenius equation. The temperature had significant effect on the rate constant k. When the temperature increased, solute movement became faster and the collision frequency between solute and absorbent surface became higher, thus making adsorption capacity bigger. It is well known that physical adsorption is a reversible dynamic procedure, and it can reach equilibrium quickly. The activation energy for physical adsorption procedure is usually no more than 4.2kJ mol^{-1} because physical adsorption procedure only requires weak force. In contrast, chemical adsorption needs high activation energy (Aksu, Z. 2002). According to the Arrhenius equation we obtained Ea was 37.20kJmol^{-1}. This further proved our previous hypothesis that the adsorption procedure was chemical adsorption.

3.2 Thermodynamic studies on the adsorption of Zn^{2+} onto chitosan-aluminium oxide composite material

Data in Table 2 indicated that the adsorption capacity of Zn^{2+} on the composite material increased with the increase of the initial concentration of Zn^{2+} in solution, and then it reached a maximum value. This was due to that the

amount of composite material was at a fixed value and thus the number of adsorption sites was at a fixed too. At the beginning of the adsorption, the composite materials could provide enough sites, thus the adsorption capacity of composite materials was high (Cheng, Y. N., & Ding, Y. C. 2009); however, the active sites became insufficient when the initial concentration of Zn^{2+} was high and the adsorption sites could be saturated under such situation. That's why when the concentration of Zn^{2+} became $0.09mol.L^{-1}$ or higher, the adsorption capacity of Zn^{2+} on the composite materials became constant.

Form table 2, we can further explore the relation between different initial concentration and temperature and adsorption amount. Date in table 2 was fitted according to two different models, Freundlich adsorption model and Langmuir adsorption model. The expressions of the two models are listed below.

$$\text{Freundlich adsorption model to meet: } lgQ_m = blgC_m + lga \tag{4}$$

$$\text{Langmuir adsorption model to meet: } C_{eq}/Q_{eq} = C_{eq}/Q_m + 1/K_L Q_m \tag{5}$$

Where, Q_m is the saturated adsorption capacity $(mmol.g^{-1})$; C_{eq} and Q_{eq} are the equilibrium concentration of metal ions $(mmol.L^{-1})$ and the adsorption capacity $(mmol.g^{-1})$, respectively, K_L $(L.mmo^{-1})$ is the Langmuir constant $(L.mmo^{-1})$.

Form the table 3, we can see that all the correlation coefficient of Langmuir equation were better than 0.999. The adsorption of Zn^{2+} onto the composite material was consistent with the Langmuir model, in stead of Freundlich model. Fig 3 shows Langmuir adsorption model for Zn^{2+} adsorption. This suggested that the adsorption procedure was consistent with a monolayer adsorption model, meaning one adsorption site only absorbs one Zn^{2+} ion and when all of the adsorption sites were occupied, the adsorption reached dynamic equilibrium (Chen, S. W., Shi, W. J., Song, W., Qin, Q., Zhang, Y. Z., & Gao, J. C. 2009).

From table 4, we can see that: When the temperature increases, the saturated adsorption capacity of composite materials and Langmuir equilibrium constants become greater, so it is clearly that the absorption is endothermic.

The relationship between K_L and T can be obtained from the Van't Hoff equation (Atia, A., Donia, A. M., & El-Boraey, H. A. 2006).

$$lnK_L = -\Delta H^o/RT + \Delta S^o/R \tag{6}$$

Where ΔH^o $(J.mol^{-1})$ and ΔS^o $(J.mol^{-1}.K^{-1})$ are the enthalpy of adsorption and the entropy of adsorption, respectively, R is perfect gas constant, T (K) is temperature. lnK_L had a linear relationship with $1/T$ with a R^2 value of 0.9148. The slope and intercept are $-\Delta H^o/R$ and $\Delta S^o/R$, respectively, and ΔH^o and ΔS^o were determined to be 17.81 $kJ.mol^{-1}$ and $109.77 J.mol^{-1}.K^{-1}$. ΔH^o was positive, and it indicated that the adsorption of Zn^{2+} onto compound materials was endothermic, and this also explained why the rate of adsorption of Zn^{2+} onto compound materials increased with the increase of temperature. ΔS^o was also positive, and this meant an irregular increase of the randomness at the composite material -solution interface during adsorption procedure.

The results of ΔG^o were listed in Table 5. Gibbs free energy (ΔG^θ) was negative at all four temperatures. ΔG^θ decreased with the increase of temperature. It suggested that the adsorption of Zn^{2+} on the composite material was a spontaneous procedure, the spontaneous degree become greater with the increase of temperature. Increasing temperature is beneficial to the adsorption procedure.

4. Conclusion

The adsorption kinetics of Zn^{2+} onto chitosan-aluminum oxide composite materials was found to follow the pseudo-second-order kinetic model. Adsorption procedure was mainly chemical adsorption, and the apparent adsorption activation energy was measured. Thermodynamic studies indicated that the adsorption procedure conformed to the Langmuir adsorption model and the adsorption satisfied monolayer adsorption theory. The adsorption thermodynamic parameters were obtained. This adsorption reaction was found to be exothermic.

References

Aksu, Z. (2002). Determination of equilibrium kinetic and thermodynamic parameters of the batch biosorption of nickel(II)ions onto Chlorella vulgaris. *Process Biochemistry*, 38, 89-99.

Atia, A., Donia, A. M., & El-Boraey, H. A. (2006). Adsorption of Ag(I) on glycidyl methacrylate/N,N′-methylene bis-acrylamide chelating resins with embedded iron oxide. *Separation and Purification Technology,* 48, 281-287.

Burke, A., Yilmaz, E., & Hasirci, N. (2002). Iron(III) ion removal from solution through adsorption on chitosan. *Journal of Applied Polymer Science*, 84, 1185-1192.

Chen, S. W., Shi, W. J., Song, W., Qin, Q., Zhang, Y. Z., & Gao, J. C. (2009). Kinetic and thermodynamic studies.on the adsorption of acid dyes onto chitosan-β-cyclodextrin polymer. *Journal of Functional Materials*, 40, 656-659.

Cheng, Y. N., & Ding, Y. C. (2009). Kinetics, Thermodynamics Study on the Adsorption of Husk to Cadmium Ions in Water, *Journal of Anhui Agriculture Science*, 37, 3190-3192.

Chu, K H. (2002). Removal of copper from aqueous solution by chitosan in prawn shell: adsorption equilibrium and kinetics. *Journal of Hazardous Materials*, 90, 77-95.

Dhakal, R P., Inoue, K., & Yoshizuka, K. (2005). Solvent Extraction of Some Metal Ions with Lipophilic Chitin and Chitosan. *Solvent Extraction and Ion Exchange*, 23, 529-543.

Ho, Y. S. (2006). Second-order kinetic model for the sorption of cadmium onto tree fern: A comparison of linear and non-linear methods. *Water Research*, 40, 119-125.

Huang, Y. R., Li, Z. J., Wang, H. F., Miao, Z .C., & Liu, J. G. (2009). Study on adsorption and kinetics of anion starch microspheres for Cr^{3+}. *Applied Chemical Industry*, 38, 1093-1097.

Majeti, N V., & Ravi, K. (2000). A review of chitin and chitosan applications. *Reactive and Functional Polymers,* 46, 1-27.

Mayumi, M., Hiroaki, M., Shoichiro, Y., & Nobuharu, Y J. (2004). Adsorption behavior of heavymetals on biomaterials. *Journal of agricultural and food chemistry*, 52, 5606-5611.

Sun, X. L., Zeng, Q. X., & Feng, C. G. (2009). Adsorption kinetics of chromium (Ⅵ) onto an anion exchange fiber containing polyamine. *Wuli Huaxue Xuebao*, 25, 1951-1957.

Veera, M. B., Drishnaiah, A., Jonathan, L. T., & Edgar, D S. (2003). Removal of hexavalent chromium from wastewater using a new composite chitosan bisorbent. *Environmental Science and Technology*, 37, 4449-4456.

Xie, G. Y., & Du, C Q. (2009). Preparation, characterization and adsorption for Cu^{2+} of chitosan-aluminium(III) oxide composite material. *Ion Exchange and Adsorption*, 25, 200-207.

Table 1. Adsorption dynamic parameters at different temperatures

T/K	Q_{eq}/(mmol·g^{-1})	k/(g·mmol^{-1}·min^{-1})	R^2
298K	1.8372	0.01889	0.9992
308K	1.8549	0.03239	0.9999
318K	1.8591	0.04725	0.9999
328K	1.8754	0.07658	0.9999

Table 2. Influence of concentration on the adsorption capacity of Zn^{2+} onto the composite materials

C_o (mol/L)	298K		308k		318k		328k	
	C_{eq} (mmol/L)	Q_{eq} (mmol /g)	C_{eq} (mmol/L)	Q_{eq} (mmol /g)	C_{eq} (mmol/L)	Q_{eq} (mmol /g)	C_{eq} (mmol/L)	Q_{eq} (mmol /g)
0.04000	5.050	1.7475	4.1810	1.7910	3.7620	1.8119	3.1680	1.8416
0.05000	9.365	2.0317	7.6230	2.1189	6.6340	2.1683	5.2870	2.2357
0.06000	16.20	2.1900	13.860	2.3070	12.610	2.3695	10.690	2.4655
0.07000	24.24	2.2880	21.880	2.4060	20.790	2.4605	18.470	2.5765
0.08000	32.12	2.3941	30.040	2.4980	29.600	2.5200	27.130	2.6435
0.09000	42.42	2.3790	40.100	2.4950	38.710	2.5645	37.820	2.6090

Table 3. Freundlich and Langmuir equation

Temperature(K)	Freundlich equation	R^2	Langmuir equation	R^2
298k	$lgQ_{eq}=0.1461lgC_{eq}+0.1540$	0.9472	$C_{eq}/Q_{eq}=0.3966C_{eq}+0.9036$	0.9995
308k	$lgQ_{eq}=0.1440lgC_{eq}+0.1837$	0.9228	$C_{eq}/Q_{eq}=0.3784C_{eq}+0.7953$	0.9996
318k	$lgQ_{eq}=0.2175lgC_{eq}+0.1284$	0.9460	$C_{eq}/Q_{eq}=0.3746C_{eq}+0.6263$	0.9999
328k	$lgQ_{eq}=0.1328lgC_{eq}+0.1315$	0.8439	$C_{eq}/Q_{eq}=0.3681C_{eq}+0.4331$	0.9994

Table 4. Parameters and equations for Langmuir adsorption model

T/K	Langmuir equation	$Q_m/(mmol \cdot g^{-1})$	$K_L/(L \cdot mmol^{-1})$	R^2
298	$C_{eq}/Q_{eq}=0.3966C_{eq}+0.9036$	2.5215	0.4389	0.9995
308	$C_{eq}/Q_{eq}=0.3784C_{eq}+0.7953$	2.6430	0.4757	0.9996
318	$C_{eq}/Q_{eq}=0.3746C_{eq}+0.6263$	2.6699	0.5980	0.9999
328	$C_{eq}/Q_{eq}=0.3681C_{eq}+0.4331$	2.7169	0.8499	0.9994

Table 5. the results of ΔG^o at different temperatures

T/K	298K	308K	318K	328K
$\Delta G^o/(kJ \cdot mol^{-1})$	-14.90	-15.60	-17.10	-18.19
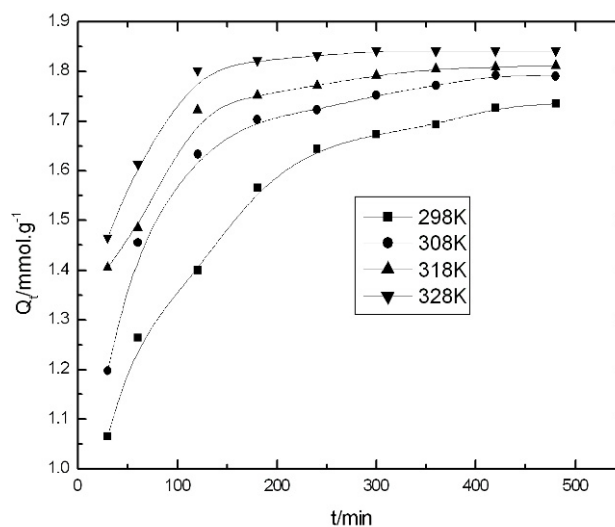
Figure 1. Adsorption rate of Zn^{2+} at different temperatures
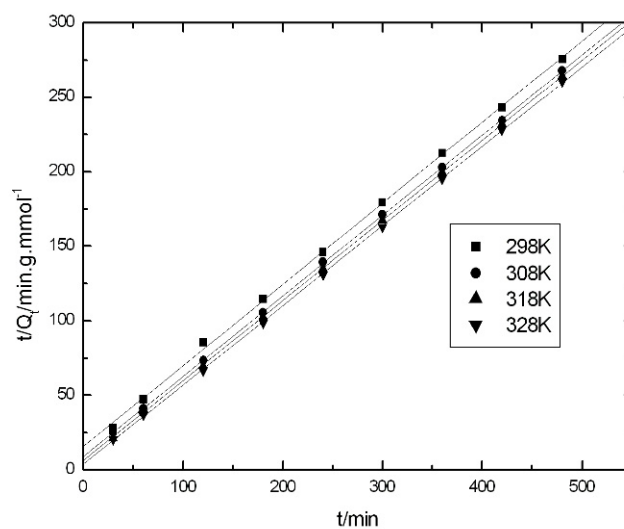
Figure 2. Pseudo second-order equation plots
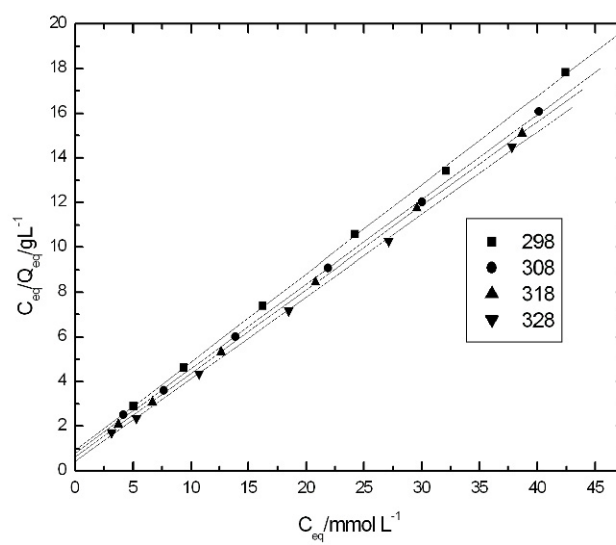
Figure 3. Fitting using Langmuir adsorption model for Zn^{2+} adsorption

Synthesis and Physicochemical Studies of Nickel(II) Complexes of Various 2-Alkyl-1-phenyl-1,3-butanediones and Their 2,2′-Bipyridine and 1,10-Phenanthroline Adducts

Oluwatola Omoregie (Corresponding author)

Department of Chemistry, Faculty of Science, University of Ibadan

Ibadan, Oyo-State, Nigeria

E-mail: tolaomoregie@yahoo.co.uk

Joseph Woods

Department of Chemistry, Faculty of Science, University of Ibadan

Ibadan, Oyo-State, Nigeria

E-mail: jaowoods@yahoo.com

Abstract

Some 2-substituted-1-phenyl-1,3-butanedionato nickel(II) complexes and their 2,2′-bipyridine (bipy) and 1,10-phenanthroline (phen) adducts have been synthesized and characterized by elemental analyses, infrared, electronic spectral studies, conductance, and magnetic susceptibility measurements. The electronic spectral data have been interpreted in terms of the $\pi_3 \rightarrow \pi_4^*$ and other transitions and the effect of the substituents at β-position on the different transitions determined. The infrared spectra of the nickel(II) complexes showed that the frequencies of the asymmetric C=O + C=C stretching vibrations were lowered from their ligand values.

Keywords: Nickel(II) complexes, 1-phenyl-1,3-butane, 2,2′-bipyridine (bipy) and 1,10-phenanthroline, Magnetic susceptibility, Conductometry

1. Introduction

β-diketone and their metal complexes are among the most widely studied coordination compounds since they have wide application in the industries as catalyst (Schwieger et al, 2009; Xingbang et al, 2009; Ferreira et al, 2002; Poncelet et al, 2005; Lassahn et al, 2005; Campelo et al, 2006) and also as precursors for chemical vapour deposition (Zhang et al, 2006; Nable et al, 2003; Banger et al, 2001; Dela Rosa et al, 2003). Thermal transfer printing materials containing metal β-diketonates exhibit good whiteness and image stability (Miura et al, 1993) and it has been found that toner containing metal complexes of β-diketones are stable, controllable and capable of producing clear colour images even at high temperature and high humidity without producing copier stain (Hiroshi and Katsuhiko, 1987).

Studies on the effect of substituents on the spectra properties of metal β-diketonates have been reported (Nakamoto et al, 1959; Nakamoto et al, 1962; Patel and Woods, 1990; Woods and Patel, 1994) but there is dearth of information on 2-substituted-1-phenyl-1,3-butanedionato nickel(II) complexes and their 2,2′-bipyridine and 1,10-phenanthroline adducts. In continuation of our studies on β-diketones and their derivatives (Woods et al, 2009a; Woods et al, 2009b), we report the results of our investigations on bis (2-substituted-1-phenyl-1,3-butanedionato) nickel(II) complexes Ni(R-bzac)$_2$ (R = H, Me, Et, n-Pr, i-Pr and n-Bu) and their adducts with 2,2′-bipyridine and 1,10-phenanthroline.

2. Experimental

2.1 Reagents

1-phenyl-1,3-butanedione (bzacH) (Aldrich chemicals), potassium carbonate, nickel(II) acetate, nickel(II) chloride, methyl iodide, ethyl iodide, n-propyl iodide, i-propyl iodide, n-butyl iodide (Aldrich chemicals), 2,2′-bipyridine and 1,10-phenanthroline (Analytical grade).

2.2 Preparation of the Ligands

The 2-alkyl-1-phenyl-1,3-butanediones were prepared according to a literature procedure (Patel and Woods, 1990).

2.3 Preparation of Ni(Me-bzac)₂.2H₂O

3 mL 2-Me-1-phenyl-1,3-butanedione(3.39 g, 19.2 mmol) dissolved in 10 mL methanol was added to nickel(II) chloride hexahydrate (2.28 g, 9.60 mmol) in 3 mL water, while stirring and the pH was raised to 8. The Precipitated solids were washed with 40% methanol and dried over silica gel. Similar procedure was used for preparation of the other nickel(II) complexes.

2.4 Preparation of Ni(Me-bzac)₂bipy

The 2,2′-bipyridine adduct of Ni(Me-bzac)₂.2H₂O was prepared by mixing 1.2 mL Me-bzacH (1.25 g, 7.07 mmol) and 2,2′-bipyridine (0.55 g, 3.53 mmol) in 80 mL methanol. Nickel(II) acetate tetrahydrate (0.88 g, 3.53 mmol) dissolved in 12 mL 50% methanol was added dropwise to the mixture and stirred for 1 hour. The precipitates obtained were filtered, washed with few drops of acetone and dried in vacuo. Similar procedure was used for preparation of the other 2,2′-bipyridine and 1,10-phenanthroline adducts except 2,2′-bipyridine and 1,10-phenanthroline adducts of Ni(bzac)₂.2H₂O which were prepared by mixing the base with the complex prior to dissolution in the solvent.

2.5 Physical Measurements

Elemental analyses for C, H and N were determined by the analytical laboratory of Geological Survey of Ethiopia while nickel was determined using a complexometric method (Vogel, 1986). The analytical and physical data are presented in Tables 1 and 2. The room temperature magnetic susceptibilities of the compounds were measured by MSB-AUTO (Sherwood scientific).

The electrolytic conductivities of the soluble compounds in nitromethane at room temperature were determined using Digital conductivity meter (Labtech).

The solution spectra of the compounds in methanol and chloroform were recorded on a Unicam UV-Visible Spectrophotometer using 1cm glass cell.

The reflectance spectra of the nickel(II) complexes were recorded on a Perkin Elmer Lambda 950 UV/VIS spectrophotometer at the Department of Chemical Engineering, Faculty of Technology, Addis Ababa University, Ethiopia using calcium carbonate as reference. The infrared spectra of the compounds as pressed KBr disc were recorded on Perkin Elmer Spectrophotometer BX FT-IR.

3. Results and Discussion

The reaction of 2-alkyl-1-phenyl-1,3-butanedione with metal salt is represented by equation 1 while that of the metal complex and base is represented by equation 2. The adducts prepared directly from metal salt are represented by equation 3. Reasonable yield of the precipitates were obtained.
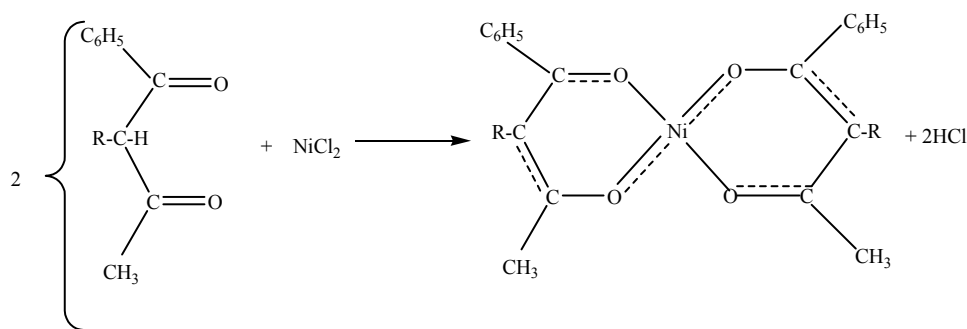
R = H, Me, Et, n-Pr, i-Pr and n-Bu

EQUATION 1:   PREPARATION OF NICKEL(II) COMPLEX

R = H, Me, Et, n-Pr, i-Pr and n-Bu

where ⌒ = Beta-diketone and ⌒ =Bipyridine/phenanthroline
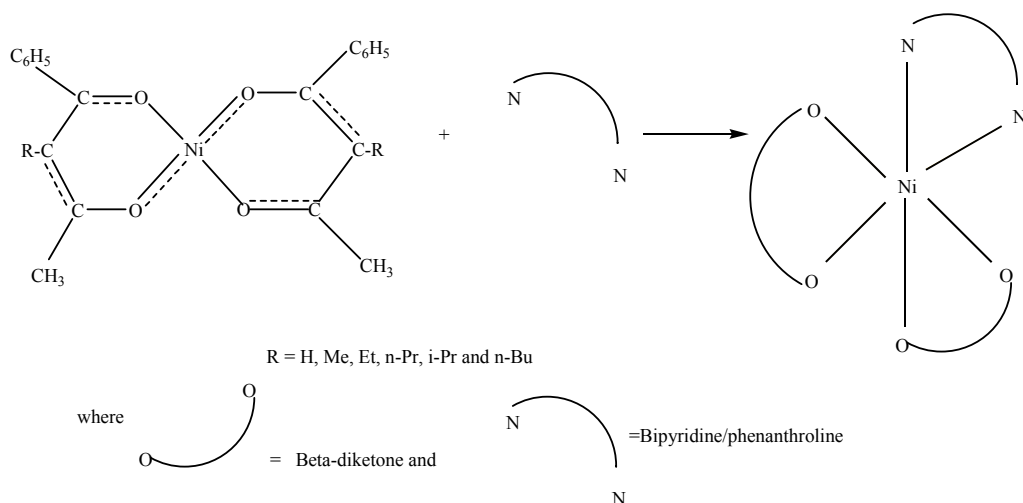
EQUATION 2:   PREPARATION OF NICKEL(II) ADDUCT

R = H, Me, Et, n-Pr, i-Pr and n-Bu

where ⌒ = Beta-diketone and ⌒ =Bipyridine/phenanthroline
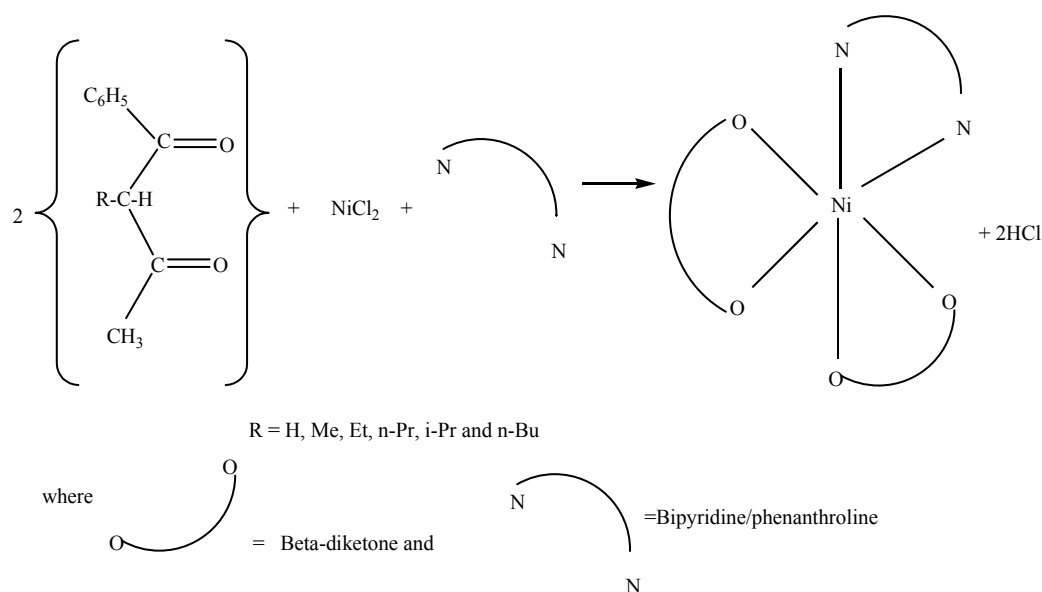
EQUATION 3:   PREPARATION OF NICKEL(II) ADDUCT

The analytical data, colours, %yields, melting points/decomposition temperatures and room temperature magnetic moments (μ_{eff}) of the complexes are given in Table 1. All the compounds were obtained as various shades of green except few that were pinkish in colour. They exhibited good solubility in chloroform and methanol except few. The microanalytical data for the compound agree with the calculated values (Table 2).

The principal infrared bands are presented in Table 3. Infrared studies on diketones have shown that electron releasing substituents give rise to low $\nu_{as}(C=O)+\nu_{as}(C=C)$ (Hancock and Thornton, 1969; Patel and Adimado, 1979). Infrared spectra of 2-substituted-1-phenyl-1,3-butanediones studied showed a decrease in frequency as the electron in the system increases except Me-bzacH and i-Pr-bzacH which showed an increase in frequency. Reduction of the frequency of $\nu_{as}(C=O)+\nu_{as}(C=C)$ is an indication of the positive inductive effect of the alkyl group on the system. Single bands of $\nu_{s}(C-O)+\delta C-H$ were observed in all the ligands except i-Pr-bzacH had two distinct bands. Reduction of the coupled $\nu_{s}(C-O)+\delta C-H$ vibrations of 2-substituted-1-phenyl-1,3-butanedione was observed as the length of the alkyl group increases except i-Pr-bzacH which had increased frequency. The reduction in frequency also indicates the positive inductive effect of the alkyl group on the system. The methyl deformation bands of the ligands studied were observed in the 1421-1359 cm^{-1} region (Wood and Patel, 1994; Patel and Woods, 1990; Tanaka et al,

1969; Koshimura et al, 1973; Nakamoto et al, 1961). These bands were observed as double bands except n-Bu-bzacH which had a single absorption band. The infrared spectra of the nickel(II) complexes showed that the frequencies of the asymmetric C=O + C=C stretching vibrations were lowered from the ligand values in the order: $Ni(n-Pr-bzac)_2.2H_2O > Ni(Me-bzac)_2.2H_2O > Ni(Et-bzac)_2.2H_2O > Ni(i-Pr-bzac)_2.2H_2O > Ni(bzac)_2.2H_2O > Ni(n-Bu-bzac)_2.2H_2O$. The order shows that the substituted Ni(II) complexes have larger bathochromic shift than the unsubstituted complex except $Ni(n-Bu-bzac)_2.2H_2O$ which had hypsochromic shift. The larger bathochromic shift probably indicates the positive inductive effect of the alkyl group on the system. The $\nu_{as}(C=O)+ \nu_{as}(C=C)$ stretching vibrations of these nickel(II) complexes were observed in the range 1560-1726 cm^{-1} while $\nu_s(C-O)+\delta C-H$ were observed in the 1450-1492 cm^{-1} region with $Ni(bzac)_2.2H_2O$ $Ni(Et-bzac)_2.2H_2O$, and $Ni(n-Bu-bzac)_2.2H_2O$ having multiple bands. A decrease in $\nu_s(C-O)+\delta C-H$ of 2-substituted-1-phenyl-1,3-butanedionato nickel(II) complexes was observed as the length of the alkyl group increases except $Ni(Et-bzac)_2.2H_2O$ and $Ni(n-Bu-bzac)_2.2H_2O$ which had increased frequency. The decrease in frequency indicates the positive inductive effect of the alkyl group on the system (Bamkole and Ogunkoya, 1981). The frequency of the methyl deformation band decreases as the length of the alkyl group increases with the exception of $Ni(n-Pr-bzac)_2.2H_2O$ and $Ni(n-Bu-bzac)_2.2H_2O$ which had increased frequency.

The $\nu_{as}(C=O)+ \nu_{as}(C=C)$ vibrations of most of the adducts were observed at higher frequency relative to the parent complexes except $Ni(Me-bzac)_2bipy$, $Ni(Et-bzac)_2bipy$, $Ni(n-Pr-bzac)_2bipy$, $Ni(n-Bu-bzac)_2bipy$, $Ni(n-Bu-bzac)_2phen$ and $Ni(bzac)_2phen_2.2H_2O$ which had bathochromic shifts while $[Ni(bzac)(bipy)(H_2O)_2](bipy)$ and $Ni(Et-bzac)_2phen$ had no shift. The strength of the bonds in the adducts and the electron density on nickel(II) ion could be inferred from these shifts (Holtzclaw and Collman, 1957). The $\nu_{as}(C=O)+ \nu_{as}(C=C)$ vibrational modes of metal β-diketonate observed at lower frequency shifts could be an indication of stronger Ni-O bonds in the chelate ring due to increased electron delocalization as a result of weaker Ni-N (base) interactions(Patel and Woods, 1990). The $\nu_s(C-O)+\delta C-H$ and $\delta_{as}(CH_3)+\delta_s(CH_3)$ of the 2,2′-bipyridine adduct of $Ni(R-bzac)_2$ were observed at higher frequency relative to the $Ni(bzac)_2$ adducts except $\delta_{as}(CH_3)+\delta_s(CH_3)$ of the $Ni(n-Pr-bzac)_2bipy$ which occurred at lower frequency. This is attributed to the positive inductive effect of the alkyl groups. The magnitude of the shift of $\nu_s(C-O)+\delta C-H$ was the same for methyl, ethyl and n-Propyl substituents ($\Delta \nu = +34$) while those of the i-Propyl and n-Butyl were ($\Delta \nu = +2$) and ($\Delta \nu = +29$) respectively. Higher frequency shifts of varying magnitude were observed in the $\delta_{as}(CH_3)+\delta_s(CH_3)$ of the 2,2′-bipyridine adducts relative to $[Ni(bzac)(bipy)(H_2O)_2](bzac)$ with the exception of $Ni(iPr-bzac)_2bipy$ which had lower frequency shift. The shift is in the order: $Ni(nPr-bzac)_2bipy(\Delta \nu = +5) > Ni(Me-bzac)_2bipy = Ni(Et-bzac)_2bipy(\Delta \nu = +3) > Ni(iPr-bzac)_2bipy(\Delta \nu = -14)$. Higher frequency shift of $\delta_{as}(CH_3)+\delta_s(CH_3)$ of the 1,10-phenanthroline adducts of 2-substituted-1-phenyl-1,3-butanedionato nickel(II) complexes relative to $Ni(bzac)_2phen$ were also observed. Strong bands in the 773-774 cm^{-1} region were assigned to CH deformation bands of 2,2′-bipyridine while the 1,10-phenanthroline adducts had very prominent bands around 714-732 cm^{-1} and 849-856 cm^{-1} region which were attributed to CH deformation bands. The coupled vibrations of Ni-O and Ni-N stretching vibrational modes appeared below 700 cm^{-1} in all the adducts.

The solution spectra of the Me-bzacH in methanol showed a splitting of the π_3-π_4* transition whereas bzacH, Et-bzacH, n-Pr-bzacH, i-Pr-bzacH, n-Bu-bzacH had just a single band. The electronic spectra of 2-substituted-1-phenyl-1,3-butanedione in chloroform showed π_3-π_4* transition in the 32,258-35,336 cm^{-1} region which had hypsochromic shift in methanol except Me-bzacH and i-Pr-bzacH with bathochromic shift while bzacH had no shift.

The phenyl-substituted ligands had bands in the 38,000-46,000 cm^{-1} region, which may be attributed to primary bands in the benzene π system (Ogden and Selbin, 1968). The synthesized ligands showed similar bands in the region 39,526-44,248 cm^{-1} which have been assigned to π-π* transition of the phenyl ring.

Hypsochromic shifts of the π_3-π_4* transition bands were 1,10-observed on substituting the 2-position of 1-phenyl-1,3-butanedione with methyl, ethyl, n-propyl and i-propyl in chloroform and methanol. Hypsochromic shifts of the π_3-π_4* transition bands could be attributed to the positive inductive effect of the alkyl groups leading to higher frequency shift (Graddon and Schulz, 1965).

The solution spectra in methanol showed that the π_3-π_4* transitions of the nickel(II) complexes are lowered from the ligand values in the order: $Ni(Et-bzac)_2.2H_2O(\Delta \nu = +2958) > Ni(i-Pr-bzac)_2.2H_2O(\Delta \nu = +2515) > Ni(Me-bzac)_2.2H_2O(\Delta \nu = +2501) > Ni(n-Pr-bzac)_2.2H_2O(\Delta \nu = +1331) > Ni(bzac)_2.2H_2O(\Delta \nu = +1202)$. The order shows that the substituted Ni(II) complexes have larger bathochromic shift than the unsubstituted complex, $Ni(bzac)_2.2H_2O$ except $Ni(n-Bu-bzac)_2.2H_2O$ which had π_3-π_4* hypsochromic shifts in chloroform and methanol.

Upon adduct formation π_3-π_4* hypsochromic shifts were observed in all the adducts in methanol except $Ni(n-Pr-bzac)_2bipy$, $Ni(n-Bu-bzac)_2bipy$ and $Ni(n-Bu-bzac)_2phen$ which had bathochromic shifts. π_3-π_4*

hypsochromic shifts were also observed in the adducts in chloroform except Ni(Et-bzac)$_2$bipy, Ni(Et-bzac)$_2$phen and Ni(n-Bu-bzac)$_2$bipy which had bathochromic shifts and Ni(n-Me-bzac)$_2$bipy which had no shift. The hypsochromic shifts probably indicate weaker bonds in the chelate ring due to reduced electron delocalization as a result of stronger Ni-bipy or Ni-phen interaction. The ligand field spectra of the 2,2′-bipyridine and 1,10-Phenanthroline adducts of the nickel(II) complexes studied had bands in the 11,494-12,853 cm^{-1}, 13,158-19,305 cm^{-1} and 20,080-20,161cm^{-1} in which have been assigned to $^3A_{2g}(F) \rightarrow ^3T_{2g}(F)$, $^3A_{2g}(F) \rightarrow ^3T_{1g}(F)$, $^3A_{2g}(F) \rightarrow ^3T_{1g}(P)$ respectively for octahedral geometry (Lever, 1986; Osowole et al, 2000).

The reflectance spectra of the ligands showed single bands of the π_3-π_4* transition in bzacH, n-Pr-bzacH, and n-Bu-bzacH while Me-bzacH and Et-bzacH had multiple bands, these occurred in the 31,056-35,587 cm^{-1} region. A split of π_3-π_4* band was also observed in Ni(Et-bzac)$_2$.2H$_2$O and Ni(n-Pr-bzac)$_2$.2H$_2$O while π-d/C.T. transition was observed in Ni(Et-bzac)$_2$.2H$_2$O at 30,395 cm^{-1}. π_3-π_4* bathochromic shifts were observed in the Nickel(II) complexes except Ni(bzac)$_2$.2H$_2$O, Ni(Et-bzac)$_2$.2H$_2$O and Ni(n-Pr-bzac)$_2$.2H$_2$O which had hypsochromic shifts.

Upon adduct formation π_3-π_4* hypsochromic shifts were observed in [Ni(bzac)(bipy)(H$_2$O)$_2$](bipy), Ni(bzac)$_2$bipy, Ni(Me-bzac)$_2$bipy, Ni(Et-bzac)$_2$bipy, Ni(n-Pr-bzac)$_2$phen, Ni(n-Bu-bzac)$_2$bipy and Ni(n-Bu-bzac)$_2$phen. The hypsochromic shifts probably indicate weaker bonds in the chelate ring due to reduced electron delocalization as a result of stronger Ni-phen or Ni-bipy interaction. [Ni(phen)$_2$(H$_2$O)$_2$](bzac)$_2$, Ni(bzac)$_2$phen, Ni(Me-bzac)$_2$phen, Ni(Et-bzac)$_2$phen and Ni(n-Pr-bzac)$_2$bipy had bathochromic shifts. The reflectance spectral data showed that the visible bands of the adducts were also typical of octahedral geometry (Lever, 1986; Osowole et al, 2000).

The room temperature magnetic moments of the synthesized nickel(II) complexes were in the range 3.02-3.26 B.M. which is indicative of octahedral geometries except Ni(n-Pr-bzac)$_2$.2H$_2$O with moment of 4.11 B.M. The spin only ($\mu_{s.o}$) value of 2.83 B.M is expected for nickel(II) complexes. Experimental moments of 2.9-3.3 B.M. are normally observed for octahedral nickel(II) complexes due to spin-orbit coupling of the $^3A_{2g}$ and $^3T_{2g}(F)$ terms while moments of 3.2-4.1 B.M. are observed for tetrahedral nickel due to orbital contributions. In the synthesized complexes, lower moments were observed on substituting the 2-position of Ni(bzac)$_2$ with alkyl groups except Ni(Et-bzac)$_2$.2H$_2$O and Ni(n-Pr-bzac)$_2$.2H$_2$O which had increased moments. Reduction in moment may probably be due to increase in electron density around the metal leading to reduction in orbital contribution and therefore lower moment. The adducts studied displayed effective magnetic moments (μ_{eff}) in the range 1.81-3.31 B.M. The magnetic moments between 1.81-2.65 B.M. which are lower than the spin only value were observed for Ni(Me-bzac)$_2$phen and Ni(n-Bu-bzac)$_2$phen. The lowering of the moment observed in the compounds studied may be attributed to interconversion of stereochemistries and /or dimerization (Osowole et al, 2000). A decrease in moment was observed on comparing the 2,2′-bipyridine adduct of 2-substituted-1-phenyl-1,3-butanedionato nickel(II) complexes with Ni(bzac)$_2$bipy. The 1,10-phenanthroline adduct of nickel(II) 2-substituted-1-phenyl-1,3-butanediones also exhibited decreased moment. Reduction in moment is attributed to increase electron density around the nickel leading to reduction in orbital contribution and therefore lower moments are obtained.

The molar conductivities of these complexes are very low with Λ_m values of 14.1-32.5 ohm^{-1}cm^{2}mole^{-1}, which suggests that they are non-electrolytes. The molar conductances of the soluble adducts in nitromethane clearly indicate that they were non-electrolytes except [Ni(bzac)(bipy)(H$_2$O)$_2$](bzac), [Ni(phen)$_3$](bzac)$_2$ and [Ni(phen)$_2$(H$_2$O)$_2$](bzac)$_2$ which are electrolytes.

4. Conclusion

The electronic and infrared spectral data and magnetic measurement are consistent with the adoption of an octahedral geometry for the Nickel(II) compounds except Ni(n-Pr-bzac)$_2$.2H$_2$O which has tentative four coordinate tetrahedral geometry. The conductance measurement showed that the compounds are non-electrolytes except [Ni(bzac)(bipy)(H$_2$O)$_2$](bzac) which is a 1:1 electrolyte, [Ni(phen)$_3$](bzac)$_2$ and [Ni(phen)$_2$(H$_2$O)$_2$](bzac)$_2$ are 1:2 electrolytes.

References

Bamkole T.O. and Ogunkoya L. (1981). *Introductory Organic Chemistry*.2nd ed. Ibadan: Day star press (Publisher), 89.

Banger, K.K., Kornilov, A., Claessen, R.U., Eisenbraun, E.T., Kaloyeros, A.E., Toscano, P.J., Welch, J.T. (2001). The first metal complex containing a silylated β-diketonate ligand: bis(2,2,6,6-tetramethyl-2-sila-3,5-heptanedionato) copper(II). *Inorg. Chem. Commun*, 4, 496-500.

Bassett, J., Denney, R.C., Jeffery, G.H., Mendham, J. (1986). *Vogel, Textbook of Quatitative Inorganic Analysis*; Eds.; Longman Scientific and Technical: London, 316-322.

DelaRosa, M.J., Banger, K.K., Higashiya, S., Ngo, S. C. (2003). Structural investigations of copper(II) complexes containing fluorine-substituted β-diketonate ligands. *Journal of Fluorine Chemistry*, 123, 109–117.

Ferreira, L.C., Costa, M.A.S., Guimaraes, P.I.C., and Luiz Claudio de Santa Maria. (2002). Comparative study of homogeneous and heterogeneous styrene polymerizations with Ni(acac)$_2$/MAO catalytic system. *Polymer,* 43(14), 3857-3862.

Graddon, D.P. and Schulz, R.A. (1965). Adducts of copper(II)β-diketone chelates with heterocyclic bases. II. Chelates with 3-alkylacetylacetones. *Australian Journal of Chemistry*, 18, 1731-1742.

Greenwood, N.N., Earnshaw, A. (1997). *Chemistry of the elements*. 2nd ed. Butterworths and Heinemann., 1193.

Hancock, R.D. and Thornton, D.A. (1969). The influence of substituents of the infrared spectra of metal(III)β-ketoenolates. *Journal of Molecular Structure*, 4, 377-382.

Hiroshi, F., Katsuhiko, T. (1987). Toner for development of electrostatic images. *Chemical Abstracts*, 106, 205178t.

Holtzclaw, H.F. Jr. and Collman, J.P. (1957). Infrared absorption of metal chelate compounds of 1,3-diketones. *Journal of American Chemical Society*, 79, 3318-3322.

Campelo, J.M., Jaraba, M., Luna, D., Luque, R., Marinas, J.M. and Romero, A.A. (2006). Structural and catalytic properties of amorphous mesoporous AlPO$_4$ materials prepared in the presence of 2,4-pentanedione and 2,5-hexanedione as aluminium chelating agents. *Studies in Surface Science and Catalysis*, 162, 315-322.

Koshimura, H., Saito, J. and Okubo, T. (1973). Effect of substituents on the keto-enol equilibrium of alkyl substituted β-diketones. *Bulletin of the chemical society of Japan*, 46, 632-634.

Lassahn, P.G., Lozanm, V., Timco, G.A., Christian, P., Janiak, C. and Winpenny, R.E.P. (2005). Homo- and Heterometallic carboxylate cage complexes as precatalysts for olefin polymerization –Activity enhancement through "inert metals". *Journal of Molecular Catalysis*, 222(1), 260-267.

Lever A.B.P. (1986). *Inorganic Electronic Spectroscopy*, 4th Ed.; Elsevier: London, 481-579.

Miura, N., Komamura, T., Abe, T. (1993). Metal ion sources for dye diffusion thermal transfer printing. Hard Copy, 93, 314-317.

Nable, J., Gulbinska, M., Suib. S.L. and Galasso, F. (2003). Aluminium oxide coating on nickel substrate by metal organic chemical vapour deposition. *Surface and Coatings technology*, 173(1), 74-80.

Nakamoto K., Morimoto Y. and Martell A.E. (1962). Infrared spectra of metal chelate compounds. V. Effect of substituents on the infrared spectra of metal acetylacetonates. *Journal of Physical Chemistry*, 66, 346-348.

Nakamoto, K., McCarthy, P.J. Ruby, A. and Martell, A.E. (1961). Infrared spectra of metal chelate compounds. II. Infrared spectra of acetylacetonates of trivalent metals. *Journal of American Chemical Society*, 83, 1066-1069.

Nakamoto, K., McCarthy, P.J. Ruby, A. and Martell, A.E. (1959). Metal-Oxygen stretching frequencies in the metal chelate compounds of β-diketones. *Nature*, 183, 459.

Ogden, D. and Selbin, J. (1968). Ultraviolet spectra studies of β-ketoenolate complexes of oxovanadium (IV). *Journal of Inorganic and Nuclear Chemistry*, 30, 1227-1236.

Osowole, A.A., Woods, J.A.O. and Odunola, O.A. (2000). Synthesis and characterization of Synthesis and physico-chemical properties of some copper(II) β-ketoamines and their adducts with 2,2′-bipyridine and 1,10-phenanthroline.some Nickel(II) β-ketoamines and their adducts with 2,2′-bipyridine and 1,10-phenanthroline. *Synthesis and Reactivity of Inorganic and Metal Organic Chemistry*, 32(4), 783-799.

Patel K.S. and Woods J.A.O. (1990). Synthesis and properties of nickel(II) complexes of various 3-alkyl-2,4-pentanediones and their adducts with 2,2′-bipyridine and 1,10-phenanthroline. *Synthesis and Reactivity in Inorganic and Metal-Organic Chemistry*, 20 (4), 409-424 and the references therein.

Patel, K.S. and Adimado, A.A. (1979). Physicochemical studies of metal β-diketonate-V. Spectral and magnetic properties of the Al(III), Cr(III), Mn(III), Fe(III) and Co(III) complexes of 1-(2-thienyl)-1,3-butanedione and 4,4,4-trifluoro-1-(2-thienyl)-1,3-butanedione. *Journal of Inorganic and Nuclear Chemistry,* 42, 1241-1246.

Poncelet, G., Centeno, M.A. and Molina, R. (2005). Characterization of reduced α-alumina-supported nickel catalysts by spectroscopic and chemisorption measurements. *Applied Catalysis*, 288(A), 232-242.

Schwieger, S., Herzog, R., Wagner, C., Steinborn, D. (2009). Platina-β-diketones as catalysts for hydrosilylation and their reactivity towards hydrosilanes. *Journal of Organometallic Chemistry*, 694(22), 3548-3558

Tanaka, M., Shono, T. and Shinra, K. (1969). Tautomerism in 3-substituted 2,4-pentanediones and their copper chelates. *Bulletin of the Chemical Society of Japan*, 42, 3190-3194.

Woods J.A.O. and Patel K.S. (1994). Nickel(II) complexes of some 3-substituted-2,4-pentanediones and their adducts with 2,2′-bipyridine and 1,10-phenanthroline. *Synthesis and Reactivity in Inorganic and Metal-Organic Chemistry*, 24(9), 1557-1571.

Woods, J.A.O, Omoregie, H.O., Retta, N., Chebude, Y., Capittelli, F. (2009a). Synthesis and physicochemical studies of Nickel(II) complexes of 2-substituted-1,3-diphenyl-1,3-propanedione, their 2,2′-bipyridine and 1,10-phenanthroline adducts and X-ray structure of (2,2′-bipyridine)bis(1,3-diphenyl-1,3-propanedionato) Nickel(II). *Synthesis and Reactivity in Inorganic*, Metal-Organic, and Nano-Metal Chemistry, 39, 694-703.

Woods, J.A.O, Omoregie, H.O., Retta, N., Chebude, Y., Capittelli, F. (2009b). Synthesis and characterization of some Nickel(II) and Copper(II) complexes of 2-substituted-4,4,4-trifluoro-(2-thienyl)butane-1,3-dione (TTAH), their 2,2′-bipyridine and 1,10-phenanthroline adducts and X-ray structure of (2,2′-bipyridine)bis(4,4,4-trifluoro-(2-thienyl)butane-1,3-dionato) Nickel(II). *Synthesis and Reactivity in Inorganic, Metal-Organic, and Nano-Metal Chemistry,* 39, 704-717.

Xingbang H., Jianyong M., Yong S., Hang C., Haoran L. (2009). Acetylacetone–Fe catalyst modified by imidazole ionic compound and its application in aerobic oxidation of β-isophorone. *Catalysis Communications*, 10(14), 25 .

Zhang, Y.C., Tang, J.Y., Wang, G.L., Zhang, M. and Hu, X.Y. (2006). Facile synthesis of submicron Cu_2O and CuO crystallites from a solid metallorganic molecular precursor. *Journal of Crystal Growth*, 294(2), 278-282.

Table 1. Analytical and physical data of Nickel(II) complexes of 2-substituted-1-phenyl-1,3-butanedione and their adducts

Compound	Colour	M.P. (°C)	Yield (%)	μ_{eff} (B.M.)
$Ni(bzac)_2 2H_2O$	Light green	165-167	93.90	3.11
$[Ni(bzac)(bipy)(H_2O)_2]$ (bipy)	Light green	210-212	38.76	3.04
$Ni(bzac)_2bipy$	Green	215	6.79	3.29
$[Ni(phen)_3](bzac)_2$	Pink	106-108	28.94	3.44
$[Ni(phen)_2(H_2O)_2](bzac)_2$	Pink	205	37.00	3.09
$Ni(bzac)_2phen$	Y green	237-239	52.26	3.05
$Ni(Me-bzac)_2.2H_2O$	Light green	158-160	11.34	3.10
$Ni(Me-bzac)_2bipy$	Light green	310-312	55.03	2.99
$Ni(Me-bzac)_2phen$	D.Pink	323-325	30.04	2.65
$Ni(Et-bzac)_2.2H_2O$	Light green	179-181	54.29	3.26
$Ni(Et-bzac)_2bipy$	Light green	296-298	30.33	3.11
$Ni(Et-bzac)_2phen$	Light green	240-242	35.97	3.31
$Ni(i-Pr-bzac)_2.2H_2O$	Light green	222-224	91.96	3.02
$Ni(i-Pr-bzac)_2bipy$	D.green	146-148	46.54	3.03
$Ni(i-Pr-bzac)_2phen$	Dark green	168-170	42.50	3.04
$Ni(n-Pr-bzac)_2.2H_2O$	Light green	304	50.56	4.11
$Ni(n-Pr-bzac)_2bipy$	Light green	301-303	42.50	3.15
$Ni(n-Pr-bzac)_2phen$	Dark green	336-338	46.90	3.28
$Ni(n-Bu-bzac)_2 2H_2O$	Bright green	155-157	59.40	3.23
$Ni(n-Bu-bzac)_2bipy$	Dark green	279-281	25.40	3.07
$Ni(n-Bu-bzac)_2phen$	Dark green	255-257	13.69	1.81

D=Dirty, Y=yellowish **%=**percentage

Table 2. Microanalytical data of nickel(II) complexes of 2-substituted-1-phenyl-1,3-butanedione and their adducts

Compound	M.Wt	% Calculated (Observed)			
		C	H	N	Ni
Ni(bzac)₂2H₂O	417.13	57.58 (57.33)	5.33 (5.13)	- -	14.07 (13.79)
[Ni(bzac)(bipy)(H₂O)₂](bipy)	573.30	62.85 (62.94)	5.29 (4.99)	4.88 (5.10)	10.24 (10.00)
Ni(bzac)₂bipy	537.27	67.06 (66.91)	4.89 (5.14)	5.21 (5.08)	10.93 (10.34)
[Ni(phen)₃](bzac)₂	957.73	70.22 (70.16)	4.85 (4.62)	8.77 (8.62)	6.13 (5.56)
[Ni(phen)₂(H₂O)₂](bzac)₂	777.53	67.96 (67.74)	4.94 (4.82)	7.20 (7.16)	7.55 (7.98)
Ni(bzac)₂phen	561.29	68.47 (68.25)	4.68 (4.56)	4.99 (5.02)	10.46 (10.39)
Ni(Me-bzac)₂.2H₂O	445.19	59.35 (59.33)	5.90 (5.82)	- -	13.19 (13.02)
Ni(Me-bzac)₂bipy	565.33	67.98 (68.05)	5.36 (5.07)	4.95 (5.21)	10.39 (10.60)
Ni(Me-bzac)₂phen	589.35	69.29 (69.01)	5.14 (4.89)	4.75 (4.53)	9.96 (10.18)
Ni(Et-bzac)₂.2H₂O	473.25	60.91 (60.69)	6.40 (6.13)	- -	12.41 (12.30)
Ni(Et-bzac)₂bipy	593.39	68.81 (68.58)	5.78 (5.57)	4.72 (4.42)	9.89 (10.10)
Ni(Et-bzac)₂phen	617.41	70.03 (69.78)	5.56 (5.34)	4.54 (4.31)	9.51 (9.79)
Ni(i-Pr-bzac)₂.2H₂O	501.39	62.29 (62.59)	6.85 (7.11)	- -	11.71 (11.73)
Ni(i-Pr-bzac)₂bipy	621.45	69.57 (69.68)	6.18 (6.30)	4.51 (4.66)	9.45 (9.69)
Ni(i-Pr-bzac)₂phen	645.47	70.71 (70.96)	5.95 (6.16)	4.34 (4.46)	9.10 (8.82)
Ni(n-Pr-bzac)₂.2H₂O	501.39	62.29 (62.59)	6.85 (7.11)	- -	11.71 (11.73)
Ni(n-Pr-bzac)₂bipy	621.45	69.57 (69.68)	6.18 (6.30)	4.51 (4.66)	9.45 (9.69)
Ni(n-Pr-bzac)₂phen	645.47	70.71 (70.96)	5.95 (6.16)	4.34 (4.46)	9.10 (8.82)
Ni(n-Bu-bzac)₂.2H₂O	529.37	63.52 (63.39)	7.25 (7.08)	- -	11.09 (11.32)
Ni(n-Bu-bzac)₂bipy	649.51	70.27 (70.01)	6.53 (6.38)	4.31 (4.59)	9.04 (8.80)
Ni(n-Bu-bzac)₂phen	673.53	71.33 (71.03)	6.30 (6.07)	4.16 (3.95)	8.72 (8.94)

Table 3. Relevant Infrared Spectra bands (cm^{-1}) of Nickel(II) complexes of 2-substituted-1-phenyl-1,3-butanedione and their adducts

Formula	C=O, C=C	ν_s(C-O)+δC-H	δ_{as}(CH$_3$)+δ_s(CH$_3$)	γ(C-H)Phen/bipy
bzacH	1599m, 1540b	1484m	1413m, 1360m	-
Ni(bzac)$_2$.2H$_2$O	1595s, 1560m	1487m, 1452m	1409b	-
[Ni(bzac)(bipy)(H$_2$O)$_2$](bzac)	1595s, 1569s	1456m	1414b	773s
Ni(bzac)$_2$bipy	1596s, 1570s	1456s	1415s	773w
[Ni(phen)$_3$](bzac)$_2$	1652w, 1626w	1482vw	1426m, 1399m	849s, 726s
[Ni(phen)$_2$(H$_2$O)$_2$](bzac)$_2$	1594s, 1565s	1458m	1400vs	852s, 727s
Ni(bzac)$_2$phen	1711s, 1592w	1486vw, 1460w	1406b	849s, 728m
Me-bzacH	1729m, 1666m	1450s	1408vw, 1372s	-
Ni(Me-bzac)$_2$.2H$_2$O	1584m, 1578s	1472s	1407s, 1354s	-
Ni(Me-bzac)$_2$bipy	1556s	1490vw,1472vw	1417m, 1342vw	774s
Ni(Me-bzac)$_2$phen	1624w, 1594s	1485w,1456m	1423vw,1400vs	850s, 727vs
Et-bzacH	1723m, 1677m	1449m	1420w, 1359m	-
Ni(Et-bzac)$_2$.2H$_2$O	1598s, 1560s	1489m, 1454s	1405s	-
Ni(Et-bzac)$_2$bipy	1557vs	1490vs, 1472vw	1417s	774vs
Ni(Et-bzac)$_2$phen	1598s, 1570s	1456s	1408s	852m, 714m
i-Pr-bzacH	1764w, 1687b	1490vw, 1448vs	1411w, 1373m	-
Ni(i-Pr-bzac)$_2$.2H$_2$O	1654w, 1584m	1472vs	1407vs, 1354vs	-
Ni(i-Pr-bzac)$_2$bipy	1663s, 1600vs	1458w, 1444w	1400s	770vs
Ni(i-Pr-bzac)$_2$phen	1665b, 1628b	1459vw	1424s	851vs,724vs
n-Pr-bzacH	1720m, 1676m	1458m	1421w,1384m	-
Ni(n-Pr-bzac)$_2$.2H$_2$O	1569b	1488w	1415b,1342w	-
Ni(n-Pr-bzac)$_2$bipy	1556b	1490w, 1472w	1419s, 1342m	774s
Ni(n-Pr-bzac)$_2$phen	1570b, 1517w	1498vw	1413s, 1344m	856s, 732s
n-Bu-bzacH	1718w, 1685w	1459w	1421w	-
Ni(n-Bu-bzac)$_2$.2H$_2$O	1726w, 1676w	1492m, 1454m	1410b	-
Ni(n-Bu-bzac)$_2$bipy	1591vw, 1557s	1485w, 1452vw	1416s,1342w	774s
Ni(n-Bu-bzac)$_2$phen	1593vs, 1568v	1486m, 1459s	1410vs	849s, 728s

Table 4. The electronic solution spectra of Nickel(II) complexes of 2-substituted-1-phenyl-1,3-butanedione and their adducts

Emperical Formula	π_3-π_4*(cm^{-1})		d-d	
	CHCl$_3$	CH$_3$OH	CHCl$_3$	CH$_3$OH
bzacH	32,258(7247)	32,258(18259)	-	-
Ni(bzac)$_2$.2H$_2$O	31,646(61419)	31,056(31780)	15,480(37)	19,305(62)
				14,286(45)
[Ni(bzac)(bipy)(H$_2$O)$_2$](bzac)	33,113(40581)	33,113(27405)	17,182(25)	17,668(21)
			12,843(5)	12,853(4)
				11,521(7)
Ni(bzac)$_2$bipy	33,3113(29467)	32,895(41812)	17,212(11)	17,361(83)
				12,821(47)
				11,765(54)
[Ni(phen)$_3$](bzac)$_2$	34,247(?)	34,014(43955)	20,080(?)	15,748(71)
			12,500(?)	13,158(69)
				11,765(69)
[Ni(phen)$_2$(H$_2$O)$_2$](bzac)$_2$	34,247(25953)	34,247(34536)	17,730(18)	17,483(31)
			12,821(7)	12,579(13)
				11,765(34)
Ni(bzac)$_2$phen	34,014(?)	34,247(22)752	17,241(26)	17,241(?)
			12,987(7)	12,626(?)
				11,494(?)
Me-bzacH	34,364(?)	33,557(?)	-	-
31,056(?)				
Ni(Me-bzac)$_2$.2H$_2$O	-	31,056(29975)	-	20,161(64)
				15,853(50)
Ni(Me-bzac)$_2$bipy	33,557(36196)	33,333(21213)	15,974(31)	16,611(6)
Ni(Me-bzac)$_2$phen	34,602*	34,483*	18,149(4)	18,149(22)
Et-bzacH	32,680(?)	34,014(?)	-	-
Ni(Et-bzac)$_2$.2H$_2$O	34,602*	31,056(339)	15,924(20)	15,674(1)
Ni(Et-bzac)$_2$bipy	33,557(3638)	33,333(20555)	15,934(23)	16,474(1)
Ni(Et-bzac)$_2$phen	34,483*	34,483(?)	15,974(23)	16,949(?)
i-Pr-bzacH	35,336(?)	35,088(?)	-	-
Ni(i-Pr-bzac)$_2$.2H$_2$O	-	32,573(?)	-	14,430(?)
Ni(i-Pr-bzac)$_2$bipy	32,895(?)	34,602(?)	15,823(?)	16,340(?)
				13,369(?)
Ni(i-Pr-bzac)$_2$phen	-	33,333*	16,779(?)	15,528(?)
				13,369(?)
n-Pr-bzacH	35,088(?)	35,461(?)	-	-
Ni(n-Pr-bzac)$_2$.2H$_2$O	-	34,130(?)	-	14,903(?)
Ni(n-Pr-bzac)$_2$bipy	33,557(25232)	33,223(?)	15,949(20)	16,393(?)
Ni(n-Pr-bzac)$_2$phen	34,247(?)	34,364(?)	15,974(?)	15,480(?)
n-Bu-bzacH	33,003(?)	33,784(?)	-	-
Ni(n-Bu-bzac)$_2$.2H$_2$O	34,602(?)	34,722*	15,674(?)	15,848(?)
Ni(n-Bu-bzac)$_2$bipy	33,557(65368)	33,557(22886)	16,207(27)	17,212(6)
Ni(n-Bu-bzac)$_2$phen	34,965*	34,483(?)	16,892(33)	16,722(?)
				13,423(8)

Table 5. The electronic solid reflectance spectra of Nickel(II) complexes of 2-substituted-1-phenyl-1,3-butanedione and their adducts

| Emperical Formula	π_3-π_4*(cm^{-1})	d-d
bzacH	31,056	-
Ni(bzac)$_2$.2H$_2$O	35,211	21,053, 19,417, 11,962
[Ni(bzac)(bipy)(H$_2$O)$_2$](bzac)	35,842, 31,250	19,881, 13,605, 12,594
Ni(bzac)$_2$bipy	35,971, 31,153	21,598, 13,680, 12,330
[Ni(phen)$_2$(H$_2$O)$_2$](bzac)$_2$	31,153	20,877, 14,493,12,771
Ni(bzac)$_2$phen	32,573	19,493, 13,532, 12,788
Me-bzacH	35,587, 32,680	-
Ni(Me-bzac)$_2$.2H$_2$O	34,965	21,739, 19608, 11,990
Ni(Me-bzac)$_2$bipy	35,842, 31,056	19,920, 13,514, 12,484
Ni(Me-bzac)$_2$phen	32,258	20,576, 14,771,12,755
Et-bzacH	35,088, 31,153	-
Ni(Et-bzac)$_2$.2H$_2$O	35,211, 31,153	19,569, 13,333, 12,034
Ni(Et-bzac)$_2$bipy	35,587, 31,055	19,763, 13,532, 12,674
Ni(Et-bzac)$_2$phen	33,223	19,531, 13,495, 12,658
n-Pr-bzacH	33,003	-
Ni(n-Pr-bzac)$_2$.2H$_2$O	33,898, 31,347	19,380, 14,205, 11,696
Ni(n-Pr-bzac)$_2$bipy	31,250	19,841, 13,587, 12,330
Ni(n-Pr-bzac)$_2$phen	34,130	19,608, 13,495, 12,315
n-Bu-bzacH	33,670	-
Ni(n-Bu-bzac)$_2$.2H$_2$O	31,153	21,231, 19,048, 12,121
Ni(n-Bu-bzac)$_2$bipy	31,250	19,881, 13,569
Ni(n-Bu-bzac)$_2$phen	33,113	19,960, 19,011
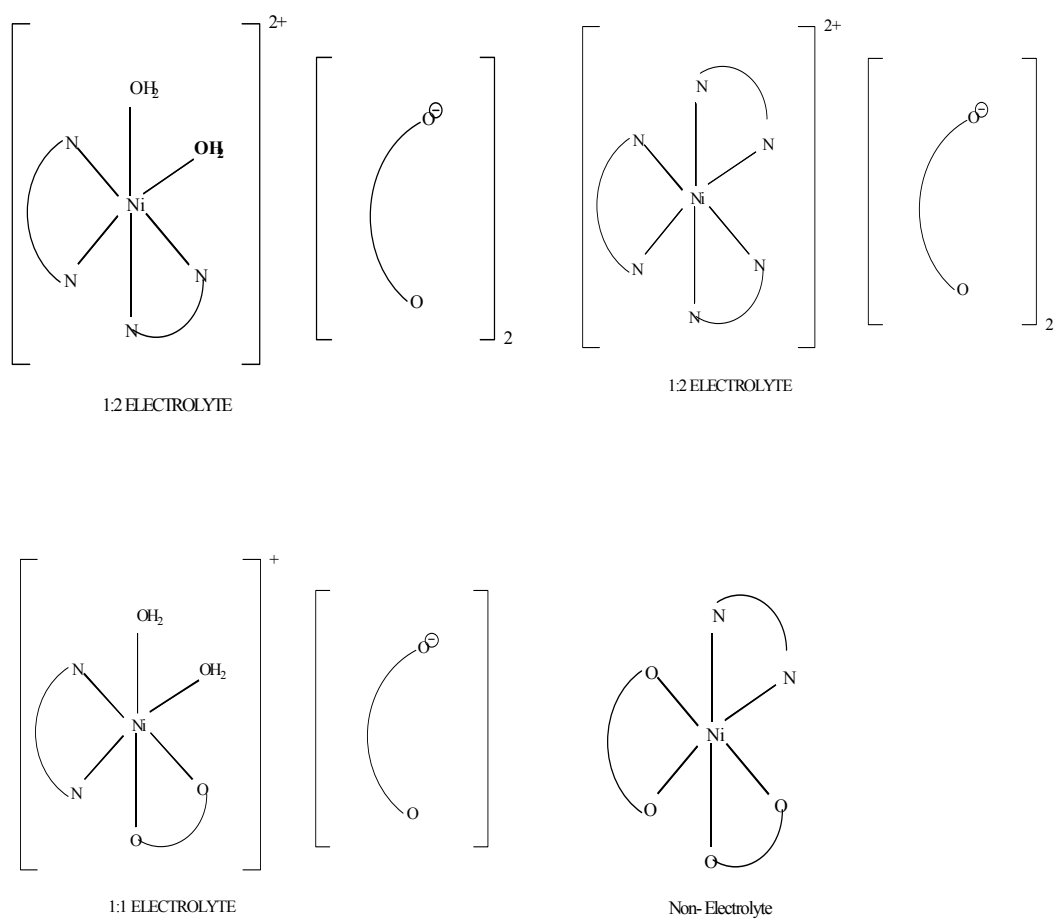
Figure 1. Proposed structures for Nickel adducts

pH Metric Studies of Interaction of Synthesized Ligands 2-amino-4-hydroxy-6-methylpyrimidine and 1-(4-hydroxy-6-methylpyrimidino)-3-phenylthiocarbamide with Cu(II), Cd(II), Cr(II), Cations At 0.1 M Ionic Strength

Dipak T. Tayade

Department of Chemistry, S. R. R. Lahoti Science College

Morshi, (MS), INDIA

Dinesh A. Pund

Department of Chemistry, J. Darda college of Engee. & technology

Yevatmal, (MS), INDIA

E-mail: dinesh_pund@rediffmail.com

Rahul A. Bhagwatkar (Corresponding author)

Department of Chemistry, S. R. R. Lahoti Science College, Morshi, (MS), INDIA

Tel: 91-997-016-5107   E-mail: bhagwatkar83@gmail.com

Dinesh B. Rathod

Department of Chemistry, S. S. K. Innani. Mv. Karanja Lad, (MS), INDIA

Neha A. Bhagwatkar

Department of Chemistry, Shivagi Science College, Amravati, (MS), INDIA

Abstract

Guanidine was successfully interacted with acetoacetic ester to synthesize 2-amino-4-hydroxy-6-methylpyrimidine (L_1) which on further treatment with phenylisothiocyanate furnishes 1-(4-hydroxy-6-methylpyrimidino)-3-phenylthiocarbamide (L_2). The interactions of Cu(II), Cd(II), Cr(II) metal ions with L_1 and L_2 have been studied at 0.1 M ionic strength in 70 % Dioxane-water mixture by Bjerrum method as adopted by Calvin and Wilson, It is observed that Cu(II), Cd(II), Cr(II) metal ions form 1:1 and 1:2 complexes with ligands (L_1 and L_2). The data obtained were used to estimate and compare the values of proton-ligand stability constant (pK.) and metal-ligand stability constants (log k).The effect of substituents were studied from estimated data (pK & log k).

Keywords: Pyrimidines, Thiocarbamide, Acetoacetic ester, Ionic strength, pH metry

1. Introduction

Pyrimidino and thiocarbamido nucleus containing heterocycles possesses pharmaceutical, medicinal agricultural industrial and biotechnological significance(Barnes, D. M., 2002; Cyril V., 1977; Ghaigy, 1965; Bossinger, 1972; Seidal, 1964). Recently 2-amino-4-hydroxy-6-methylpyrimidine was successfully condensed with various isothiocyanates in acetone, ethanol, dioxane mediums to obtain 1-(4-hydroxy-6-methylpyrimidino)-3-substitutedthiocarbamides.(Patil, 2006) When above reaction mixture was condensed in acetone-ethanol medium in 1:1 molar praportion the yield and purity increases with decrease in time span.

The manifold research work has been done on the study of metal and nitrogen heterocyclic ligands containing complexes(Irving H, 1954; Martell, 1962). Many workers have reported their results on metal-ligand stability constants. With the view to understand the bio-inorganic chemistry of metal ions, Banarjee et al (1968) have synthesized a number of mixed-ligand alkaline earth metal complexes. The studies of metal-ligand complexes in solution having number of metal ions with ligands carboxylic acids, oximes, phenols etc. would be interesting which throw a light on the mode of storage and transport of metal ions in biological kingdom. Bejerrum's (1941) dissertation describes the initiative to develop this field. Metal complexation not only brings the reacting molecules together to give activated complexes (Irving H, 1953) but also polarized electrons from the ligands towards the metal. The relation between stability and basicity of the ligands is indicated by the formation constant and free energy change value. Bulkier group increases the basicity of ligands as well as stability. The stability of the complexes is determined by the nature of central metal atom and ligand. The stability of complexes is influenced by the most important characteristics degree of oxidation, radius and electronic structure. Irving and Williams had studied the order of stability of metal complexes of transition metal ions by comparing the ionic radius and second ionization potentials of metal ions, as it is valid for most nitrogen and oxygen donor ligands. Narwade et al (1985) have investigated metal-ligand stability constants of some lanthanides with some substituted sulphonic acids. Bodkhe et al (2003) have reported the metal-ligand stability constants of some β-dikctones. Tekade et al (2005) have investigated stability constants of some substituted pyrazolines, isoxalline and diketone. Prasad et al (2005) have studied mixed ligand complexes of alkaline earth metals, Mg(II). Ca(II), Sr(II) and Ba(II) with 5-nitrosalicyladehyde and β-diketones. Recently, Thakur et al (2010) studied the interaction between some lanthanide and radioactive metal ion with substituted Schiff's bases at 0.1 M ionic strength pH metrically and spectrophotometrically.

In present work an attempt has been made to study the interactions between Cu(II), Cd(II), Cr(II) and 1-(4-hydroxy-6-methylpyrimidino)-3-substitutedthiocarbamide (L_1 and L_2) at 0.1 M ionic strength pH metrically in 70% dioxane-water mixture.

2. Materials and Methods

All the chemicals used were analar grade (India make) alkyl/arylisothiocyanates were prepared according to the literature, melting points of all synthesized compounds were determined in open capillary and uncorrected. IR spectra were recorded on Perkin-Elmer spectrophotometer in the range 4000-400 cm^{-1} in KBr pellets. PMR spectra were recorded with TMS as internal standard using CDCl$_3$ and DMSO. The purity of the compounds was checked on silica gel-G plates by TLC.

2.1 Synthesis of 2-amino-4-hydroxy-6-methyl pyrimidine [L_1]

The interaction of guanidine with acetoacetic ester had been carried out in acetone-ethanol (1:1)medium for eight hours in water bath. The precipitate was filtered. It was crystallized by precipitation method. (By precipitating it with acetic acid from its alkaline solution). Reaction yielded 79 %, m.p. was 168^{0}C. Product was off-white solid, soluble in hot acetone, benzene, hot ethanol and dioxane and insoluble in water and chloroform. When hot aqueous solution of the product was treated with aqueous ferric chloride (5%) gave red colouration, indicating the presence of phenolic -OH group. Desulphuration was noticed when the product was warmed with alkaline plumbite solution. It formed picrate (m.p. 183°C). The reaction scheme was shown in Scheme-I. The spectral data for IR (Table 1), ^{1}H-NMR (Table 2) and CHNS-O analysis (Table 3) was reported.

2.2 Synthesis of 1-(4-hydroxy-6-methylpyrimidino)-3-phenylthiocarbamide [L_2]

The interaction of 2-amino-4-hydroxy-6-methylpyrimidine with phenylisothiocyanates has been carried out in acetone-ethanol medium in 1:1 molar proportion in the boiling water bath for four hours, filter the reaction mixture to separate out 1-(4-hydroxy-6-methylpyrimidino)-3-phenylthiocarbamide [L_2], washed several times with 10 ml of water and crystallized with ethanol. Reaction yielded 62 %, m.p. was 132^{0}C. Product was brown solid, soluble in hot acetone, benzene, ethanol and dioxane and insoluble in water and chloroform. When hot aqueous solution of the product was treated with aqueous ferric chloride (5%) it gave red colouration, indicating the presence of phenolic -OH group. Desulphuration was noticed when the product was warmed with alkaline plumbite solution. It formed picrate (m.p. 142°C). The reaction scheme was shown in Scheme-II. The spectral data for IR (Table 1), ^{1}H-NMR (Table 2) and CHNS-O analysis (Table 3) was reported.

3. pH metric analysis

Systronic microprocessor based instrument with accuracy in 0.01 unit with glass and saturated calomel electrode was used for the titrations. It was calibrated with the buffer solution of pH 7.00 and 9.20 at 28 ± 0.1 °C before titrations.

Titrations were carried out in an inert atmosphere by bubbling a constant flow of nitrogen gas.

The experimental procedure involved the titrations of

i)   Free acid $HClO_4$ (0.01 M)

ii)   Free acid $HClO_4$ (0.01 M) and ligand (20 x 10^{-4})

iii)   Free acid $HClO_4$ (0.01 M) and ligand (20 x 10^{-4}) and metal ion (4 x 10^{-4} M) with standard NaOH solution

The ionic strength of all the solution was maintained constant (0.1 M) by adding appropriate amount of $NaClO_4$ solution. All the titrations were carried out in 70 % dioxane-water mixture and the reading were recorded for each 0.1 ml addition. The graph of volume of alkali (NaOH) against pH were plotted (Fig. 1 to Fig. 6).

4. Results and Discussion

4.1 Proton-ligand stability constants:

The 1-(4-hydroxy-6-methylpyrimidino)-3-substitutedthiocarbamide was monobasic acids having only one dissociable H^+ ion from OH group. It can therefore, be represented as HL

$$HL \rightleftharpoons H^+ + L^-$$
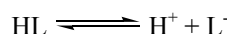
The titration curves of the acid and ligand deviate at about 3.0 pH. The deviation between acid curves from ligand for all the systems showed the dissociation of H^+ ions from -OH groups of ligands.

The proton-ligand formation number ($\overline{n}_A$) were calculated by Irving and Rossotti expression.

$$\overline{n}_A = \gamma - \frac{(V_2 - V_1) \, x \, (E^0 + N)}{(V^0 + V_1) \, T_L^0}$$

Where,

V^0 = Initial volume of solution (50 ml)

E^0 = Initial concentration of free acid ($HClO_4$)

T_L^0 = Concentration of ligand in 50 ml solution

γ = Number of dissociable protons from ligand

N = Avagadros Number

$(V_2 - V_1)$ = Volume of alkali (NaOH) consumed by acid and ligand on the same pH.

The pK values were calculated from the formation curves between pH Vs $\overline{n}_A$ noting the pH at which $\overline{n}_A$ = 0.5 (half integral method) and point wise calculations which are represented in Table 4. It is observed that, the order of pK values of ligands is found to be as, pK L_2 > pK L_1. The reduction in pK values of L_1 is attributed to the presence of electron withdrawing -OH group.

4.2 Metal-Ligand Stability Constants

The stepwise formation constants of Cu(II), Cd(II), Cr(II) metal ions with ligands (L_1 and L_2) in 70% dioxane-water mixture were determined. The values of log K_1 and log K_2 were directly computed from the formation curve ($\overline{n}_A$ Vs pH) using half integral method. The most accurate values were calculated by point wise calculations which are presented in Table 5.

5. Conclusion

From the titration curves, it is observed that the departure between acid + ligand (A+L) curve and acid + ligand + metal (A+L+M) curve for all systems started from pH = 3.0. This indicated the commencement of complex formation. Also change in colour from yellow to red in the pH range from 3 to 11 during titration showed the complex formation between metal and ligand.

Observation of Table 5 and 6 shows that the less difference between log K_1 and log K_2 values indicates the complex formation between metal ion and ligand occurring simultaneously. The values of log K_1 and log K_2 (Table 4) the stability of complexes was decided. For 2-amino-4-hydroxy-6-methylpyrimidine (L_1) the difference between the values of log K_1 and log K_2 is higher with Cu(II) complex than Cd(II) and Cr(II). It indicates that Cu(II) forms

more stable complex with Ligand-1 (L_1) than Cd(II) and Cr(II). And for 1-(4-hydroxy-6-methylpyrimidino)-3-phenylthiocarbamide (L_2) the difference between the values of log K_1 and log K_2 is higher with Cd(II) complex than Cu(II) and Cr(II) complexes. Cd(II) forms more stable complex with ligand 2 than Cu(II) and Cr(II) metal ions.

References

Banarjee A. K. and Rao T. V. R. (1968). *J. Indian Chem. Soc.*, 63, 480.

Barnes, D. M., Jianguo Ji, Fickes, M. G. (2002). *J. Am. Chem. Soc.*, 124, 13097-13105.

Bjerrum J. (1941). *Metal amine formation in aqueous solutions,* P. Haase and Sons, Copenhagen.

Bodkhe P. S., Patil K. N., Narwade M. L. and Doshi, A. G. (2003). *Aisan J. Chem.*, Vol. 15, No. 3 & 4, 1739-1743.

Bossinger, C.D. and Tekeshi E. (1972). *Chem. Abstr.*, 77, 343590.

Cyril V., Milam, M. (1977). *Chem. Abstr.*, 86, 190015.

Florence A. T. and Attwood D. (1981). *Physical principle's of pharmacy,* Macmillan. London.

Fukuda V., Morishita R. and Sone K. (1985). *Bull. Chem. Sep. Jpn.*, 49, 1017.

Ghaigy, A. G. (1965). *Siess Patent,* 393, 344.

Gudadhe S., Narwade M. L. and Jamode V, S. (1985). *Acta. Ciencia. Indica* (Chem.), 11, 234.

Irving H. and Rossotti H. (1954). *J. Chem. Soc.,* 2904.

Irving H. and William R J. P. (1953). *J. Chem. Soc.*, 3192.

Jansen J. C. and Reedijk. J. (1974). *2. Naturforsch. Teil B.*, 29, 527 (Eng.).

Jolly V. S. Arora G. D. and Taiwar P. (1990). *J. Indian Chem. Soc.,* 61, 1001.

Kadu M. V. and Jamode V. S. (1999). *Asian, J. Chem.*, 11, 420.

Martell A. E. and Calvin M. (1962). *Chemistry of metal chelate compounds.* Prentice Hall. Inc. England. Cliffs. N. J.

Narwade M. L. and Wankhade A. S. (1993). *J. Indian Chem. Sot*, 70, 709.

Narwade M. L., Chincholkar M. M. and Sathe S. W. (1985). *J. Indian Chem. Soc.,* 62, 194.

Natrajan C. and Thormaraj P. (1991). *Indian J. Chem.,* 30A, 722.

Patil S. U. (2007). *Synthesis and studies on solute-solventinteraction of bromoacetophenones and coumaren-3-ones and their antimicrobialactivity.* Ph. D. Thesis, Amravati University, Amravati.

Patil, S. U., Raghuvanshi, P. B. (2006). *Asian J. Chem.*, 18(1), 747-749.

Pfeiffer. (1940). *Angew Cham.,* 53, 93.

Poddar S. N., Dey K. and Poddar N. G. (1970). *Indian J. Chem.*, 8, 364.

Prasad R. N., Agrawal M., Ratnani R. and Sarswal K. (2005). *J. Indian Chemical Soc*, Vol. 82, PP. 137 – 139,.

Rana A. K. and Shah J. R. (1986). *J. Indian Chem. Soc.*, 63, 281.

Saha N. Dalia M. and Sinha S. (1986). *Indian J. Chem.*, 25A, 629.

Sawalakhe P. D. and Narwade M. L. (1995). *J. Indian Chem. Soc.*, 70, 25.

Sawalakhe P.D. (1992). *Studies in melal-ligand complexes with some substituted-1.3-diones and 3,5-diarylpyrazole and pyrazoline.* Ph. D. Thesis, Amravati University, Amravati.

Schwarzenbach and Ankerman. (1948). *Helv. Chim. Acta.*, 31, 1029.

Seidal, M., Betiver, F. E., S. (1964). *African Patent*, 68, 03, 47.

Shuter Ya. A. (1974). *Zh. Obshch. Khim.,* 44, 379.

Tekade P. V., Patil K. N., Narwade M. L. (2005). *Acta Ciencia Indica.*, *Vol.* XXXIC No. 4, 287.

Thakur S. D., Munot K. P., Raghuvanshi P. B., Tayade D. T. (2010). *Acta Ciencia Indica, Vol.* XXXC No. 3, 425.

Table 1. IR spectra of synthesized compounds in (cm^{-1})

Compound	ν (N-H)	ν (C=N)	ν(N-C=N)	ν (>C-O)	ν (>C=S)
[3(L$_1$)]	3180.9	1638.2	1579.6	1252.8	---
[5(L$_2$)]	3170.3	1631.5	1562.3	1222.8	1162.2

Table 2. ^{1}H-NMR spectra of synthesized compounds in (ppm)

Compound	(Ar-OH)	(N-H)	(Ar-H)	(pyrimidino-H)	(-CH3)
[3(L$_1$)]	10.80	9.76	6.20	7.74	2.19-2.59
[5(L$_2$)]	10.55	9.56	6.92	7.31	2.58

Table 3. CHNS-O analysis of synthesized compounds in (ppm)

Compound	**[3(L$_1$)]**		**[5(L$_2$)]**	
	Calculated (%)	Found (%)	Calculated (%)	Found (%)
Carbon	48.00	47.33	56.47	56.14
Hydrogen	05.60	05.12	2.75	2.55
Nitrogen	33.06	32.92	21.96	21.66
Sulphur	---	---	12.55	12.12

Table 4.

Ligands	System	pK	
		Half internal method	Point wise method
L$_1$	2-amino-4-hydroxy-6-methylpyrimidine	5.421	5.612
L$_2$	1-(4-hydroxy-6-methylpyrimidino)-3-phenylylthiocarbamide	6.751	7.332

Table 5. Metal-ligand stability constants (log K)

System	log K$_1$	log K$_2$
Cu(II) - ligand - 1	3.6970	2.5198
Cd(II) - ligand - 1	3.5969	2.5198
Cr(II) - ligand - 1	3.6969	2.3198
Cu(II) - ligand - 2	3.9968	2.8197
Cd(II) - ligand - 2	4.2969	2.3198
Cr(II) - ligand - 2	3.9969	2.8198

Table 6. Metal-ligand stability constants (log K)

System	log K$_1$ - log K$_2$	log K$_1$ / log K$_2$
Cu(II) - ligand -1	1.1772	1.4672
Cd(II) - ligand -1	1.0771	1 .4275
Cr(II) - ligand -1	1.3771	1.5936
Cu(II) - ligand -1	1.1771	1.4175
Cd(II) - ligand -1	1.9771	1.8523
Cr(II) - ligand -1	1.1771	1.4174

Fig. 1
SYSTEM - Cu(II)-(L₁)
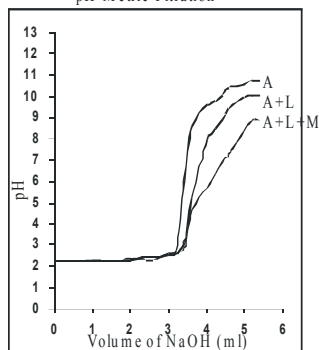pH Metric Titration

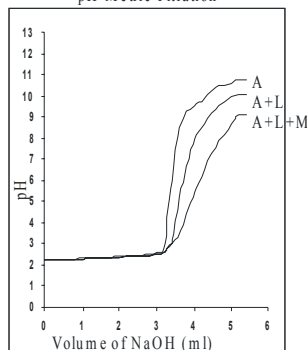Fig. 2
SYSTEM - Cd(II)-(L₁)
pH Metric Titration

Fig. 3
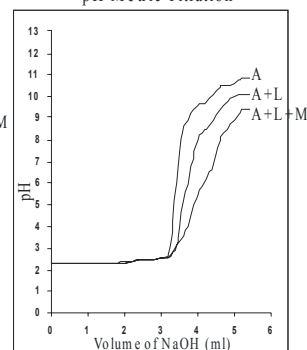SYSTEM - Cr(II)-(L₁)
pH Metric Titration

Fig. 4
SYSTEM - Cu(II)-(L₂)
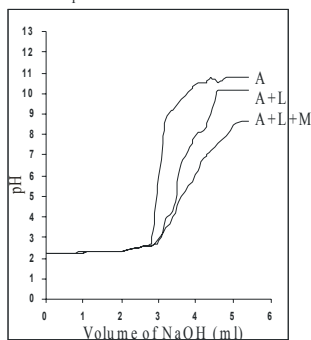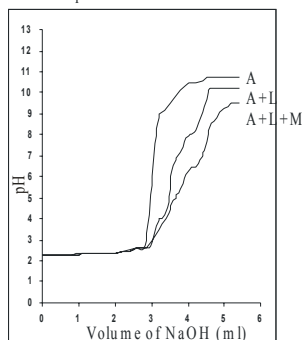pH Metric Titration

Fig. 5
SYSTEM - Cd(II)-(L₂)
pH Metric Titration

Fig. 6
SYSTEM - Cr(II)-(L₂)
pH Metric Titration
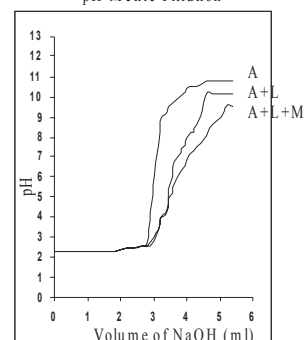
Where, A - Acid, L - Ligand, M - Metal

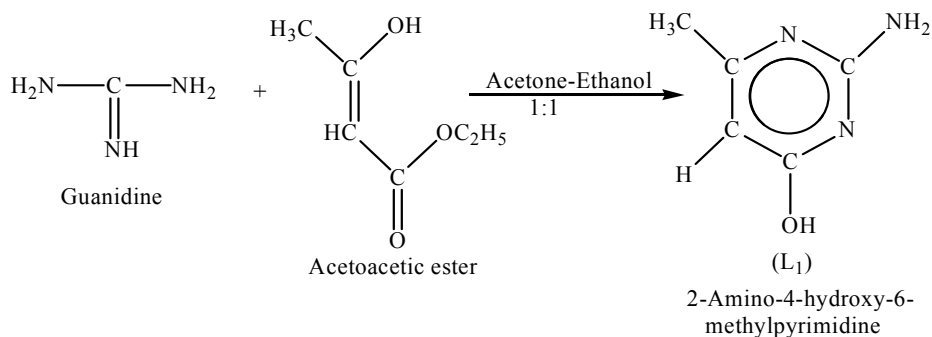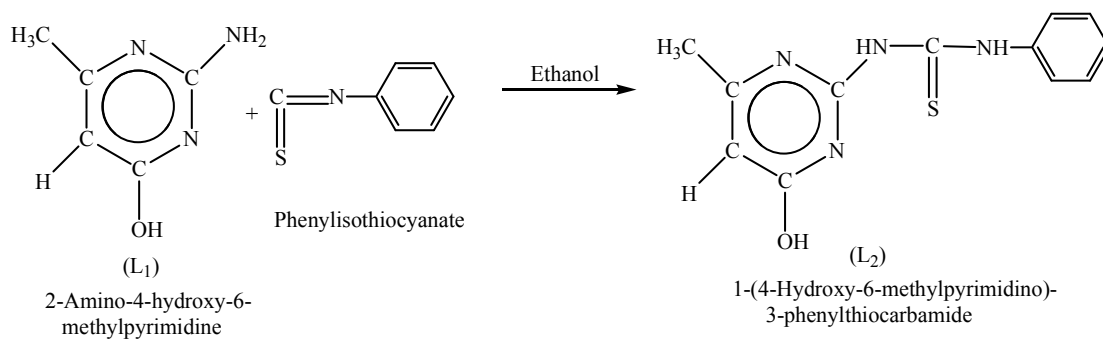Guanidine   Acetoacetic ester   (L₁)

2-Amino-4-hydroxy-6-
methylpyrimidine

SCHEME-I

(L₁)
2-Amino-4-hydroxy-6-
methylpyrimidine

Phenylisothiocyanate

(L₂)
1-(4-Hydroxy-6-methylpyrimidino)-
3-phenylthiocarbamide

SCHEME-II

Synthesis of 3-substitutedmethylene-2*H*-thiopyrano[2,3-*b*] Pyridine-4(3*H*)-ones and Their Antifungal Activity *In Vitro*

Yajun Zheng

School of Pharmacy, Pharmaceutical Sciences College of Hebei University

Baoding 071002, Hebei, China

E-mail: hainideyajun@163.com

Zhengyue Ma

School of Pharmacy, Pharmaceutical Sciences College of Hebei University

Baoding 071002, Hebei, China

E-mail: mazhengy@126.com

Xinghua Zhang & Ning Yang

School of Pharmacy, Pharmaceutical Sciences College of Hebei University

Baoding 071002, Hebei, China

Gengliang Yang (Corresponding author)

School of Pharmacy, Pharmaceutical Sciences College of Hebei University

Baoding 071002, Hebei, China

E-mail: ygl@hbu.edu.cn

Abstract

Six (Z)-3-substitutedmethylene-2*H*-thiopyrano[2,3-*b*]pyridin-4(3*H*)-ones were designed and synthesized. Their structures were confirmed by MS and ^{1}H-NMR and element analysis. Their antifungal activity was tested by micro dilution broth susceptibility for eight kinds of fungi, and the results showed that the target compounds exhibited activity against fungi tested to some extent. The compound 5a had the best antifungal effect among of the target compounds.

Keywords: 2*H*-thiopyrano[2,3-*b*]pyridin-4(3*H*)-one, Synthesis, Antifungal activity

1. Introduction

In recent years, invasive fungal infections, especially in those individuals with immunocompromised hosts such as cancer patients and patients with AIDS (N. H. Georgopapadakou, 1996), have continued to increase in incidence. Pyridine derivatives had been reported to possess important biological activities, such as antihypertensive, antitumor, antifungal and so on (Tian Laijin, 2004; Wang Dawei, 2004). Some of 4-oxothiopyrano[2,3-*b*]pyridine derivatives were recently reported as potential antihypertensive agents(A. D. Settimo, 2000; P. L. Ferrarini, 2000). *α,β*-unsaturated compounds have also exhibited excellent antitumor, antiinflammatory, antimalaria and other pharmacological effects (T Al Nakibl, 1990; Prithwiraj De, 2010; Bimal K. Banik, 2010; Giovanna Damia, 2009; Peng-Cheng Lv, 2010). At present, the (Z)-3-substitutedmethylene-2*H*-thiopyrano[2,3-*b*]pyridine -4(3*H*)-ones are rarely reported, and their antifungal activity are not reported. On this basis, we design and synthesis of six (Z)-3-substitutedmethylene-2*H*-thiopyrano[2,3-*b*]pyridin-4(3*H*)-ones. Firstly the intermediate of 2*H*-thiopyrano[2,3-*b*]pyridin-4(3*H*)-one was synthesized from the 2-chloronicotinic acid. Secondly, the target compounds were obtained by the reactions of aldehyde with 2*H*-thiopyrano[2,3-*b*]pyridin-4(3*H*)-one in ethanol. The antifungal activity of the target compounds *in vitro* was measured by consecutive double dilution. The synthetic route was outlined in Figure 1.

2. Experimental

2.1 Chemistry material

2-chloronicotinic acid (chemically pure) were from SHANDONG KEHUI Chemical Co., LTD (SHANDONG, China), and the other reagents were almost from TIANJIN Chemical LLC (TIANJIN, China). ^{1}H-NMR spectra were recorded in CDCl$_3$ on Bruker Avance DMX 600 using TMS as an internal standard (Bruker, Billerica, MA, USA). Mass spectral data were obtained by LC-MSD Trap XCT G2446A (Agilent Technologies, USA). Melting points were determined SGW X-4 microscopic melting point (Shanghai Precision & Scientific Instrument Co., Ltd, China). Elemental Analysis (C, H, N, S) was realized on Carlo Erba 1106 EAinstrument.

2.2 Preparation of 2-mercaptonicotinic acid

A suspension of 2-chloronicotinic acid 1 (15.7 g, 100 mmoles) and thiocarbamide (13.7 g, 180 mmoles) in 170 mL of water was strong mixing reflux for 4 hours. After cooling, the solid precipitate product was collected and washed with water to give 14.8 g (95% yield) of pure 2.

2.3 Preparation of 2-(2-carboxyethylthio)nicotinic acid

3-chloropropionic acid (11.7 g,108 mmoles) and sodium iodide in 50 mL of water and sodium hydrogen carbonate (9 g, 108 mmoles) were added to a solution of 2-mercaptopyridine-3-carboxylic acid (13.9 g, 90 mmoles) in 90 mL of 10% potassium hydroxide aqueous solution. The reaction mixture was stirred at 60℃ for 4 hours, cooled and acidified with concentrated hydrochloric acid to pH 3. The solid precipitate product was collected and washed with water to give 18.7 g (92% yield) of pure 3.

2.4 Preparation of 2H-thiopyrano[2,3-b]pyridin-4(3H)-one

A solution of 3 (19.3 g, 85 mmoles) and anhydrous sodium acetate (13.9 g, 170 mmoles) in 72mL of acetic anhydride was refluxed at 160℃ for 1.5 hours. After cooling, the reaction mixture was diluted with water, basified with 30% ammonium hydroxide solution to pH 8-9, extracted with ethyl acetate. The combined extracts were washed with water, dried and evaporated to give 9.7 g of crude 4. Purification was made by filtration on a silica gel chromatographic column, using petroleum ether 60-80℃/ethyl acetate 10:1 as the eluting system. The product recovered from the less mobile fraction gave 3.5 g (25％ yield) of pure 4.

2.5 Synthesis of (Z)-3-(2-methylpropylidene)-2H-thiopyrano[2,3-b]pyridin-4(3H)-one (5a-5f)

A solution of potassium hydroxide (1.3 g, 24 mmoles) and compound 4 (3.3 g, 20 mmoles) in 7 mL of water and 12 mL of ethanol were taken into a 50 mL round-bottomed flask, after which, isobutyraldehyde (2.1 g, 20 mmoles) was added over 10 minutes at room temperature, and then the mixture was stirred for 3 hours at temperature 25-30℃. After cooling, the solid precipitate product was collected to give 4.5 g of crude 5a. Purification was made by filtration on a silica gel chromatographic column, using petroleum ether 60-80℃/ethyl acetate 10:1 as the eluting system. The product recovered from the less mobile fraction gave 3.1 g (62％ yield) of pure 5a.

2.5.1 (Z)-3-(2-methylpropylidene)-2H-thiopyrano[2,3-b]pyridin-4(3H)-one (5a)

Pale yellow viscous liquid, yield 62%; ^{1}H-NMR(600 MHz; CDCl$_3$)δ: 1.15(d, J=6.63 Hz, 6H, H-10), 2.78(sext.t, J=13.21, 6.58 Hz,1 H, H-9), 3.93(s, 2 H, H-2), 6.72(d, J=10.06 Hz, 1 H, H-8), 7.18(dd, J=7.90, 4.63 Hz,1 H, H-6), 8.40(dd, J=7.90, 1.86 Hz, 1 H, 5-H), 8.53(dd, J=4.62, 1.86 Hz, 1 H, 7-H); APCI(m/z+H): 220.0; Anal. calcd for C$_{12}$H$_{13}$ClNOS(%): C, 65.72; H, 5.97; N, 6.39; S, 14.62; Found (%): C, 65.83; H, 5.95; N, 6.40; S, 14.65.

2.5.2 (Z)-3-(furan-2-ylmethylene)-2H-thiopyrano[2,3-b]pyridin-4(3H)-one (5b)

Yellow crystals; mp 100-102℃; yield 59%; ^{1}H-NMR(600 MHz, CDCl$_3$)δ: 4.02(s, 2 H, H-2), 6.21(d, J=3.04 Hz, 1 H), 6.36-6.34(m, 1 H, H-10), 7.38(d, J=1.50 Hz, 1 H), 7.49(dd, J=8.14, 4.50 Hz, 1 H, H-6), 7.64(s, 1 H, H-8), 8.78(dd, J=4.49, 1.82 Hz, 1 H, H-5), 8.81(dd, J=8.18, 1.82 Hz, 1 H, H-7); APCI(m/z+H): 244.0; Anal. calcd for C$_{13}$H$_9$ClNO$_2$S(%): C, 64.18; H, 3.73; N, 5.76; S, 13.18; Found (%): C, 64.21; H, 3.72; N, 5.77; S, 13.15.

2.5.3 (Z)-3-(4-methoxybenzylidene)-2H-thiopyrano[2,3-b]pyridin-4(3H)-one (5c)

Yellow crystals; mp 109-110℃; yield 70%; ^{1}H-NMR(600 MHz, CDCl$_3$)δ: 3.94(s, 2 H, H-2), 3.82(s, 3 H, H-11), 6.92-6.89(m, 2 H, H-10), 7.20(t, J=5.78 Hz, 2 H, H-9), 7.50(dd, J=8.25, 4.42 Hz, 2 H, H-6, H-8), 8.79(dd, J=4.49, 1.88 Hz, 1 H, H-5), 8.83(dd, J=8.06, 1.89 Hz, 1 H, H-7); APCI(m/z+H): 484.0; Anal. calcd for C$_{16}$H$_{13}$ClNO$_2$S(%): C, 67.82; H, 4.62; N, 4.94; S, 11.32; Found (%): C, 677.80; H, 4.59; N, 4.95; S, 11.33.

2.5.4 (Z)-3-(4-nitrobenzylidene)-2H-thiopyrano[2,3-b]pyridin-4(3H)-one (5d)

Yellow crystals,mp 159-160℃, yield 68%; ^{1}H-NMR(600 MHz, CDCl$_3$)δ: 4.10(s, 2 H, H-2), 7.48(d, J=8.65 Hz, 2 H, H-9), 7.52(dd, J=8.14, 4.50 Hz, 1 H, H-6), 7.74(s, 1 H, H-8), 8.19(d, J=7.69 Hz, 2 H, H-10), 8.79(dd, J=8.15, 1.87

Hz, 1 H, H-5), 8.82(dd, *J*=4.50, 1.86 Hz, 1 H, H-7); APCI(m/z+H): 299.0; Anal. calcd for $C_{15}H_{10}ClN_2O_3S$(%): C, 60.39; H, 3.38; N, 9.39; S, 10.75; Found (%): C, 60.36; H, 3.37; N, 9.40; S, 10.73.

2.5.5 (Z)-3-(benzo[d][1,3]dioxol-5-ylmethylene)-2H-thiopyrano[2,3-b]pyridin-4(3H)-one (5e)

Yellow crystals; mp 110-112 ℃; yield 57%; ^{1}H-NMR(600 MHz, CDCl₃)*δ*: 8.83(dd, *J*=8.16, 1.86 Hz, 1 H,H-7), 8.79(dd, *J*=4.48, 1.86 Hz, 1 H, H-5), 7.54(s, 1 H, H-8), 7.50(dd, *J*=8.12, 4.49 Hz, 1 H, H-6), 5.97(s, *J*=5.78 Hz, 2 H, H-10), 3.91(s, 2 H, H-2), 6.78(td, *J*=10.30, 7.79 Hz, 3 H, H-9, H-11, H-12); APCI(m/z+H): 298.0; Anal. calcd for $C_{16}H_{11}ClNO_3S$(%): C, 64.63; H, 3.73; N, 4.71; S, 10.78; Found (%): C, 64.61; H, 3.70; N, 4.72; S, 10.81.

2.5.6 (Z)-3-(4-(dimethylamino)benzylidene)-2H-thiopyrano[2,3-b]pyridin-4(3H)-one (5f)

Pale yellow oily; yield 66%; ^{1}H-NMR(600 MHz, CDCl₃)*δ*: 2.94(s, 6 H, H-11), 3.88(s, 2 H, H-2), 6.74(d, *J*=8.50 Hz, 2 H, H-10), 7.13(d, *J*=8.57 Hz, 2 H, H-9), 7.47(dd, *J*=8.11, 4.48 Hz, 1 H, H-6), 7.45(s, 1 H, H-8), 8.81(dd, *J*=8.08, 1.88 Hz, 1 H, H-7), 8.76(dd, *J*=4.49, 1.87 Hz, 1 H, H-5); APCI(m/z+H): 297.1; Anal. calcd for $C_{17}H_{16}ClN_2OS$(%): C, 68.89; H, 5.44; N, 9.45; S, 10.82; Found (%): C, 68.88; H, 5.48; N, 9.39; S, 10.86.

2.6 Antifungal Activity in Vitro

In vitro antifungal activities were measured by means of the minimal inhibitory concentrations (MIC) by consecutive double dilution method. The MIC means the lowest concentration of an antimicrobial agent that prevents visible growth of a microorganism in broth dilution susceptibility test (Marcelo C. Murguı´a, 2008).The MIC was determined according to the national committee for clinical laboratory standards (NCCLS) recommendation. Eight human opportunistic pathogenic fungi (*C.parapsilosis*, *C.glabrata*, *C.albicas*, *C.tropicalis*, *C.neoformans*, *C.Krusei*, *A.niger*, *M.gypseum*) were tested, All experiments were performed in comparison with Fluconazole, a known antifungal agent (Odds, F. C, 1986, Hoban, D. J, 1999). The six new compounds were dissolved in dimethyl sulfoxide (DMSO) (1 mL), further progressive dilutions by RPMI 1640 gave there quired concentrations (64, 32, 16, 8, 4, 2, 1, 0.5, 0.25, 0.125 μg/mL); the fungi were prepared and adjusted to a final concentration of 0.5×104-2.5×104 CFU/mL. MIC values were determined by visual observation after 2-7 d of incubation.

3. Results and discussions

In order to make the reaction proceed easy, we put sodium iodide into the synthetic process of compound 3 on the basis of literature (A. D. Settimo, 2000; P. L. Ferrarini, 2000). The compounds 5a-5f were synthesized by *Knoevenagel* reaction of compounds **4**. With active methylene compound 4 and aldehyde condensation in the presence of alkaline catalysts are *α,β*- unsaturated ketones.

The results of antifungal activities *in vitro* were shown in Table 1. The results showed that the target compounds exhibited activity against fungi tested to some extent. And all the target compounds had no activity against *C.neoformans*. The compound 5a showed a similar level of activity with Fluconazole when against *M.gypseum* and *C.Krusei*, and showed moderate activity against *C.glabrata*.

In conclusion, The target compounds had an antifungal effect on most tested fungi *in vitro*. Compound 5a had the best antifungal effect among of the target compounds. Further biological evaluation of the compounds is in progress.

References

A. D. Settimo, A. M. Marini, G. Primofiore, *et al*. (2000). Synthesis of Novel *5H,11H*-Pyrido[2',3': 2,3]thiopyrano[4,3-*b*]indoles by Fischer-Indole Cylization. *J. Heterocyclic Chem.*, (37)379-382.

Bimal K. Banik, Indrani Banik, Frederick F.Becker. (2010). Asymmetric synthesis of anticancer *β*-lactams via Staudinger reaction: Utilization of chiral ketene from carbohydrate. *Eur. J. Med. Chem.*, (45)846-848.

Giovanna Damia, Maurizio D'Incalci. (2009). Contemporary preclinical development of anticancer agents—What are the optimal preclinical models. *Eur. J. Cancer*, (45)2768-2781.

Hoban, D. J., Zhanel, G. G., Karlowsky, J. A. (1999). In Vitro Susceptibilities of Candida and Cryptococcus neoformans Isolates from Blood Cultures of Neutropenic Patients. *Antimicrobial Agents and Chemotherapy*, 43: 1463.

Lv Pengcheng, Li Huanqiu, Sun Juan, *et al*. (2010). Synthesis and biological evaluation of pyrazole derivatives containing thiourea skeleton as anticancer agents. *Bioorganic and Medicinal Chemistry*, (18)4606-4614.

Marcelo C. Murguı´a, Laura M. Machuca, *et al*. (2008). Synthesis and Properties of Novel Antifungal Gemini Compounds Derived from *N*-Acetyl Diethanolamines. *Journal of Surfactants and Detergents*, (11)223–230.

N. H. Georgopapadakou, T. J. Walsh. (1996). *Antimicrobial Agents and Chemotherapy*, (2) 09.

Odds, F. C., Cheesman, S. L., Abbott, A. B. (1986). Antifungal effects of fluconazole (UK 49858), a new triazole antifungal, *in vitro*. *Journal of Antimicrobial Chemotherapy*, 18: 473.

P L Ferrarini, C Mori, M Badawneh, *et al*. (2000). Synthesis and *β*-blocking activity of (R,S)-(E)-oximeethers of 2,3-dihydro-1,8-naphthyridine and 2,3-dihydrothiopyrano[2,3-*b*]pyridine: potential antihypertensive agents-Part IX. *Eur. J. Med. Chem.*, (35)815-826.

Prithwiraj De, Michel Baltas, Delphine Lamoral-Theys, *et al.* (2010). Synthesis and anticancer activity evaluation of 2(4-alkoxyphenyl)cyclopropyl hydrazides and triazolo phthalazi-nes. *Bioorganic and Medicinal Chemistry*, (18)2537-2548.

T Al Nakibl, V Bezjakl, MJ Meeganz, *et al*. (1990). Synthesis and antifungal activity of some 3-benzylidenechroman-4-ones, 3-benzylidenethiochroman-4-ones and 2-benzylidene-1-tetralones. *Eur. J. Med. Chem.*, (25)455-462.

Tian Laijin, Sun Yuexi, Zheng Xiaoliang, *et al*. (2004). Synthesis, Characterization and *In vitro* Antitumor Activity of Bis(triorganotin)2,3-Pyridinedicarboxylates. *Chinese Journal Inorganic Chemistry*, (22)629-632.

Wang Dawei, Zhao Baoxiang, Wang Kaiming, *et al*. (2004). Synthesis of a new class of antifungal drug Butenafine's analogues. *Chinese Journal of Shandong University (Natural Science)*, (39)99-101.

Table 1. Antifungal activity of compounds synthesized *in vitro*

Compound	MIC$_{100}$/(μg·L^{-1})							
	Cp	Cg	Ca	Ct	Cn	CK	An	Mg
5a	64	32	64	>64	—	64	>64	64
5b	>64	>64	>64	>64	—	>64	>64	>64
5c	>64	>64	>64	>64	—	>64	>64	>64
5d	>64	>64	>64	>64	—	>64	>64	>64
5e	>64	>64	>64	>64	—	>64	>64	>64
5f	>64	>64	>64	>64	—	>64	>64	>64
Flu	4	16	0.5	2	4	64	>64	64

Abbreviations: Cp, *C.parapsilosis*; Cg, *C.glabrata*; Ca, *C.albicas*; Ct, *C.tropicalis*; Cn, *C.neoformans*; CK, *C.Krusei*; An, *A.niger*; Mg, *M.gypseum*; Flu, Fluconazole.
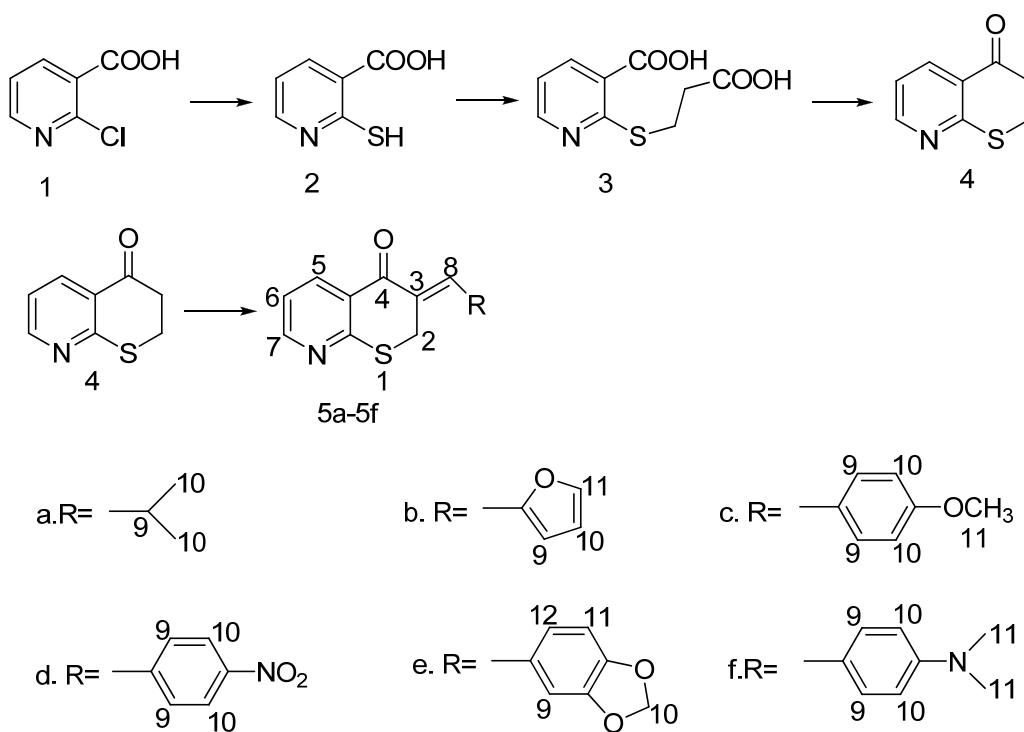
Figure 1. Synthesis route of target compounds

Quantification of Full Range Ethanol Concentrations by Using pH Sensor

Najah M. Mohammed Al-Mhanna (Corresponding author)

Institute of Bioprocess Engineering, Department of chemical and bioengineering

University of Erlangen-Nuernberg, Paul-Gordan Str. 3, 91052 Erlangen, Germany

Tel: 499-131-852-3017   E-mail: najah.mohammed@bvt.cbi.uni-erlangen.de,najah.almhanna@yahoo.de

Holger Huebner

Institute of Bioprocess Engineering, Department of chemical and bioengineering

University of Erlangen-Nuernberg, Paul-Gordan Str. 3, 91052 Erlangen, Germany

Tel: 499-131-852-3006   E-mail: holger.huebner@bvt.cbi.uni-erlangen.de

Abstract

A differential pH measurement device was used to achieve operation conditions of alcohol dehydrogenase reaction. Optimum operating conditions were temperature of 30°C, 10 µl of alcohol dehydrogenase enzyme volume (with a final activity of 563.75 units ml-1) per 50 µl of sample, NAD^+ concentration of 0.05 mM and 20 mM glycine-pyrophosphate buffer solution of pH 9.1. In this method a range of ethanol concentrations from 0 - 99,985 %, which means 0.000001714 - 17.14 M, were used. The maximum obtained change in pH, delta pH, was (-33) mPH. A calibration curve of logarithmic values of ethanol concentrations against change in pH for standard ethanol samples was done. Since this calibration curve is a linear with a correlation coefficient (R) of 0.998, this calibration curve can be used in quantification of ethanol concentration. End point of equilibrium concentrations of reactants and products of ethanol oxidation reaction was measured within spectrophotometer. The results indicated 100 seconds of process time is required to reach the end point for all ethanol standard samples. This required time was satisfied with results of measuring change in pH within differential pH analyzer system.

Keywords: Ethanol analysis, Oxidation enzymatic reaction, Ethanol quantification, Differential pH measurement device

1. Introduction

Ethanol is one of the most important substances with different application. For instance, bioethanol is rapidly rising its market share because of application of new technologies i.e. flexible fuel technology. However, for any application of ethanol it is necessary to detect and quantify ethanol with high accuracy. Therefore many methods were used to determine the concentration of ethanol in case when it is either a main product or a byproduct. The available techniques of ethanol detection include gas chromatography, electrochemical and enzymatic assay. The most important methods can be found in previous literatures (Goodman and Jacksonville, 1975; Bauer and Magers, 1985; Watanabe et al 1985; Laccheri, 1987; Moldowan, 1987; Stefan and Luc, 1997; Kempa, 2004; Hernandez, 2005; Olt, 2007; Beutler, 1984; Bernt and Gutman, 1974; Majki and Berkec, 1980).

Many difficulties and disadvantages are accompanied these methods. Some of them, especially the non-enzymatic methods, are complex and time consuming. They require previous separation process (distillation, pervarporation), expensive instrumentation and trained operators. Such disadvantages can be overcome by the use of enzymatic methods. In such enzymatic methods, most enzyme-catalyzed reactions can be followed by simple, widely available spectroscopic or electrochemical methods (Azevedo et al 2005).

Optical methods require an apparatus, such as a spectrophotometer. Moreover, such methods cannot be applied to turbid samples, such as blood or food samples. Furthermore, for carrying out the enzymatic reaction, a troublesome procedure involving dissolution of various reagents and distribution of the resulting solutions into reaction vessels in amounts specified beforehand is required, and the reagent solutions, such as prepared NAD^+ solution have poor storage stability. For these and other reasons, those methods are not suitable for general use. In order to overcome

these difficulties, the combined use of an enzymatic method and an electrochemical method for determining alcohols have been desired (Watanabe et al 1985).The optical density in such assay must be read at 340 nm, precluding the use of widely available and relatively inexpensive photoelectric colorimeters that do not allow precise determination in the UV range (Rodionov et al 2002). Additionally, in order to increase accuracy, there is a need to dilute the samples, due to the limitation of Lambert-Ber-Law's linearity.

Other spectroscopic methods (colorimetric, chemiluminescent and fluorescent methods) can be used to detect the production of H_2O_2 during the oxidation of ethanol. Most spectrometric methods are based on a bienzymatic system, comprising AOX and a peroxidase enzyme. The need for fast, cheap, sensitive and continuous analyzing methods with a high sample throughput led to application of immobilized enzyme reactors into flow system based analysis (Rodionov et al 2002).

Use of enzyme electrode or biosensor to detect changes in either oxygen concentration or H_2O_2 concentration in reactions, catalyzed by immobilized alcohol oxidase, suffers from some difficulties. Measurements based on oxygen have practical inconveniences and limitations. The response is low, and the dependency on oxygen can reduce the accuracy and reproducibility of the device. Moreover, because of a high background signal, the minimum detectable concentration is not very low. The detection of H_2O_2 is the most commonly used alternative to overcome these drawbacks. These techniques, however, usually suffer from low sensitivity (Rodionov et al 2002; Majki and Berkec, 1980).It has been reported that when ethanol was oxidized just in buffer by AOX, immobilized in 31 μl bioreactors, the conversion started to decrease after 3 h of continuous operation and after 4 h more than 80 % of the initial conversion were lost. Also one of the main factors that affect the performance of a biosensor is the enzyme immobilization procedure itself (Azevedo et al 2005).

There seems to be no fully satisfactory method for wide range ethanol concentrations quantification available yet. The above mentioned methods are not only limited for a certain range of ethanol concentration, but also they have difficulties or problems as mentioned above. Furthermore, some of them are expensive.

Therefore, the aim of this study was to develop a simple enzymatic method for detection and quantification of a full range of ethanol concentrations without diluting of samples. During this method a reduction in the cost of the ethanol assay will be done by using a small quantity of one enzyme and very low NAD^+ concentration. The measurements will be achieved by using a simple device, a differential pH analyzer system CL10.

The basic principle of this method is to assay ethanol sample by measuring pH variation produced in the medium during the enzymatic oxidation of ethanol to acetaldehyde. This reaction is achieved in presence of alcohol dehydrogenase enzyme. The following reaction represents reaction mechanism:

$$CH_3CH_2OH + NAD^+ \leftrightarrow CH_3CHO + NADH + H^+ \tag{1}$$

2. Experimental Procedure

2.1 Instruments

2.1.1 Differential pH analyzer system CL10 (Eurochem, Italy).

This device mainly consists of one mixing chamber, five peristaltic pumps and two capillary glass electrodes of pH sensor. This apparatus is controlled by using the CL10 Manger program. Figure 1 shows the schematic diagram of this apparatus. Details on the principle of its work, measurement and control can be found in different publications (Luzzana et al 1983; Rovida et al 1984; Luzzana et al 2001).

2.1.2 Spectrophotometer

In order observe the enzymatic reaction of ethanol oxidation to acetaldehyde; spectrophotometer type (Specord 205 from Analytic Jena AG, Germany) was used. A rise in absorbance, which is stoichiometric with amount of formed NADH, can be measured within spectrophotometer.

2.1.3 Curtipot program

A program was designed in order to execute pH and acid-base titration curves: Analysis and Simulation (Gutz, 2008).

2.2 Materials

β-nicotinamide-adeninedinucleotide (NAD+), Alcohol dehydrogenase enzyme ADH (EC 1.1.1.1), NADH were purchased from Sigma-Aldrich Company. High purity grade ethanol (99.985%) was used in preparing standard ethanol samples. These samples of different concentrations (0.00001714 - 17.14 M) were obtained by blending ethanol with bidest water of 0.005 microsiemens (μS). Buffer solution with pH of 9.1 at 25° C was composed from 0.02 M of glycine and 0.02 M of sodium pyrophosphate. Solution of alcohol dehydrogenase enzyme with a final

activity of (563.75 units/ml) was prepared by dissolving enzyme in a mixture of 25 % of glycerol/water. Magic N50 solution was prepared by blending 50 µl of 50 mM NAD^+ with 100 ml of the used buffer and 850 ml of pure water. This NAD^+ solution was called by authors Magic N50 solution because the effective of its low concentration in analyzing full ranges of ethanol concentrations. KIT assay (K-ETOH, Megazyme International Ireland Ltd, 2006) was used in order to make economic comparison.

2.3 Procedure

The differential pH device was set to a temperature of 30° C, a waiting time of 4 seconds and maximum reaction time (cycle time) of 300 seconds. First runs were done with buffer only as system check-up. For ethanol quantification, 50 µl of sample were well mixed with 10 µl of alcohol dehydrogenase enzyme to get 60 µl of enzyme-ethanol complex in glass tube. 250 µl of Magic N50 solution was injected into the mixing chamber which contained 1090 µl of buffer. After 40 seconds the measurement cycle was started and about 315 µl of this solution were then automatically distributed into electrodes 1 and 2. 50 µl of enzyme-ethanol complex solution were added to 775 µl of remaining solution in mixing chamber. The difference in pH of electrode 1 and electrode 2 was observed. The pH deviation is a result of ethanol conversion to acetaldehyde.

By the same procedure, differences in pH were measured for buffer solution devoid of sample and for buffer with only 250 µl of Magic N50. These measurements were done in order to see the substances effect on system measurement.

Additionally, the reaction was observed by measuring the absorption of solution caused by the consumption of NAD^+, or the formation of NADH during the conversion of ethanol to acetaldehyde within spectrophotometer at 340 nm of ultraviolet light.

3. Results and discussion

The differential pH analyzer system CL 10 was achieved detection of differences in pH between solutions. Thus, this device was used to measure change in pH, which is caused by enzymatic alcohol dehydrogenize reaction, for samples containing 0 – 99,985 % of alcohol.

After construction of delta pH value of buffer, the obtained delta pH values were in range from -0.891 mpH to -33.269 mpH for a full ethanol concentrations range of 0.00001714 M - 17.14 M respectively. These obtained delta pH values are sufficient to be used in quantifying any ethanol concentration in sample. The required time to reach constant delta pH value, end point, is inversely proportional to the ethanol concentration and it is not exceed 100 seconds. These results can be shown in figure 2.

The results indicated a nonlinear relationship between the alcohol concentration and the obtained change in pH as shown in figure 3. The non linearity was because of change in ethanol concentration which caused a change in the enzymatic reaction order from first to zero order. As approved, the order of reaction will be changed from first order reaction for low substrate concentration to zero order for high substrate concentration (Dunn et al 2003; Murry, 2003; Lee 2001). Such nonlinear plot can not be used as a calibration curve for ethanol determination.

Since ethanol concentration is stoichiometric to librated H^+ according to equation1 and pH of solution is a logarithmic function of $[H^+]$, a calibration curve was done by plotting the logarithmic value of ethanol concentrations against change in pH as shown in figure 4. This figure shows a linear relationship which can be used in quantification of ethanol concentration. Figure 4 consist of two parts a and b. Part a can be used for obtained change in pH up to -2.7 mpH while part b can be used for obtained change in pH starting from -3 up to -33 mpH as shown in figures (4.a & 4.b). The correlation coefficient of the linear regression of calibration curve, R, was 0.988 which means that the difference between predicted values and observed values of ethanol concentration is too low. This suggestive of a good model fit. In addition to that Chi square test was applied in order to evaluate the calibration curve precision. Degree of freedom, n-1, for seven standard samples of ethanol is 6. Therefore, for 6 degree of freedom and 0.05 probability, Chi critical table value is 12.592 (Snedecor and Corchran, 1989).The Chi square value was calculated 0.002 as shown in table 1. Since Chi square value is less than Chi critical table value, null hypothesis is accepted. That means there is no significant difference between the expected and observed values. In order to estimate the precision and the accuracy of the measurements, statistical evaluation for the results was made. In table 2, maximum standard deviation and maximum coefficient of variation for three replicates of measurements were 0.7 and 5.8% respectively. This low coefficient of variation range demonstrates that the measurements had little dispersion from the mean value which makes the results more precise and confidential.

To value the results, the oxidation reaction of ethanol to acetaldehyde was observed by measuring the change in absorption within spectrophotometer at 340 nm. The change in absorption of solution was caused by the formation of NADH from NAD^+ during the conversion of ethanol to acetaldehyde. The absorption values can be shown in

figures 5 and 6. The results showed that the time required reaching end point of the reactions for standard ethanol samples was not exceeding 100 seconds. These results are satisfied the results obtained by measuring change in pH within differential pH analyzer system.

Curtipot program was used to estimate the capacity of the buffer and to measure the equivalent end point of traditional titration curve. The result indicated that the buffer of 0.02 M of glycine and 0.02 M of pyrophosphate will have one equivalent point, although it contained polyprotic acids, when it was titrated with 0.1 M of NaOH. This means it actually behaves like monoprotic acid and it is stable for the measurements as shown in figure 7.

In order to see the stability of differential pH analyzer system CL10, the following two experiments have been done in absent of ethanol oxidation reaction. The changes in pH were measured for systems consist of either buffer only or by adding 250 µl of Magic N50 solution to the buffer. The results indicated that glycine-pyrophosphate buffer was suitable to be used for this system as there was no noise in measurement. Also there was no noticeable influence of the Magic N50 solution on the measurement. The ability of these preparations to influence the measurement can be seen in figure 8.

Additional experiments had been done for samples of ethanol concentrations from 0.1714 to 17.14 M. In these experiments Magic N50 solution was prepared from NAD^+ solution of 100mM. The obtained delta pH values were increased by a factor of 1.6 in comparison with those using 50 mM of NAD^+ as shown in figure 9. The general behavior was still nonlinear. This indicates that there is no reason to increase the amount of NAD^+ for this ethanol essay as that will lead to increase the essay costs and will be on expensive of time too. The set up of differential pH analyzer device CL10 has a limit of 300 seconds of maximum reaction time. However, Magic N50 solution of 100 mM NAD^+ or more could be used if somebody wants a wide range of delta pH for his own standard calibration curve.

4. Economic aspect

In order to evaluate the economic aspect of this new method, a comparison with KIT method (K-ETOH) of Megazyme International Ireland Ltd was done. The results of this economic study (calculation is not showed) indicated that assaying 373 samples by using KIT method require using 1865mg NAD^+, 5.6mg alcohol dehydrogenase (ADH) enzyme and 154.4mg aldehyde dehydrogenase (AL-DH) enzyme. However, applying the present method for assaying same number of samples utilizes 155mg NAD^+ and 4.7mg alcohol dehydrogenase enzyme. Aldehyde dehydrogenase enzyme was not used in the present method.

The above calculation demonstrates the following:

1. There is a factor of 12 in the number of samples that can be assayed for the same amount of NAD^+, which means a noticeable cost reduction.

2. In addition to that, KIT assay uses two enzymes, alcohol dehydrogenase ADH and aldehyde dehydrogenase AL-DH, while we just have used one enzyme, alcohol dehydrogenase. It could be seen that the amount of alcohol dehydrogenase enzyme for our method is slightly less than of that used in KIT method.

Additional cost by applying Kit assay is to be considered due to the use of NADH. The use of KIT assay also needs an additional calibration curve of NADH absorbent because of the necessity of accurate quantification within spectrophotometer.

5. Conclusions

It is possible to detect full range of ethanol concentration with lowering the cost. The recent method is a development for enzymatic methods by reduction the number of required enzymes to one. Also there is no need to dilute samples during the analysis. This will decrease the errors which are happened by users often. Using logarithmic values of ethanol concentrations in making calibration curve bring new approach in concentration quantification by using change in pH. This work offers the basis to start studies of full range concentrations quantification within differential pH measurement sensor device. Therefore, work in optimization is recommended.

Acknowledgements

References

Azevedo, A. M., Miguel, F., Joaquin, M.S. & Fonseca, L. P. (2005). Ethanol biosensors based on alcohol oxidase. *Biosensors and Bioelectronics*, 21, 235-247.

Bauer, R. & Magers, T. (1985). *Enzymatic ethanol test*. European patent 0164008, A2; B1.

Bernt, E. & Gutman, I. (1974). Determination with alcohol dehydrogenase and NAD. In: *Methods in enzymatic Analysis*. 3 rd edn, Edited by H. U. Bergmeyer, Academic press, New York: Vol. 3, pp. 1499-1502.

Beutler, H. (1984). In *Methods of Enzymatic Analysis*. 3rd edition , VCH, Weinheim-Deerfield Beach, FL-Basel,6, 598-606.

Dunn, L.J., Heinzle, E., Ingham, J. & Prenosil, J.E. (2003). *Biological reaction engineering*. Second edition, Wiley-Vch, pp. 68-72.

Goodman, D. & Jacksonville, F. (1975). *Method for determining the ethanol content of alcoholic beverages*. US patent 3896659.

Gutz, I. G. R. (2010). Curtipot program, Version 3.5.4, pH and Acid-Base titration curves: *Analysis and Simulation* [Online]. Available: http://www2.iq.usp.br/docente/gutz/Curtipot_.html

Hernandez, F. (2005). *Devices and methods for measuring ethanol content in blood*. European patent 1873528 A1.

Kempa, E. (2004). *Probe device for measuring ethanol concentrations in an aqueous solution*. European patent 1439383 A.

K-ETOH, Ethanol assay procedure. (2006, 11/06). Megazyme International Ireland Ltd.

Laccheri, E. (1987). Reagent for the enzymatic determination of primary c1-c4 alcohols and related method. European patent 0240964 A1.

Lee, J. (2001). *Biochemical engineering*.© by James M.Lee,Department of chemical engineering, Washington State University, Pullman ,WA 99164-2710, Chapter 2.pp. 19-69.

Luzzana, M., Agnellini D.& Cremonesi, P. (2001). Enzymatic reaction for the determination of sugars in food samples using the differential pH technique. *Journal of Analyst*, 126, 2149-2152.

Luuzzana, M., Dossi, G., Mosca, A., Granelli, A., Berger, D., Rovida, M., Ripamonti, M., Musetti, A.& Rossi-Bernardi, L. (1983). Measurement of glucose in plasma by a differential pH technique. *Clinical Chemistry*, 29, No.1, 80-85.

Majki, N. & Berkec, I. (1980). Spectrophometric determination of ethanol by an enzymatic method with 2,2 –azino-di-(3-ethylbenz-thiazoline, 6-sulfonate). *Anal.Chim.Acta.*, 115, 401-405.

Moldowan, M. J. (1987). *Composition and method for ethanol determination*. US patent 4642286.

Murray, R. (2003). *Harpers illustrated biochemistry.* 26 edition, McGraw-Hill Companies, Chapter 8, pp. 64-66.

Olt, R. (2007). *Method and means for the enzymatic determination of ethanol*. German patent, WO2007134683.

Rodionov, Yu.V., Keppen, O.I. & Sukhacheva. (2002). A photometric assay for ethanol. *Applied Biochemistry. & Microbiology*, 38, No.4, 395-396.

Rovida, E., Luzzana, M. & Ripamonti, M. (1984). The determination of ethanol in whole blood by differential pH measurements, *Scand.J.Clin.Lab.Invest*, 44, 617-621.

Snedecor, G. & Cochran, W. (1989). *Statistical Methods*, Eighth Edition, Iowa State University Press.

Stefan, S. & Luc, T. (1997). *Spectroscopic method*. US patent 5679955.

Watanabe, M., Suzuki, T. & Kageyama, M. (1985). *Testing material for detecting alcohols*. European patent 0154409.

Table 1. Statistical evaluation of the calibration curve: Chi square worksheet direction

Ethanol sample (mM)	Mean value of obtained change in pH(mpH)	Observed log[ethanol] (O)	Expected log[ethanol] (E)	(O-E)^2/E
17147	33.269	4.234	4.226	0.008
1714.7	24.519	3.234	3.289	-0.055
171.47	13.640	2.233	2.124	0.110
17.147	5.876	1.233	1.292	-0.059
1.715	2.479	0.069	0.094	-0.026
0.172	1.623	-0.931	-0.983	0.052
0.017	0.892	-1.931	-1.904	-0.028
				$\sum$ (O-E)^2/E = 0.002 =Chi square value

Mean values were multiplied by (-1) as the measurements were in (–mpH).

Table 2. Statistical evaluation of the measurements

Ethanol sample (mM)	17147	1714.7	171.47	17.147	1.715	0.172	0.017
Mean value of obtained change in pH(mpH)	33.269	24.519	13.64	5.876	2.479	1.623	0.892
Number of replicates	3	3	3	3	3	3	3
Standard deviation	0.377	0.116	0.703	0.247	0.098	0.079	0.052
Coefficient of variation %	1.1	0.05	5.2	4.2	3.9	4.9	5.8

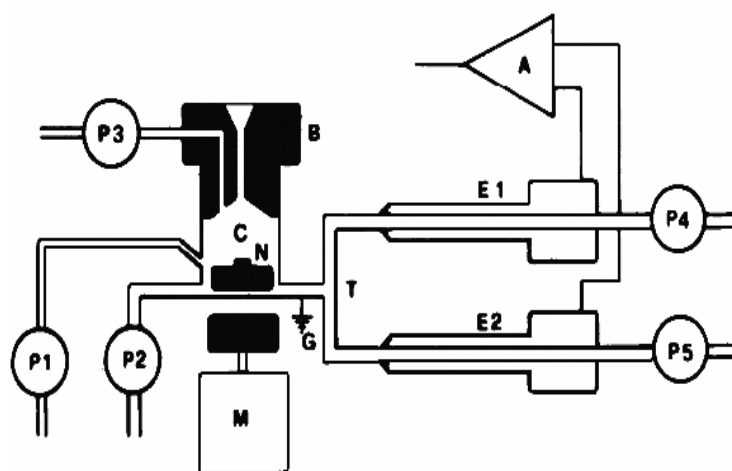Mean values were multiplied by (-1) as the measurements were in (–mpH).

Figure 1. Schematic diagram of the differential pH analyzer system CL10.P1 to P5,peristaltic pumps; C, mixing chamber ;M, stirring motor ; N, magnetic stirrer ; E1 and E2 , class capillary electrodes pH sensors ; A, differential amplifier (Luzzana et al 1983).
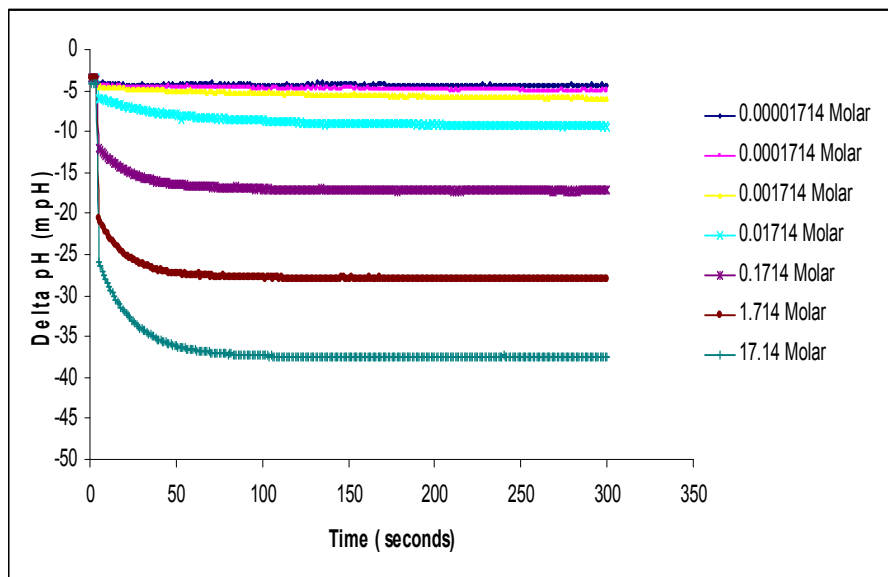
Figure 2. Delta pH (mpH) measured with time within differential pH analyzer system CL10 for different ethanol concentrations samples by using Magic N50 solution of 50mM NAD^+. Each point is an average value of three measuring values
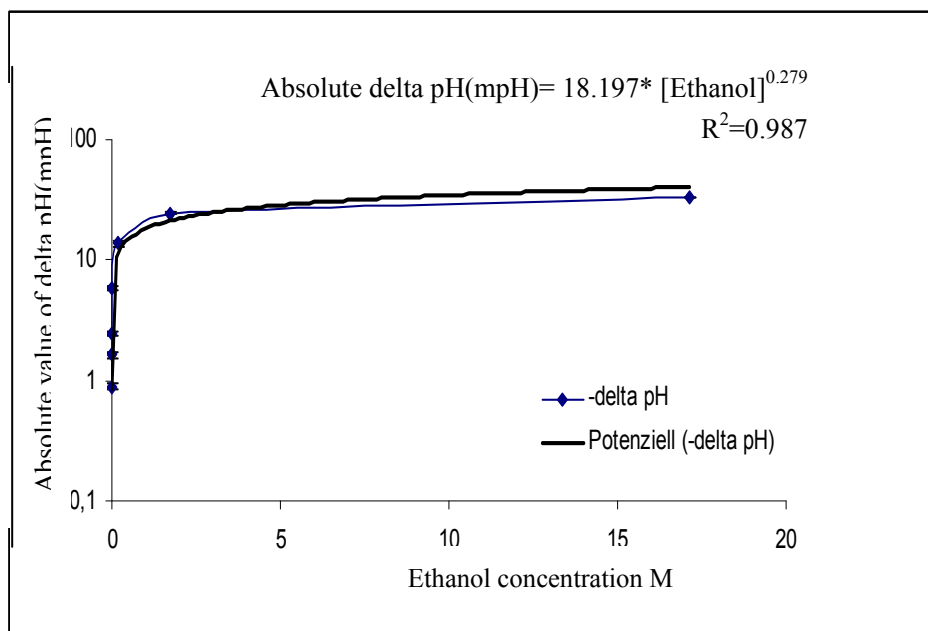

Figure 3. Delta pH (mpH) measured against different ethanol concentrations by Differential pH analyzer system CL10 .Each point is an average value of three measuring values. The absolute values were obtained by multiplying the values of change in pH by (-1)
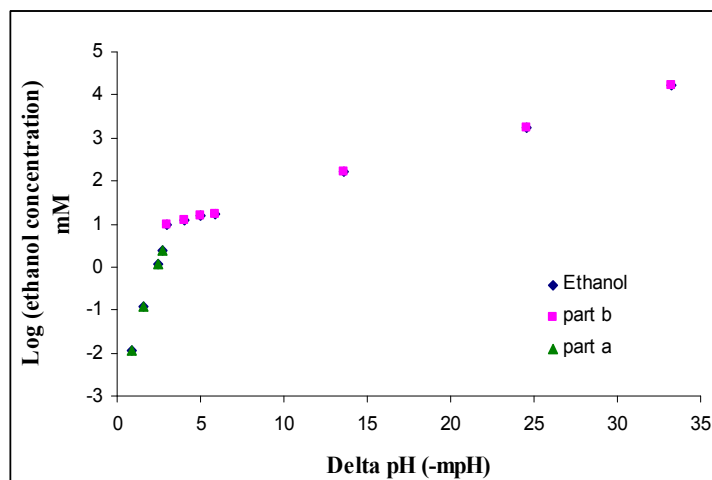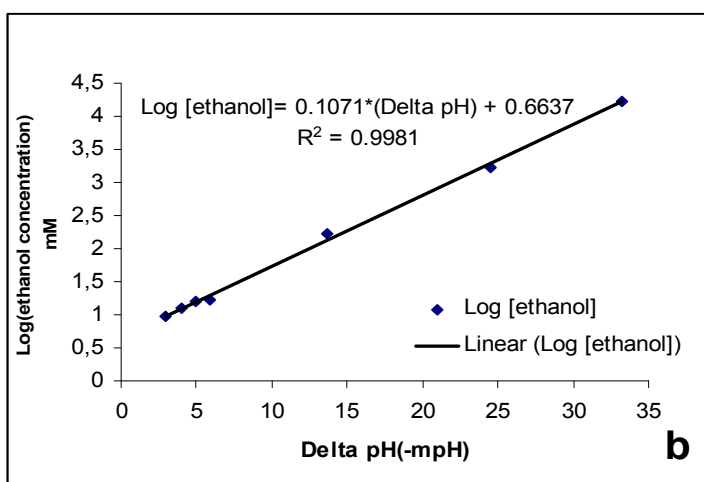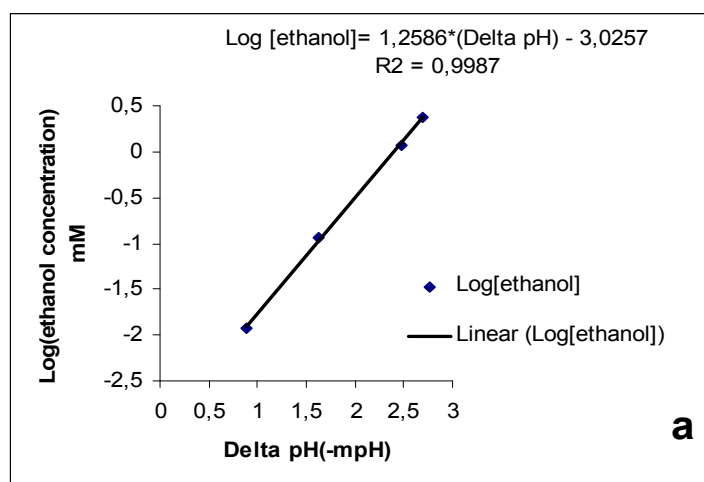
Figure 4. Calibration curves between logarithmic values of ethanol concentrations against change in pH. Linear relationship was obtained. Change in pH is absolute value which was obtained by multiply the obtained change in pH, delta pH, by (-1)

Figures (4.a and 4.b) Calibration curves between logarithmic values of ethanol concentrations against change in pH. Change in pH is absolute value which was obtained by multiply the obtained change in pH, delta pH, by (-1).

(a) can be used for obtained change in pH up to -2.7 mpH

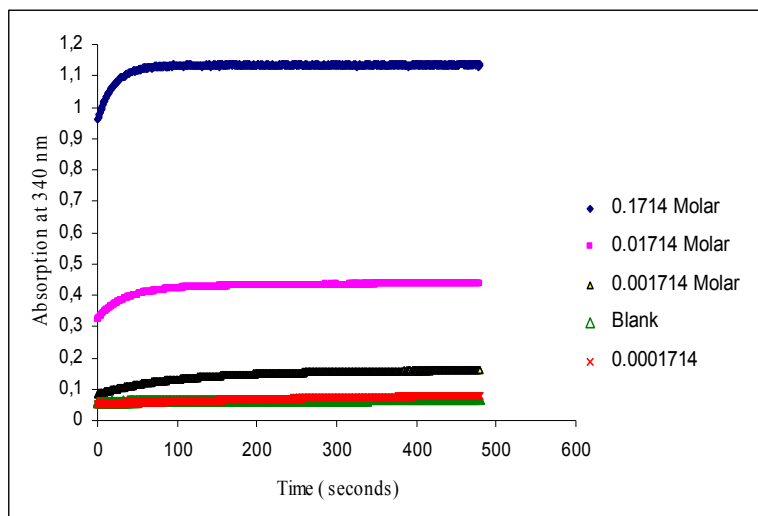(b) can be used for obtained change in pH starting from -3 mpH.

Figure 5. Absorption of formed NADH against time within spectrophotometer during Enzymatic Oxidation of different ethanol concentrations
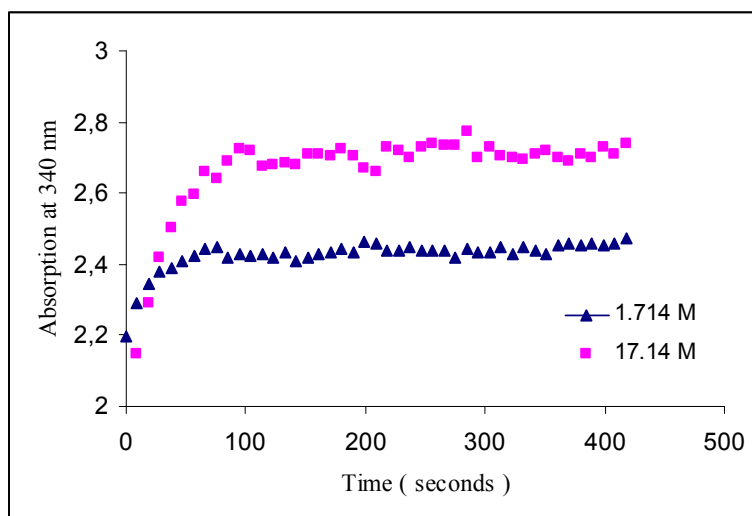

Figure 6. Absorption of formed NADH against time within spectrophotometer during Enzymatic Oxidation of different ethanol concentrations
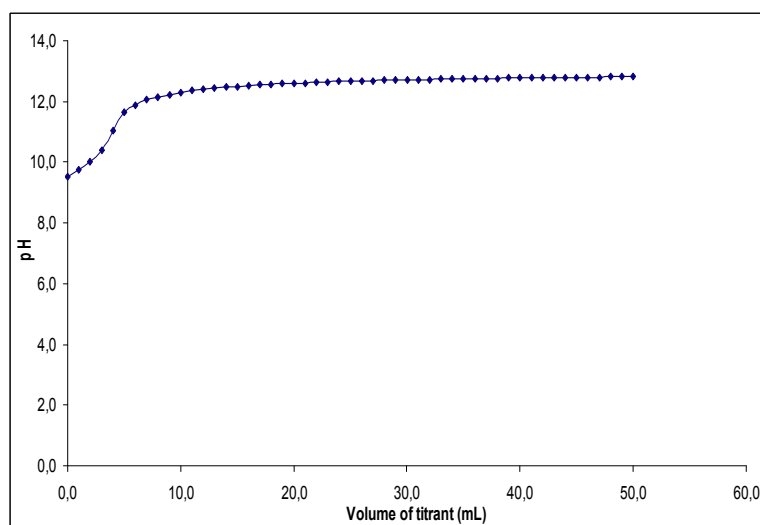

Figure 7. Titration of pyrophosphate-glycine buffer of (20mL, 0.02mol/L) with (0.1 mol/L NaOH)
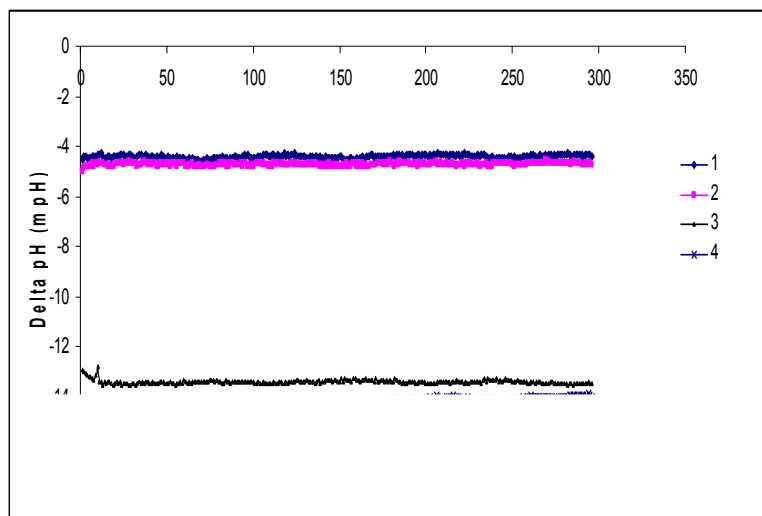
Figure 8. Observation of stability of differential pH analyzer system CL10.This measurements was devoid from ethanol oxidation reaction by using:

1. only buffer
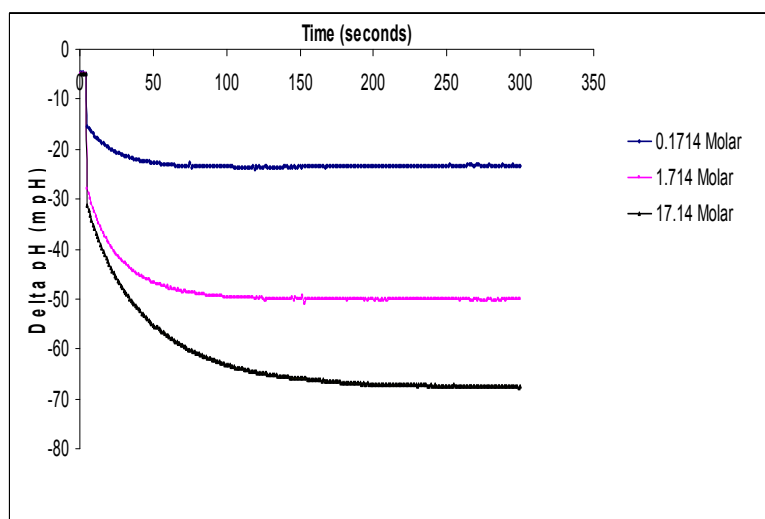
2. adding 250µl Magic N50 solution to the buffer

Figure 9. Delta pH (mpH) measured with time within differential pH analyzer system CL10 for three different ethanol concentrations samples by using Magic N50 solution of 100mM NAD+

Metal Fractionation in Soil Profiles in Umutu Oil Field, Northwest Niger Delta Nigeria

Edwin O. Adaikpoh

Department of Geology, Delta State University

Abraka. PMB 1. Abraka. Delta State, Nigeria

Tel: 234-803-727-4021   E-mail: adaikpoh_edwino@yahoo.com

Abstract

Exploitation of petroleum began recently in Umutu area, a part of the prolific Niger Delta Oil province, Nigeria. Soil profiles at six locations in this area were investigated to determine the current status of Cr, Cu, Cd, Co, Ni, Zn, Pb, Mn and Fe, and their bioavailability, in order to have reference data for future monitoring of their bioaccumulation. The procedure used sequential extraction technique. Except for the high contents of Cu, Cd, Co, Zn, and Pb in Site B (an auto-mobile mechanic waste dumpsite), mean metal levels in mgkg^{-1} for Umutu soils are Cd (0.65-1.83), Cu (2.20- 6.30), Pb (4.06-5.90), Cr (7.10-15.60), Ni (1.10-2.00), Zn (33.00- 45.00), Co (0.01- 0.06), Fe (1126.22-2955.87) and Mn (1.83-18.81). Sequential extraction shows that the bioavailability of Cr except for Site E (all horizons) and Site D (0-15cm) are high. That of Fe is also high at depths of 0-15cm. Monitoring programme is herein suggested.

Keywords: Bioavailability, Metal fractionation, Niger Delta, Sequential extraction, Umutu oil field

1. Introduction

Elements pathway of moving from rocks breakdown to plants, then to animals and humans illustrates the natural form of elements availability and therefore the natural control of human health by the solid geology of the environment. In the process of exploitation and consumption of nature's resources, man has over the years modified the availability of elements to humans (sometimes with some health implications) by introducing higher than normal concentrations of elements in the soils of certain localities where industrial, agricultural and other human activities are high. The accumulation can be through the air and/or through spills.

Anthropogenic contamination sources of trace metals in soils include industrial waste, domestic waste and urban infiltration as well as inputs from vehicle exhausts, use of pesticides, burning of fossil fuels, open air incineration of waste and petroleum activities (Enger and Smith, 2006). The most important sources of trace metals include paper mills, organic chemicals, alkalis, petroleum refining, asbestos products, cements, basic steel works, fertilizers, motor vehicles, textile mill products and leather industries.

Most trace elements are essential for the healthy development of plants, animals and humans but they can be toxic and harmful if available in certain concentrations. Accumulation of lead for example causes damage to the brain and kidney while cadmium causes kidney and lung damage as well as high blood pressure (Enger and Smith, 2006). Hence it is advisable to monitor the levels of these trace elements in the soils in areas of high population density and high human activities.

However, knowledge of the total contents of heavy metals present in the soil provides limited information about their behaviour and bioavailability (Iwegbue, 2007). Heavy metals are associated with various soil components in many ways and these determine their reactivity, mobility and bioavailability (Kabala and Singh, 2001, Alloway, 1995). Alloway (1995) described the mechanisms of adsorption and desorption and stated that the processes controlling the availability of both naturally occurring and contaminant (trace and major) elements to plants and their leaching down the soil profile to the groundwater are those which influence the sorption and desorption of these elements within the soil.

Developed countries have a long history of assessing and monitoring the levels of toxic trace elements in their environments. Apart from few recent studies in the urban cities, the status of trace elements in developing countries and especially those areas with the bulk of agricultural activities is rather unknown. This study presents the status of metals and their bioavailability in soils of a rural agricultural area in a developing country (Nigeria). Oil exploitation (with gas being flared) has just started in this area of study and the population is fast increasing. This paper documents the present status of Cr, Cu, Cd, Co, Ni, Zn, Pb, Mn and Fe, and provides reference data for future monitoring of their bioaccumulation.

1.1 Study Area

Umutu Field is one of Shell's concessions within the Niger Delta. It lies between latitude 5°35' and 5°40' north; and longitude 6°10' and 6°20' east (Shell Petroleum Development Company's Grids 418000-428000N and 205000-212000E). It lies within the Niger Delta basin, stretching through Umuaja and Umutu (Figure 1). Accessibility in the area is a major road connecting the oil cities in the Niger Delta with the central regions of Nigeria, and few access routes developed during drilling operation by SPDC. The region is an important wetlands zone referred to as inland area of the coast. The physiography, drainage, climate and vegetation are well described (Orubu, 1981; Etu-Efeotor and Odigi, 1983; Kaizer and Adaikpoh, 2005).

2. Method of Study

2.1 Sampling Method

Samples were collected from six sites: Umutu outskirt (A), Umutu automobile mechanic waste dumpsite (B), Railway profile (C), Obinomba farmlands (D), Akoko farmlands (E) and Obi-Ebele farmlands (F).

At least five random samples were used as composite sample for any sampling point. Sample points were 10m apart within 100 x 100 m of each of the sites. At each sampling point, samples were taken from 0-15 cm, 15-30 cm and 30-50 cm depths. Soils collected from same depths were combined to form the representative sample for that horizon, for that site.

The samples were air-dried. Part of each was sieved for grain-size analysis while the other part was ground to pass through 2 mm sieve and used for chemical analysis.

2.2 Analysis Procedure

The procedure for the chemical analyses is as described by Iwebue, 2007. This procedure separates the metals into fractions as follows: F1= Water soluble metals which are reversible, physically sorbed, and water extractable; F2 = Exchangeable metals which are extractable with $MgCl_2$ at pH of 7; F3 = Specifically sorbed and carbonate bound metals extracted with NH_4OAc at pH of 5; F4 = Metals specifically sorbed on iron and manganese oxides extractable with hydroxylamine chloride; F5 = Metals strongly complexed by organic matter and extractable with H_2O_2 in 1 mol l^{-1} HNO_3 and F6 = Residual metals extractable with HF and aqua regia.

Two grams of soil was placed in 50 ml polycarbonate centrifuge tube and subjected to the following extraction procedure:

Water soluble fraction F1; the metals in the soil was extracted with 20 ml of deionised water (DI) for 2 h

Exchangeable fraction F2; the metal from F1 residue were extracted with 20 ml of 1 mol l^{-1} $MgCl_2$, pH of 7 for 1 h.

Carbonate- bound fraction F3; the metals from F2 residue were extracted with 20 ml of 1 mol l^{-1}NH_4Ac at pH of 5 for 5 h.

Fe-Mn oxides-bound fraction F4; the metals from F3 residue were extracted with 20 ml 0.04 mol l^{-1}$NH_2OH.HCl$ in 25% (v/v) HOAc at 96^{0}C with occasional agitation.

Organic-bound fraction F5; the metals from F4 residue were extracted wit 15 ml 30% H_2O_2 at pH of 2 (adjusted with HNO_3) for 5.5 h (water bath, 85°C). After cooling, 5 ml of 3.2 mol l-1 HH_4OAC in 20% HNO_3 was added and shaken for 30 min before final dilution to 20ml with DI.

Residual fraction F6; the metals from F5 residue was digested using a HF-HCl/HNO_3 procedure.

All solid phases (except for F6) were washed with 10 ml of DI water before further extraction. The washes were collected and analysed with supernatant from the previous fraction. After each extraction, the supernatant was separated by centrifugation for 30 min at 7500 x g. To verify the sum of the metals recovered in the sequential extraction steps, separate total concentrations of the metal were determined on the subsample after an HF/aqua regia digestion.

Quality control was assured by the use of triplicates, standard reference materials (light sand soil CRM 142R) and the procedural blanks. For all elements analysed, the coefficient of variation on the triplicates analyses of the soil samples are less than 5%. The total concentrations of the metals in the supernatants from each step were analysed with Atomic Absorption spectrophotometer (Varian Techtron a 975). The recovery of trace metals in the sequential extraction steps was within 100 ±10 %.

3. Result and Discussion

3.1 Result

Soils within the area are characterized by yellowish red colour, 20 ± 5.5 % clay, 42 ± 3.8 % silt and 45 ± 12.2 % sand. Other physicochemical characteristics are documented by Kaizer, and Osakwe (2007) as organic matter 8 ± 2.2, pH 5.38 ±1.56 and exchangeable cation 16.60 ± 2.24 Cmol kg^{-1}

3.1.1 Total metal concentration

The total metal contents and the sum of metal contents from sequential extraction are presented for each horizon and each site in Table 1. Generally, metal contents decrease with depth. Site B has anomalously high concentrations of all the metals except for Cr, Ni and Fe. This could be due to effluents from dumps from auto-mobile mechanic waste. A similar high concentration for some of these elements was reported (Iwebue, 2007) for mechanic dumpsites in Port Harcourt, Nigeria. The concentration for other areas studied are : Cd (0.65-1.83 mgkg^{-1}); Cu (2.20-6.30 mgkg^{-1}); Pb (4.06-5.90 mgkg^{-1}); Cr (7.10-15.60 mgkg^{-1}); Ni (1.10-2.00 mgkg^{-1}); Zn (33.00-45.00 mgkg^{-1}); Co (0.01-0.06 mgkg^{-1}); Fe (1126.22-2955.87 mgkg^{-1}) and Mn (1.83-18.81 mgkg^{-1}). These are within the range for agricultural soils (Lindsay, 1979; Kabata-Pendias and Pendias, 1992; Alloway, 1995; Adriano, 2001).

Metal partition in soil

Results from speciation studies are illustrated in Figures 2-10, and descriptive trend is as thus;

Water soluble fraction (F1)

This fraction represents those metals soluble in water. Metal contents that fractionate in this phase are highly mobile and are readily available to plants and organisms. For the different sites, mean fractional content of the metals are : Cr (0.36-2.55 % except in site B with Cr of 11 %); Zn (1.27-6.71 %); Cu (0.62-2.55 %); Cd (6.07-7.71 %); Co (5.56-16.67 %); Fe (6.57-11.73); Mn (1.47-10.15 %); Pb (1.11-3.99 %); while Ni (0.75% only occurs in Site B). Generally, all metals content of this phase decrease with depth and below the top horizon (0-15ft).

Exchangeable fraction (F2)

Metal contents that fractionate in this phase have high mobility. Changes in major cationic composition may cause a release due to ionic exchange. They are also readily available to plants and organisms. Besides the mean fractional contents of Co of 9.09 % and 4.76 % for Sites A and B respectively, Co was not partitioned in this geochemical phase. Mean fractional contents of other metals for the sites in this geochemical phase are Cr (0.62-3.96 %); Ni (0.00-1.69 %); Zn (4.05-13.50 %); Cu (2.21-6.31 %); Cd (7.96-21.72 %); Fe (9.73-15.15); Mn (6.29-11.85 %); Pb (2.36-6.00 %). These values are higher than those of water soluble fraction.

The fractionation of lead and cadmium in F1 and F2 phases where elements are readily available to plants and organisms may call for concern because according to Alloyway (2005), cadmium and lead are the elements in contaminated soils that are considered to constitute the widest possible health risk to humans through the plant uptake-dietary route.

Carbonate-bound fraction (F3)

Metal contents that fractionate in this phase have medium mobility. They are not readily available to plants. Mean fractional contents of metals for the sites in this geochemical phase are Cr (4.82-9.42 %); Ni (0.13-6.42 %); Zn (7.90-18.02 %); Cu (3.00-7.74 %); Cd (8.10-20.72 %); Fe (11.74-21.37); Mn (6.21-18.04 %); Pb (6.21-17.73%). Co did not partition in this fraction except for Site A where 9.09 % of the total content for that site occurs.

Fe-Mn oxides-bound fraction (F4)

Mean fractional contents of metals for the sites in this geochemical phase are Cr (20.59-38.67 %); Ni (11.88-23.21 %); Zn (29.59-35.33 %); Cu (10.03-22.99 %); Cd (15.29-22.37 %); Co (16.67-62.50 %); Fe (12.95-32.66); Mn (16.42-31.06 %); Pb (27.09-41.57 %). Except for Site E and F, the highest percentages of Cr in the soil occur in this phase. Relatively high percentages (only in some cases second to organic-bound phase and / or residual phase) of Fe and Mn occur in this phase. Metal contents that fractionate in this phase have medium mobility, and changes in redox condition may cause a release. However, some of these metals precipitate if sulphide minerals present are insoluble.

Organic-bound fraction (F5)

Metal contents that fractionate in this phase have medium mobility and with time, decomposition/ oxidation of organic matter matter will occur. Mean fractional contents of metals for the sites in this geochemical phase are Cr (15.74-32.43 %); Ni (2.03-5.26 %); Zn (8.42-12.78 %); Cu (20.77- 47.53 %); Cd (2.55-11.05 %); Co (25.00 - 77.78 %); Fe (28.27- 44.39); Mn (21.33-35.91 %); Pb (3.41-11.11 %). Relatively high percentages of Cr occur in this phase.

Residual fraction (F6)

Metal contents that fractionate in this phase are fixed in the crystal lattice, have low mobility and can only be available after weathering or decomposition of the crystals.

Mean fractional contents of metals for the sites in this geochemical phase are Cr (19.81-54.29 %); Ni (66.42-83.89 %); Zn (23.34-40.61 %); Cu (30.10-53.55 %); Cd (25.60 - 53.50 %); Co (0.00-50.00 %); Fe (26.01-42.64 %); Mn (20.14-30.99 %); Pb (36.74-48.19 %). Ni, Cu, Zn, Cd and Pb have their highest percentages in this phase.

3.1.2 Mobility factors of metals

The mobility factor was calculated according to Narwal et al., 1999 and Kabala and Singh, 2001 as

(F1+F2+F3) X 100% / (F1+F2+F3+F4+F5+F6)

The mobility factors for sites and depths are shown in Table 2.

Except for Site E (all horizons) and Site D (0-15cm), the mobility factors of Cd are high in Umutu soils. That of Fe is also high at depth 0-15cm. High values of mobility factor for a heavy metal is an evidence of relative high mobility and bio-avaiability (Kabala and Singh, 2001). Mobility factors decrease with depth for all metals and sites except for Cr (Site C and F), Cu (Site A), Cd (Site A), Pb (Site C), Mn (Site A, C, D, E and F) and Co (all sites and all horizons).

3.2 Discussion

Site B is an auto-mobile mechanic waste dumpsite and its soil has high metal contents which may have been due to the waste. This should be noted in any future consideration of these results as reports from a baseline study. The Cd content for the Fe-Mn oxide phase is relatively high. Similar results have been reported by Horsefall and Spiff (2005), and Osakwe and Egharevba (2008). This fraction changes with variation in redox conditions becoming more soluble under reducing conditions and less soluble under oxidizing ones. Therefore, an increase in reducing conditions of the soil could increase metal mobility with increased toxicity. The contamination risk of the metals is in the order of Cu < Ni < Cd < Fe < Mn < Cr < Zn < Pb < Co. Relatively significant amount of Cu (20.77- 47.53%) occurs in the organic fraction. High Cu in organic fractions of soil extracts have been reported by Osakwe and Egharevba (2008), Tessier *et al*. (1980), Ma and Rao (1997) and Ryan *et al*. (2002). This is expected because of the high values for formation constant of Cu-organic complexes.

From the trends of fractional distribution (Figures 2-10) only Mn, Cu and Fe show similar tends of Residual > Organic complexed > Oxide extractable > Carbonate bound > Exchangeable > Water soluble. This trend is similar to reports of Iwebue (2007).

The highest bioavailable fractions of the metals Cr (Site B), Ni and Cu (site C), Fe and Pb (Site F) occur in depths of 0-15cm (Table 1). Cd and Co have their highest bioavailable fractions in depths of 15 - 30cm in site B and A respectively. Only Mn has its highest bioavailable fraction in depths of 30- 45cm (Site E). This shows that these metals are most mobile at the surface horizons. Similar results have been reported by Iwegbue (2005), *Kuo et al*. (1983), and Kabala and Sigh (2005). These Authors emphasized the predominance of heavy metal accumulation in the surface horizons and the lack of metal redistribution in soil profile. The 0.01- 0.06 mgkg^{-1} metal content of Co (apart from the waste dumpsite) is low and Co is not bioavailable above the depth of 30cm in Sites D, E, and F. Fe has high metal content (1126.22-2955.87 mgkg^{-1}) and also is highly bioavailable with mobility factors ranging from 25.84 to 33.69.

4. Conclusion

Agricultural areas can be prone to heavy metal contamination when industrial and mining activities are introduced. The consequences of bioaccumulation of these heavy metals are obvious. This paper documents the current status of Cr, Cu, Cd, Co, Ni, Zn, Pb, Mn and Fe as well as their bioavailability, and provides reference data for future monitoring of their bioaccumulation in soils of Umutu Oil Field, Niger Delta Nigeria. As oil flaring unfortunately continues in Nigeria, future studies should be those that measure changes of metal contents, physico-chemical parameters, soil organic content, pH, PAHs, conductivity, temperature, etc. as well as assessing the chronic and acute effects of the contaminants on the terrestrial ecosystem. Sampling should be done on a seasonal basis of 4 months in wet season and 4 months in dry season. Sampling points should be radial with progressively increasing radii of 1, 50, 100, 150 and 200 kilometers from the flaring point. Samples should be collected from depths of 15cm (where most of the plants' roots are).

References

Adriano, D. C. (2001). *Trace Elements in terrestrial Environments* (2nd ed.), New York: Springer-Verlag.

Alloway, B. J. (Ed.) (1995). *Heavy metals in Soils*. (2nd ed.) London: Blackie Academic and Professional.

Enger, E. D. & Smith, B. F. (2002). *Environmental Science*. (8th ed.). McGraw-Hill.

Etu-Efeotor, J. O., & Odigi, M. I. (1983). Water supply problems in Eastern Niger Delta: *Nigeria Journal of Mining Geology*, 20, 183-193.

Horsefall, M.. & Spiff, A. (2005). Speciation and bioavailability of heavy metals in sediments in Diobu River, Port Harcourt , Nigeria. *European Journal of Sciecientific research*, (3). 20-36.

Iwebue, C. M. A. (2007). Metal fractionation in soil profiles at automobile mechanic waste dumps. *Waste management and Research*, 25, 585-593.

Kabala, C., & Singh, B. R. (2001). Fractionation and mobility of copper, lead and zinc in soil profiles in the vicinity of a copper smelter. *Journal of Environmental Quality*, 30, 485-495.

Kabata-Pendias, A. & Pendias, I. I. (1992). *Trace elements in soils and plants*. (2nd edn.). Boca Ration Fl.: CRC Press

Kaizer, A. N., & Osakwe S A. (2007). Water chemistry in the Upper and Middle Ethiope River, Southwest Nigeria. *Nigerian Journal of Science and Environment*, 6, 146-157.

Kaizer, A.N., & Adaikpoh E.O. (2005). Some geotechnical properties of soils around Umutu and environs, southwest Nigeria. *Journal of Applied Science & Environmental. Management*, 10, (4) 41-45.

Kuo, S., Heilman, P. E. & Baker, A. S. (1983). Distribution and forms of copper, zinc, cadmium, iron and manganese in soils near a copper smelter. *Journal of Soil Science*, 135. 101 – 109.

Lindsay, W. L. (1979). *Chemical equilibrian in soils*. New York: John Wiley and Sons.

Ma, L. Q. & Rao, G. N. (1997). Chemical fractionation of Cd, Cu, Ni and Zn contaminated soils. *Journal of Environmental Quality*, 26. 259-264.

Narwal, R. P., Singh, B. R., & Salbu, B. (1999). Association of cadmium, zinc, copper and nickel with components in naturally heavy metal rich soils studied by parallel and sequential extraction. *Communication in Soil Science and Plant Analysis*. 30. 1209-1230.

Orubu, A. O. (1981). *A Short Geography of Bendel State*. Ibadan: University Press, (Chapter 3).

Osakwe, S. A., & Egharevba, F. (2008). Sequential fractionation of cadmium, copper, lead and chromium in soils around municipal solid waste dumps in Agbor, Nigeria. *Journal of chemical Society of Nigeria*, 33(2). 139 – 147.

Ryan, P. C., Wall, A. J., Hiller, S., & Clerk, L. (2002). Insights into sequential chemical extraction procedure for quantitative XRD: a study of trace metal partitioning in soils and sediments related to frog malformation. *Chemical Geology*, 184. 337-357.

Tessier, A., Campbell P. G. C., & Bisson, M. (1980). Trace metal speciation in the Yamaska and St. Francis River (Quebec). *Canadian Journal of Earth Science*, 17, 90-105.

Table 1. Total metals contents in soils of Umutu area and sum of their sequential extracts

Total metal content contents (mgkg^{-1}).										
	Depth (Cm)	Cd	Cu	Pb	Cr	Ni	Zn	Co	Fe	Mn
SITE A	0-15	1.43	3.22	4.38	12.30	1.50	45.00	0.05	2114.38	15.12
	15-30	1.41	3.26	5.26	10.60	1.30	42.30	0.04	2955.87	15.68
	30-50+	0.95	3.34	5.56	7.60	1.30	42.30	0.05	1806.66	14.33
SITE B	0-15	34.00	386.12	496.85	14.60	1.90	430.95	0.14	2813.44	14.76
	15-30	41.22	362.77	466.61	8.60	1.80	462.86	0.14	2098.11	13.00
	30-50+	36.75	320.34	400.12	8.20	1.80	431.43	0.17	2629.60	8.92
SITE C	0-15	1.83	6.30	5.90	10.70	2.00	46.00	0.05	2053.17	16.01
	15-30	1.28	6.10	5.63	10.80	1.90	43.20	0.06	2099.85	13.38
	30-50+	1.62	5.56	5.30	11.00	1.80	42.00	0.05	2006.28	10.22
SITE D	0-15	1.04	3.52	5.30	9.20	1.50	41.60	0.03	1931.21	17.98
	15-30	0.94	3.34	4.98	8.20	1.40	40.80	0.03	2183.58	17.27
	30-50+	0.83	3.06	4.73	7.10	1.20	40.80	0.03	1967.22	13.55
SITE E	0-15	0.83	2.75	5.21	15.20	1.40	38.20	0.03	2399.88	18.81
	15-30	0.82	3.56	4.73	15.60	1.30	34.40	0.02	2381.46	15.15
	30-50+	0.65	2.20	4.06	14.60	1.10	33.00	0.05	1555.93	15.00
SITE F	0-15	1.40	3.50	5.15	12.50	1.70	42.50	0.01	1300.47	4.06
	15-30	0.96	3.18	4.22	8.30	1.60	40.50	0.03	1231.48	1.83
	30-50+	0.93	3.06	4.07	7.90	1.40	39.40	0.06	1126.22	2.08
Sum of fractions F1 –F6 (mgkg^{-1}).										
		Cd	Cu	Pb	Cr	Ni	Zn	Co	Fe	Mn
SITE A	0-15	1.24	3.36	3.21	13.10	1.50	44.00	0.06	2105.62	16.67
	15-30	1.49	3.10	4.88	9.40	1.20	41.00	0.03	2961.56	15.13
	30-50+	0.98	3.06	5.41	8.20	1.40	40.40	0.06	1799.52	11.04
SITE B	0-15	32.55	380.54	500.17	14.50	1.90	422.61	0.13	2808.47	19.03
	15-30	38.64	361.43	460.07	8.30	1.70	450.62	0.14	3008.80	19.04
	30-50+	32.66	322.00	404.43	7.90	1.70	438.22	0.15	2625.41	10.98
SITE C	0-15	1.95	6.24	5.24	10.20	2.00	44.30	0.04	2041.79	12.16
	15-30	1.44	5.90	5.55	10.00	2.00	41.80	0.08	2098.89	11.79
	30-50+	1.62	5.30	5.23	10.60	1.90	40.50	0.05	2014.33	10.06
SITE D	0-15	1.14	3.58	5.15	8.90	1.60	41.40	0.02	1929.37	20.91
	15-30	1.00	3.20	4.63	8.20	1.40	41.20	0.03	2166.57	20.53
	30-50+	0.98	2.88	4.60	7.00	1.30	40.20	0.04	1971.65	18.54
	0-15	0.84	2.60	5.06	14.30	1.50	37.00	0.03	2395.27	21.19
	15-30	0.88	2.54	4.69	15.00	1.30	33.60	0.01	2363.52	11.73
SITE E	30-50+	0.75	2.18	3.77	14.80	1.00	31.50	0.05	1575.66	9.61
	0-15	1.32	3.54	5.10	12.50	1.80	42.80	0.01	1297.46	5.73
	15-30	1.06	3.16	4.28	8.50	1.60	40.10	0.03	1213.93	2.89
SITE F	30-50+	0.98	3.00	4.12	7.90	1.60	39.50	0.05	1114.10	5.08

Table 2. Mobility factor for metals in soils of Umutu and environs, northwest Nigeria

	Cr			Ni			Cd		
Depth (Cm)	**0-15**	**15-30**	**30-45**	**0-15**	**15-30**	**30-45**	**0-15**	**15-30**	**30-45**
Site									
A	8.47	11.91	6.71	1.34	0.00	0.00	42.98	39.6	26.53
B	26.92	12.65	7.59	9.47	8.24	5.88	54.36	54.84	39.16
C	11.86	11.90	11.04	10.00	2.00	1.05	43.37	41.67	43.21
D	10.11	16.08	5.14	3.75	3.57	8.46	33.33	33.66	18.18
E	8.39	8.53	10.2	9.33	6.92	1.00	28.92	26.14	16.00
F	8.40	8.47	10.25	3.89	9.38	3.75	43.18	37.74	40.40
	Cu			Zn			Fe		
Depth(Cm)	**0-15**	**15-30**	**30-45**	**0-15**	**15-30**	**30-45**	**0-15**	**15-30**	**30-45**
Site									
A	9.85	9.97	4.92	25.91	21.81	12.72	31.68	33.69	30.90
B	14.17	8.33	10.00	30.91	20.00	16.36	24.50	31.04	25.14
C	16.53	11.68	8.3	38.2	38.18	31.93	28.34	29.41	30.63
D	15.08	8.15	5.21	24.54	17.28	20.00	21.38	32.63	27.88
E	13.46	4.72	7.76	26.35	25.45	14.54	32.99	25.84	19.69
F	12.68	5.99	1.67	25.46	7.28	9.09	40.86	30.28	27.66
	Co			Mn			Pb		
Depth(Cm)	0-15	15-30	30-45	0-15	15-30	30-45	0-15	15-30	30-45
Site									
A	16.67	33.33	16.67	24.36	26.57	25.63	16.20	12.30	9.24
B	12.9	14.29	20.00	30.74	28.73	28.23	22.45	21.43	22.45
C	0.00	12.50	20.00	24.18	26.55	33.20	25.00	25.59	23.33
D	0.00	0.00	25.00	26.06	29.08	28.43	18.45	18.36	16.3
E	0.00	0.00	20.00	30.11	32.98	39.13	20.36	16.20	6.10
F	0.00	0.00	20.00	26.35	33.56	33.46	30.59	25.47	11.17
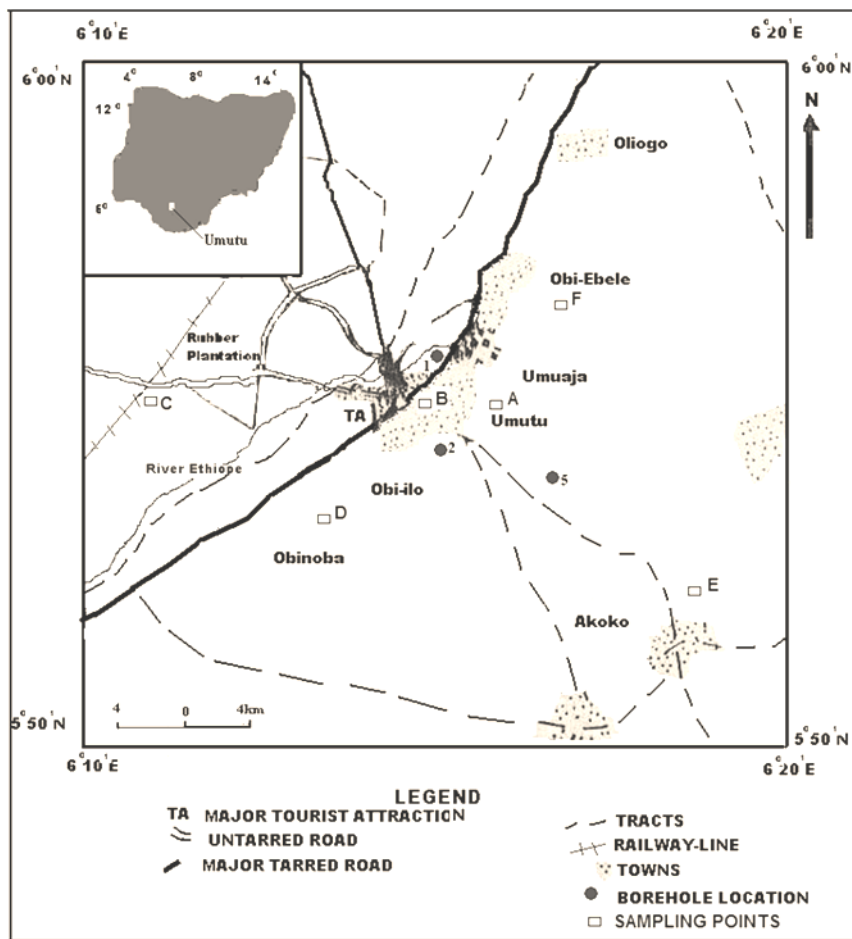
Figure 1. Map of Umutu Area
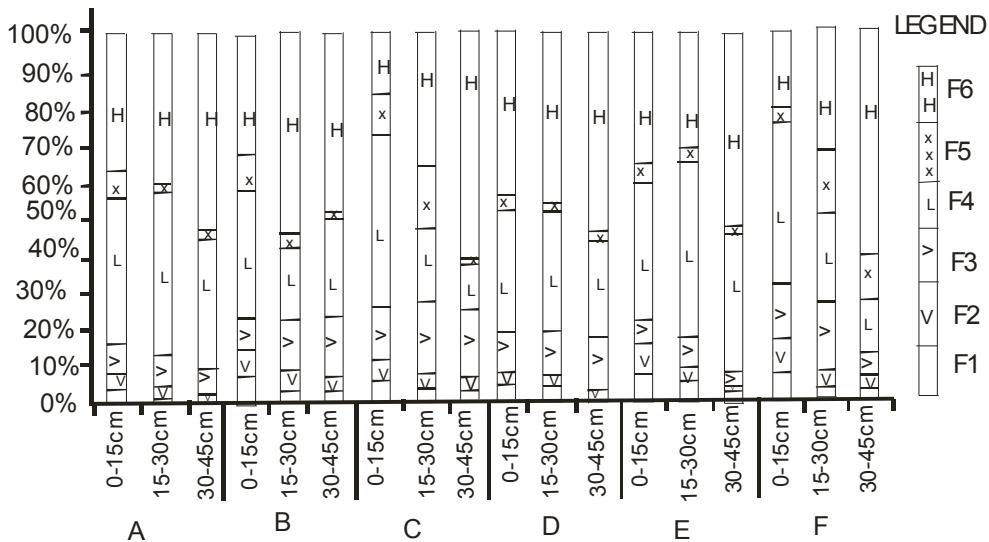
Figure 2. Percentage of lead in various geochemical phases of the soil from sequential extraction
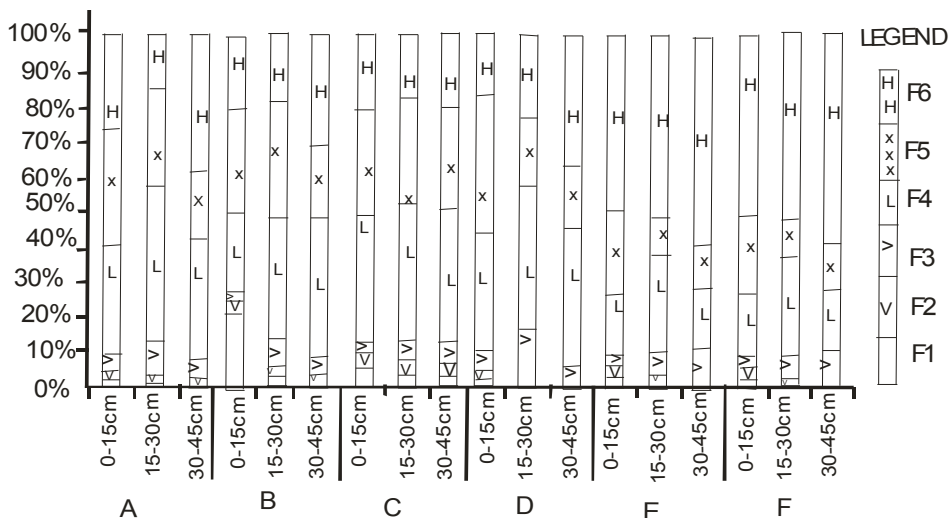
Figure 3. Percentage of chromium in various geochemical phases of the soil sequential extraction
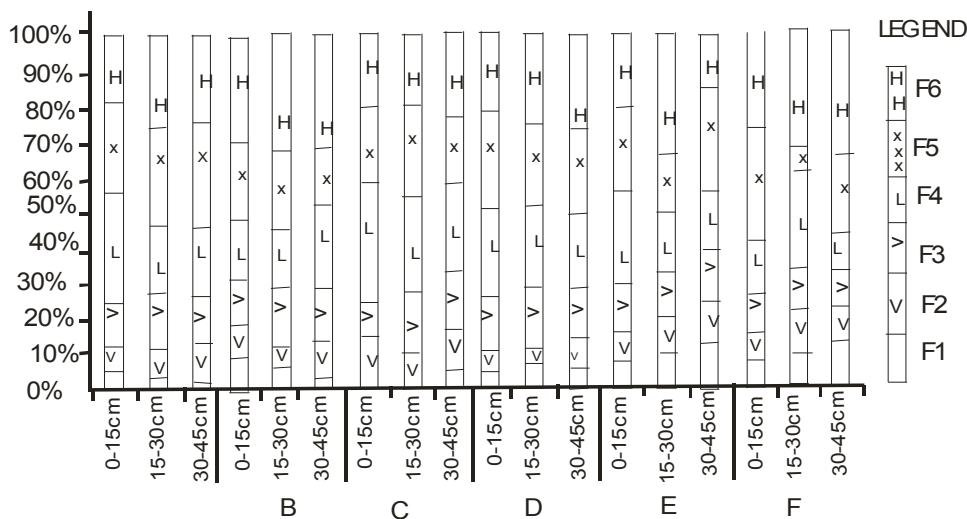

Figure 4. Percentage of manganese in various geochemical phases of the soil from sequential extraction
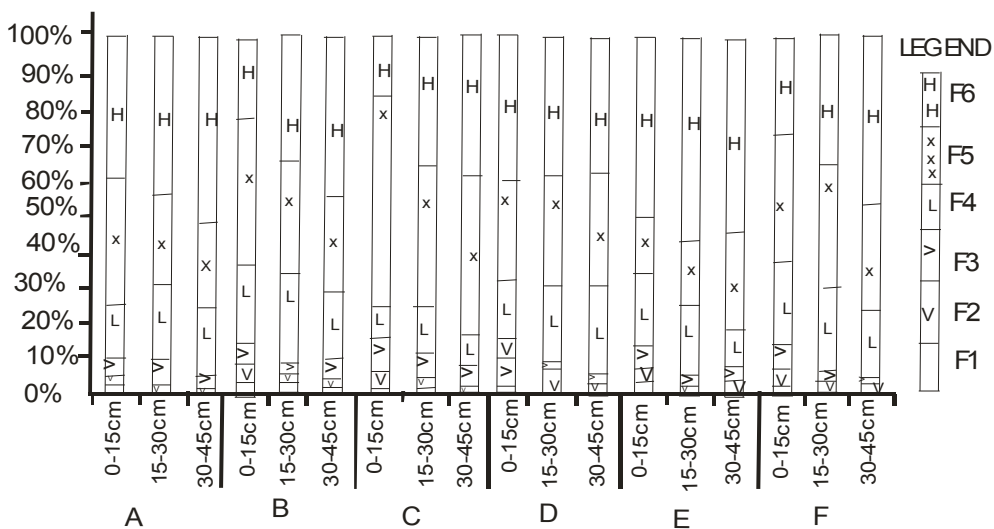

Figure 5. Percentage of copper in various geochemical phases of the soil from sequential extraction
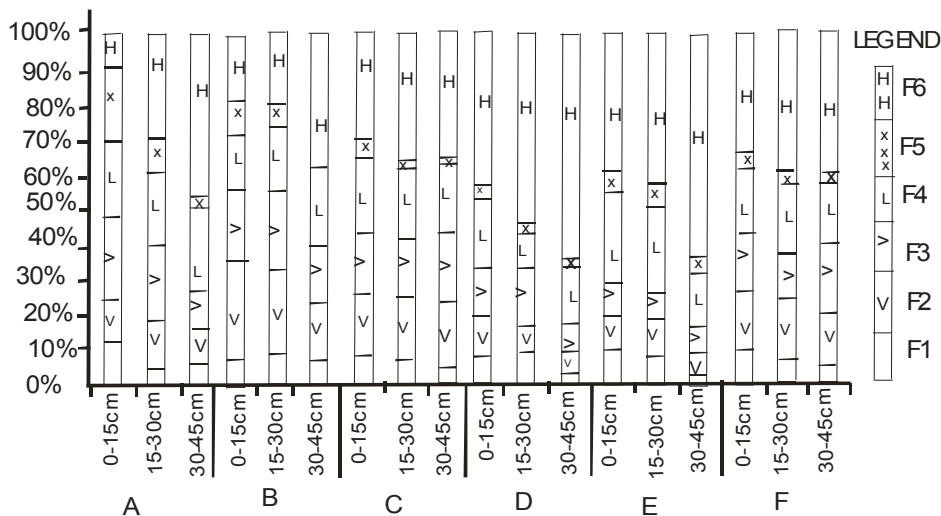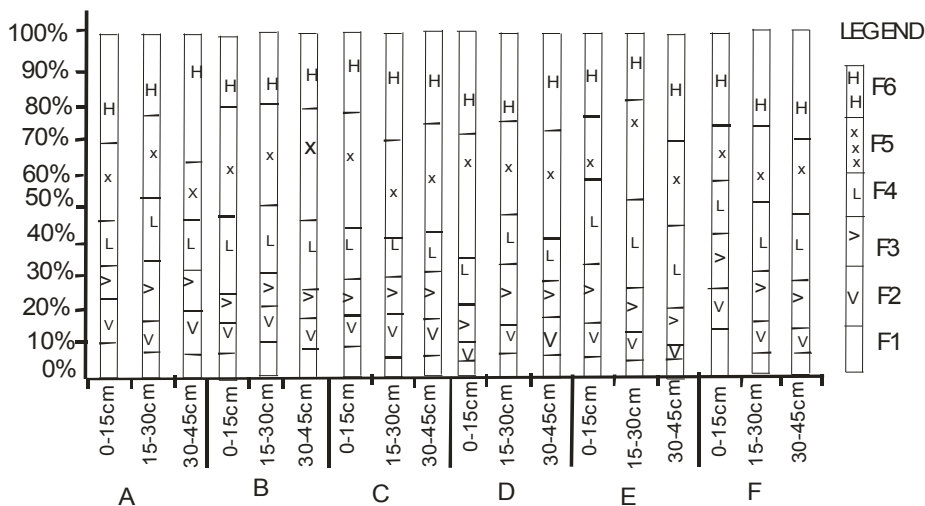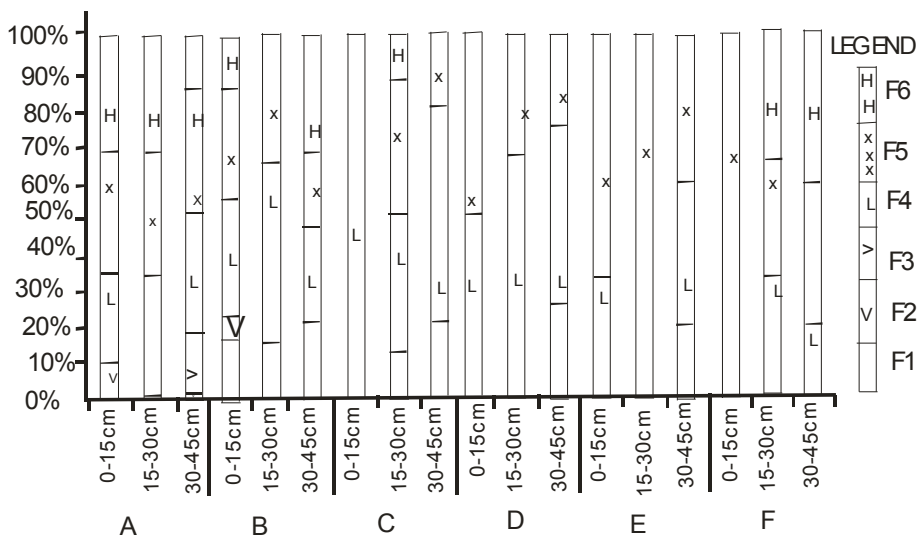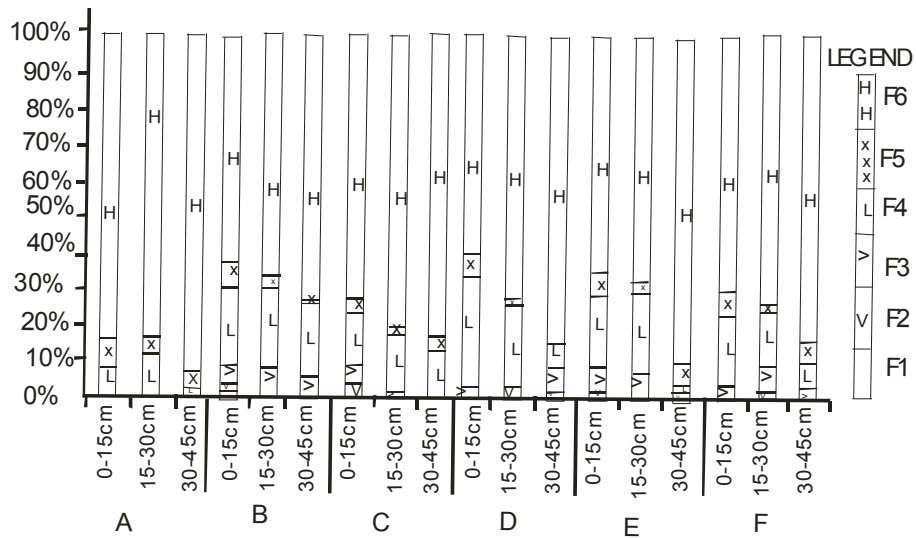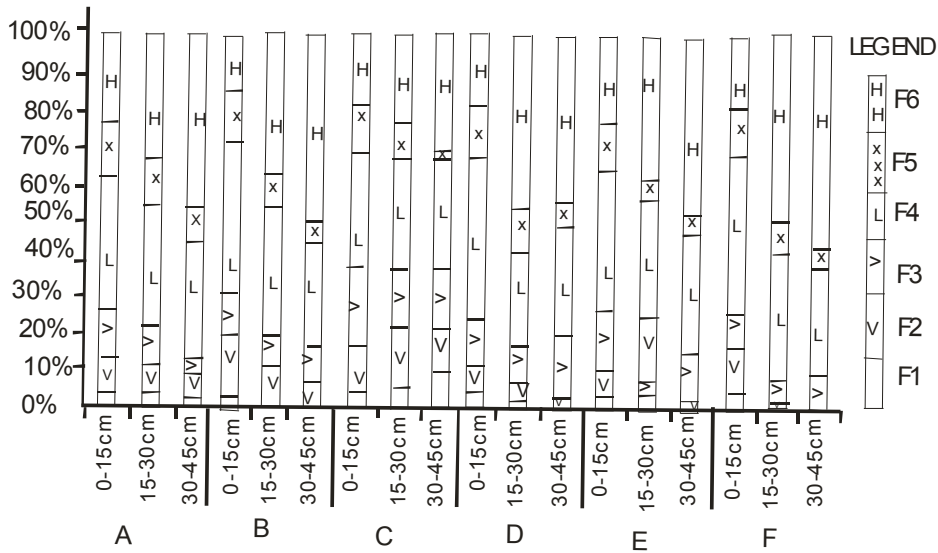
Figure 6. Percentage of cadmium in various geochemical phases of the soil sequential extraction

Figure 7. Percentage of iron in various geochemical phases of the soil sequential extraction

Figure 8. Percentage of cobalt in various geochemical phases of the soil sequential extraction

Figure 9. Percentage of nickel in various geochemical phases of the soil from sequential extraction

Figure 10. Percentage of zinc in various geochemical phases of the soil from sequential extraction

Effects of Tween-80 on the Dissolution Properties of Daidzein Solid Dispersion *in Vitro*

Lijuan Hu, Na Zhang (Corresponding author) & Gengliang Yang

Hebei Province Key Laboratory of Quality Analysis and Control

College of Pharmaceutical Sciences, Hebei University, Baoding 071000, China

Tel: 86-312-597-1107   E-mail: nzhang@hbu.edu.cn

Jingyu Zhang

Baoding Food and Drug Administration, Baoding 071000, China

Tel: 86-312-335-3188   E-mail: 363188478@qq.com

Abstract

Objective Solid dispersions of daidzein (DZ) were prepared using tween-80 as the surfactant to improve its dissolution and solubility. **Methods** Using tween-80 as the surfactant and polyethylene glycol (PEG)-10000 as the carrier, solid dispersions of DZ were prepared by solvent method. Infrared spectroscopy (IR) and X-ray diffraction spectroscopy were applied to determine the status of DZ in carriers. **Results** When appropriate amount of Tween-80 was added into the solid dispersion, the dissolution of DZ could be improved obviously. The data of IR showed the absence of well-defined drug-polymer interactions. The data of X-ray diffraction showed that the drug might exist in the form of amorphism or molecule in solid dispersions. **Conclusion** Appropriate amount of Tween-80 could increase the dissolution rate of DZ.

Keywords: Daidzein, PEG, Tween-80, Solid dispersion, Dissolution rate, IR, X-ray diffraction

Daidzein, extracted from Traditional Chinese Medicine (Guo, 1996, PP. 146-148), was synthesized in 1972 by China. DZ could expand coronary artery, reduce myocardial oxygen consumption, increase the coronary and cerebral blood flow, and ameliorate the symptoms of patients with hypertension such as headache, dizziness, nuchal rigid pain and so on obviously. It could significantly alleviate angina pectoris, possessed anti-arrhythmia and antioxidant properties, enhanced the body's immune system, and had pharmacological effects of lowering blood sugar. In clinical practice, it was principally applied as target medicine for angina pectoris, hypertension and cardiovascular disease (He, 2000, PP. 58-59). In addition, DZ could also improve the menopausal syndrome, strengthen calcium absorption, and had preventive and therapeutic effects on neurological sensory deafness and sudden deafness. However, due to its strong liposolubility, slow dissolution rate, poorly oral absorption and low bioavailability, the pharmacological effects were interfered. In recent years, , there has been a trend in the studies of solid dispersion using a single carrier or mixed carriers with surfactant, and meanwhile, the surfactant could promote the bioavailability of drug in gastrointestinal tract (Zhou, 2003, PP. 42-44). In the present paper, DZ solid dispersion was prepared by solvent method, using polyethylene glycol (PEG) as carrier, and surfactant Tween-80 was added during the preparation process. Effects of Tween-80 on the dissolution of DZ in PEG solid dispersion were investigated.

1. Apparatus and materials

1.1 Instrument

T6 UV spectrophotometer (Beijing Persee General Instrument Co., Ltd.); ZRS-8G Intelligent Dissolution Tester (Tianjin Tiandatianfa Technology Co., Ltd.); RE-2000A rotary evaporator (Gongyi Yuhua Instrument Co., Ltd.); DZF-6050 vacuum oven (Gongyi Yuhua Instrument Co., Ltd.); 100 mesh standard inspection sieve (pore size 0.15 mm, Shangyu Huafeng Hardware Instrument Co., Ltd. in Zhejiang); FT-IR 8400S Fourier Transform Infrared Spectrometer (Shimadzu, Japan); Y-2000 X-ray diffractometer (Dandong Ray Instruments Co., Ltd.).

1.2 Materials

DZ (Yangling Dongke Madison Pharmaceutical Co., Ltd.); PEG (relative molecular weight of 10,000, Tianjin Kermel Chemical Reagent Development Corporation); anhydrous ethanol (Chongqing Chemical Reagent Factory);

Tween-80 (Tianjin Donghua Reagents Factory); potassium dihydrogen phosphate (Beijing Chemical Factory); sodium hydroxide (Tianjin North Tianyi Chemical Reagent Factory.)

2. Experimental Methods

2.1 Determination of detection wavelength

Appropriate amount of DZ, PEG and Tween-80 were weighed accurately and added to pH 6.8 phosphate buffer and anhydrous ethanol 9:1 (v /v) mixed solutions. Solutions with proper concentration were prepared, and the same mixed solvent as blank. They were scanned at the wavelength from 200 to 400 nm. As seen from Figure 1, DZ had two absorption peaks at the wavelength of 248 and 305 nm while PEG and Tween-80 had none. Because PEG and Tween-80 both had absorption at the wavelength of 248 nm, and had none at 305 nm, 305 nm was selected as detection wavelength. Figure 1 shows the UV spectra of DZ, PEG and Tween-80.

2.2 The calibration curve

DZ was recrystallized with anhydrous ethanol. Accurately weighted DZ (Dried to constant weight) 0.025 g was added into a 100 ml volumetric flask, and dissolved and diluted with anhydrous ethanol to the scale as stock solution. 0.1, 0.1, 0.2, 0.5, 0.7 and 1.0 ml of stock solution were added to 50, 25, 25, 25, 25 and 25 ml volumetric flask respectively, and anhydrous ethanol were supplemented to the flaks until 5, 2.5, 2.5, 2.5, 2.5 and 2.5 ml, respectively. Finally, pH 6.8 phosphate buffer solution was added to the final scale, respectively. Absorption at the wavelength of 305 nm was determined respectively. Linear regression was undertaken using drug concentration (C) and absorbance (A), and DZ calibration curve, $Y = 23.58834X-0.01941$ (r = 0.9999, linear range of 0.5~10 mg/L, n=6) was obtained.

2.3 Preparation of solid dispersions

Three groups of 1:2, 1:5 and 1:8 (w/w) of the DZ and PEG-10000 solid dispersion were prepared. Each group had three samples. One sample among each group was added to rotary evaporator with 50 mL anhydrous ethanol, heated by water bath to dissolve. The resultant solution was evaporated till constant weight, and frozen for 24 h. The obtained solid dispersion was placed into a vacuum oven for 12 h, grinded, and then undertaken 100 mesh sieve for further investigation. Solid dispersion preparation of the rest two samples among the three groups used the same proportion of DZ and PEG, with 0.4g and 0.8g Tween-80 respectively, and 50 mL anhydrous ethanol. The following steps were the same as the first group, and the solid dispersion of Tween-80 and DZ with surfactant was prepared.

2.4 Determination of dissolution

Dissolution medium was 1000 mL pH 6.8 phosphate buffer at the temperature of 37±0.5 ℃ with the paddling speed of 100 rpm. 5 mL solution was sampled at accurate time of 5, 10, 20, 40, 60, 90 and 120 min, and meanwhile the same volume of phosphate buffer was supplemented at the same temperature. The sample was rapidly filtered through a 0.45 μm microporous membrane. Proper amount of filtrate was selected to determine the absorbance at the wavelength of 305 nm. Drug concentration was obtained from the calibration curve, and then the drug dissolution rate was calculated. Pharmaceutical raw material and solid dispersions were all weighted according to the equivalence to 10 mg of DZ raw material. Sample of each group was replicated 6 times. Dissolution curves of drug were undertaken regression analysis using SPSS 13.0 software, and the equations with the largest R^2 were selected as the fitting equation of each dissolution curve.

2.5 FTIR spectra

FTIR spectra of DZ raw material, PEG and DZ PEG solid dispersion were investigated using potassium bromide tablet method. 1~2 mg sample was grinded into powders with an agate mortar, and 100~200 mg grinded and dried KBr was added. They were mixed evenly, prepared into transparent tablets with the thickness of 1 mm and the diameter of 10 mm by pressure machine and tested. Sample dosage and tablet thickness was considered to be good when FTIR spectrum with the baseline of over 80 % and the maximum absorption peak of about 20 % transmittance was obtained.

2.6 X-ray diffraction

DZ, PEG and solid dispersions were undertaken X-ray diffraction analysis respectively. Test condition: Cu target; pressure, 30 kV; pressure: 30 kV; tube current: 20 mA; scanning speed: 2 °/min; scan range: 5 °~90 °.

3. Results and discussion

3.1 Dissolution test in vitro

Figure 2 describes the dissolution profiles of pure DZ, and its solid dispersions. The dissolution rate of DZ solid dispersion with or without Tween-80 increased with the decreasing ratio of drug to PEG, and the drug dissolution rates were classified in this order: DZ<(drug: PEG, W/W) 1:2 <(drug: PEG, W/W) 1:5 <(drug: PEG, W/W) 1:8,

which might be attributed to the facts that the increment of carrier impeded the contact among drug molecule, and reduced the possibility of forming large particle size drug crystal. Consequently, the practical size of drug crystal decreased, or more drugs were dispersed in the form of molecule, and thus the drug dissolution rate increased.

After adding Tween-80, drug dissolution rate with relative more PEG content was classified in the order: (drug: PEG: Tween-80, W/W/W) 1:5:0.8 <(drug: PEG, W/W) 1:5 <(drug: PEG: Tween-80, W/W/W) 1:5:0.4; (drug: PEG: Tween-80, W/W/W) 1:8:0.8 <(drug: PEG: Tween-80, W/W/W) 1:8:0.4 <(drug: PEG, W/W) 1:8; X-ray diffraction data also proved this point (Figure 4), which indicated that Tween-80 could enhance the dissolution of DZ. But Tween-80 content shouldn't be too high. Too much Tween-80 could defer the dissolution of DZ, which might be ascribed to the facts that Tween-80 was sticky liquid, and when its content was relatively high, DZ was dried slowly, which afford enough time for the crystal to grow, made the drug failed to completely disperse in the carrier in the form of amorphism, and thus affected drug dissolution; Proper Tween-80 dosage not only couldn't affect the drying time of solid dispersion, but also could lower the surface tension during evaporating, in order to make the drug to distribute evenly and prevent further aggregation of drug particles. Drug dissolution rate with relative less PEG content was classified in the order: (drug: PEG, W/W) 1:2< (drug: PEG: Tween-80, W/W/W) 1:2:0.8 < (drug: PEG: Tween-80, W/W/W) 1:2:0.4, and the dissolution with Tween-80 increased. However, too much addition had less effects compared to the less amount of Tween-80, possibly because the dissolution at the ratio of 1:2 was low by itself. Effects of Tween-80 on the solubilization of DZ tended to be more conspicuous, and because Tween-80 was sticky solution, too much addition wouldn't be obvious compared to the less addition. Table 1 summarizes the results of Fitting equations of PEG solid dispersions and DZ dissolution curves. Drug dissolution curves of solid dispersion with or without Tween-80 at each ratio accorded with cubic curve, quadric curve and power function curve.

3.2 FTIR spectra

Figure 3 shows the FTIR spectra of different samples. Each solid disperse was basically similar in infrared spectra, and the spectra of solid disperses were very similar to that of PEG. PEG accounted for the larger proportion, and therefore each peak position of PEG covered that of drug. Hydrogen bond and other bonding interaction between DZ and PEG had not been found. All results indicated that there was no chemical change between DZ and PEG, but only physical interaction.

3.3 X-ray diffraction spectra

As seen from Figure 4, PEG had a distinct diffraction peak at about 20° or 23°, while drug had many peaks at about 10°, 18°, 19° and 25°. In the diffraction spectrum 3~11, peaks of DZ diminished significantly, and even disappeared, which suggested that carrier existed in the form of crystal, and drug might be dispersed in the carriers in the form of amorphism or molecule. All these also explained the reason why PEG solid disperse enhanced the dissolution of DZ significantly.

4. Conclusions

Using PEG 10000 as carrier, DZ solid dispersion prepared by solvent method could enhance the dissolution rate of DZ. The dispersion level of DZ in solid dispersions increased with the increasing weight ratio of PEG 10000. Appropriate amount of Tween-80 could enhance the dissolution of drug, but too much could impede inversely. In the present paper, the Tween-80 level was enhanced to 2.0 g, but could not be dried completely, and therefore its dosage shouldn't be too high. The optimum level of Tween-80 still needs further investigation.

During the preparation process of DZ solid dispersion, there had been no chemical bonding between DZ and PEG 10000, and preparation process didn't change the molecular structure of DZ. Because only the dissolution of DZ solid dispersion in vitro was observed, further investigation should be carried out on the comparison of dissolution in vitro among the current existing DZ dosage in the market in order to provide theoretical basis for the development of new DZ formulations.

References

Guo, J.P., & Sun, Q.R. (1996). Chemical composition and clinical application research status of Pueraria. *The Journal of Pharmaceutical Practice*, 14(3):146-148.

He, W.S. (2000). Clinical pharmacology research progress of effects of Pueraria and its extract on cardiovascular and cerebrobascular diseases. *Journal of Integrative Medicine on Cardio-/ Cerebrovascular Disease*, 17(3):58-59.

Zhou, Y.S., Jia, Y.Y., & Shen, X.Q. (2003). Studies on preparation and dissolution in vitro of puerarin solid dispersions. *Chinese Pharmaceutical Journal*, 38(1):42-44.

Table 1. Fitting equations of dissolution profiles of DZ and PEG solid dispersions at each ratio

Ratio	Equation	R^2	P
1:2	$Y=-7.412+1.404X-0.02X^2+0.003X^3$	1.000	0.000
1:5	$Y=-31.79+6.083X-0.371X^2+0.011X^3$	0.999	0.000
1:8	$Y=54.092-0.241X^2+0.007X^3$	0.998	0.000
1:2:0.4	$Y=11.478-0.077X^2+0.004X^3$	0.998	0.000
1:5:0.4	$Y=-0.583-0.03X^2+0.003X^3$	0.997	0.000
1:8:0.4	$Y=109.993-12.249X+0.362X^2$	0.995	0.000
1:2:0.4	$Y=-4.623+0.722X+0.005X^3$	0.998	0.000
1:5:0.4	$Y=2.573X^{0.013}$	0.996	0.000
1:8:0.4	$Y=-8.722+2.587X-0.208X^2+0.007X^3$	0.998	0.000
DZ	$Y=-0.144+0.393X-0.02X^2$	0.998	0.000
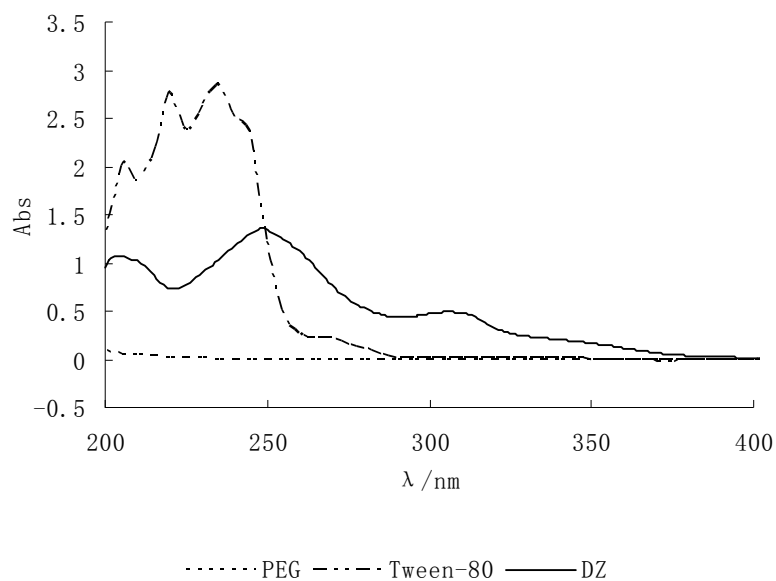
Figure 1. UV spectra of DZ, PEG and Tween-80
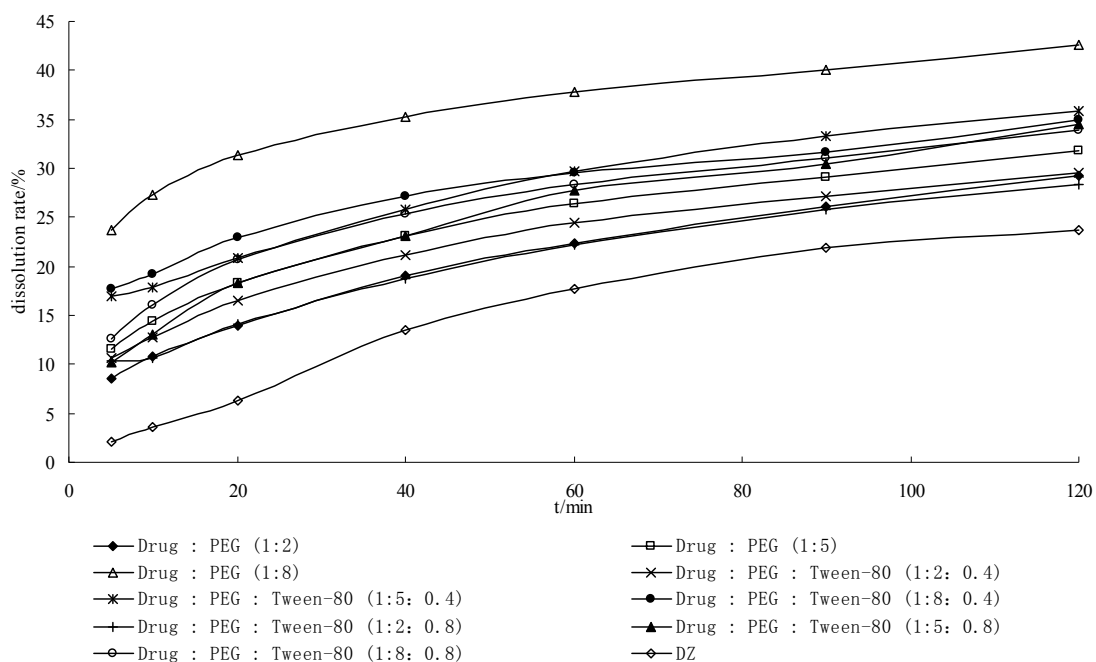
Figure 2. Dissolution profiles of DZ and PEG solid dispersions at each ratio
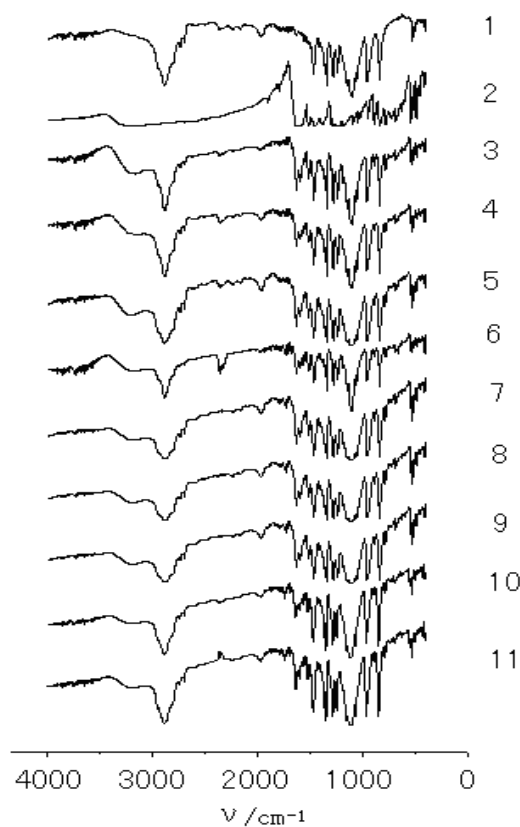
Figure 3. FTIR spectra of different samples: (1) PEG, (2) DZ, (3) Drug: PEG (1:2), (4) Drug: PEG (1:5), (5) Drug: PEG (1:8), (6) Drug:PEG:Tween-80 (1:2:0.4), (7) Drug:PEG:Tween-80 (1:5:0.4), (8) Drug:PEG:Tween-80 (1:8:0.4), (9) Drug:PEG:Tween-80 (1:2:0.8), (10) Drug:PEG:Tween-80 (1:5:0.8), (11) Drug:PEG:Tween-80 (1:8:0.8)
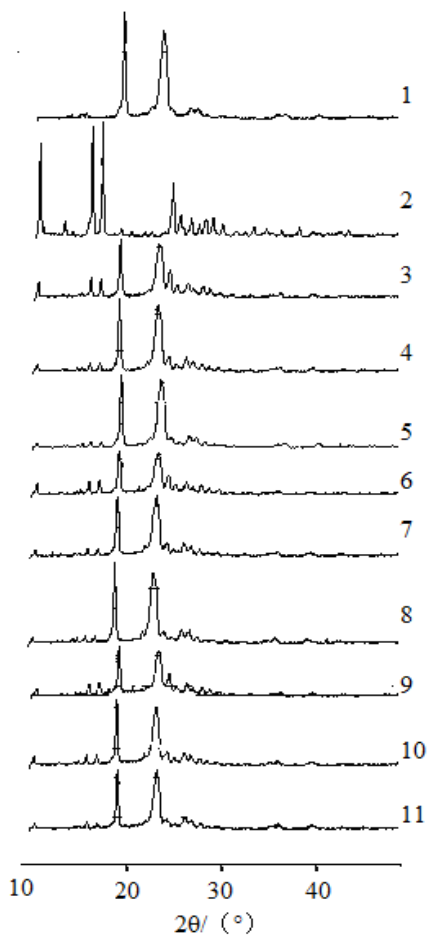
Figure 4. X-ray diffraction spectra of different samples: 1) PEG, (2) DZ, (3) Drug: PEG (1:2), (4) Drug: PEG (1:5), (5) Drug: PEG (1:8), (6) Drug:PEG:Tween-80 (1:2:0.4), (7) Drug:PEG:Tween-80 (1:5:0.4), (8) Drug:PEG:Tween-80 (1:8:0.4), (9) Drug:PEG:Tween-80 (1:2:0.8), (10) Drug:PEG:Tween-80 (1:5:0.8), (11) Drug:PEG:Tween-80 (1:8:0.8)

Synthesis and Antimicrobial Study of New
8-bromo-1,3-diaryl-2,3-dihydro-1H-naphtho[1,2e][1,3]oxazines

Anil N. Mayekar

Department of Studies in Chemistry, University of Mysore

Manasagangotri-570 006, India

SeQuent Scientific Limited, 120 A and B, Industrial Area

Baikampady, New Mangalore-575 011, India

Tel: 91-824-240-2306　　　E-mail: anilmayekar@gmail.com

H. S. Yathirajan (Corresponding author)

Department of Studies in Chemistry, University of Mysore

Manasagangotri-570 006, India

Tel: 91-821-241-9656　　　E-mail: yathirajan@hotmail.com

B. Narayana

Department of Chemistry, Mangalore University

Mangalagangotri-574 199, India

Tel: 91-824-228-7262　　　E-mail: nbadiadka@yahoo.co.uk

B. K. Sarojini

Department of Chemistry, P. A. College of Engineering, Nadupadavu

Mangalore-574 153, India

Tel: 91- 824-2284701　　　E-mail: bksaroj@yahoo.com

N. Suchetha Kumari

Department of Biochemistry, Justice K.S. Hegde Medical Academy, Deralakatte

Mangalore-574 162, India

Tel: 91-824-220-2471　　　E-mail: suchetha.shetty@rediffmail.com

William T. A. Harrison

Department of Chemistry, University of Aberdeen, Meston Walk, Aberdeen AB24 3UE, Scotland

Tel: 44-(0)1224-272-897　　　E-mail: w.harrison@abdn.ac.uk

Abstract

A series of new 8-Bromo-1,3-bis(aryl)-2,3-dihydro-1H-naphtho[1,2-e][1,3]oxazines **2a–n** have been synthesized, in which 6-bromonaphthol undergoes a ring closure reaction with substituted aryl and heteroarylaldehydes to give naphthoxazine derivatives. Some of these were hydrolyzed to obtain the aminobenzylnaphthols **3c** and **3l** which are further condensed with different aryl/heteroarylaldehydes to yield **4a–e.** The structures were confirmed through elemental analysis, spectral studies and single crystal X-ray study. The compounds were screened for their antibacterial and antifungal activity and some of them exhibited promising activity.

Keywords: 8-Bromo-1,3-diaryl-2,3-dihydro-1*H*-naphtho[1,2e][1,3]oxazine,   Ring-closure   reaction, Aryl/heteroarylaldehydes, Single crystal X-ray, Antimicrobial activities

1. Introduction

Heterocycles containing the oxazine nucleus are found to possess a wide range of biological applications (Takimoto & Calvo, 2008; Ohnacker, & Scheffler, H. 1960). Efavirenz, a trifluoromethyl-1,3-oxazin-2-one, is a non-nucleoside reverse transcriptase inhibitor which shows high activity against a variety of HIV-1 mutant strains (Young *et al*., 1995). 1,3-Oxazine derivatives are also known as progesterone receptor agonists (Zhang *et al*., 2003). Oxazine derivatives have shown analgesic, antipyretic anticonvulsant and antimicrobial activity (Clauson-Kaas *et al.*, 1968; Singh *et al.,* 1995; Latif et al., 1982). Oxazine with naphthalene ring, called naphthoxazine are used in the treatment of Parkinson's disease (Millan *et al*., 2004; Joyce *et al*., 2003). Naphthoxazines are also known for their psycho stimulating and antidepressant activity (Nozulak & Giger, 1987). Dihydrofuronaphth[1,3]oxazines have shown anti-tumor activity (Benameur *et al*., 1996). The stereoelectronic effects in ring-chain tautomerism of 1,3-diarylnaphth[1,2-*e*][1,3]oxazines and 3-alkyl-1-arylnaphth[1,2-*e*][1,3]oxazines is reported (Szatmari *et al*., 2004). The studies on the synthesis of 1,3-diarylnaphthoxazines (Turgut *et al.,* 2007) and substituent effects in the ring-chain tautomerism are reported (Szatmari *et al*., 2003). The synthesis and conformational analysis of naphth[1',2':5,6][1,3]oxazino[3,2-c][1,3]benzoxazine and naphtha[1'2':5,6][1,3]oxazino[3,4-c][1,3] benzoxazine derivatives have been reported (Heydenreich *et al*., 2006). Only few reports are available regarding their biological activity. Hence, there is enough scope to explore new oxazine derivatives for biological activities. In this connection, the present paper describes the synthesis and antimicrobial study of new 8-bromo-1,3-diaryl-2,3-dihydro-1*H*-naphth[1,2e][1,3]oxazines.

2. Experimental

TLC was run on a Merck silica gel 60 F254 coated aluminum plates and melting points were taken in open capillary tubes and are uncorrected. Elemental analysis was carried out using Flash EA 1112 Series, CHNSO Analyzer (Thermo). IR spectra in KBr pellets were recorded on Jasco FT/IR-4100 FTIR spectrophotometer. ^{1}H NMR spectra were recorded in CDCl3 and in DMSO-d6 on a Bruker DRX-300 (300 MHz) spectrometer using TMS as internal standard and Mass spectra were recorded on a Jeol SX 102/Da-600 mass spectrometer/data system using Argon/Xenon (6kv,10mA) as FAB gas.

2.1 General procedure for the synthesis of 8-bromo-1,3-bis(aryl)-2,3-dihydro-1H-naphtho[1,2-e][1,3]oxazines (2a-n)

To 6-bromo-2-naphthol (2.23 g, 0.01 mol) in methanol (10 ml) was added aryl or heteroarylaldehyde (0.02 mol; freshly distilled if a liquid) and 10 ml of 25-30% methanolic ammonia. The mixture was left to stand at ambient temperature for 2-3 days, during which the crystalline products separated out. The crude product were filtered off, washed with cold methanol and purified by recrystallization.

8-Bromo-1,3-bis(phenyl)-2,3-dihydro-1H-naphtho[1,2-e][1,3]oxazine (2a)

^{1}H NMR (CDCl3, δ ppm): 5.52 (s, 1H, CH), 5.64 (s, 1H, CH), 7.21-8.1(m, 15H, ArH), 8.14 (s, 1H, naphthalene ring proton). ^{13}C-NMR (CDCl3, δ ppm): 53.49, 79.09, 113.68, 114.31, 114.80, 115.75, 116.03, 116.93, 120.31, 124.19, 125.78, 127.78, 128.20, 128.56, 129.74, 130.12, 130.29, 134.01. MS FAB: 416 M$^+$, 418 [M+2]$^+$.

8-Bromo-1,3-bis(2-chlorophenyl)-2,3-dihydro-1H-naphtho[1,2-e][1,3]oxazine (2b)

^{1}H NMR (CDCl3, δ ppm): 5.97 (s ,1H , CH), 6.05 (s,1H, CH), 6.85-7.92 (m, 13H, ArH), 8.95 (s, 1H, naphthalene ring proton), 11.85 (s, 1H, NH). ^{13}C-NMR (CDCl3, δ ppm): 53.55, 80.01, 113.68, 114.31, 114.80, 115.75, 116.03, 116.93, 120.31, 124.19,124.89, 125.78, 127.78, 128.20, 128.56, 129.74, 130.12, 130.29, 134.01,136.10, 136.44, 136.52, 146.23. MS FAB: 452 M$^+$, 454 [M+2]$^+$.

8-Bromo-1,3-bis(3-methoxyphenyl)-2,3-dihydro-1H-naphtho[1,2-e][1,3]oxazine (2c)

^{1}H NMR (CDCl3, δ ppm): 3.53 (s, 3H, OCH3), 3.69 (s, 3H, OCH3), 5.96 (s, 1H, CH), 6.02 (s, 1H, CH), 6.81-7.90 (m, 12H, ArH), 9.06 (s, 1H, naphthalene ring proton), 12.60 (s, 1H, NH). ^{13}C-NMR (CDCl3, δ ppm): 53.49, 55.57, 67.76, 80.57,110.51, 110.74, 111.23, 114.46, 116.03, 116.72, 119.95, 120.43, 120.85, 121.19, 121.43,123.22, 123.67, 127.96, 128.50,128.72, 129.08, 129.49, 130.48, 133.02 156.74, 159.27. MS FAB: 476 M$^+$, 478 [M+2]$^+$.

8-Bromo-1,3-bis(4-methoxyphenyl)-2,3-dihydro-1H-naphtho[1,2-e][1,3]oxazine (2d)

^{1}H NMR (CDCl3, δ ppm): 3.46 (s, 3H, OCH3), 3.62 (s, 3H, OCH3), 5.96 (s, 1H, CH), 6.06 (s, 1H, CH), 6.74-7.89(m, 12H, ArH), 9.07 (s, 1H, naphthalene ring proton), 12.61 (s, 1H, NH). ^{13}C-NMR (CDCl3, δ ppm): 53.49, 55.46, 55.57, 80.27, 110.74, 111.23, 114.46, 116.72, 119.95, 120.43, 120.85, 121.19, 121.43,123.22, 123.67, 127.96,128.72, 129.49, 130.48, 133.02 156.77, 159.28. MS FAB: 476 M$^+$, 478 [M+2]$^+$.

8-Bromo-1,3-bis(3-bromophenyl)-2,3-dihydro-1H-naphtho[1,2-e][1,3]oxazine (2e)

^{1}H NMR (CDCl$_3$, δ ppm): 5.51 (s, 1H, CH), 5.67 (s, 1H, CH), 7.16-8.16(m, 13H, ArH).

^{13}C-NMR (CDCl$_3$, δ ppm): 53.49, 79.09, 113.68, 114.31, 114.80, 115.75, 116.03, 116.93,

199.86,120.31, 123.6,124.19, 125.78, 127.24,127.78, 128.20, 128.56, 129.74,130.06, 130.12, 130.29, 130.68, 131.68,134.01. MS FAB: 574 M$^+$, 576 [M+2]$^+$.

8-Bromo-1,3-bis(2-furyl)-2,3-dihydro-1H-naphtho[1,2-e][1,3]oxazine (2f)

^{1}H NMR (CDCl$_3$, δ ppm): 5.96 (s, 1H, CH), 6.06 (s, 1H, CH), 6.74-7.89 (m, 11H, ArH).

^{13}C-NMR (CDCl$_3$, δ ppm): 53.49, 79.09, 105.68, 105.81, 114.80, 115.75, 120.31, 124.19, 125.78, 127.78, 128.20, 128.56, 129.74, 130.12, 130.29, 134.01, 141.58, 141.62, 153.6, 155.2. MS FAB: 396 M$^+$, 398 [M+2]$^+$.

8-Bromo-1,3-bis(3,4-dimethoxyphenyl)-2,3-dihydro-1H-naphtho[1,2-e][1,3]oxazine (2g)

^{1}H NMR (CDCl$_3$, δ ppm): 3.62-3.91 (m, 12H, OCH$_3$), 5.42 (s ,1H , CH), 5.65 (s, 1H, CH), 6.51-7.89 (m, 11H, ArH).
^{13}C-NMR(CDCl3, δ ppm): 53.49, 55.61, 80.09, 110.74, 114.46, 116.03, 116.72, 119.95, 120.43, 120.85, 121.19, 121.43,123.22, 123.67, 127.96, 128.50,128.72, 129.08, 129.49, 130.48, 133.02, 156.30, 156.32. MS FAB: 536 M$^+$, 538 [M+2]$^+$.

8-Bromo-1,3-bis(2-methoxyphenyl)-2,3-dihydro-1H-naphtho[1,2-e][1,3]oxazine (2i)

^{1}H NMR (CDCl3, δ ppm): 3.62 (s, 3H, OCH3), 3.68 (s, 3H, OCH3), 5.96 (s, 1H, CH), 6.06 (s,1H, CH), 6.74-7.89(m, 12H, ArH), 9.07(s, 1H, ArH). ^{13}C-NMR (CDCl$_3$, δ ppm): 53.49, 55.57, 67.76, 80.57,110.51, 110.74, 111.23, 114.46, 116.03, 116.72, 119.95, 120.43, 120.85, 121.19, 121.43, 123.22, 123.67, 127.96, 128.50, 128.72, 129.08, 129.49, 130.48, 133.02 156.74, 159.27. MS FAB: 476 M$^+$, 478 [M+2]$^+$.

8-Bromo-1,3-bis(4-chlorophenyl)-2,3-dihydro-1H-naphtho[1,2-e][1,3]oxazine (2j)

^{1}H NMR (CDCl$_3$, δ ppm): 5.55 (s ,1H , CH), 5.59 (s, 1H, CH), 7.21-7.94 (m, 12H, ArH),

8.61(s,1H,ArH). ^{13}C-NMR (CDCl$_3$, δ ppm): 53.49, 79.09, 113.68, 114.31, 114.80, 115.75, 116.03, 116.93, 120.31, 124.19, 125.78, 127.32, 127.78, 128.20, 128.56, 129.74, 130.12, 130.29, 134.01, 134.12. MS FAB: 485 M$^+$, 487 [M+2]$^+$.

8-Bromo-1,3-bis[4-(methylthio)phenyl]-2,3-dihydro-1H-naphtho[1,2-e][1,3]oxazine (2k)

^{1}H NMR (CDCl$_3$, δ ppm): 2.47 (s, 3H, SCH$_3$), 2.50 (s, 3H, SCH3), 5.55 (s ,1H , CH), 5.61 (s, 1H, CH), 7.11-7.62 (m, 4H, ArH), 7.62-7.67 (m, 6H, ArH), 7.9 (d, 2H, J=8.7, ArH), 8.15 (s, 1H, ArH). ^{13}C-NMR (CDCl$_3$, δ ppm): 13.8, 55.36, 79.26, 113.68, 114.31, 114.80, 115.75, 116.03, 116.93, 120.31, 124.19, 125.78,126.35,127.12, 127.78, 128.20, 128.56, 129.74, 130.29, 136.18. MS FAB: 508 M$^+$, 510 [M+2]$^+$.

8-Bromo-1,3-bis(3-methylphenyl)-2,3-dihydro-1H-naphtho[1,2-e][1,3]oxazine (2l)

^{1}H NMR (CDCl$_3$, δ ppm): 2.35 (s, 3H, CH$_3$), 2.37 (s, 3H, CH$_3$), 5.96 (s ,1H , CH), 6.06 (s, 1H, CH), 6.74-7.89(m, 12H, ArH), 9.07 (s, 1H, naphthalene ring proton), 12.61 (s, 1H, NH). ^{13}C-NMR (CDCl$_3$, δ ppm): 21.20, 55.49, 79.09, 110.68, 114.31, 114.80, 115.75, 116.03, 116.93, 120.31, 124.19, 125.78, 126.32, 126.98, 127.22, 127.78, 128.20, 128.56, 129.74, 130.12, 130.29, 134.01, 138.23. MS FAB: 444 M$^+$, 446 [M+2]$^+$.

8-Bromo-1,3-bis(3-pyridinyl)-2,3-dihydro-1H-naphtho[1,2-e][1,3]oxazine (2m)

^{1}H NMR (CDCl$_3$, δ ppm): 5.66 (s ,1H , CH), 5.68 (s, 1H, CH), 7.18-7.97(m, 9H, ArH), 8.52 (t, 1H, J=8.0 Hz, py proton), 8.64 (t, 1H, J=7.9 Hz, py proton), 8.70 (d, 1H, J=7.2 Hz, py proton), 8.82 (d, 1H, J=7.2 Hz, py proton). ^{13}C-NMR (CDCl$_3$, δ ppm): 51.67, 84.55, 113.06, 117.37, 120.36, 123.11, 124.15, 125.14, 128.72,128.91, 129.74, 130.16, 130.20, 130.67, 133.87, 136.67, 137.42, 147.81, 148.90, 149.82, 150.78, 152.42.MS FAB: 418 M$^+$, 420 [M+2]$^+$.

2.2 General procedure for the synthesis of 1-(aminosubstituted methyl)-2-naphthols 3c and 3l

2c or **2l** (1 mmol) were suspended in 20 % HCl (20 mL) and the mixture was stirred and refluxed for 6 h, whereby the crystalline hydrochloride of **3c**, **3l** separated out. The product was filtered off and washed with EtOAc. The solid was suspended in H$_2$O and the mixture was treated with conc. NH$_4$OH (3 mL) and extracted with EtOAc. After drying (over Na$_2$SO$_4$) and evaporation of the EtOAc phase, crude crystalline compounds were obtained, which were further purified by recrystallization.

1-[Amino(3-methoxyphenyl)methyl]-6-bromo-2-naphthol (3c)

^{1}H NMR (CDCl$_3$, δ ppm): 1.58 (bs, 2H, NH$_2$), 3.73 (s, 1H, OCH$_3$), 6.05 (s, 1H, CH), 6.79 (d, 1H, J=8.1 Hz, ArH), 6.96-7.02 (m, 2H, ArH), 7.14-7.25 (m, 2H, ArH), 7.38 (d, 2H, J=9.3 Hz, ArH), 7.58 (t, 1H, J=9.3 Hz, ArH), 7.85 (s, 1H, ArH).MS FAB: 358 M$^+$, 360 [M+2]$^+$.

IR (KBr, γ$_{max}$ cm^{-1}): 3358, 3187, 1508. Elemental analysis % Calculated (Found) for C$_{18}$H$_{16}$BrNO$_2$: C- 60.35(60.33), H- 4.50(4.49) and N-3.91(3.89). m.p:138-140 °C

1-[Amino(3-methylphenyl)methyl]-6-bromo-2-naphthol (3l)

^{1}H NMR (CDCl$_3$, δ ppm): 1.58 (bs, 2H, NH$_2$), 2.39 (s, 1H, CH$_3$), 6.01 (s, 1H, CH), 7.06-7.25 (m, 5H, ArH), 7.37 (d, 1H, J=9 Hz, ArH), 7.55 (d, 1H, J=9 Hz, ArH), 7.60 (d, 1H, J=9 Hz, ArH), 7.93 (s, 1H, ArH) MS FAB: 342 M$^+$, 346 [M+2]$^+$.

IR (KBr, γ$_{max}$ cm^{-1}): 3356, 3329, 1511. Elemental analysis % Calculated (Found) for C$_{18}$H$_{16}$BrNO : C- 63.17(63.16), H- 4.71(4.69) and N-4.09(4.07). m.p.:118-120 °C.

2.3 General procedure for the synthesis of 8-bromo-1,3-diaryl-2,3-dihydro-1H-naphtho[1,2e][1,3]oxazines (4a-e)

To a solution of the appropriate aminonaphthol **3c** or **3l** (1 mmol) in absolute MeOH (20 mL), an equivalent amount of aryl- or heteroarylaldehyde was added, and the mixture was left to stand at ambient temperature for 48h. The crystalline product separated were filtered off and then recrystallized in methanol.

8-Bromo-1-(3-methoxyphenyl)-3-(4-chlorophenyl)-2,3-dihydro-1H-naphtho[1,2-e][1,3]oxazine (4a)

^{1}H NMR (CDCl$_3$, δ. ppm): 3.76 (s, 3H, OCH$_3$), 5.61 (s ,1H , CH), 5.89 (s, 1H, CH), 6.81- 6.86(m, 4H, ArH),7.05-7.69(m, 6H, ArH), 7.90(d, 1H, J=6.9Hz, ArH), 7.95(d, 1H, J=7.8Hz, ArH), 8.90 (s, 1H, naphthalene ring proton). ^{13}C-NMR (CDCl$_3$, δ ppm): 53.49, 55.15, 79.09, 113.68, 114.31, 114.80, 115.75, 116.03, 116.93, 120.31, 124.19, 124.67,125.78, 127.78, 128.20, 128.56, 129.74, 130.12, 130.29, 134.01, 152.63, 158.93. MS FAB: 480 M$^+$, 482 [M+2]$^+$.

8-Bromo-1-(3-methoxyphenyl)-3-(3-methylphenyl)-2,3-dihydro-1H-naphtho[1,2-e][1,3]oxazine (4b)

^{1}H NMR (CDCl$_3$, δ ppm): 2.37 (s, 3H, CH$_3$), 3.77 (s, 3H, OCH$_3$), 5.59 (s ,1H , CH), 5.70 (s, 1H, CH), 6.77-7.91(m, 12H, ArH), 8.6 (s, 1H, naphthalene ring proton). ^{13}C-NMR (CDCl$_3$, δ ppm): 20.12, 53.97, 55.22, 81.95, 113.68, 114.31, 114.80, 115.75, 116.03, 116.93, 117.06, 119.65, 120.31,121.42, 121.42,123.31, 124.70, 125.78, 127.78, 128.20, 128.56, 129.74, 130.12, 130.29, 134.01, 158.63. MS FAB: 460 M$^+$, 462 [M+2]$^+$.

8-Bromo-1-(3-methoxyphenyl)-3-pyridin-3-yl-2,3-dihydro-1H-naphtho[1,2-e][1,3]oxazine (4c)

^{1}H NMR (CDCl$_3$, δ. ppm): 3.79 (s, 3H, OCH$_3$), 5.61 (s ,1H , CH), 5.74 (s, 1H, CH), 6.83(d, 2H, J=9.9Hz, ArH),7.24-7.40(m, 6H, ArH), 7.69(d, 1H, J=6.7Hz, ArH), 7.92-7.95(m, 2H, ArH), 8.61(s, 1H, ArH), 8.85 (s, 1H, ArH). ^{13}C-NMR(CDCl$_3$, δ. ppm): 51.67, 54.43, 80.58, 114.31, 115.75, 116.03, 116.93,117.42, 120.31, 123.11, 124.19, 125.18, 127.78, 128.20, 128.91, 129.74, 130.12, 130.29, 130.67, 134.01,136.67,137.89,149.30, 149.82. MS FAB: 447 M$^+$, 449 [M+2]$^+$.

8-Bromo-1-(3-methylphenyl)-3-pyridin-3-yl-2,3-dihydro-1H-naphtho[1,2-e][1,3]oxazine (4d)

^{1}H NMR (CDCl$_3$, δ. ppm): 2.37 (s, 3H, CH$_3$), 5.61 (s, 1H, CH), 5.74 (s, 1H, CH), 6.83(d, 2H, J=8.9Hz, ArH), 7.24-7.40(m, 6H, ArH), 7.86-7.95(m, 3H, ArH), 8.61(s, 1H, ArH), 8.85 (s, 1H, ArH). ^{13}C-NMR(CDCl$_3$, δ. ppm): 20.23, 54.33, 80.18, 114.21, 115.65, 116.01, 116.84, 117.39, 120.31, 123.21, 124.17, 125.09, 127.76, 128.18, 128.91, 129.69, 130.12, 130.27, 130.65, 134.12, 136.77, 137.91, 149.28, 149.82. MS FAB: 431 M$^+$, 433 [M+2]$^+$.

8-Bromo-1-(3-methylphenyl)-3-(4-chlorophenyl)-2,3-dihydro-1H-naphtho[1,2-e][1,3]oxazine (4e)

^{1}H NMR (CDCl$_3$, δ. ppm): 2.39 (s, 3H, CH$_3$), 5.55 (s, 1H, CH), 5.59 (s, 1H, CH), 7.20-7.92(m, 12H, ArH), 8.3 (s, 1H, ArH). ^{13}C-NMR (CDCl$_3$, δ. ppm): 20.22, 53.49, 79.09, 113.68, 114.31, 114.80, 115.75, 116.03, 116.93, 120.31, 124.19, 124.67,125.78, 127.78, 128.20, 128.56, 129.74, 130.12, 130.29, 134.01, 152.63, 158.93. MS FAB: 464 M$^+$, 466 [M+2]$^+$.

2.4 Pharmacology

2.4.1 Antibacterial studies

The newly synthesized compounds were screened for their antibacterial activity against *Escherichia coli* (ATTC-25922), *Staphylococcus aureus* (ATTC-25923), *Pseudomonas aeruginosa* (ATCC-27853) and *Klebsiella pneumoniae* (recultured) bacterial strains by serial plate dilution method (Barry, 1991; James *et al.*, 1991). Serial dilutions of the drug in Mueller Hinton broth were taken in tubes and their pH was adjusted to 5.0 using phosphate buffer. A standardized suspension of the test bacterium was inoculated and incubated for 16-18 h at 37°C.

A number of antimicrobial discs are placed on the agar for the sole purpose of producing zones of inhibition in the bacterial lawn. Twenty milliliters of agar media was poured into each Petri dish. Excess of suspension was decanted and plates were dried by placing in an incubator at 37°C for an hour. Using a punch, wells were made on these seeded agar plates and minimum inhibitory concentrations of the test compounds in dimethylsulfoxide (DMSO) were added into each labeled well. A control was also prepared for the plates in the same way using solvent DMSO. The Petri dishes were prepared in triplicate and maintained at 37°C for 3-4 days. Antibacterial activity was determined by measuring the diameter of inhibition zone. Activity of each compound was compared with ciprofloxacin as standard (Fenlon, & Cynamon, 1986). Zone of inhibition was determined for newly synthesized compounds at 10 μg/ml concentration and the results are presented in **Table 4**.

2.4.2 Antifungal studies

Newly prepared compounds were also screened for their antifungal activity against *Aspergilus flavus* (NCIM No.524), *Aspergilus fumigates* (NCIM No. 902), *Penicillium* (*S.aurus*) (recultured) and *Trichophyton mentagrophytes* (recultured) in DMSO by serial plate dilution method (Arthington-Skaggs *et al*., 2000; Verma *et al*., 1998). Sabourands agar media was prepared by dissolving peptone (1 g), D-glucose (4 g) and agar (2 g) in distilled water (100 ml) and adjusting the pH to 5.7. Normal saline was used to make a suspension of spore of fungal strains for lawning. A loopful of particular fungal strain was transferred to 3 ml saline to get a suspension of corresponding species. Twenty milliliters of agar media was poured into each Petri dish. Excess of suspension was decanted and plates were dried by placing in incubator at 37°C for 1 h. Using a punch, wells were made on these seeded agar plates minimum inhibitory concentrations of the test compounds in DMSO were added into each labeled well. A control was also prepared for the plates in the same way using solvent DMSO. The Petri dishes were prepared in triplicate and maintained at 37°C for 3-4 days. Antifungal activity was determined by measuring the diameter of inhibition zone at 10 μg/ml concentration. Activity of each compound was compared with Fluconazole as standard. Zone of inhibitions were determined and the results are given in **Table 5**.

3. Results and discussion

The reaction sequence employed for synthesis of the title compounds are shown in **scheme 1** and **scheme 2**. 8-Bromo-1,3-bis(aryl)-2,3-dihydro-1*H*-naphtho[1,2e][1,3]oxazines **(2a-n)** were obtained by treating 6-bromonaphthol with aryl aldehydes in presence of methanolic ammonia at room temperature for 2-3 days. The reaction leads to the generation of two chiral centers in the structure which would result in a mixture of diastereomers. The newly synthesized compounds were characterized based on their elemental analysis and spectral (^{1}H NMR, ^{13}C NMR and FAB mass) data. The characterization data of all the new compounds are presented in **Table 1.** The formation of 8-Bromo-1,3-bis(phenyl)-2,3-dihydro-1H-naphtho[1,2-e] [1,3]oxazine **(2a)** and 8-bromo-1,3-bis(3-methoxyphenyl)-2,3-dihydro-1*H*-naphtho[1,2-*e*][1,3]oxazine **(2c)** was confirmed through elemental analysis, spectral data and single crystal X-ray studies (Jasinsik *et al*., 2010; Sarojini *et al*., 2007). In ^{1}H NMR, the peaks due to two OCH$_3$ groups appeared as singlet at δ 3.53 and 3.69. Two singlets were observed at δ 5.96 and δ 6.02 representing N-CH- and O-CH- protons of oxazine ring respectively. The aromatic protons resonated as multiplet at δ 6.81-7.90 accounting for 12 protons. A singlet was observed at δ 9.06 representing naphthalene ring proton and a broad singlet at δ 12.06 accounted for NH proton. While ^{13}C NMR showed signals at 53.49 and 55.57 due to two OCH$_3$. The other signals at 67.76 and 80.57 were due to C-atoms of N-CH- and O-CH-. The aromatic carbon signals appeared at 110.51, 110.74, 111.23, 114.46, 116.03, 116.72, 119.95, 120.43, 120.85, 121.19, 121.43,123.22, 123.67, 127.96, 128.50,128.72, 129.08, 129.49, 130.48, 133.02 156.74, 159.27 accounting for 22 carbon atoms. The structure of this compound was also confirmed through single crystal X-ray studies (Sarojini *et al.,* 2007).

The naphthoxazine **2c** and **2l** were subjected to acid hydrolysis to get Betti bases (Betti, 1941). [1-α-aminobenzyl]-6-bromo-2-naphthols **3c**, **3l** in good yield. In the ^{1}H NMR spectrum of **3c**, the NH$_2$ protons resonated at δ 1.58 as a broad singlet and methoxy protons resonated as a singlet at δ 3.73 integrating for three protons while the singlet due to -N-CH- appeared at δ 6.05. The signal for naphthalene ring proton appeared as follows; C4-H appeared at δ 6.79 as doublet J=8.1Hz and C5-H as singlet at δ 7.85. The C7-H proton resonated at δ 7.38 as doublet with J=9.3 Hz. The C5 –H phenyl ring proton resonated at δ 7.58 J=9.3 Hz as triplet. The FAB mass of this compound showed the molecular ion peak at m/z = 358 and the other peak was observed at 360 (M+2) indicating the presence of bromine. The reactions of the Betti bases **3c, 3l** with equivalent amounts of arylaldehydes/heteroaldehydes afforded the corresponding 8-bromo-1,3-diaryl-2,3-dihydro-1*H*-naphtho[1,2e][1,3]oxazines **(4a-e) (Table 2).** The characterization data of all the compounds are given in **Table 3.** In a typical example, the ^{1}H NMR of **4d** showed a singlet at δ 2.37 accounting for three protons, indicating the presence of CH$_3$. The N-CH- and O-CH- protons resonated as singlets at δ 5.61 and 5.74 respectively. The C5-H proton appeared as a singlet at δ 8.61 and a singlet was observed at δ 8.85 representing

the pyridine ring proton. In ^{13}C-NMR the signal at δ 20.23 accounting for CH_3 and at δ 54.33 and 80.18 for N-CH- and O-CH- were observed. The FAB mass of this compound showed the molecular ion peak at m/z = 431.

Compound *8-Bromo-1,3-bis(4-fluorophenyl)-2,3-dihydro-1H-naphtho[1,2-e][1,3]oxazine* (**2h**) was obtained as colourless blocks by recrystallization from acetonitrile solution and characterized through single crystal X-ray study, which reveals the following: $C_{24}H_{16}BrF_2NO$, M_r = 452.28, triclinic, $P\bar{1}$ (No. 2), a = 8.7436 (8) Å, b = 10.7804 (10) Å, c = 11.6475 (13) Å, α = 102.536 (5)°, β = 109.154 (6)°, γ = 104.135 (6)°, V = 951.31 (18) Å^3, Z = 2, ρ_{calc} = 1.579 g cm^{-3}, μ = 2.195 mm^{-1}, $F(000)$ = 456, Nonius Kappa CCD diffractometer, Mo Kα radiation, λ = 0.71073 Å, T = 120 K, $R(F)$ = 0.033, $wR(F^2)$ = 0.082, S = 1.04. All the bond lengths and bond angles fall within their expected ranges of values (Allen *et al.,* 1987). The molecular structure of **2h** is shown in **Fig. 1** and intermolecular N–H⋯π interactions are shown in **Fig. 2**. The conformation of the six-membered C1/C10/C11/N1/C12/O1 oxazine ring approximates to a half-chair, with C1/C10/C11/O1 roughly coplanar (r.m.s. deviation = 0.021 Å) and C12 and N1 displaced from their mean plane by +0.384 (6) Å and –0.328 (6) Å, respectively. The C11–N1–C12 bond angle of 110.9 (3)° and the bond angle sum of 331° for N1 are strongly indicative of sp^3 hybridization for the nitrogen atom and its attached H atom (coordinates freely refined) occupies a *pseudo* axial site. The dihedral angles between the C1–C10 naphthalene ring system and the pendant C13–C18 and C19–C24 fluorobenzene rings were 20.50 (17) and 74.05 (16)°, respectively. In the crystal, inversion dimers arise, being linked by pairs of N–H⋯π (Page & Rzepa, 1996) interactions [N–H = 0.85 (4) Å, H⋯π = 2.49 (4) Å, N–H⋯π = 166 (3)°, where π is the centroid of the C4–C9 ring at the symmetry position [1–x, –y, 1–z], as shown in **Fig. 2**. Any aromatic π–π stacking effects in the crystal of **2h** must be very weak, with a minimum centroid–centroid separation of 3.926 (2) Å. All the H atoms were located in difference maps and their positions and U_{iso} values were freely refined. [X-ray crystallographic files, in Cif format, for the structure determinations of **2h** (**CCDC 760555**) has been deposited with the Cambridge Crystallographic Data Center, CCDC: 26091. Copies of this information may be obtained free of charge from the Director, CCDC, 12 Union Road, Cambridge, CB2 1EZ (fax: ? 44-1223-336033; email: deposit@ccdc.cam.uk or http://www.ccdc.cam.ac.uk.].

Compounds were also screened for their antibacterial and antifungal activity. Almost all the compounds tested showed moderate to good activity against the bacterial and fungal strains. Compounds **2h, 2j, 2l** and **4e** showed promising results. The good activity could be attributed to the presence of phenyl ring substituted with fluoro, chloro and methyl groups attached to the oxazine ring. Replacing one of the aryl substituent with a different aryl/heteroaryl group showed increase in the activity of **4a, 4b, 4c, 4d** and **4e**.

In the antifungal activity study, compound **4e** emerged with good activity against fungal strains, particularly against *Aspergilus flavus*. This may be due to the presence of 3-methylphenyl and 4-chlorophenyl groups attached to the naphthoxazine ring.

4. Conclusions

The present study reports the synthesis of series of new naphthoxazine derivative. Structure of compound **2h** was elucidated through single crystal X-ray diffraction. The newly synthesized compounds were screened for their biological activity. Some of the new compounds found to exhibit good activity against tested bacterial and fungal strains. Compounds having fluoro, chloro and methyl substituted phenyl group attached to naphthoxazine showed promising activity. However it is a preliminary study and these newly synthesized compounds should be subjected to detailed pharmacological and toxicological evaluation for their application in clinical use.

References

Allen, F.H., Kennard, O., Watson, D.G., Brammer, L., Orpen, A.G., Taylor, R. (1987). Tables of bond lengths determined by X-ray and neutron diffraction. Part 1. Bond lengths in organic compounds. *Journal of the Chemical Society, Perkin Transactions II*, S1-S19.

Arthington-Skaggs, B.A.; Motley, M.; Warnock, D.W.; Morrison, C. J. (2000). Comparative evaluation of PASCO and national committee for clinical laboratory standards M27-A broth microdilution methods for antifungal drug susceptibility testing of yeasts. *Journal of Clinical Microbiology,* 38:2254-2260.

Barry, A.L. (1991). *Procedure for testing antimicrobial agents in agar media*, in: Corian V.L. (Ed), *Antibiotics in Laboratory Medicine*, Williams and Wilkins, Baltimore, MD.

Benameur, L., Bouaziz, Z., Nebois, P., Bartoli, M.H., Boitard, M., Fillion, H. (1996). Synthesis of furonaphth[1,3]oxazine and furo[1,3]oxazinoquinoline derivatives as precursors for an o-quinonemethide structure and potential antitumor agents. *Chemical and Pharmaceutical Bulletin.*, 44: 605-608.

Betti, M. (1941). Organic Synthesis Collective 1, 381.

Clauson-Kaas, N., Denss, R., Ostermayer, F., Renk, E. F. (1968). U.S Patent. 3, 410, 852.

Fenlon, C.H., Cynamon, M.H. (1986). Comparative in vitro activities of ciprofloxacin and other 4-quinolones against Mycobacterium tuberculosis and Mycobacterium intracellulare. *Antimicrobial Agents and Chemotherapy,* 29:386-388.

Heydenreich, M., Koch, A., Klod, S., Szatmari, I., Fulop, F., Kleinpeter, E. (2006). Synthesis and conformational analysis of naphth[1',2':5,6][1,3]oxazino[3,2-c][1,3]benzoxazine and naphth[1'2':5,6][1,3]oxazino[3,4-c][1,3]benzoxazine derivatives. *Tetrahedron*. 62:11081–11089.

James, D., Lowry, M., Jaqua, M. J., Selepak, S. T. (1970). Detailed Methodology and Implementation of a Semi automated Serial Dilution Micro technique for Antimicrobial Susceptibility Testing. *Applied Microbiology,* 20: 46-53.

Jasinski, J. P., Pek, A. E., Mayekar, A. N., Yathirajan, H. S., Narayana, B. (2010). 8-Bromo-1,3-diphenyl-2,3-dihydro-1H-naphtho[1,2-e][1,3]oxazine. *Acta Crystallographica,* E66:o2053-o2054.

Joyce, J.N., Presgraves, S., Renish, L., Borwege, S., Osredkar, T., Hagner, D., Replogle, M., PazSoldan, M., Millan, M.J. (2003). Neuroprotective effects of the novel D_3/D_2 receptor agonist and antiparkinson agent, S32504, in vitro against 1-methyl-4-phenylpyridinium (MPP+) and in vivo against 1-methyl-4-phenyl-1,2,3,6-tetrahydropyridine (MPTP): a comparison to ropinirole. *Experimental Neurology*, 184:393-407.

Latif, N., Mishriky, N., Assad, F.M. (1982). Carbonyl and thiocarbonyl compounds. XIX. Intramolecular cyclization of (2-nitroetheny1)aryl N-arylcarbamates : synthesis of newer series of 3,4-dihydro-2H-1,3-oxazin-2-ones and their antimicrobial activities. *Australian Journal of Chemistry.* 35:1037-1043.

Millan, M.J., Di Cara, B., Hill, M., Jackson, M., Joyce, J.N., Brotchie, J., McGuire, S., Crossman, A., Smith, L., Jenner, P., Gobert, A., Peglion, J.L., Brocco, M. (2004). S32504, a Novel Naphtoxazine Agonist at Dopamine D_3/D_2 Receptors: I. Cellular, Electrophysiological, and Neurochemical Profile in Comparison with Ropinirole. *Journal of Pharmacology and Experimental Therapeutics,* 309:921-935.

Nozulak, J., Giger, R.K.A. (1987). Naphthoxazines and their use as psychostimulating and antidepressant agents. U.S. Patent. 4,656,167.

Ohnacker, G., Scheffler, H. (1960). Derivatives of 4-oxo-2,3-dihydro-(benzo-1,3-oxazines). US Patent 2943087.

Page, C. S., Rzepa, H. S. (1996). *Electronic Conference on Trends in Organic Chemistry (ECTOC-1),* Eds. Rzepa, H. S.; Goodman, J. M.; and Leach, C. (CD-ROM), Royal Society of Chemistry publications. [Online] Available: http://www.ch.ic.ac.uk/ ectoc/papers/47/ on 29 December 2009.

Szatmari, I., Martinek, T. A., Lazar, L., Fulop, F. (2003). Substituent effects in the ring-chain tautomerism of 1,3-diaryl-2,3-dihydro-1H-naphth[1,2-e][1,3]oxazines. *Tetrahedron,* 59:2877-2884.

Sarojini, B. K., Narayana, B., Mayekar, A. N., Yathirajan, H. S., Bolte, M. (2007). 6-Bromo-2,4-bis(3-methoxyphenyl)-3,4-dihydro-2H-1,3-naphthoxazine. *Acta Crystallographica,* E63:o4739.

Singh, C., Parwana, H. K., Singh, G. (1995). Synthesis of 3,6-diaryl-2h, 3h, 4h, 5h, 6h-[1,3]-oxazine-2-thiones as potential anticonvulsants. *Indian Journal of Pharmaceutical Sciences*, 57:198-202.

Szatmari, I., Martinek, T. A., Lazar, L., Koch, A., Kleinpeter, E., Neuvonen, K., Fulop, F. (2004). Stereoelectronic effects in ring-chain tautomerism of 1,3-diarylnaphth[1,2-*e*][1,3]oxazines and 3-alkyl-1-arylnaphth[1,2-*e*][1,3]oxazines. *Journal of Organic Chemistry,* 69:3645–3653.

Takimoto, C.H., Calvo, E. (2008). *Principles of Oncologic Pharmacotherapy* in Pazdur R., Wagman, L.D., Camphausen, K.A., Hoskins, W.J. (Eds) *Cancer Management: A Multidisciplinary Approach*. 11 edition.

Turgut, Z., Pelit, E., Koycu, A. (2007). Synthesis of new 1,3-disubstituted-2,3-dihydro-1H-naphth[1,2e] [1,3]oxazines. *Molecules,* 12:345-352.

Verma, R.S., Khan, Z.K., Singh, A.P. (Ed). (1998). *Antifungal Agents: Past, Present and Future Prospects, National Academy of Chemistry and Biology*, Lucknow, India. 55.

Young, S.D., Britcher, S.F., Tran, L.O., Payne, L.S., Lumma, W.C., Lyle, T.A., Huff, J.R., Anderson, P.S., Olsen, D.B., Carrol, S.S., Pettibone, D.J., O'Brien, J.A., Ball, R.G., Balani, S.K., Lin, J.H., Chen, L.W., Schleif, W.A., Sardana, V.V., Long, W.J., Byrnes, V.W., Emini, E.A. (1995). A novel, highly potent nonnucleoside inhibitor of the

human immunodeficiency virus type 1 reverse transcriptase. *Antimicrobial and Agents Chemotherapy,* 39:2602-2605.

Zhang, P., Terefenko, E. A., Fensome, A., Wrobel, J., Winneker, R., Zhang, Z. (2003). Novel 6-aryl-1,4-dihydrobenzo[*d*][and]oxazine-2-thiones as potent, selective, and orally active nonsteroidal progesterone receptor agonists. *Bioorganic and Medicinal Chemistry letters,* 13:1313-1316.
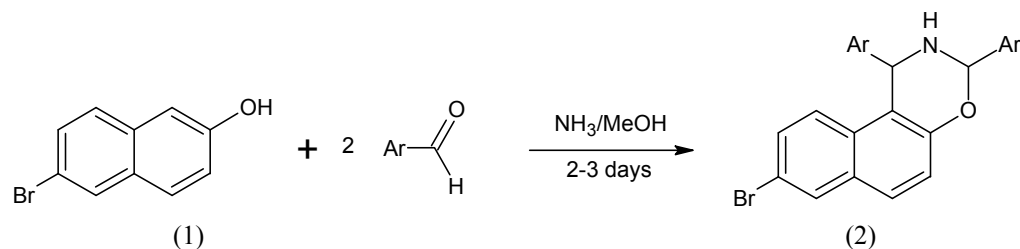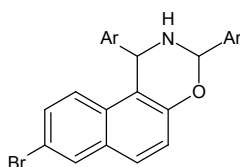

Scheme 1
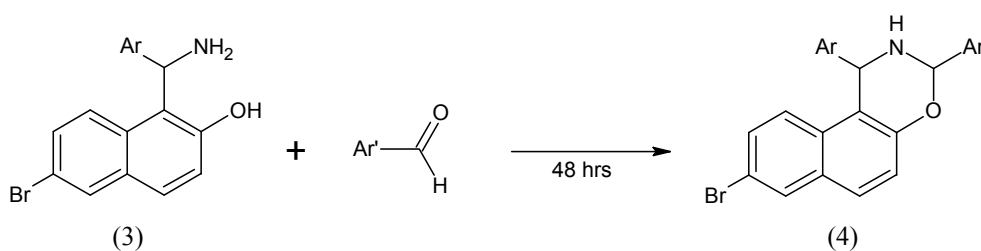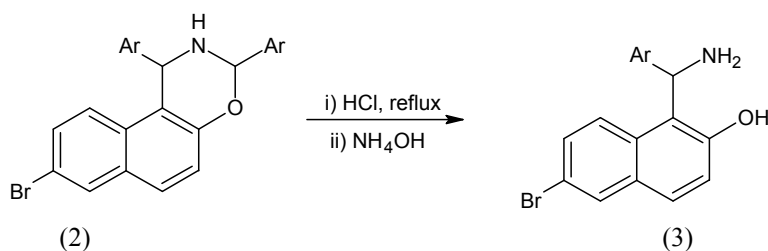
Scheme 2

Table 1. Characterization data of compounds 2a-n

Compd.	Ar	m. p. (°C)	Yield %	Mol. formula	Elemental analysis % found (calculated)		
					C	H	N
2a		150-152	51	$C_{24}H_{18}BrNO$	69.19 (69.24)	4.31 (4.35)	3.34 (3.36)
2b		106-108	46	$C_{24}H_{16}BrCl_2NO$	59.39 (59.41)	3.31 (3.32)	2.89 (2.88)
2c		88-90	52	$C_{26}H_{22}BrNO_3$	65.48 (65.55)	4.61 (4.66)	2.90 (2.94)
2d		162-164	56	$C_{26}H_{22}BrNO_3$	65.50 (65.55)	4.60 (4.66)	2.92 (2.94)
2e		148-150	40	$C_{24}H_{16}Br_3NO$	50.20 (50.21)	2.79 (2.80)	2.43 (2.43)
2f		118-120	65	$C_{20}H_{14}BrNO_3$	60.61 (60.62)	3.52 (3.56)	3.51 (3.53)
2g		132-134	48	$C_{28}H_{26}BrNO_5$	62.65 (62.69)	4.88 (4.88)	2.59 (2.61)
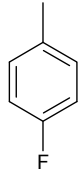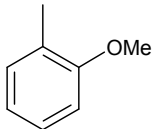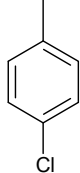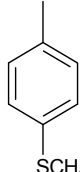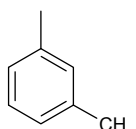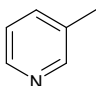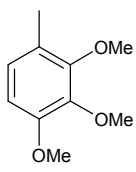
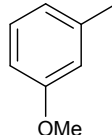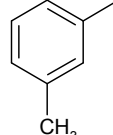|						
2h		162-164	50	$C_{24}H_{16}BrF_2NO$	63.70 (63.73)	3.55 (3.56)	3.01 (3.09)
2i		130-132	49	$C_{26}H_{22}BrNO_3$	65.51 (65.55)	4.60 (4.66)	2.93 (2.94)
2j		172-174	60	$C_{24}H_{16}BrCl_2NO$	59.38 (59.41)	3.31 (3.32)	2.85 (2.88)
2k		156-158	41	$C_{26}H_{22}BrNOS_2$	61.39 (61.41)	4.33 (4.36)	2.71 (2.75)
2l		124-126	49	$C_{26}H_{22}BrNO$	70.26 (70.27)	4.96 (4.99)	3.11 (3.15)
2m		118-120	40	$C_{22}H_{16}BrN_3O$	63.15 (63.17)	3.84 (3.85)	10.01 (10.04)
2n		138-140	48	$C_{30}H_{30}BrNO_7$	60.39 (60.41)	5.03 (5.06)	2.31 (2.34)

Table 2. Substituents Ar and Ar' of compounds 4a-e

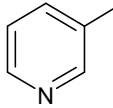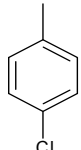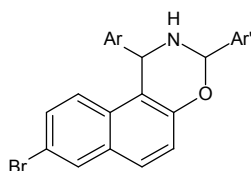| Compound	4a	4b	4c	4d	4e
Ar	OMe	OMe	OMe	CH₃	CH₃
Ar'	Cl	CH₃	N	N	Cl
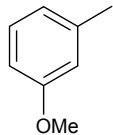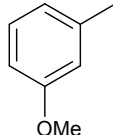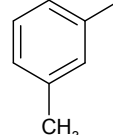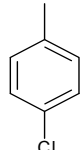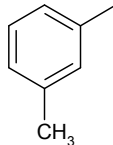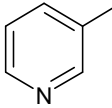
Table 3. Characterization data of compounds 4a-e

Compound	m.p. (°C)	Yield %	Mol. formula	Elemental analysis % found (calculated)		
				C	**H**	**N**
4a	152-154	68	$C_{25}H_{19}BrClNO_2$	62.44 (62.45)	3.96 (3.98)	2.90 (2.91)
4b	114-116	69	$C_{26}H_{22}BrNO_2$	67.81 (67.83)	4.79 (4.81)	3.01 (3.04)
4c	134-136	52	$C_{24}H_{19}BrN_2O_2$	64.42 (64.42)	4.27 (4.28)	6.24 (6.26)
4d	120-122	60	$C_{24}H_{19}BrN_2O$	66.81 (66.83)	4.42 (4.44)	6.48 (6.49)
4e	156-158	65	$C_{25}H_{19}BrClNO$	64.59 (64.60)	4.10 (4.12)	3.02 (3.01)

Table 4. Antibacterial activity of the compounds 2a-n and 4a-e at 10 µg/ml concentration. (Diameter of zone of inhibition in mm)

Compound	*E.coli*	*S.aureus*	*K.pneumoniae*	*P.aeruginosa*
2a	-	-	-	-
2b	11	9	10	11
2c	6	9	10	10
2d	12	13	9	13
2e	-	-	-	-
2f	9	8	8	6
2g	12	11	11	10
2h	18	15	16	12
2i	12	13	9	11
2j	16	19	11	18
2k	-	-	-	-
2l	16	15	16	16
2m	11	10	10	10
2n	13	15	11	12
4a	14	14	12	10
4b	16	14	11	12
4c	14	12	14	14
4d	12	15	14	14
4e	18	12	18	16
Ciprofloxacin	24	27	24	20

Table 5. Antifungal activity of the compounds 2a-n and 4a-e at 10 µg/ml concentration. (Diameter of zone of inhibition in mm)

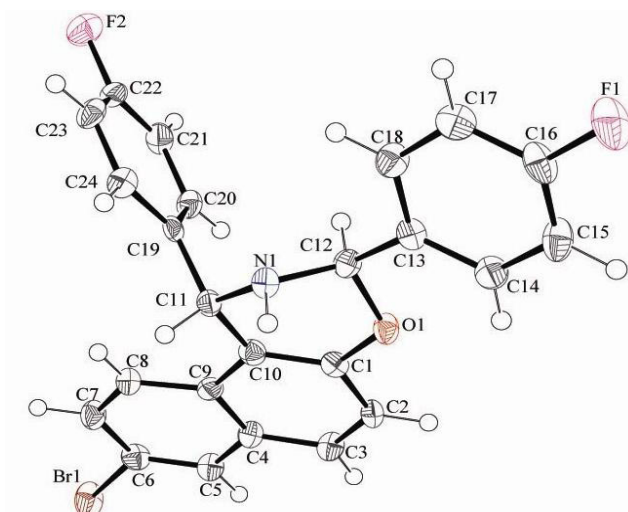| Compound	*Penicillium*	*Trichophton*	*Aspergilus Flavus*	*Aspergilus Fumigatus*
2a	-	-	-	-
2b	11	9	10	11
2c	6	9	10	10
2d	12	13	9	13
2e	-	-	-	-
2f	9	8	8	6
2g	12	11	11	10
2h	19	15	18	12
2i	15	13	9	11
2j	16	12	18	12
2k	-	-	-	-
2l	16	15	16	16
2m	11	10	10	10
2n	13	15	11	12
4a	14	14	12	14
4b	16	14	11	12
4c	14	12	14	14
4d	10	15	14	14
4e	16	15	18	18
Fluconazole	21	18	21	20

Figure 1. Molecular structure of 2h showing 50% displacement ellipsoids for the non-hydrogen atoms
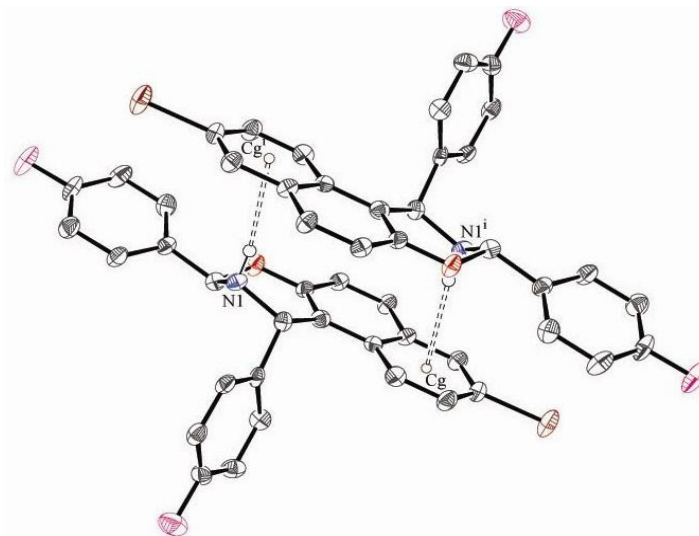

Figure 2. N–H···π interactions in the crystal of 2h

Application of Sulfonic Acid Functionalized Nanoporous Silica (SBA-Pr-SO₃H) for One-Pot Synthesis of Quinoxaline Derivatives

Ghodsi Mohammadi Ziarani (Corresponding author)

Department of Chemistry, Alzahra University

Vanak Square, Tehran, PO Box: 1993891176, Iran

Tel: 98-21-8804-1344   E-mail: gmziarani@gmail.com

Alireza Badiei

School of Chemistry, College of Science, University of Tehran, Tehran, Iran

E-mail: abadiei@khayam.ut.ac.ir

Mahbobeh Haddadpour

Department of Chemistry, Alzahra University, Vanak Square, Tehran, Iran

Abstract

Sulfonic acid functionalized SBA-15 (SBA-Pr-SO₃H) with pore size 6 nm was proved to be an efficient heterogeneous nanoporous solid acid catalyst in the synthesis of quinoxaline derivatives from the reaction of *o*-Phenylenediamines with 1, 2-diketone compounds in very good yields.

Keywords: One pot synthesis, Quinoxaline derivatives, SBA-Pr-SO₃H, Nanoporous solid acid catalyst

1. Introduction

Quinoxalines exhibit a wide range of biological activities. In the core part of many agrochemicals and pharmaceuticals were found quinoxaline ring.(Sakata *et al.* 1988; Sato *et al.* 1996; Seitz *et al.* 2002; Gazit *et al.* 1996) Similarly, it was found that quinoxaline ring also exists in antibiotics, such as actinomycin, levomycin, and echinomycin (Brown *et al.* 2004) . Its derivatives have been used as anti-viral (Lindsley *et al.* 2005) and anticancer agents (Loriga *et al.* 1997). In addition, they are used in dyes (Katoh *et al.* 2000) and organic semiconductors (Dailey *et al. 2001*). In the literature, different methods for the preparation of quinoxaline derivatives have been published (Porter *et al.*1984). The general method for the synthesis of quinoxalines is the condensation of aryl 1, 2-diamines with 1, 2-dicarbonyl compounds in refluxing ethanol in the presence of acetic acid (Brown *et al.* 2004). The yields of products were not good. Improved methods have been reported using the different catalysts including I₂ (Bhosale *et al.* 2005, More *et al.* 2005), SA (Darabi *et al.* 2007), Montmorillonite K-10 (Huang *et al.* 2008), polyaniline-sulfate salt (Srinivas *et al.* 2007), H₆P₂W₁₈O₆₂. 24H₂O (Heravi *et al.* 2007), InCl₃ (Hazarika *et al.* 2007), MnCl₂ (Heravi *et al.* 2008), CuSO₄.5H₂O (Heravi *et al.* 2007), Zn[(L)proline] (Heravi *et al.* 2007), CAN (More *et al.* 2006), Ga(OTf)₃ (Cai *et al.* 2008), PEG-400 (Zhang *et al.* 2010), Pd(OAc)₂ (Robinson *et al.* 2005), MnO₂ (Raw *et al.* 2003), keggin heteropoly acid (Huang *et al.* 2009), and IBX (Heravi *et al.* 2006) have been explored. In continuation of our studies (Mohammadi *et al.* 2008, 2009), on the application of nanoporous heterogeneous solid catalyst to organic synthesis, in this paper we want to report an efficient method for the preparation of quinoxaline derivatives using SBA-Pr-SO₃H as a nanoporous heterogeneous acid catalyst. There are only a few reports about the application of several types of sulfonic acid functionalized ordered mesoporous silicas as nano acid catalyst in chemical transformations (Van Rhijn *et al.* 1998, Das *et al. 2006*). For example, SBA-Pr-SO₃H has been used in the synthesis of chromenes from chromanols (Kureshy *et al.* 2009), and the von Pechmann Reaction (Karimi *et al.* 2008).

The high ordered nanoporous silica, such as MCM-41(Beck *et al.* 1992), LUS-1(Reinert *et al.* 2003, Bonneviot *et al.* 2001) and SBA-15 (Zhao *et al.* 1998) are unique inorganic solid supports that have very high surface area with controllable pore sizes between 2 to 30 nm. They can be used as catalysts (Trong On *et al.* 2001, Mohammadi *et al.* 2007), for the preconcentration of metals (Ganjali *et al.* 2006, 2004, 2006), and as modified carbon electrodes (Badiei *et al.* 2005, Zhang *et al.* 2006, Walcarius *et al.* 1999). The SBA-15 is new nanoporous silica with hexagonal structure, large pore, high surface area, high thermal stability and also diffusion free due to thicker pore walls and larger pore

size respectively. This can be prepared by using commercially available triblock copolymer Pluronic P126 as a structure directing agent (Zhao *et al.* 1998). Integration of acidic functional groups (e.g., -SO$_3$H) into SBA-15 has been explored to produce promising solid acids. The sulfonic acid functionalized SBA-15 were usually synthesized through direct synthesis or post-grafting (Lim *et al.* 1998, Wight *et al.* 2002).

2. Experimental section

Characterization

IR spectra were recorded from KBr disk using a FT-IR Bruker Tensor 27 instrument. Melting points were measured by using the capillary tube method with an electro thermal 9200 apparatus. The ^{1}H NMR (250 MHz) was run on a Bruker DPX, 250 MHz. Weight change curve in nitrogen was measured on a TA instrument of TGA Q50 V6.3 with maximum heating rate of 20°C/min. Nitrogen adsorption and desorption isotherms were measured at -196°C using a Japan Belsorb II system after the samples were vacuum dried at 150°C overnight.

2.1 Preparation of SBA-15

The synthesis of SBA-15 was carried out in accordance to the earlier reports (Zhao *et al.* 1998). In a typical synthesis batch, triblock copolymer surfactant as a template (P123 = EO$_{20}$PO$_{70}$EO$_{20}$, M$_{ac}$=5800) (4.0 g) was dissolved in 30 g of water and 120 g of 2 M HCl solution. Then, TEOS (tetraethylorthosilicate) (8.50 g) was added to reaction mixture which was stirred for 8 h at 40 °C. The resulting mixture was transferred into a Teflon-lined stainless steel autoclave and kept at 100 °C for 20 h without stirring. The gel composition P123: HCl: H$_2$O: TEOS was 0.0168 : 5.854 : 162.681: 1 in molar ratio. After cooling down to room temperature, the product was filtered, washed with distilled water and dried overnight at 60 °C in air. The as-synthesized sample was calcinated at 550 °C for 6 h in air atmosphere to remove the template.

2.2 Functionalization of the SBA-15 by organic groups

Functionalization of the SBA-15 catalyst was schematically shown in Fig. 1. The calcinated SBA-15 (2 g) and (3-mercaptopropyl)trimethoxysilane (10 ml) in dry toluene (20 ml) were refluxed for 24 h. The product was filtered and extracted for 6h in CH$_2$Cl$_2$ using a soxhlet apparatus, then dried under vacuum. The solid product was oxidized with H$_2$O$_2$ (excess) and one drop of H$_2$SO$_4$ in methanol (20 ml) for 24 h at rt and then the mixture was filtered and washed with H$_2$O, and acetone. The modified SBA-15-Pr-SO$_3$H was dried and used as nanoporous solid acid catalyst in the following reaction.

2.3 General procedure for the preparation of quinoxaline derivatives

The SBA-Pr-SO$_3$H (0.02 g) was activated in vacuum at 100°C and then after cooling to room temperature, 1,2-dicarbonyl (1 mmol), aromatic 1,2-diamine(1 mmol), dichloromethane (5 ml) was added to the catalyst. The mixture of reaction was stirred at the room temperature. The progress of reaction was monitored by TLC. The reaction mixture was filtered in order to recover the catalyst and the filtrate was evaporated on vacuum to obtain the crude product which is recrystallized from ethanol to afford pure quinoxaline **3**. The catalyst was washed subsequently with diluted acid solution, distilled water and then acetone, dried under vacuum and re-used for several times without loss of significant activity.

2.4 Spectral Data for Selected Products

3a: 2, 3-Diphenyl-quinxaline, White solid; m.p: 128-129 °C**; IR (KBr, cm^{-1}):** ν_{max}= **3054**, 1544, 1343, 767, 730 cm^{-1}. **^{1}H NMR (250 MHz, CDCl$_3$):** δ = 7.42-7.53 (m, 6H), 7.61-7.67 (m, 4H), 7.87-7.94 (m, 2H), 8.28-8.34 (m, 2H) ppm. **MS (m/e):** 282 (M$^+$), 205, 179, 156, 140, 76, 50.

3b: 6-Nitro- 2, 3-diphenylquinoxaline; Light brown solid; **m.p:** 101-193 °C; **IR (KBr, cm^{-1}):** ν_{max}= **3059**, 2923, 1522, 1342, 697 cm^{-1}. **^{1}H NMR (250 MHz, CDCl$_3$):** δ (ppm) = 9.2 (d, 1H), 8.53 (dd, 1H), 8.39 (d, 1H), 7.6 (m, 4H), 7.42 (m, 6H). **MS (m/e):** 327 (M$^+$), 297, 281, 224, 207, 178, 140, 75, 51.

3c: 6-Methyl-2, 3-diphenylquinoxaline; Light yellow solid; **m.p:** 117-118 °C; **IR (KBr, cm^{-1}):** ν_{max}= 3055, 2921, 1617, 1486, 1341, 752, 699 cm^{-1}. **^{1}H NMR (250 MHz, CDCl$_3$):** δ (ppm) = 8.07 (d, 1H), 7.94 (s, 1H), 7.57-7.61 (dd, 1H), 7.48-7.52 (m, 4H), 7.29-7.35 (m, 6H), 2.35 (s, 3H, CH$_3$). **MS (m/e):** 296 (M$^+$), 219, 192, 165, 89.

3d: 2, 3- Bis(4-methoxy-phenyl)-6-nitroquinoxaline; Yellow solid; **m.p:** 192-194 °C; **IR (KBr, cm^{-1}):** ν_{max}= 2930, 1603, 1523, 1341, 1174, 1024, 836 cm^{-1}. **^{1}H NMR (250 MHz, CDCl$_3$):** δ (ppm) = 9.1 (d, 1H), 8.49 (dd, 1H), 8.24 (d, 1H), 7.56 (m, 4H), 6.98 (m, 4H). **MS (m/e):** 387 (M$^+$), 356, 342, 327, 312, 296, 282,207, 44.

3e: 2, 3- Bis(4-methoxy-phenyl)-6-nitroquinoxaline; Yellow solid; **m.p:** 192-194 °C; **IR (KBr, cm^{-1}):** ν_{max}= 2930, 1603, 1523, 1341, 1174, 1024, 836 cm^{-1}. **^{1}H NMR (250 MHz, CDCl$_3$):** δ (ppm) = 9.1 (d, 1H), 8.49 (dd, 1H), 8.24 (d, 1H), 7.56 (m, 4H), 6.98 (m, 4H). **MS (m/e):** 387 (M$^+$), 356, 342, 327, 312, 296, 282, 207, 44.

3f: 2, 3- Bis(4-fluoro-phenyl)quinoxaline; White solid; **m.p:** 135-137 °C; **IR (KBr, cm^{-1}):** ν_{max}= 3063, 1600, 1552, 1510, 1343, 1225, 842, 764 cm^{-1}. **^{1}H NMR (250 MHz, CDCl$_3$):** δ (ppm) = 8.2 (dd, 2H), 7.82 (dd, 2H), 7.52 (dd, 4H), 7.05 (dd, 4H). **MS (m/e):** 318 (M$^+$), 300, 223, 197, 177, 159, 76, 50.

3g: 2, 3- Bis(4-fluoro-phenyl)-6-nitroquinoxaline; Light yellow solid; **m.p:** 173-175 °C; **IR (KBr, cm^{-1}):** ν_{max}= 3054, 2930, 1606, 1513, 1342, 1248, 833 cm^{-1}. **^{1}H NMR (250 MHz, CDCl$_3$):** δ (ppm) = 9.1 (d, 1H), 8.56 (dd, 1H), 8.3 (d, 1H), 7.6 (m, 4H), 7.1 (m, 4H). **MS (m/e):** 363 (M$^+$), 348, 333, 317, 297, 242, 196, 75.

3h: 2, 3- Bis(4-fluoro-phenyl)-6-methyquinoxaline; White solid; **m.p:** 165-167 °C; **IR (KBr, cm^{-1}):** ν_{max}= 3056, 1566, 1524, 1384, 1221, 1159, 836 cm^{-1}. **^{1}H NMR (250 MHz, CDCl$_3$):** δ (ppm) = 8.05 (d, 1H), 7.92 (s, 1H), 7.59-7.63 (dd, 1H), 7.63-7.51 (m, 4H), 7.01-7.09 (m, 4H), 2.62 (s, 3H). **MS (m/e):** 332 (M$^+$), 313, 237, 211, 183, 166, 89, 75.

3i: 2, 3- Bis(4-chloro-phenyl) quinoxaline; White solid; **m.p:** 194-196 °C; **IR (KBr, cm^{-1}):** ν_{max}= 3061, 1590, 1488, 1341, 1087, 828, 759 cm^{-1}. **^{1}H NMR (250 MHz, CDCl$_3$):** δ (ppm) = 8.14-8.18 (dd, 1H),7.77-7.81 (dd, 1H), 7.45-7.49 (dd, 2H), 7.33-7.36 (dd, 2H); **MS (m/e):** 350 (M$^+$), 331, 315, 279, 239, 213, 178,151, 76, 50.

3j: 2, 3- Bis(4-choloro-phenyl)-6-nitroquinoxaline; Yellow solid; **m.p:** 174-176 °C; **IR (KBr, cm^{-1}):** ν_{max}= 3088, 1527, 1341, 1090, 832 cm^{-1}. **^{1}H NMR (250 MHz, CDCl$_3$):** δ (ppm) = 9.05 (d, 1H), 8.51-8.55 (dd, 1H), 8.26-8.29 (d, 1H), 7.54-7.6 (m, 2H), 7.05-7.12 (m, 2H). **MS (m/e):** 396 (M$^+$), 364, 350, 316, 240, 213, 178, 75, 50.

3k: 2, 3- Bis(4-Chloro-phenyl)-6-nitroquinoxaline; Yellow solid; **m.p:** 174-176 °C; **IR (KBr, cm^{-1}):** ν_{max}= 3088, 1527, 1341, 1090, 832 cm^{-1}. **^{1}H NMR (250 MHz, CDCl$_3$):** δ (ppm) = 9.05 (d, 1H), 8.51-8.55 (dd, 1H), 8.26-8.29 (d, 1H), 7.54-7.6 (m, 2H), 7.05-7.12 (m, 2H). **MS (m/e):** 396 (M$^+$), 364, 350, 316, 240, 213, 178, 75, 50.

3l: 2, 3- Bis(4-Chloro-phenyl)-6-methylquinoxaline; White solid; **m.p:** 176-178 °C; **IR (KBr, cm^{-1}):** ν_{max}= 2923, 1484, 1340, 1088, 831 cm^{-1}. **^{1}H NMR (250 MHz, CDCl$_3$):** δ (ppm) = 8.05 (d, 1H), 7.92 (s, 1H), 7.59-7.63 (dd, 1H), 7.63-7.51 (m, 4H), 7.3-7.35 (m, 4H), 2.62 (s, 3H); **MS (m/e):** 364 (M$^+$), 349,329, 293, 227, 192, 165, 146, 89, 76.

3. Results and Discussion

At the beginning of this work, the condensation reaction of *o*-Phenylenediamines with benzil in the presence of nanoporous acid catalyst of SBA-Pr-SO$_3$H was employed as the model reaction to screen the suitable reaction conditions (scheme 1). A plausible mechanism was shown in scheme 2. Among different conditions, we found using CH$_2$Cl$_2$ as solvent in room temperature give the best result on the yields and time of the reaction (Table 1) and then these conditions were chosen as the optimized condition. Thus, under the optimized reaction conditions, this reaction was effected using various 1,2-diamines and 1,2-dicarbonyl compounds, and the results were summarized in Table 2. It can be seen when the electron-donating substituents present in diamine part, increased yields of products were observed, whereas the effect was reverse with the electron withdrawing substituent. On the other hand, substituents on aromatic 1, 2-diketone had no significant effect on the product yields.

The efficiency of various catalysts in synthesis of quinoxalines derivatives has been compared in Table 3. The best yield and short reaction time is attributed to the high efficiency of the nano-catalyst of SBA-Pr-SO$_3$H.

Preparation and characterization of catalyst

Pure Nanoporous compound SBA-15 was synthesized with triblock poly(ethylene oxide)-b-poly(propyleneoxide)-bpoly(ethyleneoxide) copolymer (Pluronic, EO$_{20}$PO$_{70}$EO$_{20}$, P123) as the template (Zhao *et al.* 1998). A schematic illustration for the preparation of SBA-Pr-SO$_3$H was shown in Fig. 1. First, the calcined SBA-15 silica was functionalized with (3-mercaptopropyl)trimethoxysilane (MPTS) and then, the thiol groups were oxidized to sulfonic acid by hydrogen peroxide.

The TGA analysis of SBA-Pr-SO$_3$H confirmed the amount of organic groups on SBA-15. The weight reduction in the temperature range between 200-600°C (about 15%) indicated that the amount of organic group was 1.2 mmol/g.

The nitrogen adsorption–desorption isotherm SBA-Pr-SO$_3$H (Fig. 2) shows type-IV adsorption behavior with the hysteresis loops appearing at relatively high pressure, suggesting that the prepared samples have regular mesoporous framework structures. The surface area, average pore diameter calculated by the BET method and pore volume of SBA-Pr-SO$_3$H are 440 m^{2}g^{-1}, 6.0 nm and 0.660 cm^3 g^{-1}, respectively, which are smaller than those of SBA-15 due to the immobilization of sulfonosilane groups into the pores. Table 4 shows the obtained results from the nitrogen adsorption studies at -196 °C.

4. Conclusion

In summary, we have described the use of nano acid Catalyst of SBA-Pr-SO$_3$H in the synthesis of quinoxaline derivatives under mild conditions. SBA-Pr-SO$_3$H was proved to be an efficient heterogeneous nanoporous solid acid

catalyst with pore size of 6 nm. Furthermore, excellent yields, mild reaction conditions, short reaction times and easy work-up procedures make it, a facile and superior method for the synthesis of quinoxalines as compared in Table 3.

Acknowledgements

References

Badiei, A., Norouzi, P., Tousi, F. (2005). Study of Electrochemical Behavior and Adsorption Mechanism of $[Co(en)_2Cl_2]^+$ on Mesoporous Modified Carbon Paste Electrode. *Eur. J. Sci. Res.,* 12, 39-45.

Beck, S., Vartuli, J. C., Roth, W. J., Kresge, C. T., Leonowicz, M. E., Schmitt, K. D., Chu, C. T-W., Olson, D. H., Sheppard, E. W., McCullen, S. B., Higgins, J. B., Schlenker, J. L. (1992). A new family of mesoporous molecular sieves prepared with liquid crystal templates. *J. Am. Chem. So*c., 114, 10834-10843.

Bhosale, R. S., Sarda, S. R., Ardhapure, S. S., Jadhav, W. N., Bhusare, S. R., Pawar, R. P. (2005). An efficient protocol for the synthesis of quinoxaline derivatives at room temperature using molecular iodine as the catalyst. *Tetrahedron Lett*., 46, 7183-7186.

Bonneviot, L., Morin, M., Badiei, A. (2001). Mesostructured Metal or Non-Metal Oxides and Method for Making Same. Patent WO 01/55031 A1.

Brown In, J. D., Taylor, C. E., Wipf, P., Eds. (2004). *The Chemistry of Heterocyclic Compounds Quinoxalines*: Supplements II, John Wiley and Sons: New Jersey.

Brown, D. J. (2004). Q*uinoxalines: Supplement II. In The Chemistry of Heterocyclic Compounds*; Taylor, E. C., Wipf, P., Eds.; John Wiley & Sons: New Jersey.

Cai, J.-J., Zou, J.-P., Pan, X.-Q., Zhang, W. (2008). Gallium (III) triflate-catalyzed synthesis of quinoxaline derivatives. *Tetrahedron Lett*., 49, 7386–7390.

Dailey, S., Feast, W. J., Peace, R. J., Sage, I. C., Till, S., Wood, E. L. (2001). Synthesis and device characterisation of side-chain polymer electron transport materials for organic semiconductor applications. *J. Mater. Chem.*, 11, 2238-2243.

Darabi, H. R., Mohandessi, S., Aghapoor, K., Mohsenzadeh, F. (2007). A recyclable and highly effective sulfamic acid/MeOH catalytic system for the synthesis of quinoxalines at room temperature, *Catal. Commun.,* 8, 389-392.

Das, B., Venkateswarlu, K., Holla, H., Krishnaiah, M. (2006). Sulfonic acid functionalized silica: A remarkably efficient heterogeneous reusable catalyst for α-monobromination of carbonyl compounds using *N*-bromosuccinimide, *J. Mol. Catal. A: Chem.,* 253, 107-111.

Gangali, M. R., Hajiagha Babaei, L., Badiei, A., Mohammadi Ziarani, G., Tarlani, A. (2004). Novel Method for the Fast Preconcentration and Monitoring of a ppt Level of Lead and Copper with a Modified Hexagonal Mesoporous Silica Compound and Inductively Coupled Plasma Atomic Emission Spectrometry, *Anal. Sci.,* 20, 725-729.

Ganjali, M. R., Daftari, A., Hajiagha Babaei, L., Badiei, A., Saberyan, K., Mohammadi Ziarani, G., Moghimi, A. (2006). Pico level monitoring of silver with modified hexagonal mesoporous compound (MCM-41) and inductiviely coupled plasma atomic emission spectrometry, *Water, Air, Soil Pollut.,* 173, 71-80.

Ganjali, M. R., Hajiagha Babaei, L., Badiei, A., Saberian, K., Behbahani, S., Mohammadi Ziarani, G., Salavati-Niasari, M. (2006). A novel method for fast enrichment and monitoring of hexavalent and trivalent chromium at the PPT level with modified silica MCM-41 and its determination by inductively coupled plasma optical emission spectrometry, *Quim. Nova*, 29, 440-443.

Gazit, A., App, H., McMahon, G., Chen, J., Levitzki, A., Bohmer, F. D. (1996). Tyrphostins. 5. Potent inhibitors of platelet-derived growth factor receptor tyrosine kinase: Structure-activity relationships in quinoxalines, quinolines, and indole tyrphostins. *J. Med. Chem*., 39, 2170-2177.

Hazarika, P., Gogoi, P., Konwar, D. (2007). Efficient and green method for the synthesis of 1,5-benzodiazepine and quinoxaline derivatives in water. *Synth. Commun*., 37, 3447-3454.

Heravi, M. M., Bakhtiari, Kh., Bamoharram, F. F., Tehrani, M. H. (2007). Wells-Dawson type heteropolyacid catalyzed synthesis of quinoxaline derivatives at room temperature Monatsh. *Chem*., 138, 465-467.

Heravi, M. M., Bakhtiari, Kh., Oskooie, H. A., Taheri, Sh. (2008). $MnCl_2$-promoted synthesis of quinoxaline derivatives at room temperature, Heteroat. *Chem.*, 19, 218-220.

Heravi, M. M., Taheri, Sh., Bakhtiari, Kh., Oskooie, H. A. (2007). On Water: A practical and efficient synthesis of quinoxaline derivatives catalyzed by CuSO$_4$.5H$_2$O, *Catal. Commun*., 8, 211-214.

Heravi, M. M., Tehrani, M. H., Bakhtiari, Kh., Oskooie, H. A. (2007). Zn[(L)proline]: A powerful catalyst for the very fast synthesis of quinoxaline derivatives at room temperature, *Catal. Commun*., 8, 1341-1344.

Heravi, M., Bakhtiari, Kh., Tehrani, M. H., Javadi, N. M., Oskooie, H. (2006). Facile synthesis of quinoxaline derivatives using o-iodoxybenzoic acid (IBX) at room temperature, *ARKIVOC*, xvi 16-22.

Huang, T.- K., Shi, L., Wang, R., Guo, X.- Z., Lu, X.- X. (2009). Keggin type heteropolyacids-catalyzed synthesis of quinoxaline derivatives in water, *Chin. Chem. Lett.*, 20, 161–164.

Huang, T. K., Wang, R., Shi, L., Lu, X. X. (2008). Montmorillonite K-10: An efficient and reusable catalyst for the synthesis of quinoxaline derivatives in water, *Catal. Commun.*, 9, 1143-1147.

Karimi, B., Zareyee, D. (2008). Design of a Highly Efficient and Water-Tolerant Sulfonic Acid Nanoreactor Based on Tunable Ordered Porous Silica for the von Pechmann Reaction, *Org. Lett.*, **10**, 3989-3992.

Katoh, A., Yoshida, T., Ohkanda, J. (2000). Synthesis of quinoxaline derivatives bearing the styryl and phenylethynyl groups and application to a fluorescence derivatization reagent. *Heterocycles*, 52, 911-920.

Kureshy, R. I., Ahmad, I., Pathak, K., Khan, N. H., Abdi, S. H. R., Jasra, R. V. (2009). Sulfonic acid functionalized mesoporous SBA-15 as an efficient and recyclable catalyst for the synthesis of chromenes from chromanols, *Catal. Commun.*, 10, 572-575.

Lim, M. H., Blanford, C. F., Stein, A. (1998). Synthesis of Ordered Microporous Silicates with Organosulfur Surface Groups and Their Applications as Solid Acid Catalysts, *Chem. Mater.* **10**, 467-470.

Lindsley, C. W., Zhao, Z., Leister, W. H., Robinson, R. G., Barnett, S. F., Defeo-Jones, D., Jones, R. E., Hartman, G. D., Huff, J. R., Huber, H. E., Duggan, M. E. (2005). Allosteric Akt (PKB) inhibitors: Discovery and SAR of isozyme selective inhibitors. *Bioorg. Med. Chem. Lett*., 15, 761-764.

Loriga, M., Piras, S., Sanna, P., Paglietti, G. (1997). Quinoxaline chemistry. Part 7. 2-[aminobenzoates]- and 2-[aminobenzoylglutamate] quinoxalines as classical antifolate agents. Synthesis and evaluation of in vitro anticancer, anti-HIV and antifungal activity. *Farmaco*, 52, 157-166.

Mohammadi Ziarani G., Badiei A., Miralami A. (2007). The study of solvent effect on the diastereoselectivity of Diels-Alder reaction in the presence of nanoporous silica-supported cerium sulfonate catalyst, *Eur. J. Sci. Res.*, 18, 282-286.

Mohammadi Ziarani, G., Badiei, A., Abbasi, A., Farahani, Z. (2009). Cross-aldol Condensation of Cycloalkanones and Aromatic Aldehydes in the Presence of Nanoporous Silica-based Sulfonic Acid (SiO$_2$-Pr-SO$_3$H) under Solvent Free Conditions. *Chin. J. Chem.*, 27, 1537-1542.

Mohammadi Ziarani, G., Badiei, A., Khaniania, Y., Haddadpour, M. (2010). One Pot Synthesis of Polyhydroquinolines Catalyzed by Sulfonic Acid Functionalized SBA-15 as a New Nanoporous Acid Catalyst under Solvent Free Conditions, *Iran. J. Chem. & Chem. Eng.*, 29, 1-10.

Mohammadi Ziarani, G., Badiei, A., Miralami, A. (2008). A study of the Diastereoselectivity of Diels-Alder reactions on the Ce-SiO$_2$ as support. *Bull. Korean Chem. Soc.*, 29, 47-50.

More, S. V., Sastry, M. N. V., Wang, C. C., Yao, C. F. (2005). Molecular iodine: A powerful catalyst for the easy and efficient synthesis of quinoxalines, *Tetrahedron Lett.,* 46, 6345-6348.

More, S. V., Sastry, M. N. V., Yao, C. F. (2006). Cerium (IV) ammonium nitrate (CAN) as a catalyst in tap water: A simple, proficient and green approach for the synthesis of quinoxalines, *Green Chem*., 8, 91-95.

Porter, A. E. A. (1984). *In Comprehensive Heterocyclic Chemistry;* Katritsky, A. R., Rees, C.W., Eds.; Pergamon: Oxford, pp 157–197.

Raw, S. A., Wilfred, C. D., Taylor, R. J. K. (2003). Preparation of quinoxalines, dihydropyrazines, pyrazines and piperazines using tandem oxidation processes*, Chem. Commun,* 2286.

Reinert, P., Garcia, B., Morin, C., Badiei, A., Perriat, P., Tillement, O., Bonneviot, L. (2003). Cationic templating with organic counterion for superstable mesoporous silica, Nanotechnology in mesostructure Materials, *Stud. Surf. Sci. Catal.,* 146, 133-136.

Robinson, R. S., Taylor, R. J. K. (2005). Quinoxaline synthesis from α-hydroxy ketones via a tandem oxidation process using catalysed aerobic oxidation, *Synlett,* 1003-1005.

Sakata, G., Makino, K., Kurasawa, Y. (1988). Recent Progress in the Quinoline Chemistry. Synthesis and Biological Activity. *Heterocycles,* 27, 2481-2515.

Sato, N. (1996). In *Comprehensive Heterocyclic Chemistry* II; Katritzky, A. R., Rees, C. W., Scriven, E. F., Eds.; Elsevier Science Ltd: Oxford, Chapter 6.03, p 6.

Seitz, L. E., Suling, W. J., Reynolds, R. C. (2002). Synthesis and antimycobacterial activity of pyrazine and quinoxaline derivatives. *J. Med. Chem*., 45, 5604-5606.

Srinivas, C., Kumar, C. N. S. S. P., Jayathirtha Rao, V., Palaniappan, S. (2007). Efficient, convenient and reusable polyaniline-sulfate salt catalyst for the synthesis of quinoxaline derivatives, *J. Mol. Catal. A: Chem.,* 265, 227-230.

Trong On, D., Desplantier-Giscard, D., Danumah, C., Kaliaguine S. (2001). Perspectives in catalytic applications of mesostructured materials, *Appl. Catal. A: Gen.*, 222, 299-357.

Van Rhijn, W. M., De Vos, D., Sels, B. F., Bossaert, W. D., Jacobs, P. A. (1998). Sulfonic acid functionalised ordered mesoporous materials as catalysts for condensation and esterification reactions, *Chem. Commun.,* 317-318.

Walcarius, A., Despas, C., Bessiere, J. (1999). Selective monitoring of Cu((II)) species using a silica modified carbon paste electrode, *Anal. Chim. Acta*, 385, 79-89.

Wight, A. P., Davis, M. E. (2002). Design and preparation of organic-inorganic hybrid catalysts, *Chem. Rev.* 102, 3589-3614.

Zhang, H.-X., Cao, A.-M., Hu, J.-S., Wan, L.-J., Lee, S.-T. (2006). Electrochemical sensor for detecting ultratrace nitroaromatic compounds using mesoporous SiO_2-modified electrode, *Anal. Chem*., 78, 1967-1971.

Zhang, X. Z., Wang, J. X. , Sun, Y. J., Zhan, H. W. (2010). Synthesis of quinoxaline derivatives catalyzed by PEG-400, *Chin. Chem. Lett.* 21, 395–398.

Zhao, D., Huo, Q., Feng, J., Chmelka, B. F., Stucky, G. D. (1998). Nonionic triblock and star diblock copolymer and oligomeric sufactant syntheses of highly ordered, hydrothermally stable, mesoporous silica structures, *J. Am. Chem. Soc.* 120, 6024-6036.
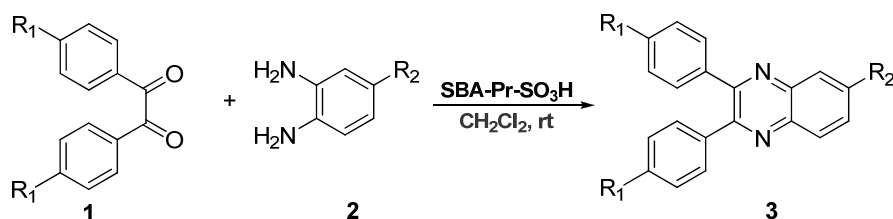
Scheme 1. Synthesis of quinoxaline derivatives using SBA-Pr-SO₃H as efficient nano acid catalyst
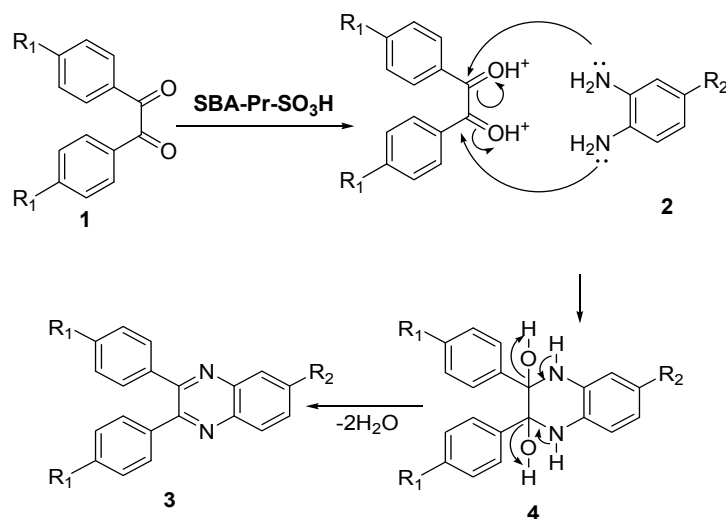
Scheme 2. The proposed mechanism

Table 1. The Optimization of reaction conditions in the synthesis 2, 3- Diphenyl-quinxaline 3

no	Solvent	T°C	time	Yield %
1	_	25	24 h	60
2	_	80	5 h	60
3	CH_2Cl_2	25	10 min	95

Table 2. The SBA-Pr-SO₃H catalyzed the synthesis of quinoxaline derivatives

Entry	R_1	R_2	Product	Time (min)	Yeild (%)	mp °C	mp Lit.
1	H	H	3a	10	95	128-129	129-128[1]
2	H	NO₂	3b	20	90	191-193	194-193[1]
3	H	CH₃	3c	5	98	117-118	118-117[1]
4	OCH₃	H	3d	15	95	150-152	152-151[1]
5	OCH₃	NO₂	3e	25	90	192-195	194-192[1]
6	OCH₃	CH₃	3f	15	95	124-126	125-127[1]
7	F	H	3g	5	97	135-137	135-137[1]
8	F	NO₂	3h	10	90	173-175	174-176[1]
9	F	CH₃	3i	5	95	165-167	165-167[1]
10	Cl	H	3j	10	95	194-196	195-196[2]
11	Cl	NO₂	3k	15	90	174-176	176[2]
12	Cl	CH₃	3l	5	95	176-178	180[2]

[1] (Heravi *et al* ARKIVOC, 2006), [2] (Heravi, *et al* Catal. Commun., 2007)

Table 3. Comparison of efficiency of various catalysts in synthesis of quinoxaline derivatives 3c

Entry	Catalyst	Condition	Time	Yield (%)	Ref.
1	polyaniline-sulfate salt	CH_2Cl_2	15 min	92	[1]
2	Montmorillonite K-10	H_2O	2.5 h	100	[2]
3	molecular iodine	DMSO	50 min	90	[3]
4	Keggin type heteropolyacids	H_2O	1 h	92	[4]
5	PEG-400	free	10-60 min	93	[5]
6	SBA-Pr-SO₃H	CH_2Cl_2	5 min	98	This work

[1](Srinivas *et al.* 2007), [2](Huang *et al.* 2008), 3(Bhosale *et al.* 2005), [4](Huang *et al.* 2009), [5](Cai *et al.* 2008)

Table 4. Porosimetery values for SBA-15 and functionalized SBA-15

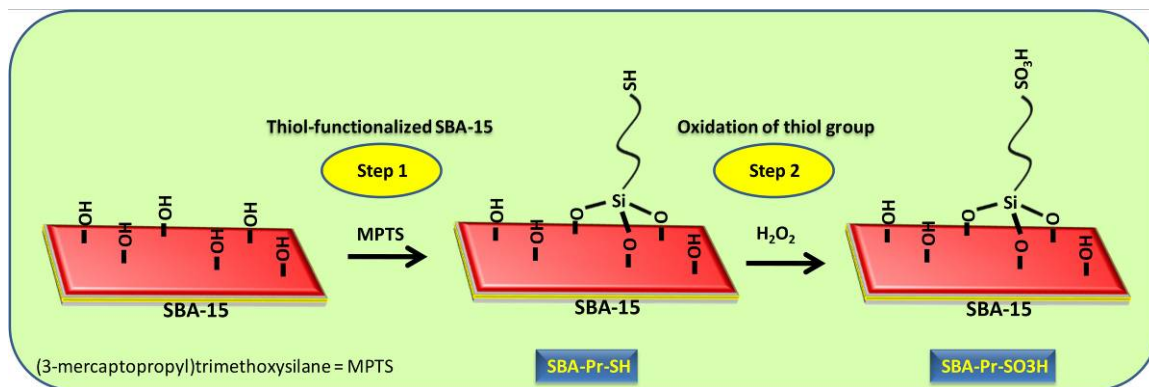|	Surface area (cm^2g^{-1})	Pore volume (cm^3g^{-1})	Pore radius (nm)
SBA-15	649	0.806	3.1
SBA-Pr-SO₃H	440	0.660	3.0

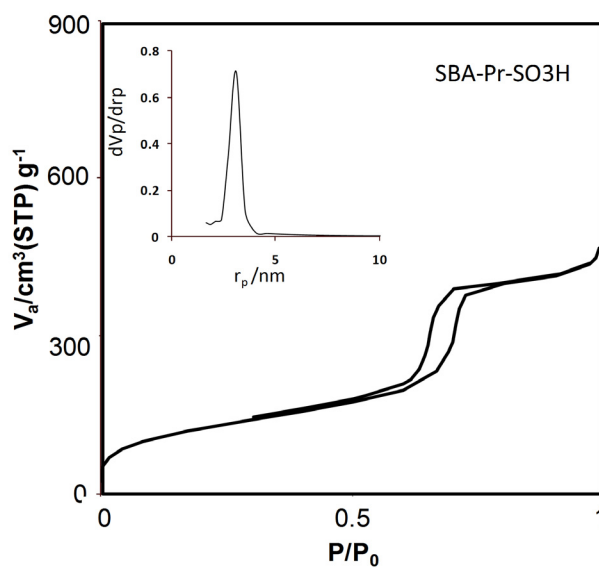Figure 1. Schematic illustration for the preparation of SBA-Pr-SO$_3$H

Figure 2. N$_2$ adsorption-desorption isotherms and pore size distribution (inset) SBA-Pr-SO$_3$H

Sodium Monobromoisocyanurate: A New Catalyst for Direct Synthesis of Aryl Thiocyanates

J. Anil Kumar (Corresponding author)

Research and Development, Acacia Life Sciences, Pvt Ltd

IDA Nacharam, Hyderabad, 500076, India

N. Srinivasan (Corresponding author)

Research and Development, Acacia Life Sciences, Pvt Ltd

IDA Nacharam, Hyderabad, 500076, India

Ch. Shanmugham

Research and Development, Acacia Life Sciences, Pvt Ltd

IDA Nacharam, Hyderabad, 500076, India

E-mail: drjak18@gmail.com

Abstract

An efficient and highly selective methods for the preparation of arylthiocyanates by thiocyanation with ammonium Thiocyanates in the presence of sodium mono bromoisocyanurate as a catalyst in methanol under mild conditions to afford the corresponding aryl and para substituted thiocyanates. The use of sodium mono bromoisocyanurate is simple and more convenient.

Keywords: Aromatic system, Aryl thiocyanates, Sodium monobromoisocyanurate (SMBI), Thiocyanation

1. Introduction

The thiocyanation of aromatics and hetero aromatics is an important carbon-hetero atom bond formation in organic synthesis. It was of interest to probe the direct thiocyantion of aromatic and hetero aromatic compounds. (Roberto, Margarita. 2000) Nucleophilic thiocyanation of phenol ethers using hypervalent iodine (III) reagents has been reported recently, thus thiocyanation of aromatic systems is of importance. Consequently several methods have been developed for the thiocyanation of arenes using a variety of reaction conditions. In contrast only a limited number of reagents such as N-Chlorosucinamide (NCS), N-Bromosuccinamide (NBS), (Yadav, J, Reddy, B. V. S, 2004) Ferric (III) chloride-promted efficient thiocyanation of aryl alkenes. (Nair, V. George., 1999; Grant, M. S, Snyder, H. R. 1960) Ceric ammonium nitrate (CAN) etc. have reported for thiocyanation of indoles and arenes.

2. Experimental

Our preliminary studies were carried out with indole (1) (3 equivalents) and of ammonium thiocyanate (3 equivalents) and sodium monobromoisocyanurate (SMBI) (1.0 equivalent) in the required minimum volume of methanol at 50 ^{O}C for 6 hours as a model substrate in order to establish the best reaction conditions. The reaction went to completion within 6 hrs at 50 ºC and the products 3-thiocyanato indole (2) was obtained in 85-90% yield (scheme 1 Table 1, entry a).

Like indoles, isatins also worked under similar conditions to give 5-thiocyanato derivatives (Table 1, entries C). Similarly anilines in the presence of SMBI and ammonium thiocyanate resulted also in the formation of aryl thiocyanates in high yield (entries d, e, and f Table 1, Scheme 2)

In the case of aryl amines, the products were obtained with high para selectivity. In all cases the products were characterized by ^{1}H NMR, IR and mass spectroscopic data and also by comparison with authentic samples.

In conclusion we have developed an efficient and improved procedure for thiocyanation of indoles and aryl compounds using sodium monobromoisocyanurate: The mild reaction condition, easy isolation of products, high yields (80-90 %), economically viability of the catalyst and wide applicability for various reactants and wide applicability of various reactants are important features of this protocol.

Melting Points were recorded Buchi R-535 apparatus and are uncorrected.IR spectra were recorded on Perkin-Elmer FT/IR-2400 spectrometer with KBr optics. ^{1}H and ^{13}C NMR spectra were recorded on a Varian Gemini – 200 spectrometer in CDCl3 using TMS as an internal standard. Mass spectra were recorded an Finnigan MAT 1020 Mass spectrum operating at 70 eV.

3. General Procedure

The indole 1(1mmol) and ammonium thiocyanate (3 mmol) were dissolved in minimum amount of methanol and treated with SMBI (3 mmol) in methanol (50 mL) at 50 ºC for 6 hrs. It was then distilled of then diluted with water (100ml) and extracted with CH_2Cl_2 (5 x25mL) .The solvent was evaporated and the residue was then recrystallised from Chloroform: Methanol.

4. Results and Discussion

3-Thiocyanato - 1H- indole (2a)

Solid; mp 125-127º C

IR(KBr):3341,3107,2924,2853,2157,1618,1503,1455,1217,758,668,589 cm-1.

^{1}H NMR (200 MHz, CDCl3) = 7.23-7.45(m, 4H), 7.80(d, 1H, J = 8.0Hz).

EIMS: m/z (%) : 174 (M^+,30)155 (25),141(30),97(20),85(27),71(36),57(94),43(100).

2-Methyl-3-thiocyanato-1H-indole (2b)

Solid; mp 102-103º C

IR(KBr):3324,2933,2151,1618,1543,1408,1229,740,651 cm-1.

^{1}H NMR (200 MHz, CDCl3) = 2.48(s, 3H) 7.15(m, 3H), 7.70(d, J = 8.1Hz 1H).8.48 (brs, 1H, NH)

EIMS: m/z (%): 188 (M^+, 100)156 (18), 77(14).

5-Thiocyanato-2, 3-indolidine (2c)

Solid; mp 203-204º C

IR(KBr):3447, 2924, 2165,1618,1460,771 cm-1.

^{1}H NMR (200 MHz, DMSO-$d6$) = 7.05 (d, 1H, J = 8.1Hz, 1H), 7.65-7.75(m, 2H) 11.35   (brs, 1 H, NH)

EIMS: m/z (%) : 204 (M^+,20)180 (80),176(35),135.(30),109(10),88(100),71(60),43(50).

2-Chloro – 3-methyl-4-thiocyanatoaniline (2d)

Solid; mp 112-113º C

IR(KBr):3382,2148,1632,1578,1461,1394,1302,1109,811,593 cm-1.

^{1}H NMR (200 MHz,CDCl$_3$) = 2.45(,3H),3.85(brs,2H,NH2),6.60(d,J=8.2Hz,1H),   7.35(d,J = 8.2Hz,1H)

References

Ardeshir Khazaei, Abdolhamid Alizadeh, Ramin Ghorbani Vaghei. (2001). *Molecules,* 6, 253-257.

Biswanath Das, Avula Satya Kumar. (2010). *Synth. Commun*, *40*. 337– 341.

Chakrabarthy, M, Sarkar, S. (2003). *Tetrahedron Lett*, *44*, 8131-8133.

Cheeseman, G.W.H, Hawi, A.A, Varvounis, G. (2009). *Journal of Heterocyclic Chemistry*, 22, 423-427

Emil Popovski, Jane Bogdanov, Metodija Najdoski, Evamarie Hey- Hawkins. (2006). *Molecules*, 6, *11*, 279-285.

Grant, M. S, Snyder, H. R. (1960). *J. Am. Chem. Soc*, *82*, 2742-2744.

Guy, R. G, Thompson, J. J. (1978). *34*, 541-546.

Habib Firouzabadi, Nasser Iranpoor, Sara Sobhani. (2004). *Synthesis*, 292-294.

Hamid R. Memarian, Iraj Mohammadpoor-Baltork, Kobra Nikoofar. (2008). *15*, 456-462.

Hitomi Suzuki, Hajime, Abe. (1996). *Synth. Commun*, *26*, 3413-3419.

Hosseini-Sarvari, Mona; Tavakolian, Mina. (2008). *Journal of Chemical Research*, *6*, 318-321.

Iranpoor Nasser, Firouzabadi Habib, Azadi Roya. (2006). *Tetrahedron Lett*, *47*, 5531-5534.

James, H. Clark, Craig, W. Jones. Catherine, V. A. Duke, Jack, M. Miller. (1989). *J. Chem. Soc*., *Chem. Commun*., 81-82.

Jeremy Chmielewski, Michelle Haun Krista Topmiller, Jacob Ward, Kevin M. Church. (2002). *Synth. Commun*, *32*, 343 – 353.

Jhillu S. Yadav, Basi V. Subba Reddy, Bala Murali Krishna, B. (2008). *Synthesis*, 3779-3782.

Jhilu S. Yadav, Basi V. Subba Reddy, Ummareddy V.Subba Reddy, Darshanoju N. Chary. (2008). *Synthesis*, 1283-1287,

Kelly, T.R. Kim, T.R, Curtis, A.D.M. (1993). *J.Org.Chem*, 58, 5855-5858.

Kita Y, Takada T, Mishra S, Whelan BA, Tohma H. (1995). *J.Org.Chem.60*, 7144-7148.

Kobra, Memarian, Hamid. R. (2007). *Canadian Journal of Chemistry*, *85*, 930-937.

Krishnan, P, Gurjar, V. G. (1993). *Journal of Applied Electrochemistry*, *23*, 268-270.

Kumar, Atul, Pathak, Seema, R. (2005). *Letters in Organic Chemistry*, *2*, 745-748.

Memarian HR, Mohammadpoor-Baltork I, Nikoofar K. (2008). *Ultrason Sonochem, 15*, 456-462.

Nair, V. George. Nair, L.G, Panicker, S. B. (1999). *Tetrahedron Let,. 40*, 1195-1196.

Om Prakash, Harpreet Kaur, Hitesh Batra, Neena Rani, Shiv P. Singh, Robert, M. Moriarty. (2001). *J. Org. Chem*, *66*, 2019–2023.

Pan, X.Q, Lei, M.-Y, Zou, J.-P, Zhang, W. (2009). *Tetrahedron Lett*, *50*, 347-349.

Pierre-Yves Renard, Hervé Schwebel, Philippe Vayron, Eric Leclerc, Sonia Dias, Charles Mioskowski. (2001). *Tetrahedron Lett*, *42*, 8479-8481.

Roberto Margarita, Chiara Mercanti, Luca Parlanti, Giovanni Piancatelli. (2000). *European J. Org. Chem*, *10, 1865*-1870.

Saldabol N.O, Popelis, J.; Slainska, V. (2002). *Chemistry of heterocyclic compounds*, *38*, 873-881.

Toste, F. Dean, Stefano, V.D, Ian, W.J.Still. (1995). *Synth.Commun*, *25*, 1277-1286.
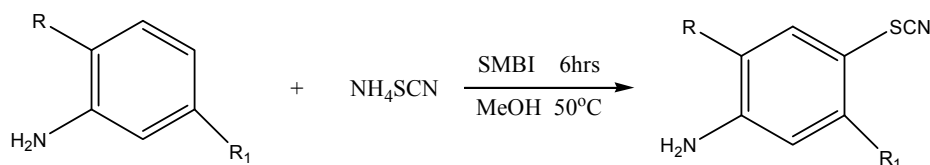
Vara Prasad, J. V. N, Panapoulous, A, John R. Rubin. (2000). *Tetrahedron Lett*, *41*, 4065-4068.

Yadav, J, Reddy, B. V. S, Manoj Kumar Gupta. (2004). *Synthesis*, 1983-1986.

Yadav, J.S, Reddy, B.V.S, Shubashree, S, Sadashiv, K. (2004). *Tetrahedron Lett*, *45*, 2951-2954.
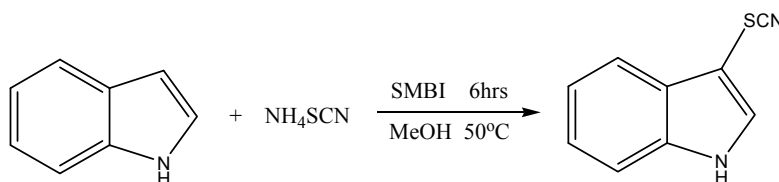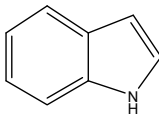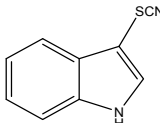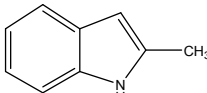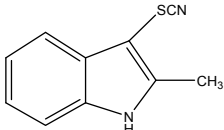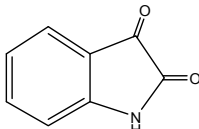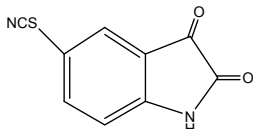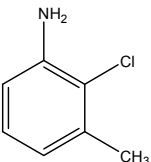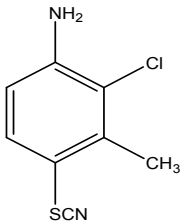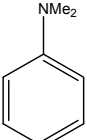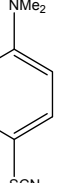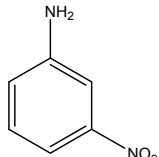
Scheme 1
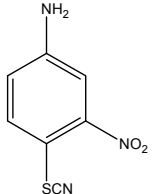

Scheme 2

Table 1. Thiocyanation of aryl and hetero aromatic compounds

Entry	Indole 1	Product[a] 2	Time (h)	Yields (%)[b]
a			6.0	80
b			9.0	90
c			12.0	80
d			5.5	75
e			6.0	80
f			3.0	80

[a] All products were characterized by ^{1}H NMR,IR and mass spectroscopy.

[b] Isolated yields

Solvent Extraction of Sodium Permanganate by Mono-benzo 3*m*-Crown-*m* Ethers (*m* = 5, 6) into 1,2-Dichloroethane and Nitrobenzene: a Method which Analyzes the Extraction System with the Polar Diluents

Yoshihiro Kudo (Corresponding author)

Graduate School of Science, Chiba University

Chiba, 263-8522, Japan

Tel: 81-43-290-2786   E-mail: iakudo@faculty.chiba-u.jp

Kyohei Harashima

Department of Chemistry, Faculty of Science

Chiba University, Chiba, 263-8522, Japan

Shoichi Katsuta & Yasuyuki Takeda

Graduate School of Science, Chiba University

Chiba, 263-8522, Japan

Abstract

Analytical equations were derived for the extraction of univalent metal salts (MA) by crown ethers (L) into polar diluents. Then, $NaMnO_4$ was extracted at 25 °C by benzo-15-crown-5 and -18-crown-6 ethers (B15C5 and B18C6) from a water (w)-phase into a 1,2-dichloroethane (DCE)-one. So, the extraction constants of K_{ex1} and K_{ex2} were determined, where $K_{ex1} = [NaLMnO_4]_{DCE}/[Na^+][L]_{DCE}[MnO_4^-]$ and $K_{ex2} = [NaL^+]_{DCE}[MnO_4^-]_{DCE}/[Na^+][L]_{DCE}[MnO_4^-]$ $(= K_{ex1}/K_{NaLMnO4}{}^{DCE})$. From the calculation processes of these K_{ex} values, $K_{D,MnO4}$ and $K_{MLA}{}^{DCE}$ values with MLA = $NaLMnO_4$ were obtained and also $K_{NaL}{}^{DCE}$ values were estimated from the thermodynamic cycle of $K_{ML}{}^{DCE} = K_{ex2}/K_{D,M}K_{D,A}$. Here, the $K_{MLA}{}^{DCE}$, $K_{D,A}$ or $K_{D,M}$, and $K_{ML}{}^{DCE}$ values denote an ion-pair formation constant of MLA in the DCE-phase, a distribution constant of A^- or M^+ between the w- and DCE-phases, and a complex formation one of a complex ion ML^+ in the DCE-phase, respectively. The same values were obtained for the w/nitrobenzene (NB) extraction systems. By comparing the $K_{NaL}{}^{org}$ and $K_{D,NaL}$ $(= [NaL^+]_{NB}/[NaL^+]$: distribution constant into NB) values with those previously-reported by other methods, the validity of the equations was confirmed. Additionally, extraction-abilities of the extraction systems with DCE and NB were examined, using component equilibrium constants reported before.

Keywords: Extraction constant, Distribution constant, Pairing anion, Sodium permanganate, Crown ether, 1,2-Dichloroethane, Nitrobenzene

1. Introduction

Extraction of alkali metal salts (MA) by crown compounds (L) into less-polar diluents, such as benzene, chloroform, and 1,2-dichloroethane (DCE), has been studied in more detail by considering an ion-pair formation between a complex ion ML^+ and a pairing anion A^- in water (w) and a distribution of the thus-formed ion pairs MLA into the diluents (Takeda et al., 2004; Yajima et al., 2000). In such extraction systems, especially the extraction into DCE has been also analyzed by taking other processes into account: a distribution of M^+ or A^- between the w- and DCE-phases, a dissociation of MLA into ML^+ and A^- in the DCE-one, and so on (Kikuchi and Sakamoto, 2000; 1998). These facts suggest that DCE makes treatments for chemical equilibria in the extraction systems either more-complicate or -simple, probably depending on experimental conditions. The former cases (Takeda et al., 2004; Yajima et al., 2000) are more-informative for the equilibria of species in the w-phase, while the latter ones (Kikuchi and Sakamoto, 2000; 1998) are more-informative for those in the diluent. Hence, if both the cases are combined, then it is more-convenient for the study of the extraction systems. Also, few systematic studies for data-handling of

the MA-extraction by L into polar diluents, such as nitrobenzene (NB) (Danesi et al., 1975; Makrlík et al., 1999), have been reported. However, these data-handlings seem to be either over-approximated (Kikuchi and Sakamoto, 2000; 1998; Danesi et al., 1975) or very complicate computation (Makrlík et al., 1999) for the determination of some equilibrium constants relevant to these extraction systems.

Moreover, the diluents, DCE and NB, have been well used for electrochemical studies of ion transfers of alkali and alkaline-earth metal ions across w/DCE and w/NB interfaces (Koryta, 1984; Sabera et al., 1992; Yoshida et al., 2002; Olaya et al., 2010) and of their transfers facilitated by L and other ligands (Sabera et al., 1992; Uehara et al., 2007; Kakiuchi, 2004). Especially, the ion-transfer behavior of univalent cations is very important for the determination of many equilibrium constants, such as complex formation (or stability) and acid-dissociation ones, in both the phases (Reymond et al., 2000), because standard potentials at the interfaces for the ion transfer (Koryta, 1984; Sabera et al., 1992) are always required for the calculation of these constants. Additionally, the potentials for A^- transfers across the w/DCE and w/NB interfaces are very interesting in examining properties of A^--solvent and -w interactions and standardizing the ion-transfer behavior of M^+ and R_4N^+ at the interfaces (Sladkov et al., 2004).

In the present paper, we derived fundamental equations for a detailed analysis of the above extraction systems with DCE or NB as the polar diluent, examined usefulness of these equations, and then tried to elucidate extraction-abilities of the systems. Here, $NaMnO_4$ and benzo-15-crown-5 and -18-crown-6 ethers (B15C5 and B18C6, respectively) were employed as MA and L, respectively. In these processes, extraction constants (K_{ex1}/mol^{-2} dm^6 and K_{ex2}/mol^{-1} dm^3, respectively) for the extraction of $NaLMnO_4$ and sodium complex ions NaL^+ (with MnO_4^- as a counter ion) into the diluents, distribution constants ($K_{D,A}$ and $K_{D,NaL}$, respectively) of MnO_4^- and NaL^+ between the w-phase and the two diluents, and the ion-pair formation constants ($K_{MLA}{}^{org}$/mol^{-1} dm^3) of NaL^+ with MnO_4^- in the diluents were determined. Also, using the reported values for the distribution constant ($K_{D,M}$, converted into the potential at the interface) of Na^+ between the two phases, we estimated the complex formation constants ($K_{ML}{}^{org}$/mol^{-1} dm^3) of Na^+ with L in the w-saturated DCE and NB. The $K_{D,NaL}$ (into NB) and $K_{NaL}{}^{org}$ values were compared with those reported previously, in order to examine the validity of the present method based on the equations derived here.

2. Theory

2.1 Fundamental equations

The following equilibria were considered for the analysis of the present extraction system with the polar diluent.

$$L \rightleftharpoons L_o \tag{1}$$

$$M^+ + L \rightleftharpoons ML^+ \tag{2}$$

$$M^+ + A^- \rightleftharpoons MA \tag{3}$$

$$ML^+ + A^- \rightleftharpoons MLA \tag{4}$$

$$MLA \rightleftharpoons MLA_o \tag{5}$$

$$MLA_o \rightleftharpoons ML^+{}_o + A^-{}_o \tag{6}$$

Here, the subscript "o" denotes the o-phase. For these equilibria, the corresponding equilibrium constants were

$$K_{D,L} = [L]_o/[L] \tag{E1}$$

$$K_{ML} = [ML^+]/[M^+][L] \tag{E2}$$

$$K_{MA} = [MA]/[M^+][A^-] \tag{E3}$$

$$K_{MLA} = [MLA]/[ML^+][A^-] \tag{E4}$$

$$K_{D,MLA} = [MLA]_o/[MLA] \tag{E5}$$

$$(K_{MLA}{}^{org})^{-1} = [ML^+]_o[A^-]_o/[MLA]_o. \tag{E6}$$

Also, the entry of A^- and $A^-{}_o$ or ML^+ and $ML^+{}_o$ in Eqs. (2)–(4) and (6) means the presence of the distribution equilibrium of A^- or ML^+ into the o-phase, respectively (see 4.3). Equations of mass and charge balances for such equilibria were

$$[M]_t \approx [M^+] + [ML^+] + [MLA] + [MA] + [MLA]_o + [ML^+]_o \tag{7}$$

$$[L]_t = [L] + [ML^+] + [MLA] + [L]_o + [MLA]_o + [ML^+]_o \tag{8}$$

$$[A]_t = [A^-] + [MLA] + [MA] + [A^-]_o + [MLA]_o \tag{9}$$

and

$$[M^+] + [ML^+] = [A^-] \tag{10}$$

$$[ML^+]_o \approx [A^-]_o. \tag{11}$$

It is assumed here that $[ML^+]_o \gg [M^+]_o$. Using Eqs. (10) and (11), the ionic strength-values of each phase were calculated from $[A^-]$ ($= I$) for the w-phase and $[ML^+]_o$ or $[A^-]_o$ ($= I_o$) for the o-phase, respectively.

Eqs. (7)–(9) were rearranged into

$$[M^+] = \frac{[M]_t - \sum[MLA_n]_o}{1 + K_{MA}[A^-] + (K_{ML}/K_{D,L})[L]_o(1 + K_{MLA}[A^-])} \tag{12}$$

$$[L]_o = \frac{[L]_t - \sum[MLA_n]_o}{1 + K_{D,L}{}^{-1} + (K_{ML}/K_{D,L})[M^+](1 + K_{MLA}[A^-])} \tag{13}$$

$$[A^-] = \frac{[A]_t - \sum[MLA_n]_o}{1 + [M^+]\{K_{MA} + (K_{ML}K_{MLA}/K_{D,L})[L]_o\}} \tag{14}$$

with $\sum[MLA_n]_o = [MLA]_o + [ML^+]_o \approx [MLA]_o + [A^-]_o$ {see Eq. (11)}.

2.2 For determination of compositions of extracted species

The overall extraction equilibria (Yajima et al., 2000; Danesi et al., 1975) are expressed as

$$M^+ + L_o + A^- \rightleftharpoons MLA_o \tag{15}$$

and

$$M^+ + L_o + A^- \rightleftharpoons ML^+{}_o + A^-{}_o. \tag{16}$$

The equilibrium constants for their mixtures are defined as follows:

$$K_{ex}{}^{mix} = \sum[MLA_n]_o/[M^+][L]_o[A^-] = K_{ex1} + K_{ex2}/[A^-]_o \qquad (n = 0, 1) \tag{17}$$

with

$$K_{ex1} = [MLA]_o/[M^+][L]_o[A^-] = K_{ML}K_{MLA}K_{D,MLA}/K_{D,L} \tag{E15}$$

and

$$K_{ex2} = [ML^+]_o[A^-]_o/[M^+][L]_o[A^-] = K_{ex1}/K_{MLA}{}^{org} \tag{E16}$$

at I_o and I. Therefore, if the K_{ex1} and $[ML^+]_o$ {$= (K_{ex}{}^{mix} - K_{ex1})([M^+][L]_o[A^-])$ in each run} values are determined (see *2.3* for K_{ex1}), then we can easily obtain the K_{ex2} from a set of $[M^+]$, $[L]_o$, $[A^-]$, and $[ML^+]_o$ and accordingly the $K_{MLA}{}^{org}$ values at I_o.

By plotting $\log(D_{mix}/[A^-])$ or $2\log D_{mix}$ against $\log[L]_o$ based on Eq. (17), its slope generally gives the composition of the ion-pair complex or the complex ion (with the counter ion A^-) extracted into the o-phase, respectively. This detail is as follows. A distribution ratio of the mixtures with M^+, D_{mix}, is defined as $\sum[MLA_n]_o/([M]_t - \sum[MLA_n]_o) = \sum[MLA_n]_o/[M^+](1 + f_{AL})$ and, when $1 \gg f_{AL}$, it is nearly equal to $D_1 + D_2$, where f_{AL}, D_1, and D_2 denote $K_{MA}[A^-] + (K_{ML}/K_{D,L})[L]_o(1 + K_{MLA}[A^-])$ in Eq. (12), $[MLA]_o/[M^+]$ in Eq. (E15), and $[ML^+]_o/[M^+]$ in Eq. (E16), respectively. One can see that, generally, D_{mix} becomes D_1 in the higher range of $[L]_o$, while it does D_2 in the lower range. In other words, the relation $\log\{(D_1 + D_2)/[A^-]\} \approx \log(K_{ex1} + K_{ex2}/[A^-]_o) + \log[L]_o$ is primarily derived from Eq. (17) and then becomes

$$\log(D_1/[A^-]) \approx \log K_{ex1} + \log[L]_o \tag{17a}$$

at the conditions of $D_1 \gg D_2$ and $K_{ex1} \gg K_{ex2}/[A^-]_o$. Similarly it becomes

$$2\log D_2 \approx \log K_{ex2} + \log[L]_o \tag{17b}$$

at the conditions of $D_1 \ll D_2$ and $K_{ex1} \ll K_{ex2}/[A^-]_o$ and by assuming that $[A^-]_o/[A^-] \approx [ML^+]_o/([M^+] + [ML^+]) \approx [ML^+]_o/[M^+] = D_2$ {see Eq. (11); $[M^+] \gg [ML^+]$ in Eq. (10)}. Therefore, in the plots based on Eqs. (17a) and (17b), their slopes have to show unity for the extraction of MLA and ML^+ into the o-phases, respectively.

2.3 For determination of K_{ex1} and $K_{D,A}$

From Eq. (17), we can obtain its other form:

$$K_{ex}{}^{mix} = K_{ex1} + K_{D,A}/[M^+][L]_o, \tag{18}$$

where $K_{D,A}$ refers to the distribution constant of A^- between the w- and o-phases and defined as $[A^-]_o/[A^-]$ {$\approx$ $[ML^+]_o/[A^-]$ from Eq. (11)}. Then, taking logarithms of both side of the equation, we have immediately

$$\log K_{ex}{}^{mix} = \log (K_{ex1} + K_{D,A}/[M^+][L]_o). \tag{19}$$

Therefore, a non-linear regression analysis of the plot of $\log K_{ex}{}^{mix}$ against $-\log [M^+][L]_o$ yields these K_{ex1} and $K_{D,A}$ values. Also, if the $K_{D,M}$ value, defined as $[M^+]_o/[M^+]$, is available, then we can easily estimate the $K_{ML}{}^{org}$ value at I_o, using the thermodynamic cycle of

$$K_{ex2} = K_{D,M}K_{D,A}K_{ML}{}^{org}. \tag{E16a}$$

3. Experimental

3.1 Chemicals

Sodium permanganate solution was prepared from $NaMnO_4 \cdot H_2O$ (Aldrich, 97%) by the same procedure as that for the $KMnO_4$ solution (Kudo et al., 2003). Commercial B15C5 and B18C6 (Aldrich, 98%) were dried at room temperature under reduced pressure (Kudo et al., 2003). DCE or NB (Kanto, Guaranteed reagent) were washed three times with water and then saturated with water (Kudo et al., 2003). All other chemicals were analytical grade and used without further purification. Water, by which all the aqueous solutions were prepared, was obtained by distilling once tap water and then passing through a Milli-Q Lab system (Millipore).

3.2 Solvent extraction experiments

Initial concentrations of $NaMnO_4$ in w were in the range of 3.4×10^{-4}–9.0×10^{-2} mol dm^{-3}; those of L in w were in that of 9.2×10^{-5}–2.5×10^{-2} mol dm^{-3}. The pH readings of the aqueous permanganate solutions at 25 °C were in the range of 5–6: these values were obtained with a Horiba pH/ion meter (type F-23), using a Horiba glass electrode (type 6366-10D).

Five cm^3 of the aqueous $NaMnO_4$ solution was mixed with 5 cm^3 of the aqueous L solution and then 10 cm^3 of DCE or NB was added into its mixture in the stoppered-glass tube of about 30 cm^3. Its tube was agitated at 25 ± 0.3 °C about 10 minutes (Kudo et al., 2003) and then centrifuged. After the DCE- or NB-phase was subdivided by 2–9 cm^3 into another tube, 4–7 cm^3 of w was added into it, and then back-extracted into the w-phase by vigorously shaking the tube. The total concentration, $[MnO_4^-]_t$, of MnO_4^- back-extracted into the w-phase was spectrophotometrically determined at 525 nm (Kudo et al., 2003): absorbance $= 2.40 \times 10^3[MnO_4^-]_t - 2 \times 10^{-5}$ at correlation coefficient (R) $= 0.999_8$. This $[MnO_4^-]_t$ was defined to be $[NaLMnO_4]_o + [NaL^+]_o$ {$= \Sigma[NaL(MnO_4)_n]_o$}, where it was assumed that $[NaL^+]_o \approx [MnO_4^-]_o$ {see Eq. (11)}. As the case may be, operations for the back-extraction from the DCE- or NB-phase and the spectrophotometric determination of MnO_4^- were repeated. The spectrophotometric measurements were performed at 25 °C by using a Hitachi U-2001 spectrophotometer equipped with a 1-cm quartz cell.

Decomposition of MnO_4^- was not detected spectrophotometrically and potentiometrically to 6 h after the dilution of the aqueous $NaMnO_4$ solution (Kudo et al., 2003) and accordingly the extraction experiments of $NaMnO_4$ by L into DCE or NB and the determination of amounts of MnO_4^- extracted were finished for about 6 h.

3.3 Computation of $[Na^+]$, $[L]_o$, and $[MnO_4^-]$ at extraction equilibrium

The molar concentrations at equilibrium, $[Na^+]$, $[L]_o$, and $[A^-]$ with $A^- = MnO_4^-$, were computed by the following successive approximation. First, $[Na^+]$ was computed by using Eq. (12) with the approximation (ap. 1) of $1 >> K_{MA}[A^-] + (K_{ML}/K_{D,L})[L]_o(1 + K_{MLA}[A^-])$. Secondly, $[L]_o$ was computed by introducing $[Na^+]$ into Eq. (13) with the approximation (ap. 2) of $1 >> K_{MLA}[A^-]$. Lastly, $[A^-]$ was computed by introducing $[Na^+]$ and $[L]_o$ into Eq. (14). Then, the second $[Na^+]$ was computed by introducing $[L]_o$ and $[A^-]$ into Eq. (12) without the ap. 1. Similarly, the second $[L]_o$ was computed by introducing $[A^-]$ and the second $[Na^+]$ into Eq. (13) without the ap. 2. Moreover, the second $[A^-]$ was computed by introducing the second $[Na^+]$ and $[L]_o$ into Eq. (14). These calculations were repeated until $[Na^+]$, $[L]_o$, and $[A^-]$ became constant values: namely, the $(N-1)$-th $[Na^+]$ = the N-th $[Na^+]$, where N means the number of run and $[Na^+]$ is replaced by $[L]_o$ and $[A^-]$. Using these values and the experimental $\Sigma[NaLA_n]_o$ one, we computed the $K_{ex}{}^{mix}$ value from Eq. (17). Such calculations were performed on other data sets. In the calculation of $[Na^+]$, $[L]_o$, and $[A^-]$, constant values were employed for K_{ML} and $K_{D,L}$, while K_{MA} and K_{MLA} were computed from their values at $I \to 0$, according to I for the w-phase.

4. Results and Discussion

4.1 Composition of the complexes extracted

The plots of $\log (D_{mix}/[MnO_4^-])$ versus $\log [L]_o$ based on Eq. (17a) yielded the slope of 0.92 and the intercept of 2.1

at $R = 0.997$ for L = B15C5, while those of $2\log D_{mix}$ versus $\log [L]_o$ based on Eq. (17b) yielded the slopes of 1.10 and the intercepts of -1.5 at $R = 0.993$ for B18C6 in the extraction into DCE, 1.10 and 0.4 at $R = 0.999$ for B15C5, and 0.99 and 0.9 at $R = 0.974$ for B18C6 in that into NB (Figure 1). According to Eqs. (17a) and (17b), these intercepts correspond to the $\log K_{ex1}$ value for the former system and the $\log K_{ex2}$ ones for the latter three systems, respectively. Also, the higher slopes of the NaMnO$_4$ extraction systems with both B18C6 into DCE and B15C5 into NB predict that the corresponding intercepts $> \log K_{ex2}$ and accordingly their experimental deviations from the prerequisite of $1 \gg f_{AL}$ in Eq. (17) are somewhat large, compared with the deviation for the extraction by B18C6 into NB. The results indicate the extraction of the complexes composed of Na:L:A = 1:1:1 and Na:L = 1:1. Taking the above facts into account, we determined the K_{ex1} and K_{ex2} values for MLA and ML$^+$ by using Eqs. (19) and (E16), respectively (see *4.2*).

4.2 Extraction of NaLMnO$_4$ and NaL$^+$ into DCE and NB

Plots of $\log K_{ex}^{mix}$ versus $-\log [Na^+][L]_o$ for the w/DCE and w/NB extraction systems gave the K_{ex1} and $K_{D,A}$ values by the non-linear regression analysis based on Eq. (19) (Figure 2 as an example). Table 1 lists these values determined, together with other component equilibrium constants available in the references (Kudo et al., 2008; 2006a; 2007; 1991; 1996; Katsuta and Takeda, 2003); 15C5 and 18C6 in this table denote 15-crown-5 and 18-crown-6 ethers, respectively. In addition to the values in Table 1, the $\log K_{NaMnO4}$ values at the given I, estimated from the value at $I \to 0$ (Kudo et al., 2003), were 0.82 for the DCE extraction systems with B15C5 and B18C6, 0.87 for NB with B15C5, and 0.89 for NB with B18C6 on the average.

In the w/DCE extraction, the $\log K_{ex1}$ value of Na(B15C5)A with A$^-$ = MnO$_4^-$ was comparable with that of Na(B18C6)A (Table 1). We can see this result from the fact that a difference in $\log K_{D,NaLA}$ between Ls cancels out that in the sum of $\log K_{NaL}$ and $\log K_{NaLA}$ between them {see Eq. (E15)}. In the w/NB extraction, the $\log K_{ex1}$ value of Na(B18C6)A was larger than that of Na(B15C5)A. This difference (= 1.24) mainly comes from that {= 0.81 + 3.19 − (0.45 + 2.51) = 1.04} between the sums of $\log K_{NaL}$ and $\log K_{NaLA}$, although there are differences between the experimental conditions of I and I_o (see Table 1).

The K_{ex2} is immediately resolved as $K_{ML}K_{MLA}K_{D,MLA}/K_{D,L}K_{MLA}^{org}$ from Eqs. (E15) and (E16). Hence, we can see that a difference in K_{ex2} between L = B15C5 and B18C6 for the DCE extraction comes from that in $K_{NaLMnO4}^{DCE}$ (see *4.4*). For the NB extraction, differences in both K_{ex1} and K_{ex2} between their Ls are mainly due to those in the sum of K_{NaL} and $K_{NaLMnO4}$ (Table 1). On the other hand, we can adopt the cycle of Eq. (E16a). That is, fixing MA to NaMnO$_4$, the extraction-ability depends on only the magnitude of K_{NaL}^{org}, because the product $K_{D,Na}K_{D,MnO4}$ is an intrinsic value for NaMnO$_4$ and the diluent.

The $\log K_{ex1}$ values for Na(B15C5)MnO$_4$ and Na(B18C6)MnO$_4$ in the DCE extraction were smaller than those (= 3.728 at $I = 0.022$ mol dm^{-3} and 3.501 at $I = 0.081$) (Kudo et al., 2006b) for Na(B15C5)Pic and Na(B18C6)Pic, respectively: here Pic$^-$ denotes picrate ion. Obviously, these differences are due to those in $\log K_{D,NaLA}$ between these systems: $\log (K_{D,NaLPic}/K_{D,NaLMnO4}) = 1.37$ for L = B15C5 and 1.76 for B18C6. These results are the same as those reported previously for the extraction systems with 15C5 and 18C6 (Kudo et al., 2003; 2008).

The $\log K_{D,NaLMnO4}$ values for the w/DCE extraction were much smaller than the $\log K_{D,NaLPic}$ ones which were reported to be 2.60 for L = B15C5 and 2.09 for B18C6 (Kudo et al., 2006b). These results indicate that an interaction of w-molecules with NaLMnO$_4$ in the w-phase is larger than that with NaLPic (Kudo et al., 2008). The same results for $K_{D,NaLA}$ with L = 15C5 and 18C6 have been reported (Kudo et al., 2008). Also, the $\log K_{D,NaLMnO4}$ values for given L were in the relation of DCE < NB, suggesting that an interaction of NaLMnO$_4$ with NB is larger than that with DCE (see *4.3* for $K_{D,MnO4}$ and $K_{D,NaL}$).

4.3 Distribution of single MnO$_4^-$ and NaL$^+$ between water and DCE or NB

As can be seen from Table 1, the $K_{D,MnO4}$ values for the extraction systems with B15C5 are somewhat smaller than those for the systems with B18C6. These findings suggest a pairing cation-dependence of $\log K_{D,A}$ in the present extraction experiments, as well as in the extraction ones of NaMnO$_4$ into the same diluents {$\log K_{D,A} = -4.6$ (into DCE); -3.22 (NB), unpublished data by Kudo}. The $K_{D,A}$-difference for the w/DCE extraction can be expressed as $\log \{K_{D,A}(B15C5)/K_{D,A}(B18C6)\} = \log \{([Na^+]_{DCE} + [Na(B15C5)^+]_{DCE})/([Na^+]_{DCE} + [Na(B18C6)^+]_{DCE})\}$, when [A$^-$] has a common value between the extraction systems, and, according to Eq. (11), it becomes $\log (K_{NaL}^{DCE}[B15C5]_{DCE}/K_{NaL}^{DCE}[B18C6]_{DCE})$ (see *4.5* for K_{NaL}^{org}). Therefore, assuming that $[B15C5]_{DCE} = [B18C6]_{DCE}$, we obtained -0.8 as $\log \{K_{D,A}(B15C5)/K_{D,A}(B18C6)\}$, being equal to the experimental difference (= -0.8, see Table 1). The same is true of the w/NB distribution: the value was calculated to be -0.4 against the experimental value of -0.5. These facts may mean that these values should be standardized by the $(C_6H_5)_4As^+B(C_6H_5)_4^-$ assumption (Rais, 1971). The $\log K_{D,A}$ values with A$^-$ = MnO$_4^-$ were comparable with that ($\log K_{D,ClO4} \approx -2.58$ at 20 °C) measured at the w/DCE interface by cyclic voltammetry (Olaya et al., 2010). The same is true of the $\log K_{D,ClO4}$ value (-1.4 at 25

°C) obtained from solvent extraction into NB (Rais, 1971). The $K_{D,MnO4}$ values indicate that an interaction of MnO_4^- with DCE is smaller than that with NB (Table 1), as well as that of ClO_4^-.

The complex-cation distribution constant can be calculated from the thermodynamic cycle of $K_{D,ML} = K_{D,I}K_{ex2}/K_{ML}K_{D,A}$ (= $[ML^+]_o/[ML^+]$). So, their values were log $K_{D,NaB15C5} = 1.0_1$, log $K_{D,NaB18C6} = 1.4_6$ in the w/DCE extraction, log $K_{D,NaB15C5} = 2.6_2$, and log $K_{D,NaB18C6} = 2.5_7$ in the w/NB one. As similar to the distribution of MnO_4^-, the $K_{D,NaL}$ values show that an interaction with NaL^+ was in the relation of DCE < NB. The log $K_{D,NaL}$ values for the w/NB extraction are comparable with those recalculated from those determined by the ion-transfer polarography at the w/NB interface: log $K_{D,NaL}$(recalculated) = 2.1 for L = B15C5 and 2.67 for B18C6 (Kudo et al., 1996). These facts indicate that the present method is comparable with the electrochemical method at the interface and also suggest that the $K_{D,NaL}$ values corresponding to the w/DCE extraction are valid ones.

For given L, the log $K_{D,NaL}$ values were comparable with the log $K_{D,NaLMnO4}$ ones (Table 1), except for the extraction by L = B18C6 into DCE. These facts indicate that the interaction of NaL^+ with DCE or NB is similar to that of $NaLMnO_4$. On the other hand, a difference in L = B18C6 between $K_{D,NaL}$ and $K_{D,NaLA}$ suggests any change, such as a distortion of the $Na(B18C6)^+$ conformation, due to the ion-pair formation with MnO_4^-.

We estimated from the above values the log $K_{D,A}$ and log $K_{D,NaL}$ values at I and $I_o \to 0$ using the relation log $K_{D,A}{}^0$ {= log $(y_-{}^{org}[A^-]_o/y_-[A^-])$} = log $K_{D,A}$ + log $(y_-{}^{org}/y_-)$ or log $K_{D,ML}{}^0$ = log $K_{D,ML}$ + log $(y_+{}^{org}/y_+)$. Here, $K_{D,A}{}^0$, $y_-{}^{org}$, and y_- (or $K_{D,ML}{}^0$, $y_+{}^{org}$, and y_+) denote $K_{D,A}$ at I and $I_o \to 0$, ionic activity coefficients of A^- (or ML^+) in the organic solvents (or diluents), and those in w, respectively; the extended Debye-Hückel law was applied for the y-calculation of MnO4− and the Davies equation, log $y_+ = -(constant)(+1)^2\{\sqrt{I}/(1+\sqrt{I}) - 0.3I\}$, for that of NaL^+. Consequently, the log K_D values agreed with the log $K_D{}^0$ ones within the error of about ±0.01. From this result, the $K_{D,A}$ and $K_{D,NaL}$ values seem to be independent of the I and I_o conditions under the present experimental concentration-ranges.

4.4 Ion-pair formation of NaL^+ with MnO_4^- in water-saturated DCE and NB

The log $K_{NaLMnO4}{}^{org}$ values estimated from Eq. (E16) are listed in Table 1 (see *4.2*). Small I_o values suggest that these log $K_{NaLA}{}^{org}$ values are very close to those at $I_o \to 0$. For a given L, log $K_{NaLA}{}^{DCE}$ was larger than or nearly equal to log $K_{NaLA}{}^{NB}$. Since DCE and NB have less-donor properties, this ion-pair formation seems to be affected by the amounts ($[w]_{t,o}$) of water saturated in both the diluents: $[w]_{t,DCE} = 0.127$ mol dm^{-3} (Kikuchi et al., 2001) and $[w]_{t,NB} = 0.178$ mol dm^{-3} (Iwachido et al., 1980) at 25 °C. That is, the above findings suggest that the hydration effect to Na^+ caught in L is stronger in NB than in DCE.

For a given diluent, the log $K_{NaLMnO4}{}^{DCE}$ values showed also the relation of L = B15C5 > B18C6. This fact reflects the degree of hydration to NaL^+ in the DCE-phase and its size (cavity size: B15C5 < B18C6). On the other hand, the same discussion does not hold for the same reaction in the w-saturated NB: its hydration number (h) for $NaL(OH_2)_h{}^+$ has been reported to be L = B15C5 ($h = 0.8$) ≤ B18C6 (1.1) (Iwachido et al., 1980) and it is easily predicted that $Na(B15C5)^+ < Na(B18C6)^+$ in size. These fact and prediction are in conflict with the experimental result for $K_{NaLMnO4}{}^{NB}$. This disagreement suggests, as described previously (Kudo et al., 2006a) for log $K_{NaLMnO4}$ in Table 1, that the shielding effect of B15C5 to the charge on Na^+ is greater than the size effect of B18C6; it is well known that Na^+ more size-fits the cavity of B15C5 than that of B18C6. Now, we can not explain the reason why the shielding effect to NaL^+ in the DCE-phase does not clearly function or the relation between the $K_{NaLMnO4}{}^{NB}$ values is similar to those between the $K_{NaLMnO4}$ ones (see Table 1).

The log $K_{NaLMnO4}{}^{NB}$ values for L = B18C6 were much larger than those of the more-bulky ion-pair complex, Na(DB18C6)A with $A^- = Pic^-$ and 2,2',4,4',6,6'-hexanitrodiphenylaminate (Dpa^-), where DB18C6 denotes dibenzo-18C6: $K_{Na(DB18C6)Pic}{}^{NB} = 10^{2.48}$ mol^{-1} dm^3 at 22 ± 1 °C by solvent extraction experiments (Danesi et al., 1975) and $K_{Na(DB18C6)Dpa}{}^{NB} = 10$ at 25.00 °C by conductance measurements (Iwachido et al., 1980). From differences in size among these A^-, we can suppose easily the order in size of the ion-pair complex being $Na(B18C6)MnO_4 < Na(DB18C6)Pic < Na(DB18C6)Dpa$. These results indicate that a major interaction between NaL^+ and MnO_4^- in the diluents is the Coulombic force. This is also supported by the fact that the log $K_{Na(B18C6)A}{}^{DCE}$ value (= 4.5) with $A^- = MnO_4^-$ (crystal radius: $r_c = 2.40$ Å) (Marcus, 1997) was a little larger than that (= 4.38 at $I_o \to 0$) (Kikuchi and Sakamoto, 2000) with $A^- = Pic^-$ ($r_c = 3.35$ Å) (Marcus, 1997).

4.5 Complex formation of L with Na^+ in water-saturated DCE and NB

When the $K_{D,Na}$ values of Na^+ into DCE and NB are available in some way, we can immediately calculate the $K_{ML}{}^{org}$ values for Na^+ with L in these diluents using Eq. (E16a). The thus-obtained values were log $K_{NaL}{}^{DCE} = 9.5$ for L = B15C5, 10.3 for B18C6, log $K_{NaL}{}^{NB} = 7.4$ for B15C5, and 7.8 for B18C6, where log $K_{D,Na} = -9.99$ at 25 °C for the ion transfer at the w/DCE interface (Sabela et al., 1992) or −10.502 at 22 °C (Ulmeanu et al., 2002) and −6.0 for the w/NB extraction (Rais, 1971). These relations, $K_{NaL}{}^{DCE} \gg K_{NaL}{}^{NB}$, suggest the hydration of w-molecules saturated in

the diluents to Na^+ or L (see *4.4*). The log $K_{NaB18C6}^{DCE}$ value was larger than that (9.43) reported previously (Kikuchi and Sakamoto, 2000). This fact can be due to a difference between the mass-balance equations: for example, $[B18C6]_{DCE}$ in the reference (Kikuchi and Sakamoto, 2000) must correspond to $[B18C6]_{DCE}$ + [B18C6] + $[Na(B18C6)^+]$ + [Na(B18C6)A] in Eq. (8), namely $[B18C6]_{DCE}$(the ref.) $\geq [B18C6]_{DCE}${Eq. (8)}. The log $K_{NaB18C6}^{NB}$ value (7.8) thus-determined was in accord with that (7.91) determined at $I = 0.05$ mol dm^{-3} {$(C_4H_9)_4N^+B(C_6H_5)_4^-$} by ion-transfer polarographic measurements (Kudo et al., 1996). Similarly, the log $K_{NaB15C5}^{NB}$ value (7.4) was close to that (6.8, 6.82, 6.9$_2$) determined by the same and voltammetric measurements (Kudo et al., 1991; 2001; Harris et al., 1992). The above results indicate that the present method is suitable for the estimate of some equilibrium constants at least.

5. Conclusion

It was demonstrated experimentally that the present method is useful for the determination of the composition of extracted species, MLA and ML^+, and the equilibrium constants, K_{ex1}, K_{ex2}, $K_{D,A}$, K_{MLA}^{org}, $K_{D,ML}$, and K_{ML}^{org}, relevant to them. Comparable results with those by other measurements were obtained with respect to the $K_{D,NaL}$ and K_{NaL}^{org} values. The method is effective for studying the extraction-ability of MA by neutral ligands into polar diluents. The pairing cation-dependence of $K_{D,A}$ shows that a further study will be required for the magnitude of $K_{D,A}$ and for other A^- (, M^+, and ML^+).

References

Danesi, P. R., M.-Gorican, H., Chiarizia, R., et al. (1975). Extraction selectivity of organic solutions of a cyclic polyether with respect to the alkali cations. *J Inog Nucl Chem*, 37, 1479-1483.

Daňková, M., Vaňura, P., & Makrlík, E. (1999). Extraction of cesium by the nitrobenzene solution of sodium bis-1,2-carbollylcobaltate in the presence of 18-crown-6. *J Radioanal Nucl Chem*, 240, 747-750.

Harris, N. K., Jin, S., Moody, G. J., et al. (1992). Facilitated ion transfer of alkali metal cations from water to a nitrobenzene phase containing various crown ethers. *Anal Sci*, 8, 545-551.

Iwachido, T., Minami, M., Kimura, M., et al. (1980). The coextraction of water into nitrobenzene with alkali and alkaline earth metal salts of 2,2',4,4',6,6'-hexanitrodiphenylamine in the presence of several crown ethers and cryptands. *Bull Chem Soc Jpn*, 53, 703-708.

Kakiuchi, T. (2004). Electrochemical instability in facilitated transfer of alkaline-earth metal ions across the nitrobenzene|water interface. *J Electroanal Chem*, 569, 287-291.

Katsuta, S., & Takeda, Y. (2003). Transfer activity coefficients of crown ethers and their alkali metal ion complexes between water and polar nonaqueous solvents. *Bunseki Kagaku* (in Japanese), 52, 89-105.

Kikuchi, Y., & Sakamoto, Y. (1998). Fundamental equilibrium analysis on the ion-pair extraction of dibenzo-18-crown-6 complex of alkali metal ions with picrate ion into 1,2-dichloroethane. *Anal Chim Acta*, 370, 173-179.

Kikuchi, Y., & Sakamoto, Y. (2000). Complex formation of alkali metal ions with 18-crown-6 and its derivatives in 1,2-dichloroethane. *Anal Chim Acta*, 403, 325-332.

Kikuchi, Y., Arayashiki, Y., & Anada, T. (2001). Hydration to benzo-15-crown-5, benzo-18-crown-6 and the benzo-18-crown-6-potassium ion complex in the low-polar organic solvents. *Anal Sci*, 17, 421-424.

Koryta, J. (1984). Electrochemical polarization phenomena at the interface of two immiscible electrolyte solutions –II. Progress since 1978. *Electrochim Acta*, 29, 445-452.

Kudo, Y., Takeda, Y., & Matsuda, H. (1991). Ion-transfer-polarographic study of distribution equilibrium of metal complex cations with several crown ethers between nitrobenzene and water. *Bunseki Kagaku* (in Japanese), 40, 779-784.

Kudo, Y., Miyakawa, T., Takeda, Y., et al. (1996). Ion-transfer polarographic study of the distribution of alkali and alkaline-earth metal complexes with 3*m*-crown-*m* ether derivatives (*m* = 6, 8) between water and nitrobenzene phases. *J Incl Phenom Mol Recognition Chem*, 26, 331-341.

Kudo, Y., Imamizo, H., Kanamori, K., et al. (2001). On the facilitating effect of neutral Macrocyclic ligands on the ion transfer across the interface between aqueous and organic solutions part III. competitive facilitated ion-transfer. *J Electroanal Chem*, 509, 128-138.

Kudo, Y., Usami, J., Katsuta, S., et al. (2003). Solvent extraction of permanganates (Na, K) by 18-crown-6 ether from water into 1,2-dichloroethane: elucidation of an extraction equilibrium based on component equilibria. *Talanta*, 59, 1213-1218.

Kudo, Y., Fujihara, R., Ohtake, T., et al. (2006a). Ion-pair formation of 3*m*-crown-*m* ether (*m* = 5, 6) and its monobenzo derivative complex ions with several pairing anions in water. *J Chem Eng Data*, 51, 604-608.

Kudo, Y., Usami, J., Katsuta, S. et al. (2006b). On the difference between ion-pair formation constants of crown ether-complex ions with picrate ion in water determined by solvent extraction and by potentiometry. *J Mol Liquids*, 123, 29-37.

Kudo, Y., Fujihara, R., Katsuta, S., et al. (2007). Solvent extraction of sodium perrhenate by 3*m*-crown-*m* ethers (*m* = 5, 6) and their mono-benzo-drivatives into 1,2-dichloroethane: elucidation of an overall extraction equilibrium based on component equilibria containing an ion-pair formation in water. *Talanta*, 71, 656-661.

Kudo, Y., Fujihara, R., Ohtake, T., et al. (2008). Evaluation of the hydrophilic property of sodium ion-pair complexes with 3*m*-crown-*m* ethers (*m* = 5, 6) and their benzo-derivatives by solvent extraction. *Anal Sci*, 24, 999-1003.

Marcus, Y. (1997). *Ion Properties*, New York: Marcel Dekker Inc., Table 3.

Olaya, A. J., Méndez, M. A., C.-Salazar, F., et al. (2010). Voltammetric determination of extreme Gibbs ion transfer energy. *J Electroanal Chem*, 644, 60-66.

Rais, J. (1971). Individual extraction constants of univalent ions in the system water-nitrobenzene. *Collect Czech Chem Commun*, 36, 3253-3262.

Reymond, F., Fermín, D., Lee, H. J., et al. (2000). Electrochemistry at liquid/liquid interface: methodology and potential applications. *Electrochim Acta*, 45, 2647-2662.

Sabela, A., Mareček, V., Samec, Z., et al. (1992). Standard Gibbs energies of transfer of univalent ions from water to 1,2-dichloroethane. *Electrochim Acta*, 37, 231-235.

Sladkov, V., Guillou, V., Peulon, S., et al. (2004). Voltammetry of tetraalkylammonium picrates at water|nitrobenzene and water|dichloroethane microinterfaces; influence of partition phenomena. *J Electroanal Chem*, 573, 129-138.

Takeda, Y., Taguchi, R., & Katsuta, S. (2004). Study on solute-solvent and solute-solute interactions for the dibenzo-24-crown-8-alkali metal picrate extraction system. *J Mol Liquids*, 115, 139-147.

Uehara, A., Kasuno, M., Okugaki, T., et al. (2007). Electrochemical evaluation of the distribution of a metal ion at the aqueous|organic solution interface in chelate extraction. *J Electroanal Chem*, 604, 115-124.

Ulmeanu, S. M., Jensen, H., Samec, Z., et al. (2002). Cyclic voltammetry of highly hydrophilic ions at a supported liquid membrane. *J Electroanal Chem*, 530, 10-15.

Yajima, S., Yahata, T., & Takeda, Y. (2000). Extraction of alkali metal (Na-Cs) picrates with dibenzo-18-crown-6 into various organic solvents. elucidation of fundamental equilibria which govern the extraction-ability and -selectivity. *J Incl Phenom Macrocyclic Chem*, 38, 305-322.

Yoshida, Y., Yoshida, Z., Aoyagi, H., et al. (2002). Evaluation of Gibbs free energy for the transfer of a highly hydrophilic ion from an acidic aqueous solution to an organic solution based on ion pair extraction. *Anal Chim Acta*, 452, 149-161.

Table 1. Equilibrium constants for the extraction of $NaMnO_4$ by L into DCE and NB and their component equilibrium constants at 25 °C

L	log K_{ex1}	log K_{ex2}	log K_{ML}	log K_{MLA} (I)[a]	log $K_{D,MLA}$
Diluent: DCE					
15C5[b]	2.02	---[c]	0.70	1.49 (0.010)	−0.15
B15C5	2.24 ± 0.02[d]	−3.7$_5$ ± 0.3$_1$[e]	0.45[f]	2.47[g] (0.0084)	1.23
18C6[j]	2.57	---[c]	0.73	2.29 (0.0062)	−0.42
B18C6	2.26 ± 0.04[d]	−2.2$_3$ ± 0.3$_0$[e]	0.81[f]	3.13[g] (0.0077)	0.33
Diluent: NB					
B15C5	3.79 ± 0.08[d]	−0.2$_3$ ± 0.2$_1$[e]	0.45[f]	2.51[g] (0.0015)	2.4
B18C6	5.03 ± 0.09[d]	0.6$_1$ ± 0.3$_1$[e]	0.81[f]	3.19[g] (0.00031)	2.59

Table 1. Continued

L	log $K_{D,L}$	log $K_{D,A}$	log $K_{MLA}{}^{org}$ $(I_o)^a$
Diluent: DCE			
15C5[b]	0.02	---[c]	---[c]
B15C5	1.910[h]	-3.3 ± 0.3[d]	6.0[i] (4.5×10^{-6})
18C6[j]	0.03	---[c]	---[c]
B18C6	2.009[h]	-2.5 ± 0.2[d]	4.5[i] (2.3×10^{-5})
Diluent: NB			
B15C5	1.6[h]	-1.7 ± 0.2[d]	4.0[i] (3.5×10^{-5})
B18C6	1.57[h]	-1.2 ± 0.2[d]	4.4[i] (1.8×10^{-5})

a. Average values in each phase. b. Kudo et al., 2008. c. Not determined. d. Determined by the non-liner regression analysis. e. Calculated from each value. f. Katsuta and Takeda, 2003. g. Kudo et al., 2006a. h. Kudo et al., 2007; 1991; 1996. i. Calculated from log $K_{MLA}{}^{org}$ = log K_{ex1} − log K_{ex2}. See *4.4* in the text. j. Kudo et al., 2007.
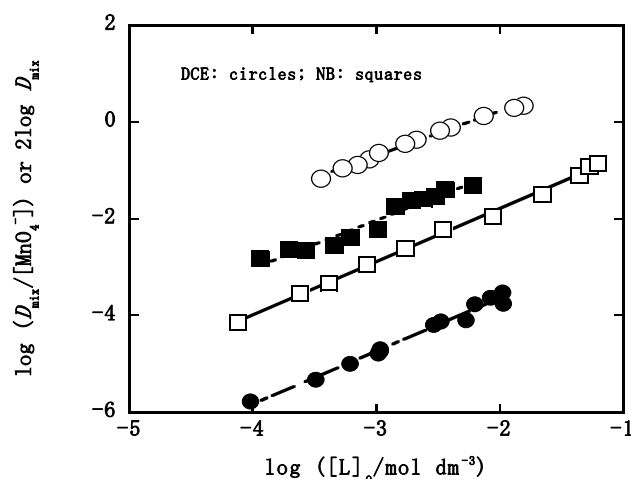

Figure 1. Plots of log $(D_{mix}/[MnO_4^-])$ or 2log D_{mix} versus log $[L]_o$ for the NaMnO$_4$-L extraction systems
The circles and squares refer to the extraction into DCE and NB, respectively. Also, the open and full symbols denote the extraction by L = B15C5 and B18C6, respectively. Only the open-circle symbol is the case for the log $(D_{mix}/[MnO_4^-])$-versus-log $[L]_o$ plot.

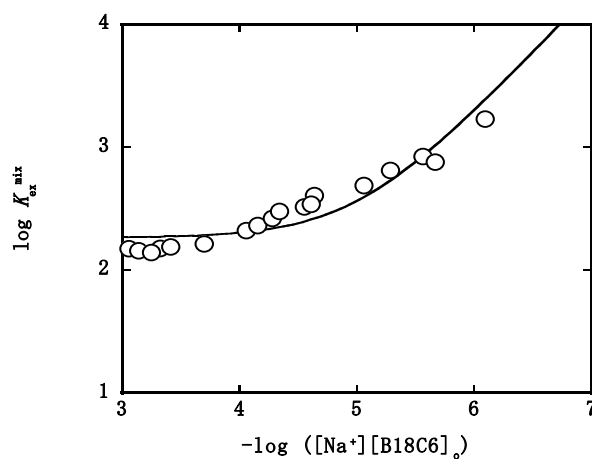Figure 2. Plot of log $K_{ex}{}^{mix}$ versus −log $([Na^+][L]_o)$ for the NaMnO$_4$ extraction by L = B18C6 into DCE
A curve shows the regression line of the plot analyzed by Eq. (19): *R* = 0.936.

Strategies for Controlling and Monitoring Water Quality in the Central African Water Distribution Company (SODECA)

Alafei Nama Janice Sandrine (Corresponding author) & Hong Jun

China University of Geosciences, School of Environmental Studies

388 Lumo Road, Hongshan Administrative District, Wuhan 430074, Hubei, China

Tel.: 86-27-5983-9746　　　E-mail: namajanice@yahoo.fr

Yves Yalanga

Central African Water Distribution Company (SODECA)

Tel.: 236-7550-5086　　　E-mail: yves_yalanga@yahoo.fr

Abstract

The present study investigated the strategies for controlling and monitoring water quality in the Central African Water Distribution Company. Several important monitoring measurements were done to ascertain the water quality at different stages of the production line, such as physico-chemical, limnology and bacteriological. According to the results, sometimes the frequency of controls undergoes a modification in time. This justifies the reduction of the number of controls. The breaking-off the reagent causes also a reduction of the number of analyses. The frequency of physicochemical control is much more respected compared to the bacteriological and limnologic controls. Therefore, it is recommended to have laboratory equipment with high technical instrument, and highly trained work force; the regular supply of reagents used in analyses of quality control; the revision of method, mode of analyses of control, monitoring and distribution.

Keywords: Drinking water quality, Monitoring, Strategy, SODECA

1. Introduction

Water quality is the physical, chemical, and biological characteristics of water. For example, water that is to be used for drinking should not contain any chemicals or micro-organisms that could be hazardous to health. Reference is frequently made to a set of standards from which compliance can be assessed. The most common standards used to assess water quality relate to drinking water, safety of human contact and for the health of ecosystems. Safe and potable water is the basis for good human health. Water provides essential elements, but when polluted it may become the source of undesirable substances dangerous to human health (Karavoltsos et al., 2008). On a continuing basis around the world an estimated 1.8 million people die every year from diarrheal diseases (including cholera). The majority of these deaths are among children in developing countries and up to 39% of diarrheal disease could be prevented by household water treatment by chlorination (WHO, 2004a). By contrast, drinking water safety is largely

taken for granted by many citizens of affluent nations. The availability of drink water delivered to households without of consumers becoming ill may be one of the key defining characteristics of developed nations in relation to the majority of the world. Valuing that enormous benefit appropriately must be a core value guiding risk management in the drinking water business. (Hrudey et al., 2006). Therefore, appropriate systems are designed to facilitate sustainable monitoring of regular and emergency release attributes with human health factors, and economic impacts. The data from these monitoring facilities help decision makers identify problems, documentation, and demonstrate overall trends in water quality. Thus, it is crucial to review the current network design procedures and develop basic guidelines in the design, expansion, and relocation of surface water quality monitoring networks from time to time. In recent years, the adequacy of collected water quality data and the performance of existing monitoring networks have been extensively evaluated for two basic reasons. First, an efficient information system is required to satisfy the needs of water quality management plans and to aid in the decision making process (Harmancioglu et al., 1998). Secondly, this system has to be realized under the constraints of limited financial resources, sampling and analysis facilities, and manpower. To ensure cost-effectiveness, an evaluation strategy adopted for a water quality monitoring network should cover all relevant technical design features, including selection of sampling sites, sampling frequencies, variables to be monitored, sensors synergy, and sampling duration (Loftis and Ward, 1980). As a result, existing monitoring networks will have to be adapted to new requirements. In the majority

of cases, the location and the density of monitoring points will need to be adapted to provide adequate spatial coverage (surveillance monitoring) and to capture the effect of individual (main) pressures (operational and investigative Monitoring). Furthermore, more substances should be monitored in a more systematic manner, particularly those listed as priority substances. From a technical perspective, the main challenges will comprise establishing new monitoring networks (selection of representative monitoring points), developing information systems for managing an increasing volume of data coming from different producers (Chery *et al.*, 2005), developing new analytical methods and controlling measurement uncertainty (Coquery *et al.*, 2005). From an economic perspective, the challenge will be to minimize monitoring cost. In some cases, organizational changes might also be necessary, with possible redistribution of tasks and responsibilities within or between organizations, be they private, public, national and/or regional. (Graveline *et al.*, 2010). Harmancioglu *et al.*, (1998) summarized the technologies and solutions for planning and designing various water quality monitoring networks. Information retrieval from the monitoring networks has turned out to be critical, recently leading the development of a variety of visualization techniques that might be useful for demonstrating important aspects of a water quality monitoring network (Boyer *et al.*, 2000).

Central African Republic Government has endorsed the basic principles of the World Water Vision; by creating National Water and Sanitation body (CNEA) that is responsible for defining and monitoring national policy on water and sanitation, ensuring the coordination of various sector's institutions and implementing the program of the International Decade for Drinking Water and Sanitation (IDWSSD, 1981-1990). It also adopted in 1983 the first strategic national policy documentation on water and sanitation. Therefore, the Central Africa Water Distribution Company (SODECA) was established to provide good water quality to the people. Its water quality laboratory is to provide city staff and citizens with the high quality water and data needed to ensure the safety of the water supply, make informed decisions, and maintain regulatory compliance for potable water. However, financial problems and outdated facilities have negatively affected this primary function of the company.

This study reviews the organization and working procedures of SODECA; highlighting the control system of water quality at this company based on the design of a monitoring program that efficiently and effectively generates data that serve management decision needs such as:

- Establishing, reviewing, and revising water quality standards

- Determining water quality standards attainment

- Identifying causes and sources of water quality impairments

1.1 Strategies for controlling and monitoring

Scientists use water quality data, collected in extensive monitoring and research programs, to assess the condition of aquatic ecosystems, and the effectiveness of environmental policies and management practices. Monitoring strategies are designed to characterize water quality, identify impacts from a variety of sources, provide a systematic and integrated framework for gathering necessary information to support decision making process. And ensure that at all times, the water supplied to the country's population is consistent with current standards. SODECA performs quality checks on inlet water at factory and consumer taps to determine the physicochemical and bacteriological aspect of the water produced at any given point in time.

1.1.1 Type of control analysis

In order to effectively monitor the water quality, SODECA has established a testing program; physico-chemistry, limnology and bacteriology. This laboratory is required to perform such checks regularly to ensure better water quality supply.

1.1.1.1 Physicochemical control

Physicochemical control is performed at all stages of processing and distribution of water in order to judge the effectiveness of treatment adopted and to verify whether the water supplied has the characteristics required for drinking water. The parameters monitored are: pH, turbidity, alkalinity, conductivity, temperature, total hardness, iron, manganese, color, nitrates, nitrites, sulfur and phosphate (Grelaud & Oudar, 1996).

1.1.1.2 *Bacteriological* control

Drinking water may be a means of transmitting many serious infectious diseases. Therefore drinking water bacteriological quality is of great importance, and the monitoring of bacterial indicators such as total coliforms, and fecal coliforms must be especially in ensuring that the bacteriological quality of water produced and distributed within the international limit of less than 100ml total coliform and fecal in 100 ml of sample. These analyses were carried out

in 'SODECA' and 'Institute Pasteur'. These controls are based on study of colonies such as yeasts and moulds, coliform and total bacteria: and carried out twice a month if there's availability of reagents.

A further examination is conducted monthly at the 'Institute Pasteur', for research on germs witnessing a fecal contamination such as *Escherichia coli*, fecal *streptococci*, and *Clostridium* sulfite reducers, total aerobic bacteria at 30°C, total aerobic bacteria at 37°C, heat-resistant coliforms and coliforms. These analyses were performed at the source point in the treated water, on points of special water fountains, and then selected in each distribution area reservoir, especially toward the ends of the network (Grelaud & Oudart, 1996).

1.1.1.3 Limnological test

Limnological analysis is conducted twice a month in rainy period on raw water, and weekly in case of proliferation in the SODECA laboratory, in order to identify the types of algae that can give the water unpleasant taste and odor and initiate anti-algal (Onpe, 1996).

2. Materials and Methods

2.1 Methods of physicochemical Analysis

2.1.1 Volumetric method

The principle consists of adding in a known and precise volume of standard solution (deci normal in general) to water under analysis. The end of reaction is highlighted by a color indicator or a sudden change in pH. This method allows the determination of complete alcalimetric title (CAT), oxidizability of potassium permanganate ($KMnO_4$), Total Hydrometric title (THT) and total calcium hardness (THCA). (Afnor, 1990 and Jean Rodier, 1984)

2.1.2 Nephelometric Method

It is based on the comparison of light diffracted by the sample to a reference standard in the same conditions. This method allows the determination of water turbidity (Afnor, 1990 & Rodier, 1984).

2.1.3 Colorimetric method

This is one of the most used methods in water analysis. Its principle consists of developing a specific reaction color of an element of concern in the samples, and comparing the intensity of the color obtained with a set of standard. The standard color may result from the use of colored screens. This method is applied for measuring pH, residual chlorine, etc. (Afnor, 1990 & Rodier, 1984).

2.1.4 Potentiometric Method

This method measures the potential difference between a working electrode and a reference electrode under the same conditions. It is used for determining conductivity, temperature, pH etc. (Afnor, 1990 & Rodier, 1984).

2.1.5 Photometric method

It is the most accurate analytical method in water analysis. It requires the preliminary implementation of a specific colored reaction of the element sought. It relies on the fact that the dye solution passes through a beam of light, absorbs an amount equivalent to the concentration of elements in it. This method allows the determination of: Fe^{2+}, SO_4^{2-}, Cl^-, S^{2-}, Al^{3+}, NO_3^-, PO_4^{3-}, etc. (Afnor, 1990 & Rodier, 1984).

2.2 Bacteriological analysis method

2.2.1 Millipore sampler's method is used at Central African Water Distribution Company (SODECA) to detect the water contaminants in drinking water. This method identifies the different germs on a specific culture medium that could be their colors.

- Yellow Sampler is specific for yeasts and molds;
- Blue for total coli form colonies;
- Red for total bacteria colonies.

The sampler is immersed in water for few moments and incubated at specific temperatures to find out the specific gems in the water sample. (Grelaud & Oudart, 1996).

2.2.2 Method of analysis conducted at the 'Institute Pasteur'

The microbiological monitoring of water supplied at 'Institute Pasteur' involves the collection, incubation, enumeration isolation, identification and interpretation of results by the following methods:

- Incorporation in agar;
- Membrane filtration;
- Incorporation in agar deep tube.

The main steps in the analysis are: collection, the setting in culture, the enumeration in insulation, identification, and interpretation of results.

2.3 Limnological analysis method

Limnological analysis is to identify the algal species that disrupt the treatment process by clogging filters, odor, taste changes and the risk of proliferation in drinking water pipes in case of infiltration. Its principle is to spin a certain volume of the sample and observe under a microscope the nerve between the blade and the slide in order to identify the different species present in the water sample (Hach, 1986).

3. Results and Discussions

3.1 Results

3.1.1 Frequencies of analyses of water control

The frequency of analyses on water is shown in table 1.

The parameters are grouped as types.

Type I: Temperature, pH, turbidity, CAT, Conductivity.

Type II: Oxidizability KMnO4.

Type III: Rates of alumina sulphate treatment.

Type IV: Identifying algal (twice monthly).

Type V: Fe^{2+}, NO_2^-, NO_3^-, S^{2-}, Mn^{2+}, NH_4^+, PO_4^{3-}, SO_4^{3-}, THT, THMg, THCA, Ca^{2+}, Mg^{2+}, True Color.

Table 2 shows the number of physicochemical parameters controls carried out during three successive months. The Central African Water Distribution Company conducted 133 inspections in November, 126 inspections in December and further 128 inspections in January. The November data lacks some water controls parameters, probably due to the lack of reagents.

Table 3 shows that no Limnological control was performed during the month of November, however only one Limnological control was done during the months of December and January.

Table 4 shows that during November to January, the determination of treatment rates of alumina sulphate was regular. The absence of determination of calcium hypochlorite and lime treatment rates was reported as done to the failure of proportioning pumps.

3.1.2 Frequencies of analyses of water during treatment

The numbers of determination of the physicochemical parameters of water during treatment are more or less good, owing to the fact that certain parameters are below the control standard (Table 5 and 6).

3.1.3 Frequencies of analysis of treated water (From the factory)

Table 7 shows values of various parameter groups:

Type I: Cl_2, temperature, pH, turbidity, CAT, Conductivity.

Type II: Oxidizability KMnO4.

Type III : Cu^{2+}, Al^{3+}, NO_2^-, S^{2-}, Cl^-, Fe^{2+}, Mn^{2+}, NH_4^+, NO_3^-, PO_4^{3-}, SO_4^{2-},THT, THMg, THCa, HCO_3^-, Ca^{2+}, Mg^{2+}.

Table 8 shows, all the parameters are within the acceptable levels, except the residual chlorine and oxidability in KMnO4.

3.1.4 Frequencies of analyses of treated water (From the factory and on the distribution networks)

Table 9 shows the different parameters like Physico-chemistry: Cl_2, pH, temperature, turbidity, CAT, NO_3^-, Al^{3+}, Cu^{2+}, SO_4^{2-}, Fe^{2+}, Color.

Bacteriology: Yeasts and molds, coliforms and total bacteria are determined in SODECA laboratory, while fecal streptococci, Clostridium sulfite reducers, total coliforms, total aerobic bacteria at 30 ° C, and total aerobic bacteria at 37 ° C are determined at 'Institute Pasteur'.

In addition table 10 and 11 shows the results of inspections carried out at the 'Institute Pasteur' in Bangui.

3.2 Discussions

3.2.1 Statistics of controls carried out, and their interpretations

Statistical analyses were done on the data obtained for November to January during 2003 to 2007 period and are illustrated in figures (1- 6).

3.2.2 Statistics of control of raw water

3.2.2.1 Total number and frequency control physicochemical variables and their percentages

In the years 2003-2004 and 2005-2006, the frequency of controls carried out was in conformity with the standard established initially by the water distribution firm in Central African .On the other hand, the years 2004-2005 and 2006-2007 present data parameters was lower than the known standard of controls. This fall could be due to a temporary halt of production during the year 2004-2005 and also the non availability of stock reagents of analyses at the water supply company in Central Africa. With the approach of the rupture, sometimes the frequency of controls undergoes a modification in time. This justifies the reduction of the number of controls. However, it should be recognized that the frequency of analyses is a very significant aspect in monitoring raw water quality which constantly varies in its characteristics. The regular knowledge of the physicochemical quality of raw water allows water handler to re-examine the treatment process with the aim of improve quality of water distributed for human consumption (Figure 1).

3.2.2.2 Totals number of limnologic frequency and a number of control and their percentages

As illustrated by the peaks, no limnologic control was carried out during the year 2003-2004. This is because the SODECA had technical problems within that period. However, in the years 2004-2005, 2005-2006, 2006-2007, these analyses were carried out in accordance with the established frequency. A good identification is not possible unless the base collected after centrifugation is appreciable. Nevertheless, it is found that, the water becomes less turbid in dry periods, thus making the base a little tricky to obtain as show in figure 2.

3.2.2.3 Totals of frequency and a number of determination of the rate of Treatments and their percentages

The number of determination of treatment rates is constant during each year, while remaining very far below the established standard. From table 4, it is obvious that tests of chlorination and neutralization are non-existent. This result could be the disturbance during coagulation, due to inadequate pH of flocculation. Therefore, improper clarification a related to disinfection are caused by under dosage or over dosage (Figure 3).

3.2.3 Statistics of control of water in treatment progress

3.2.3.1 Total frequency and number of controls during water treatment and their percentages

In the first three years controls were more or less constant, although remaining below the standard. In the year 2006-2007, a considerable drops in the number of controls were observed, which could be related to a modification of the frequency of analyses for saving in reagents. The failure of this control may cause a disruption in processing as show in Figure 4.

3.2.4 Statistics of treated water (from the factory)

3.2.4.1 Total frequency and number of physicochemical controls of the processed water and their percentages

The physicochemical controls carried out on the water processed in the factory during 2003-2004 and 2004-2005 periods are in conformity with the established frequency. The deficits recorded in controls during the two last years are due to the breaking-off of the reagents, mainly the reagent Diethylparanylendiamine (**DPD N1)** on which it possible to control the effectiveness of disinfection (Figure 5).

3.2.5 Statistics of treated water (from the factory and on the distribution .networks)

3.2.5.1 Total frequency and number of physicochemical controls and their percentages

The physicochemical controls carried out on the distribution network during the first three years are in conformity with the standards adopted by the water company in Central Africa. It would be judicious to double the frequency of these monitoring for more rigorous oversight of the state of the network because the dilapidated distribution network may lead to the alteration of the water quality flowing through it. The breaking-off of the reagents caused a reduction of the number of analyses on the physicochemical parameters such as: Fe^{2+}, Cl_2, NO_2^-, Al^{3+}, SO_4^{2-}, and Cl^- during the year 2006-2007 (Figure 6).

3.2.5.2 Total numbers of frequency and bacteriological controls and their percentages

The frequency of controls decreases year after year due to the following reasons: the irregularity in the payment of the invoices by the 'Institute PASTEUR' consequently denies it services to the 'SODECA' at times; the breaking-off of the Millipore samplers for bacteriological controls by the SODECA laboratory; the bacteriology is significant in the confirmation of the portability of water. So, it must be carried out as regularly as possible (Figure 7).

4. Conclusions and Suggestions

Water is an essential element of life, not only for human organisms but for all living beings. The consumption of unsafe water which can cause a variety of health problems to man's, if it contains impurities. Therefore, a regular control and monitoring of water quality is essential. The frequency of controls on water quality must be established so that the excess amount of a given element can be detected very quickly. Monitoring the quality of water produced and distributed to the public is of great importance to the health of consumers. However, controls must be strengthened from the raw water intake to the consumer's tap. Based on the results obtained in this study, the following conclusions can be drawn:

- Sometimes the frequency of controls undergoes a modification in time. This justifies the reduction of the number of controls.

- The breaking-off of the reagent causes also a reduction of the number of analyses.

- The frequency of physicochemical control is much more respected compared to the bacteriological and limnologic controls.

And yet, the respect of the frequency of the analyses is a very significant aspect of monitoring. However, the regularity and the insurance in the realization of the physicochemical and bacteriological analyses constitute a guarantee in the control of quality of water produced.

Therefore, the 'SODECA' will have to pay much more attention on the following points in order to perform efficiently and effectively.

- The equipment of its laboratory with high technical instrument and highly trained work force;

- The regular supply of reagents of analyses for quality control;

- More qualified personnel should be involved in management, in order to gain the confidence of consumers on quality control issues;

- The revision of method, mode of analyses of control, monitoring and distribution;

- The sensitizing of the population on the importance of quality of drinking water.

Acknowledgement

References

Association Française de Normalisation (AFNOR). (1990). 4^{éme} édition, Tome I et II. Eaux méthodes d'essais. P: 414 et 734.

Boyer, J.N., Sterling, P. & Jones R.D. (2000). Maximizing Information from a Water Quality Monitoring Network through Visualization Techniques. *Estuarine, Coastal, and Shelf Science*, 50, 39-48.

Cosgrove,W. & Rijsberman, F.R. (2000). World Water Vision: Making Water everybody's Business London. *World Water Council*, Earthscan Publications Ltd.

Chery, L. & Thouin, C. (2005). 6th Int. EWRA Conf., European Water Resources Association. [Online] Available: http://www.ewra.net/.

Coquery, M., Morin, A., Be´cue, A. & Lepot, B. (2005). *Trends Anal. Chem.*, 24, 117.

Degremont. (1989). 9^{éme} édition, Tome 1 et 2. Mémento technique de l'eau.

Gadgil, A. (1998). Drinking water in developing countries. *Annual Review of Energy and the Environment,* 23, 253–286.

Grelaud, M. & Oudart, I. (1996). Traitement des eaux potables n°1et 2. Institut de Formation Professionnelle. P : 96 et 120.

Graveline, N., Maton, L., Lu¨ckge, H., Rouillard, J., Strosser, P., Palkaniete, K., Rinaudo, J.D., Taverne, D. & Interwies, E. (2010). An operational perspective on potential uses and constraints of emerging tools for monitoring water quality. *Trends in Analytical Chemistry*, Vol. 29, No. 5

Hach. (1989). Mémento technique de l'eau. 9^{éme} édition, Tome 1 et 2.

Harmancioglu, N.B. & Alpaslan, N. (1992). Water Quality Monitoring Network Design: A Problem of Multi-Objective Decision Marking. *Water Resources Bulletin*, 28(1), 179-192.

Harmancioglu, N.B., Fistikoglu, O., Ozkul, S.D., Singh, V.P. & Alpaslan, M.N. (1998). *Water Quality Monitoring Network Design*. Kluwer Academic Publishers, Dorbrecht, the Netherlands.

Hrudey, S.E., Hrudey, E. J., Pollard, S.J.T. (2006). Risk management for assuring safe drinking water. *Environment International*, 32, 948–957

Karavoltsosa, S., Sakellaria, A., Mihopoulosb, N., Dassenakisa, M., Scoullosa, M.J. (2008). Evaluation of the quality of drinking water in regions of Greece. *Desalination*, 224, 317–329

Loftis, J.C. & Ward, R.C. (1980). Cost Effective Selection of Sampling Frequencies for Regulatory Water Quality Monitoring. *Environment International*, 3, 297-302.

Office National de l'Eau Potable (ONEP). (1996). Les algues dans les retenues de barrage utilisées pour la production d'eau potable au Maroc. Royaume du Maroc production d'eau. P : 104.

Rodier, J. (1984). *Analyse de l'eau*. 7eme édition. DUNOD Paris, 1365p.

WHO (World Health Organization). (2004a). *Water, Sanitation and Hygiene Links to Health, Facts and Figures*. World Health Organization

Table 1. Frequency of parameters used to control raw water

Periods	Monitored Parameters
Daily	Type I and Type III
Weekly	Type II
Monthly	Type IV
Quarterly	Type V

Table 2. Number of determinations of physicochemical parameters during three months

	November 06	December 06	January 07
Temperatures	30	31	31
pH	30	31	31
Turbidity	30	31	31
Conductivity	30	31	31
Oxidizability	2	2	4
Fe^{2+}	0		
NO_2^-	0		
NO_3^-	0		
S^{2-}	0		
Mn^{2+}	1		
NH_4^+	1		
PO_4^{3-}	1		
SO_4^{2-}	1		
THT	1		
THM_g	1		
THC_a	1		
C_a^{2+}	1		
M_g^{2+}	1		
HCO_3^-	1		
Color	1		
Total	133	126	128

Table 3. Determination of number of limnological control over three months

	November 06	December 06	January 07
Control Number	0	1	1
Total	**0**	**1**	**1**

Table 4. Determination of the rate of treatments carried out of the principal chemicals

Chemicals	*November 06*	*December 06*	*January 07*
Alumina Sulphate	30	31	31
Calcium hypochlorite	0	0	0
Lime	0	0	0
Total	30	31	31

Table 5. Frequency of physicochemical parameters used

Daily parameters	**pH**	**Turbidity**	**Cl_2** (case of pre chlorination)
Frequencies	1 time / h	1 time / day	1 time / h

Table 6. Number of inspections conducted by the 'SODECA' company

	November 06	December 06	January 07
pH	**48**	**44**	**45**
Turbidity	**30**	**31**	**31**
Cl_2	**-**	**-**	**-**
Total	**78**	**75**	**76**

Table 7. Frequency of physicochemical parameters

Periods	Monitored Parameters
Daily	Type I
Weekly	Type II
Quarterly	Type III

Table 8. The number of controls of the physicochemical parameters

	November 06	December 06	January 07
Cl_2	76	98	103
Temperature	30	31	31
Turbidity	30	31	31
pH	30	31	31
Conductivity	30	31	31
CAT	30	31	31
Oxidizability	2	2	4
Cu^{2+}	-	-	-
Al^{3+}	1		
NO_2^-	1		
NO_3^-	1		
Fe^{2+}	1		
Cl^-	1		
NH_4^+	1		
PO_4^{3-}	1		
SO_4^{2-}	1		
Mn^{2+}	1		
THT	1		
THMg	1		
THCa	1		
HCO_3^-	1		
Ca^{2+}	1		
Mg^{2+}	1		
Total	243	255	262

Table 9. Frequency of parameters used

Monitored Parameters	Monthly
Physico-chemistry	1 time
Bacteriology (SODECA company)	2time
Bacteriology (institute Pasteur)	1time

Table 10. The number of physicochemical controls carried out

	December 06	January 07
Temperature	1	1
Turbidity	1	1
pH	1	1
CAT	1	1
Iron	0	1
Cl_2	1	1
NO_2^-	0	1
Al^{3+}	0	1
Cu^{2+}	-	-
SO_4^{2-}	1	1
Cl^-	1	1
Color	1	1
Total	**8**	**11**

Table 11. The number of bacteriological controls carried out at the institute Pasteur

	Bacteriology (Institut pasteur)
November 06	0
December 06	1
January 07	1
Total	**2**
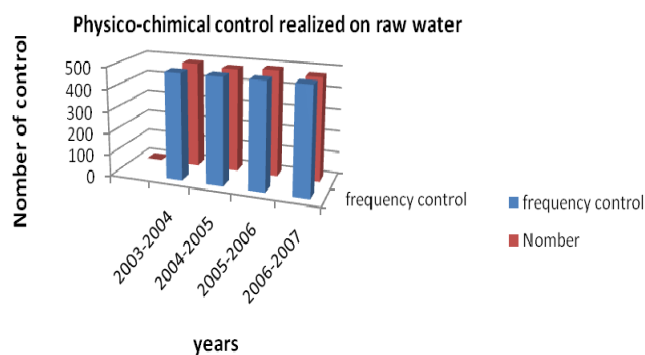
Figure 1. Evolution of physicochemical controls
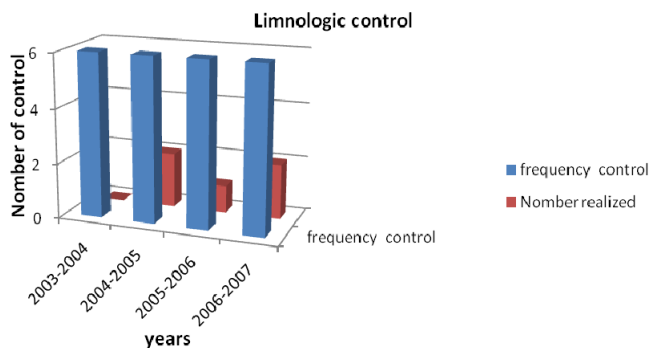
Figure 2. Evolution of the Limnologic control
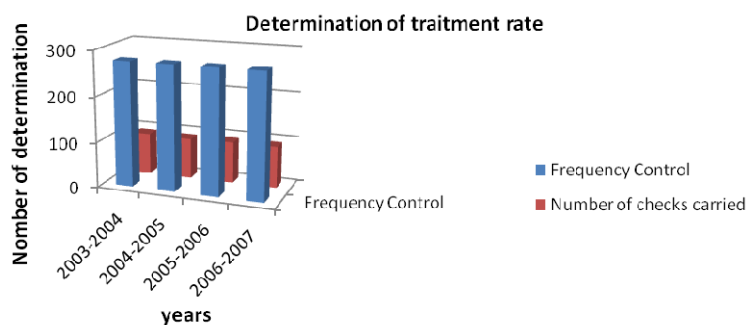
Figure 3. Evolution of the treatment rates
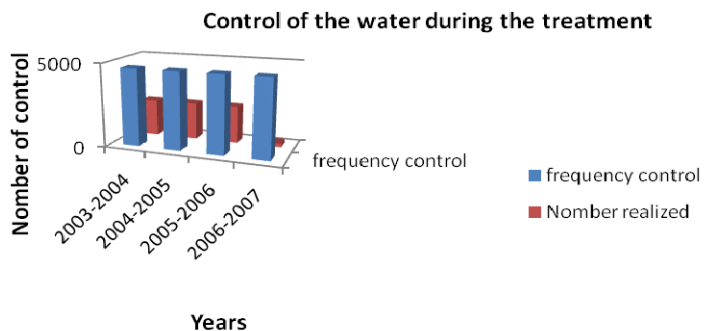
Figure 4. Evolution of control of the water during the treatment
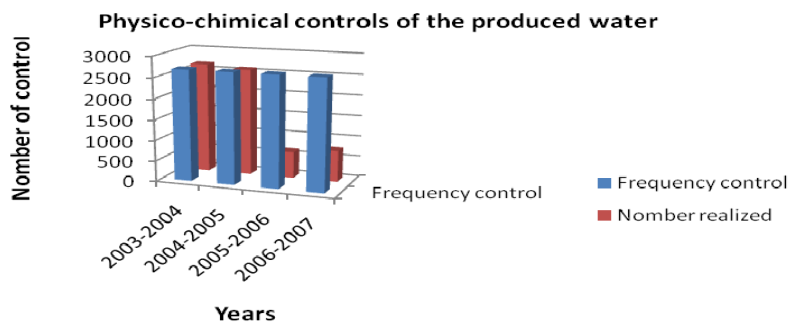
Figure 5. Evolution of physicochemical controls of the produced water
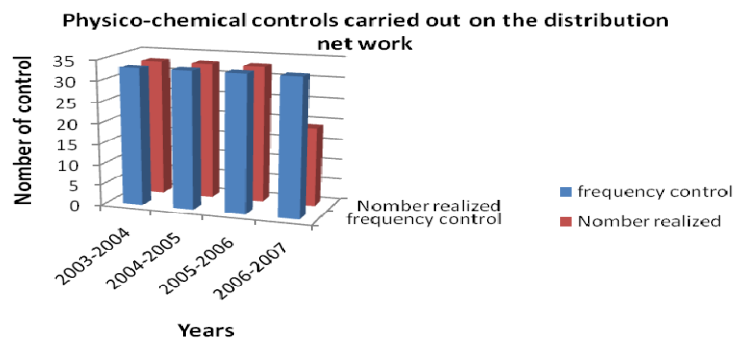
Figure 6. Evolution of physicochemical controls of the treated water
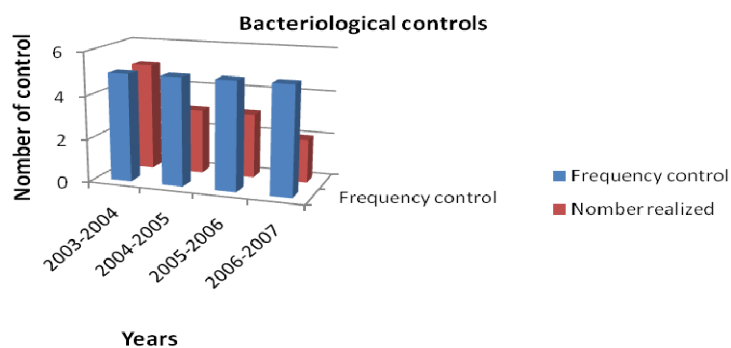
Figure 7. Evolution of bacteriological controls

One-pot Multi-component Synthesis of Amidoalkyl Naphthols with Potassium Hydrogen Sulfate as Catalyst under Solvent-free Condition

Xiao-hua CAI

College of Chemistry and environmental Science, Guizhou University for *Nationalites*

Guiyang 550025, China

Tel: 86-851-361-0313   E-mail: caixh1111@163.com

Hui GUO

College of Pharmaceutical Sciences, Zhejiang University of Technology

Hangzhou 310014, China

E-mail: gh635@zjut.edu.cn

Bing XIE

College of Chemistry and environmental Science, Guizhou University for *Nationalites*

Guiyang 550025, China

Tel: 86-851-361-0313   E-mail: bing_xie1963@hotmail.com

Abstract

One-pot multicomponent condensation of β-naphthol, aromatic aldehydes, acetamide or urea was carried out in the presence of potassium hydrogen sulfate under solvent-free condition to afford the corresponding amidoalkyl naphthols in 83%~96% yields.

Keywords: Amidoalkyl naphthol, Multicomponent reaction, Potassium hydrogen sulfate

1. Introduction

The multicomponent reactions are responsible for this higher efficiency (Bienaymè, H. C. et. al 2000), not only because of intrinsic aspects of the reaction such as superior atom economy (Trost, B. M., 1991, Trost, B. M. 1995, Trost, B. M. 2002), atom utilization and selectivity, as well as lower level of by-products, but also because of extrinsic aspects of the processing reaction, such as simpler procedures and equipment (Mitchell, M. C. et. al 2001, Jähnisch, K. et. al 2004), lower costs, time, and energy, as well as more environmentally friendly criteria. It is noteworthy that 1-carbamato-alkyl-2-naphthols can be converted to important biologically active 1-aminomethyl-2-naphthol derivatives by carbamate hydrolysis. The hypotensive and bradycardiac effects of these compounds have been evaluated (Szatmári, I.; et. al 2004, Shen, A. Y. et. al 1999, Shaterian, H. R. et. al 2008).

Amidoalkyl naphthols can be prepared by multicomponent condensation of aldehydes, β-naphthols and acetonitrile or different amides in the presence of Lewis or Brösted acids such as Iodine (Das, B. et al 2007, Nagawade R. R. et. al 2007), FeCl$_3$·SiO$_2$ (Shaterian, H. R. et. al 2008), K$_5$CoW$_{12}$O$_{40}$·3H$_2$O (Nagarapu, L. et. al 2007), HClO$_4$–SiO$_2$ (Mahdavinia, G. H. et. al 2008), Brösted acidic ionic liquid (Hajipour, A. R. et. al 2009), P$_2$O$_5$ (Nandi, G. C. et. al 2009), cyanuric chloride (Mahdavinia, G. H. et. al 2009), montmorillonite K10 (Kantevari, S. et. al 2007), sulfamic acid (Patil, S. B. et. al 2007), thiamine hydrochloride (Min L. et. al 2009), Sr(OTf)$_2$ (Su, W. K. et. al 2008), silica sulfuric acid (Srihari, G. et. al 2007). Yb(OTf)$_3$ (Kumar, A. et. al 2009), Ce (SO$_4$)$_2$ (Selvam, N. P. et. al 2006), etc. However, some of the reported protocols suffer from certain drawbacks such as prolonged reaction time, use of dichloromethane like carcinogenic solvent, unsatisfactory yield, high temperature (120~125 ℃) and use of toxic, highly acidic, expensive catalysts and additional microwave or ultrasonic irradiation. Therefore, the discovery of clean procedures and the use of green and eco-friendly catalysts with high catalytic activity and short reaction times for the production of amidoalkyl naphthols have gained considerable attention.

Potassium hydrogen sulfate is a cheap and efficient catalyst for the condensation reactions (Huang, Z. Y. et. al 2005, Shi, F. et. al 2007, Tu, S. J. et. al 2004, CaiP, X. –H. et. al 2006). In the present study, a simple and green procedure for the synthesis of amidoalkyl naphthols by the condensation of aldehydes with β-naphthol, acetamide or urea in the presence of potassium hydrogen sulfate (KHSO$_4$) under solvent-free conditions at 100 ℃ has been reported (Figure 1).

Benzaldehyde was selected as a representative aldehyde along with of β-naphthol, acetamide and KHSO$_4$ were reacted under solvent-free conditions at 100 ℃ in order to optimize the reaction conditions. The condensation of mixture of benzaldehyde **1a** (1 mmol) with β-naphthol **2** (1 mmol) and acetamide **3** (1.1 mmol) in the presence of KHSO$_4$ (0.15 mmol) was carried out at 100 ℃ for 1.0 h under solvent free conditions. The reaction proceeded smoothly and gave the corresponding amidoalkyl naphthol **4a** as the sole product in 90% isolated yield (Table 1). Water was added to the reaction mixture and simply filtering the mixture and gave the crude product, which was purified by crystallization from 30% ethanol to obtain **4a** as white solid.

In order to demonstrate the generality of the process, some examples illustrating the present method for the synthesis of amidoalkyl naphthols **4** was studied (Table 1). The reaction of β-naphthol **2** with various aromatic aldehydes bearing electron withdrawing groups (such as nitro, halide), electron releasing groups (such as, methyl or methoxy groups) and acetamide was carried out in the presence of KHSO$_4$ as a catalyst. In all cases, clean and the complete conversion leading to the corresponding amidoalkyl naphthols as observed in shorter reaction times (0.5~1.5 h). Aromatic aldehydes with electron-withdrawing groups reacted faster than aromatic aldehydes with electron-donating groups, as would be expected. Similar results were obtained under the same conditions when urea was used in place of acetamide.

2. Experimental

General procedure: KHSO$_4$ (0.15 mmol) was added into a mixture of aldehyde (1 mmol), β-naphthol (1 mmol) and acetamide or urea (1.1 mmol), then the reaction mixture was heated to 100 ℃ and maintained for the appropriate time (Table 1). After completion of the reaction (monitored by TLC), the reaction mixture was diluted with water, and the resulting solid product was collected by filtration, which was purified by recrystallization from EtOH/H$_2$O.

N-[(4-Fluorophenyl)(2-hydroxynaphthalen-1-yl)methyl]acetamide **4e**, ^{1}H NMR (400 MHz, CDCl$_3$, δ ppm): 10.16 (s, 1H), 8.08 (d, J = 8.2 Hz, 1H), 7.88 (d, J = 12.2 Hz, 1H),7.81-7.65 (m, 2H), 7.38-7.05 (m, 8H), 2.02 (s, 3H); ES-MS, m/z: 308 (M−H, 100%); Anal. Calcd for C$_{19}$H$_{16}$FNO$_2$: C, 73.77; H, 5.21; N, 4.53; F, 6.14. Found: C, 73.72; H, 5.25; N, 4.52; F, 6.14.

[(Furan-2-yl)(2-hydroxynaphthalen-1-yl)methyl]urea **4q**: ^{1}H NMR (400 MHz, CDCl$_3$, δ ppm): 10.20 (s, 1H), 7.67–7.08 (m, 7H), 6.73 (s, 2H), 6.35 (br. s, 1H), 6.22 (m, 1H), 6.09 (m, 1H), 5.73 (br. s, 1H). ES-MS, m/z: 281 (M−H, 100%). Found (%): C, 67.89; H, 5.06; N, 9.85. Calc. for C$_{16}$H$_{14}$N$_2$O$_3$ (%): C, 67.92; H, 5.02; N, 9.89.

3. Conclusion

In conclusion, a novel and highly efficient methodology for the synthesis of amidoalkyl naphthols by condensation reaction of aldehydes, β-naphtol and acetamide or urea in the presence of catalytic amounts of KHSO$_4$ under solvent-free conditions is reported. This method offers significant advantages, such as, high conversions, easy handling and shorter reaction times, which makes it a useful and attractive process for the rapid synthesis of substituted amidoalkyl naphthols.

References

Bienaymè, H. C., Hulme, G., Oddon, P. (2000). Schmitt. Maximizing synthetic efficiency: multi- component transformations lead the way, *Chem. Eur. J.*, 6: 3321-3329.

CaiP, X. –H., Xie, B., PGuoP, H. (2006). Synthesis of α,α'-bis(R-benzylidene) cycloalkanones catalyzed by potassium hydrogen sulfate under solvent-free conditions. *Chem. Pap.*, 60: 318-320.

Das, B., Laxminarayana, K., Ravikanth, B., Rao, R. (2007). Iodine catalyzed preparation of amidoalkyl naphthols in solution and under solvent-free conditions. *J. Mol. Catal. A: Chem.*, 261: 180-183.

Hajipour, A. R., Ghayeb, Y., Sheikhan, N., Ruoho, A. E. (2009). Brønsted acidic ionic liquid as an efficient and reusable catalyst for one-pot synthesis of 1-amidoalkyl 2-naphthols under solvent-free conditions. *Tetrahedron Lett.*, 50: 5649-5651.

Huang, Z. Y., Zhang, M., Wang, Y., Qin, Y. (2005). KHSO$_4$-mediated condensation reactions of tert-butanesulfinamide with aldehydes. preparation of tert-butanesulfinyl aldimines, *Synlett*, 1334-1336.

Jähnisch, K., Hessel, V., Löwe, H. (2004). Baerns, M. Chemie in mikrostrukturreaktoren. *Angew. Chem.*, 116:

410-451.

Kantevari, S., Vuppalapati, S. V. N., Nagarapu, L. (2007). Montmorillonite K10 catalyzed efficient synthesis of amidoalkyl naphthols under solvent free conditions. *Catal. Commun.*, 8: 1857-1862.

Kumar, A., Rao, M. S., Ahmad, I., Khungar, B. (2009). A simple and facile synthesis of amidoalkyl naphthols catalyzed by Yb(OTf)$_3$ in ionic liquids. *Can. J. Chem.*, 87: 714-719.

Lei, M., Ma, L., Hu, L. H. (2009). Thiamine hydrochloride as a efficient catalyst for the synthesis of amidoalkyl naphthols. *Tetrahedron Lett.*, 50: 6393-6397.

Mahdavinia, G. H., Bigdeli, M. A. (2009). Wet cyanuric chloride promoted efficient synthesis of amidoalkyl naphthols under solvent-free conditions. *Chin. Chem. Lett.*, 20: 383-386.

Mahdavinia, G. H., Bigdeli, M. A., Heravi, M, M. (2008). Silica supported perchloric acid (HClO$_4$–SiO$_2$): A mild, reusable and highly efficient heterogeneous catalyst for the synthesis of amidoalkyl naphthols. *Chin. Chem. Lett.*, 19: 1171-1174.

Mitchell, M. C., Spikmans, V., Manz, A., de Mello, A. (2001). Microchip-based synthesis and total analysis systems (μSYNTAS): chemical microprocessing for generation and analysis of compound libraries. *J. Chem. Soc. Perkin Trans., 1*: 514-518.

Nagarapu, L., Baseeruddin, M., Apuri, S., Kantevari, S. (2007). Potassium dodecatungstocobaltate trihydrate (K$_5$CoW$_{12}$O$_{40}$ · 3H$_2$O): A mild and efficient reusable catalyst for the synthesis of amidoalkyl naphthols in solution and under solvent-free conditions. *Catal. Commun.*, 8: 1729-1734.

Nagawade R. R. and Shinde. D. B. (2007). Synthesis of amidoalkyl naphthols by an iodine-catalyzed multicomponent reaction of β-naphthol. *Mendeleev Commun.*, 17: 299-300.

Nandi, G. C., Samai, S., Kumar, R., Singh, M. S. (2009). Atom-efficient and environment-friendly multicomponent synthesis of amidoalkyl naphthols catalyzed by P$_2$O$_5$. *Tetrahedron Lett.*, 50: 7220-7222.

Patil, S. B., Singh, P. R., Surpur, M. P., Samant, S. D. (2007). Ultrasound-promoted synthesis of 1-amidoalkyl-2-naphthols via a three-component condensation of 2-naphthol, ureas/amides, and aldehydes, catalyzed by sulfamic acid under ambient conditions. *Ultrason. Sonochem.*, 14: 515-518.

Selvam, N. P., Perumal, P. T. (2006). A new synthesis of acetamido phenols promoted by Ce(SO$_4$)$_2$. *Tetrahedron Lett.*, 47: 7481-7483.

Shaterian, H. R., Yarahmadi, H., Ghashang. M. (2008). An efficient, simple and expedition synthesis of 1-amidoalkyl-2-naphthols as 'drug like' molecules for biological screening. *Bioorg. Med. Chem. Lett.*, 18: 788-792.

Shaterian, H. R.; Yarahmadi, H. (2008). A modified reaction for the preparation of amidoalkyl naphthols. *Tetrahedron Lett.*, 49: 1297-1300.

Shen, A. Y., Tsai, C. T., Chen, C. L. (1999). Synthesis and cardiovascular evaluation of N-substituted aminonaphthols. *Eur. J. Med. Chem.*, 34: 877-882.

Shi, F., Jia, R. H., Zhang, X. J., Tu, S. J., Yan, S., Zhang, Y., Jiang, B., Zhang, J. Y., Yao, C. S. (2007). Extension of the Biginelli-type reaction: one-pot synthesis of pyrimido-pyrimidines and spirobi [pyrimidine]s using potassium hydrogen sulfate as a catalyst, *Synthesis*, 2782-2790.

Srihari, G.; Nagaraju, M.; Murthy, M. M. (2007). Solvent-free one-pot synthesis of amidoalkyl naphthols catalyzed by silica sulfuric acid. *Helv. Chim. Acta.*, 90: 1497-1504.

Su, W. K., Tang, W. Y., Li, J. J. (2008). Strontium(II) triflate catalysed condensation of β-naphthol, aldehyde and urea or amides: a facile synthesis of amidoalkyl naphthols. *Chem. Res.*, 123-128.

Szatmäri, I., Fülöp, F. (2004). Syntheses and Transformations of 1-(α-Aminobenzyl)-2-naphthol Derivatives. *Curr. Org. Synth.*, 1: 155-165.

Trost, B. M. (1991). The atom economy: a search for synthetic efficiency. *Science*, 254: 1471-1477.

Trost, B. M. (1995). Atom cconomy-a challenge for organic synthesis: homogeneous catalysisleads the way. *Angew. Chem.*, 107: 285-307.

Trost, B. M. (2002). On inventing reactions for atom economy. *Acc. Chem. Res.*, 35: 695-705.

Tu, S. J., Fang, F., Zhu, S. L., Li, T. J., Zhang, X. J., and Zhuang, Q. Y. (2004). A new Biginelli reaction procedure using potassium hydrogen sulfate as the promoter for an efficient synthesis of 3,4-dihydropyrimidin-2(1H)-one. *Synlett*, 537-539.

Table 1. Synthesis of Amidoalkyl Naphthols with Potassium Hydrogen Sulfate as Catalyst under Solvent-free Condition

Product[a]	R_1	R_2	Time (h)	Yield[b] (100%)	Mp (℃)
4a	C_6H_5	CH_3	1.0	90	232-233
4b	$4\text{-}MeC_6H_5$	CH_3	1.0	91	223-224
4c	$4\text{-}ClC_6H_5$	CH_3	0.5	95	233-234
4d	$4\text{-}MeOC_6H_5$	CH_3	1.0	94	172-174
4e	$4\text{-}FC_6H_5$	CH_3	0.5	95	205-207
4f	$4\text{-}NO_2C_6H_5$	CH_3	0.5	96	239-240
4g	$3\text{-}NO_2C_6H_5$	CH_3	0.5	93	238-240
4h	$4\text{-}BrC_6H_5$	CH_3	0.5	92	230-231
4i	$2\text{-}ClC_6H_5$	CH_3	0.5	93	194-195
4j	$3\text{-}MeOC_6H_5$	CH_3	1.0	88	192-194
4k	2-Furyl	CH_3	1.5	83	218-220
4l	C_6H_5	NH_2	1.0	90	173-174
4m	$4\text{-}ClC_6H_5$	NH_2	0.5	94	170-171
4n	$4\text{-}NO_2C_6H_5$	NH_2	0.5	96	181-183
4o	$3\text{-}NO_2C_6H_5$	NH_2	1.0	95	186-188
4p	$4\text{-}BrC_6H_5$	NH_2	1.0	92	173-175
4q	2-Furyl	NH_2	1.5	85	162-163

[a]All known compounds were characterized by comparing their spectral data with those reported
[b]Isolated yields.
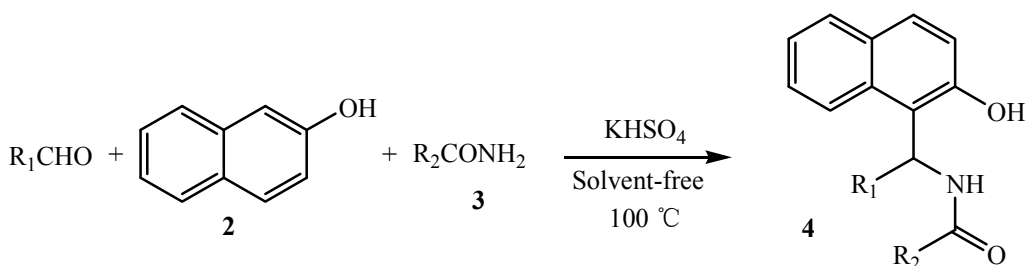
Figure 1. Synthesis of amidoalkyl naphthols by the condensation of aldehydes with β-naphthol, acetamide or urea in the presence of (KHSO$_4$) under solvent-free conditions

One-Pot Synthesis of Aromatic Hydroxyketones under Microwave Irradiation and Solvent-Free Conditions

Yuqing Cao (Corresponding author)

College of Pharmacy, Hebei University

Baoding 071002, Hebei, China

E-mail: pharm_hbu@yahoo.com

Fangrui Song

College of Pharmacy, Hebei University

Baoding 071002, Hebei, China

E-mail: fangrui102@163.com

Liya Xu, Dingxiang Du, Xiaojun Yang & Xiangtao Xu

College of Pharmacy, Hebei University

Baoding 071002, Hebei, China

Abstract

An efficient one-pot synthesis of aromatic hydroxyketones with carboxylic acids as acylating agents without solvent under microwave irradiation was reported. The reaction time was only 1-5 min. Besides, this method has a feature of high yields, low cost, easy manipulation and less pollution.

Keywords: One-pot synthesis, Microwave irradiation, Aromatic hydroxyketones, Carboxylic acids, Solvent-free

1. Introduction

Aromatic hydroxyketones are valuble intermediates in the synthesis of pharmaceuticals (Szmant, H. 1989), perfumery (Naeimi, H. et.al 2006), acetophenone resins (Heitling, E. et.al 2004), etc. The classic synthesis commonly involves two steps, esterification of phenols and fries rearrangement which is an intermolecular Friedel-Crafts acylation of phenolic ester (Kozhevnikova, E. F. et.al 2004,Vogt, A. et.al 1995). The disadvantages associated with classic procedures include the use of toxic acid chlorides or acid anhydrates as acylating agents (Rupinder, K. L. et.al 2006, Ludwigshafen, J. M. et.al 1985) and aluminum trichloride as Lewis acids (Miller, E. et.al 1943) and an excess amount of reagents for separation of phenolic ester, which entains environment pollution and tedious workup. Recently, zeolite H-beta (Hoefnagel, A. J. 1993) and montmorillonite clay (Bolognini, M. et.al 2004) are reported to be used as catalysts for synthesis of aromatic hydroxyketones, but these catalysts both need special treatment before use such as calcination at a high temperature. Moreover, the whole reaction process normally requires long reflux times at oil bath. The drawbacks as above described have prompted considerable researches into the development of a new method which is low cost, easy manipulation and less pollution.

Microwave irradiation as a new technology has been widely used in various organic reactions, such as substitution (Mojtahedi, M. M. et.al 1999), addition (Mojtahedi, M. M. et.al 1999), dehydration (Bandgar, B. P. et.al 1999), rearrangement (Khadikar, B. M. et.al 1999) and redox (Palombi, L. et.al 1997). Solvent-free could avoid the use of auxiliary reagents that may be toxic or flammable, and also simplify the follow-up operation. The synthesis without solvent under microwave irradiation has been of growing interest as an efficient, economic and, clean procedure (Pasha, M. A. et.al 2007, Gopalakrishnan, M. et.al 2005). Carboxylic acids are common precursors of acid chlorides and anhydrides and their reactions produced water as the only by-product (Naeimi, H. et.al 2006). From an environment point of view, the aromatic acylation with carboxylic acids has also attracted interest.

In this paper, the mixture of phenols, carboxylic acids, phosphoric acid and phosphorus pentoxide (85% H_3PO_4/P_2O_5) were irradiated in a microwave oven, the target products were obtained by one-pot.

2. Experimental

2.1 General

All reactions were performed in a modified commercial domestic microwave oven (Midea PJ21C-BF) which was equipped with a reflux device. TLC was used to monitor the reaction process. TLC was GF254 thin- layer chromatography with petroleum ether/ethyl acetate (4:1v/v) used as eluent. Melting points were determined on a microscopy apparatus (SGW X-4). IR spectra were recorded on a Bio-Rad FTS-40 spectrometer (KBr). All the liquid parent materials are fresh distilled. The products were characterized by comparison of their melting points and boiling points with the literature values.

2.2 General procedure for the preparation of o-/p- Hydroxyacetophenone

A mixture of phenol (9.4g), acetic acid (7.0mL), 85% H_3PO_4 (2mL) and P_2O_5 (0.9g) was irradiated at middle power (231W) in a 50mL one-necked, round-bottomed flask equipped with a reflux device which was placed into a 200mL beaker. The progress of the reaction was monitored by TLC. Upon completion, the products were poured into water (200mL). Extracted the acylation products from water with ether. The water layer was rejected. Distilled the ether layer to remove ether. The p-hydroxyacetophenone (p-HAP) 9.8g (72%yield) was obtained by filtration and purification. m.p.108-109 ^{o}C.(lit m.p.109 ^{o}C); The organic phase detached from the filtration was distilled. Collecting the distillation of 215-218 ^{o}C to obtain the o-hydroxyacetophenone (o-HAP) 2.4g (18%yield). (lit b.p.213 ^{o}C). The IR spectra of the products were accordant with the standard IR spectra respectively.

3. Results and Discussion

Carboxylic acids are less reactive than acid chlorides or acid anhydrates, in the present case, however, the high charge density of the aromatic ring in phenols makes carboxylic acids the best candidate for the electrophilic reaction. Microwave irradiation promoted this electrophilic acylation, because the water as its only by-product was easily removed under microwave irradiation.

3.1 The catalytic medium for the preparation of aromatic hydroxyketones

In our study, the mixture of phosphoric acid and phosphorus pentoxide (85% H_3PO_4/P_2O_5) was choosen as a catalytic medium which was mild, cheap and, easy to be got. More importantly, phosphoric acid and phosphorus pentoxide both were easily washed away by water. The weight ratio of 85% H_3PO_4 to P_2O_5 was 4:1. P_2O_5 mainly played a role of dehydrating agent, since the use of P_2O_5 alone always failed to promote acylation. Phosphoric acid was crucial to the catalytic effectiveness. As a liquid catalyst, it not only promoted acylation but also supplied convenience for the mixing of solids reactants. This catalytic medium has an efficiency under microwave irradiation. Large amount of the catalyst might make reactants darked and parched like the phenomenon reported in previous literature in short times and low power (Kozhevnikova, E. F. et.al 2004), we guessed it may result from the polymerization of olefine ketone which is easily produced under excessive catalyst. The optimal molar ratio of H_3PO_4 to aromatic substrate is 0.3:1.

With carboxylic acids as acylating agents, this "protonic-acid catalytic method" is a preferred one because of its simplicity. There is no large amount of metal salts formed after reaction like Lewis acids. Furthermore, the usage amount of catalyst was largely reduced. This not only saved the production cost, but also decreased the pollution to environment.

3.2 Effect of power and reaction time on yield of products

The power and reaction time both have an obvious effect on yield of products. Taking phenol to react with acetic acid for example, as is shown in table 1, the yield was higher at 231W than that at 119 W, however, when the power was 385 W or upwards, lots of side products formed due to the oxidation of phenols and other side reactions. Microwave irradiation can produce lots of heat in short time, so the temperature is not easy to control if the reaction time is too long. The optional microwave irradiation power was 231W and the reaction time was 2min.

3.3 Acylation of various phenols with acetic acid

Various phenols were treated with acetic acid along with a catalytic amount of catalyst under microwave irradiation and solvent-free conditions. As shown in table 2, most phenols afforded their corresponding aromatic hydroxyketones in excellent yields by one-pot and the reaction time was only 1-3min which was greatly reduced compared with long reflux times by conventional heating. The phenols with electron-donating groups such as –OCH_3 were more reactive than those with electron-withdrawing groups such as –Cl, that mainly because the electron-donating groups could increase the electron density of aromatic ring which caused the reaction easier. When a –NO_2 on the aromatic ring (entry9), the reaction did not afford the corresponding hydroxyketone. Most phenols could obtain their $ortho$-acylated products in high yields. Due to the poor regioselectivity of phenol (entry1)

and catethol (entry2), the acylation result was a mixture of *ortho*-acylated and *para*-acylated products. However, the regioselectivity of phenol and catethol was enhanced and the *para*-isomer was obtained in high yields under this reaction conditions. In addition, the naphthols and heteroaromatic compound substituted with hydroxyl group also can react in excellent yields.

3.4 Acylation of phenol with various carboxylic acids

In continuation, the acylation of phenol with propionic acid, butanoic acid, valeric acid, succinic acid and benzoic acid in the presence of catalyst without solvent under microwave irradiation was tried, respectively. These reactions also produced *para*-acylated compounds in high yields and in short times except succinic acid. Succinic acid was a binary acid, because of the high charge density of phenol, the diphenyl succinate was easily formed under this reaction conditions. The obtained results of other carboxylic acids were shown in table 3. Thereinto, *p*-hydroxypropiophenone (entry1) is a key intermediate for preparation of ritodrine which is an agonist for β_2 acceptor of adrenalin. Compared with the previous method (Rupinder, K. L. et.al 2006, Ludwigshafen, J. M. et.al 1985, Miller, E. et.al 1943), this new method only took 2 min to finish the reaction with yield of 79%. In an environmentally benign, it is more favourable for large-scale chemical industry production. In addition, microwave irradiation has greatly promoted the smooth progress of the reaction between phenol and solid carboxylic acids such as benzoic acid (entry4) without solvent. Easy sublimation of benzoic acid at 100℃ made the yield lower than that of aliphatic carboxylic acids in table 3.

4. Conclusions

In this paper, we reported an efficient one-pot synthesis of aromatic hydroxyketones with carboxylic acids as acylating agents without solvent under microwave irradiation. In competition with the previous method, it not only simplies the procedure but also diminishes the waste problem of the aforementioned known reactions with metal chlorides. Besides, the reaction time was greatly reduced, from many hours to 1-5 min.

References

Bandgar, B. P., Sadavarte, V. S., & Sabu, K. R. (1999). Microwave activation in organic synthsis: Natural Indian Clay, EPICR EPZGR EPZIOR as novel heterogeneous catalysis for rapid synthesis of nitriles from aldoximes in absence of solvent. *Synthetic Communications*, 29, 3409-3413.

Bolognini, M., Cavani, F., & Cimini, M. (2004). An environmentally friendly synthesis of 2,4-dihydroxybenzophenone by the single-step O-mono-benzoylation of 1,3-dihydroxybenzene (resorcinol) and Fries rearrangement of intermediate resorcinol monobenzoate: the activity of acid-treated montmorillonite clay catalysis. *Comptes Rendus Chimie*, 7, 143-150.

Gopalakrishnan, M., Sureshkumar, P., Kanagarajan, V., & Thanusu, J. (2005). Aluminium metal power (atomized) catalyzed Friedel-Crafts acylation in solvent-free conditions: A facile and rapid synthesis of aryl ketones under microwave irradiation. *Cataysisl Communications*, 6, 753-756.

Heitling, E., Roessner, F., & Van Steen, E. (2004). Origin of catalyst deactivation in fries rearrangement of phenyl acetate over zeolite H-Beta. *Journal of Molecular Catalysis A: Chemical*, 216, 61-65.

Hoefnagel, A. J. (1993). Direct Fries reaction of resorcinol with benzoic acids catalyzed by zeolite H-beta. *Applied Catalysis A: General*, 97, 87-102.

Khadikar, B. M., & Madyar, V. R. (1999). Fries rearrangement at atmospheric pressure using microwave irradiation. *Synthetic Communications*, 29, 1195-1200.

Kozhevnikova, E. F., Raficc, E., & Kozhevnikov, I. V. (2004). Fries rearrangement of arylesters catalysed by heteropoly acid catalyst regeneration and reuse. *Applied Catalysis A: General*, 260, 25.

Kozhevnikova, E. F., Raficc, E., & Kozhevnikov, I. V. (2004). Fries rearrangement of arylesters catalysed by heteropoly acid catalyst regeneration and reuse. *Applied Catalysis A: General*, 260, 25.

Ludwigshafen, J. M., Mutterstadt, W. W., & Ludwigshafen, W. K. (1985). *Preparation of o-acylphenols and p-acylphenols*, US, 4508924.

Miller, E., & Hartung, W. H. (1943). *O*-propiophenol and *p*-propiophenol. *Organic Synthesis*, 2, 543-545.

Mojtahedi, M. M., Saidi, M. R., & Bolourtchian, M. (1999). A novel method for synthesis of disubstituted ureas and thioureas under microwave irradiation. *Journal of Chemical Research*, 710-711.

Mojtahedi, M. M., Saidi, M. R., & Bolourtchian, M. (1999). Microwave-assisted aminolysis of epoxies under solvent-free conditions catalyzed by montmorillonite clay. *Journal of Chemical Research*, 128-129.

Naeimi, H., & Moradi, L. (2006). Efficient and mild synthesis of *ortho*-hydroxyaryl ketones catalyzed by zinc chloride under solvent-free condition and microwave irradiation. *Catalysis Communication*, 7, 1067-1071.

Naeimi, H., & Moradi, L. (2006). Facile, convenient and regioselective direct *ortho*-acylation of phenols and naphtols catalyzed by Lewis acids under free solvent and microwave conditions. *Journal of Molecular Catalysis A: Chemical*, 256, 242-246.
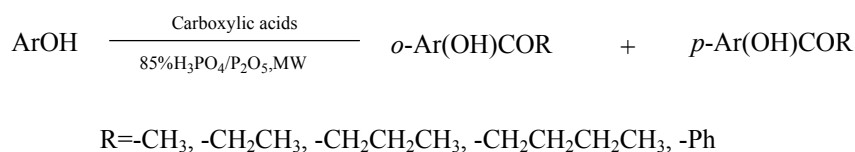
Palombi, L., Bonadies, F., & Scettri, A. (1997). Microwave-assisted oxidation of saturated and unsaturated alcohols with t-butyl hydroperoxide and zeolites. *Tetrahedron*, 53, 15867-15876.

Pasha, M. A., Manjula, K., & Jayaskankara, V. P. (2007). Antimony catalyzed simple, efficient and solvent-free Friedel-Crafts acylation of aromatics under microwave irradiation. *Journal of Saudi Chemistry Society*, 11, 327-330.

Rupinder, K. L., Sachin, D., & Caroline, P. O. (2006). Synthesis, biochemical evaluation and rationalization of the inhibitory activity of a series of 4-hydroxyphenyl ketones as potential inhibitors of 17β-hydroxysteroid dehydrogenase type 3 (17β-HSD3). *Bioorganic and Medicinal Chemistry Letters*, 16, 4519-4522.

Szmant, H. (1989). Organic building blocks for the chemical industry. Wiley. NewYork: pp. 503.

Vogt, A., Kouwenhoven, H. W., & Prins, R. (1995). Fries rearrangement over zeolitic catalysis. *Applied Catalysis A: General*, 123, 37-39.

$$\text{ArOH} \xrightarrow[\text{85\%H}_3\text{PO}_4/\text{P}_2\text{O}_5,\text{MW}]{\text{Carboxylic acids}} o\text{-Ar(OH)COR} \quad + \quad p\text{-Ar(OH)COR}$$

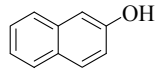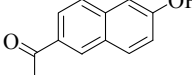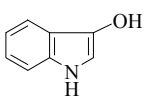R=-CH$_3$, -CH$_2$CH$_3$, -CH$_2$CH$_2$CH$_3$, -CH$_2$CH$_2$CH$_2$CH$_3$, -Ph
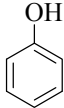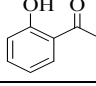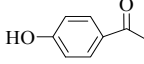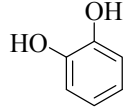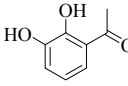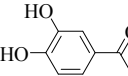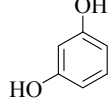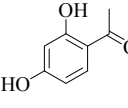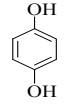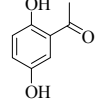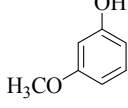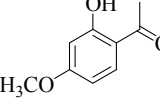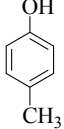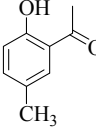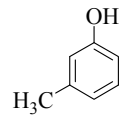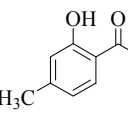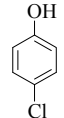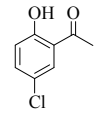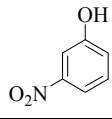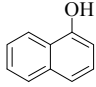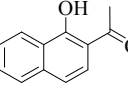
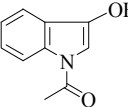Scheme 1. Friedel-Crafts acylation between phenols and carboxylic acids

Table 1. Effect of the power and reaction time on yield of aromatic ketones

Power (W)	Time (min)	Yield (%)	Power (W)	Time (min)	Yield (%)
119	5	79	385	1	75
231	1	72	385	2	83
231	3	90	539	1	70
231	5	87	700	30s	68

Table 2. Acylation of phenols with acetic acid to aromatic hydroxyketones

Entry	Substrate	Product	Time (min)	Power (W)	Yield (%)	M.p/b.p(℃) Found/Reported[c,d]
1			2	231	90	Liq/213[a]
						108-109/109
2			2	231	89	96-97/97-98
						118-119/119-121
3			2	231	87	143-145/144-146
4			2	231	89	203-205/204-206
5			1	231	95	48-49/47-50
6			3	231	87	43-44/42-44
7			2	231	90	Lip/245[a]
8			2	385	72	52-54/54-56
9		——[b]	4	385	0	——[b]
10			3	119	72	98-100/98
11			3	119	70	169-170/171
12			2	119	75	139-140/140-142
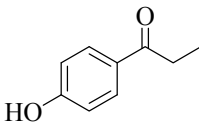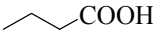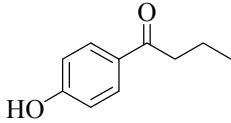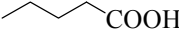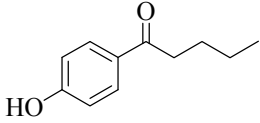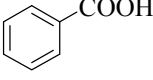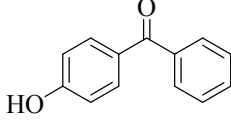
[a] boiling points were determined.

[b] "——" represents no corresponding hydroxyketone obtained.

[c] Adrich catalog handbook of fine chemicals, 1996-1997.

[d] melting or boiling points from Chemical Abstracts

Table 3. Acylation of phenol with various carboxylic acids to aromatic hydroxyketones

Entry	Substrate	Product	Time (min)	Power (W)	Yield (%)	M.p/b.p(℃) Found/Reported
1	∧COOH		2	231	79	89-90/91[8]
2	∧∧COOH		3	231	81	146-147/148[a]
3	∧∧∧COOH		3	231	83	59-60/60-62[a]
4	C6H5COOH		5	385	60	130-132/132-135[a]

[a] Adrich catalog handbook of fine chemicals, 1996-1997.

Study of the Effect of Weathering in Natural Environment on Polypropylene and Its Composites: Morphological and Mechanical Properties

Mashael Al-Shabanat

Princess Nora Bint Abdurrahman University, Science College – Chemistry Department

Riyadh, Saudi Arabia

E-mail: ma.naif@hotmail.com

Abstract

Three kinds of samples of PP, first was pure PP, second was PP with the basic stabilization and third with the talc as inorganic filler. The samples were produced using injection molding. The stability of prepared samples in natural weathering condition of Riyadh, in Saudi Arabia was studied. FT-IR and SEM were used to analyze the structural change. Stress at break, elongation at break and young's modulus measured as mechanical properties. However, talc was found to be able to stabilize PP a little.

Keywords: Polypropylene, Natural weathering, Exposure, Photo oxidation

1. Introduction

Polypropylene is widely applicable polymer material because of having many kinds of advantage such as easy processability and low production cost (Azuma *et al*. 2009). The composite with mineral has been considered a useful way to improve some properties. Polypropylene / talc composite has been widely studied by many researchers (Dence *et al*. 2005, Obata *et al*. 2001, Naiki *et al*. 2001) and has been extensively used as applicable materials for automotive, electric and other industrial components. Most automotives parts would be exposed to natural weathering like heat, humidity, rain, sunshine and atmospheric pollutants such as sand, dust and hydrocarbons, all of this weather factors can be responsible for severe damage. Weatherability is one of important properties for industrial materials (Azuma *et al*. 2009). Although the wavelength of the sunshine at the earth's surface is over 290nm, the sunshine is enough to initial the degradation (Al-Madfa *et al*. 1998). The degradation of Polypropylene and its composites have been studied by many researchers. Abu-Sharkh & Hamid 2003, prepared composites of polypropylene (PP) from date and UV stabilizers .They investigated the stability of the composites in natural weathering conditions of Saudi Arabia and in accelerated weathering conditions. The composites were found to be much more stable than PP under the severe natural weathering conditions of Saudi Arabia and in accelerated weathering trials. Compatibilized samples were generally less stable than uncompatibilized ones as a result of the lower stability of the maleated polypropylene. Irgastab and Tinuvin are found to be efficient stabilizers for PP/cellulose fibre composites. In addition to enhanced stability imparted by the presence of the fibres in the composites, enhanced interfacial adhesion resulting from oxidation of the polymer matrix can be the source of retention of mechanical strength.

Xue *et al*. 2007, developed aspen fiber–polypropylene composites (APC). The mechanical properties of APCs with five different fiber-loadings were evaluated at the room temperature, 4 °C, and 40 °C. Environmental effects on the mechanical properties of APCS were experimentally quantified after conditioning the APCs with two different fiber-loadings in the following temperature and humidity for over 7000 h: (1) hot/dry at 40 °C and 30% relative humidity (RH), (2) hot/wet at 40 °C and 82% RH, (3) cold/dry at 4 °C and 30% RH, and (4) cold/wet at 4 °C and 82% RH. The tensile moduli, flexural moduli, and the flexural strength increased as the woodfiber content increased in the composites. The tensile strength decreased as the fiber content increased. The tensile strength was shown to slightly improve with an addition of a coupling agent between the aspen fibers and polypropylene. The simple empirical micromechanics Halpin–Tsai model for randomly distributed short fiber reinforced composites was employed to predict the homogenized elastic moduli of APC, by optimizing the interfacial model parameter. Scanning electron microscopy (SEM) micrographs confirmed that an addition of the adhesion promoter maleated anhydride polypropylene (MAPP) between the aspen fibers and polymeric matrix improved the interfacial bonding.

The effect of talc as a filler on degradation of polyolefin has been studied. Yang *et al*. 2005, focused on the natural photo-oxidation of HDPE composites, with several inorganic fillers. Among them, talc as inorganic filler. Fourier transform spectroscopy (FTIR), ultraviolet spectroscopy (UV), scanning electron microscopy (SEM) and pyrolysis

gas chromatography–mass spectroscopy (PGC–MS) were used to analyse the structural changes, the reflection and absorbance of ultraviolet light, the surface morphologies and the volatile oxidation products of samples during natural aging. After 180 days of exposure, the results showed that some inorganic filler, e.g., $CaCO_3$ and wollastonite, can stabilize HDPE a little. In HDPEs filled with these fillers lower degrees of degradation were observed. In contrast, other inorganic fillers more or less accelerated the photo-oxidation degradation. They are act as photo-oxidation catalysts with the rank of kaolin > diatomite > mica> black mica> talc. Inorganic fillers also have some effects on the crystallinity of HDPE after photo-oxidation. The surfaces of the composites after exposure became rough and with cracks, but showed different damage patterns. A seriously damaged surface did not definitely correspond to a great oxidation degree. The remaining volatile oxidation products of the photo-oxidised composites were proven to be mostly a series of *n*-alkanes. A hypothesis was proposed that the relative absorbances to UV light in 290–400 nm by these fillers are the key factors influencing the photo-oxidation.

In other study of Azuma *et al.* 2009, the comparisons of degradation behavior of polypropylene(PP) and PP/talc composites were carried out with one outdoor weathering test at Hidaka, Saitama, Japan and three accelerated weathering (xenon, metal halide and carbon arc lamps) tests, respectively. The outdoor exposure vigorously advanced these degradations with the lowest amount of UV exposure energy. It was found that the degradation rates were affected by the visible light intensity in the light sources. In the case of the existence of talc compound, the degradation was synergistically accelerated by the exposures of the sunshine, the xenon and the metal halide lamps having higher visible light intensities. In addition, the degradations of the PP and the PP/talc composites were found to be synergistically accelerated by sunlight exposure and the acid rain, too. Leong *et al.* 2004, prepared two kinds of composites, namely single-filler polypropylene (PP) composites (containing either talc or calcium carbonate) and hybrid-filler PP composites (consist of a mixture of talc and calcium carbonate). These specimens were subjected to natural weathering i.e. tropical climate in Penang, Malaysia for 6 months. After 6 months of exposure, the mechanical properties of single-filler PP composites deteriorated due to severe physical and chemical degradation. However, the hybrid-filler PP composites were found to show better retention in mechanical properties albeit having undergone some degree of surface-degradation as well. It is believed that in hybrid composites, the interparticle cavities, created by low interaction between CaCO3 fillers and the matrix, would dampen crack propagation from the surface to the interior of the samples, thus minimizing internal damage. Talc particles in the inner parts of the specimen would in turn act as the main reinforcement, which explains the retaining of mechanical properties in hybrid composites.

In this study, the degradation and stabilization of PP, PP/the basic stabilization and PP/ talc composites under natural weathering of Riyadh city in Saudi Arabia will be investigated by studding the morphology and the mechanical properties.

2. Experimental

2.1 Materials and Preparation

The Polypropylene used was supplied by Saudi Basic Industries Corporation (SABIC). The brand name for it is PP520L. It is homo polymer and the details of it are given in Table 1. The additives used in a composite were the basic stabilization and talc (Luzenac, France). The surface of talc had not been subjected to any chemical treatment. The prepared samples in this study are three. The first, polypropylene without any additives. The second, polypropylene with basic stabilization and the third, talc filled polypropylene (10%).The samples are denoted as (PP, PPW and TPP) respectively. Injection molding was carried out using a Battenfeld BSKN 400/100HK KS, Germany. The molding conditions are listed in Table 2.

2.2 Exposure Procedure

The samples were exposed to natural weathering (all environmental effects such as rain, sunlight, wind etc.) at Riyadh city in Saudi Arabia. The natural exposure was conducted for a period of 6 months from April to September 2009, the details of climate condition of Riyadh city in this period is given in Table 3 [Online] . The specimens were attached to a rack with a rack holder and were placed on the roof of our research building. Samples were collected every 2months to study of the effect of weathering .

2.3 Characterization

Fourier transform infra-red (FTIR) analysis were done for weathered and unweathered samples in the wavenumber range of 4000-400 cm^{-1} to gives out the indication of formation of the oxidation products by using Fourier-transform infrared (FTIR) spectroscopy (Thermo Nicolet, FT-IR Nexus). Scanning electron microscopy (SEM) on the surface of specimens before and after the exposure were carried out to study effect of natural weathering on structure and morphology by using Jeol JSM-6360LV Scanning Electron Microscope.

2.4 Mechanical Testing

Tensile properties, elongation at break, tensile stress at break and young's modulus were measured using an Instron corporation machine with a series IX automated materials testing system in accordance with ASTM D 638. For tensile tests, the crosshead speed was 5 mm/min and preparation of samples in dog bone shape.

3. Results and Discussion

3.1 Characterization

3.1.1 FT-IR Spectra

The IR spectra of PP,PPW and TPP before and after the exposure were recorded as seen Fig. 1. For the infrared spectrum of PP, there are beaks near 2976, 1460, and 1380 cm^{-1}. In addition, medium intensity beaks are observed near 1155 and 970 cm^{-1}, attributable to the asymmetry stretching vibration of CH_3 ($1460cm^{-1}$) , the symmetry bending vibration of CH_3($1380cm^{-1}$), vibration of the rocking of CH_3 & $-CH_2$ and the stretching of $CH-CH_2$ & $CH-CH_3$($1155,970$ and 841 cm^{-1}) (Socrates 2001;p. 268-169 and Othman *et al*. 2006). When comparing the IR spectra of PP with its composites, no obvious changes between the spectra of PPW and PP. In the case of TPP, there are several shifting obtained for some beaks. All the regions of spectra listed in Table 4.

After 6 months of exposure, various chemical reaction take place which result in the change of FT-IR spectra . Several peaks in the carbonyl region (1684-1725) cm^{-1} in spectrum of PP, which are attributed to carboxylic acid and conjugated ketone, respectively. In addition, a beak at 1635 cm^{-1}, which is attributed to vinyl group. For PPW and TPP spectra, It is clear that there are beaks appear at the carbonyl region (1722)cm^{-1} of PPW and (1726) cm^{-1} of TPP which are attributed to carboxylic acid. In the hydroxyl region, the IR spectra of both composites have shown weak and broad peak in the ranges of (3400-3460) cm^{-1} (Tidjani 2000, Tidjani & Arnaud 1995).

The presence of carbonyl, acid and ketone species acknowledges the presence oxidation products in the weathered samples (Leong *et al*. 2004). The little changes during the natural photo-oxidation of PPW and TPP indicate that these samples more stable than PP. It can say that the additives materials of PP in the composites Played positive roles on the stability of PP. On the other hand, the difference in intensity in the carbonyl region of PPW and TPP spectra indicates that the TPP sample was better than PPW to resist photo-oxidation. This means that the role played by the talc was more positive.

3.1.2 Scanning Electron Microscope (SEM)

Figs 2, 3, 4 and 5 show surfaces before and after exposure. As seen in Fig. 2 Which shows the surface of samples before exposure. The surface looks smooth relatively. After 2 months of exposure, the surfaces became rough as seen in Fig. 3, this could means that it is still at the initial stages of degradation by natural photo-oxidation.

From Fig. 4 which shows PP and its composites after 4 months of exposure, it is clear that there are cracks and unidirectional micro fissures could be seen on the surface of degraded samples which increased strongly after 6 months and some particles can be observed as seen in Fig 5, which may be caused by the fracture of large amount of fragments from surface. All of this surface damages form spontaneously during UV exposure as a result of the surface layers, which lead to shrinkage (Rabello & White 1997). Although surface cracks are evident in all samples after being weathered for 6 months, the severity of the cracks varies from one another where the least damage done by weathering is on TPP that contain talc particles as a filler of PP. This results in lower damage of PP matrix comparing with PPW and PP.

3.2 Mechanical Testing

From Fig. 6 which shows the tensile stress at break as a function of Weathering Time (month), it is clear that the initial stress at break (before exposure) of TPP is the highest comparing to PP and PPW. This indicates that the polymer became harder. After exposure, the stress at break decreases of all samples over a period of 6 months due to the effects of polymer degradation where could be attributed to the natural photo-oxidation of the polymer , which result in chain under UV exposure. This leads to physical deterioration of the polymer (Tidjani 1997). On the other hand, The TPP sample seemed to have better retention of tensile strength compared to another samples, it can thus be hypothesize that talc, which is platy in natural, would act as the reinforcing filler in the composites.

Fig. 7 shows the elongation at break Versus Weathering Time (month). Remarkably, the initial elongation at break value of the PP sample (before exposure) is much higher than that of another sample. This indicates that the composites is more brittle especially, TPP which has the lowest value of elongation at break. This is a consequence of the much lower ductility of the composites resulting from the presence of the additives. After exposure, although initially the deformability of PP itself is the highest compared to other samples, the effects of weathering caused its elongation at break to decline to a point below that of composites after 2 months of weathering time. This means

that the PP becomes very brittle after short exposure times. This is a consequence of the large drop in molecular weight associated with degradation. Regarding PPW which seemed more brittle comparing to PP before exposure, showed similar behavior of PP sample after exposure especially after 4 months of weathering time. Decline in elongation at break with increasing in the weathering time of PP and PPW, this is caused by extensive chain scission in the samples, causing the breakdown of tie chain molecules and entanglements, which are especially detrimental to the ductility of the polymer. On the contrary, TPP remains constant in the first 2 months of weathering. After this period of weathering, TPP sample shows little change then keep remaining constant after 6 months. This can be explained, it is possible that the interfacial adhesion can be enhanced by degradation following formation of the carbonyl group in PP which are more compatible with talc particle. However, when comparing to their resistance of change during exposure, it can be very obvious that the TPP shows more resistance and the change in elongation at break versus exposure time decreases slightly where seemed more stability of degradation than another samples as a result of the presence of talc particles.

From Fig. 8 which shows the young's modulus versus weathering Time (month), it is clear that PPW before weathering seemed the softest where the values of young's modulus are the least compared to other samples while the TPP composite seemed the most rigid and the PP has an average behavior between them. Although, PPW is still the softest after weathering, but the rigidity of it increases gradually with increasing exposure time while for the other two samples, the rigidity decreases with increasing exposure time then increases after 4 months of exposure significantly especially for TPP and this result indicates that all samples became more rigid. This could be attributed to the surface cracks that have formed the polymer. However, longer exposure times lead to the development of more and more surface cracks which in turn allow degradation process to take place, which causes a ductile to brittle transition of the polymer, thus rendering it to lose its soft.

4. Conclusion

PP and its composites were prepared and the effect of natural weathering on morphology and mechanical properties of them were investigated. From the above results, it can be concluded:

- As evidenced from FT-IR, the natural weathering exposure of PP and its composites are caused degradation judging by the formation of photo-oxidation products.

- From SEM analyses on the surface, the photo- oxidation of materials begins from the surface and then develops along the depth gradually.

- Several changes observed in mechanical properties as a result of degradation of polymer.

- The results showed that the talc play a role in improving the stability of PP slightly, but the relationship between shape, size, the treatment of the talc surface and preparation method of composites and stability of polymer needs further research.

References

Abu-Sharkh, B. F., & Hamid, H. (2004). Degradation study of date palm fiber/polypropylene composites in natural and artificial weathering: mechanical and thermal analysis. *Polymer Degradation and Stability*, 85, 3, 967-973

Al-Madfa, H., Mohamed, Z., & Kassem, M.E. (1998). Weather ageing characterization of the mechanical properties of the low density polyethylene. *Polymer Degradation and Stability*, 62, 105-9.

Azuma, Y., Takeda, H., Watanabe, S., & Nakatani, H. (2009). Outdoor and accelerated weathering tests for polypropylene and polypropylene/talc composites: A comparative study of their weathering behavior. *Polymer Degradation and Stability*, 94, 2267-2274.

Dence, M., Musil, V., & Smit I. (2005). Polypropylene/talc/SEBS(SEBS-g-MA). *Composites. Part A, Applied Science Manufacturing*, 36, 1282-90.

Leong, Y.W., Abu Bakar, M.B., Mohd Ishak, Z.A., & Ariffin, A. (2004). Characterization of talc/calcium carbonate filled polypropylene hybrid composites weathered in a natural environment. *Polymer Degradation and Stability*, 83, 411-422.

Naiki, M., Fukui, Y., Matsumura, T., Nomura, T., & Matsuda, M. (2001). The effect of talc on the crystallization of isotactic polypropylene. *Journal of Applied Polymer Science,* 79,1693-703.

Obata,Y., Sumitomo, T., Masuda, M., & Nomura, T. (2001). The effect of talc on the crystal orientation in polypropylene/ethylene-propylene rubber/talc polymer blends in injection molding. *Polymer Engineering and Science*, 41, 408, 16.

Othman, N., Ismail, H., & Mariatti, M. (2006). Effect of compatibilisers on mechanical and thermal properties of bentonite filled polypropylene composites. *Polymer Degradation and Stability*, 91,1761-74.

Rabello, M.S., & White, J.R. (1997). Photodegradation of polypropylene containing a nucleating agent. *Journal of Applied polymer Science*, 64,2505-17.

Socrates, G. (2001). *Infrared and Raman Characteristic Group Frequencies*. (3rd ed.) Chichester: John Wiley & Sons Ltd, (Chapter 21; page 268-269).

Tidjani, A. (1997). Photooxidation of polypropylene under natural and accelerated weathering conditions. *Journal of Applied Polymer Science,* 64, 2497- 503.

Tidjani, A. (2000). Comparison of formation of oxidation products during photo-oxidation of linear low density polyethylene under different natural and accelerated weathering condition. *Polymer Degradation and Stability*, 68,465-9.

Tidjani, A., & Arnaud, R. (1995). Formation of treeing figures during the photooxidation of polyolefins. *Polymer* , 36 , 2841-4.

Xue, Y., Veazie, D.R., Glinsey, C., Horstemeyer, M.F., & Rowell, R.M. (2007). Environmental effects on the mechanical and thermomechanical properties of aspen fiber-polypropylene composites. *Composites Part B: Engineering,* 38, 2, 152-158.

Yang, R., Yu, J., Liu, Y., Wang, K. (2005). Effects of inorganic fillers on the natural photo-oxidation of high-density polyethylene. *Polymer Degradation and Stability*, 88, 2, 333-340.

[Online] Available: http://en.wikipedia.org/wiki/Riyadh#Climate.

Table 1. Product data for PP 520L

Property	Unit	Value	Test Method
Melt Flow Rate (216 Kg & 230°C)	g/10 min	10	ASTMD-1238
Tensile Strength @Yield	MPa	35	ASTMD-638
Tensile Elongation @ Yield	%	10	ASTMD-638
Flexural Modulus (1%SECANT)	MPa	1600	ASTMD-790A
Notched Izod Impact Strength @ 23°C	J/ m	23	ASTMD-256
Heat Distortion Temperature @ 455 KPa	°C	105	ASTMD-648
Victa Softing Temperature	°C	155	ASTMD-1525B
Hardness	Rockwell	102R	ASTMD-785

Table 2. Molding conditions

Injection Pressure	500 Pa	Temperature Zone 1	180 °C
Holding Pressure	500 Pa	Temperature Zone 2	200 °C
Cooling Time	10 s	Temperature Zone 3	215 °C
Holding Time	10 s	Nozzle Temperature	235 °C

Table 3. Details of the climate condition in Riyadh city

Month	Apr	May	Jun	Jul	Aug	Sep
Record high °C	42.0	45.1	47.1	48.0	47.8	44.5
Average high °C	33.3	39.1	42.4	43.5	43.2	40.3
Daily mean °C	26.8	32.7	35.4	36.6	36.3	33.2
Record low °C	11.0	18.0	16.0	23.6	22.7	16.1
Average low °C	20.3	25.7	27.6	29.1	28.8	25.7
Rainfall mm	22.3	4.6	0.0	0.0	0.2	0.0
Humidity %	28	17	11	10	12	14
Location of Riyadh city: in the midst of Saudi Arabia Coordinates: 24°38′N 46°43′E24.633°N 46.717°E						
Riyadh city have many dust storms. The dust is often so thick that visibility is under 10 meters.						

Table 4. The regions of spectra of PP, PPW and TPP before weathering

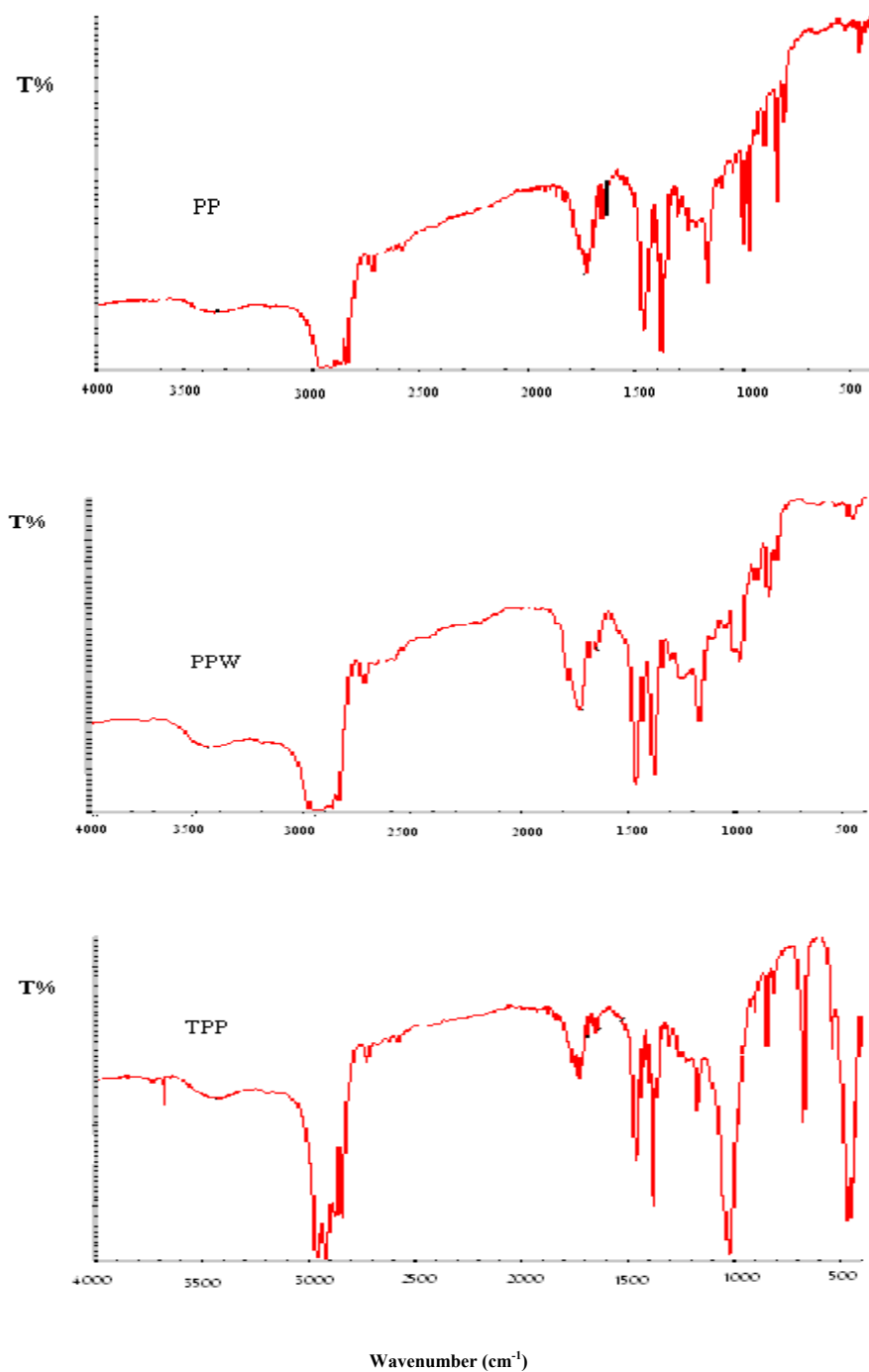| PP	PPW	TPP	Comment
2976	2975	2975	————
1460	1448	1446	Shifting (PPW,TPP)
1380	1380	1380	————
1155	1155	1160	Shifting (TPP)
970	970	979	Shifting (TPP)
841	841	841	————
————	————	3668(stretching)	These beaks attributed to OH group of octahedral layers of the talc surface

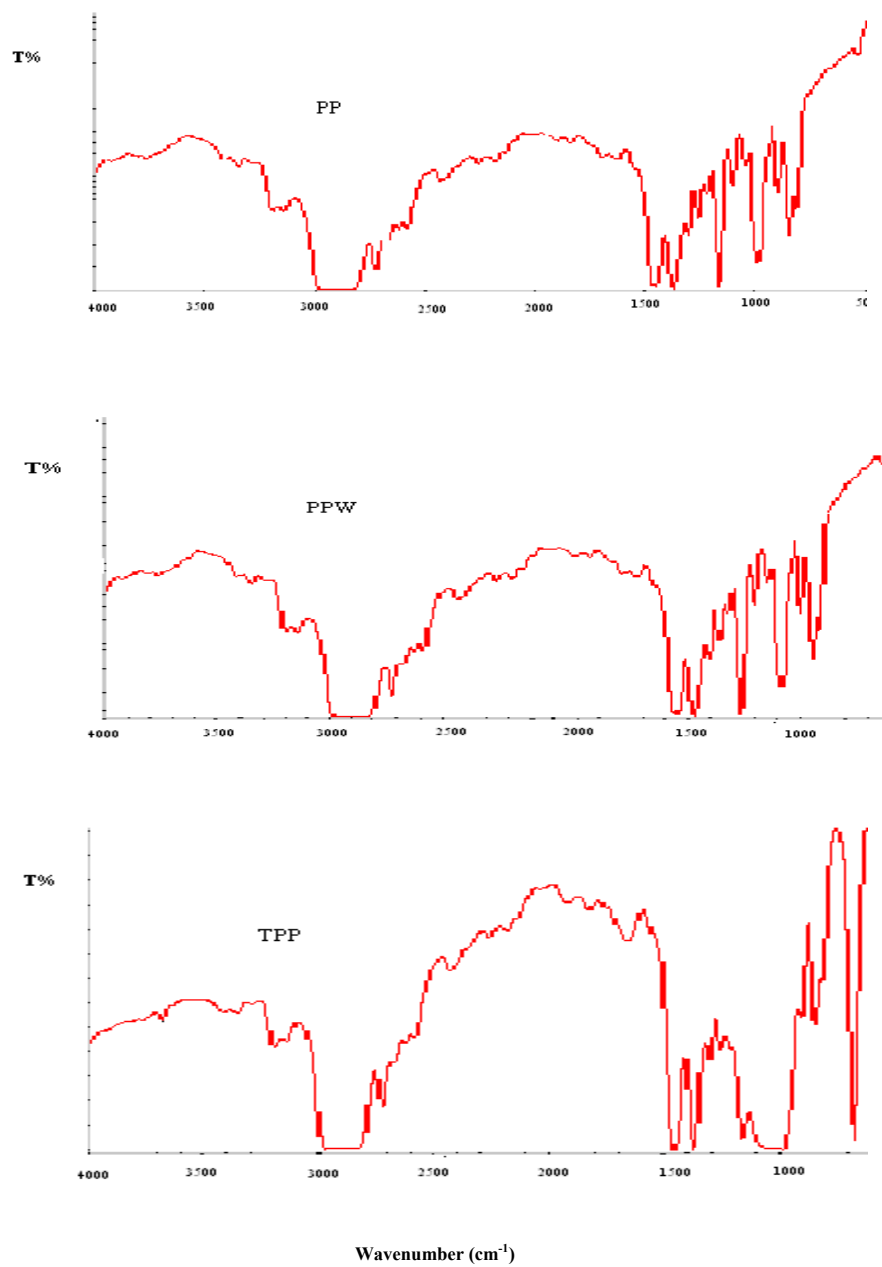Figure 1. PP, PPW and TPP before exposure

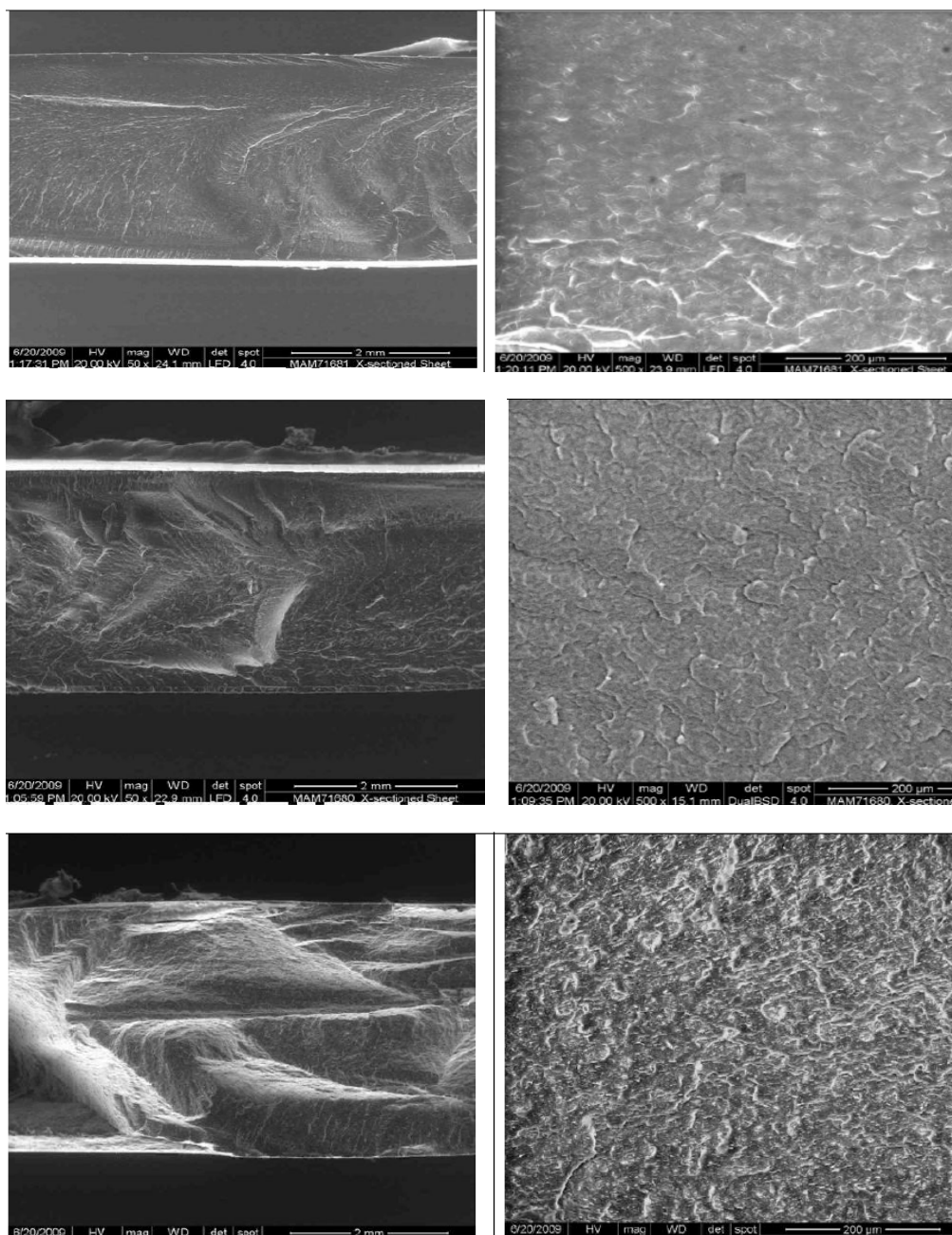Figure 1. (Continued); after 6 month from exposure

Figure 2. Surface aspects before exposure

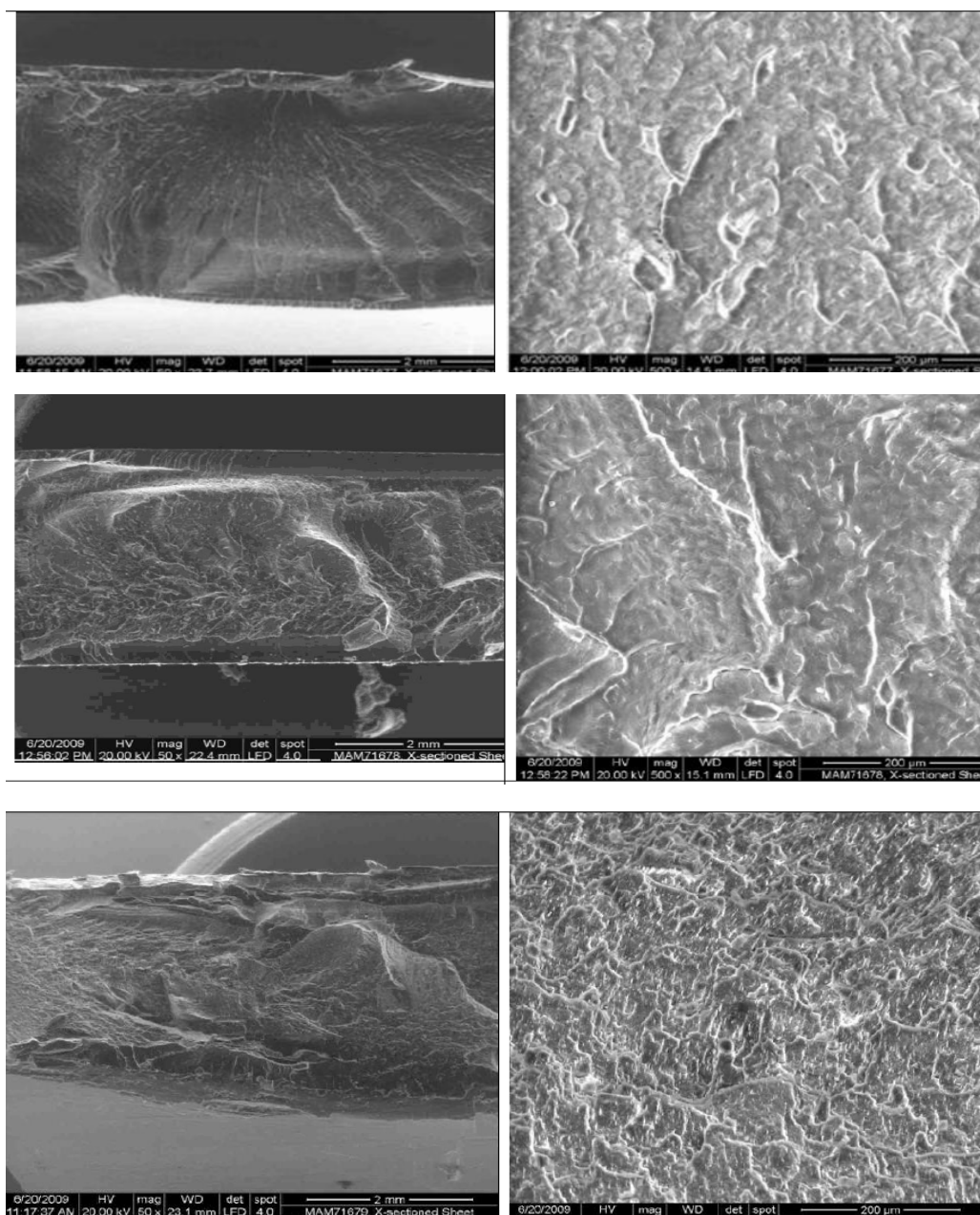(above) PP, (middle) PPW and (below) TPP.

Figure 3. Surface aspects after 2 months of exposure
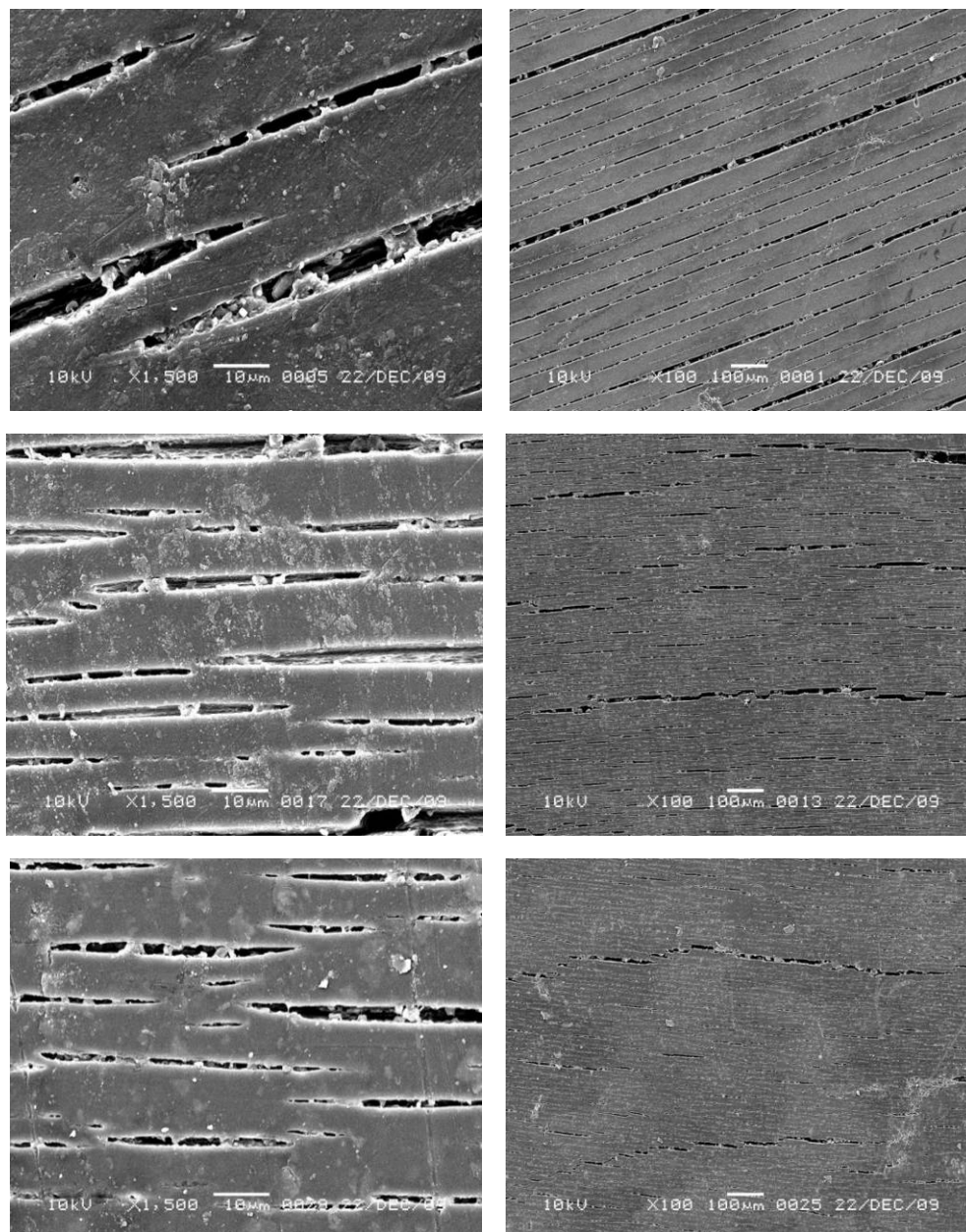
(above) PP, (middle) PPW and (below) TPP.

Figure 4. Surface aspects after 4 months of exposure
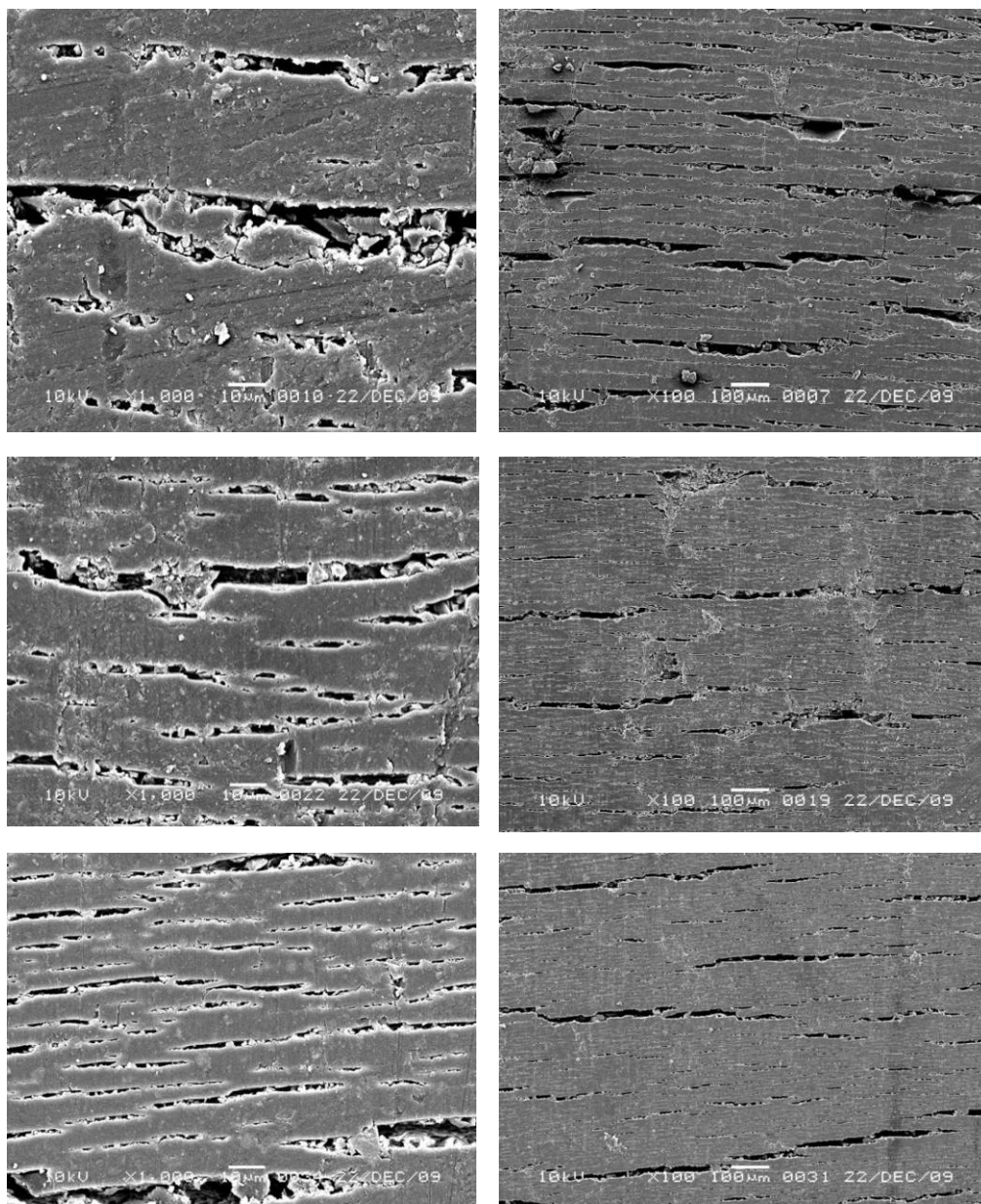
(above) PP, (middle) PPW and (below) TPP.

Figure 5. Surface aspects after 6 months of exposure

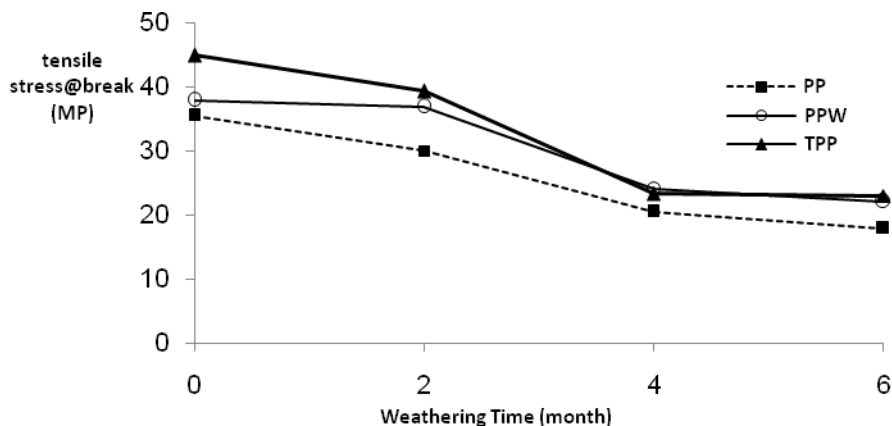(above) PP, (middle) PPW and (below) TPP.

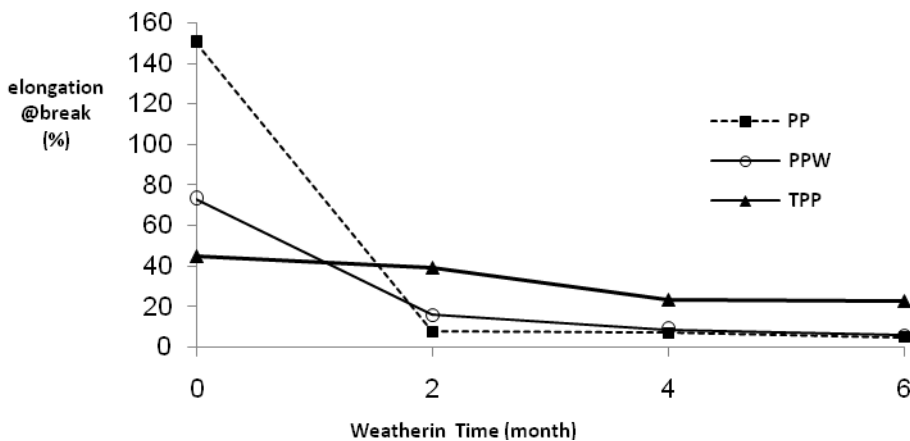Figure 6. Tensile stress at break as a function of Weathering Time (month)

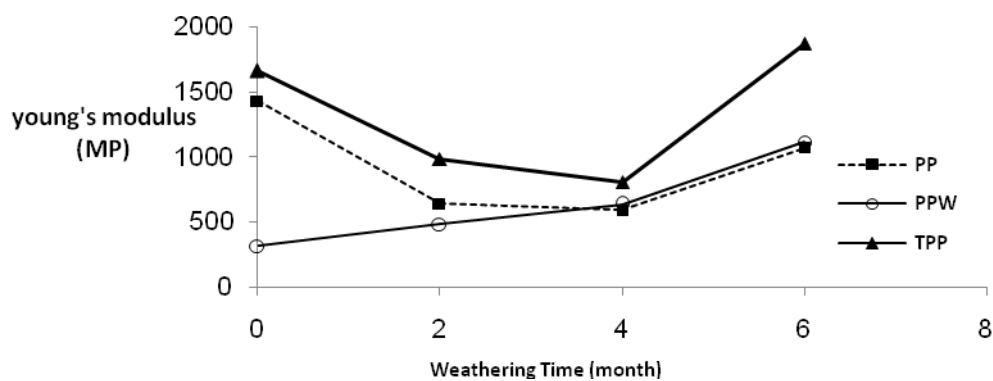Figure 7. Elongation at break as a function of Weathering Time (month)

Figure 8. Young's modulus   as a function of Weathering   Time (month)

First Photolysis of Benzidine Schiff Base in Non Aqueous Solvents

Sulaiman G. Muhamad

Chemistry Dept, College of Science, Salahaddin University-Kurdistan, Iraq

Tel: 964-66-250-4921   E-mail: gafff2002@yahoo.com

Abstract

The first photolysis of synthesized Schiff base [Bis-(2-chlorobenzalidene) benzidine] in the presence of various solvents (methanol, acetonitrile and n-hexane) was carried out under UV-light radiation. The data obtained by UV-Visible spectroscopy was used to determine the kinetic parameters of the Schiff base photolysis. It was found that the degradation of Schiff base in all solvents followed a first order reaction. The results show the rate of photolysis depends on the polarity of solvents. The effect of temperature on the photolysis process in methanol has been studies at different temperature ranging from 10ºC to 50ºC. The activation energy has been determined. The intermediates formed in the Schiff base photolysis processes were detected and identified, using High Performance Liquid Chromatography analytical technique coupled with UV-visible spectrophotometer.

Keywords: Photolysis, Schiff base, Effect of solvents effect of temperature

1. Introduction

Compounds which posses R-CH=N-R' as a general formula are called Imines or Schiff bases and can be efficiently prepared by condensation of an aromatic aldehyde or ketone with an appropriate aromatic amine at an optimum pH of 4-6 using dry alcohol as a solvent (S.A Niazi et al., 2010) . Schiff bases have played and continue to play an important role in the development of coordination chemistry (A. A. Osowle, 2008). Schiff bases and their metal complexes are becoming increasingly important in recent years due to their biological activity (F.M. Morad eta al., 2007)and their uses as catalysts (J. Zhang, Y. Tang et al. 2005) and as compounds of interesting photoluminescent(V. Papper et al. ,2003) and electroluminescent (T. Maindron et al ,2004)properties.

In spite of the relatively large number of thermal hydrolysis (Z.Huang et al., 2001), thermal decomposition (A. M. Aly et al., 2009) and ionization (J.Donoso et al., 1986) reports on Schiff base compounds, less work was published on photolysis and kinetic studies.

Effect of the medium on kinetics and mechanism of chemical transformations is one of the key problems of the modern physical chemistry. The polarity of a medium and temperature changing play the most important role in this phenomenon. Effects of solvent (R.Kumar and M. Yusuf, 2009) and temperature (K. M. Shareef et al., 2010) on photolysis were extensively studied of organic compounds while comparatively little is known on Schiff-base.

Photolysis is the process that involves the use of light to degrade molecular compounds toward their basic constituents, often carbon dioxide and water. During photolysis, a direct photochemical transformation takes place, when energy from light attacks bonds within a molecular compound, thereby degrading the compound (F. Al-Momani , 2003) .The first one is that the organic compound to be eliminated must be able to absorb light in competition with other compounds of the effluent to be treated. The second one is that the organic compounds generate a wide variety of photochemical reactions that can produce products more complex for degradation. In addition, not all the radiation emitted by the source of radiation is fully exploited .Only the radiation absorbed and only a part of this produce chemical changes .This means that some reactions of photodegradation have very slow kinetics (DI Wolfgang **,** 2006).

A number of papers have been published on the direct photolysis of chemicals in water using the Hg-lamp (K. G. Mostafa, 2007, J.P. Escalanda, 2008, S.T. Ong, 2009). Photochemistry of some 2-butenyl/butynyl-bischromones has been investigated by Kumar and Yusf (R.Kumar and M. Yusuf, 2009) in benzene and isopropanol-THF (1:1). Photolysis conversion of the bischromones is found to be dependent upon the nature of the intermediate spacer and H-donating capability of the solvent. L. Scrano et al (L. Scrano et al., 2002) reported the direct photolysis of acifluorfen in different solvents (water, methanol, acetonitrile and n-hexan) by UV mercury lamp. On the other hand,J. Sanz-Asensio et al (J. Sanz-Asensio et al.1999) reported a comparative photolysis kinetic study of ethiofencarb [2-ethylthiomethyl(phenyl)-*N*-methylcarbamate] in aqueous and non-aqueous media (hexane and methanol). In the present work the first photolysis of Bis-(2-chlorobenzalidene)benzidine have been carried out in different solvent and at different temperature.
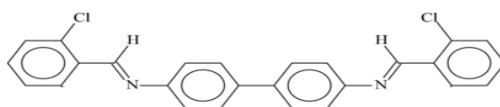
2. Experiment

2.1 Chemicals

Benzidine, 2-chloro benzoic acid and 2-chlorobezaldehyde supplied by Fluka AG. Methanol and acetonitrile were HPLC grade and purchased from Tedia Company-USA .Other solvents used were obtained from BDH chemicals.

2.2 Preparation of Schiff Base

The Schiff base was prepared by adding 25 cm^3 of 2-chlorobezaldehyde methanolic solution (0.02 mol) to the same volume of methanolic solution of benzidine (0.0l mol). The mixture was stirred for one hour at room temperature (30^0 C). The resulting solution was evaporated under vacuum to remove the solvent. The yellow product was collected by filtration, washed several times with methanol and recrystallized from hot methanol and then dried under vacuum .Melting point of Schiff base is 234-237° C. Chemical structure of Schiff base has been shown in below.

Chemical structure of Bis-(2-chlorobenzalidene)benzidine Schiff base

2.3 Photolysis procedure

The photolysis experiments were carried out at room temperature (30ºC) in a laboratory-made photoreactor including a 35 ml cylindrical photochemical cell.20ml of solution (50 mg/l of Schiff base in different solvents) was added to the photochemical cell then irradiated immediately by 100-Hg UV lamp (230V, 50Hz and 1 Am, without selector from Osram- Germany). The effect of temperature on catalytic photodegradation was monitored by adjusting the temperature of circulating water between (10° to 50° C).

2.4 Analytical methods and instruments

Infrared spectra of the Schiff base were carried out on I.R 300 spectrophotometer from Thermo Mattson -USA by using KBr disk. Melting point was measured on Toshinwal-Electrothermal melting point apparatus. Electronic spectra were reworded in the range 200-300 nm by uv-visibl Cesil 3021 spectrophotometer, from England using 10 mm quartz cell. Concentration changes of the Schiff base were determined by monitoring the Schiff base absorption peak at 209nm in methanol, 212nm in acetonitrile and 213nm in n-Hexan from calibration curve. A calibration curve was found to be linear in the range of 0.75 to 100 mg/l with a good correlation (R^2=0.962). Circulating thermostat type Julabo F10-Germany was used for controlling the reaction temperature. PerkinElmer series 200 HPLC connected with UV-visible spectrophotometer detector and analytical column (PRT 720041, ET2501814 Nucleosil 120-5 C18 Machereg) was used for detection the Schiff base and some photolysis intermediates with the conditions *of Mobile phase:* Methanol/Water (70:30 v/v) ,*Flow rate:* 0.1 ml/min ,*Detector wavelength:* 254 nm, *Injection volume*: 20µl, *Operating temperature*: 30 ºC

3. Results and discussion

3.1 I.R spectra

The formation of Schiff base is inferred by the appearance of strong band in the IR spectrum at 1618 cm- due to azomethine group (A. A. Ahmed and S. A. BenGuzzi, 2008) as shown in Fig. 1.

3.2 Electronic absorption spectra

Ultraviolet-Visible absorption spectral of Schiff base displays absorption bands at 209,252, and 281nm in methanol (206,212 250 and 284 nm in acetonitrile and 203,213, 249 and 285 nm in n-hexane) as shown in Fig. 2, 3 and 4. The 209 nm band of the Schiff base spectrum in methanol (212 nm and 213 nm in acetonitrile and n-hexane respectively) represent the π→π* transition of substituted aromatic compounds. The n→π* transition at 281 nm of Schiff base spectrum in methanol (284 nm and 285 nm in acetonitrile and n-hexane respectively) corresponds to non bonding electron of azomethine group (A. A. Osowle, 2008) as shown in figs. 2,3and 4.

3.3 Photolysis of Schiff base

The spectra of Schiff base in all solvents indicate that during the photolysis, the intensities of the absorption bands exhibit sudden variation, after which their intensities tend to decrease gradually. Figs. 2, 3 and 4 show a variation in absorption spectra of Schiff base in methanol, acetonitrile and n-hexane respectively at various time intervals of irradiation.

The absorption maximum at 209 nm in methanol, 212 nm in acetonitrile and 213nm of Schiff base spectra are always decreased in intensity with irradiation time indicating the decreasing of Schiff base concentration during the photolysis. Fig. 5 shows the photolysis of 50 mg/l of Schiff base in different solvents at room temperature (30 C^o).

3.4 Kinetic studies

The graphical method was employed to predict the order of the reaction. The plot of ln C/C∘ versus irradiant time, (where, C is the concentration of Schiff base at time, C∘ is the initial concentration of Schiff base), gives a straight line behavior, which suggests the first-order kinetics of the photolysis (Ch. Boughelouma and A. Messalhib , 2009) as shown in Fig. 6.

By application of first order equation (**ln (ClCo) =-kt**) the reaction rate constants (k) of the photolysis processes are calculated from the slope of the straight line and the reaction half time ($t_{1/2}$) are calculated by equation **$t_{1/2}$=0.693/k** as shown in table 1.

The results in Fig. 6 and table 1 showed that the photolysis of the Schiff base in acetonitrile is faster than the photolysis in n- hexane and slower than the photolysis in methanol. This means that the rate of photolysis of Schiff base increase with increasing the polarity of solvent and consistent with previous photolysis studies (S. K. Pramanikabc and S.Dasb, A. Bhattacharyyaa , 2008) . A possible explanation for the higher photolysis rate in polar solvents is due to the contribution of an oxygen independent mechanism which enhanced photolysis reaction (R.Kumar and M. Yusuf, 2009) and polar solvents would achieve better stabilization of the free ions (L. Scrano, 2002).

3.5 Effect of Temperature

The activation emerge (Ea) of photolysis process in methanol was determined after determination of photolysis reaction rate constant at 10, 20,30,40,50ºC, the values of the rate constant (k)were plotted in the form lnk versus 1/T (K), as shown in Fig. 7.

The energy of activation (Ea) was determined according to Arrhenius equation **lnk = lnA+ (Ea/RT)** (A.Atita, 2008) ,where A is an empirical constant depending on compound and nonthermal system conditions, R is the universal gas constant (J/K, mol^{-1}) and T is the temperature (K). The activated energy of Schiff base photolysis calculated and equal to 0.2399 KJ.mol^{-1}.The low values of Ea might be considered that the photolysis process in this work is generally temperature independent (N. Mittal**,** 2009) .Other workers also determined low activation energies for catalytic photolysis of organic compounds. (A.Atita, 2008 , B. Dabrowski, 2005)

3.6 Photolysis intermediates

Figure.8 shows the HPLC chromatogram of Schiff base before photolysis (time=0) the peak at retention time 2.34 min (peak 1) belongs to the Schiff base as a reactant. After 60 min of photolysis the area of this peak was decreased indicating the decreasing of Schiff base concentration, as shown in fig .9. In fig.9 the new peaks appear in a chromatogram corresponding to the intermediate compounds produce during the photolysis reaction. A peak of retention time 1.51 min was due to 4-hydroxy-2-chlorobenzoic acid (peak 4), while a peak of retention time 1.93 min corresponds to 2-chlorobenzoic acid (peak 2).The formation of 2-chlorobenzoic acid can be explained by considering the oxidation of 2-chlorobenzaldehyd .This suggestion is agreement with that reported by Miray and Nikola (M. Bekbolet, and N. Getoff , 2002), that have reported benzoic acid and 2-chlorobenzoic acid as the main degradation products of 2-chlorobenzaldihyd.While the formation of 4-hydroxy-2-chlorobenzoic acid might be formed by attack of an · OH radical (M. Bekbolet, and N. Getoff , 2002)on 2-chlorobenzoic acid. It must be pointed out that other intermediates were detected, although attempts to identify them were unsuccessful.

References

A. A. Ahmed and S. A. BenGuzzi. (2008). Synthesis and Characterization of Some Transition Metals Complexes of Schif Base Derived From Benzidine and Acetylacetone. *J. of Sci. and Appl.*, 2 (1)83-90.

A. A. Osowle. (2008). Syntheses and Characterization of Some Tetradentate Schiff-Base Complexes and Their Heteroleptic Analogues. *E-Journal of Chemistry*, 5(1) 130-135.

A. Atita, S.H. Kadhim and F. H. Hussin. (2008). hotocatalytic Degradation of Textile Dyeing Wastewater Using Titanium Dioxide and Zinc Oxide. *E-J. of Chem.*, 5(2) 219-223.

A. M. Aly, A. H. Osman, B. Abd El-mottaleb and B. A. Gouag. (2009). THERMAL STABILITY AND KINETIC STUDIES OF COBALT (II), NICKEL (II), COPPER (II), CADMIUM (II) AND MERCURY (II) COMPLEXES DERIVED FROM N-SALICYLIDENE SCHIFF BASES. *J. Chil. Chem. Soc.*, 54(4)349-353.

B. Dabrowski, J. Hupka, M. Żurawaska and J. D. Miller. (2005). LABORATORY AND PILOT SCALE PHOTODEGRADATION OF CYANIDE–CONTAINING WASTEWATERS. *Physicochemical Problems of Mineral Processing*, 39, 229-248.

Ch. Boughelouma and A. Messalhib. (2009). Photocatalytic Degradation of Benzene Derivatives on TiO_2 Catalyst. *Physics Procedia*, 2, 1055–1058.

DI Wolfgang Gernjak. (2006). Ph.D Thesis, *SOLAR PHOTO FENTON TREATMENT OF EU PRIORITY SUBSTANCES*, University of Bodenkultur Wien.

F. Al-Momani. (2003). *Combination of photo-oxidation processes with biological treatment*, PhD Thesis, University of Barcelona.

F.M. Morad, M.M.El.ajaily, S. B. Gweirif. (2007). Preparation, Physical Characterization and Antibacterial Activity of Ni (II) Schiff Base Complex. *J. of Sci. and Appl.*, 1(1)72-78.

J. Donoso, F. Munioz, A.G. Vado, G. Echevarria. (1986). Study of the Hydrolysis and Ionization Constants of Schiff base from Pyridoxal 5'-phosphate and n-hexylamine in Partially Aqueous Solvents. *Biochem. J.,* 238, 137-144

J.P. Escalanda, J. E .Gianotti, A. Pajares, W. A. Massad,F. A.Guerri and N. A. Garcia. (2008). Photodegradation of the Acaricide Abamectin: A Kinetic Study. *J. Agric. Food Chem.*, 56, (16)134-139.

J. Sanz-Asensio, M. Plaza-Medina, M. T. Martínez-Soria and M. Pérez-Clavijo. (1999). Study of photodegradation of the pesticide ethiofencarb in aqueous and non-aqueous media, by gas chromatography–mass spectrometry. *Journal of Chromatography A*, 840, 235-247.

J. Zhang, Y. Tang, J.Q. Xie, J.Zhang, W Zeng and C.-Weihu. (2005). Study on phenol oxidation with H_2O_2 catalyzed by Schiff base manganese complexes as mimetic peroxidase. *J. Serb. Chem. Soc.*, 70(10) 1137–1146.

K. G. Mostafa,T. Yoshioka, E. Konohira and E. Tanoue. (2007). Photodegradation of Fluorescent Dissolved Organic Matter in River Waters. *Geochem. J.*, 41, 323- 331.

K. M. Shareef, S. M.A.Naman and S. G.Muhamad. (2010). Temperature And pH Affecting The Catalytic Photodegradation of 2,4-D and MCPA pesticides in Aqueous Medium. *J. of Koya unv.*, 15, 152-159.

L. Scrano, S. A. Bufo, M. D'Auria, P. Meallier, A. Behechti, and K. W. Shramm. (2002). Photochemistry and Photoinduced Toxicity of Acifluorfen, a Diphenyl-Ether Herbicide. *J. ENVIRON. QUAL.*, 31, 268- 274.

M. Bekbolet, and N. Getoff. (2002). Degradation of chlorinated benzaldehydes in aqueous solutions by UV-irradiation. *International J. of Phtoenergy*, 4, 133-139.

N. Mittal, A.Shah, P. B. Punjabi and V.K. Sharma. (2009). PHOTODEGRADATION OF ROSE BENGAL USING MnO_2. *Rasayan J.chem*, 2, 516-520.

R.Kumar and M. Yusuf. (2009). Photolysis of some 2- butenyl/butynyl bischromones: Effect of solvent polarity, *Org. Commun.*, 2(1)7-19.

S.A Niazi, C. Javali, Paramesh and M Shivaraja. (2010). A Study of Influence of Linkers and Substitution on Antimicrobial Activity of Some Schiff Base. *International Journal of Pharmacy and Pharmaceutical Sciences*, 2,108 -112.

S. K. Pramanikabc and S.Dasb, A. Bhatacharya. (2008). Potodegradation of the herbicide penoxsulam in aqueous methanol and acetonitrile. *J. of Environ. Sci. and Health*, Part B, 43, 569 – 575.

S.T. Ong, C.K. Lee and Z. Zainal. (2009). A Comparison of Sorption and Photodegradation Study in the Removal of Basic and Reactive Dyes. *Australian Journal of Basic and Applied Sciences*, 3(4)3408-3416.

T. Maindron, Y. Wang, J.P. Dodelet, K. Miyatake, A.R. Hlil, A.S. Hay,Y. Tao, M. D'Iorio. (2004). Highly electroluminescent devices made with a conveniently synthesized triazole-triphenylamine derivative, *Thin Solid Films*, 466,209– 216.

V. Papper, V. Kharlanov, S.Schädel, D. Maretzki and W. Rettig. (2003). New fluorescent probes for visual proteins. Part II. 5-(Oxo) penta-2, 4-dienyl-p-(N ,N-dimethyl amino)benzoate, *Photochem. Photobiol. Sci.*, 2, 1272–1286.

Z.Huang, D.Wan, and J.Huang. (2001). Hydrolysis of Schiff Bases promoted by *UV Light Chemistry Letters*, 9,708-709.

Table 1. Kinetic parameters for photolysis of Schiff base in different solvents

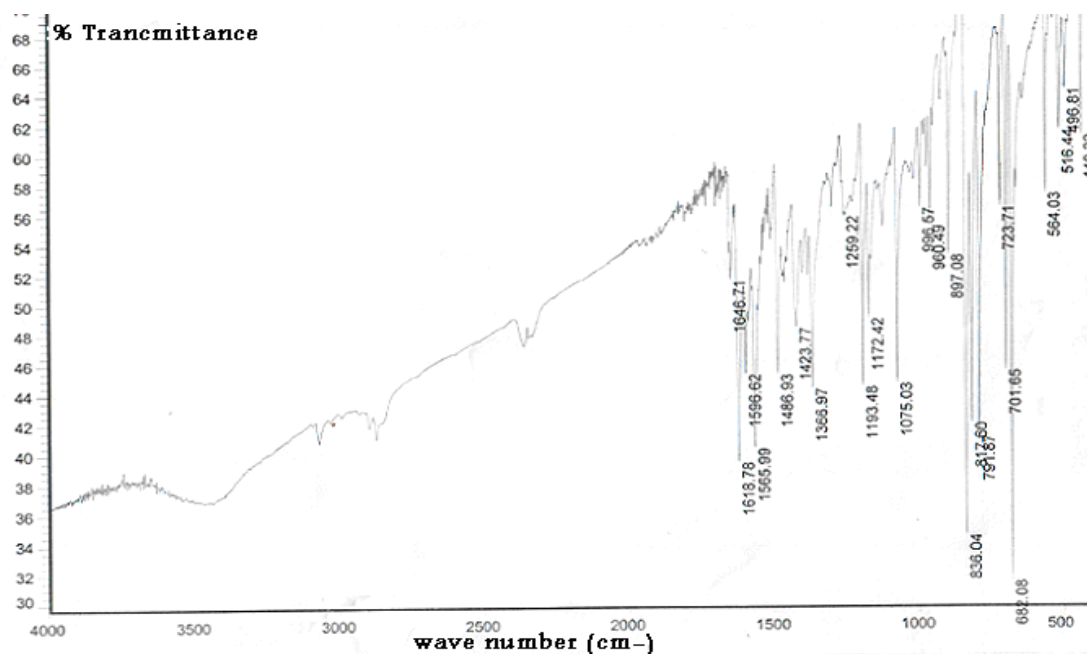| Solvents	$k(min^{-1})$	R^2	$t_{1/2}$ (min)
Methanol	0.0170	0.9185	40.70
Acetonyrtile	0.0128	0.9044	54.14
n-Hexan	0.0098	0.9001	70.71

Figure 1. IR absorption spectrum of Schiff base in KBr disk

Figure 2. UV-Visible absorption spectra of 50 mg/l of Schiff base in Methanol at various irradiation times
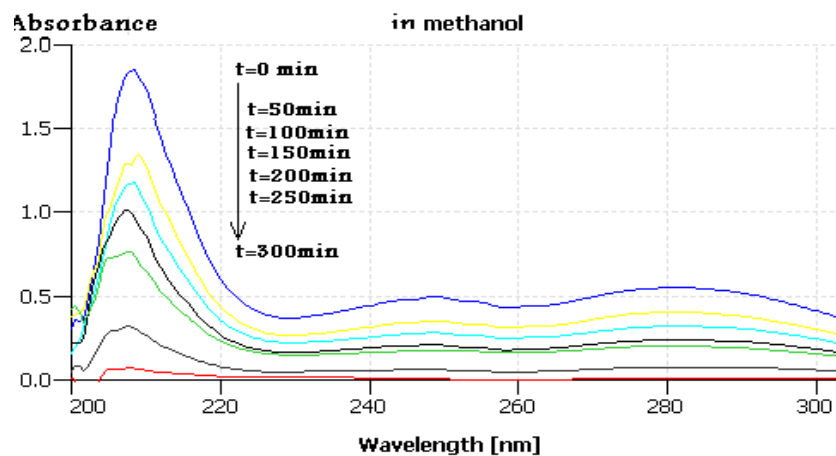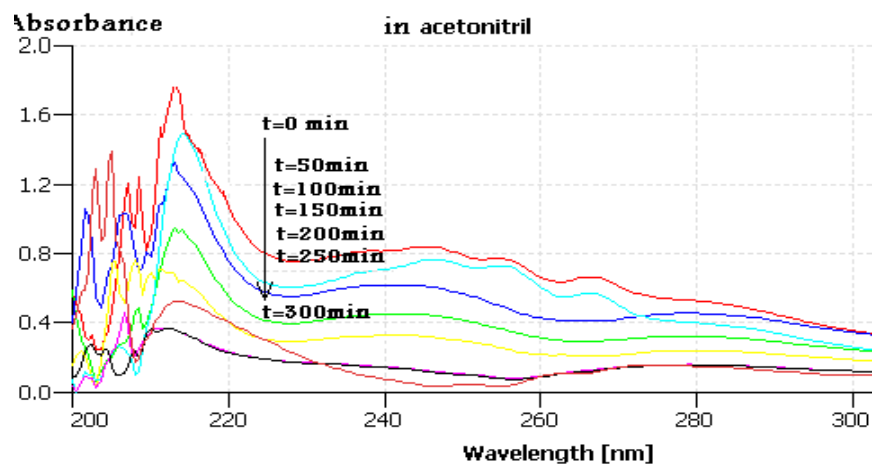
Figure 3. UV-Visible absorption spectra of 50 mg/l of Schiff base in acetonitrile at various irradiation times
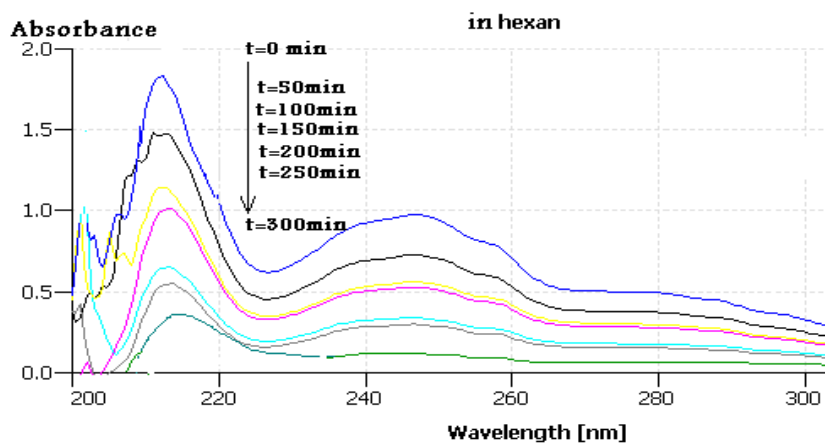
Figure 4. UV-Visible absorption spectra of 50 mg/l of Schiff base in n-hexane at various irradiation times
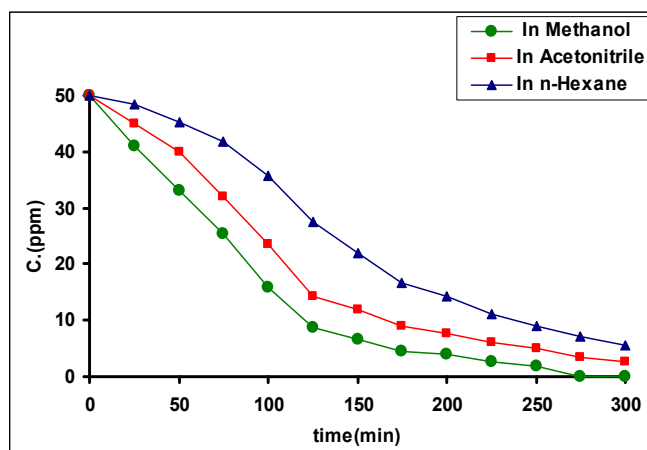
Figure 5. Direct photolysis of 50 mg/l Schiff base in different solvents at room temperature
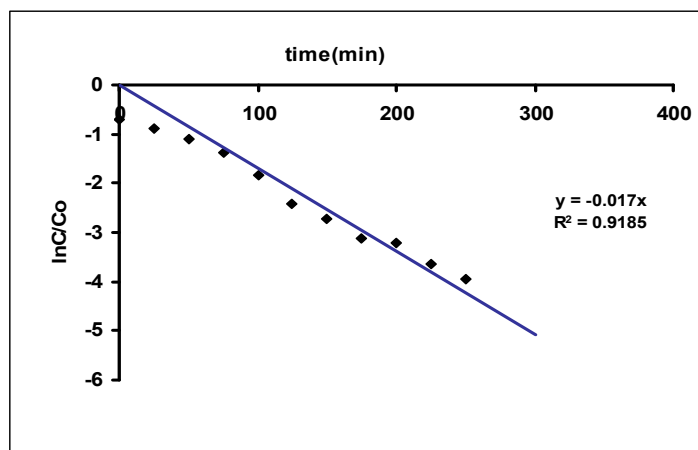
Figure 6. Plotting of ln C/C0 of Schiff base versus time of photolysis in methanol

Figure 7. ln k versus 1/T of Schiff base photolysis in methanol

Figure 8. HPLC chromatogram of Schiff base before photolysis

Figure 9. HPLC chromatogram of Schiff base after 60 min of photolysis in methanol

Kinetics and Mechanism of Oxidation of Sodium Sulfanilate by Dihydroxydiperiodat Onickelate(IV) in Aqueous Medium

Haixia Shen, Jinhuan Shan, Jiying Zhang & Xiaoqian Wang

College of Chemistry and Environmental Science, Hebei University

Baoding 071002, China

E-mail: shanjinhuaner@yahoo.com.cn

Abstract

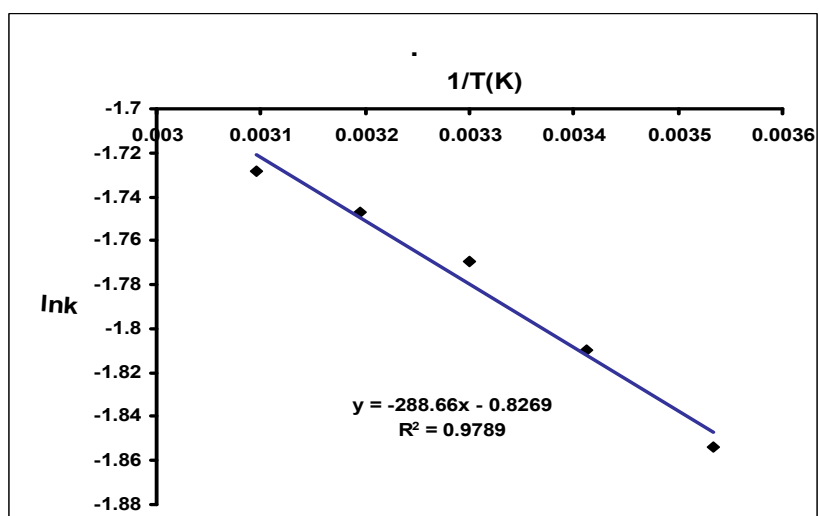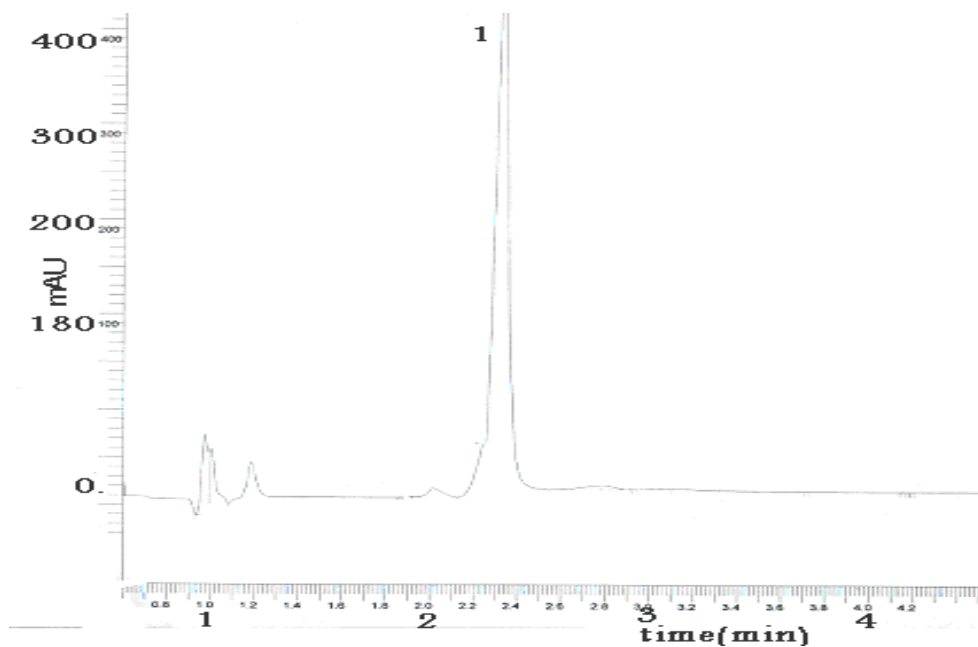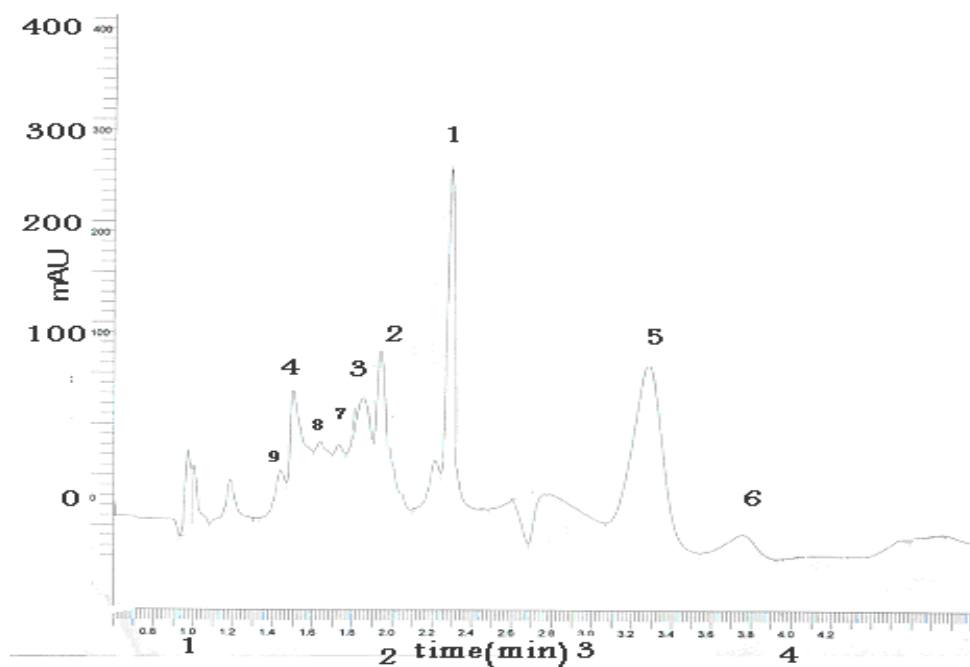The kinetics of oxidation of sodium sulfanilate by dihydroxydiperiodatonickelate(IV)(DPN) was studied spectrophotometrically in alkaline medium. The reaction rate showed first order dependence in oxidant and fractional order in reductant. The corresponding reaction mechanism involving a pre-equilibrium of adduct formation between the complex and reductant was proposed. The rate equations derived from mechanism can explain all experimental observations. The activation parameters along with rate constants of the rate-determining step were calculated.

Keywords: Dihydroxydiperiodatonickelate(IV), Sodium sulfanilate, Oxidation, Kinetics and mechanism

1. Introduction

In recent years, the study of the highest oxidation state of transition metals has intrigued many researchers. This can provide new and valuable information in some fields. Transition metals in a higher oxidation state can generally be stabilised by chelation with suitable polydentate ligands. Metal chelates such as diperiodatocuprate(III) (Niu, W. J., Zhu, Y., Hu, K. C., Tong, C. L. and Yang, H. S. 1996, p.899-904), diperiodatoargentate(III) (Shi, T. S. 1990, p.471-479) and diperiodatonickelate(IV) (Chandraiah, U., Murthy, C. P. and Sushama, K. 1989, p.162-164) are good oxidants in a medium with an appropriate pH value. Ni(IV) complexes have been employed as oxidizing agents for the investigation of some organic compounds such as tetrahydrofurfuryl alcohol (Li, Z. T., Wang, F. L. and Wang, A. Z. 1992, p.933-941), L-leucine (Mahesh, R. T., Pol, P. D. and Nandibewoor, S. T. 2003, p.1341-1352), 4-hydroxycoumarin (Shettar, R. S. and Nandibewoor, S. T. 2005, p.137-143), gabapentin (Hiremath, C. V., Hiremath, D. C. and Nandibewoor, S. T. 2007, p.246-253)etc.

Sodium sulfanilate(SS) is an important and interesting compound, which finds a number of applications in the syntheses of organic dyes, resist agent and whitening agent. It can be used as pesticide to control wheat rust disease. In addition, SS is also an ideal material intermediate for perfume, food additive pigment, pharmaceutical and building materials. The study of SS becomes important because of its biological significance. In this paper, the kinetics and mechanism of oxidation of sodium sulfanilate by dihydroxydiperiodatonickelate(IV) is presented.

2. Experimental

2.1 Reagents and instrumentation

All the reagents used were of A.R. grade. All solutions were prepared with doubly distilled water. The solution of oxidation was prepared (Baker, L. C. W., Mukerjee, H. G. and Sarkar, S. B. and Choudhury, B. K. 1982, p.618-619) and standardized (Murthy, C. P., Sethuram, B. and Rao, T. 1986, p.1212-1218) by the method reported earlier. Its UV spectrum were found to be consistent with that reported in the literature. The concentration of DPN was derived from its absorption at 410 nm. The solution of oxidation was always freshly prepared before use. The ionic strength μ was maintained by adding KNO_3 solution and the pH of the reaction mixture was adjusted with a KOH solution. The kinetic measurements were performed on a UV-vis spectrophotometer (TU-1901, Beijing Puxi Inc., China), which had a cell holder kept at constant temperature ($\pm$ 0.1°C) by circulating water from a thermostat (BG-chiller E$_{10}$, Beijing Biotech Inc., Beijing).

2.2 Kinetics measurements

All kinetics measurements were carried out under pseudo-first order conditions. 2ml of the oxidation solution containing a definite concentration of Ni(IV), OH$^-$, IO$_4^-$ was transferred to upper branch of the λ-type tube and 2ml of SS solution with an appropriate concentration was transferred separately to the lower branch of this tube. After thermal equilibration at the desired temperature in a thermostat, the two solutions were mixed well and immediately

transferred into a 1cm thick rectangular quartz cell in a constant temperature cell-holder (±0.1°C). The reaction process was monitored automatically by recording with a TU-1900 spectrophotometer. All other species did not absorb significantly at this wavelength. Details of the determinations are described elsewhere(Shan, J. H., Wang, L. P., Shen S. G. and Sun H. W. 2003, p.265-272).

3. Results and discussion

3.1 Evaluation of pseudo-first order rate constants

Under the conditions of $[SS]_0 \gg [Ni(IV)]_0$, the plots of $\ln(A_t-A_\infty)$ versus time were straight lines, details of the evaluation are described in our previous work(Qian, J., Gao, M. Z., Shan, J. H. Shen, S. G. and Sun H. W. 2003, p.248-249).

3.2 The dependence of rate on the concentration of SS

At constant temperature, k_{obs} values increase by increasing the concentration of SS while keeping the concentration of [Ni(IV)], [OH⁻], [IO₄⁻], and μ constant. The order with respect to SS was fractional (Figure 1). The plots of $1/k_{obs}$ versus $1/[SS]$ were straight lines with a positive intercept(**Figure 1** r≥0.997) (**Figure 2** r≥0.996).

3.3 The dependence of rate on the concentration of IO_4^-

At constant concentration of [Ni(IV)], [SS], [OH⁻], μ and temperature, the experimental results indicate that k_{obs} decreases while increasing the concentration of [IO₄⁻]. The order with respect to [IO₄⁻] was negative fractional and the plot of $1/k_{obs}$ versus [IO₄⁻] was linear (**Figure 3** r = 0.999) (**Figure 4** r = 0.997).
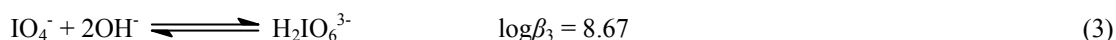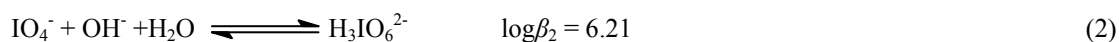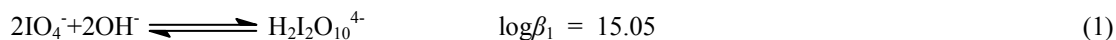
3.4 The dependence of rate on the concentration of OH^-

At constant [Ni(IV)], [SS], [IO₄⁻], μ and temperature, k_{obs} values decreased rapidly with the increase in [OH⁻], and then increased slowly with the increase in [OH⁻], The concentration of OH⁻ was about 0.0569 mol·L⁻¹ at the turning point in which the rate was the slowest.(**Table 1**).

3.5 The dependence of rate on the ionic strength

With other conditions fixed, the reaction rate increased with increase in ionic strength when SS was oxidized by Ni(IV), indicating that there was a positive salt effect to sodium sulfanilate (**Table 2**).

3.6 Discussion of the reaction mechanism

In alkaline solution, equilibria (1-3) were observed and the corresponding equilibrium constants at 298.2 K were determined by Aveston(Aveston, J. 1969, p.273-275).

$$2IO_4^- + 2OH^- \rightleftharpoons H_2I_2O_{10}^{4-} \qquad \log\beta_1 = 15.05 \qquad\qquad (1)$$

$$IO_4^- + OH^- + H_2O \rightleftharpoons H_3IO_6^{2-} \qquad \log\beta_2 = 6.21 \qquad\qquad (2)$$

$$IO_4^- + 2OH^- \rightleftharpoons H_2IO_6^{3-} \qquad \log\beta_3 = 8.67 \qquad\qquad (3)$$

The distribution of all species of periodate in alkaline solution can be calculated from the equilibriums (1)-(3). The dimer $H_2I_2O_{10}^{4-}$ and IO_4^- species can be neglected, the main iodic acid species is $H_3IO_6^{2-}$ and $H_2IO_6^{3-}$. According to the literature, the main existent form of oxidant was $[Ni(OH)_2(H_2IO_6)_2]^{4-}$ over the experimental concentration range of OH⁻.

Neglecting the concentration of ligand dissociated from Ni(IV), the main species of periodate are $H_2IO_6^{3-}$ and $H_3IO_6^{2-}$, here:

$$[IO_4^-]_t \cong [H_3IO_6^{2-}] + [H_2IO_6^{3-}] \qquad\qquad (4)$$

Equations (5) and (6) can be obtained from (2), (3), (4):

$$[H_2IO_6^{3-}] = \frac{\beta_3[OH^-]}{\beta_3 + \beta_3[OH^-]} \cdot [IO_4^-]_t = f([OH^-]) \cdot [IO_4^-]_t \qquad\qquad (5)$$

$$[H_3IO_6^{2-}] = \frac{\beta_2}{\beta_2 + \beta_3[OH^-]} \cdot [IO_4^-]_t = \phi([OH^-]) \cdot [IO_4^-]_t \qquad\qquad (6)$$

Here, $[IO_4^-]_t$ represents the concentration of original over all periodate ions which is approximately equal to the sum of $[H_2IO_6^{3-}]$ and $[H_3IO_6^{2-}]$. In the [OH⁻] range used in this work, the main specie of periodate is $H_2IO_6^{3-}$. Based on the discussion, the formula of the Ni(IV) periodate complex may be represented by either $[Ni(OH)_2(H_3IO_6)_2]^{2-}$ or

the less protonated ionic species $[Ni(OH)_2(H_2IO_6)_2]^{4-}$. We preferred to use the latter to represent DPN because it is close to that suggested by Mukherjee(Mukherjee, H. G., Mandal, B. and De, S. 1984, p.426-428).

Based on the above discussion, two simultaneous reaction mechanisms were proposed:

Mechanism I: In a less alkaline medium:

$$[Ni(OH)_2(H_2IO_6)_2]^{4-}+OH^- \xrightleftharpoons{K_1} [Ni(OH)_2(HIO_6)]^{2-}+H_2IO_6^{3-}+H_2O \tag{7}$$

(DPN) (MPN)

$$NH_2C_6H_6SO_3^-(\text{or } R^-)+H_2O \xrightleftharpoons{K_2} NH_3^+C_6H_6SO_3^-+OH^- \tag{8}$$

$$[Ni(OH)_2(HIO_6)]^{2-}+NH_3^+C_6H_6SO_3^- \xrightarrow{K_3} \text{complex} \tag{9}$$

(MPN)

$$\text{complex} \xrightarrow{k} Ni(II)+\text{product} \tag{10}$$
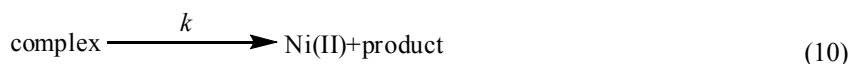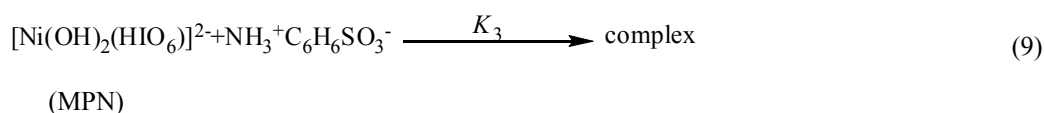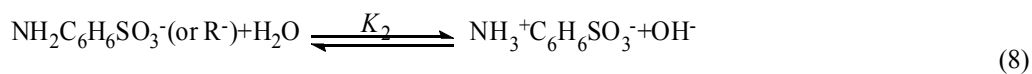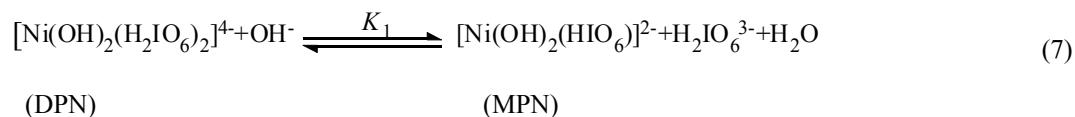
Here, reaction (9) was the rate-determining step.

$$[Ni(IV)]_T = [DPN]_e + [MPN]_e + [\text{complex}]_e$$

Subscripts t and e stand for total concentration and concentration at equilibrium respectively.

As the rate of the disappearance of $[Ni(IV)]_t$ was monitored, the rate of the reaction can be derived as:

$$-\frac{d[Ni(IV)_t]}{dt} = \frac{kK_1K_2[OH^-][R^-]}{K_1K_2[R^-][OH^-] + K_1[OH^-] + [H_2IO_6^{3-}]}[Ni(IV)]_t \tag{11}$$

$$\therefore k_{obs} = \frac{kK_1K_2K_3[R^-]}{K_1K_2K_3[R^-] + K_1[OH^-] + [H_2IO_6^{3-}]} \tag{12}$$

$$\frac{1}{k_{obs}} = \frac{1}{k} + \frac{K_1[OH^-]+f(OH^-)[IO_4^-]}{kK_1K_2K_3[R^-]} \cdot \frac{1}{[R^-]} \tag{13}$$

$$\frac{1}{k_{obs}} = \frac{K_1K_2K_3[R^-]+K_1[OH^-]}{kK_1K_2K_3[R^-]} + \frac{f(OH^-)}{kK_1K_2K_3[R^-]} \cdot [IO_4^-] \tag{14}$$

Mechanism II. In a more alkaline medium:

$$[Ni(OH)_2(H_2IO_6)_2]^{4-}+OH^- \xrightleftharpoons{K_1} [Ni(OH)_2(HIO_6)]^{2-}+H_2IO_6^{3-}+H_2O \tag{15}$$

(DPN) (MPN)

$$[Ni(OH)_2(HIO_6)]^{2-}+NH_2C_6H_6SO_3^-(\text{or } R^-) \xrightarrow{K_2} \text{complex} \tag{16}$$

(MPN)

$$\text{complex} \xrightarrow{k} Ni(II)+\text{product} \tag{17}$$
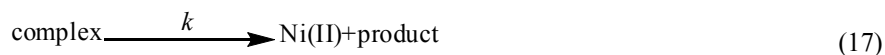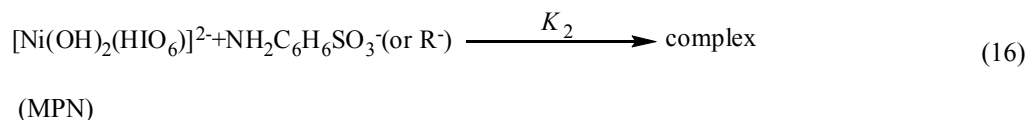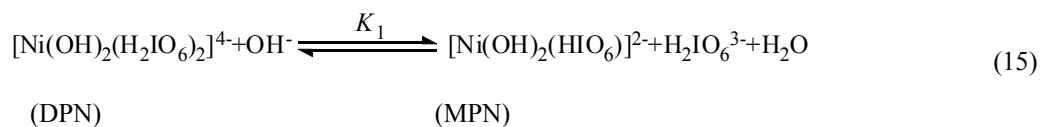
The total concentration of Ni(IV) at time t can be written as :

$$[Ni(IV)]_T = [DPN]_e + [MPN]_e + [complex]_e$$

Since reaction (15) is the rate-determining step, the rate of disappearance of $[Ni(IV)]_t$ is monitored as:

$$\therefore k_{obs} = \frac{kK_1K_2[OH^-][R^-]}{K_1K_2[R^-][OH^-] + K_1[OH^-] + [H_2IO_6^{3-}]} \tag{18}$$

$$\frac{1}{k_{obs}} = \frac{1}{k} + \frac{f([OH^-])[IO_4^-]_t + K_1[OH^-]}{kK_1K_2[OH^-]} \cdot \frac{1}{[R^-]} \tag{19}$$

$$\frac{1}{k_{obs}} = \frac{1+K_2[R^-]}{kK_2[R^-]} + \frac{f([OH^-])}{kK_1K_2[OH^-][R^-]} \cdot [IO_4^-]_t \tag{20}$$

In this report, Equations (12) and (18) can explain k_{obs} values decreased rapidly with the increase in $[OH^-]$ up to 0.0569 mol·L^{-1}, after that point, it increased gradually with the continuous increase in $[OH^-]$. Equations (14) and (20) show that the plots of $1/k_{obs}$ versus $[IO_4^-]$ should also be linear. Equations (13) and (19) show that the order in SS should be fractional order and $1/k_{obs}$ versus $1/[SS]$ should be linear. The rate equations derived from the reaction mechanisms are consistent with our experimental results. The activation energy and the thermodynamic parameters were evaluated by the previously published method (Shan, J. H. and Liu, T. Y. 1994, p.1140-1144). (Table 3)

4. Conclution

Among various species of Ni(IV) in alkaline liquids, monoperiodatonickelate is considered as the active species for the title reaction. The rate constant of slow step and other equilibrium constants involved in the mechanism are evaluated and activation parameters with respect to the slow step of the reaction were computed. The overall mechanistic sequence described here is consistent with mechanistic studies and kinetic studies.

References

Aveston, J. (1969). Hydrolysis of Potassium Periodate: Ultracentrifugation Potentiometric Titration and Raman Spectra. *J. Chem. Soc.*, (A): 273-275.

Baker, L. C. W., Mukerjee, H. G. and Sarkar, S. B. and Choudhury, B. K. (1982). Synthesis & characterisation of lithium bexaorth periodatonickelate(IV). *Indian J. Chem.*, 21(A): 618-619.

Chandraiah, U., Murthy, C. P. and Sushama, K. (1989). Kinetics of oxidation of lactic,mandelic & glycollic acids by diperiodatonickelate(IV) in alkaline medium. *Indian J. Chem.*, 28(A), 162-164.

Hiremath, C. V., Hiremath, D. C. and Nandibewoor, S. T. (2007). Ruthenium(III) catalysed oxidation of gabapentin (neurontin) by diperiodatonickelate(IV) in aqueous alkaline medium: A kinetic and mechanistic study. *J. Mol. Catal. A: Chem.*, 269, 246-253.

Li, Z. T., Wang, F. L. and Wang, A. Z. (1992). Kinetics and mechanism of oxidation of tetrahydrofuryl alcohol by dihydroxydiperiodatonickelate(IV) complex in aqueous alkaline medium. *Int. J. Chem. Kinet.*, 24, 933-941.

Mahesh, R. T., Pol, P. D. and Nandibewoor, S. T. (2003). Kinetics and mechanism of oxidation of L-leucine by alkaline diperiodatonickelate(IV): A free radical intervention, deamination, and decarboxylation. *Monatsh. Chem.*, 134, 1341-1352.

Mukherjee, H. G., Mandal, B. and De, S. (1984). Preparation and Studies of the Complex Periodatoferrate(III) Hexahydrare and Periodatonickelate(IV) Monohydrate. *Indian J. Chem.*, 23(A): 426-428.

Murthy, C. P., Sethuram, B. and Rao, T. (1986). Oxidation by tetravalent nickel part 1: kineties of electron transfor from some aliphatic alcoholos to Ni (IV) in aqueoous alkaline media. *Z Phys Chem. (Leizig).*, 287: 1212-1218.

Niu, W. J., Zhu, Y., Hu, K. C., Tong, C. L. and Yang, H. S. (1996). Kinetics of oxidation of SCN$^-$ by diperiodatocuprate(III) (DPC) in alkaline medium. *Int. J. Chem. Kinet.*, 28, 899-904.

Qian, J., Gao, M. Z., Shan, J. H. Shen, S. G. and Sun H. W. (2003). Kinetics of Oxidation of ethanolamine by dihydroxydiperiodatonickelate(IV) in alkaline media. *J. Guangxi Normal Univ.*, 21(1): 248-249.

Shan, J. H. and Liu, T. Y. (1994). Kinetics and mechanism of substitution reactions of bis(N,N-diethyldithiocarbamato)alkylxanthatocobalt(III) with dipropylamine and di-n-butylamine in methanol.

ACTA Chem Sin., 52: 1140-1144.

Shan, J. H., Wang, L. P., Shen S. G. and Sun H. W. (2003). Kinetics and Mechanism of Oxidation of Some Hydroxy Butyric Acid Salts by Ditelluratocuprate(III) in Alkaline Medium. *Turk J. Chem.*, 27: 265-272.

Shettar, R. S. and Nandibewoor, S. T. (2005). Kinetic, mechanistic and spectral investigations of ruthenium(III)-catalysed oxidation of 4-hydroxycoumarin by alkaline diperiodatonickelate(IV) (stopped flow technique). *J. Mol. Catal. A: Chem.*, 234, 137-143.

Shi, T. S. (1990). Studies of unsual oxidation states of transition metals (I)----kinetics and mechanism of oxidation of potassium thiocyanate by diperiodatoargentate(III) ion in alkaline medium. *Sci. China, Ser. B Chem.*, 12, 471-479.

Table 1. k_{obs} varying with [OH$^-$] at 298.2 K

[Ni(IV)]= 7.83×10^{-6} mol/L; [SS]= 8.00×10^{-3} mol/L; [IO$_4^-$]= 2.00×10^{-3} mol/L; μ=0.167 mol/L

10^2[OH$^-$]/(mol/L)	1.09	1.69	3.19	4.69	5.69	6.69	8.19	9.69	10.7
$10^2 k_{obs}$/s^{-1}	5.09	4.35	3.40	3.22	3.02	3.12	3.26	3.37	3.41

Table 2. k_{obs} varying with ionic strength at 298.2 K

[Ni(IV)]= 7.83×10^{-6} mol/L; [SS]= 6.00×10^{-3} mol/L; [OH$^-$]=1.69×10^{-2} mol/L; [IO$_4^-$]= 2.00×10^{-3} mol/L

10μ/(mol·L^{-1})	0.249	0.449	0.749	1.15	1.75
$10^2 k_{obs}$/s^{-1}	2.06	2.60	3.05	3.53	3.68

Table 3. Rate constants (k) and activation parameters of the rate-determining step at 298.2 K

	T/K	293.2	298.2	303.2	308.2	313.2
$10^2 k$/s^{-1}	In a less alkaline medium	2.36	3.53	6.26	8.97	15.1
	In a more alkaline medium	1.92	2.84	4.69	7.08	12.7
Thermodynamic activation parameters	In a less alkaline medium	E_a= 70.97 kJ·mol^{-1}, $\Delta H^{\neq}$= 68.49 kJ·mol^{-1}, $\Delta S^{\neq}$= -42.64 J·K^{-1}·mol^{-1}				
	In a more alkaline medium	E_a= 71.51 kJ·mol^{-1}, $\Delta H^{\neq}$= 69.03 kJ·mol^{-1}, $\Delta S^{\neq}$= -42.70 J·K^{-1}·mol^{-1}				

The plots of ln k vs. 1/T have following intercept (a) slope (b) and relative coefficient (r).
In a less alkaline medium: a= 25.33 b= -8536 r= 0.998
In a more alkaline medium: a= 25.33 b= -8601 r= 0.99
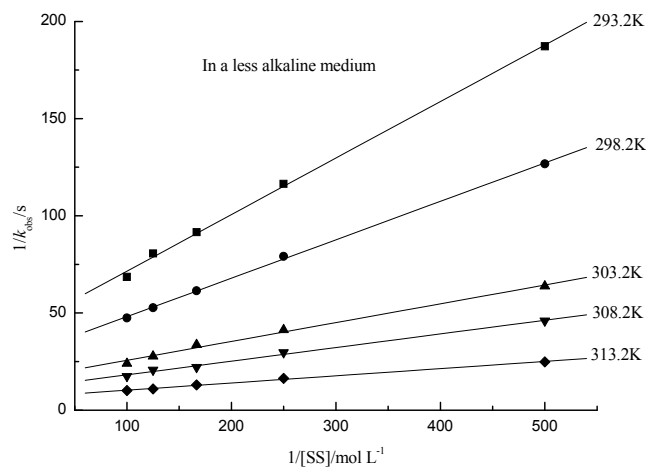
Figure 1. Plots of $1/k_{obs}$ versus $1/[SS]$ at different temperatures

$[Ni(IV)]= 7.83\times10^{-6}$ mol/L; $[OH^-]= 1.69\times10^{-2}$ mol/L; $[IO_4^-]= 2.00\times10^{-3}$ mol/L; $\mu= 3.99\times10^{-2}$ mol/L
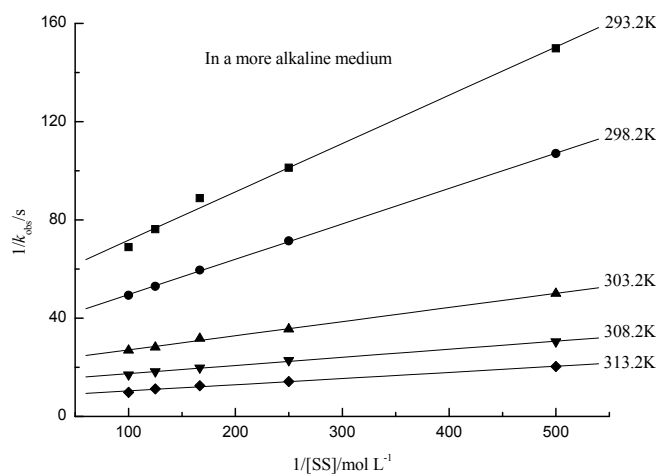
Figure 2. Plots of $1/k_{obs}$ versus $1/[SS]$ at different temperatures

$[Ni(IV)]= 7.83\times10^{-6}$ mol/L; $[OH^-]= 8.19\times10^{-2}$ mol/L; $[IO^{4-}]= 2.00\times10^{-3}$ mol/L; $\mu= 9.39\times10^{-2}$ mol/L
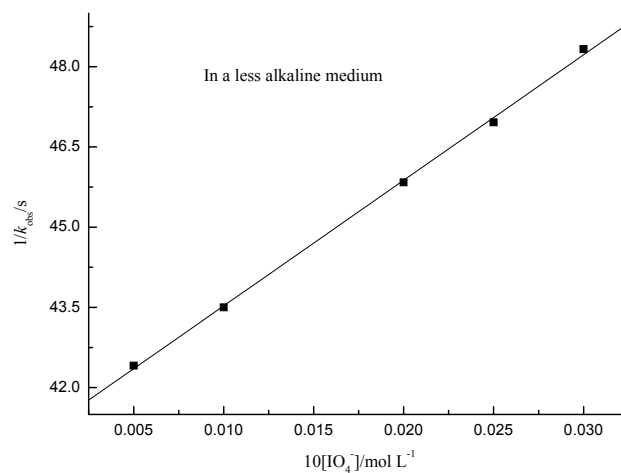
Figure 3. Plot of $1/k_{obs}$ versus $[IO^{4-}]$ at 298.2K

$[Ni(IV)]= 7.83\times10^{-6}$ mol/L; $[SS]= 6.00\times10^{-3}$ mol/L; $[OH-]= 1.69\times10^{-2}$ mol/L; $\mu= 2.54\times10^{-2}$ mol/L
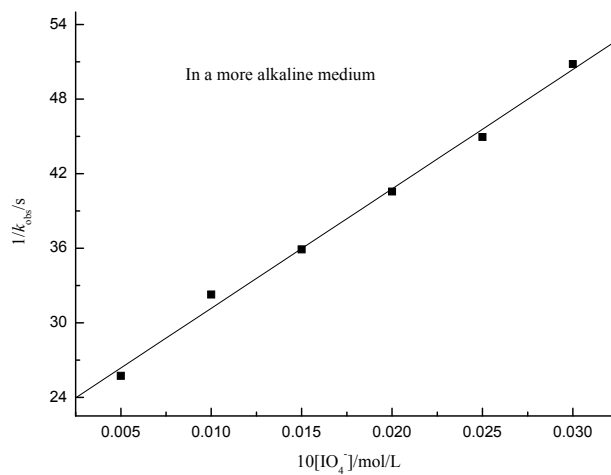
Figure 4. Plot of $1/k_{obs}$ versus $[IO^{4-}]$ at 298.2K

$[Ni(IV)]= 7.83\times10^{-6}$ mol/L; $[SS]= 6.00\times10^{-3}$ mol/L; $[OH-]= 8.19\times10^{-2}$ mol/L; $\mu= 9.19\times10^{-2}$ mol/L

Solvent-Free and Microwave-Assisted Synthesis of Aryl Thiocyanates

Yuqing Cao (Corresponding author)

College of Pharmacy, Hebei University

Baoding 071002, Hebei, China

E-mail: pharm_hbu@yahoo.com

Liya Xu

College of Pharmacy, Hebei University

Baoding 071002, Hebei, China

E-mail: xuliyaabcd@126.com

Fangrui Song, Dingxiang Du, Xiaojun Yang & Xiangtao Xu

College of Pharmacy, Hebei University

Baoding 071002, Hebei, China

Abstract

Aryl thiocyanates are important intermediates in organic synthesis, and are more widely used. This paper reported the solvent-free conditions, microwave assisted synthesis method, and a series of aromatic thiocyanates were synthesized by the solvent-free conditions, microwave assisted synthesis method. Under microwave irradiation, directly putting the active aromatic compounds and thiocyanates into the flask, then adding the phase transfer catalyst, the reaction can be done in some minutes. Yield can reach up to 80% or more. This method is simple, efficient, environmentally friendly, and meets the requirements of the development of green chemistry.

Keywords: Microwave irradiation, Polyethylene glycol 400, Thiocyanates, Solvent-free

1. Introduction

Aryl thiocyanates are well-known in the area of organosulfur chemistry (Bhalerao, D. S. et. al 2010). Aryl thiocyanates have found a wide variety of applications as insecticides (Buchel, K. H. 1970), biocidal(Gerson, C. et. al 2000), antiasthmatic(Akio, M. et. al 1991), vulcanization accelerators(Gorl, U. et. al 1992), and starting materials for the preparation of heterocycles(Batanero, B. et. al 2002). Aryl thiocyanates are also considered to be an important class of compounds in some anticancer natural products formed by deglycosylation of glucosinolates derived from cruciferous vegetables (Ju, Y. et. al 2006).

Direct introduction of sulfur into aromatic rings is an interesting objective (Khazaei, A. et. al 2001). A number of general methods are commonly utilized for this purpose, such as, displacement of leaving groups with thiocyanates ions (Bacon, R. G. R. 1961), (KSCN, NaSCN, $Zn(SCN)_2$, NH_4SCN, Me_3SiNCS, $Me_3SiNCS/TiCl_4$, Me_3SiNCS/Bu_4NF). And sulfonation (lan , W. J. Still, ea. tl. 2001). The former would be more useful for our purpose, but the low nucleophilicity of the –SCN ion requires relatively harsh reaction conditions. Thiocyanates can also be obtained from alcohols, silylethers using in situ formed electrophilic phosphorane $Ph_3P(SCN)_2$ (Karade, N. N. et. al 2005) or amines. However, the results are not reproducible because of the low thermal stability of the required intermediate $(SCN)_2$. The toxicity of the starting material, $Ph_3P(SCN)_2$, is also a major drawback in this thiocyanation method. And the thiocyanates group is unstable when heated or submitted to acidic conditions, so the reaction can give mixtures of thiocyanates and isothiocyanates, or can proceed selectively to either isomer. Overall, developing efficient, selective, and eco-friendly synthetic methods for applications in organic synthesis is an ongoing program in our research group. Herein, we now report an eco-friendly, facile method of direct introduction of sulfur into aromatic rings by Utilization of microwave irradiation and polyethylene glycol (PEG).And the results shown in Table 1.

Until now, the application of phase-transfer catalyst (PTC) has drawn a great deal of attention, and substantial interest has been devoted to the utilization of PEG. Attractive features of PEG include their low cost, readily availability and apparent lack of significant toxicological properties (Du, Y.F.ea.tl 2004). In many cases, they are

good alternative substitutes for the traditional PTC, such as the crown ether, which is toxic and expensive, and quaternary ammonium salts or quaternary phosphonium compounds, which are predominantly used in a liquid-liquid two-phase reaction. In contrast with crown ethers, PEG has more powerful ability to solubilise the inorganic salts in a nonpolar organic solvent due to the fact that they have two terminal polar hydroxyl groups.

2. Experimental

General procedure

All reactions were performed in a commercial domestic microwave oven (Midea PJ21C-BF). The reaction process was monitored by GF254 TLC using petroleum ether/ethyl acetate (10:1 v/v) as the eluant. Melting points were determined on a microscopy apparatus (SGW X-4) and uncorrected. The products were characterized by comparison of their melting points and boiling points with the literature values.

Synthesis of 1-methoxy-4-thiocyanatobenzene is given as a representative example. Anisole (0.562 g, 0.0052 mol), KSCN (1.516 g, 0.0156 mol) and PEG 400 (0.104 g, 0.00026 mol) were taken in a conical flask, mixed thoroughly and subjected to microwave irradiation at 231W for 3 min. The progress of the reaction was monitored by TLC. After completion of the reaction, water (10 mL) was added to the reaction mixture, stirred well and extracted with CH_2Cl_2 (2×30 mL). The combine organic extract was dried over anhydrous sodium sulphate, concentrated in vacuum. The products were dried in a vacuum tank. All the liquid parent materials were freshly distilled. The products were also characterized by comparison of their melting points and boiling points with the literature values.

3. Result and Discussion

In table 1, a variety of aromatic compounds including methoxybenzenes and heteroaromatics were successfully thiocyanated by utilization of microwave irradiation and polyethylene glycol(PEG).We have not identified the species responsible for carrying out the thiocyanation, but we can rule out thiocyanogen. The electron density on the aromatic ring was shown to have considerable effect on the yield of thiocyanation reaction. Highly activated methoxybenzenes (entries 1-3) could be converted to the corresponding aryl thiocyanates in excellent yields. It was noteworthy that only para substitution products were formed in the case of anisole (entry 1). The heteroaromatics (entry 6-7) yielded thiocyanation products in lower yields.

With a medium molecular weight, PEG is a particularly desirable phase-transfer catalyst for non-aqueous heterogeneous reactions. It is important that features of PEG include its low cost, stability, ready availability and apparent lack of significant toxicological problems, so the application of PEG as an eco-friendly PTC for activation of reaction has now become a very popular and useful method. These reactions may not be completed if there is no catalyst. So, PEG400 as a phase transfer to this reaction has been studied, and the effects of PEG400 were shown in Table 2. The best amount to use was 5 mol%. It was found that lower dosage of PEG400 could not catalyse the reaction effectively and higher dosage would undoubtedly lead to more loss of products during the washing procedure. In our opinion, this reaction can be made easier because PEG400 may be work as a solvent and disperse reactants.

4. Conclusions

In summary, we have found that aryl thiocyanates can be synthesized in high yields under microwave irradiation using readily available, inexpensive, ecofriendly PEG. This method is inexpensive, practical and with less pollution and easy work-up.

References

Akio, M., & Masaaki, K. (1991). US, Patent 5, 155, 108, *Chem.Abstr.*, 114, 102028e.

Bacon, R. G. R. (1961). *Organic sulfur compounds*. New York: Pergamon, (Chapter 27, p 304).

Batanero, B., Braba, F., & Martina, A. (2002). Preparation of 2,6-dimethyl-4- arylpyridine-3,5-dicerbonitrile: a paired electrosynthesis. *J. Org. Chem.*, 67(7), 2369–2371.

Bhalerao, D. S., & Akamanchi, K. G. (2010). Mild and efficient method for α-thiocyanation of ketones and β-dicarbonyl compounds using bromodimethylsulfonium bromide-ammonium thiocyanate. *synthetic communications*, 40, 799-807.

Buchel, K. H. (1970). *Chemie der Pflanzen Schutz-Und Schadlingsbe Kampfungsmittle*. Springer: Berlin Heidelberg, New York, 457–459.

Du, Y. F., Cao, Y. Q., Dai,Z., & Chen, B. H. (2004). A study on the heterogeneous reaction of trialkylsilyl chlorides with inorganic salts and monocarboxylates catalysed by PEG400. *Journal of chemical research*, 3, 223–225.

Gerson, C., Sabater, J., Scuri, M., Torbati, A., Coffey, R., Abraham, J. W., Lauredo, I., Forteza, R., Wanner, Salathe,

A., Abraham, M., & Conner, G. E. (2000). The lactoperoxidase system functions in bacterial clearance of airways (see comments). *Am. J.Respir. Cell Mol. Biol.*, 22, 665–671.

Gorl, U., & Wolff, S. (1992). DE 4, 100, 217, *Chem.Abstr.*, 117, 152581n.

Ju, Y., Kumar, D., & Arma, R. S. (2006). Revisiting nucleophilic substitution reactions: microwave-assisted synthesis of azides, thiocyanates, and sulfones in an aqueous medium. *The Journal of Organic Chemistry,* 71(17), 6697-6700.

Karade, N. N., Tiwari, G. B., Shirodkar, S. G., & Dhoot, B. M. (2005). Tiwari Efficient and Mild Oxidative Nuclear Thiocyanation of Activated Aromatic Compounds Using Ammonium Thiocyanate and Diacetoxyiodobenzene. *Synthetic Communications*, 35, 1197–1201.

Khazaei, A., Alizadeh, A., & Vaghei, R. G. (2001). Preparation of arylthiocyanates using N, N′-dibromo-N, N′-bis(2,5-dimethylbenzenesulphonyl) ethylenediamine and N, N-dibromo-2,5- dimethylbenzenesulph- onamide in the presence of KSCN as a novel thiocyanating reagent. *Molecules*, 6(3), 253–257.

Lan, W. J. Still & Iain, D. G. Watson. (2001). An efficient synthetic route to aryl thiocyanates from arenesulfinates. *Synthetic Communications*, 31(9), 1355–1359

Table 1. Microwave-assisted synthesis of thiocyanates

Entry	Substrate	Product	Time (min)	Yield (%)	m.p./^{o}C Found/Reported
1			5	85	40-41/33-44
2			3	89	50-53/ 51-53
3			4	87	66-68/ 68–69
4			5	84	61-62/63-64
5			4	80	72-74/ 73-74
6			5	75	132-135/134-136[b]
7			6	73	105-106/106-107
8			6	70	89-90/91

[b] the structure of product determined by boiling point

Table 2. The amount of PEG400[a]

Power(w)	Time(min)	Amount of PEG400 (mol%)	Yield (%)
116	3	1	70
116	3	3	80
116	3	5	93
116	3	6	92
116	3	7	91

[a]anisole

Complexation Reaction Using Ammonium Based Chloride Compounds for Preparation of Eutectic Mixtures

Ahmad Adlie Shamsuri (Corresponding author)

Laboratory of Industrial Biotechnology, Institute of Bioscience

Universiti Putra Malaysia, 43400 UPM Serdang

Selangor Darul Ehsan, Malaysia

E-mail: adlie@putra.upm.edu.my

Dzulkefly Kuang Abdullah

Laboratory of Industrial Biotechnology, Institute of Bioscience

Universiti Putra Malaysia, 43400 UPM Serdang

Selangor Darul Ehsan, Malaysia

Abstract

In this study, we are interested in the eutectic processing of chloride compounds and decided to focus on ammonium based compounds that can provide sufficient insight in the fundamental chemistry. 10 types of ammonium based chloride compounds namely ammonium chloride, methanaminium chloride, dimethylammonium chloride, trimethylammonium chloride, tetramethylammonium chloride, dodecyltrimethylammonium chloride, hexadecyltrimethylammonium chloride, phenyltrimethylammonium chloride, benzyltrimethylammonium chloride and (vinylbenzyl)trimethylammonium chloride were used in this study. This research led to a hypothesis that the ammonium based chloride compounds could be reacted with urea through complexation reaction giving eutectic mixtures. However, functional groups have plays an important role to influence melting points of these eutectic mixtures. This is regarded to be a motivating finding that will be important for the most future research work involving complexation reaction for the production of eutectic mixtures.

Keywords: Eutectic mixture, Ammonium based chloride compounds, Complexation reaction, Ionic liquids

1. Introduction

Eutectic mixtures which are materials consisting of components that form a low melting point mixture, provide a unique substance for developing advanced materials and usually cheaper with less time-consuming than the development of new materials. It is composed of a mixture with a melting point much lower than each of the individual components. For example, changing metal such as tin and lead into metallic eutectic is a common way to make them low melting point material usually used in soldering (Kanchanomai, et al., 2002). Other eutectic mixture is sodium chloride and water; it has a eutectic point of -21.2°C (Chen, et al., 2005) it is used to aid ice removal or to produce low temperatures ice. Eutectic mixtures are simple to prepare, the components of the eutectic can be easily mixed and converted without further purification. Most recently, eutectic mixtures were utilized to produce ionic liquids that might be used as green solvents (Hou, et al., 2008).

Since little information using common ammonium based compounds as eutectic components is known concerning the chloride compounds (except for choline chloride) related to the preparation of eutectic mixture. Therefore, we have produced some eutectic mixtures using common ammonium based chloride compounds. Previous study has shown that complexation reaction was used to produce eutectic mixture by means of ammonium based chloride compounds such as choline chloride with urea as complexing agent (Abbott, et al., 2003), although low melting point of eutectic mixture was observed in that study, but we have found that the role of functional groups in ammonium based chloride compounds for producing eutectic mixtures through complexation reaction is still not fully discovered and identified. In this study, eutectic mixtures have been prepared via complexation reaction by

means of ammonium based chloride compounds with different functional groups; its physical appearance and melting point were also studied.

2. Materials and methods

2.1 Materials

Ammonium chloride, methanaminium chloride, dimethylammonium chloride, trimethylammonium chloride, tetramethylammonium chloride, dodecyltrimethylammonium chloride, hexadecyltrimethylammonium chloride, phenyltrimethylammonium chloride, benzyltrimethylammonium chloride and (vinylbenzyl)trimethylammonium chloride were supplied by Sigma Aldrich. Urea was also obtained from Sigma Aldrich. All chemicals purity ≥98.0% and were recrystallized before use.

2.2 Preparation of eutectic mixture

Preparation of eutectic mixture via complexation reaction was done according to (Abbott, et al., 2007). In this study, ammonium based chloride compounds were mixed in the flask with urea as 1:2 mole ratios, respectively. The flask was immersed in oil bath at 100°C and stirred for at least 1 hour. Then, the reaction mixture was dried for overnight at 100°C in a vacuum oven to obtain the final product and prior to the melting point measurements.

2.3 Melting point characterization

Differential scanning calorimetry (DSC) analysis was conducted on a Mettler Toledo DSC822^e apparatus using the STAR analysis software under a constant stream of nitrogen at flow rate of 50 mL/min. The samples were tightly sealed in aluminium pans. The samples were first heated to 100°C to eliminate the thermal history. The analyses were carried out in a temperature range of 25 to 350ºC with a heating rate of 10ºC/min to obtain the melting point, T_m which were determined from thermograms during the programmed reheating steps.

3. Results and discussion

3.1 Physical appearance

Table 1 shows the physical appearances profile of eutectic mixtures at room temperature (25ºC). All prepared eutectic mixtures are solid at ambient temperature corresponding to physical properties of its individual components. Ammonium based chloride compounds are composed of nitrogen cations and chloride ions, so, they have tendency to form eutectic mixture with complexing agent (urea) assisted by elevated temperature (Abbott, et al., 2003). It can also be seen in Table 1 all eutectic mixtures are solid possibly due to high melting points. Nonetheless, DSC thermal analysis was carried out to determine the melting points accurately.

3.2 DSC characterization

Table 2 shows the melting points of pristine eutectic components were supplied by Sigma Aldrich MSDS, which obviously high. DSC is a well known as technique which gives an exhaustive overview the relevant thermal analysis (Ford & Timmins, 1989). The calorimetric data was obtained by heating the eutectic mixtures; all melting points corresponding with the peaks of DSC traces were listed in Table 3. Each melting point of DSC traces means a crystalline melting point of the eutectic mixtures. From this result, it can be observed that the melting points of eutectic mixtures are different from its pristine eutectic components. In other words, melting points of eutectic mixtures are significantly lower than its individual components. Therefore, in this study all eutectic mixtures were indicating absolute eutectic behaviour due to the reduction in melting points. In Table 3 it seems that the complexation reaction has been taking place which chloride ions complexed with urea. The reasons why they have low melting points are basically the endothermic shifted to the lower temperature after complexing agent was given to the ammonium based chloride compounds. Mostly the chloride ions could be reacted with urea through complexation reaction assisted by high temperature condition. The complexation reaction of chloride ions with urea is actually driven by hydrogen bonding between them (Abbott, et al., 2003).

Although hydrogen bonding is fully known as strong bond between the hydrogen atom with the organic constituents such as nitrogen, oxygen, and fluorine (Brady, et al., 2000), essentially, hydrogen bonding also could be formed between the hydrogen atoms with the electronegative constituent such as chloride ions. In this case, the hydrogen atoms of complexing agent are attached to the chloride ions from ammonium based chloride compounds that relatively electronegative to form chloride ions complex. Since eutectic mixtures consist of nitrogen cations and complex anions so, when higher temperature was applied, these structures possible dissociated cations from anion relations owing to the larger size ratios thus, offered weak interactions, as a result increased degrees of freedom and amounts motion of nitrogen cations and complex anions. Apart from that, the reason we have chosen 1:2 mole ratio is when chloride compound or complexing agent are more or less than that composition the tendency to form

complex anions are low (Abbott, et al., 2003). Formation of hydrogen bonding between eutectic components in the eutectic mixtures has been shown in Figure 1.

In the pristine ammonium based chloride compounds phase, the interactions between cations and anions are generally stronger, which are normally held together by strong ionic bond. As a result, compounds in these structures tend to have higher melting points compared to the nitrogen cations and complex anions of the eutectic mixtures. The highest melting point is can be observed for eutectic mixture of ammonium chloride and urea which contained fully hydrogen atoms. Hence, nitrogen cations with the hydrogen atoms in the all side group causing the melting point slightly decreased to a value below its origin. Eutectic mixtures with ammonium based chloride compounds that consisted of methyl branches such as methanaminium chloride, dimethylammonium chloride, trimethylammonium chloride and tetramethylammonium chloride have significant results related to the melting point reduction compared with ammonium chloride. A completely unexpected observation can be seen for eutectic components of dodecyltrimethylammonium chloride and hexadecyltrimethylammonium chloride give important results, due to their melting points far away from individual components eventhough they have longest alkyl chains contrasted to tetramethylammonium chloride. While, with phenyl and benzyl functional group as can be seen on eutectic mixture of phenyltrimethylammonium chloride and benzyltrimethylammonium chloride with urea, respectively were demonstrating higher melting point than (vinylbenzyl)trimethylammonium chloride.

The melting points of these eutectic mixtures are dependent upon the interaction lattice energies of the ammonium based chloride compounds with complexing agent and the entropy changes arising from forming eutectics, therefore the reduction of melting point are measure of the entropy change (Abbott, et al., 2004). However, first it is important to relate the structure of the ammonium based chloride compounds to the melting points of the eutectic mixtures. The DSC results clearly show to relate to the differences of chemical structure between each eutectic mixture. In other words, the highest of the melting point may suggest the existence of inappropriate character of the functional groups in the nitrogen cations (Abbott, et al., 2001) in term of reducing the melting point. The appropriate functional groups of ammonium based chloride compounds will create the suitable eutectic components for preparation of low melting points eutectic mixtures.

In addition, melting points of eutectic mixtures also decrease with the larger more asymmetric nitrogen cations (Buzzeo, et al., 2004), which the highest melting points are observed with the more symmetric nitrogen cations. This may be a reason for the highest melting points of eutectic components such as ammonium chloride and tetramethylammonium chloride also the lowest melting points of dimethylammonium chloride and hexadecyltrimethylammonium chloride. On the other hand, in comparison with phenyl and benzyl functional group, the lower melting point is observed for (vinylbenzyl)trimethylammonium chloride, possibly due to the larger size of nitrogen cations providing greater asymmetry. Based on this study, the order of melting point reduction for varying functional groups for the ammonium based chloride compounds has been shown in Figure 2.

4. Conclusions

This study was indicated that eutectic mixtures were successfully produced by using ammonium based chloride compounds and complexing agent specifically urea. Based on these results, it is clear that ammonium based chloride compounds can undergo reactions with the urea through complexation reaction. The most important and intriguing discovery from this research is the fact that the functional groups of ammonium based chloride compounds are necessarily have play an important role to influence the melting point. The order of melting point reduction for varying functional groups is hydrogen > alkyl > phenyl > benzyl > vinylbenzyl > fatty alkyl. Eutectic components should be having appropriate functional group that will not influence functionality of nitrogen cations so that can reduce melting points of eutectic mixtures to the lowest points. This information is regarded as the motivating finding that will be the most important for future studies involving complexation reaction therefore, could be useful for fundamental chemistry especially if wanted to generate low melting points of eutectic mixtures for developing advanced materials such as ionic liquids.

References

Abbott, A. P., Capper, G., Davies, D. L., Munro, H. L., Rasheed, R. K., & Tambyrajah, V. (2001). Preparation of novel, moisture-stable, Lewis-acidic ionic liquids containing quaternary ammonium salts with functional side chains. *Chemical Communications, 19*, 2010-2011.

Abbott, A. P., Capper, G., Davies, D. L., Rasheed, R. K., & Tambyrajah, V. (2003). Novel solvent properties of choline chloride/urea mixtures. *Chemical Communications, 1*, 70-71.

Abbott, A .P., Boothby, D., Capper, G., Davies, D. L., & Rasheed, R. K. (2004). Deep Eutectic Solvents Formed between Choline Chloride and Carboxylic Acids: Versatile Alternatives to Ionic Liquids. *Journal of the American Chemical Society, 126*, 9142-9147.

Abbott, A. P., Capper, G., McKenzie, K. J., & Ryder, K. S. (2007). Electrodeposition of zinc-tin alloys from deep eutectic solvents based on choline chloride. *Journal of Electroanalytical Chemistry, 599*, 288-294.

Brady, J. E., Russel, J. W., & Holum, J. R. (2000). *Chemistry: Matter and Its changes.* New York, United States: John Wiley & Sons Inc. pp. 45-46.

Buzzeo, M. C., Evans, R. G., & Compton, R. G. (2004). Non-haloaluminate room-temperature ionic liquids in electrochemistry–a review. *European Journal of Chemical Physics and Physical Chemistry, 5*, 1106-1120.

Chen, N., Morikawa, J., & Hashimoto, T. (2005). Effect of cryoprotectans on eutectics of NaCl–$2H_2O$/ice and KCl/ice studied by temperature wave analysis and differential scanning calorimetry. *Thermochimica Acta, 431*, 106-112.

Ford, J. L., & Timmins, P. (1989). *Pharmaceutical Thermal Analysis - Techniques and Applications.* Chichester, England: Ellis Horwood. pp. 60-63.

Hou, Y., Gu, Y., Zhang, S., Yang, F., Ding, H., & Shan, Y. (2008). Novel binary eutectic mixtures based on imidazole. *Journal of Molecular Liquids, 143*, 154-159.

Kanchanomai, C., Miyashita, Y., & Mutoh, Y. (2002). Strain-rate effects on low cycle fatigue mechanisms of a eutectic Sn–Pb solder. *International Journal of Fatigue, 24*, 987-993.

Table 1. Physical appearances of eutectic mixtures at room temperature (25ºC)

Eutectic mixture	Appearance
ammonium chloride + urea	White solid
methanaminium chloride + urea	White solid
dimethylammonium chloride + urea	White solid
trimethylammonium chloride + urea	White solid
tetramethylammonium chloride + urea	White solid
dodecyltrimethylammonium chloride + urea	White solid
hexadecyltrimethylammonium chloride + urea	White solid
phenyltrimethylammonium chloride + urea	White solid
benzyltrimethylammonium chloride + urea	White solid
(vinylbenzyl)trimethylammonium chloride + urea	White solid

Table 2. Melting points of eutectic components as obtained from MSDS data

Eutectic component	Melting point, T_m (ºC)*
ammonium chloride	340
methanaminium chloride	229-233
dimethylammonium chloride	170-173
trimethylammonium chloride	283-284
tetramethylammonium chloride	>300
dodecyltrimethylammonium chloride	246
hexadecyltrimethylammonium chloride	232-237
phenyltrimethylammonium chloride	246-248
benzyltrimethylammonium chloride	239
(vinylbenzyl)trimethylammonium chloride	240
urea	132-135

* obtained from Sigma Aldrich

Table 3. Melting points of eutectic mixtures as determined from DSC data

Eutectic mixture	Melting point, T_m (ºC)
ammonium chloride + urea	286.51
methanaminium chloride + urea	210.28
dimethylammonium chloride + urea	123. 61
trimethylammonium chloride + urea	215.12
tetramethylammonium chloride + urea	240.06
dodecyltrimethylammonium chloride + urea	145.75
hexadecyltrimethylammonium chloride + urea	120.09
phenyltrimethylammonium chloride + urea	213.16
benzyltrimethylammonium chloride + urea	180.48
(vinylbenzyl)trimethylammonium chloride + urea	170.55
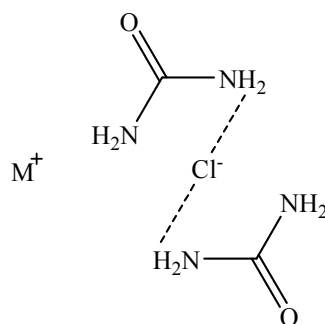
M^+ = ammonium based cation

Figure 1. Formation of hydrogen bonding between eutectic components in the eutectic mixtures
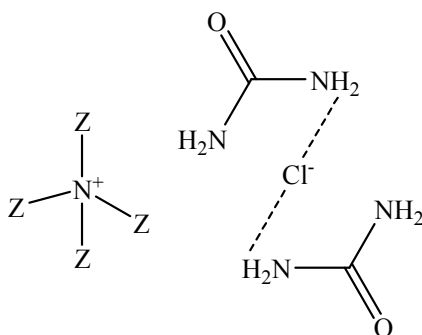
Z = hydrogen > alkyl > phenyl > benzyl > vinylbenzyl > fatty alkyl

Figure 2. The order of melting point reduction for varying functional groups

Effect of Gramicidin D on the Compressibility and Volume Fluctuations of DPPC – Peptide Bilayers: A Densitometry and Sound Velocimetry Study

Linus N. Okoro

American University of Nigeria

Yola, Nigeria

Tel: 234-805-604-8688　　　E-mail: linus.okoro@aun.edu.ng

Abstract

The effects of increasing gramicidin D (gD) concentration on the partial specific volume, v^o, and the adiabatic compressibility coefficient of the lipid, β_S^{lipid} of the bilayer reveals a continual decrease in v^o and β_S^{lipid} (within the range of concentration studied) with concentration, except between 5 and 7.5 %, where a very slight decrease was observed. At gD concentrations higher than 5 mol%, the isothermal compressibility coefficient, β_T^{lipid} is greater than β_S^{lipid} at the gel-fluid region by $\sim 10 - 20$ % in the entire temperature range covered. The maximum value of the relative volume fluctuation of 12 % is reached for DPPC at the main transition, and is strongly dampened upon addition of gD. A gradual decrease in the calculated relative volume fluctuations with gD concentration at T_m is observed between concentrations 1 and 10 mol%.

Keywords: Gramicidin D (gD), Phospholipid, DPPC, Pressure perturbation calorimetry, Ultrasound velocimetry, Densitometry, Fluctuations

1. Introduction

In 1939 the French-American microbiologist Rene Dubos isolated the substance tyrothricin and later showed that it was composed of two substances, gramicidin (20%) and tyrocidine (80%). These were the first antibiotics to be manufactured commercially. Gramicidin is a heterogeneous mixture of antibiotic compounds, Gramicidins A, B and C, making up 80%, 6%, and 14% respectively [Bourinbaiar 1997], all of which are obtained from the soil bacterial species *Bacillus brevis* and called collectively Gramicidin D. Gramicidin D are linear pentadecapeptides; that is chains made up of 15 amino acids [Burkhart, 1999]. This is in contrast to gramicidin S, which has a cyclic peptide chain. Gramicidin is active against Gram-positive bacteria, except for the Gram-positive bacilli, and against selected Gram-negative organisms, such as Neisseria bacteria.

Gramicidin has the general formula: formyl-L-**X**-Gly-L-Ala-D-Leu-L-Ala-D-Val-L-Val-D-Val-L-Trp-D-Leu-L-**Y**-D-Leu-L-Trp-D-Leu-L-Trp-ethanola mine. X and Y depend upon the gramicidin molecule. There exists valine and isoleucine variants of all three gramicidin species and 'X' can be either valine or isoleucine. Y determines which is which; in the place of Y, Gramicidin A contains Tryptophan, B contains Phenylalanine and C contains Tyrosine. The alternating stereochemical configurations (in the form of D and L) of the amino acids is vital to the formation of the β-helix. The chain assembles inside of the hydrophobic interior of the cellular lipid bilayer to form a β-helix. The helix itself is not long enough to span the membrane but it dimerises to form the elongated channel needed to span the whole membrane.

1.1 Lipid – Gramicidin Interaction

The primary interest of gramicidin lies in its ability to form ion channels in lipid membranes. Gramicidin has been reported to form specific channels across the cell membrane and to enhance the transport of cations [Woolf 1994]. Gramicidin has no charged or hydrophilic side chains, and its aqeous solubility is low. As both the amino and carboxy termini of the molecule is blocked, gramicidin has been found to partition strongly into the hydrophobic region of phospholipid membranes and to maintain the liquid - crystalline state [Short 1987, Glowka 2005]. Extensive studies have been made on the influence of gramicidin on lipid polymorphism and of the ordering effects on the lipid chains [Killian 1992, Rice 1979, Kharakoz 1993, Szule 2003]. Gramicidin S has been found to progressively decrease the phase transition of DMPC vesicles as well as to decrease the degree of cooperativity of the main phase transition and to increase the volume compressibility of the vesicles [Krivanek 2001, Lewis 1999].

The PFG-NMR method has been used in microscopically oriented bilayers to investigate the effect of the Gramicidin D on the lateral diffusion of DMPC [Orädd 2004]. No evidence of linear aggregate of gramicidin in the gel phase was found. Aggregation of gramicidin A in phospholipids has been reported [Ivanova 2003].

It has equally been observed that gramicidin insertion into the DMPC bilayer structure has significant influence on the lipid bilayer structure and temperature, pressure phase behaviour [Zein 2000, Eisenblätter 2006]. Further, the interaction between integral proteins and lipids has been found to depend on the relative length of their hydrophobic core, a concept known as the 'hydrophobic matching' (Woolf 1996). Gramicidin modulates the spontaneous curvature properties of the phospholipid assemblies [Szule 2003]. The effect of gramicidin D on the conductance and electroporation thresholds of planar bilayer membranes has been examined and was found to change their mechanical properties [Troiano 1999]. It has been shown as well, that the presence of peptide or proteins in the membrane can significantly affect the dynamic structure of the bulk lipid [Ge 1994].

The goal of this study is to incorporate different gramicidin D concentrations into DPPC bilayer, and to determine the effects of increasing concentrations of gramicidin D on the lipid bilayer membrane compressibility and volume fluctuations in their different transition phases. To this end, molecular acoustics (ultrasound velocimetry and densitometry) was utilized at varying significant gramicidin D concentrations. This is the first time the two methods could be employed simultaneously for the study of DPPC – gramicidin D interactions, to the best of my knowledge. This study has been able to reveal a considerable influence of gramicidin D on the mechanical, volume and compressibility properties of DPPC bilayer.

2. Materials and methods

2.1 Sample Preparation

1,2-Dipalmitoyl-3-*sn*-phosphatidylcholine (DPPC) was purchased from Avanti Polar Lipids (Alabaster, AL, USA), while Gramicidin D as a lyophilized solid was obtained from Sigma-Aldrich. Both were used without further purification. Multilamellar vesicles (MLV) of DPPC and melittin with designated mole ratios were mixed in chloroform-methanol mixture (3:1 v/v) and dried as a thin film under a stream of nitrogen and then freeze-dried in a freeze-dryer (Christ, Osterode, Germany) under high vacuum overnight. The lipid films were hydrated in a Tris buffer (10 mM Tris-HCl, 100 mM NaCl, pH 7.4), followed by vortexing at ~60°C (above the main phase transition temperature, T_m, of DPPC (~41.5°C [Cevc 1987, Okoro 2008], and five freeze-thaw cycles, resulting in homogeneous multilamellar vesicles (MLVs). Large unilamellar vesicles (LUVs) of uniform shape and size used in the ultrasound velocity and the density measurements were prepared from the MLVs by extrusion [MacDonald 1991] using a Mini-Extruder (Avanti Polar Lipids Inc., Alabaster, AL, USA), and passing them through 100 nm Nuclepore® Polycarbonate Track-Etch™ Membranes (Whatman GmbH, Dassel, Germany) at ~60°C. The final DPPC concentration used in the ultrasound velocity and the density measurements was 5 mg/mL.

2.2 Ultrasound velocity and density measurements

The ultrasound velocity u of the vesicles was determined simultaneously using a differential ultrasonic resonator device ResoScan (TF Instruments, Heidelberg, Germany, operating in a frequency range of 7.2 – 8.5 MHz. [Eggers 1969, Eggers 1973, Stuehr 1965].

Ultrasonic measurements are extremely sensitive to temperature changes. Reproducibility and accuracy is therefore crucially dependent on TFI's Ultra-high Precision Peltier-Thermostat that reaches temperature constancy better than 1 mK (0,001 °C), and features a fast heating, cooling and equilibration time between 5 and 85 °C.

The sound velocity of the lipid dispersion was determined relative to that in the buffer solution at the same temperature in terms of the velocity number, $[u]$, defined as [Stuehr 1965].

$$[u] = (u - u_0)/u_0 c \tag{1}$$

Where u and u_0 denote the sound velocity in the solution and in the solvent, respectively, and c is the solute concentration in mol/L.

The densities, ρ and ρ_0, of the lipid solution and the solvent, respectively were measured by a high-precision density meter DMA 5000 (Anton Paar, Graz, Austria) based on the mechanical oscillator principle [Kratky 1973], corrected for viscosity-induced errors.

The partial molar volume, V^0, of the lipid is evaluated from the density data by the given relation:

$$V^\circ = \left(\frac{\partial V}{\partial n}\right) \cong \frac{M}{\rho_0} - \frac{\rho - \rho_0}{\rho_0 c} \tag{2}$$

Where V is the volume, n the number of solute molecules in moles, and M is the molar mass of the solute. The very right term is valid only for diluted lipid suspensions as used in this study.

The adiabatic compressibility coefficient, $\beta_S = -1/V\,(\partial V/\partial p)_S$ (V, p and S are the volume, the pressure and entropy, respectively), the speed of sound propagation, u, in the medium, and the density, ρ are related by the expression:

$$\beta_S = 1/\,u^2\,\rho \tag{3}$$

In molecular acoustics, due to the additivity of all components of the system, the partial molar adiabatic compressibility, K_S^{o}, is generally used, which is given by;

$$K_S^{\mathrm{o}} = \left(\frac{\partial K_S}{\partial n}\right) = \left(\frac{\partial V^{\mathrm{o}}}{\partial p}\right)_S \cong \beta_{S,0}\left(2\left(V^{\mathrm{o}} - [u]\right) - \frac{M}{\rho_0}\right), \tag{4}$$

where $K_S = \beta_S V$ is the adiabatic compressibility and $\beta_{S,0}$ is the adiabatic compressibility coefficient of the solvent. By dividing the partial molar quantities V^{o} and K_S^{o} by the molar mass of the solute we obtain the partial specific values, i.e., the partial specific volume, v^{o}, and the partial specific adiabatic compressibility, k_S^{o}. Accordingly, the concentration, c, in Eq. 1 becomes c/M, which is then expressed in mg/mL.

The sound velocity was determined with a relative error better than 10^{-3} %, corresponding to a precision higher than 5×10^{-5} mL/g in $[u]$. The density values were measured with relative error smaller than 10^{-3} %, so the accuracy in v^{o} is better than 10^{-4} mL/g. Therefore, considering the relative errors of $[u]$ and v^{o}, the certainty in k_S^{o} taken from Eq. 4 is within 10^{-12} mL/gPa. In both methods, the corresponding values were measured at discrete temperatures (read with an accuracy of 10^{-3} °C), resulting in an average temperature scan rate of ~12 °C/h.

The adiabatic compressibility of the lipids, β_S^{lipid}, is defined as

$$\beta_S^{\mathrm{lipid}} = -\frac{1}{v^{\mathrm{o}}}\left(\frac{\partial v^{\mathrm{o}}}{\partial p}\right)_S \tag{5}$$

which is related to the partial specific adiabatic compressibility, k_S^{o}, by

$$k_S^{\mathrm{o}} = v^{\mathrm{o}}\,\beta_S^{\mathrm{lipid}} \tag{6}$$

β_S^{lipid} can thus be directly obtained from combined ultrasound velocity and density measurements.

Lipid bilayer thermotropic main phase transitions are considered to be of weak first-order, i.e., they show typical features of first-order phase transitions, such as abrupt changes in specific volume or a peak in the enthalpy and entropy, but also significant fluctuations in volume and lamellar d-spacing, which are typical for a second-order phase transition. The isothermal compressibility, K_T, is directly proportional to the volume fluctuations of the system [Wilson 1957, Hill 1960]. In a system exhibiting a first-order transition, K_T diverges at the phase transition temperature, whereas it exhibits a power-law behavior ($K_T \propto |T\text{-}T_c|^{-\gamma}$), with a particular critical exponent ($\gamma = 1.24$ for 3D systems) in the critical-point region of a second-order phase transition [Stanley 1971, Winter 1999]. By the ultrasound velocity and the density measurements, however, only the adiabatic compressibility, K_S, can be determined (see Eqn. 3 and 4). The isothermal compressibility can be calculated from [Hill 1960]

$$K_T = K_S\,\frac{C_p}{C_V} \tag{7}$$

where C_p and C_V are the heat capacities at constant pressure and volume, respectively, which, using Maxwell relations, can also be expressed as

$$K_T = K_S + \frac{T}{C_p}\left(\frac{\partial V}{\partial T}\right)_p^2 = K_S + \frac{TE^2}{C_p} \tag{8}$$

with the thermal expansion $E = (\partial V/\partial T)_p$. Hence, the isothermal compressibility can be obtained from the adiabatic one when the thermal expansion and the heat capacity data are available. Differentiating Eqn. 8 yields the exact differential of K_T, dK_T, which is given as:

$$dK_T = dK_S + \frac{E^2}{C_p} dT + 2\frac{TE}{C_p} dE - \frac{TE^2}{C_p^2} dC_p \tag{9}$$

For convenience, Eqn. 8 is adapted through Eqn. 9 by thermodynamic treatment to a form where the corresponding partial specific quantities are taken [Chalikian 2003]:

$$k_T^\circ = k_S^\circ + \frac{T\alpha_0^2}{\rho_0 c_{p,0}}\left(2\frac{e^\circ}{\alpha_0} - \frac{C_p^\circ}{\rho_0 c_{p,0}}\right) \tag{10}$$

k_T° is the partial specific isothermal compressibility, α_0 ($\alpha = E/V$) and $c_{p,0}$ are the thermal expansion coefficient and the specific heat capacity of the solvent, respectively; e° and C_p° are the partial specific expansivity and the partial specific heat capacity of the lipid, respectively; the latter is given by [Privalov 1980]

$$C_p^\circ = \frac{\Delta C_p}{m} + \frac{v^\circ}{v_0^\circ} c_{p,0} \tag{11}$$

where m is the mass of the solute.

The corresponding isothermal compressibility of the lipid, $\beta_T^{\text{lipid}} = k_T^\circ/v^\circ$ (note that β_T^{lipid} differs from the partial specific isothermal compressibility coefficient, β_T°, which is defined as $\beta_T^\circ = 1/M\ (\partial\beta_T/\partial n) = \beta_T\ v^\circ/V$), can be obtained from Eqn. 10 and is given as:

$$\beta_T^{\text{lipid}} = \beta_S^{\text{lipid}} + \frac{T\alpha_0^2}{v^\circ \rho_0 c_{p,0}}\left(2\frac{e^\circ}{\alpha_0} - \frac{C_p^\circ}{\rho_0 c_{p,0}}\right) \tag{12}$$

For simplification, we denote in Eqn. 12 the second and third term as β_e^{lipid}, and β_C^{lipid}, respectively:

$$\beta_T^{\text{lipid}} = \beta_S^{\text{lipid}} + \beta_e^{\text{lipid}} - \beta_C^{\text{lipid}} \tag{13}$$

Hence, the isothermal compressibility coefficient, β_T^{lipid}, is given as a sum of the adiabatic compressibility, β_S^{lipid}, an expansion term, β_e^{lipid}, and a heat capacity term, β_C^{lipid}. Interestingly, as can be seen from Eqs. 10 and 12, the heat capacity term has a compensating effect, balancing that of the thermal expansion on the adiabatic compressibility.

The thermodynamic parameters C_p, K_T and E are directly related to corresponding fluctuation parameters [Cooper 1984]: i) the square average of the enthalpy fluctuations, its variance, $\langle\Delta H^2\rangle$, is determined by the heat capacity, C_p, of the system, ii) the square average of the volume fluctuations $\langle\Delta V^2\rangle$ as given by the respective isothermal compressibility, K_T, and iii) the covariance between H and V, $\langle\Delta H\,\Delta V\rangle$, is related to the thermal expansion, E:

$$\langle\Delta H^2\rangle = RT^2 C_p \tag{14a}$$

$$\langle\Delta V^2\rangle = RTK_T \tag{14b}$$

$$\langle\Delta H\,\Delta V\rangle = RT^2 E = RT^2 V\alpha \tag{14c}$$

As seen from Eqn. 14c, the thermal expansion couples contributions from the heat capacity and the isothermal compressibility.

3. Results and discussion

3.1 Ultrasound and density measurements on DPPC – gramicidin D (gD) mixtures

The determination of mechanical parameters of DPPC – gD is crucial for an evaluation of the size of distorted membrane structure around proteins or peptides (Hianik 1995). Figure 1a shows the temperature dependent velocity number [u] for the DPPC – gramicidin mixtures. At points distant from the lipid main phase transition temperature, T_m, [u], a gradual decrease of [u] with rise in temperature is observed, leading to the typical anomalous dip (Mitaku 1978, Kharakoz 1993, Schrader 2002, Krivanek 2008) in the vicinity of T_m for pure lipids. The lowest value of [u] at T_m is ~-0.15mL/g for pure DPPC, which is consistent with Mitaku and co-workers data (Mitaku 1978). It should be

noted, however, that the size and the width of the dip in [u] depends on the sample preparation [Mitaku 1978], which is related to the different degree of cooperativity of the main phase transition, on the lipid concentration [Kharakoz 1993], and on the ultrasound frequency applied for the measurement itself [Mitaku 1982], which is related to the heat exchange within the period of the sound wave [Osdol 1989, Heimburg 1996]. The dip in the ultrasonic number profiles will be more pronounced at lower frequencies, because C_p assumes higher values, leading to an increase of the adiabatic compressibility at lower frequencies. The frequency dependence of the ultrasonic absorption coefficient of DPPC suspensions has been measured. The excess absorption data has been described by a relaxation term with a discrete relaxation time, displaying some evidence of critical slowing down near the phase transition [Heimburg 1996].

In addition, inadequately high temperature scan rates might induce a slight shift in the dip minimum position toward higher temperatures [Kaatze 2006], since lipid bilayers are not able to thermally equilibrate rapidly due to molecular processes slowing down during the main phase transition.

Addition of 1 mol% gramicidin produced a significant change in [u], and a peak broadening is observed leading to a comparatively increased [u] at T_m with a dip of ~-0.1mL/g. The dip continues to decrease with increase in gramicidin concentration, with the highest value and broadest peak at 10 mol%. In the gel phase, in general, we observe that [u] is smaller below T_m and larger above T_m for both DPPC – gramicidin mixtures than for the pure DPPC LUVs. In addition, for the DPPC – gramicidin mixtures in the gel phase, there is no clearly defined trend in [u] unlike in the transition region. It is of interest to note that the minimum in the [u] value generally reflects effects from changes in heat capacity, C_p, [u] and the isothermal compressibility β_T upon approaching Tm.

The temperature dependence of the partial specific volume, ν^o, is shown in figure 1b. An increase of ν^o with temperature is observed throughout the whole melting transition regime. A step-like change at the transition temperature T_m is observed for pure DPPC and for DPPC – gramicidin concentrations of 1 and 2.5 mol%. Changes in [u] and ν^o with increase in gramicidin concentration are clearly observed at T_m and above the T_m region indicating, increased volume fluctuations in this temperature region. The $\Delta\nu^o$ for pure DPPC at the gel/fluid transition was found to be ~0.045, which corresponds to an ~4% bilayer volume increase. The partial specific volume ν^o is larger below T_m and smaller above T_m for the DPPC – gramicidin mixtures, similar to the behavior of [u].

The partial specific adiabatic compressibility, k_S^o, has been determined from equation 6. Figure 2a gives the temperature dependence of k_S^o for the DPPC – gramicidin mixtures. As expected, the k_S^o for pure DPPC has the highest value increasing from 2.35 mL/gPa at 10 ^{o}C and abruptly reaching 5.5 mL/gPa (57%) at T_m. It shows a slight drop right beyond T_m, and finally continues to increase with increasing temperature to reach its maximum value of 6.3 mL/gPa at 80 ^{o}C.

Generally, a significant broadening of the transition peak, a shift to lower temperatures and a decrease of k_S^o in the lipid melting transition region with increasing gD concentration was observed. Increase in compressibility of the lipid vesicle with increasing gramicidin concentration below T_m suggests a decrease in the lipid bilayer order. The opposite holds true for $T > T_m$, where k_S^o decreases with increasing gD concentration.

The temperature dependence of β_S^{lipid} for the DPPC – gD mixtures is displayed in figure 2b. As can be seen it has the same shape as k_S^o (Eqn. 10), which includes the anomalous peak at the main phase transition.

At 25 and 60 ^{o}C, β_S^{lipid} for pure DPPC is 3.2 x 10^{-10} Pa^{-1} and 5.6 x 10^{-10} Pa^{-1}, respectively. The value for β_S^{lipid} of 3.4×10^{-10} Pa^{-1} at 30 °C is in good agreement with β_S^{lipid} = 3.5×10^{-10} Pa^{-1} obtained by Mitaku and coworkers (Mitaku 1978), but 5.3×10^{-10} Pa^{-1} at 50 °C is higher compared to the literature value of 4.6×10^{-10} Pa^{-1}, which might be due to different vesicle preparations (LUV in our study and MLV in the reference mentioned (Mitaku 1978)). Also for k_S^o, the anomalous increase of β_S^{lipid} around T_m is still significant at 1 and 2.5 mol% of gD and markedly diminishes for higher gD concentrations.

A summary of the effects of increasing gramicidin concentration on ν^o and β_S^{lipid} of the bilayer at 25 and 60°C is shown in figures 3a & 3b, respectively. The data reveal a continuous decrease in ν^o and β_S^{lipid} with gD concentration in the fluid phase (except between 5 and 7.5%, where we observe only a very slight decrease) and a slight increase with concentration in the gel phase. The increase of β_S^{lipid} with increasing gD concentration, in the gel phase probably reflects the disordering effect which gD imposes on ordered phospholipid bilayers in this phase region. The data thus clearly show that incorporation of gD also drastically changes the temperature-dependent gel phase behavior of DPPC. It has been reported that incorporation of gD leads to a decrease of the molecular order of the acyl chains in the gel phases, whereas in the fluid phase, the mean order parameter increases (Eisenblätter 2006). Incorporation of gD into fluid-like DPPC has been shown to have a significant rigidifying effect on the conformational order in a cooperative manner along the entire acyl chain. Furthermore, it can be seen that, as

expected, both v^o and β_S^{lipid} generally increase with increasing temperature, and the slope of $\beta_S^{\text{lipid}}(T)$ decreases with increase in gD concentration.

3.2 Isothermal Compressibility and Volume fluctuations of DPPC – gD mixtures

Figure 4a displays the temperature dependences of the isothermal compressibility of DPPC-gD LUVs at different gD concentrations. We observed that the isothermal compressibility peak at the main transition drops drastically (~ 75 %) upon addition of gramicidin concentrations as low as 1 mol%. This decrease in β_T^{lipid} corresponds to a similar strong decrease (80 %) of the thermal expansion coefficient, indicating the close relationship between the corresponding fluctuations ($\langle \Delta V^2 \rangle$ *vs.* $\langle \Delta H \Delta V \rangle$) (Krivanek 2008).

Between 1 and 10 mol% gD, only a slight decrease in β_T^{lipid} at the main transition region with increasing gD concentration is observed, and almost no change between 5 and 7.5 mol%, as already observed in β_S^{lipid}. At gD concentrations higher than 5 mol%, β_T^{lipid} is greater than β_S^{lipid} at the gel-fluid region by ~ 10 - 20% in the whole temperature range covered. Significant differences in β_T^{lipid} and β_S^{lipid} are seen in the gel and fluid phases of the lipid bilayer, as the solvent and lipid membranes are adiabatically uncoupled in the MHz region in the ultrasound experiment. These differences become dramatic in the gel-fluid transition region, indicating a significant degree of slow relaxational processes in the   s time range in the transition region. β_T^{lipid} in both the gel phase (25 ^{o}C) and in the fluid phase (60 ^{o}C) of the DPPC-gD mixtures between 1 and 10 mol% reveal continuous increase with increase in gD concentration (Fig. 5a). Above the main transition, at 60 ^{o}C, only the β_T^{lipid} value of 10 mol% gramicidin surpasses the value for pure DPPC.

Given that the partial specific volume, vo, is largely determined by the lipid term (Eqn. 2), which reflects the "real" volume of the lipid molecule, Eqn. 3 can be modified to convey the relative volume fluctuations as

$$\sqrt{\frac{\langle \Delta V^2 \rangle}{V^2}} = \sqrt{\frac{RT\beta_T^{\text{lipid}}}{Mv^o}} \tag{15}$$

Fig. 4b displays the calculated temperature dependence of the relative volume fluctuations for the DPPC-gD mixtures. The figure clearly shows that the relative volume fluctuations of pure DPPC are drastically increased at the main transition, reaching up to 12 %, and are strongly damped upon addition of gramicidin D to 2.6% at 10 mol% gD. Furthermore, the volume fluctuations in both the gel phase (25 ^{o}C) and in the fluid phase (60 ^{o}C) reveal a continuous and gradual increase with increase in gD concentration between 1 and 10 mol% (Fig. 5b). Again, it can be clearly seen that the volume fluctuations are larger in the fluid phase than in the gel phase.

3.3 Conclusion

In this work, the isothermal compressibility and the volume fluctuations of DPPC – gramicidin bilayer membranes in their different phases was determined by using molecular acoustics (ultrasound velocity and densitometry). The effect of increasing gramicidin concentration on v^o and β_S^{lipid} of the bilayer at T_m region has revealed a continuous decrease in v^o and β_S^{lipid} (within the range of concentrations studied) with increase in gD concentration except between 5 and 7.5 %, where only a very slight decrease was observed. Another observation was that the isothermal compressibility peak at the main transition drops drastically (~75%) upon addition of gramicidin concentrations as low as 1 mol%. In addition, at gD concentrations higher than 5 mol%, it was found that β_T^{lipid} is greater than β_S^{lipid} in the gel-fluid coexistence region by 10 – 20 % in the whole temperature range covered.

The maximum value of the relative volume fluctuation of 12 % is reached for pure DPPC at the main transition, and is strongly damped upon addition of gD. A gradual decrease in the calculated relative volume fluctuations with gD concentration at T_m is observed between concentrations 1 and 10 mol%.

References

Bourinbaiar, A. S., & C. F. Coleman. (1997). The effect of gramicidin, a topical contraceptive and antimicrobial agent with anti-HIV activity, against herpes simplex viruses type 1 and 2 in vitro. *Arch Virol,* 142, 2225-2235.

Burkhart, B. M. (1999). Gramicidin D conformation, dynamics and membrane ion transport. *Biopolymers,* 51, 129-144.

Cevc, G., & Marsh D. (1987). *Phospholipid Bilayers*, John Wiley and Sons, New York.

Chalikian, T. V. (2003). Volumetric Properties of Proteins. *Annu. Rev. Biophys. Biomol. Struct,* 32, 207-235.

Cooper, A., (1984). Protein fluctuations and the thermodynamic uncertainty principle. *Prog. Biophys. Molec. Biol.,* 44, 181-214.

Eggers, F., & Kustin K. (1969). Ultrasonic methods. *Methods Enzymol*, 16, 55-80.

Eggers, F., & Funk T. (1973). Ultrasonic measurements with millilitre liquid sample in the 0.5 − 100 MHz range. *Rev. Sci. Instr*, 44, 969-978.

Eisenblätter, J., & Winter R. (2006). Pressure effects on the structure and phase behaviour of DMPC-Gramicidin lipid bilayers: A synchrotron SAXS and ^{2}H-Nmr spectroscopy study. *Biophys. J.*, 90, 956-966.

Ge, M. T., & Freed J.H. (1999). Electron spin resonance study of aggregation of gramicidin in dipalmitoylphosphatidylcholine bilayers and hydrophobic mismatch. *Biophys. J.*, 76, 264-280.

Glowka, M. L., Olzzak, A. Bojarska, J., Szczesio, M., Duax, W.L., Burkhart, B.M., Pangborn, W.A., Langs, D.A., & Wawrzak, Z. (2005). Structure of gramicidin D-Rbcl complex at atomic resolution from low–temperature synchrotron data: interactions of double-stranded gramicidin channel contents and cations with channel wall. *Biological crystallography,* 61, 433-441.

Heimburg, T. & Marsh D. (1996). Thermodynamics of the interaction of proteins with lipid membranes. *In* Biological Membranes: *A Molecular Perspective from Computation and Experiment.* K. M. Merz, and B. Roux. editors. Birkhauser, Boston. 405-462.

Hianik, T. & Passechnik V.I. (1995). Bilayer Lipid Membranes: *Structure and Mechanical Properties*, Kluwer Academic, Dordrecht/ Boston/London.

Hill, T. L. (1960). *An Introduction to Statistical Thermodynamics*. Dover, New York.

Ivanova, V. P., Makarou, I.M., Schäffer, T.E., Heimburg T. (2003). Analysis, heat capacity profile of peptide containing membranes cluster formation of gramicidin A. *Biophys. J.*, 84, 2427-2439.

Kaatze, U., O'Driscoll, B., Hanke, E., Jäger, M & Buckin V. (2006). Ultrasonic calorimetry of membranes. *Pharmaceutical Technology Europe,* 1-5.

Kharakoz, D. P., Colotto, A., Loher, K., & Laggner, P. (1993). Fluid-gel interphase line tension and density fluctuations in dipalmitoylphosphatidylcholine multilamellar vesicles: an ultrasonic study. *J. Phys. Chem.*, 97, 9844-9851.

Killian, J. A. (1992). Gramicidin and gramicidin-lipid interactions. *Biochim Biophys. Acta*, 1113, 391-425.

Kratky, O., Leopold H., & Stabinger H. (1973). The determination of partial specific volume of protein by the mechanical oscillator technique. *Methods Enzymol*, 27, 98-110.

Krivanek, R., Rybar P., Prenner, E.J & McElhaney R.E. (2001). Interaction of the antimicrobial peptide gramicidin S with dimyristoyl-phoshatidyl choline bilayer membranes: A densitometry and sound velocimetry study *Biochim. Biophys. Acta,* 1510, 452-463.

Krivanek, R., Okoro, L., & Winter, R. (2008). Effect of cholesterol and ergosterol on the compressibility and volume fluctuations of phospholipid-sterol bilayers in the critical point region − A molecular acoustic and calorimetric study. *Biophys. J.*, 94, 3538-3548.

Lewis, R. N. A. H., Prenner, E.J., Kondejewski, L.H., Flash C.R., Mendelsohn, R., Hodges, R.S., & McElhaney, R.N. (1999). Fourier transform infrared spectroscopic studies of the interaction of Antimicrobial peptide Gramicidin S with micelles and with lipid monolayer and bilayer membranes. *Biochemistry.* 38, 15193-15203.

MacDonald, R. C., MacDonald, R.I., Menco, B.P.M., Takeshita, K., Subbarao, N.K., & Hu, L.R. (1991). Small-volume extrusion apparatus for preparation of large unilamellar vesicles. *Biochim. Biophys. Acta.* 1061, 297-303.

Mitaku, S., Ikegami, A & Sakanishi, A. (1978). Ultrasonic studies of lipid bilayer phase transition in synthetic phosphatidylcholine liposomes. *Biophys. Chem*, 8, 295-304.

Mitaku, S., & Data, T. (1982). Anomalies of nanosecond ultrasonic relaxation in the lipid bilayer transition. *Biophys. Biochim. Acta*, 688, 411-421.

Orädd, G., & Lindblom, G. (2004). Nmr studies of lipid lateral diffusion in the DMPC/gramicidin D/water system: peptide aggregation and obstruction effects. *Biophys. J.*, 87, 980-987.

Okoro, L., & Winter, R. (2008). Pressure Perturbation Calorimetric Studies on Phospholipid-Sterol Mixtures. *Z. Naturforsch,* 63b, 769-778.

Osdol, V. W. W., Biltonen, R.L., & Johnson, M.L. (1989). Measuring the kinetics of membrane phase transition. *J. Bioenerg. Biophys. Methods*, 20, 1-46.

Privalov, P. L. (1980). Scanning microcalorimeters for studying macromolecules. *Pure Appl. Chem*., 52, 479-497.

Rice, D. & Oldfield, E. (1979). Deuterium nuclear magnetic resonance studies of the interaction between dimyristoylphosphatidylcholine and gramicidin A. *Biochemistry*, 18, 3272-3279.

Schrader, W., Ebel, H., Grabitz, P., Hanke, E., Heimburg, T., Hoeckel, M., Kahle, M., Wente, F., & Kaatze, U. (2002). Compressibility of Lipid mixtures studied by calorimetry and ultrasonic velocity measurements. *J. Phys. Chem*, 106, 6581-6586.

Short, K. W., Wallace, B.A., Myers, R.A., Fodor, S.P.A., & Dunker, A.K. (1987). Comparison of lipid/gramicidin dispersion and co-crystals by Roman scattering. *Biochemistry*, 26, 557-562.

Stanley, H. E. (1971). *Introduction to Phase Transitions and Critical Phenomena*. Oxford University Press, NY.

Stuehr, J., & Yeager, E. (1965). The Propagation of Sound in Electrolytic Solutions. *In Physical Acoustics*. Vol. 2A. W. P. Mason. editor. Academic Press, NY.

Szule, J. A., & Rand, R.P. (2003). The effects of gramicidin on the structure of phospholipid assemblies. *Biophys. J.*, 85, 1702-1712.

Troiano, G. C., Stebe, K.J., Raphael, R.M., & Tung, L. (1999). The effects of gramicidin on electroporation of lipid bilayers. *Biophys. J.*, 76, 3150-3157.

Wilson, A. H. (1957). *Thermodynamics and statistical mechanics*. Cambridge University Press, Cambridge.

Winter, R., Gabke, A., Czeslik,C., & Pfeifer, P. (1999). Power-law fluctuations in phase-separated lipid membranes. *Phys. Rev.,* E. 60, 7354-7359.

Woolf, T. B. & Roux, B. (1994). Molecular dynamic simulations of the gramicidin channel in a phospholipid bilayer. *Proc. Natl. Acad. Sci., USA*. 91, 11631-11635.

Woolf, T. B. & Roux, B. (1996). Structure, energetics and dynamics of lipid-protein interactions: a molecular dynamics study of the gramicidin A channel in a DMPC bilayer. *Proteins,* 24, 92-114.

Zein, M. & Winter, R. (2000). Effect of temperature, pressure and lipid acyl-chain length on the structure and phase behaviour of phospholipid-gramicidin Bilayers", *Phys. Chem. Chem. Phys.,* 2, 4545-4551.
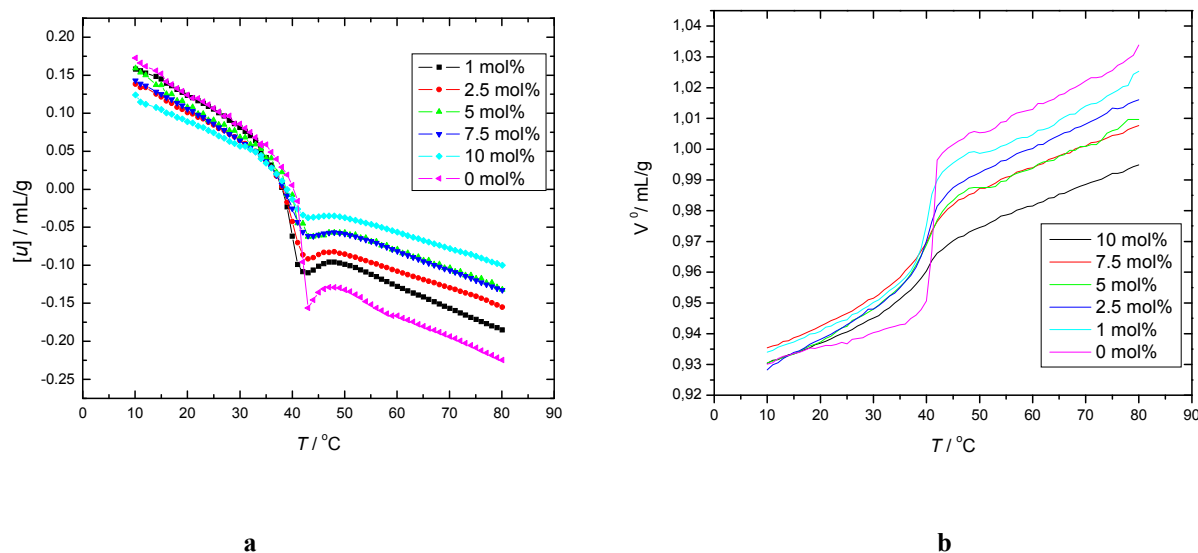
a   b

Figure 1. a) The temperature dependence of the ultrasound velocity number, [*u*], for DPPC – gD mixtures. b) The temperature dependence of the partial specific volume, *v*o, for DPPC – gD mixtures
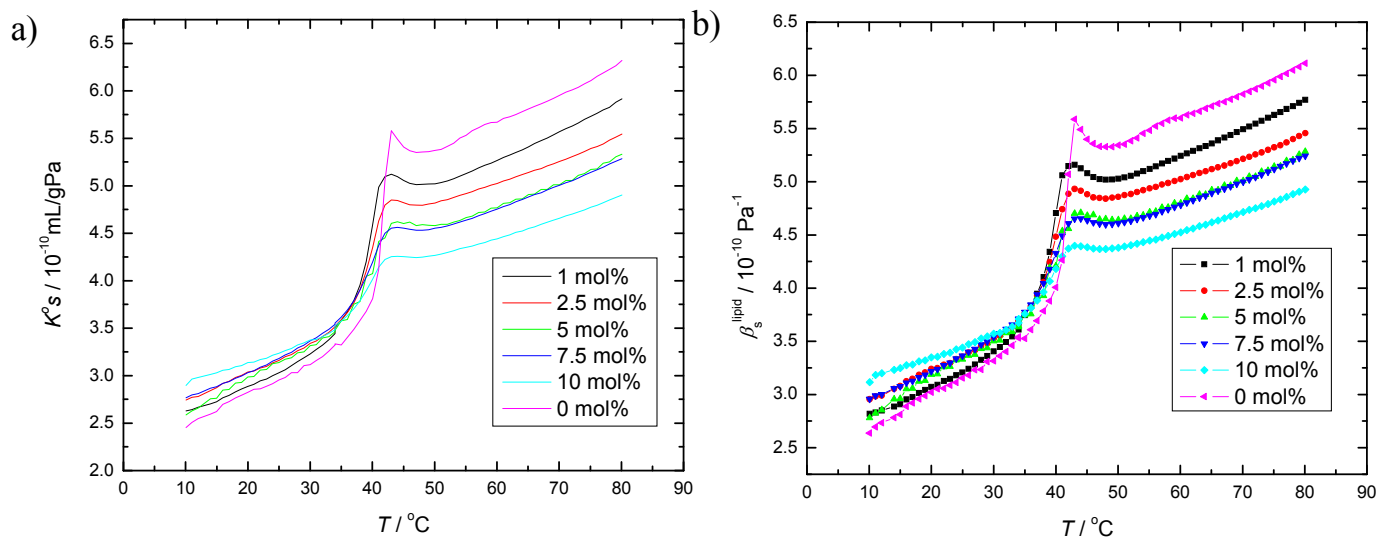
Figure 2. a) The temperature dependence of the partial specific adiabatic compressibility, k_S^o, of DPPC-gramicidin mixtures at different gramicidin mole fractions, X_{gD} and (**b**) the adiabatic compressibility coefficient, β_S^{lipid}, of DPPC LUVs at various gramicidin mole fractions
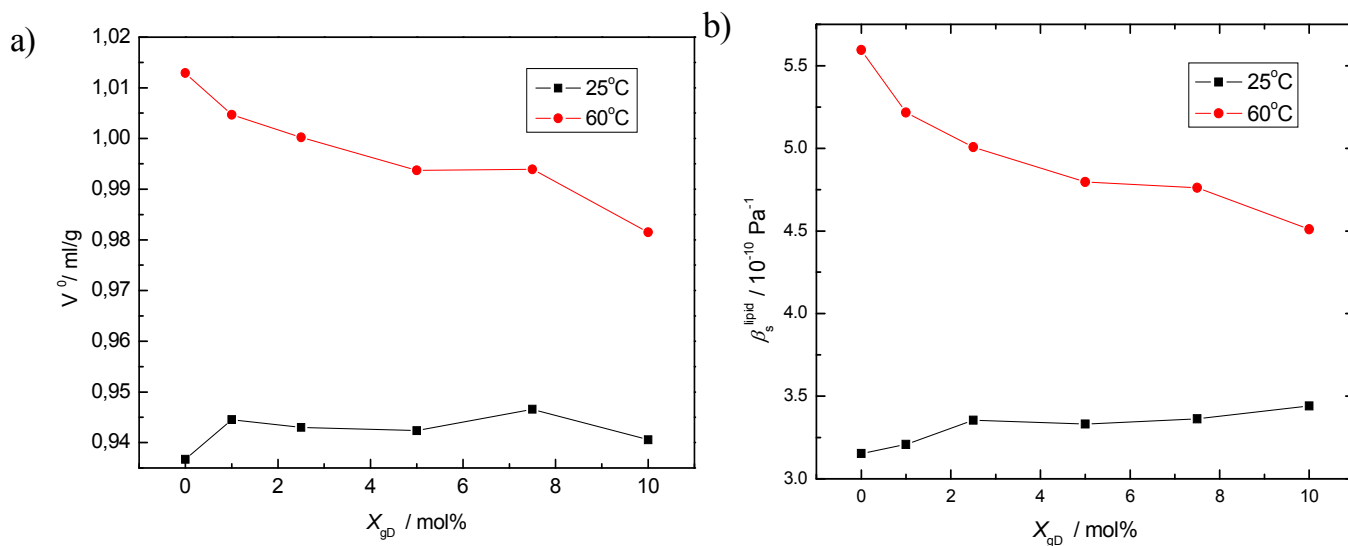

Figure 3. a) The partial specific volume and (b) the adiabatic compressibility coefficient of DPPC-gD mixtures as a function of gD concentration at 25 ^{o}C and 60 ^{o}C.
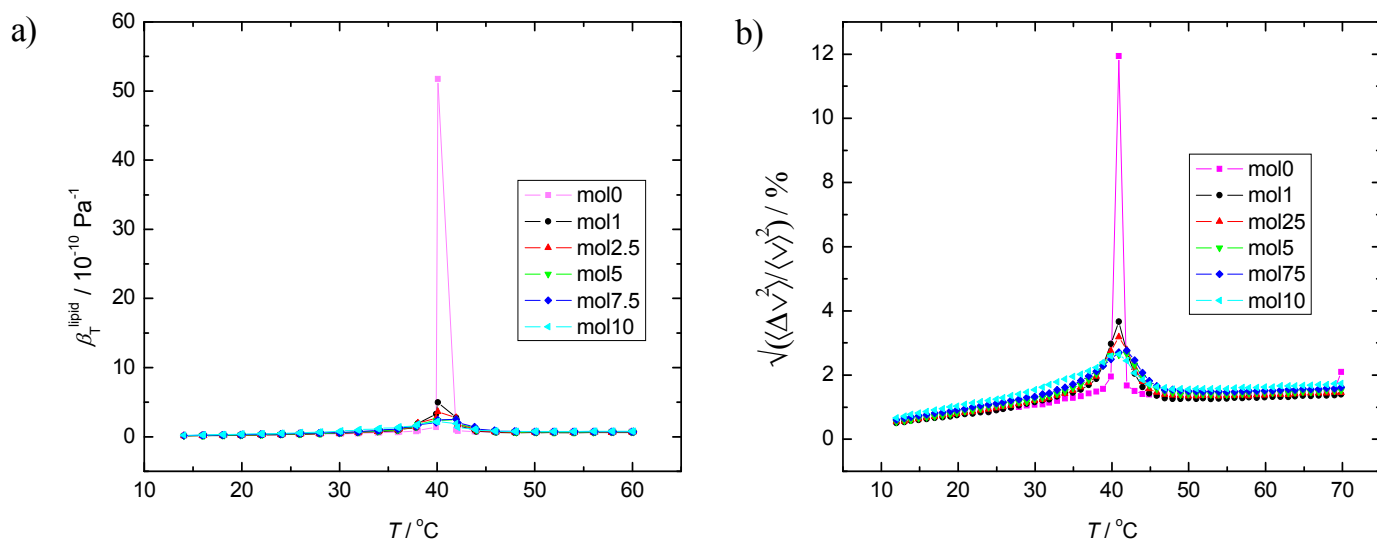
a)

b)

Figure 4. The temperature dependence of (a) the isothermal compressibility coefficient of the lipids β_T^{lipid} and (b) the calculated relative volume fluctuations for DPPC-gD mixtures at different gD molar fractions, X_{gD}
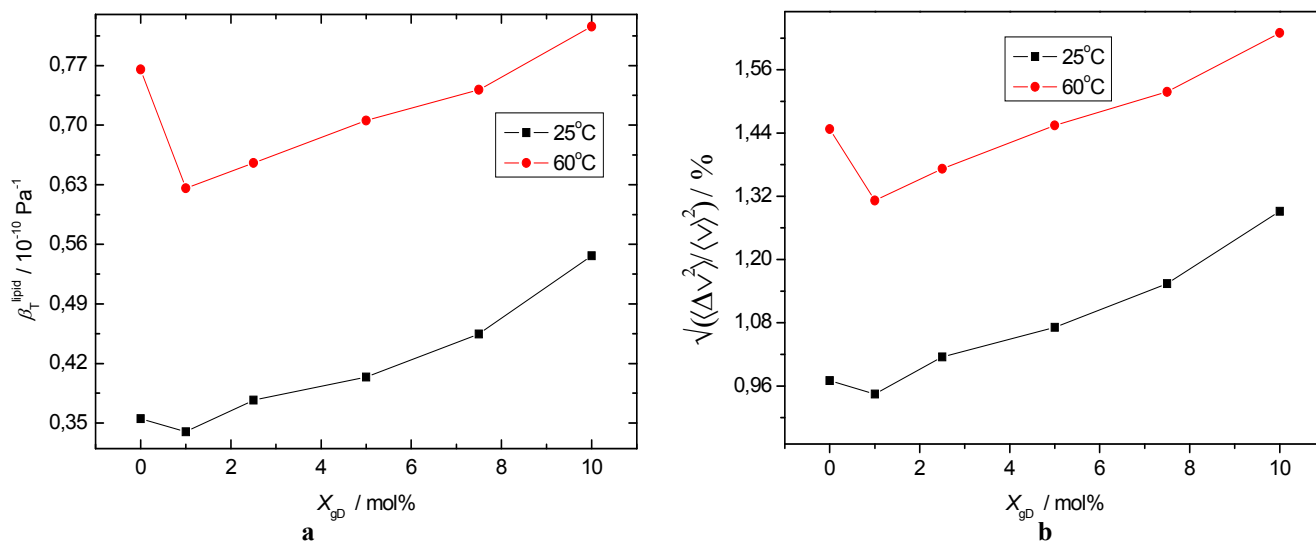

Figure 5. a) The temperature dependence of the calculated isothermal compressibility coefficient of the lipids, β_T^{lipid}, at 25 and 60 °C for DPPC-gD mixtures at different gD mole fractions, X_{gD}. (b) the temperature dependence of the calculated relative volume fluctuations at 25°C and 60°C for DPPC-gD mixtures at different gD mole fractions, X_{gD}

Application of Composite Addictives in Paper-Making Using Slag-wool Fiber

Ying Han

School of Business Administration, Northeastern University, Shenyang, China

Tel: 86-24-2332-7070   E-mail: hanying139@163.com

Wen-Jiang Feng (Corresponding author)

College of Physics Science and Technology, Shenyang Normal University, China

Tel: 86-24-6265-2182   E-mail: wjfeng@yahoo.com.cn

Wei Cheng

School of Business Administration, Shenyang University, China

Tel: 86-24-8659-3289   E-mail: chengweigood@yahoo.cn

Feng Chen

School of Business Administration, Northeastern University, Shenyang 110004, China

Tel: 86-24-2332-7070   E-mail: chenfengfly@yahoo.cn

Rong-Rong Chen

School of Business Administration, Northeastern University, Shenyang 110004, China

Tel: 86-24-2332-7070   E-mail: rrchen79@yahoo.cn

Abstract

The composite paper was made successfully from the heterogeneous mixture of common pulp and slag-wool fibers, without/with different amounts of composite addictives. These physical properties, including tensile strength, folding endurance, and smoothness, etc., were investigated in detail. All physical properties of the composite paper, made from the 30% slag wool fibers & 70% paper pulp, and no any composite addictive, decrease sharply, in comparison with common paper. While for the same paper with addition of optimum amount (0.5%) of composite addictives, the tensile strength increases by 15%, while the folding endurance, by 40%. Therefore, it is vital to introduce composite addictives in the process of composite papermaking. The aforementioned investigation can reduce the amount of paper pulp, and therefore, protect our forest resource.

Keyword: Blast-furnace slag, Slag wool fiber, Addictive, Tensile strength

1. Introduction

Blast-furnace slag (BFS) is a by-product in the manufacture of pig iron. It is formed by the reaction of limestone with materials rich in SiO_2 and Al_2O_3 at 1350–1550 °C. It has been often used as a pozzolanic admixture in Portland cement paste [Uchigawa, 1986; Mehta 1989; Pal *et al*., 2003; Cheng *et al*., 2003; Barnett *et al*., 2006]. The major components of blast-furnace slag are SiO_2, CaO, MgO, and Al_2O_3.

In China annual granulated BFS production capacity is around 15 million tons, which becomes a threat to the environment [Wang *et al*., 2004]. Therefore, it is vital for China to make the best of BFS. Unfortunately, BFS in China has little application in all fields except for Portland cement. On the other hand, as the second papermaking country [Hu et al., 2001], China has destroyed amounts of forests, together with deadly emission of waste liquid from papermaking process.

As is known, slag wool fibers (SWF) can be produced by means of re-melting and throwing BFS. In the previous

report [Zhou *et al.* 1997], SWF can be easily obtained by directly throwing the high-temperature (1300 °C or so) liquid BFS, which is a common industrial waste from steel factory or thermoelectricity factory. As inorganic fibers, SWF is very brittle, difficult to bind with organic fibers. However, unlike plant fibers or traditional filler such as calcium carbonate, SWF can be prepared non-noxiously, without environment pollution. According to report [Nie *et al.*, 2005], SWF can be employed as a new papermaking material between plant fibers and traditional fillers. After superfine ground, SWF gives a length-diameter ratio of 10, with a mean diameter of 10–15 μm, the same size as plant fibers serving as papermaking material. The previous report reveals [Nie *et al.*, 2005] that the SWF substitute range of paper pulp is 10–30%, which can protect the rare forest resource. Besides, the substitute of SWF for common pulp can lower the cost of papermaking and the amount of industrial waste. Commonly, SWF is much shorter and more brittle than plant fibers, which indicates difficult binding between SWF and common organic fibers. In the present paper, the investigation mainly is focused on the home-made composite addictives as new-type paper strength agents. The physical properties, including tensile strength, folding endurance, and smoothness, etc., were studied on different conditions. Our investigation is beneficial to the SWF-plant fibers composite paper, which can be promising to solve the BFS problem, and lower the environment pollution from papermaking process.

2. Experimental

2.1 Materials and reagents

Kraft Pulp: from Russia, 45° Schoppe rriegler (SR); SWF: thrown by high-temperature BFS; and home-made composite addictives

2.2 Equipments

ZT4-00 23 liters laboratory beater; Screen: ZQS5 with ø 300; One-side glazed dryer: CSG 356×457mm; Hand sheet former: ZQJ1-B with ø 200 mm

2.3 Procedures

2.3.1 Preparation of beating and handsheets

Fiber stuff was fully soaked in water. Kraft pulp was beaten up to about 45°SR by ZT4-00 23 beater, with a wet-weight of 6 g. The impurities in SWF, such as sands, can be removed by wet cyclone separator. After that, the SWF was treated by some organic agent, and then beaten by the beater to about 7°*SR*, with the wet-weight of 0.3 g. Both kinds of pulp were mixed according to the ratio, and the SMF was fully dispersed into the plant pulp. After the addictives were added into the composite pulp one by one, and mixed homogeneously, the handsheets were conducted on the sheet former, with the weight of 60 g/m^2. Finally, the formed sheet can be obtained after the handsheets were dried on the one-side glazed dryer [Qu, 1992].

2.3.2 Measurements of beating degree were conducted on the Schoppe Rriegler Apparatus.

2.3.3 Measurements of physical properties of paper were based on the methods listed by *Measurement Standard Compile of Papermaking Industry*.

3. Results and discussion

3.1 Paper properties without composite addictives

For the common paper sheet and that of adding 30% SWF, the physical properties were measured and listed as Table 1.

As illustrated from Table 1, each property indexes are dramatically changed after 30% SWF were added into the composite pulp. That is, the opacity and the thickness increase while the weight is unchanged. Besides, the tensile strength and the folding endurance are much lowered, or rather, the former decrease by 24%, the latter, 90%. Due to short and brittle SWF, as well as difficult to bind with plant fibers, it is reasonable for the strength indexes, such as tensile strength and folding endurance, to be lowered with increasing SWF content. In order to promote the strength of the composite paper solve this problem, it is indispensable to add some composite addictive.

3.2 Effect of composite addictives

3.2.1 Tensile strength and folding endurance

For the composite paper with 30% SWF and different amounts of composite addictives, the tensile strength and folding endurance were measured and shown in Fig. 2 and 3, respectively. With increasing the composite addictive, the tensile strength and the folding endurance dramatically increase, as shown in Fig. 1 and 2. When 0.5% composite addictives is added, the tensile strength is increase by 15%, and the folding endurance, by 40%. With further increasing the composite addictives, both the tensile strength and folding endurance are lowered. As we know, the composite addictives employed are macromolecule polymer. Little amounts of composite addictives can

promote the binding between SWF and plant fibers, while large amounts of them will make the composite pulp viscous. That is to say, the large viscousness can trap the fibers dispersion, and lower sheet formation, which lowers strength properties.

From the chemical point, the ammonia, from the composite addictives, combines with hydroxide radical, from cellulose and hemicelluloses molecular, by means of H-bind [Ma *et al.*, 2004]. That is, the cations from molecular absorbs the anions from SWF, which can promote the number as well as the strength of molecular binding, leading to a reversible change of physical property [David *et al.*, 1991; Henry, 1964]. Moreover, due to the presence of electrostatic repulsive force, the composite addictives have a good dispersity, which can make fibers fully dispersed and bound. So, the good dispersity and H-bind can promote paper formation and the physical strength. That is, the paper strength became dramatically increased after adding the composite into the composite pulp.

3.2.2 Other properties

For the composite paper with 30% SWF and different amounts of composite addictives, the physical properties are shown in Table 2.

As shown in Table 2, after the composite addictives were added, little change occurs to the weight, the thickness and the opacity of the composite paper. Generally speaking, these physical properties are concerned with the pulp composition, or rather the content of SWF. Based on the same content (30%) SWF, these properties are reasonably unchanged.

3.3 SEM analysis

SEM was conducted on the composite paper with the 30% content of SWF. The morphologies of SEM are shown in Fig. 3 and 4, respectively.

Comparing Fig. 3 with 4, we can observe the dispersion state of fibers. That is, without the present of composite addictives, the fibers diffuse randomly, while the fibers can disperse homogenously after adding the addictives. Obviously, it is the addition of the composite addictives that can promote the strength indexes of the composite paper. In other words, after added into the paper pulp, the addictives can disperse on the surface of as well as into the fibers, and chemically cross link with the fibers [*Yang et al.*, 2005]. Therefore, the net-like amorphous crossing is formed, which can confine the motion between fibers, and consequently, lower the expanding of fibers and companding deformation of sheets [Wu *et al*., 2005]. The paper strength is obviously improved.

4. Conclusion

Composite paper was made successfully from the heterogeneous mixture of common pulp and slag-wool fibers without/with the presnce of composite addictives. All properties of the composite paper, made from the 30% slag wool fibers and no any composite addictive, decrease sharply, in comparison with common paper. While for the paper with addition of optimum amount (0.5%) of composite addictives, the tensile strength increases by 15%, while the folding endurance, by 40%. Therefore, it is vital to introduce composite addictives in the composite paper making, which can reduce the amount of pulp, and therefore, protect our environments.

References

Barnett, S.J., Soutsos, M.N., Millard, S.G., Bungey J.H. (2006). Strength development of mortars containing ground granulated, blast-furnace slag: Effect of curing temperature and determination of apparent activation energies. *Cement and Concrete Research*, 36: 434–440.

Cheng, T.W., Chiu, J.P. (2003). Fire-resistant geopolymer produced by granulated blast furnace slag. *Minerals Engineering*, 16: 205–210.

David P, Nancy S Clungeon, Stephen A Fischer. (1991). Reducing organic chloride contaminats in polyamionamide-epichlorhydrin wet-strength resins. *TAPPI*, 74(12): 135–138.

Henry P.W. (1964). Water-dispersible acide-form melamineformalde hyderesins. US, 3117106. 1964-01-07.

Hu, Z.A., Xu X.Q. (2001). Exploration on Blast-furnace slag papermaking process. *China Resource Comprehensive Utilization,* (7): 32–33.

Ma, Y.S., Qiu H.Y. (2004). Advance of Mechanism of Dry Strength Additives. *Paper and Paper Making*, (2), 26–27.

Mehta, P.K. (1989). In Proceedings of the 3rd International Conference on Fly Ash, *Silica Fume, and Natural Pozzolans in Concrete*. Tronheim, Norway. 1–43.

Nie Y.J. (2005). *Study on Mineral Composition Fiber Using in Papermaking*. Nanjing, China: Nanjing Forestry University Press.

Pal, S.C., Mukherjee, A., Pathak, S.R. (2003). Investigation of hydraulic activity of ground granulated blast furnace slag in concrete. *Cement and Concrete Research,* 33: 1481–1486.

Qu W.J. (1992). *Pulp Screen Experiments*. Beijing, China: China Light Industry Press.

Uchigawa, H. (1986). In Proceedings of the 8th International Congress on the Chemistry of Cement. *Rio de Janeiro*, 3: 249–256.

Wang, L., Tian P., Yao Y. (2004). Application of ground granulated blast furnace slag in high-performance concrete in China. *International Workshop on Sustainable Development and Concrete Technology,* (3): 309–317.

Wu C.L., Li X.P., Wang J.Yo. (2005). Wet Strengthening Agents in Paper Makingand Its Developing Prospect. *Paper and Paper Making*, (60): 35–38.

Yang K.J., Su W.Q. (2005). Mechanism and research status of wet strength agent. *South West Pulp and Paper*, 34(5): 16–19.

Zhou L.M., Wen G.P. (1997). Development of blast-furnace slag fiber. *New Building Materials*, (4): 34–37.

Table 1. Comparison of physical property indexes of paper sheets without/with adding 30% SWF

SWE content (%)	Weight (g/m^2)	Thickness (mm)	Whiteness (%)	Tensile Strength (Km)	folding endurance (Time)	Smoothness (Sec)	Opacity (%)
0	61.01	0.119	78.45	5.01	465	9.1	76.5
30	59.96	0.139	76.9	3.80	43	2.9	80.0

Table 2. All physical property indexes of the composite paper after adding the composite addictives

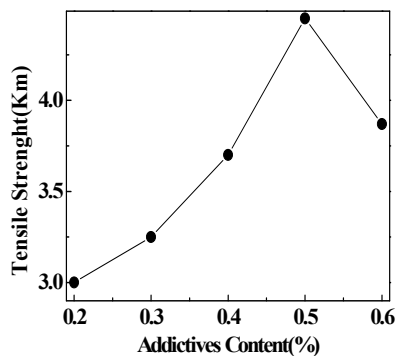| SWF content (%)	Addictives content (%)	weight (g/m^2)	Thickness (mm)	Whiteness (%)	Smoothness (Sec)	Opacity (%)
30	0.2	62.6	0.149	73.4	0.6	81.5
	0.3	59.2	0.162	70.2	1.6	80.5
	0.4	56.6	0.148	74.2	1.3	78.0
	0.5	63.5	0.160	74.5	1.5	80.0

Figure 1. Tensile strength v.s. different amount of composite addictives
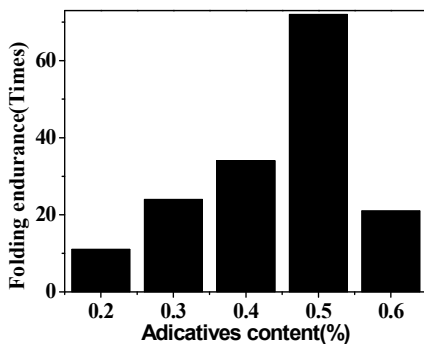

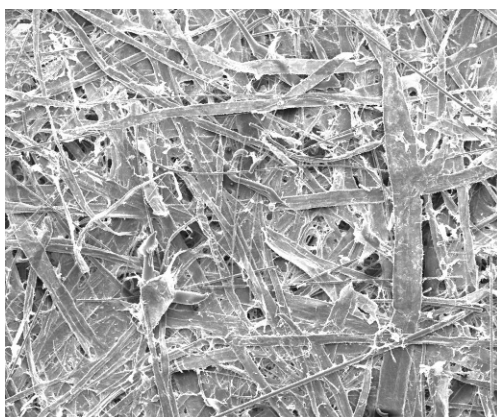Figure 2. Folding endurance v.s. different amount of composite addictives

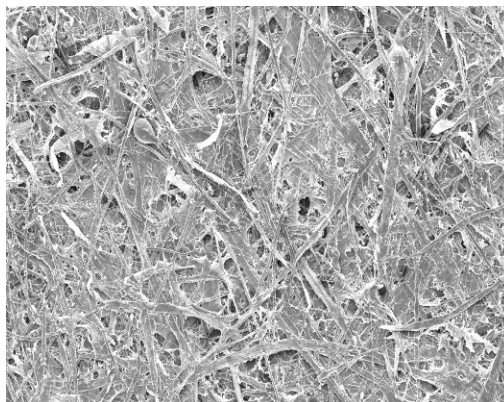Figure 3. (a) Fiber SEM images without addition of composite addictives

Figure 3. (b) Fiber SEM images with addition of composite addictives

Synthesis of New Bioactive Sulfur Compounds Bearing Heterocyclic Moiety and Their Analytical Applications

Mohammad. S. T Makki (Corresponding author) & Reda. M.Abdel-Rahman

Department of Chemistry, Faculty of Science, King Abdulaziz University

P.O. Box 80203, Jeddah 21589, Kingdom of Saudi Arabia

E-mail: mmakki@kau.edu.sa

Mohammad.S. El-Shahawi

(On leave) Department of Chemistry, Faculty of Science at Damiatta, Mansoura University

Mansoura, Egypt

E-mail: mohammad_el_shahawi@yahoo.co.uk

Abstract

Some new bioactive sulfur compounds bearing heterocyclic nitrogen moieties such as 3- imino –2-thioxo-4,5-dihydro- thiazolidin – 4-one (**3**), 3-imino – 2-thioxo -3,4,5,6-tetrahydro-1, 3-thiazine-4, 6- (2 H)dione (**4**), N- substituted – pyrazol -3,5-dione (**10**) , 1,3 –disubstituted -2-thioxo-pyrimidin-4,6 –dione (**11**) and di –(3, 5-diaminopyrazolin-1-yl)thioketone (**13**) derived from dithioc formic acid hydrazide (**1**) and thiocarbohydrazide (**7**) were prepared via condensation of compound **1** or **7** with acyclic and cyclic oxo compounds (e.g. aldehydes and ketones) in 1:1 and 1:2 molar ratios, and addition of iso thiocyanate or treatment with active methylene compounds followed by ring closing reactions in different media (Schemes I & II). The biocidal effect of some compounds towards some bacteria and fungi was evaluated. Compound **4** was used as selective chelating agent for spectrophotometric determination of mercury (II) ions. The limit of detection (LOD) and quantification (LOQ) of the developed spectrophotometric method were found to be equal to 0.16 and 0.52 μg mL^{-1} mercury (II), respectively. Compound **4** was also physically immobilized onto polyurethane foam (PUFs) and was successfully used as solid sorbent in packed column for removal of mercury (II) ions from wastewater.

Keywords: Heterocyclic compounds, Biocidal effects, Mercury (II) determination, Wastewater

1. Introduction

Recently, great attention has been oriented towards cyclic and acyclic heterocyclic systems containing nitrogen, oxygen or sulfur. Such class of compounds has wide applications as pharmaceutical drugs, biological activities, as anti HIV, anticancer, efficient plant protection and as analytical reagents for trace and ultra trace heavy metal determination and pre concentration in aqueous media (Ramadan, et al., 1993, PP. 291 -303; Piper, et al., 1997, PP. 377 -384; Abdel-Rahman, 2000, PP. 315 -357; Abdel-Rahman, 2001, PP. 18 -22; PP.195 -204, PP.410 -410; El-Gendy, et al., 2003, PP.2055 -2071; Gladis and Rao, 2004, PP. 60 -65; Yonetoku, et al., 2006; Sharma et al., 2006, PP. 1139 -1143; Kadi and El-Shahawi, 2009, PP.613 -620; Hamza et al., 2010, PP. 69 -74. The presence of proton at nitrogen and/ or sulfur atoms, provide these compounds with the ability to form metal complexes with heavy metal ions [13-17]. **(**Zaki et al., 1995, PP. 127 -138; Jozlowski, et al., 2002, pp. 677 -682; Pandy, et al., 2006, PP. 107 -109; Pulakesh, 2007, PP. 544 -547; Sadasivan and Alaudeen, 2007, PP. 1959 -1962).

The great electrophilicity of nitrogen atom compared to that of sulfur atom makes the latter more acidic and an active centre in the nucleophilic attack. The fact that, the sulfur anion formed is more stabilized by negative charge distribution as reported (Sbirna, et al., 2005, PP. 389 -392) as shown in equation (1):

$$(1)$$
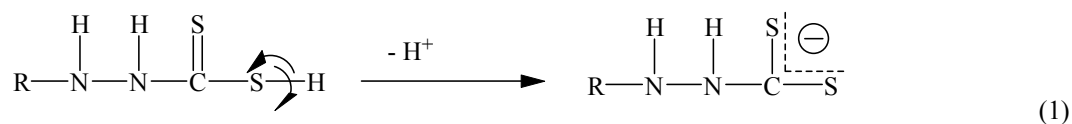
Thus, in the case of dithioic acid hydrazides, the orientation of heterocyclization reactions will start from **S** on alkylation or from **N** on condensation (Sadasivan and Alaudeen, 2006, PP. 1145 -1148). The starting materials, dithioic formic acid hydrazide **1** and thiocarbohydrazide **7** possess two donor sites situated at -NH and / or =NH group in addition of sulfur (Sadasivan and Alaudeen, 2006, PP. 1145 -1148).

Recently, a series of cyclic and acyclic systems close to the title compounds has been used extensively in the literature as biocidal reagents (Sadasivan and Alaudeen, 2006, PP. 1145 -1148). Such compounds have been used as complexing agents for pre concentration, and subsequent determination of trace and ultra trace concentrations of toxic ions via both S and N as donor atoms (Hassanien, 2003, PP. 1987 -1997; Shindhu, et al., 2005, PP. 472- 474) as shown below:

<Figure 1>

Considering the biocidal and complexation properties of these compounds and as a part of our search for novel mono- and di-thiocarbohydrazide and alkyl, acyl derivatives, the present article reports the synthesis of heterocyclic nitrogen compounds containing sulfur using dithioic formic acid hydrazide (**1**) and thiocarbohydrazide (**7**) as starting materials via condensation with oxygenated compounds. Moreover, one of the compounds prepared by this methodology was tested as chelating agent for the pre concentration and subsequent determination of mercury (II) ion in water.

2. Experimental

2.1 Reagents and materials

All chemicals and solvents used were of analytical reagent (A.R) grade quality and were used as received. Most of the chemicals were provided by Merck (Darmstadt, Germany). Doubly deionized water was used throughout. Low density polyethylene (LDPE) bottles, Nalgene were used and carefully cleaned first with hot detergent, soaked in 50% HCl (Analar), HNO_3 (2.0 mol L^{-1}), subsequently washed with dilute HCl (0.5 mol L^{-1}) and finally rinsed with distilled water. The sample solution was stored in LDPE bottles and stored at -20°C in a freezer. Stock solutions (0.1 %w/v) of the steroid reagent were prepared in ethanol. A stock solution of $HgCl_2$ (1mg/mL) was prepared by dissolving an accurate weight of the salt in doubly distilled water (100 mL). Britton – Robinson (B –R) buffers of pH 2-11 were prepared from the acid mixture of phosphoric acid, boric acid, acetic acid (0.04 mol L^{-1}) and adjusting the pH to the required value with sodium hydroxide (0.20 mol L^{-1}). A series of standard diluted mercury (II) solutions were then prepared in doubly distilled water.

2.2 Apparatus and measurements

A Perkin Elmer (Lambda EZ-210) double beam spectrophotometer (190-1100 nm) with 1cm (path width) was used for recording the electronic spectra of the comounds. A Perkin Elmer model RXI-FT-IR system 55529 was used for recording the IR spectra of the prepared compounds. A Brucker advance DPX 400 MHz model using TMS as an internal standard was used for recording the ^{1}HNMR spectra of the compounds on deuterated DMSO. A GC-MS-QP 1000-Ex model was used for recording the mass spectra of the compounds. Melting points were determined with an electro thermal Bibbly Stuart Scientific Melting Point SMPI (US). Molecular weights of the compounds were preformed on Micro analytical center, Cairo University, Egypt. Microanalysis (Sulfur %) was performed by microanalytical center Ain-Shams University-Cairo-Egypt. A digital pH-meter (model MP220, Metter Toledo) was used for pH measurements.

2.3 Organic preparation

Mono-hydrazones (2a – d) and bis-hydrazones (5 a and 5b)

A mixture of **1** and the selected aromatic / heteroaldehydes and / or cyclic biketones (1:1) and/ or 1,2-biketones (1:1 molar ratio) and a cyclic biketones (2:1 molar ratio) in ethanol- acetic acid (1:1, 100 mL) was refluxed for 1 h, cooled then poured onto an ice bath. The solid precipitate was collected and crystallized from the appropriate solvent to give **2a-d** and/ or **5a** and **5 b,** respectivel**y**.

N ^{1}-Arylidene-dithioic formic acid hydrazones (2 a-d):

2 a: This compound was crystallized from ethanol as yellow crystals. Yield = 80%, m.p. 150-151 ^{0}C. $C_6H_7N_3S_2$ (185) Calcd.: S, 34.59. Found S, 33.95.

2 b*: This compound was crystallized from ethanol as pale yellow crystals. Yield (85.2%), m.p. 105-106 ^{0}C. IR: ν cm^{-1} = 3500 (OH), 3120 (NH), 1595 (C=N), 1380 (NCSN), 1185 (C-S), 1055 (- C-O-Me). $C_9H_{10}N_2S_2$ O_2 (242) Calcd.: S, 26.44. Found S, 25.58.

2 c: This compound was crystallized from ethanol as pale yellowish crystals. Yield (90.05%), m.p. 220-221^{0}C. $C_{11}H_{14}N_2S_2 O_3$ (286) Calcd.: S, 22. 37. Found S, 22.18.

2d: This compound was crystallized from ethanol as faint yellow crystals. Yield (60.2%), m.p. 225-226 ^{0}C. UV, λ_{nm} (DMF): 380, IR: ν cm^{-1} = 3315 (NH of indole),3155 (NH of NHCS) 1686 (C=O), 1551 (C=N), 1432 (NCSN), 1190 (C-S), 826 (phenyl CH). ^{1}H NMR (DMSO): δ: 4.2 (s, 1H, SH), 6.8-7.2, 7.5-7.8 (each m, 4 H of aromatic CH), 10.2 and 14.5 (each s, 2H, NH of indole and acid hydrazide). MS, m/z (Int. %): 249 (0.0), 203 (M$^+$-HCSH, 100), 157 (5.15), 145 (31.91), 131 (15.18), 102 (87.31), 90 (27.13), 77 (5.98). $C_9H_7N_3S_2$ O (237) Calcd.: S, 27.0. Found S, 26.59.

Bis - N-arylidene-dithioic formic acid hydrazones (5a, 5b):

5a: This compound was crystallized from methanol as pale yellow crystals. Yield (65.03%), m.p. 145-146^{0}C. $C_6H_{10}N_4S_4$ (266) Calcd.: S, 48.12. Found S, 47.95.

5b: This compound was crystallized from methanol as pale yellow crystals. Yield (80.1%), m.p. 190-191 ^{0}C. IR: ν cm^{-1} = 3139 (NH), 1596 (C=N)), 1350 (NCSN), 1213(C-S), 793, 763 (phenyl CH). $C_{16}H_{14}N_4S_4$ (390) Calcd.: S, 32.82 . Found S, 32.80.

N^1 – (Phenyl amino carbothia) dithioic formic acid hydrazides (**6a**)

Phenyl isothiocyanate (0.01 mmol) was added to a solution of **1** (0.01m mol) in DMF (50 mL) and refluxed for 20 min. After cooling, the reaction mixture was poured onto ice. The solid precipitate was collected and crystallized from DMF as deep yellow crystals. Yield (83.2%), m.p. 240-241 ^{0}C. IR: ν cm^{-1} = 3195, 3103 (NH, NH), 1342 (NCSN), 1191 (C-S), 776 (phenyl CH). ^{1}H NMR (DMSO): δ = 7.2-7.4, 7.5-7.6 (each m, 10H, two phenyl), 8.1 (s, 1H, NH), 9.2 (s, 1H, SH), 10.8, 11.4 (each d, 2H, NH-NH). $C_8H_9N_3S_3$ (243) Calcd.: S, 39.5. Found S, 38.98.

*N^1 – (*4- Chlorophenyl *amino carbothia) .)dithioic formic acid hydrazides* (**6 b**)

This compound was prepared by mixing 4-chlorophenyl isothiocyanate (0.01 mmol) with a solution of **1** (0.01m mol) in DMF (50 mL) and refluxed for 20 min. After cooling, the reaction mixture was poured onto ice and the solid precipitate was filtered and crystallized from DMF as deep yellow crystals. Yield (63.0%), m.p. 215-216 ^{0}C. IR: ν cm^{-1} = 3180, 3165 (NH, NH), 1355 (NCSN), 1185 (C-S), 777 (phenyl CH), 624 (C-Cl).$C_8H_8N_3S_3Cl$ (277.5) Calcd. S, 34.65. Found S, 34.45.

3-Imino-2--thioxo-4, 5-dihydro-thiazolidin-4-one (3)

An equimolar mixture of **2a** and monochloroacetic acid with anhydrous sodium acetate (5 g) in ethanol (50 mL) was refluxed for 4 h. After cooling, the reaction mixture was poured onto ice and the resulting solid precipitate was collected and crystallized from acetic acid as yellow crystals. Yield (50.12%), m.p. 260-261 ^{0}C. IR: ν cm^{-1} = 3110 (NH), 1710 (C=O), 1603 (C=N), 1356 (NCSN), 1480 (deformation CH$_2$) . MS: m/z (Int.%):227 (M+2, 5.18), 92 ($C_5H_4N_2$), 56 (100, C_2H_2NO).$C_8H_7N_3S_2O$ (225.11) Calcd.: S, 28.44 Found S, 28.01.

2-Thioxo-3-(2-oxoindolin-3-imino)-3,4,5,6- tetrahydro-1,3- thiazin-4,6-dione (**4**)

An equimolar mixture of **2d** and diethylmalonate was added to sodium ethoxide solution in absolute ethanol (0.2 mmol, 100 mL). The reaction mixture was refluxed for 4 h, cooled then poured onto ice-HCl. The produced solid was filtered and crystallized from THF as strong yellow crystals. Yield (70.12%),m.p.280-281 ^{0}C. IR: ν cm^{-1} = 3353 (OH of thiazine-4, 6 –dione), 3056 (NH of indole), 1667, 1620 (2 C=O), 1607 (C=N), 1362 (NCSN), 1192 (C-S), 738 (phenyl CH). ^{1}H NMR (DMSO): δ =3.2 (d, 2H, cyclic O-CH$_2$-O), 6.2 (s, 1H, OH of 3-indole), 7.3-7.7 (m, 4H, of benzo-protons). MS, m/z (Int. %): 305(0.0), 271 (M-H$_2$S, 100), 203 (13.11), 157 (51.15), 131 (13.08), 102 (78.34). $C_{12}H_7N_3S_2 O_3$ (305) Calcd.: S, 20.98 Found S, 20.75.

Ketone thiocarbohydrazones (8a-d)

A mixture of compound **7** in hot water (10 mL) and the appropriate heteroaldehydes/ ketone (1:1 molar ratio) in ethanol-acetic acid (1:1, 50 mL) mixture was refluxed for 1 h, cooled and poured onto an ice bath. The produced solid precipitate was filtered and crystallized from ethanol to give **8a-d as** pale – yellow crystals.

8a: Yield (85%), m.p.182-184 ^{0}C. $C_6H_8N_4S$ O (184) Calcd.: S, 17.39. Found S, 17.11.

8b: Yield (90.02%), m.p.185-186 ^{0}C. $C_6H_8N_4S_2$ (200) Calcd.: S,32.01. Found S, 31.89.

8c: Yield (95.1%), m.p.230-231^{0}C. $C_9H_{12}N_4S$ O (224) Calcd.: S,14.28 Found S,13.99.

8d: Yield (80.0%), m.p.260-261^{0}C. UV, λ_{nm} (DMF): 420. IR: ν cm^{-1} = 3353 (NH$_2$), 3150 (NH, NH), 1684 (C=O), 1552 (C=N), 1349 (NCSN), 776 (phenyl CH). The MS, m/z (Int. %): 235(0.0), 203(18.21), 157 ($C_8H_5N_3SO$), 131 (35.13), 102 (78.11),90 (21.78). $C_9H_9N_5SO$ (235) Calcd.: S,13.61 Found S, 13.41.

Formation of N ^{1}, N ^{3} – di (iminoaryl)thioureas, (**9a-e**)

In hot ethanol, compound **7** (10 mL) was mixed with the appropriate heteroaldehydes or ketones (1:2 molar ratio) in ethanol-acetic acid (1:1, 50 mL). The reaction mixture was refluxed for 1h, cooled, and poured onto ice. The produced solid was recrystalized from isopropyl alcohol to give yellowish-crystals **9a-e.**

9a. Yield (80%), m.p.230-232 ^{0}C. $C_{17}H_{18}N_4SO_4$ (374) Calcd.: S,8.55 Found S,8.15.

9b. Yield (75.2%), m.p.195-196^{0}C. $C_{11}H_{12}N_6S$ (260) Calcd.: S,12.30 Found S,11,89.

9c. Yield (78.12%), m.p.196-197 ^{0}C. $C_{11}H_{10}N_4SO_2$ (262) Calcd.: S,12.21. Found S,11.88..

9d. Yield (75.05%), m.p.140-141 ^{0}C. $C_{11}H_{10}N_4S_3$ (294) Calcd.: S,32.65. Found S,32.45.

9e: Yield (80.0%), m.p.260-261^{0}C. IR: ν cm^{-1} = 3150, 3099 (NH, NH),1647 (C=O), 1606 (C=N), 1354 (NCSN), 1211 (C-S), 769 (benzo- CH). MS, m/z (Int. %): 364(0.0), 203(17.27), 157 (85.15) , 131 (100), 102 (38.13). 90 (11.18). $C_{17}H_{12}N_6SO_2$ (364) Calcd.: S,8.79 Found S, 8.65.

*1-(1H- 2-oxo-indol-3-hydrazono) thioxo-2,3,4,5-tetrahydropyrazol-3,5-dione (***10**)

Compound **8d** (0.01 mmol) with dimethyl malonate (0.01 mmol) in solution of sodium ethoxide (0.02 mol, 100 mL) were refluxed for 4 h. After cooling, the reaction mixture was poured onto ice-HCl. The produced solid precipitate was filtered and crystallized from acetic acid as faint yellow crystals. Yield (60.0%), m.p.185 – 186 ^{0}C. IR: ν cm^{-1} = 3200-3080 (b, OH ⇌ NH, NH), 2890 (CH$_2$), 1693, 1670 (two C=O), 1348 (NCSN), 1185 (C-S), 780 (benzo - CH). MS, m/z (Int. %): 303(0.0), 247(M-56, CN$_2$O, 21.18), 203 (10.00), 1.47 (8.11) , 111 (12.12), 97 (12.12), 56 (100). $C_{12}H_9N_5SO_3$ (303) Calcd.: S,10.56; Found S, 9.96.

*1,3-Di (1H- 2-oxo-indol-3-imino)-2- thioxobarbituric acid (***11**)

An accurate of compound **9e** (0.01 mmol) with diethyl malonate (0.01 mmol) in solution of sodium ethoxide (0.02 mol, 100 mL) were refluxed for 4 h. The reaction mixture was cooled, poured onto ice-HCl. The produced solid precipitate was filtered and crystallized from ethanol as deep yellow crystals. Yield (85.12 %), m.p.210-212 ^{0}C. IR: ν cm^{-1} = 3090 (NH), 2980 (CH$_2$), 1720, 1693, 1670   (C=O), 1600, 1595 (C=N), 1350 (NCSN), 1199(C-S), 777 (benzo- CH). $C_{20}H_{12}N_6SO_4$ (432) Calcd.: S,7.40 Found S, 7.45.

N, N-Di (acyl/thioacyl/amido)thiocarbohydazides (**12a-d**)

Carbon disulfide, phenyl isothiocyanate, adipoyl chloride or 4-methoxyphenyl chloride was added by dropwise addition to a solution of compound **7 (**0.01 mmol) in DMF (20 mL). The reaction mixtures were refluxed for 1h, cooled and poured onto ice. The formed solids were filtered and crystallized from DMF to give yellowish crystals of **12a-d**, respectively**.** .

12a. Yield (75%), m.p.155-156 ^{0}C. $C_3H_6N_4S_5$ (258) Calcd.: S,62.01   Found S,61.75.

12b. Yield (80%), m.p.195-196^{0}C. $C_{15}H_{16}N_6S_3$ (376) Calcd.: S,25.55   Found S,25.27.

12c. Yield (78.1%), m.p.150-151 ^{0}C. $C_{21}H_{42}N_4SO_2$ (414) Calcd.: S,7.72.   Found S,7.55.

12d. Yield (65.05%), m.p.165-166 ^{0}C. IR: ν cm^{-1} = 3350 -3080 (b, NH, NH), 1580 (CONH), 1335 (NCSN), 1189 (C-S), 1080 (-C-O-Me). MS, m/z (Int. %): 374 (1.15), 107 (15.31), 74 (100, CN$_2$SH$_2$). $C_{17}H_{18}N_4SO_4$) (374) Calcd.: S,8.55 Found S, 8.41.

Di (3,5- diaminopyrzolin-1-yl)thioketone, 13

An **e**quimolar mixture of **7** and malononitrile in DMF –EtOH (1:1, 100 mL, 1:1), was refluxed for 4h, cooled then poured onto ice. The solid formed was filtered and crystallized from ethanol to give **13** as deep –yellow crystals. Yield (90.2 %), m.p.110-112 ^{0}C. UV, λ$_{nm}$ nm (DMF): 375 nm. IR: ν cm^{-1}:3300 (NH$_2$), 3100 (2 NH), 1580 (C=N), 1180 (C-S). MS, m/z (Int. %): 238 (M$^+$,5.0), 203 (25.01), 157 (12.11), 143 (18.18), 56 (100, CN$_2$O). $C_7H_{10}N_8S$ (238) Calcd.: S,13.44 Found S, 13.21.

2.4 Analytical procedures

2.4.1 Recommended Spectrophotometric determination of mercury (II)

In a series of volumetric flasks (25 mL), an appropriate concentration (0.2-2.0 μgmL^{-1}) of mercury (II) solution was allowed to react with the reagent **4** solution (1.50 mL, 0.05 %w/v). To the test solution, an approximate volume (5 mL) of Britton -Robinson buffer of pH 4-5 was added. The reaction mixture was completed with distilled water to the mark of the measuring flask (10 mL) and allowed to stand for 5 min before measuring the absorbance at λ$_{max}$ 505 nm. The results were compared successfully with the concentration of mercury (II) determined with atomic absorption spectrometry.

2.4.2 Preparation of the immobilized reagent **4** polyurethane foams

The reagent **4** (0.1% w/v) in water-ethanol (1:1 v/v) was shaken with the PUFs cubes with efficient stirring for 30 min. The immobilized reagent PUFs cubes were squeezed and dried as reported (El- Shahawi, et al., 200, PP. 221 -228). The retained reagent **4** onto the PUFs cubes was determined employing the equation:

$$a = (C_o - C) \frac{v}{w} \tag{2}$$

where, C_o and C are the initial and final concentrations (mol L^{-1}) of the reagent **4** in solution, respectively, v = volume of the reagent solution (liter) and w is the mass (g) of the PUFs sorbent.

2.4.3 Analysis of mercury (II) in water samples

Tap - and mineral water samples were collected from the laboratories of Chemistry Department, King AbdulAziz University, and local market of Jeddah city, KSA, respectively. The water samples were filtered through 0.45 μm cellulose membrane filter prior to analysis and stored in LDPE sample bottles (250 mL). The recommended general spectrophotometric procedure used to prepare the standard curve was followed. The concentration of mercury (II) ions was then determined following the recommended spectrophotometric procedure used for the preparation of the standard curve and employing the equation:

$$\text{Mercury (II) concentration} = C_{std} \text{ x } A_{samp} / A_{std} \tag{3}$$

where, C_{std} is the standard concentration and A_{samp} and A_{std} are the corrected absorbance of the sample and the standard at λ_{max} 505 nm, respectively.

Alternatively, the standard addition method was employed as follows: transfer known volume (5.0 mL) of the unknown water samples to the volumetric flask (25.0 mL) adjusted to pH.5-6 with B-R buffer (10 mL). An accurate volume (1.5 mL) of the reagent was added to the test solution and the reaction mixture was made up to the mark with distilled water. Repeat the same procedures after adding various concentrations (0.2-1.0 μgmL^{-1}) of mercury (II). Measure the true absorbance displayed by the test solutions before and after the addition of the standard (0.2-1.0 μgmL^{-1}) mercury (II) solution employing single wave spectrophotometry method. The concentration of mercury (II) was then determined via the calibration curve of the standard addition procedure.

3. Results and Discussion

Heterocyclic systems containing endo- and exocylic sulfur atom show a wide spectrum of potential applications. Thus, 3-imino – 2- thioxo-4,5-dihydro-thiazolidine-4-one (**3**) and 3-imino-2-thioxo-3,4,5,6-tetrahydro -1,3-thiazine-4,6(2H)dione (**4**) were obtained from condensation of dithioic formic acid hydrazide (**1**) with aldehydes to give the thiohydrazones **2** followed by heterocyclization with chloroacetic acid in ethanol – sodium acetate medium to give **3** or with dimethyl malonate in sodium ethoxide allows the formation of compound **4** [Scheme I].

Formation of compound **3** may be takes place via the nucleophilic attack of sulfide (S$^-$) to the electropositive carbon of chloroacetic acid (CH$_2$-Cl) followed by another nucleophilic attack of more nucleophilic nitrogen of thiohydrazone (N-H) to other electrophilic carbon of acetic acid (-COOH).

Compound **4** may be formed via nucleophilic sulfur atom of dithioic moietyon a more electrophilic carbon dimethyl malonate followed by heterocyclization via second nucleophilic nitrogen on the other electrophilic carbon. On the other hand, condensation of compound **1** with cyclic 1, 2- bicarbonyl compounds as biacetyl & benzil (2**:**1 by molar ratio) afforded the bis- compounds **5a** and **5 b**, respectively. Addition of phenyl / p- chlorophenyl iso thiocyanate in warming DMF yielded N- (arylaminocarbothia) dithioic formic acid hydrazide **6** [Scheme I].

Thiocarbohyrazide (El-Gendy et al, 2001, PP. 376 -383; Rastogi and Yadav, 2005, PP. 448 -451) is one of the most important materials for building heterocyclic comounds containing sulfur and nitrogen (Hassanien, 2003, PP. 1987 – 1997; El-Gendy, et al., 2001, PP. 376 – 383). Thus, condensation of thiocarbohydrazide **7** with cyclic and a cyclic oxygenated compounds such as heteroaromatic aldehydes:pyrrole/furan/thiophene carboxaldehyde and cyclic hetero ketone e.g. indol-2,3-dione in boiling ethanol – acetic acid gave the mono hydrazone **8** (1:1 by moles) and/or the bis – hydrazone **9** (1:2 by moles) (Scheme II).

Heterocyclization of mono hydrazone **8d** was achieved via refluxing with dimethyl malonate in sodium ethylate furnished 1-[(2-oxoindol-3-ylimino) aminothia]-2,3-dihydro-pyrazol-3,5-dione (**10**). Under the same experimental conditions, refluxing compound **9e** with diethyl malonate afforded 1, 3-di(2-oxoindol-3-ylimino)-2-thioxo-4,5-dihydro-pyrimidin-4,6-dione, **11**. (Scheme II). Addition of CS$_2$ and phenyl isothiocyanate to **7**, in warming DMF yielded N, N- di (caramido) thioureas **12a** and **12 b**, respectively, while

compounds **12 c** and **12 d** were isolated from careful treatment of compound **7** with adipolyl chloride and p-methoxybenzoyl chloride in warming DMF (Scheme II). Heterocyclization of compounds **12** failed because the high acidity with electronic symmetry of molecule in addition to the resonance stabilization of the conjugated anion may be formed (Rastogi and Yadav, 2005, PP. 448 -451).Treatment of acid hydrazide with malononitrile is one of the most important routes for the synthesis of poly functional amino hetercyclic systems (Schachtner, et al., 1999, PP. 335 – 341; El-Gendy, et al., 2001, PP. 376 -383; Hassanien, 2003, PP. 1987 -1997; Rastogi and Yadav, et al., 2005, PP. 448 -451; Burghate et al., 2007, PP. 103 -108). Thus, refluxing thio carbohydrazide **7** with malononitrile in ethanol – DMF afforded di (3, 5-diaminopyrazolin-1-yl) thio ketone, **13** (Scheme II). Compound **13** was also prepared by nucleophilic attack of the first primary NH_2 to the first cyano group followed by ring closing reaction of a second nucleophilic attack of secondary NH_2 to other cyano group.

3.1 Antibacterial activity

Recent literature survey has revealed the need of new compounds endowed with antimicrobial activity. Previous investigation has shown that, some of cyclic sulfur – nitrogen compounds have excellent antimicrobial activity (Burghate, 2007, PP. 103 -108). Therefore, in this study the cyclic sulfur compounds **2, 5, 6, 8, 9** and **12** were screened as antibacterial active agents using cup – plate diffusion method (Burghate et al., 2007, PP. 103 -108). The used bacterial organisms included both gram positive and gram negative strains: e.g. *Escherichia. coli*; *Bacills. subtilis, Staphyylococcus. aureus*, *Pseudomonas .vulgaris* and *Shigella flexneri* in DMF. Streptomycin was used as standard antibiotic. The diameter of the inhibition zone in mm was measured at concentration of 100 μg mL^{-1}. The results are summarized in Table 1, where the compounds **6b** and **12 a**, showed high activity, the other compounds presented moderate or low antimicrobial activity compared to streptomycin. The activity of compounds **6b** and **12a** may be attributed to the thiourea and dithioic moieties in their structures, respectively as reported (Abuo-Rahma, et al., 2009, PP. 3879 -3886).

3.2 Analytical application of compound 6-hydroxy-3-(2-oxoindolin-3-ylidene- amino)-2-thioxo-3,4,5,6-tetrahydro -1,3-thiazin-4(3H)-one, 4

3.2.1 Spectrophotometric determination of trace amounts of mercury (II)

On mixing the compound **4** abbreviated as HOTT with mercury (II) ions in the aqueous media of pH 4-5 and shaking, for 2-3 min, a red colored complex was developed. The absorption spectrum of the reagent showed one well defined absorption peak at 336 nm (λ_2) nm, while the spectrum of the complex **4** at the same pH showed one peak at 505nm (λ_2)nm (Fig. 1). Thus, in the subsequent work, the absorbance of the aqueous solution was measured at 505 nm against a reagent blank**.** Maximum absorbance of the produced colored complex was achieved at pH 4–5. In the aqueous solutions of pH < 4, the data revealed no complex formation between compound **4** and mercury (II) ions. In acidic pH, the equilibrium of the reagent moves to left, hence the quantity of the available dissociated species of the chelating agent **4** decreases and not able to form complex with mercury (II). The absorbance of the aqueous phase of pH ≥ 6 decreased due to the formation of non- colored complex species of mercury (II) ions e.g. hydroxo-species of mercury (II).

The influence of the concentration of compound **4** revealed that, a 2 mL of 5.1×10^{-4} mol L^{-1} of the reagent was sufficient to react quantitatively (97–98%) with mercury (II) up to 10 μg mL^{-1} in the aqueous layer. The molar absorptivity (ε) at λ_{max} 505 nm calculated from the absorbance measurement was found equal to 2.5×10^4 L mol^{-1} cm^{-1}. The chemical structure of the produced mercury (II) complex species was determined by continuous variation method (Sawyer, et al., 1984) at various concentrations of the mercury (II) ions and reagent. The results revealed the formation of complex species of 1:2 molar ratio of mercury (II) to the reagent. Thus, the chemical structure of the developed colored species is most likely Hg (HOTT)$_2$.

3.2.2 Figure of merits

The values of LOD and LOQ of mercury (II) were determined employing the equations (Miller, 1994):

$$LOD = 3\,\delta\,/b \tag{4}$$

$$LOQ = 10\,\delta\,/b \tag{5}$$

where δ, is the standard deviation of the blank reading and b is the slope of the calibration plot. The LOD and LOQ values were found equal to0.16 and 0.52 μg mL^{-1} mercury (II), respectively. These values could be improved by immobilizing the reagent **4** onto PUFs sorbent in packed column for quantitative collection of trace and ultra trace amounts of mercury. The level of precision is suitable for the routine analysis of the mercury (II) in various types of water samples. The analysis of mercury (II) at the concentration levels of 1.0-15 μg mL^{-1} was achieved with a recovery percentage of 97±2.9%, (n = 5). A satisfactory recovery percentage of various mercury (II) species spiked to the tested water samples was also achieved.

3.2.3 Effect of diverse ions

The selectivity of the developed method for the determination of 10 µg mL^{-1} of mercury (II) ions in the presence of a relatively high excess (0.05-0.1 mg mL^{-1}) of some cations e.g. Li$^+$, Na$^+$, K$^+$, Ca^{2+}, PO$_4^{-3}$, Al^{3+}, Fe^{2+}, Ni^{2+}, Co$^{2+,}$ and Zn^{2+} and the anions MnO$_4^-$ and CrO$_4^{-2}$, chloride, nitrate, sulfate and fluoride was investigated. The tolerance limit was defined as the concentration of the added foreign ion causing a relative error within ± 2% of mercury (II) determination. The results revealed that, all the tested cations does not interfered even at 1:100 tolerable concentration of mercury (II) to the diverse ions, respectively. The interference of MnO$_4^-$ and CrO$_4^{-2}$ was eliminated by the addition of NaN$_3$ and sodium sulfite in HCl media (1.0 mol L^{-1}), respectively. Thus, the developed method could be extended for the analysis of mercury in various water samples.

3.2.4 Retention profile of mercury (II) onto reagent 6 loaded PUFs

In aqueous solution of pH 4-5, mercury (II) forms an orange – red colored complex species with compound **4**. Thus, the sorption profile of the aqueous solutions containing mercury (II) at pH 4-5 by the reagent **4** loaded PUFs was studied after shaking for 1h at room temperature. The amount of mercury (II) in the aqueous phase after equilibrium was determined spectrophotometrically (Marczenko, 1986). The %E and the D of mercury (II) sorption onto the PUFs decreased markedly at pH<4 and maximum uptake was achieved at pH ~ 4-5. The high retention of mercury (II) at pH 4-6 is most likely attributed to the deprotonation of the reagent **4** and the available active sites on the reagent loaded PUFs membrane that enhanced the retention of analyte via "solvent extraction and/ or chelation mechanism" (El-Shahawi, et al., 2005, PP. 221 -228). At pH>6, the sorption performance of the reagent loaded PUFs towards mercury (II) decreased markedly. This behavior is most likely attributed to the instability, hydrolysis, or incomplete extraction of the produced complex of mercury (II) –reagent **4** in the PUFs solid sorbent. These results suggested the use of the reagent **4** treated PUFs in packed column for removal of mercury from wastewater samples after percolation at 5-10 mL min^{-1} flow rate. An acceptable removal percentage (97 ± 2.5) of mercury (II) was achieved.

3.2.5 Validation

The proposed method was validated by the complete removal of the spiked mercury (II) onto tap and wastewater samples at a total concentration ≤ 15.0 µg mL$^{-1.}$ An acceptable extraction percentage (95± 3.5%, n = 5) of mercury was successfully achieved with the aid of the calibration plot and standard addition procedures. The plot of mercury (II) added to the tested water sample versus the amount of mercury (II) retained was linear with a slope of 0.998 and a correlation coefficient of r= 0.999 confirming the performance of the developed method for mercury (II) removal from water.

4. Conclusion

New bioactive sulfur compounds bearing heterocyclic moieties were prepared. Only one compound **4** was successfully used as selective chromogenic reagent for single wave spectro- photometric determination of mercury (II) in aqueous media. The presence of different tautomerism in the structure of compound **4** participates effectively on complex formation. The values of LOD and LOQ of the developed spectrophotometric were found equal to 0.16 and 0.52 µg mL^{-1} mercury, respectively. Moreover, the reagent **4** immobilized PUFs could be packed in column for on –line pre concentration and subsequent determination of mercury (II) ions at ultra trace concentrations.

References

Abdel-Rahman, R.M. (2000). Chemistry of uncondensed 1,2,4-triazines: Part II sulfur containing 5-oxo-1,2,4 – triazin-3-yl moiety. An overview. *Phosphorous, Sulfur, Silicon and the Related Elements*, 166 (1), 315-357.

Abdel-Rahman, R.M. (2001). Role of Uncondensed 1,2,4-triazine Compounds and Related Heterocyclic systems as Therapeutic Agents. A Review. Part XV. *Pharmazie*, 56(1), 18-22.

Abdel-Rahman, R.M. (2001). Role of Uncondensed 1,2,4-triazine Derivatives as Biocidal Plant Protection Agents. *Pharmazie*, 56 (3), 195- 204.

Abdel-Rahman, R.M. (2001). Chemoselective heterocyclization of pharmacological activities of new heterocycles. A Review Part V: Synthesis of biocida sulfur containing 4- thiazolidinones. *Boll. Chim. Famaceutico*, 140 (6), 401-410.

Abuo-Rahma,G, Sarhan, H, Gad, G. (2009). Design, synthesis, antibacterial activity and physicochemical parameters of novel N-4-piperazinyl derivatives of norfloxacin. *Biorg.Med.Chem*., 17, 3879-3886.

Burghate, M.K., Grandhe, S.V., Ajmire, M.G., Berad, B.N. (2007). Synthesis of (substituted) benzylidenehydrazino-5-arylamino-1,3,4-thiadiazoles and their antimicrobial activity. *J. Indian Chem. Soc.*, 84, 103-108.

El-Shahawi, M.S., Othman,A.M., Abdel-Fadeel,M.A. (2005). Kinetics, thermodynamic and chromotographic behavior of the uranyl ions sorption from aqueous thiocyanate media onto polyurethane foams. *Anal. Chim. Acta*, 546(7), 221-228.

El-Gendy Z., Morsy J.M., Allimony H.A., Ali. W.R.., Abdel-Rahman, R.M. (2001). Synthesis of heterocyclic nitrogen systems bearing systems 1,2,4- triazine moiety as anti-HIV and anti cancer drugs, Part III. *Pharmazie*, 56, 376 – 383.

El-Gendy, Z., Morsy, J.M., Allimony, H.A., Abdel-Monem, W.R., Abdel-Rahman, R.M. (2003). Synthesis of some new heterocyclic nitrogen systems bearing 1,2,4-triazine moiety as anti HIV and anti Cancer drugs- Part III. Phosphorous, *Sulfur, Silicon and the Related Elements*, 178 (9), 2055- 2071.

Gladis, J.M., Rao, T.P. (2004). Determination of trace amounts of gold in acid-attacked environmental samples by atomic absorption spectrometry with electrothermal atomization after preconcentration. *Anal. Bioanal. Chem*., 379, 60 - 65.

Hamza,A., Bashammakh, A.S., Al-Sibaai,A.A., Al-Saidi, H.M., El-Shahawi, M.S. (2010). Dual-wavelength *β*-correction spectrophotometric determination of trace concentrations of cyanide ions based on the nucleophilic addition of cyanide to imine group of the new reagent 4-hydroxy-3-(2-oxoindolin-3-ylideneamino)-2-thioxo-2H-1,3-thiazin-6(3H)-one. *Anal. Chim. Acta*, 657, 69-74.

Hassanien A.A. (2003). Phthalazinone in heterocyclic synthesis: Synthesis of some s-triazole, s-triazolothiadiazine and s- triazolothiadiazole derivatives as pharmaceutical interest. *Phosphorous, Sulfur, Silicon and Related Compounds*, 178, 1987 – 1997.

Jozlowski, C.A., Ulewicz, M., Walkowiak, W, Girek, T., Tablonska, J. (2002). The effect of tautomeric rearrangement on the separation of Zn(II) and Cd(II) in ion flotation process with 4-thiazolidinone derivatives. *Minerals Engneering*, 15, 677- 682.

Kadi, M.W., El-Shahawi, M.S. (2009). Differential pulse cathodic stripping voltammetric determination of uranium with arsenazo-III at the hanging mercury dropping electrode. *Radiochim. Acta*, 97, 613 - 620.

Miller, J.C. Miller,J.N. (1994). *Statistics for Analytical Chemistry* 4th edn. Ellis-Howood, New York, p.115.

Marczenko, Z. (1986). *Spectrophotometric determination of elements*, 3rd edition, Ellis Horwood Chichester, U.K, PP.68 -70, 203.

Pandy, J.K., Sengupta, S.K., Pandey, O.P. (2006). Synthesis and spectroscopic studies on oxo vanadium (IV) tetraza macrocyclic complexes derived from substituted β-diketones and 2, 6-diaminopyridine. *J. Indian.Chem. Soc*., 83, 107- 109.

Piper, J.R., DeGraw, J.I., Colwell, W.T., Johnson, C.A., Smith, R.L., Waud, W.R., Sirotnak, F.M. (1997). Analogues of methotrexate in rheumatoid arthritis. 2. Effects of 5-deazaaminopterin, 5, 10-Dideazaaminopterin, and Analogues on Type II Collagen-Induced Arthritis in Mice. *Eur.J. Med. Chem*., 40 (3), 377- 384.

Pulakesh, B. (2007). Synthesis and spectral properties of palladium (II) complexes derived from 5-methyl-3-formyl pyrole thiosemicarbazone and 5-alkyl/aryl dithiocarbazates. *J. Indian Chem. Soc*., 84, 544 -547.

Ramadan, A.T., Abdel-Rahman, R.M., El-Behairy, M. A., Ismail, A.I, Mahmoud, M.M. (1993). The Thermodynamics of complexation of transition and lanthanides metal ions by 3- (α-carboxy - methylaminobenzylidene hydrazine)- 5,6-diphenyl-1,2,4-triazine. *Thermochim. Acta*, 222 (2), 291-303.

Ramadan, A.T., Abdel-Rahman, R.M., Seada, M. (1992). Studies on complexes of copper (II), nickel (II), cobalt (II) and indium (III) with 3- (α-benzoyl)-benzylidenehydrazine - 5,6-diphenyl-1,2,4-triazine. *Asian J. Chem.*, 4, 569 - 574.

Rastogi, R.B, Yadav, M. J. (2005). Synthesis of some molybdenum (V) and tungsten (V) complexes of 1- aryl – 2, 5- dithiohydrazodicarbonamides. *J. Indian Chem. Soc.*, 82, 448 – 451

Sadasivan, V., Alaudeen, M. J. (2007). Synthesis and crystal structure of the zinc (II) complex of 5-(2, 3-dimethyl-1-phenyl-3-pyrazolin-5-one-4-ylhydrazono) hexahydropyrimidine-2-thioxo-4,5,6-trione. *Indian Chem. Soc.*, 46 (12) A, 1959- 1962.

Sadasivan, V., Alaudeen, M. (2006). A study on the arylazo coupling reaction of bis-(acetyl-acetone) ethylene diaminocopper (II) and bis-(acetyl)acetone)ethylenediaminenickel (II). *J. Indian Chem. Soc.*, 83, 1145- 1148.

Sawyer, D.T; W. R. Heinemann, W.R., Beebe, J. M. (1984). *Chemistry Experiments for Instrumental Methods*, John Wiley &Sons.

Sbirna, L.S., Muresan,V, Sbiren, S, Muresani, N. (2005). Complex compounds of nickel (II) with bidentate heterocyclic ligands using both S and N as donor atoms. *J. Indian Chem. Soc*, 82, 389 – 392.

Schachtner, J.E., Nienaber, J.,. Stachel, H.D., Waisser, K. (1999). Fused 1, 2-dithioles, V: Carbenoid anions as intermediates in reactions of pyrrothines and their heteroanalogues. *DiePharmazie*, 54 (5), 335 - 341.

Sharma, R.N., Giri, P., Kmari, A., R.N. Pandey, R.N. (2006). Synthesis, spectral and antifungal studies of some iron (II, III) and cobalt (II) complexes of 4-amino-3-ethyl-5-mercapto-5-triazole. *J. Indian Chem. Soc.*, 83, 1139-1143.

Sindhu S.K., Siddhu D.S., Aqarwal H., Chandra S.J. (2005). Cadmium (II) ion selective electrode based on pyridine-3-carboxaldehyde thiosemicarbazone. *J Indian Chem. Soc.*, 82, 472- 474.

Yonetoku, Y, Kubta, H, Okamoto,Y., Toyoshima, A., Funatsu, M., Ishikawa, J, Takeuchi, M, Ohta, M, Tsukamoto, S-I. (2006). Novel potent and selective calcium-release-activated calcium (CRAC) channel inhibitors. Part 1: Synthesis and inhibitory activity of 5-(1-methyl-3-trifluoromethyl-1H-pyrazol-5-yl)-2-thiophenecarboxamides. *Bioorg. Med. Chem.*, 14, 4750- 4760.

Zaki, M.T., Abdel-Rahman, R.M., El-Sayed, A.Y. (1995). Use of arylidenerhodanines for the determination of copper (II), mercury (II) and cyanide ions. *Anal. Chim. Acta*, 307, 127-138.

Table 1. Antibacterial activity of the prepared compounds

| Compound No.	Inhibition zones (mm) *				
	E.c	B.s	S.a	P.v	S.f
1	16	15	17	15	18
2e	18	15	16	15	17
5	14	16	15	14	17
6b	23	21	21	22	24
7	15	15	15	15	15
8e	16	15	14	15	15
9e	14	15	14	15	16
12a	26	24	20	21	25
12b	22	21	20	22	24
Streptomycin	25	22	21	21	30

* *E. coli*; *B. subtilis; S.. aureus*; *P.vulgaris* and *S. flexneri.*

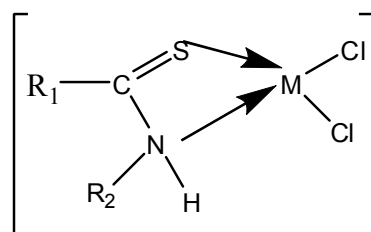Streptomycin: Reference antibiotics, Bristol-Myers Squibb, Giza, Egypt.

Highly active = inhibition zones > 19 mm; moderately active = inhibition zones 15 -19 mm and lethal active = inhibition zones 11-14 mm.
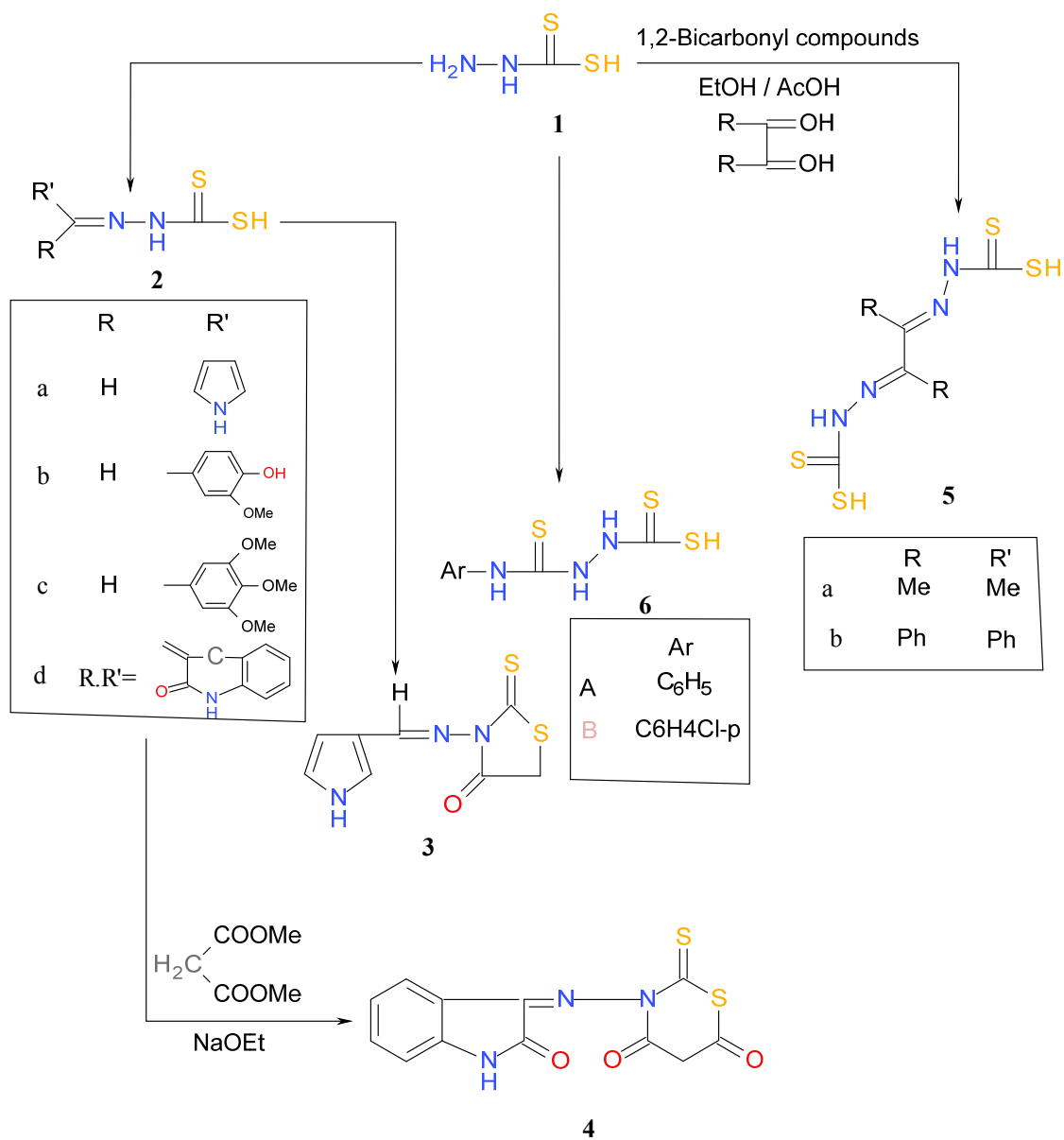
Scheme I
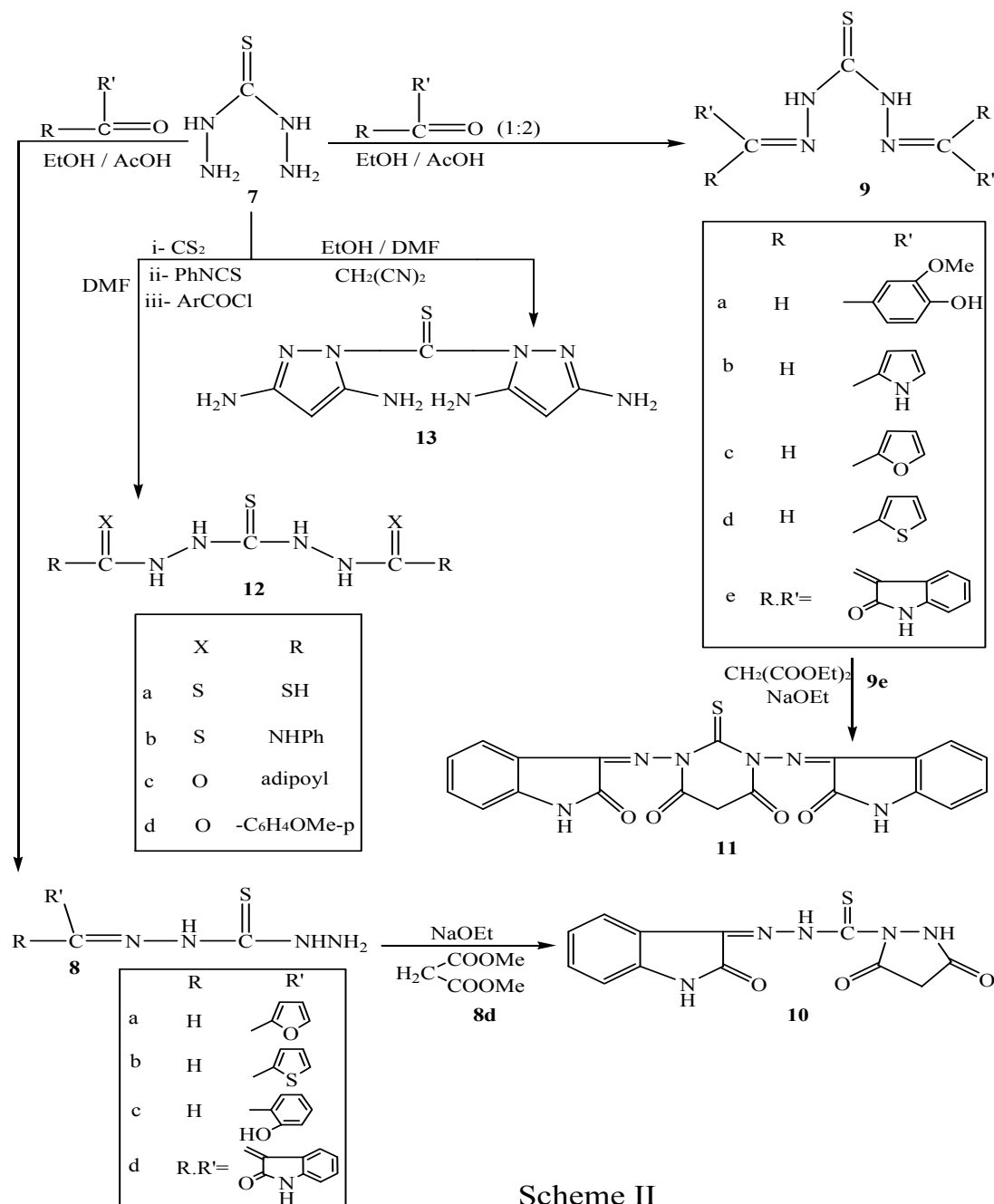
Scheme II

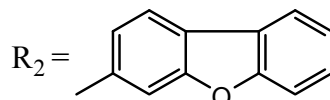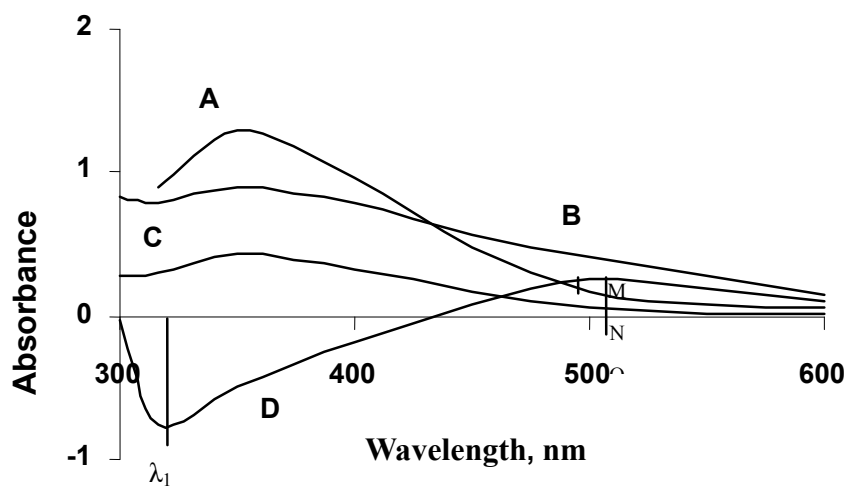$R_1 = O$-substituted heterocyclic

$R_2 =$

Figure 1.

Figure 2. Absorption spectra of reagent **4** and its mercury (II) complex at pH 5-6. Curve A is the spectrum of the reagent blank (reference water); B is mercury (II) complex (reference, water); C is the excess of reagent (reference water) and D is mercury (II) complex (reference, reagent blank).

Thermodynamics of Room Temperature Ionic Liquid BMIInCl$_4$

Jinsong Gui

College of pharmacy, Guilin medical college

PO box 541004, Guilin, China

Tel: 86-773-589-1689   E-mail: jinsonggui@163.com

Kaimei Zhu (Corresponding author)

College of pharmacy, Guilin medical college

PO box 541004, Guilin, China

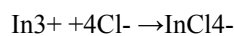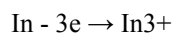Tel: 86-773-589-1689   E-mail: jinsonggui@glmc.edu.cn

Abstract

In a room temperature ionic liquid RTILs) BMIInCl4, he equilibrium constants were determined potentiometrically for the dissociation reaction: 2InCl4- = In2Cl7- + Cl- in the temperature range 313-348 K. The equilibrium constants K= [Cl-][In2Cl7-]/[InCl4-]2, pK = 76.43 – 780.9/T – 0.115T on different temperature. According to the thermodynamic relationship and the parameters of above equation, the dissociation entropy was determined.

Keywords: Thermodynamics, Equilibrium constants, BMIInCl4

1. Introduction

RTILs have received more attention because of their unusual properties lately . Sedon (1997,68, 351-356) and Gui (2010,84,760-765) reported that they have great potential as "green" solvents for industrial processes. It has been reported previously that the RTIL based on AlCl3 have been most widely studied (Endres, 2002,3, 144-154 and Ito, 2000,45,2611-22). However, there have been numerous studies in which transition metal chlorides were placed in RTILs for a variety of purposes. Hussey(1988,60,1763-1772) pointed out that InCl3 behaves much like AlCl3, that is, when the ratio of InCl3 to BMIC was equal to 1:1, InCl4- was main anion; when the ratio exceeded 1:1 anion In2Cl7- formed and when the ratio was less 1:1 some Cl- remained. In this paper RTILs BMIInCl4 was prepared .According Osteryoung' method(1979, 18, 1603-1605), on the temperature range of 313-348 K, the equilibrium constant K of the dissociation reaction was measured by following cell with liquid junction:

In│InCl3-BMIC(ref) |fritted disk |BMIC-InCl3(x)│In

In - 3e → In3+

In3+ +4Cl- →InCl4-

2InCl4- = In2Cl7- + Cl-
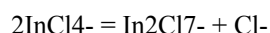
K' = [InCl4-] / [Cl4-]4 [In3+]

E = (RT/3F) ln [In3+]/[In3+(ref)]

E = (RT/3F) ln [InCl4-(ref)]/[InCl4-] + (4RT/3F) ln [Cl-]/[Cl-(ref)]

Where [ ] means a new concentration scale, which is defined that the number of moles of the species per kilogram melt .Where (ref) means reference one, x means mole fraction of InCl3 in InCl3 and BMIC mixture, Indium electrode was regarded as a reversible one and its electrode reaction is above.Corresponding Nernst Equation of this cell is received.Where E means emf of cell, [In3+(ref)] and [In3+] are activity of In3+ in reference electrode compartment and in working electrode compartment, respectively. It is noted that liquid junction potential Ej across the fritted disk may be neglected by Torsi(1971,10,1900-1902)

Through a series of the substitution of equation into equation, a pCl- electrode was yield.Hence, in this case, working electrode in the cell may be used as a pCl- one. Our purpose in the paper is to calculate the dissociation constant K and to obtain the dependence of pK on T. Considering the dissociation reaction, other thermodynamic quantities were obtained.

2. Experimental

2.1 Reagente

1-methylimidazole(AR grade reagent ACROS) and chlorobutane (AR grade reagent, Beijing Chem. Co) were used as received. The purity of Indium as reference electrode is 0.9999 produced from Kermio. Chem. Co, Tianjin. Ethyl acetate and acetonitrile were distilled and then stored over molecular sieves in tightly sealed glass bottles, respectively. Anhydrous $InCl_3$ was purchased from Aldrich, opened in the glove box filled with dry argon, and used without further purification.

2.2 Preparation of 1-methyl-3-butylimidazole chloride

1-methyl-3-butylimidazole chloride (BMIC) was synthesized by refluxing the 1-methylimidazole with a large excess four double of chlorobutane at 323K for 4 h and react 20h at room temperature. Then the excess cholrobutane was removed by evaporation and the crude product was recrystalized from acetonitrile/ethylacetate. The resulting white precipitate was isolated filtration and then dried in vacuo for 20h.The mp of the product is (T-273)=66-68K.NMR spectrum is good agreement with the literature of Dyson(1997,3465-9) and Yang et al (2004, 6: 541-543).

2.3 Prepareation of ionic liquid

All glasswares that contacted the RTLI were cleaned in hot dilution nitric acid and washed in doubly deionized water, and then were backed dry in 393k over and stored in desiccator before use. In the cell in a dry agon atmosphere glove box, BMIC were firstly prepared. $InCl_3$ mole fraction X=0.48 was simple added to cell. In order to avoid thermal decomposition, the ieces of $InCl_3$ added slowly , with stirring. The ionic liquid was formed and was brown.

2.4 Procedure of the titration

The electrochemical cell was made of Pyrex, which employed for the potentiometric titrations.The reference electrode compartment, containing X = 0.48 $InCl_3$ ionic liquid of $BMIInCl_4$ as electrolyte and coiled polishing Indium wire as reference electrode, was isolated with a fritted Pyrex disk. The electrolyte level in the reference electrode compartment was maintained very slightly higher than that of bulk solution. Initial bulk cell solution is the same with that in reference electrode compartment.

Equilibrium was reached about 1h after each addition of $InCl_3$.The potentials of cell were measured at the 313.15, 323.15, 333.15 and 343.15, 348.15K by means of a SDC-Ⅱ type digital potentiometer calibrated. The criterion for the attainment of equilibrium was taken a steady reading within ±0.5mv for a period of about 0.5 minute.The emf was measured.

3. Results and Discussion

The values of cell emfs in the temperature range of 313.15K to 348.15K are listed in Table 1, where each one is the average of four readings. Table1 illustrate the results of experimental titrations from approximately $XInCl_3$=0.48 to 0.55 in ionic liquid. The overall features of the titration jump is distinct from those obtained resulting in a greater pCl- range.When the composition range was near 50.00 mole % $InCl_3$, that is titration jump just. When composes $XInCl_3$ =(50.0±0.2)%, in the system, activity coefficient and the activity of working electrode and reference electrode were approximately equal, the first item may ignore in the eq. E = (RT/3F) ln [InCl4-(ref)]/[InCl4-] + (4RT/3F) ln [Cl-]/[Cl-(ref)]. Then emf E for the cell was given by E = (4RT/3F) ln [Cl-]/[Cl-(ref)].The number of moles of $InCl_3$ added to reach the midpoint of the titration curve was taken to be equal to number of moles of free Cl- initialling in BMIC.With this information, using E, the [Cl-] at the equivalence point was calculated. At the equivalence point [Cl-]=[In2Cl7-].Since [InCl4-] is known, that is,[InCl4-]=number of moles of mass of melt. The unite of mass was kilogram. Then the dissociation constant, K = [Cl-][In2Cl7-]/[InCl4-]2, was to be calculated.

pK = -lgK,and were readily calculated with K = [Cl-][In2Cl7-]/[InCl4-]2 (note that K expressed as above is numberically the same on other concentration scales). The values of pK in the temperature range 313.15-348.15K are fitted with the method of least squares with empirical equation of the form.So pK = A1 + A2(K/T) + A3(T/K).The values of the parameters obtained are e A1=75.461,A2=-7801.912,A3=-0.1111. The standard fit deviation is 2.175×10-2.The standard molar thermodynamic functions ΔGm°, ΔHm°, ΔSm°, for the dissociation reaction are related to the parameters of above quation.

ΔGm°= Rln10[A1(T/K)+A2+A3(T/K)2]

ΔHm°= Rln10[A2- A3(T/K)2]

ΔSm°= -Rln10[A1+2 A3(T/K)]

The values of the thermodynamic function ΔGm°, ΔHm°,ΔSm°calculated from above equations are listed in Table

2.From Table 2. $\Delta Gm° > 0$ means that the dissociation reaction can not occur spontaneously under the condition of constant temperature and pressure. The Gibbs free energy includes two factors: $\Delta Hm°$ and $T\Delta Sm°$. In dissociation reaction $\Delta Hm° > T\Delta Sm°$ leads us to conclude that enthalpy of dissociation is the dominant thermodynamic factor which hinders dissociation reaction from occurring. When InCl3 and BMIC quantities 1:1, [InCl4⁻] stable existence in system, namely BMIInCl4 is only pure solute in solution.

References

Dyson, P.J,Grossel, M.C., Srinivasan, N, Vine, T., Welton, T, Williams, D.J., White, J.P., Zigras, T.J. (1997). Chem.Soc. and Dalton trans. *Inorg.Chem*, 3465-9.

Endres, F. (2002). *CHEMPHYSCHEM*, 3, 144-154.

Gui, Jinsong. (2010). Properties of room temperature ionic liquid-3-ethyl-1-methylimidazolium ethyl sulfate. *Russian Journal of Physical Chemistry A, Focus on Chemistry*, 84(5):760-765.

Gale, R.J., Osteryoung, R.A. (1979). *Inorganic Chemisty*, 6, 1603-1605.

Hussey, C.L. (1988). *Pure Appl.Chem.*, 60, 1763-1772.

Ito, Y and Vohira, T. (2000). *Electrochemica.Acta*, 45, 2611-22.

Lu, Xingmei, Xu, Weiguo and Gui, insong, et al. (2005). Volumetric properties of room temperature ionic liquid 1. The system of {1-methyl-3-ethylimidazolium ethyl sulfate + water} at temperature in the range (278.15 to 333.15) K.J.*Chem.Thermodynamics*, 37:13-19.

Sedon, KR. (1997). *J, chem..Technol.Biotechnol*, 68,351-356.

Torsi, G and Mamantov, G. (1971). *Inorg.Chem*, 10,1900-1902.

Yang, Jiazhen, Lu, Xingmei, Gui Jinsong, et al. (2005). Volumetric properties of room temperature ionic liquid 2: The concentrated aqueous solutions of {1-methyl-3-ethylimidazolium ethyl sulfate+water} in a temperature range of 278.2K to 338.2K.J.*Chem.Thermodynamics*, 2005, 37: 1250-1255.

Yang, Jiazhen, Lu, Xingmei and Gui, JinSong, et al. (2004). A new theory for ionic liquids-the Interstice Model Part 1.The density and surface tension of ionic liquid EMISE. *Green Chem.*, 6: 541-543.

Zhang, Qingguo, Yang, Jiazhen and Lu, Xingmei, et al. (2004). Studies on an ionic liquid based on FeCl3 and its properties. *Fluid Phase Equilibria.*, 226:207-211.

Table 1. The emf values of cell at different temperatures

T/K	313.15	323.15	333.15	343.15	348.15
X(InCl3)	E/V				
0.4804	0.00001	0.000017	0.000016	0.000016	0.000016
0.4851	0.04067	0.054961	0.06545	0.08176	0.09216
0.4908	0.07742	0.081395	0.09935	0.097555	0.11321
0.4950	0.47543	0.490628	0.50593	0.480828	0.30601
0.4974	0.84194	0.860258	0.86880	0.83208	0.78388
0.5000	1.00817	1.045791	1.068348	1.063911	1.0254
0.5026	1.09712	1.100045	1.097971	1.076273	1.08171
0.5051	1.14161	1.162603	1.156253	1.147941	1.12751
0.5074	1.18452	1.182381	1.171732	1.163065	1.13348
0.5101	1.19844	1.199988	1.193125	1.181232	1.15981
0.5148	1.21745	1.211952	1.205805	1.194038	1.17421
0.5201	1.24703	1.244574	1.242285	1.222213	1.20834
0.5302	1.27104	1.267175	1.260243	1.248743	1.22327
0.5501	1.32009	1.321288	1.321745	1.309425	1.28269

Table 2. The values of thermodynamic function for dissociation reaction at different Temperatures

T/K	313.15	323.15	333.15	343.15	348.15
$\Delta Gm°/kJ.mol^{-1}$	88.22	89.01	88.45	88.15	88.00
$\Delta Hm°/kJ.mol^{-1}$	108.91	94.67	79.63	66.24	59.04
$\Delta S m°/J.K^{-1}mol^{-1}$	60.12	16.06	-27.64	-72.60	-96.50

Preliminary Design of Semi-Batch Reactor for Synthesis 1,3-Dichloro-2-Propanol Using Aspen Plus

Herliati, Robiah Yunus, A.S. Intan & Z.Z.Abidin

Department of Chemical and Environmental Engineering, Faculty of Engineering

Universiti Putra Malaysia, Serdang 43400, Selangor, Malaysia

Tel. 60-3-8946-6288   E-mail: herliati2004@yahoo.com

Dzulkefly Kuang

Department of Chemistry, Faculty of Science

Universiti Putra Malaysia, Serdang 43400, Selangor, Malaysia

Abstract

Glycerin is a key byproduct from the biodiesel production process. Due to the rapid growth in biodiesel production, the market has been flooded with the crude natural glycerin. This crude glycerin (glycerol) has a very low value because of its impurities, and consequently, a great interest has emerged in the development of technology for alternative uses of glycerol. Among the various possibilities, a technology to convert glycerol to 1,3-dichloro-2-propanol has caught our attention. This compound can be subsequently converted into epichlorohydrin, which is an important intermediate in the production of epoxy resins. 1,3-dichloro-2-propanol is currently being synthesized from propylene via allyl chloride route. However, our technology uses crude natural glycerin, the byproduct of biodiesel production plant, as the starting material and hydrochloric acid as the reagent. The present paper discusses the simulation work on the semi-batch reactor for the production of 1,3-dichloro-2-propanol using ASPEN PLUS. The simulation results were then compared with the experimental data.

Keywords: Aspen plus, Dichloropropanol, Epichlorohydrin, Semi-batch, Design

1. Introduction

Biodiesel as an alternative, environmentally friendly, and renewable energy has been produced on a large scale. However one of the main problems in the production of biodiesel is the formation of significantly amount of glycerol (10 wt%) as a by-product (McCoy, 2006; Zheng, Chen, & Shen, 2008). This has resulted in the over supply of glycerol in the industrial market and decrease the commercial value of glycerol. This scenario has attracted attention from many researchers to develop alternative routes to utilize crude glycerol in the production of useful intermediates or final products. One of the promising methods to convert glycerol to high-value chemicals is the chlorination reaction for preparing 1,3-dichloro-2-propanol or α,γ-Dichlorohydrin (α,γ-DCH), which is the an important intermediate in the process for synthesizing epichlorohydrin (Krafft, Gilbeau, Balthasart, & Paganin, 2008; Kubicek, 2005; Ma, Zhu, Yuan, & Yue, 2007; Siano et al., 2006; Tesser, Santacesaria, Di Serio, Di Nuzzi, & Fiandra, 2007). Since this compound is highly toxic, harmful if inhaled, and reported as causing cancer, this compound must be handled with care (Giri, 1997).

Tesser et al had carried out chlorination reactions experimentally for preparing α,γ-DCH from glycerol and gaseous hydrochloric acid. Their experiment focused on the determination of the reaction kinetics. The reaction was performed in the presence of malonic acid, as a catalyst, and the temperature range was set at 80-120°C. The HCL flow rate, glycerol loaded, and catalyst concentration were kept constant at 24 g/min, 200 g, and 8% (mol/mol) respectively. Based on the literature, the HCL flow rate and catalyst concentration have marked effects on the reaction selectivity of the chlorination reaction but the extent of the effect has not been reported (F.Kastanek, J.Zahradnik, J.Kratochvil, & J.Cermak., 1993). Therefore, investigating the effect of HCL flow rate and catalyst concentration on the preparation of α,γ-DCH would become the initial step taken in this study.

Consequently, the aim of this paper is to present the simulation results obtained from Aspen Plus simulator software carried out on the semi-batch stirred tank reactor by considering the effects of both HCL flow rate and catalyst concentration on reaction selectivity and yield for α,γ-DCH. The reactor block utilized in the simulation was RBatch which is suitable for a semi-batch reactor process (AspenTech., 1999)
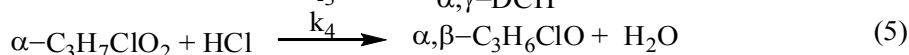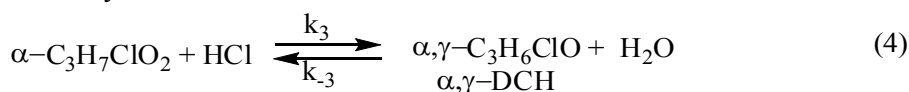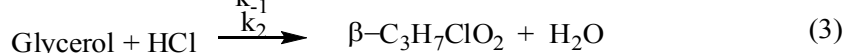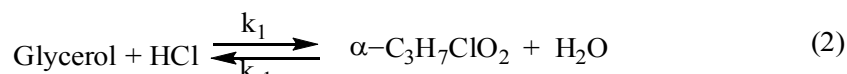
2. Modeling Approach

2.1. Chemical Reactions and Kinetic Parameters

Tesser et al. (2007) have reported that the overall reaction scheme for preparing α,γ-DCH, starting from glycerol and hydrochloric acid, is as follows:

$$\text{Glycerol} \quad\quad\quad\quad \text{1,3-dichloro-2-propanol} \tag{1}$$
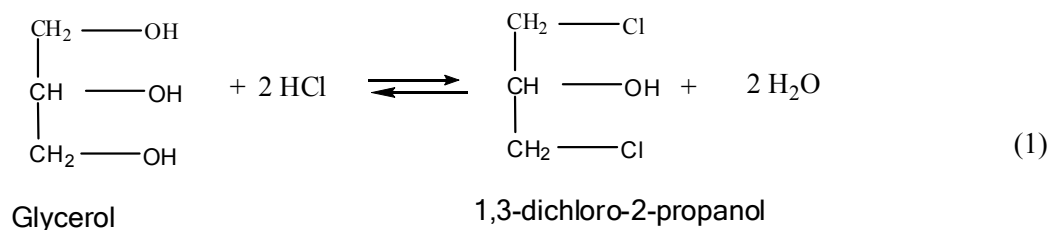
This reaction starts with the chlorination of the glycerol, which mostly forms α-monochlorohydrin (α-MCH) and water, with small quantity of β-monochlorohydrin (β-MCH), followed by a second chlorination from which the required product, α,γ-DCH was mainly obtained and very small amounts of α,β-DCH. Relation 1 can be broken down into four distinct reactions, which are as follows:

$$\text{Glycerol} + \text{HCl} \underset{k_{-1}}{\overset{k_1}{\rightleftarrows}} \alpha-\text{C}_3\text{H}_7\text{ClO}_2 + \text{H}_2\text{O} \tag{2}$$

$$\text{Glycerol} + \text{HCl} \xrightarrow{k_2} \beta-\text{C}_3\text{H}_7\text{ClO}_2 + \text{H}_2\text{O} \tag{3}$$

$$\alpha-\text{C}_3\text{H}_7\text{ClO}_2 + \text{HCl} \underset{k_{-3}}{\overset{k_3}{\rightleftarrows}} \alpha,\gamma-\text{C}_3\text{H}_6\text{ClO} + \text{H}_2\text{O} \tag{4}$$
$$\alpha,\gamma-\text{DCH}$$

$$\alpha-\text{C}_3\text{H}_7\text{ClO}_2 + \text{HCl} \xrightarrow{k_4} \alpha,\beta-\text{C}_3\text{H}_6\text{ClO} + \text{H}_2\text{O} \tag{5}$$

The kinetic parameters of the reactions are shown in Table 1 (Tesser,2007).

2.2 Aspen plus Simulation

Table 2 shows the reactor characteristic and feed materials used in the Aspen Plus simulation.

In this work, both parameters HCL flow rate and catalyst concentration (% by moles of glycerol loaded into the reactor), were varied as presented in Table 2. The simulation analyzed the effects of the parameters mentioned above on selectivity and yield of reaction. The following equations were used for selectivity and yield calculation (Felder & W, 2004):

$$\text{selectivity for } \alpha,\gamma-\text{DCH} = \frac{\text{moles of } \alpha,\gamma-\text{DCH produced}}{\text{total moles of } \alpha\text{-MCH}, \beta\text{-MCH, and } \alpha,\beta\text{-DCH produced}}$$

$$\text{Yield for } \alpha,\gamma-\text{DCH} = \frac{\text{moles of } \alpha,\gamma-\text{DCH produced}}{\text{moles of glycerol fed}}$$

3. Simulation Result and Model Validation

3.1 Model Validation

In order to validate the proposed model, experimental data from glycerol chlorination in a lab-scale semi-batch stirred tank reactor reported by Tesser et.al (2007) was used to validate the simulation. Tables 1 and 2 show the kinetic parameters and reactor characteristics used in the simulation. The simulation results in terms of reaction selectivity and glycerol conversion are compared with the experimental data. The results are shown below.

<Figure 1-Figure 3>

Figures 1 and 2 show the simulation results as compared to the experimental data for glycerol conversion and reaction selectivity at five different temperatures in the range of 80 – 120°C. Simulation results and experimental data for products composition versus time of the reaction is shown in Figure 3. These figures show that there is a strong agreement between Aspen Plus simulation results and experimental data. Thus, we can conclude that the

Aspen Plus simulation can indeed be used in our study to guide us in the analysis of the performance of the chlorination reaction using the crude glycerol.

<Figure 4>

Furthermore, several simulation runs had also been carried out in order to investigate effect of HCL flow rate and catalyst concentration on selectivity and yield for α,γ-DCH preparation. Selectivity and yield of α,γ-DCH decreased over the HCL flow rate range from 4 to 24 g/min as shown in Figure 4. It is in good agreement compared qualitatively to data from the literature. Rose (1981) reported that the gas feed rate to the stirred tank should be not more than what is called flood point of the impeller in order to prevent spinning of agitator in a bubble of the gas that have marked on the reaction (L.M.Rose, 1981). In contrast, catalyst concentration does not significantly affect the selectivity and yield for α,γ-DCH preparation as depicted in Figure 5.

<Figure 5>

4. Conclusion

In the present paper, a simulation study was carried out on the α,γ-DCH preparation in a semi batch stirred tank reactor (SBSTR) using the Aspen Plus simulation software. The resulting simulation results were used to predict the performance of SBSTR in terms of selectivity and yield. Effect of both HCL flow rate and catalyst concentration had also been investigated. While lower HCL flow rate improves the chlorination process on both the selectivity and yield of α,γ-DCH, the catalyst concentration does not have significant effect on the process. The findings from these simulation results can be used in our experimental work to develop the technology to convert crude glycerol to 1,3-dichloro-2-propanol and subsequently into epichlorohydrin, which is an important intermediate in the production of epoxy resins.

Acknowledgement

References

AspenTech. (1999). *Introduction to ASPEN PLUS, Based on Aspen Plus 10.1*.

F.Kastanek, J.Zahradnik, J.Kratochvil, & J.Cermak. (1993). *Chemical Reactors for Gas-Liquid System* (1st ed.). New York: Czech Republic.

Felder, R. M., & W, R. R. (2004). *Elementary Principles of Chemical Processes*. New York: Wiley.

Giri, A. K. (1997). Genetic toxicology of epichlorohydrin: a Review. *Mutation Research,* 386: 25-38.

Krafft, P., Gilbeau, P., Balthasart, D., & Paganin, M. (2008). Manufacturing dichloropropanol involves reacting glycerol with pressurized hydrogen chloride, followed by subjecting to a treatment for reducing weight ratio between hydrogen chloride and water, and/or between the water and dichloropropanol: WO2008110588.

Kubicek. (2005). Method of Preparing Dichloropropanol From Glycerol. *World Intellectual Property Organization* US: WO 2005/021476 A1

L.M.Rose. (1981). *Chemical Reactor Design in Practice*. New York: Amsterdam.

Ma, L., Zhu, J. W., Yuan, X. Q., & Yue, Q. (2007). Synthesis of epichlorohydrin from dichloropropanols: Kinetic aspects of the process. *Chemical Engineering Research & Design*, 85(A12): 1580-1585.

McCoy, M. (2006). *Bussiness Glycerin Surplus:* Plants are closing, and new uses for the chemical are being found. 84(6).

Siano, D., Santacesaria, E., Fiandra, V., Tesser, R., Di Nuzzi, G., Di Serio, M., & Nastasi, M. (2006). Continuous regioselective process for the production of 1,3-dichloro-2-propanol from glycerin and hydrochloric acid in the presence of organic carboxylic acid catalyst., *World Organization Patent*.

Tesser, R., Santacesaria, E., Di Serio, G., Di Nuzzi, G., & Fiandra, V. (2007). Kinetics of Glycerol Chlorination with Hydrochlorc Acid. *Ind. Eng. Chem. Res*, 46: 6456-6465.

Zheng, Y. G., Chen, X. L., & Shen, Y. C. (2008). Commodity Chemicals Derived from Glycerol, an Important Biorefinery Feedstock. *Chemical Reviews*, 108(12): 5253-5277.

Table 1. Kinetic parameters

T (^{o}C)	K_1^a	k_2^a	K_3^a	K_4^a	K_1	K_3
80	7667±940	450±41	714±227	8±3	3846	194
100	13274±1692	1089±87	1784±407	26±7	2470	146
120	27411±2861	2215±170	2179±685	31±13	1660	113

^{a} Kinetic constant are expressed in cm^3/(mol min)

Tabel 2. Set up Parameters used in the Simulation

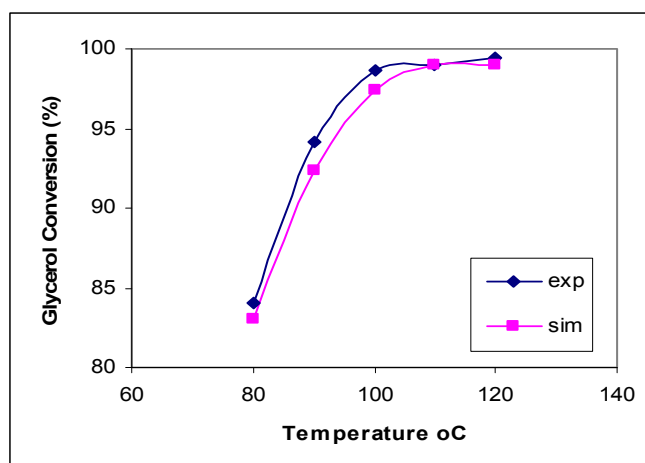| Reactor Block	RBatch
Base Method	Wilson
Input Variable	
Temperature (^{o}C)	110
Pressure (bar)	1.05
Chemical reactions	Reaction 2 to 5
Kinetics rate constant	From Table 1
Feed of Reactor	
HCL flow rate (g/min)	4, 8, 12, 16, 20, 24
Concentration of malonic acid catalyst (%)	2,4,6,8,10

Figure 1. Effect of Temperature on Glycerol conversion. Glycerol loaded: 200g; HCL flow rate: 24 g/min; Catalyst concentration: 8% by moles; reaction time: 2.5 h
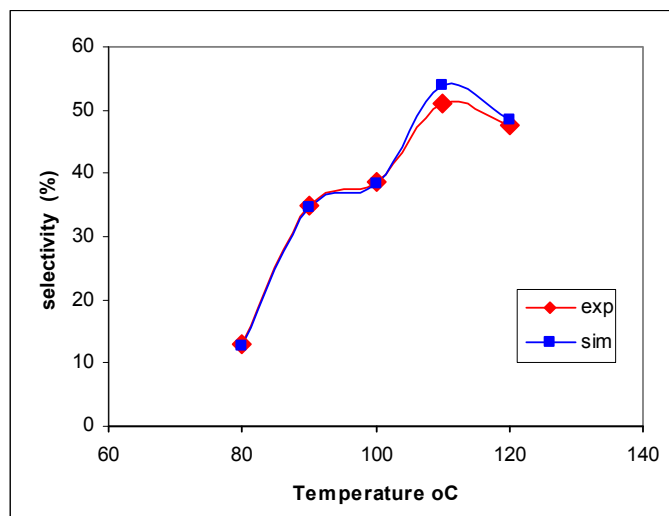
Figure 2. Effect of Temperature on reaction selectivity. Glycerol loaded: 200g; HCL flow rate: 24 g/min; Catalyst concentration: 8% by moles; reaction time: 2.5 h
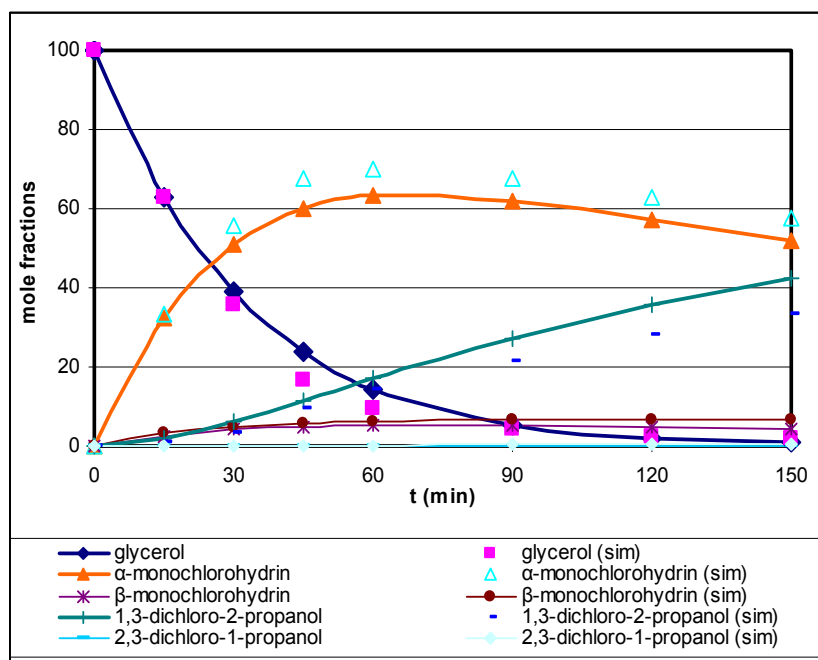

Figure 3. Evolution in time of Products composition. Glycerol loaded: 200g; HCL flow rate: 24g/min; Catalyst concentration: 8% by moles; reaction temperature: $110^{o}C$
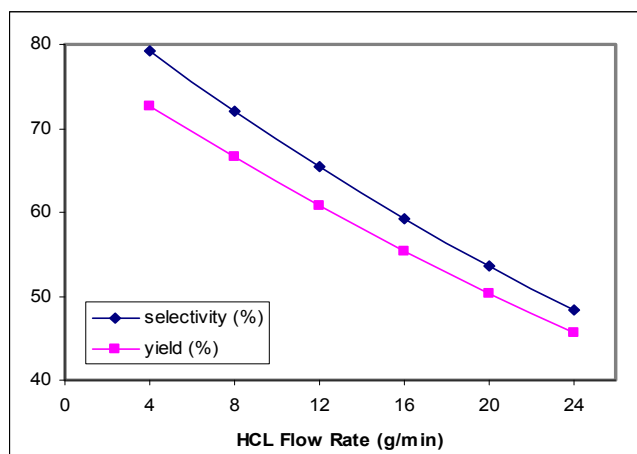
Figure 4. Effect of HCL flow rate on selectivity and yield predicted by the simulation. Glycerol loaded: 200g; Catalyst concentration: 8% by moles; reaction temperature: 110°C; reaction time: 2.5 h
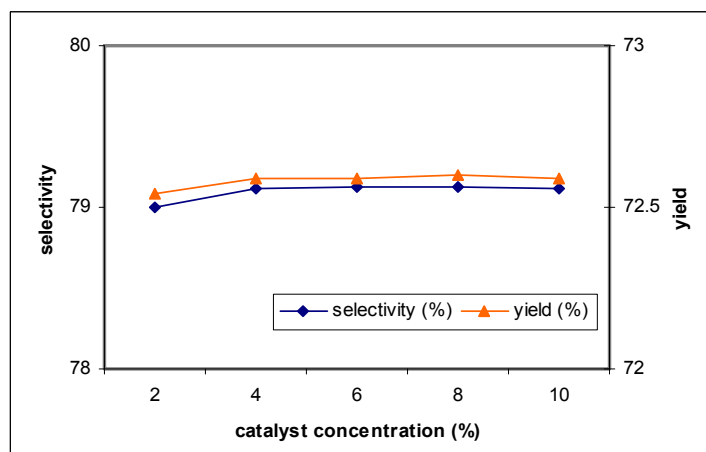

Figure 5. Effect of catalyst concentration on selectivity and yield predicted by the simulation. Glycerol loaded: 200g; HCL flow rate: 4 g/min; reaction temperature: 110°C; reaction time: 2.5 h

Simultaneous Determination of Ephedrine and Pseudoephedrine in Mice Plasma by Capillary Zone Electrophoresis

Chunmei Zhang

College of Pharmacy, Hebei University

Baoding 071002, Hebei, China

E-mail: zhangcm19850304@126.com

Huaizhong Guo (Corresponding author)

College of Pharmacy, Hebei University

Baoding 071002, Hebei, China

E-mail: ghuaizh@yahoo.com.cn

Li Guan, Weiquan Zhang, Qian Wen & Chunying Chen

College of Pharmacy, Hebei University

Baoding, Hebei, 071002, China

Abstract

A low cost, accurate, rapid and sensitive capillary zone electrophoresis (CZE) quantitative method, using thiamine hydrochloride as internal standard (IS), was developed for the simultaneous analysis of ephedrine and pseudoephedrine in mice plasma. Analytes were extracted from plasma samples by n-hexane/dichloromethane/isopropanol (2:1:0.1, v/v/v) after alkalization, and stripped with 1.5% hydrochloric acid solution. Separation was performed by CZE using 50mM borax-20mM threonine (pH 9.27) as running buffer, with voltage of +10 kV applied and UV detection wavelength at 210 nm. The total running time was within 10 min. Calibration curves for plasma samples were linear over the concentration range of 0.075-5.0 μg/mL for ephedrine and 0.0375-2.5 μg/mL for pseudoephedrine. The method had a limit of quantitation of 17.80 ng/mL for ephedrine and 22.00 ng/mL for pseudoephedrine, respectively. The method was reliable and feasible for the evaluation of pharmacokinetic profiles of drug products containing ephedrine and pseudoephedrine.

Keywords: Ephedrine, Pseudoephedrine, Capillary Zone Electrophoresis

1. Introduction

Ephedrine (E) and Pseudoephedrine (PE) are pairs of diastereoisomeric sympathomimetic amines that have human central nervous system stimulating properties, and they also can relieve the spasm of the bronchial smooth muscle (Lou Hong-gang, 2010, PP.682-688, Kang Yong, 2001, PP.37-39). Several methods have been employed for the detection of the individual component in plasma, including HPLC (Aymard G. 2000, P.25, Roman MC. 2004, PP.15-24), LC-MS/MS (Beyer J. 2007, PP.150-160, Yi Feng, 2008, P.572), GC-MS (Gunn J. 2010, PP.37-43, Nakano M. 2000, PP.583-586) and CE (Wei F. 2007, PP.38-44, Liu Gang, 2006, P.617). Recently, a GC-MS/SIM method was reported for the simultaneous determination of E and PE in humn plasma through liquid–liquid extraction and derivatization by trifluoroacetic anhydride (TFA) with a lower limit of quantitation (LOQ) of 2 and 1ng/mL for E and PE, respectively (Shen Qun, 2002). Although the method achieved sufficient detection sensitivity in short run time, it suffered from high cost and time-consuming extraction procedure. Therefore, a highly sensitive and simple CZE method was developed and validated for the simultaneous determination of E and PE in mice plasma. This developed method offered smaller sample volume requirement and shorter run time, especially lower cost. This method can be flexibly applied to a bioequivalence study.

2. Experimental

2.1 Materials and reagents

E was purchased from national institute for the control of pharmaceutical and biological products (Beijing, China), and PE was obtained from national narcotics laboratories (Beijing, China). Thiamine hydrochloride manufactured by the Medical Chemical Reagent (Tianjin, China) was used as the internal standard (IS). HPLC grade methanol was purchased from Kermel Chemical (Tianjin, China). Borax and all the other reagents used in the experiment were all of analytical grade and obtained from Huaxin Chemical Reagent (Baoding, China). Blank mice plasma was obtained from the experimental animals center of Hebei Medical University (Shijiazhuang, China). Ultrapure water was obtained from AK water treatment system (Taiwan, China).

2.2 Instrumentation

High Performance Capillary Electrophoresis system (Cailu Co. Ltd, Beijing, China) is with a 0-30 kV high voltage power supply, and a variable wavelength UV detector near the column end. Data acquisition and procession were performed using HW-2000 software (Qianpu Co. Ltd, Shanghai, China). Capillaries with 50 μm I.D. and 375 μm O.D.(Yongnian Ruifeng Photoconductive Fiber Factory, Hebei, China). Buffer pH was measured with a PHS-3C pH meter (Shanghai, China). A vortex mixer (QL-901, Haimen Medical Instrument, Jiangsu, China) was used to extract the analytes and a centrifuge (L500, Xiangyi Centrifuge Instrument Co. Ltd, Changsha, China) was used to accelerate the separation of organic and inorganic phases.

2.3 CZE conditions

Before the experiment, the capillary column should be pretreated. Firstly, the capillary column was rinsed with 1.0 M NaOH solution for 30 min and then with water until the pH value of the outlet solution reached 7.0. Secondly, the capillary was rinsed with 1.0 M HCl solution for 30 min and then with water until the pH value of the outlet solution reached 7.0.

Then, the conditions of the experiment were optimized with a fused-silica capillary of 50 cm×40 μm (40 cm effective length) in a running buffer of 50 mM borax-20 mM threonine (the pH value was adjusted to 9.27 with 1 M NaOH solution) and an applied voltage of +10 kV at room temperature. Samples were introduced by hydrodynamic injection (15 cm×30 s) and the detection wavelength was 210 nm.

2.4 Preparation of mixed stock and working solutions

The mixed stock solutions of E and PE were prepared together by dissolving accurately weighed reference standards in methanol to result in a final concentration of 1mg/mL for E and 0.5 mg/mL for PE. Standard working solutions were prepared by diluting the mixed stock solutions with methanol to get six different concentrations in a range of 0.3-20 μg/mL for E and 0.15-10 μg/mL for PE. IS working solution was prepared with 1.5% hydrochloric acid solution to the nominal concentration of 10 μg/mL.

2.5 Preparation of standard and quality control samples

100 μL of each of the above different concentration working solutions was added to 400 μL blank mice plasma to obtain the desired series plasma concentration of analytes. The plasma concentrations of calibration standards were 0.075, 0.125, 0.25, 0.5, 1.25, 5.0 μg/mL for E and 0.0375, 0.0625, 0.125, 0.25, 0.625, 2.5 μg/mL for PE, respectively. The quality control (QC) samples were prepared in the same way as the calibration standards to obtain plasma concentrations of 0.125, 0.5, 5.0 μg/mL for E and 0.0625, 0.25, 2.5 μg/mL for PE. All of these plasma samples were kept at -20 $^{\circ}$C before use.

2.6 Sample preparation

(1) Liberation and organic solvent extraction

In 15 mL centrifuge tubes, a standard sample (mentioned above) was mixed with 0.5 mL, 2 M NaOH, and the analytes were liberated from plasma by vortex-mixing for 1 min. 4 mL mixed organic solutions of n-hexane/dichloromethane/isopropanol (2:1:0.1, v/v/v) was added and vortex-mixed for 3 min, then the analytes diverted into the organic phase. After centrifugation with 5000 rmp for 6 min, the organic phase was transferred to another centrifuge tube.

(2) Back extraction

100 μL IS working solution was added and the mixture was back extracted by vortex-mixing for 3 min. Discarding the upper organic phase after centrifugation with 5000 rmp for 6 min. The lower aqueous phase was dried in 75 $^{\circ}$C water bath, and then the residues was dissolute in 10 μL ultrapure water to obtain the enriched analytes, which was analyzed by CZE subsequently.

3. Results and discussion

3.1 Optimization of CZE conditions

The influence of the separation voltage on the separation efficiency was evaluated. The separation voltage at +20, +15 and +10 kV were tested. The electropherograms in fig. 1 obviously showed that optimum separation voltage was +10 kV.

With the increasing of the injection time, the intensity of the signals of analytes increased, generally to obtain the high sensitivity. A standard mixture was injected into the capillary at different time between 10 s and 40 s by hydrodynamic injection, keeping the sampling height constant at 15 cm. The results indicate that peak areas are proportional to the injection time up to 40 s. However, when an injection time was longer than 30 s, so did peak broadening and worse resolution presented. Thus, an injection time of 30 s was selected.

3.2 Selection of sample preparation conditions

Due to the low concentration of E and PE in human plasma, the high extraction efficiency and sample enrichment is in need. The developed extraction method could avoid the interference of endogenous compounds and overcome the shortcoming of low recovery rate through the process of basification, extraction followed by acidification. Additionally, the investigation for the organic extractant indicated that the extraction efficiency with the mixture of *n*-hexane-dichloromethane-isopropanol as extractant was obviously higher than that with the cyclohexane-dichloromethane as extractant. Simultaneously, this work studied the effects of the different hydrochloric concentrations (0.3%, 0.5%, 1.0%, 1.5%, 2.0%) on the extraction efficiency for the analytes. The results indicated that the higher recoveries with the increase of the hydrochloric concentrations, but when 2.0% hydrochloric solution was used, extraction efficiency has no obvious change compared with 1.5% hydrochloric solution, so 1.5% was chosen.

3.3 Method validation

3.3.1 Separation and specificity

The CZE-based method in this paper was investigated by analyzing the blank plasma sample, spiked plasma samples and mice plasma sample, and their electropherograms were shown in Fig. 2, Fig. 3 and Fig. 4. Under the CZE conditions described above, the migration time was about 7.210 min for IS, 7.857 min for E and 9.292 min for PE, respectively. There were no interference peaks found at the migration times of the two analytes and IS.

3.3.2 Linearity

Calibration curves for plasma were good linear over the concentration range of 0.075-5.0 μg/mL for E and 0.0375-2.5 μg/mL for PE. Typical equations of calibration curves were as follows: for E, C=2.688A+0.1999 (r=0.9982), and for PE, C= 3.322A+0.1418 (r=0.9988), where A=peak-area ratio and C=concentration (μg/mL).

3.3.3 LOQ and LOD

The current assay had a LOQ calculated on the basis of a signal-to-noise (S/N) ratio of 10:1 were 17.18 ng/mL for E, and 22.00 ng/mL for PE. The LODs were 5.34 ng/mL for E and 6.60 ng/mL for PE (S/N=3). These limits are sufficient for clinical pharmacokinetic studies after oral administration of therapeutic dose.

3.3.4 Intra-day and inter-day precisions

The precision of the method was evaluated by analyzing five replicates of QC samples at low, medium and high concentrations, respectively. Intra-day precision was assessed as the relative standard deviation (RSD) resulting from the same day. Inter-day assay precision was expressed by the RSD of the mean concentrations on three consecutive days. The summary of intra-day and inter-day precisions at QC concentrations was shown in Table 1. The results were less than 5.30% and 6.75% for the two analytes, which indicated good precision.

3.3.5 Recovery

The recovery experiment was carried out to evaluate the accuracy of the method. In this study, the recovery was determined from QC samples of low, medium and high concentrations, and recovery%=measured concentration/QC sample concentration×100%. Table 2 summarized the results of recoveries of the two analytes, which were in range of 97.6-106.9% and RSD were in range of 2.46-8.29%. Thus, recoveries were within the acceptable criteria.

4. Conclusions

In our study, a low cost and accurate CZE method with high sensitivity was developed .The satisfactory results of the methodology validation indicated that the method can be applied to simultaneous determination of E and PE plasma concentrations in complex clinical samples, for example, human plasma and herbal medicine.

References

Aymard G, Labarthe B & Warot D. (2000). Sensitive determination of ephedrine and norephedrine in human plasma samples using derivatization with 9-fluorenylmethyl chloroformate and liquid chromatography. *Chromatogr, B*, 01, 25.

Beyer, J., Peters, FT., Kraemer, T. & Maurer, HH. (2007). Detection and validated quantification of nine herbal phenalkylamines and methcathinone in human blood plasma by LC-MS/MS with electrospray ionization. *Journal of Mass Spectrometry*, 02, 150-160.

Gunn J, Kriger S & Terrell AR. (2010). Identification and quantitation of amphetamine, methamphetamine, MDMA, pseudoephedrine and ephedrine in blood, plasma and serum using gas chromatography-mass spectrometry (GC/MS). *Methods Mol Biol.,* 607, 37-43.

Kang Yong. (2001). *Chinese Pharmacology*. Beijing: Science Press, PP. 37-39.

Liu Gang, Zhang Hui & Zhang Xianzhou. (2006). Determination of pseudoephedrine in human serum by HPCE. *China Pharmacist*, 07, 617.

Lou Hong-gang, Yuan Hong, Ruan Zou-rong & Jiang, Bo. (2010). Simultaneous determination of paracetamol, pseudoephedrine, dextrophan and chlorpheniramine in human plasma by liquid chromatography–tandem mass spectrometry. *Chromatography B.*, 878, 682-688.

Nakano M, Morimoto Y, Tajima S & Kosaka N. (2000). GC-MS determination of l-ephedrine and d-pseudoephedrine in human plasma. *Yakugaku Zasshi*, 06, 583-586.

Roman MC. (2004). Determination of ephedra alkaloids in urine and plasma by HPLC-UV: Collaborative study. *Journal of AOAC International*, 01, 15-24.

Shen Qun. (2002). the effect of the different compatibility of mahuangtang on ephedrine and pseudoephedrine pharmacokinetics in mice. *First Military Medical University*.

Wei F, Zhang M & Feng YQ. (2007). Combining poly (methacrylic acid-co-ethylene glycol dimethacrylate) monolith microextraction and on-line pre-concentration-capillary electrophoresis for analysis of ephedrine and pseudoephedrine in human plasma and urine. *J Chromatogr B Analyt Technol Biomed Life Sci*, 01-02, 38-44.

Yi Feng, Yu Huang & Lai Weiling. (2008). Determination of pseudoephedrine in rabbit plasma by LC-MS/MS. *Journal of Guangdong College of Pharmacy*, 06, 572.

Table 1. Intra-day and inter-day precision for E from plasma samples (n=5)

Concentratio added (µg/mL)		Intra-day (n=5)		Intra-day (n=5)	
		Measured concentration (µg/mL)	Precision (RSD %)	Measured concentration (µg/mL)	Precision (RSD %)
E	0.125	0.139±0.003	2.33	0.120±0.007	6.04
	0.5	0.447±0.016	3.50	0.478±0.021	4.30
	5.0	4.966±0.073	1.46	5.021±0.134	2.66
PE	0.0625	0.067±0.004	5.30	0.062±0.004	6.75
	0.25	0.232±0.010	4.48	0.261±0.011	4.40
	2.5	2.516±0.064	2.53	2.413±0.110	4.55

Table 2. Recoveries for E and PE for E from plasma samples (n=5)

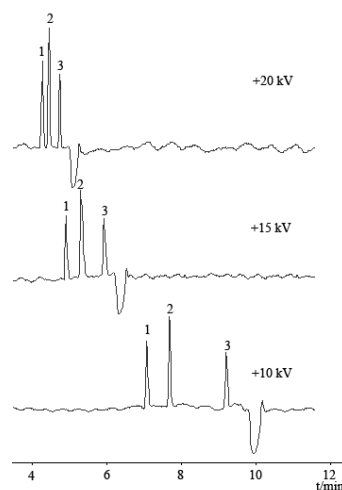| Concentration Added (µg/mL)		Measured Concentration (µg/mL)	Recovery ±s (%)	RSD (%)
E	0.125	0.134±0.009	106.9±6.94	6.50
	0.5	0.489±0.018	97.8±3.69	3.78
	5.0	5.063±0.183	101.3±3.66	3.61
PE	0.0625	0.061±0.005	97.6±8.08	8.29
	0.25	0.246±0.006	98.3±2.42	2.46
	2.5	2.520±0.131	100.8±5.24	5.20

Figure 1. The eletropherograms of analytes were at different separation voltage
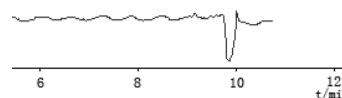Peak identification: (1) IS; (2) E; (3) PE

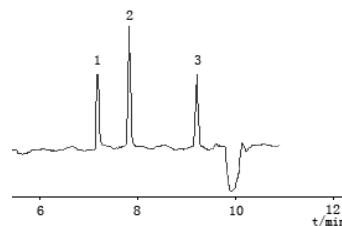Figure 2. The eletropherogram of a blank plasma

Figure 3. The eletropherogram of a blank plasma sample was added with E, PE and IS
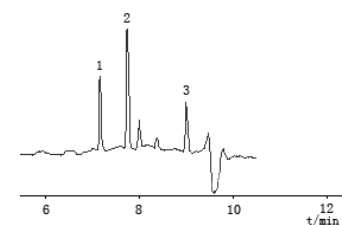Peak identification as in Fig. 1

Figure 4. The electropherograms of a plasma sample from the mice after
2 h of *ig* Maxingshigan Decoction. Peak identification as in Fig. 1

Synthesis and Physicochemical Studies of Some 2-substituted-1-phenyl-1,3-butanedionato Nickel(II) and Copper(II) Complexes And Their 2,2′-Bipyridine and 1,10-Phenanthroline Adducts

Oluwatola Omoregie (Corresponding author)

Department of Chemistry, Faculty of Science, University of Ibadan

Ibadan, Oyo-State, Nigeria

E-mail: tolaomoregie@yahoo.co.uk

Joseph Woods

Department of Chemistry, Faculty of Science, University of Ibadan

Ibadan, Oyo-State, Nigeria

E-mail: jaowoods@yahoo.com

Abstract

The nickel(II) and copper(II) complexes of 2-substituted-1-phenyl-1,3-butanedione (2-R-bzacH, R=Cl, NO_2) and their 2,2′-bipyridine (bipy) and 1,10-phenanthroline (phen) adducts have been synthesized and characterized by microanalysis, conductance, magnetic and spectral measurements. The conductivity measurements in nitromethane indicate that the complexes are non-electrolytes while all the adducts are electrolytes except $Ni(NO_2\text{-}bzac)_2bipy$ and $Cu(NO_2\text{-}bzac)_2phen$ which are non-electrolytes. The room temperature magnetic moments suggest that the $Cu(NO_2\text{-}bzac)_2$ is a dimer while the visible absorption spectra of the compounds suggest plausible 4-, 5- and 6-coordinate geometry for these compounds. The infrared spectra of the complexes showed that lower frequency shifts of varying magnitudes were observed in the carbonyl stretching frequencies on complexation.

Keywords: 2-substituted-1-phenyl-1,3-butanedione, Spectra studies, Magnetic moments, Conductance measurement

1. Introduction

A survey of the literature reveals that metal β-diketonates have found use as fuel additives, trace metal analysis by gas chromatography and numerous other extraction applications (Wenzel et al, 1985). The dissolution of chelating agents in supercritical fluids has been explored as a possible route to waste cleanup (Laintd et al, 1992; Lalntz et al, 1994; Wang et al, 1995; Wang et al, 1994). Complexes of β-diketones are reported to have potentially useful pharmacological properties (Onawumi et al, 2008).

Literature is available on the introduction of halogens and nitronium ion at the central carbon atom of β-diketones [($R_1COCH_2COR_2$) where $R_1=R_2=CH_3$](Singh and Sahai, 1967a; Singh and Sahai, 1967b; Woods and Patel,1994; Patel and Woods, 1990a; Collman et al, 1962; Ebeid et al, 1966; Tanaka et al, 1969) whereas little work has been carried out on the synthesis and characterization of the nickel(II) and copper(II) complexes of 2-substituted-1-phenyl-1,3-butanedione (2-R-bzacH, R=Cl, NO_2) and their 2,2′-bipyridine (bipy) and 1,10-phenanthroline (phen) adducts. In continuation of our work on substituted β-diketones (Woods et al, 2009a; Woods et al, 2009b), we report the results of our investigations on the nickel(II) and copper(II) complexes of some 2-substituted-1-phenyl-1,3-butanediones (2-R-bzacH, R=Cl, NO_2) and their adducts with 2,2′-bipyridine (bipy) and 1,10-phenanthroline (phen).

2. Experimental

The following reagents were used: 1-phenyl-1,3-butanedione or benzoylacetone (bzacH) (Aldrich chemicals), sulphuryl chloride, copper nitrate, nickel acetate, copper acetate, 2,2′-bipyridine and 1,10-phenanthroline (analytical grade).

2.1 Synthesis of the Ligands

The ligands, 2-chloro-1-phenyl-1,3-butanedione (Tanaka et al, 1969) and 2-nitro-1-phenyl-1,3-butanedione (Singh and Sahai, 1967a) were prepared by literature methods.

2.2 Synthesis of the Complexes and Adducts

2.2.1 Synthesis of Cu(Cl-bzac)$_2$

Cl-bzacH (2.00 mL, 12.4 mmoles) in 6 mL acetone was added to copper(II) acetate monohy drate (1.24 g, 6.2 mmoles) in 50 mL 60% methanol in drops. The mixture was stirred for 1 hour and the precipitates formed were filtered, washed with 60% methanol and dried in the vacuo.   All the other complexes were prepared using similar procedure.

2.2.2 Synthesis of Cu(Cl-bzac)$_2$phen

The phenanthroline adduct of Cu(Cl-bzac)$_2$ was prepared by adding the solid complex (0.50 g, 1.1 mmol) while stirring to phenanthroline (0.72 g, 3.6 mmol) dissolved in 10 mL hot chloroform solution. The mixture was further stirred for 15 minutes and the precipitates formed were filtered and washed with acetone. This was dried in vacuo over anhydrous calcium chloride. Other adducts were prepared using similar procedures.

2.3 Physical measurements

Elemental analyses for C, H, N were determined at Department of Chemistry, Loughborough University, UK. The % metal in the nickel(II) and copper(II) compounds were determined titrimetrically using EDTA.

The molar conductivities of the soluble compounds in nitromethane at room temperature were determined using Digital conductivity meter (Labtech).

The solution spectra of the the Ligands, nickel(II) and copper(II) compounds in methanol and chloroform were recorded on a Unicam UV-Visible Spectrophotometer using 1cm glass cell. The reflectance spectra of the Ligands, nickel(II) and copper(II) compounds were recorded on a Perkin Elmer Lambda 950 UV/VIS spectrophotometer at the Department of Chemical Engineering, Faculty of Technology, Addis Ababa University, Ethiopia using calcium carbonate as reference. The infrared spectra of the compounds as pressed KBr disc were recorded on Perkin Elmer Spectrophotometer BX FT-IR.

3. Results and discussion

Table I shows the analytical data, colours, %yield and room temperature magnetic moments (μ_{eff}) of the prepared nickel(II) and copper(II) compounds. The elemental analyses were in good agreement with those calculated for the proposed formula (Table 2). The nickel(II) compounds prepared from 2-chloro-1-phenyl-1,3-butanedione were generally pink in colour except Ni(Cl-bzac)$_2$.2H$_2$O which had green colour while those prepared from 2-NO$_2$-1-phenyl-1,3-butanedione were obtained as various shades of green except [Ni(NO$_2$-bzac)(phen)$_2$](NO$_2$-bzac) which was obtained as Light brown. All the copper(II) complexes and their adducts were obtained as varous shades of green colour.

The magnetic moment data as shown in Table 1 depicts the paramagnetic nature of the compounds. The nickel(II) compounds had values in the range 2.9-3.28 B.M. which is in agreement with the range expected for octahedral nickel(II) complexes (2.9-3.3 B.M) (Patel and Woods, 1990b). A moment of 1.73-2.2 B.M. is usually observed for magnetically dilute copper(II) compounds, with compounds whose geometry approaches octahedral having moments at the lower end while those approaching tetrahedral geometry are at the higher end (Patel and Woods, 1990c). The prepared 2-substituted-1-phenyl-1,3-butanedionato copper(II) compounds had moments in the range 1.44-2.19 B.M. The magnetic moment of Cu(NO$_2$-bzac)$_2$ (1.44 B.M.) is lower than the spin only value of 1.73 B.M. which is indicative of dimerization with the possibility of Cu-Cu linkage (Cotton and Wilkinson, 1988).

The molar conductivity of the complexes in nitromethane were in the range 17-21 ohm^{-1}cm^{2}mol^{-1} indicating that they are non-electrolytes. The adducts had values between 62-198 ohm^{-1}cm^{2}mol^{-1} except Ni(NO$_2$-bzac)$_2$bipy and Cu(NO$_2$-bzac)$_2$phen which are non-electrolytes (13 and 46 ohm^{-1}cm^2 mol^{-1} respectively).

The principal IR absorption bands of the prepared complexes are listed in Table 3. In the spectrum of NO$_2$-bzacH, the band at 1600 cm^{-1} has been assigned as ν_{as}(C=O) + ν_{as}(C=C) + ν_{as}(NO$_2$) vibrations while those at 1360 cm^{-1} and 820 cm^{-1} are assigned as ν_s(NO$_2$) and ν(C-N) or δN-O respectively. Bathochromic shifts of varying magnitude were observed in the asymmetric C-O and C-C stretching vibrations of the complexes relative to their respective ligands whereas hypsochromic shifts were observed in all the adducts relative to the complexes. Multiple bands of ν_s(C-O)+δC-H were observed in all the compounds except [Ni(Cl-bzac)(bipy)(H$_2$O)$_2$](Cl-bzac), [Ni(phen)$_2$(H$_2$O)$_2$](Cl-bzac) and [Ni(Cl-bzac)(phen)(H$_2$O)$_2$](Cl-bzac) which had single band. Studies have shown

that methyl deformation band occurred at around 1425 cm^{-1} in acetylacetone (Holtzclaw and Collman, 1957; Belford et al, 1956) while bands in the 1420-1350 cm^{-1} region have been assigned as $\delta_{as}(CH_3) + \delta_s(CH_3)$ vibrations (Singh and Sahai, 1967b; Tanaka et al, 1969; Patel and Woods, 1990b; Koshimura et al, 1973; Nakamoto et al, 1961). Furthermore, the νM-$O + \nu C$-N vibrational modes occurred below 700 cm^{-1} (Patel and Woods, 1990a; Patel and Woods, 1990c). The C-H deformation bands (δC-H) for the bipyridine appeared at around 768 cm^{-1} while that of the phenanthroline adducts were observed at 852 cm^{-1} and 727 cm^{-1}.

The electronic spectra of the ligands in CHCl$_3$ and methanol are listed in Table 4. Single bands of the π_3-π_4* were observed in the 31,250-31,154 cm^{-1} region in Cl-bzacH and NO$_2$-bzacH ligands. Bathochromic shift of the π_3-π_4* were observed in Cl-bzacH and NO$_2$-bzacH as compared to bzacH in chloroform. π_3-π_4*Hypsochromic shifts of varying magnitude were observed in the Ni(Cl-bzac)$_2$.2H$_2$O and Ni(NO$_2$-bzac)$_2$.2H$_2$O complexes in chloroform and methanol. Upon adduct formation, π_3-π_4* Hypsochromic shifts were observed in all the adducts in chloroform except [Ni(Cl-bzac)(bipy)(H$_2$O)$_2$](Cl-bzac) which had bathochromic shift.The ligand field spectra band of Ni(Cl-bzac)$_2$.2H$_2$O and Ni(NO$_2$-bzac)$_2$.2H$_2$O were typically of an octahedral geometry (Lever, 1986) while the shift observed in Cu(Cl-bzac)$_2$ and Cu(NO$_2$-bzac)$_2$ suggest a four coordinate square planar geometry. Lower frequency shifts were observed in Cu(Cl-bzac)$_2$ and Cu(NO$_2$-bzac)$_2$ in methanol relative to chloroform [18,031 cm^{-1} in chloroform→15,625 cm^{-1} in methanol for Cu(Cl-bzac)$_2$] and [18,349 cm^{-1} in chloroform→15,198 cm^{-1} in methanol for Cu(NO$_2$-bzac)$_2$] which is an indication that the complexes are square planar in structure. Nickel(II) species have a large number of stereochemical forms in which the ion occurs, hence equilibrium between these forms are usually set up which are generally temperature, solvent and sometimes concentration dependent (Bailar et al, 1973). In solution, Ni(II) β-diketonates sometimes exhibit a monomer↔trimer, square planar↔octahedral equilibrium (Cotton and Wilkinson, 1980). Three transitions are expected for an octahedral nickel(II) ion in the region 7,000-13,000, cm^{-1}, 11,000-20,000 cm^{-1}, 19,000-27,000 cm^{-1} which are assigned to the $^3A_{2g}(F) \rightarrow {}^3T_{2g}(F)$, $^3A_{2g}(F) \rightarrow {}^3T_{1g}(F)$, $^3A_{2g}(F) \rightarrow {}^3T_{1g}(P)$ respectively. In the synthesized nickel(II) adducts, bands in the 11,442-12,821 cm^{-1} and 13,908-19,455 cm^{-1} region have been assigned to $^3A_{2g}(F) \rightarrow {}^3T_{2g}(F)$, $^3A_{2g}(F) \rightarrow {}^3T_{1g}(F)$ transitions respectively(Lever, 1986; Osowole et al, 2000). The visible spectra of the synthesized copper(II) adducts had a single band between 14,006-15,625 cm^{-1} which is consistent with the adoption of square pyramidal geometry for copper(II) compounds (Odunola et al, 2003). In addition, higher frequency shifts were observed in the ligand field spectral of the copper(II) adducts in methanol as compared with chloroform. [Cu(Cl-bzac)(bipy)(H$_2$O)](Cl-bzac) had a band in the 14,205 cm^{-1} region in chlorofom and this band was shifted to 16,393 cm^{-1} in methanol. This is an indication that the compound is a five coordinate square pyramidal geometry (Patel and Woods, 1990a). The electronic reflectance spectra of the ligands, complexes and adducts in the ultraviolet region exhibited single peak between 31,056-37,453 cm^{-1} with an additional peak observed between 39,683-48,544 cm^{-1} which have been assigned to π_3-π_4* and charge transfer (CT) respectively. The visible region of the spectra showed that the nickel(II) compounds were octahedral in geometry while the copper(II) complexes and adducts were square planar and square pyramidal in geometry respectively.

4. Conclusion

Probable six coordinate octahedral geometry is suggested for all the nickel(II) compounds while a probable five coordinate, square pyramidal geometry is suggested for the copper(II) compounds except Cu(Cl-bzac)$_2$ and Cu(NO$_2$-bzac)$_2$ which are square planar in structure.

References

Bailar, J.C. Jr, Emeleus, H.J., Nyholm, R. and Trotman-Dickenson, A.F. (1973). *Comprehensive inorganic chemistry*. Pergamon: Oxford. pp 1139-1159.

Belford, R.L., Martell, A.E. and Calvin, M. (1956). Influence of fluorine substitution on the properties of metal chelate compounds- I. copper (II) chelates of bidentate ligands. *Journal of Inorganic Nuclear Chemistry*, 2, 11-31.

Collman, J.P., Marshall, R.L., Young, W.L., and Goldby, S. (1962). Reactions of metal chelates. Nitration and formylation of metal acetylacetonates. *Inorganic Chemistry*, 1(3), 704-710.

Cotton, F.A. and Wilkinson, G. (1980). *Advanced inorganic chemistry*. 4th ed. New York: Wiley and sons Inc. pp 627-628, 783-821.

Cotton, F.A. and Wilkinson, G. (1988). *Advanced Inorganic Chemistry*. 5th ed. Canada: John Wiley & Sons, Inc. 768.

Ebeid, F.M., Rihan T.I. and Hassanein, M. (1966). A simple method for preparation of metal acetylacetonates and their nitro derivatives. *Indian Journal of Chemistry*, 4, 451-452.

Holtzclaw, H.F. Jr. and Collman, J.P. (1957). Infrared absorption of metal chelate compounds of 1,3-diketones. *Journal of American Chemical Society*, 79, 3318-3322.

Koshimura, H., Saito, J. and Okubo, T. (1973). Effect of substituents on the keto-enol equilibrium of alkyl substituted β-diketones. *Bulletin of the Chemical Society of Japan*, *46, 632-634.*

Laintd, K. E., Wai, C. M., Yonker, *C.* R., and Smith, R. D. (1992). Extraction of Metal Ions from Liquid and Solid Materials by Supercritical Carbon Dioxide. *Anal. Chem.*, 64, 2875-2878.

Lalntz, K.E., and Tachlkawa, E. (1994). Extraction of Lanthanides from acidic solution using tributyl phosphate modified supercritical carbon dioxide. *Anal. Chem.*, 66, 2190-2193.

Lever A.B.P. (1986). *Inorganic Electronic Spectroscopy*, 4th Ed.; Elsevier: London, 481-579.

Nakamoto, K., McCarthy, P.J. Ruby, A. and Martell, A.E. (1961). Infrared spectra of metal chelate compounds. II. Infrared spectra of acetylacetonates of trivalent metals. *Journal of American Chemical Society*, 83, 1066-1069.

Odunola, O.A., Oladipo, M.A., Woods, J.A.O., and Gelebe, A.C. (2003). Synthesis and structural studies of some ternary copper(II) complexes containing β-diketones with 1,10-phenanthroline and 2,2′-bipyridyl and x-ray structure of [Cu(C$_6$H$_5$COCHCOCH$_3$)(bipy)Cl]. *Synthesis and Reactivity in Inorganic and Metal-Organic Chemistry*, 33(5), 857-871.

Onawumi, O.O.E., Faboya, O.O.P., Odunola, O.A., Prasad, T.K., Rajesekharan, M.V. (2008). Synthesis, structure and spectral studies on mixed ligand copper(II) complexes of diimines and acetylacetonate. *Polyhedron*, 27, 113-117.

Osowole, A.A., Woods, J.A.O. and Odunola, O.A. (2000). Synthesis and characterization of some Nickel(II) β-ketoamines and their adducts with 2,2′-bipyridine and 1,10-phenanthroline. *Synthesis and Reactivity in Inorganic and Metal-Organic Chemistry*, 32(4), 783-799.

Patel, K.S. and Woods J.A.O. (1990a). Preparation and physico-chemical studies of some 3-substituted-2,4-pentanedionato copper(II) complexes and their adducts. *Synthesis and Reactivity of Inorganic and Metal Organic Chemistry*, 20(1), 97-109.

Patel, K.S. and Woods J.A.O. (1990b). Synthesis and properties of nickel(II) complexes of various 3-alkyl-2,4-pentanediones and their adducts with 2,2′-bipyridine and 1,10-phenanthroline. *Synthesis and Reactivity of Inorganic and Metal Organic Chemistry*, 20(4), 409-424.

Patel, K.S. and Woods J.A.O. (1990c). Synthesis and physico-chemical properties of Bis(3-akyl-2,4-pentanedionato) copper(II) complexes and their adducts with 2,2′-bipyridine and 1,10-phenanthroline. *Synthesis and Reactivity of Inorganic and Metal Organic Chemistry*, 20(7), 909-922.

Singh, P.R. and Sahai, R. (1967a). Chemical and spectroscopic studies in metal β-diketonates. I. Preparation and study of halogenated metal acetylacetonates. *Australian Journal of Chemistry*, 20, 639-648.

Singh, P.R. and Sahai, R. (1967b). Chemical and spectroscopic studies in metal β-diketonates. II. Nitration of metal β-diketonates. *Australian Journal of Chemistry*, 20, 649-655.

Tanaka, M., Shono,T. and Shinra, K. (1969). Tautomerism in 3-substituted 2,4-pentanediones and their copper chelates. *Bulletin of the Chemical Society of Japan*, 42, 3190-3194.

Wang, J., Marshall, W. D. (1994). Recovery of Metals from Aqueous Media by Extraction with Supercritical Carbon Dioxide. *Anal. Chem.*, 66, 1658-1663.

Wang, S., Eishani, S., Wai, C.M. (1995). Selective extraction of mercury with ionizable crown ethers in supercritical carbon dioxide. *Anal. Chem.*, 67, 919-923.

Wenzel, T.J., Williams, E.J., Haltiwanger, R.C. and Sievers, R.E. (1985). Studies of metal chelates with the novel ligand 2,2,7-trimethyl-3,5-octanedione. *Polyhedron*, 4(3), 369-378.

Woods, J.A.O, Omoregie, H.O., Retta, N., Chebude, Y., Capittelli, F. (2009a). Synthesis and physicochemical studies of Nickel(II) complexes of 2-substituted-1,3-diphenyl-1,3-propanedione, their 2,2′-bipyridine and 1,10-phenanthroline adducts and X-ray structure of (2,2′-bipyridine)bis(1,3-diphenyl-1,3-propanedionato) Nickel(II). *Synthesis and Reactivity in Inorganic, Metal-Organic, and Nano-Metal Chemistry*, 39, 694-703.

Woods, J.A.O, Omoregie, H.O., Retta, N., Chebude, Y., Capittelli, F. (2009b). Synthesis and characterization of some Nickel(II) and Copper(II) complexes of 2-substituted-4,4,4-trifluoro-(2-thienyl)butane-1,3-dione (TTAH), their 2,2′-bipyridine and 1,10-phenanthroline adducts and X-ray structure of

(2,2′-bipyridine)bis(4,4,4-trifluoro-(2-thienyl)butane-1,3-dionato) Nickel(II). *Synthesis and Reactivity in Inorganic, Metal-Organic, and Nano-Metal Chemistry*, 39, 704-717.

Woods, J.A.O. and Patel, K.S. (1994). Nickel(II) complexes of some 3-substituted-2,4-pentanediones and their adducts with 2,2′-bipyridine and 1,10-phenanthroline. *Synthesis and Reactivity of Inorganic and Metal Organic Chemistry*, 24(9), 1557-1571.

Table 1. Analytical and physical data of nickel(II) and copper(II) complexes of 2-substituted-1-phenyl-1,3-butanedione and their adducts

Formula	M.Wt	Colour	M.P. (˚C)	Yield (%)	μ_{eff} (B.M.)
Ni(Cl-bzac)$_2$.2H$_2$O	486.09	Green	128-130	51.58	2.90
[Ni(Cl-bzac)(bipy)(H$_2$O)$_2$](Cl-bzac)	642.28	Pink	124-126	61.86	2.93
[Ni(phen)$_3$(H$_2$O)$_2$](Cl-bzac)$_2$	1026.71	Pink	138-140	40.36	3.28
[Ni(phen)$_2$(H$_2$O)$_2$](Cl-bzac)$_2$	846.49	Pink	198-200	82.67	3.08
Ni(NO$_2$-bzac)$_2$.2H$_2$O	507.10	L.Green	168	52.32	2.96
Ni(NO$_2$-bzac)$_2$.bipy	627.25	Green	218-219	77.78	3.02
[Ni(NO$_2$-bzac)(phen)$_2$](NO$_2$-bzac)	831.47	L.Brown	196-198	69.42	3.18
Cu(Cl-bzac)$_2$	454.84	Green	220-222	61.34	1.79
[Cu(Cl-bzac)(bipy)(H$_2$O)](Cl-bzac)	629.05	D.Green	175-177	89.13	2.19
Cu(Cl-bzac)(phen)(H$_2$O)](Cl-bzac)	653.06	D.Green	207-209	34.82	1.98
Cu(NO$_2$-bzac)$_2$	475.85	Green	145-147	89.13	1.44
[Cu(NO$_2$-bzac)(bipy)(H$_2$O)]	650.06	Green	170-172	56.03	1.73
Cu(NO$_2$-bzac)$_2$.phen	656.05	Green	185-187	25.67	2.01

D = dark, L = light

Table 2. Microanalytical data of nickel(II) and copper(II) complexes of 2-substituted-1-phenyl-1,3-butanedione and their adducts

Emperical formula	%Found				%Calculated			
	C	H	N	Metal	C	H	N	Metal
Ni(Cl-bzac)$_2$.2H$_2$O	50.17	4.10	-	11.78	49.41	4.16	-	12.08
[Ni(Cl-bzac)(bipy)(H$_2$O)$_2$](Cl-bzac)	55.70	4.55	4.02	9.42	56.10	4.40	4.36	9.42
[Ni(phen)$_3$(H$_2$O)$_2$](Cl-bzac)$_2$	65.69	4.03	7.83	6.22	65.51	4.33	8.18	5.72
[Ni(phen)$_2$(H$_2$O)$_2$](Cl-bzac)$_2$	62.04	3.98	7.02	6.80	62.43	4.30	6.62	6.85
Ni(NO$_2$-bzac)$_2$.2H$_2$O	46.97	4.28	5.82	11.33	47.37	3.98	5.52	11.58
Ni(NO$_2$-bzac)$_2$.bipy	56.94	4.05	9.12	9.11	57.44	3.86	8.92	9.34
[Ni(NO$_2$-bzac)(phen)$_2$](NO$_2$-bzac)	64.01	4.32	9.82	7.50	63.55	3.89	10.10	7.06
Cu(Cl-bzac)$_2$	52.24	3.84	-	13.7	52.81	3.55	-	13.96
[Cu(Cl-bzac)(bipy)(H$_2$O)](Cl-bzac)	56.83	4.07	4.15	10.19	57.28	4.17	4.45	10.09
[Cu(Cl-bzac)(phen)(H$_2$O)](Cl-bzac)	59.09	3.77	4.79	9.40	58.85	4.02	4.29	9.72
Cu(NO$_2$-bzac)$_2$	50.18	3.20	5.82	13.33	50.48	3.40	5.88	13.34
[Cu(NO$_2$-bzac)(bipy)(H$_2$O)]	55.81	3.92	9.01	9.47	55.43	4.04	8.61	9.77
Cu(NO$_2$-bzac)$_2$.phen	5858.58	3.69	8.54	9.68	58.50	3.86	8.63	9.62

Table 3. Relevant Infrared Spectra bands (cm^{-1}) of nickel(II) and copper(II) complexes of 2-substituted-1-phenyl-1,3-butanedione and their adducts

Formula	C=O, C=C	ν_s(C-O)+δC-H	δ_{as}(CH$_3$)+δ_s(CH$_3$)	δ(C-H) Phen/bipy	
bzacH	1599m, 1540b	1484m	1413m, 1360m	-	
Cl-bzacH	1749w 1724w 1686m	1449w	1359w		
Ni(Cl-bzac)$_2$.2H$_2$O	1689w1591s 1563s	1487m 1448w 1352w			
[Ni(Cl-bzac)(bipy)(H$_2$O)$_2$](Cl-bzac)	1598s 1570m 1509m	1443m	1406m 1355w	768s	
[Ni(phen)$_3$(H$_2$O)$_2$](Cl-bzac)$_2$	1626m 1587m 1516s	1462w	1424s	847s	726s
[Ni(phen)$_2$(H$_2$O)$_2$](Cl-bzac)$_2$	1736b 1627w 1594s	1457s	1399s	851s	727s
NO$_2$-bzacH	1600m 1567w	1462m	1412w1360m		
Ni(NO$_2$-bzac)$_2$.2H$_2$O	1592s 1561s 1516s	1484m 1452s	1403m		
Ni(NO$_2$-bzac)$_2$.bipy	1595vs 1570vs 1506vs	1484vs 1456s	1358w	772vs	
[Ni(NO$_2$-bzac)(phen)$_2$](NO$_2$-bzac)	1624w 1593s 1564s	1484m 1457m	1399s	851s	727s
Cu(Cl-bzac)$_2$	1553s 1516m	1487w 1443m	1395m		
[Cu(Cl-bzac)(bipy)(H$_2$O)](Cl-bzac)	1592s 1589m1521s	1490m 1448s	1385s	764s	
[Cu(Cl-bzac)(phen)(H$_2$O)](Cl-bzac)	1597m 1564m 1518s	1486m 1450m	1388s	852s	724s
Cu(NO$_2$-bzac)$_2$	1587m 1565s 1523s	1488m 1453m	1401s 1360m		
[Cu(Cl-bzac)(phen)(H$_2$O)](Cl-bzac)	1666s 1589s 1561s	1488s 1451m	1390s	774s	
Cu(NO$_2$-bzac)$_2$.phen	1716w 1595s 1568s	1486m 1450m	1387s	852s	724s

b=broad, s=strong, v=very, w=weak, m=medium

Table 4. The electronic solution spectra of nickel(II) and copper(II) complexes of 2-substituted-1-phenyl-1,3-butanedione and their adducts

Emperical Formula	$\pi_3\text{-}\pi_4*(cm^{-1})$		d-d	
	CHCl$_3$	CH$_3$OH	CHCl$_3$	CH$_3$OH
bzacH	32,258(7247)	32,258(18259)	-	-
Cl-bzacH	31,250*	32,051(?)	-	-
Ni(Cl-bzac)$_2$.2H$_2$O	33,333*	34,247*	17,422(67) 13,850(59)	15,974(16)
[Ni(Cl-bzac)(bipy)(H$_2$O)$_2$](Cl-bzac)	33,113(?)	33,784(29412) 12,690(?)	17,730(?) 12,755(41)	17,544(60)
[Ni(phen)$_3$(H$_2$O)$_2$](Cl-bzac)$_2$	34,014(?)	34,014(18085)	19,048(?) 13,908(?)	19,455(56) 12,755(8) 11,442(8)
[Ni(phen)$_2$(H$_2$O)$_2$](Cl-bzac)$_2$	34,247(31759)	34,247(26188)	17,857(89) 12,853(73)	18,450(24) 12,563(8)
NO$_2$-bzacH	32,154(27141)	32,051(22717)	-	-
Ni(NO$_2$-bzac)$_2$.2H$_2$O	34,014*	34,483*	15,723(15)	18,587(43) 12,821(15)
Ni(NO$_2$-bzac)$_2$.bipy	34,420(29568)	34,480(29765)	17,870(60) 12,600(55)	17,560(68) 12,080(40)
[Ni(NO$_2$-bzac)(phen)$_2$](NO$_2$-bzac)	34,247(30811)	34,247(39952)	17,373(98) 12,987(72)	18,587(43) 12,821(15)
Cu(Cl-bzac)$_2$	32,468(12998)	31,056(?)	12,690(113)	15,625(?) 11,848(?)
[Cu(Cl-bzac)(bipy)(H$_2$O)](Cl-bzac)	33,557(66659)	33,333(53582)	14,205(489)	16,393(161)
[Cu(Cl-bzac)(phen)(H$_2$O)](Cl-bzac)	34,014(?)	34,014(44970)	14,006(?)	16,129(137)
Cu(NO$_2$-bzac)$_2$	31,447(36456)	33,898*	18,349* 15,060(128)	15,198(70)
[Cu(NO$_2$-bzac)(bipy)(H$_2$O)]	32,258(58721)	32,680(31224)	15,625(82)	16,447(96)
Cu(NO$_2$-bzac)$_2$.phen	34,014(31249)	34,014(38037)	14,164(224)	16,287(185)

? Compounds partially soluble in the solvent.

*Shoulder

Table 5. The electronic solid reflectance spectra of nickel(II) and copper(II) complexes of 2-substituted-1-phenyl-1,3-butanedione and their adducts

Emperical Formula	π_3-π_4*(cm^{-1})	d-d
Cl-bzacH	35,971	-
Ni(Cl-bzac)$_2$.2H$_2$O	32,154	18,484, 12,019
[Ni(Cl-bzac)(bipy)(H$_2$O)$_2$](Cl-bzac)	36,364	20,325, 14,749, 12,642
[Ni(phen)$_3$(H$_2$O)$_2$](Cl-bzac)$_2$	31,056	21,645, 15,480, 12,048
[Ni(phen)$_2$(H$_2$O)$_2$](Cl-bzac)$_2$	31,348	20,790, 14,749, 12,739
NO$_2$-bzacH	37,453	-
Ni(NO$_2$-bzac)$_2$.2H$_2$O	36,900	18,349, 12,063
Ni(NO$_2$-bzac)$_2$.bipy	36,630	20,325, 13,587, 12,642
[Ni(NO$_2$-bzac)(phen)$_2$](NO$_2$-bzac)	31,157	19,802, 14,306,12,500
Cu(Cl-bzac)$_2$	34,364	20,000, 17,007, 12,121
[Cu(Cl-bzac)(bipy)(H$_2$O)](Cl-bzac)	36,101	14,724
[Cu(Cl-bzac)(phen)(H$_2$O)](Cl-bzac)	34,247	14,305
Cu(NO$_2$-bzac)$_2$	31,847	20,284, 16,155, 12,210
[Cu(NO$_2$-bzac)(bipy)(H$_2$O)]	36,101	15,325
Cu(NO$_2$-bzac)$_2$.phen	35,345	14,987
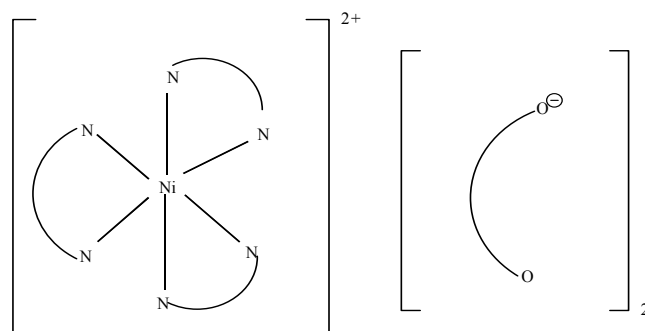
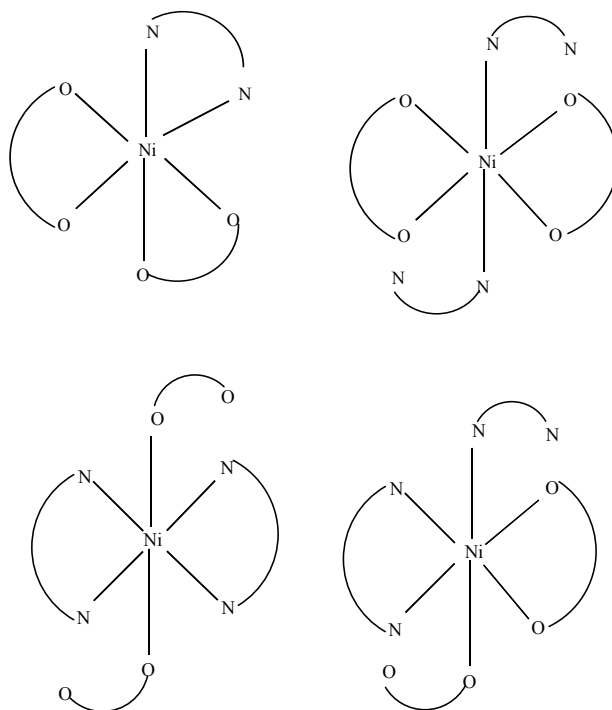1:2 ELECTROLYTE
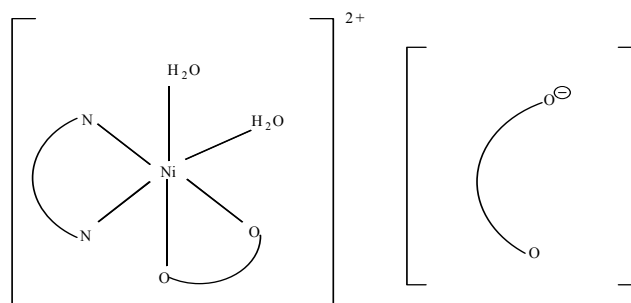
1:1 ELECTROLYTE

Figure 1. Proposed structures for Nickel adducts
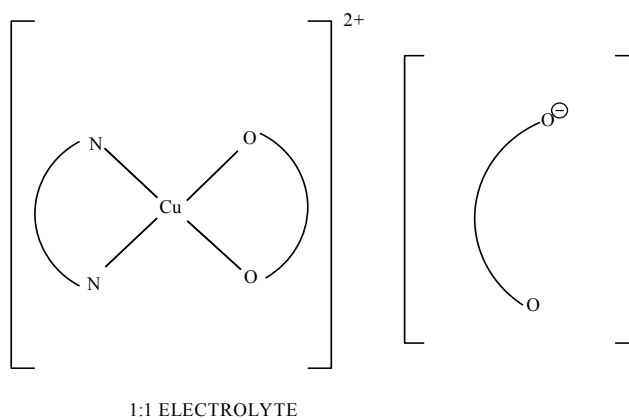
1:1 ELECTROLYTE

Figure 2. Proposed structures for Copper adducts

Direct Passerini Reaction of Aldehydes, Isocyanides, and Aliphatic Alcohols Catalyzed by Bismuth (III) Triflate

Xiao-hua CAI

College of Chemistry and environmental Science

Guizhou University for Nationalites

Guiyang 550025, China

Tel: 86-851-361-0313   E-mail: caixh1111@163.com

Hui GUO

College of Pharmaceutical Sciences

Zhejiang University of Technology

Hangzhou 310014, China

E-mail: gh635@zjut.edu.cn

Bing XIE

College of Chemistry and environmental Science

Guizhou University for Nationalites

Guiyang 550025, China

Tel: 86-851-361-0313   E-mail: bing_xie1963@hotmail.com

Abstract

Bismuth (III) triflate was found to be effective Lewis acid catalyst for direct alkylative Passerini reaction of aldehydes, isocyanides, and aliphatic alcohols. In the present reaction, α-unsaturated and aromatic aldehydes used as substrates produced the corresponding α-alkoxy amide products in good yield.

Keywords: Passerini reaction, Lewis acid catalyst, α-alkoxy amide, Bismuth (III) triflate

1. Introduction

Multicomponent reactions (MCRs), due to their productivity, simple procedures, significant advantages over conventional linear-type syntheses, and facile execution, are one of the best tools in combinatorial chemistry (Zhu, J. et. al 2005, Dömling, A. et. al 2000). Therefore, the design of novel MCRs has attracted great attention from research groups working in medicinal chemistry, drug discovery, and materials science. Isocyanide-based multicomponent reactions are used extensively in target oriented and diversity oriented organic synthesis (Dömling, A., 2006). The most widely known and best characterized isocyanide-based multicomponent reaction is the Passerini three-component reaction (P-3CR). In the Passerini 3CR, an isocyanide, a carboxylic acid, and either an aldehyde or a ketone react with one another to yield an α-acyloxycarboxamide (Dömling, A. et. al 2006). But the use of phenol or aliphatic alcohol derivatives instead of a carboxylic acid component has not been realized until recently. O-arylative Passerini-type reaction (El Kaim, L. et. al 2006, El Kaim, L. et. al 2007) was reported by the using *O*-nitrophenol derivatives in 2006, which have a more acidic proton compared to aliphatic alcohols. On the other hand, Chatani and co-workers (Tobisu, M. et. al 2007, Yoshioka, S. at. al 2005) reported that the reaction of benzaldehyde, isocyanide, and silyl-protected aliphatic alcohol can be catalyzed by triflic acid to give α-alkoxy amides in moderate yield. But the direct Passerini reaction using aliphatic alcohol derivatives instead of carboxylic acid components are still unsolved and the corresponding researches are less found. Yanai group have reported that direct alkylative Passerini reaction of aldehydes, isocyanides, and free aliphatic alcohols catalyzed by Indium triflate

(Yanai, H. et. al 2009). Therefore, the development of direct Passerini three-component type reaction of aldehydes, isocyanides, and aliphatic alcohols is still very necessary.

Bismuth (III) triflate is known as mild, soft, chemically stable Lewis acid, and used widely for condensation (Matsushita, Y. et. al 2005, Yadav, J. S. et. al 2006), addition (Ollevier, T. et. al 2009, Ollevier, T. et. al 2007), rearrangement (Ollevier, T. et. al 2006, Ollevier, T. et. al 2008) and multicomponent reactions (Ollevier, T. et. al 2003, Ollevier, T. 2006) as an effective catalyst in organic synthesis. In the present study, we were interested in the application of bismuth (III) triflate Lewis acid to the direct P-3CR of aldehydes, isocyanides, and aliphatic alcohols at reflux in THF providing to the corresponding α-alkoxy amide products (Figure 1).

To explore the effective Bismuth (III) triflate for direct O-alkylative P-3CR reaction and optimize the reaction condition, our initial attempts to examine the reaction of benzaldehyde, *tert*-butyl isocyanide and 2-propanol in THF with Bi(OTf)$_3$ as catalyst. In the presence of 20 mol % Bi(OTf)$_3$, the reaction of benzaldehyde with 1.0 molar equiv of *tert*-butyl isocyanide and 2-propanol at reflux for 10 h gave alkylative Passerini product in 40 % yield, and the product yield improved to 53% when *tert*-butyl isocyanide was added to 2.0 molar equiv. Moreover, the stepwise addition of *tert*-butyl isocyanide in reaction mixture dramatically increased the product yield. For example, in the presence of 20 mol % of Bi(OTf)$_3$, benzaldehyde was reacted with 1.0 molar equiv of *tert*-butyl isocyanide at reflux for 10 h, then further treatment by additional 1.0 molar equiv of *tert*-butylisocyanide in THF gave the corresponding product at reflux for 10 h in 75% yield.

Secondly, we checked the reaction with various aldehydes under the optimized conditions, the results exhibited the reactions with aromatic or α,β-unsaturated aldehydes to give alkylative Passerini product in good yield, such as, the reaction of cinnamaldehyde, *tert*-butyl isocyanide, and 2-propanol was nicely catalyzed by 20 mol % of Bi(OTf)$_3$ to give the corresponding α-isopropoxy alkylative amides 10 h in 82% yield. Under the same conditions, 2-naphthaldehyde and 2-furaldehyde gave Passerini products **4g** and **4h** in 73 and 78% yield, respectively. Unfortunately, with aliphatic aldehydes, the yield of O-alkylated products was not so good. For example, the reaction of cyclopentylaldehyde, *n*-propylaldehyde with *tert*-butyl isocyanide and 2-propanol, and produced the desired product **4i** and **4j** only in 50% and 44% yield.

Finally, we examined the reaction with various alcohols instead of 2-propanol, and this reaction also proceeded in secondary or primary alcohol. Under the same conditions, the reaction in cyclopentanol and cyclohexanol gave **4k** and **4l** in 72% and 67% yield, respectively. In general, the reactivity of primary alcohol such as *n*-butanol (**4m**) and *n*-propanol (**4n**) was lower than that of several secondary alcohols.

2. Experimental

In a typical procedure, a mixture of Bi(OTf)$_3$ (0.4 mmol, 20 mol %), aliphatic alcohol (2.0 mmol) in THF (30 ml), *t*-BuNC (2.0 mmol, 1.0 equiv) and aldehyde (2.0 mmol) were added. After being stirred at reflux for 10 h, the reaction mixture was treated by additional *t*-BuNC (2.0 mmol, 1.0 equiv) in THF (20 ml), and then stirred at reflux for 10 h. The resultant mixture was concentrated under reduced pressure and purified by column chromatography on silica gel and gave the corresponding direct alkylative Passerini products.

N-*tert*-Butyl-2-isopropoxy-2-phenylacetamide (**4a**) as a white crystal. Mp. 58.5~60.0 °C (57.5~59.0 °C[8]); ^{1}H NMR (400 MHz, CDCl$_3$) δ 1.07 (3H, d, J = 6.2 Hz), 1.16 (3H, d, J = 6.2 Hz), 1.29 (9H, s), 3.61 (1H, J = 6.1 Hz), 4.59 (1H, s), 6.62 (1H, brs, -NH), 7.18-7.30 (3H, m), 7.33-7.38 (2H, m); ^{13}C NMR (100 MHz, CDCl$_3$) δ 22.3 and 22.9, 29.6, 51.3, 72.0, 81.1, 125.9, 127.4, 127.8, 139.1, 171.2; ESI-MS m/z 272([M+Na]$^+$, 100%); Anal. Calcd for C$_{15}$H$_{23}$NO$_2$: C, 72.26; H, 9.29; N, 5.63. Found: C, 72.29; H, 9.20; N, 5.58.

N-*tert*-Butyl-2-(2-furyl)-2-isopropoxyacetamide (**4h**) ^{1}H NMR (400 MHz, CDCl$_3$) δ 1.18 (3H, d, J = 6.2 Hz), 1.23 (3H, d, J = 6.2 Hz), 1.42 (9H, s), 3.72 (1H, J = 6.2 Hz), 4.75 (1H, s), 6.28-6.34 (2H, m), 6.68 (1H, brs, NH), 7.33-7.37 (1H, m); ^{13}C NMR (100 MHz, CDCl$_3$) δ 22.1, 22.8, 29.2, 51.8, 72.0, 73.8, 110.1, 110.8, 143.2, 151.8, 169.0; ESI-MS m/z: 262 ([M+H]$^+$, 100%); Anal. Calcd for C$_{13}$H$_{21}$NO$_3$: C, 65.26; H, 8.85; N, 5.86. Found: C, 65.12; H, 8.91; N, 5.96.

3. Conclusion

In conclusion, we have developed a new and efficient method for the direct Passerini alkylative reaction of aldehydes, isocyanides, and aliphatic alcohols using aliphatic alcohols instead of a carboxylic acid component. In the present reaction, α-unsaturated and aromatic aldehydes used as nice substrates produced the corresponding α-alkoxy amide products in good yield. The present reaction is a highly useful method to construct the chemical library of α-alkoxy amide derivatives.

References

Dömling, A. (2006). Recent developments in isocyanide based multicomponent reactions in applied chemistry, *Chem. Rev.*, 106: 17-89.

Dömling, A., Ugi, I. (2000). Multicomponent reactions with isocyanides, *Angew. Chem. Int. Ed.*, 39: 3168-3210.

El Kaim, L., Gizolme, M., Grimaud, L. (2006). *O*-Arylative passerini reactions, *Org. Lett.*, 8: 5021-5023.

El Kaim, L., Gizolme, M., Grimaud, L., Oble, J. (2007). Smiles rearrangements in Ugi- and Passerini-type couplings: New multicomponent access to O- and N-arylamides, *J. Org. Chem.*, 72: 4169-4180.

Matsushita, Y., Sugamoto, K., Matsui, T. (2005). Bismuth triflate catalyzed mukaiyama aldol reaction in an ionic liquid, *Eur. J. Org. Chem.*, 4971-4973.

Ollevier, T., Ba, T. Y. (2003). Highly efficient three-component synthesis of protected homoallylic amines by bismuth triflate-catalyzed allylation of aldimines, *Tetrahedron Lett.*, 44: 9003-9005.

Ollevier, T., Etienne, N. (2006). synthesis of β-amino esters by bismuth triflate catalyzed three-component Mannich-type reaction, *Synlett*, 219-222.

Ollevier, T., Li, Z. Y. (2007). Bismuth triflate catalyzed cllylation of cldehydes with cllylstannane under microwave assistance, *Eur. J. Org. Chem.*, 34: 5665-5668.

Ollevier, T., Li, Z. Y. (2009). Bismuth triflate-catalyzed addition of allylsilanes to N-alkoxycarbonyl- amino sulfones: Convenient access to 3-Cbz-protected cyclohexenylamines, *Adv. Synth. Cat.*, 351: 3251-3259.

Ollevier, T., Mwene-Mbeja, T. M. (2006). Bismuth triflate catalyzed Claisen rearrangement of allyl naphthyl ethers, *Tetrahedron Lett.*, 47: 4051-4055.

Ollevier, T., Mwene-Mbeja, T. M. (2008). Bismuth triflate-catalyzed rearrangement of acetates of the Baylis–Hillman adducts into (E)-trisubstituted alkenes, *Tetrahedron*, 64: 5150-5155.

Tobisu, M., Kitajima, A., Yoshioka, S., Hyodo, I., Oshita, M., Chatani, N. (2007). Brønsted acid catalyzed formal insertion of isocyanides into a C−O bond of acetals. *J. Am. Chem. Soc.*, 129: 11431-11437.

Yadav, J. S., SubbaReddy, B. V., Gayathri, K. U., Meraj, S., Prasad, A, R. (2006). Bismuth(III) triflate catalyzed condensation of Isatin with indoles and pyrroles: A facile synthesis of 3,3-diindolyl- and 3,3-dipyrrolyl oxindoles, *Synthesis*, 4121-4123.

Yanai, H; Oguchi, T. and Taguchi, T. (2009). Direct alkylative passerini reaction of aldehydes, isocyanides, and free aliphatic alcohols catalyzed by indium (III) triflate, *J. Org. Chem.* , 74: 3927–3929.

Yoshioka, S., Oshita, M., Tobisu, M.; Chatani, N. (2005). GaCl$_3$-catalyzed insertion of isocyanides into a C−O bond in byclic ketals and acetals. *Org. Lett.*, 7, 3697-3699

Zhu, J., Bienaymë, H. (2005). *Multicomponent Reactions,* Wiley-VCH: Weinheim, Germany.

Table 1. P-3CR of Aldehydes, Isocyanides, and Aliphatic Alcohols Catalyzed by Bi(OTf)$_3$

Product[a]	R_1	R_2	Yield (%)[b]
4a	Ph	i-Pr	75
4b	p-MeOPh	i-Pr	69
4c	p-BrPh	i-Pr	76
4d	p-MePh	i-Pr	72
4e	propenyl	i-Pr	78
4f	styryl	i-Pr	82
4g	2-naphthyl	i-Pr	73
4h	2-furyl	i-Pr	78
4i	cyclopentyl	i-Pr	50
4j	n-propyl	i-Pr	44
4k	Ph	cyclopentyl	72
4l	Ph	cyclohexyl	67
4m	Ph	n-butyl	38
4n	Ph	n-propyl	32

[a]All known compounds were characterized by comparing their spectral data with those reported; [b]Isolated yields
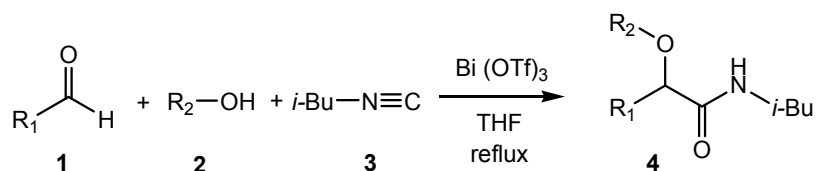
Figure 1. P-3CR of Aldehydes, Isocyanides, and Aliphatic Alcohols Catalyzed by Bi(OTf)$_3$

Call for Manuscripts

International Journal of Chemistry is a peer-reviewed journal, published by Canadian Center of Science and Education. The journal publishes research papers in the fields of applied chemistry, inorganic chemistry, analytical chemistry, organic chemistry, physical chemistry, structural chemistry, polymer chemistry, nuclear chemistry, chemical engineering and environmental chemistry. The journal is published in both printed and online versions, and the online version is free access and download.

We are seeking submissions for forthcoming issues. The paper should be written in professional English. The length of 3000-8000 words is preferred. All manuscripts should be prepared in MS-Word format, and submitted online, or sent to: ijc@ccsenet.org

Paper Selection and Publication Process

a). Upon receipt of paper submission, the Editor sends an E-mail of confirmation to the corresponding author within 1-3 working days. If you fail to receive this confirmation, your submission/e-mail may be missed. Please contact the Editor in time for that.

b). Peer review. We use single-blind system for peer-review; the reviewers' identities remain anonymous to authors. The paper will be peer-reviewed by three experts; one is an editorial staff and the other two are external reviewers. The review process may take 2-3 weeks.

c). Notification of the result of review by E-mail.

d). The authors revise paper and pay publication fee.

e). After publication, the corresponding author will receive two copies of printed journals, free of charge.

f). E-journal in PDF is available on the journal's webpage, free of charge for download.

Requirements and Copyrights

Submission of an article implies that the work described has not been published previously (except in the form of an abstract or as part of a published lecture or academic thesis), that it is not under consideration for publication elsewhere, that its publication is approved by all authors and tacitly or explicitly by the responsible authorities where the work was carried out, and that, if accepted, it will not be published elsewhere in the same form, in English or in any other languages, without the written consent of the Publisher. The Editors reserve the right to edit or otherwise alter all contributions, but authors will receive proofs for approval before publication.

Copyrights for articles published in CCSE journals are retained by the authors, with first publication rights granted to the journal. The journal/publisher is not responsible for subsequent uses of the work. It is the author's responsibility to bring an infringement action if so desired by the author.

More Information

E-mail: ijc@ccsenet.org

Website: www.ccsenet.org/ijc

Paper Submission Guide: www.ccsenet.org/submission

Recruitment for Reviewers: www.ccsenet.org/reviewer.html

International Journal of Chemistry